MULTI-SCALE MORPHODYNAMICS OF UNCONFINED COARSE-BEDDED RIVERS IN THE RUAMĀHANGA CATCHMENT

A thesis presented in partial fulfilment of the requirements for the degree of

DOCTOR OF PHILOSPHY

in

EARTH SCIENCE

at

MASSEY UNIVERSITY, PALMERSTON NORTH

NEW ZEALAND

William C. Conley, Jr.

2023

Primary Supervisors:
Professor Ian C. Fuller
Dr. Sam T. McColl

Co-supervisors:
Dr. Jon F. Tunnicliffe
Professor Mark G. Macklin
Professor Russell G. Death

Examiners:
Professor Brett Eaton
Dr. Murray Hicks
A/Prof Alan Palmer

THESIS ABSTRACT

Riverine floods are the most frequent global natural disaster and a fundamental behaviour of alluvial systems. Flood protection management tends to focus on constraining the spatial extent, frequency, and magnitude of inundation, but often neglects a second intrinsic alluvial behaviour: changes to the channels themselves. This omission can be particularly problematic for gravel-bed rivers, which are well-known for their change propensity across spatiotemporal scales due to complex sediment dynamics. Changes often vary asynchronously on timescales far greater than individual flow events with controls and processes that nest across spatial scales. Further, differential feedbacks mean that similar water discharge may result in two or more very different channel responses. This complex array of riverscape responses and biophysical feedbacks in space and time encapsulates riverscape dynamics, which lie at the heart of this thesis. The applied research of this thesis addresses important gaps regarding 1) suitability assessment of geospatial time-series data, 2) river avulsion hazard screening, 3) tectonic forcing of alluvial rivers, and 4) channel response to human forcing.

The gravel-bed rivers of New Zealand's Ruamāhanga catchment provide an excellent real-world setting to explore these gaps. The short, steep rivers draining the high-relief Tararua Range experience frequent, intense rain-driven hydrology and transit the low-relief of an active forearc basin after emerging from the mountain front. The rivers cross numerous active geologic structures including the Wairarapa Fault, known for the world's largest single-event land-based horizontal displacement (18.7 m) in 1855. Rivers draining the Tararua Range are known to have filled and expanded into the late-1860s as landslide sediments introduced to rivers during the 1855 shaking gradually worked downstream. Associated changes in river channel and floodplain forms would have generated more severe flood responses given a comparable pre-quake precipitation event. While the rivers eventually adjusted to a more relaxed state of response, their high intrinsic dynamism continues to challenge human habitation. With extensive riparian agriculture and 26% of all buildings occurring on Holocene alluvium, humans have exerted considerable control over the past sixty years using frequent (annual- to sub-annual) earth-moving to incrementally train multithreaded, wandering rivers into the narrower, straighter, and steeper forms seen today.

Confidence in localizing hazards and characterising river dynamics rests on certainty that the same locations is/are being compared through time and expressed as coregistration error for members of a time-series. I developed a numerical model to illustrate how root-mean-squared-error (RMSE) values, the customary form of error expression, from intercomparison of randomly-varied and systematically-biased datasets are substantially greater than RMSE values derived from comparison to a common reference. A case study from the Ruamāhanga catchment spanning a wide quality spectrum of archival aerial photomosaics (n = 5) indicates assumptions of residual normality are tenuous and RMSE consistently represents only 65-75% of error frequency and 30-36% of the maximum observed error magnitude. My results suggest that an empirically determined 95% confidence value is better suited to address simulated and real-world limitations. After reprocessing a subset of the historic data, some prior interpretations of channel movement were found erroneous. I propose a conceptual framework to aid fitness-for-purpose determination for different types of geospatial data quality, errors, and analyses to promote more suitable interpretations.

Globally, the direct observational record of major river relocations (avulsions) is highly limited given their infrequent occurrence on timescales from decades to millennia. Field- and model-based investigations over the last 45 years have identified a diverse array of contributing factors. These include sedimentation rates, conveyance capacities, and erodibility of existing channels relative to potential receiving areas, although to varying degrees across landscapes. My review identifies

topographic advantage as a common denominator across landscape settings and develop a relative digital elevation model (rDEM) approach for rapid, landscape-scale screening in GIS. I propose revision of the traditional two-phase avulsion model to be consistent with other threshold phenomena (e.g., landslides) that divides factors of the set-up phase into static and dynamic components. I present a simple, dichotomous conceptual framework along a gradient of sensitivity (threshold proximity) to aid resource prioritisation for follow-on investigation and/or mitigation. Explicit inclusion of coseismic displacement adds novelty, particularly as adjacent streams appear to be out-of-phase.

Control of rivers by tectonic processes is traditionally investigated at millennial and orogen scales though some recent studies have explored annual and reach scales. Nonetheless, fluviotectonic dynamics operating between these timescales are relatively unexplored, especially regarding gravel bed rivers. I relate changes from a time-series of benchmarked cross-sections to surface deformation interpreted from a high-resolution DEM for a 16-kilometre study segment that crosses four active oblique strike-slip faults and several folds. Net and total bed change within and between cross-sections exhibit a high-degree of noise and lack reach-scale patterns. In contrast, patterns of total change accumulated over the time-series show strong spatial partitioning by intersecting geologic structures. The least dynamic cross-sections are generally in proximity to uplifted axes while the most dynamic cross-sections are generally downstream of such intersections and/or coincide with inferred back-tilting. This is the first analysis to suggest morphological forcing of an alluvial river by active geologic structures is detectable at decadal-scale and persistent during an interseismic period.

Human river management is a critically important control, but seldom addressed by research across spatiotemporal scales. I address this gap by evaluating a mix of short- and long-term records to assess congruence between two common management aims: increased channel stability and reduced active footprint. Active belt width at the riverscape scale (~16 km) interpreted from a 69-year aerial photo record shows decreasing trend (-48% mean) and increasing uniformity (-62% SD) that converges on the width of the contemporary design corridor (fairway). By contrast, ultrahigh-resolution, reach-scale morphological budgeting over a series of sub-annual events finds roughly sixfold greater volumetric changes in sub-reaches with recent in-channel flood protection earthworks than adjacent untreated reaches. Treated subreaches experienced up to 16 metres of lateral bank erosion, had more instances of increased activity outside the fairway, and propagated changes into untreated areas upstream and downstream. While management actions appear collectively successful in long-term constraint of the riverscape's active belt, the same actions amplify bed changes from common flow events. I call this anti-pattern the "fairway paradox". Increased magnitude and frequency of reach-scale movements over short time periods creates maintenance dependencies and makes river responses to flooding less certain. Such scale-dependent responses mean action-effectiveness can only be assessed if aims explicitly identify spatiotemporal scale. Greater certainty regarding a river's location at any point in time may be gained by less frequent mechanical interventions. This study is the first rigorous evaluation of the effectiveness of NZ river fairway management with broad implications given the widespread application of similar river management throughout NZ.

Collectively, this thesis highlights importance of identifying different controls on river behaviour and the scales on which they operate. Substantive doubt is cast on broad application of theoretical or averaged design conditions over alluvial riverscapes with diverse and comingled controls. This is particularly important considering management has occurred under best-case conditions and a large sediment-generating earthquake is expected regionally every ~150 years. As the first work of its kind in NZ and possibly globally, this thesis provides a robust example for future multiscale investigations.

For Ada and Declan

My favourite days in the field are with you. May this work inspire lifetimes of personal growth and contribute to a safer, more aware world for your generation.

ACKNOWLEDGEMENTS

To my supervisors, especially Professor Ian Fuller and Dr. Sam McColl. I will always value your insights, patience, and critique. I will very much miss our “15-minute” chats and greatly look forward to future collaborations.

Massey University, Greater Wellington Regional Council (GWRC), and New Zealand Hydrological Society provided the funding without which this work would not have been possible. Menno Diersmann, James Fay, Brent Vermolen, Amelia Horne, Ada Conley, Declan Conley, Sam McColl, Ian Fuller, and David Feek provided field and/or data pre-processing assistance. I am grateful for data acquisition assistance provided by Land Information New Zealand (LINZ), National Institute of Water and Atmospheric Research (NIWA), GWRC, Landcare Research | Manaaki Whenua, and GNS Science. The following GWRC staff were particularly helpful for site access, acquiring reports, and data: Des Peterson, James Flanagan, Mark Hooker, Mike Gordon, Geoff Lewis, and Hamish Smith. Gareth Winter at the Wairarapa Archives was particularly helpful with historic references and insights. Thank-you to the many landowners that granted access to field sites, especially Bob Hall, Chris Southey, Dean Wilkinson, Rex Fenemor, and the Wadham family.

This work is possible because of professional and academic colleagues and instructors over the past thirty years, including:

- My fellow river curmudgeons: Sandy Allegretto, Terril Stevenson, and Marjorie Wolfe.
- Early academic inspiration provided by Paul Heller, Al Kimball, Larry Munn, Fred Servello, Andy Sheldon, and Tom Wesche.
- Pete Klingeman for recruiting me into professional service and whose boundless energy and insight touched so many.
- My PhD ‘feasibility committee’: Dave Fast, Colin Thorne, Rob Sampson, and Joe Wheaton
- Kent Houston for a conversation in Cooke City that sparked my geospatial odyssey: chocolate chip cookies and Guinness remain a delicious combination twenty-five years later.
- Professor Bernd Cyffka for being such an excellent host at the Katholische Universität Eichstätt – Ingolstadt.
- My thesis examiners for thoughtful feedback and engaging so thoroughly with this work.

Thank-you to the developers associated with following free and/or open-source software projects, including: Python and related packages (pandas, geopandas, matplotlib, numPy, shapely, scipy, and rasterio); Inkscape; QGIS; WinMerge; Bulk Rename Utility; GIMP; CloudCompare; 7zip; ImageMagick; Whitebox Tools; and Geomorphic Change Detection (GCD). I was also aided directly or indirectly by educational licenses granted for ArcGIS, GitHub, GitLab, Hilltop, Planet, and PyCharm.

To the Benoit, Cushnahan, Fouhy and Perry families whose kindness, support and friendship have helped make Aotearoa / Land of the Long White Cloud home.

Peter Lovejoy and Tommy and Megan Cushnahan for friendship, insights, and thought leadership: I’m a better person for knowing you.

To my Klickitat County ‘fire family’ and friends that helped us get here: It was an honour to serve with you and I remain in humbled by your assistance getting us packed for NZ. I miss you all.

Finally, thank-you to Scotti, Ada, and Declan for your support. What a great adventure this has been.

FOREWORD

The Wairarapa floods of 2 September 1884 caused “the rivers to swell to an *unprecedented* [emphasis added] extent” (1884c). Water rose at the rate of “a foot in ten minutes over the floors of [Masterton] shops and dwellings” (1884b) cresting with up to four feet of water inside of some structures and requiring evacuation of 120 to 150 families. Two homes were isolated when the Waipōua River channel changed course and lands along the Ruamāhanga River were “converted into an immense lake more than a mile in width” (1884b). Waters of the Waiohine reached the eves of houses at Woodside and the old river bed at the north end of Greytown became “a rushing mountain torrent” (1884a) that could not be safely crossed, forcing residents to shelter in second-story homes as the ground floors flooded. While only a handful of human lives were lost, many goods and many thousands of livestock were lost.

Early post-settlement accounts are rife with disruption, damage and occasional death resulting from flooding of the Wairarapa’s gravel bed rivers. Following construction of the first railway and road bridges in the late-1860s, the frequency of bridge damage from river flows mentioned by newspapers indicates routine occurrence. Yet the September 1884 flood produced heavier damage than most, including near-total removal of the newly constructed railway bridge across the Waipōua River, one span of the railway bridge across the Waingawa River and removal of the south approach to the road bridge over the Waipōua River (1884a). The September 1884 flood garnered national attention and, over subsequent weeks, was generally portrayed as exceptional. In stark contrast, a letter-to-the-editor published on 26 September (Correspondence, 1884) diminished such coverage, noting, “this last flood [September 1884] nothing into comparison with what has been.”

Unlike newspaper editors or most of the Wairarapa region’s human population in 1884, the author of the 26 September letter had lived in the area since January 1856. The author specifically notes witnessing three floods between 1858 and 1867 (possibly 1868) with the “plains under water, except a few patches.” Of these three events, the greatest detail is provided on the final one which also had the greatest implications for Masterton. During the third event, the Waingawa river shifted course into the Waipōua River upstream of Masterton with “but little difficulty, when it got into the old channel, in coming down the plain.” Fifteen or sixteen settlers worked for three days to “make a break-water with large boulders, walling them up” while working in water that was sometimes over their knees to counter the avulsion and return the river to its pre-flood course.

By virtue of greater extent and generating more dramatic river movements, it would be tempting to conclude the pre-1870 floods resulted from a greater quantity of rain than delivered by the 1884 storm. However, the strong potential for river channel and catchment dynamics to have influenced flood expression prevents such a conclusion. Channel filling and expansion commonly occurs over years to decades following the mass sediment delivery that accompanies large earthquakes, powerful storms, and periods of increased storm frequency, such as during climate shifts.

The pre-1870s floods followed shortly after New Zealand’s largest recorded earthquake (estimated M8.2) which occurred on the Wairarapa Fault in January 1855. Rivers draining the Tararua Range are known to have filled and expanded for over a decade following the Wairarapa quake. Such changes would have occurred as sediments from landslides (now widely recognised to co-occur with such severe shaking) initially swamped rivers in the ranges, then gradually propagated downstream. Thus, it is entirely possible for greater flooding experienced in the 1850s and 1860s to have resulted from channels that were more predisposed to flooding, possibly requiring even less precipitation than the 1884 storm.

New Zealand's mid-latitude location in the Southern Ocean along a major tectonic plate boundary makes it an inherently dynamic (and hazardous) place. The Wairarapa region's location on the fore-arc side of the axial ranges adds further complexity and amplifies geohazard hazards. It has been roughly eighty years since the most recent catchment-scale event (Masterton earthquakes of 1942) expected to radically influence channel form or process. Though localised manipulations of the Wairarapa's gravel bed rivers began 80-100 years ago, broad-scale intensive management began roughly 60 years ago. Despite occurring under best-case conditions, great ongoing effort and cost are necessary to maintain the rivers to approximate the selected design forms and dimensions. The hiatus of large sediment-generating events will eventually end, and big changes will return to Wairarapa rivers and present critical management challenges. In the absence of severe individual events, climate change is likely to produce catchment behaviours which management has not yet faced.

When I began this work in 2016 I found myself frequently having to explain its practical relevance. Even following the avulsion of the Clarence River associated with the 2016 Kaikoura earthquake, explaining continued to be required even as the analyses were completed in 2020. As I've put the finishing touches on the work the past couple of years, major events in British Columbia, Germany, Pakistan, Turkey, South Africa, New Zealand, and many other places around the globe have sadly made the work's relevance plainly apparent. With or without climate change, all locations have a bigger flood somewhere in their future and design criteria of engineered flood defenses will be exceeded. And most engineering defenses don't account for earthquake rupture or co-seismic sediment delivery. The need to better understand channel and catchment dynamics in advance is paramount and I am pleased to make such globally important contributions that increase understanding human contributions to flood risk and tectonic-forcing on river behaviours. In particular, I am proudest of the synthesis specific to the Ruamāhanga catchment and sincerely hope these findings are taken-to-heart to assist people of the Wairarapa coexist in a safer manner with their truly fantastic rivers.

Will Conley
June 2023
Eketāhuna, NZ

Contents

Chapter 1

General Introduction

Floods comprised 47% of all weather-related disasters globally between 1995 and 2015, and impacted over 2.3 billion people (UNDRR, 2015). Riverine floods are the most frequent natural disaster globally and affect the second highest number of people after droughts (Guha-Sapir, 2020). Nationally, New Zealand has the second highest natural hazards risk in the world (Lloyd's of London, 2018), with floods reported to be the costliest type (McSaveney, 2009). Consistent with global statistics, floods are New Zealand's most frequent natural disaster (Flood Risk Management and River Control Review Steering Group, 2008; McSaveney, 2009; Ministry of Business Innovation and Employment, 2020) with an 87% chance of at least one 1% Annual Exceedance Probability (AEP; a.k.a. 100-year recurrence) flood event occurring in a populated New Zealand catchment in any given year (Smart and McKerchar, 2010). While natural hazard risks, including floods, and the natural character of "rivers and their margins" are explicitly considered matters of national importance (RMA , Parliament, 1991; Part 2, Section 6), risky developments and human pressure on floodplains have grown (Smart and McKerchar, 2010). Awareness that the geographic distribution, extent, frequency and magnitude of natural disasters changes through time has increased with the Insurance Council of New Zealand (2014) explicitly emphasising the need to focus on areas where future risks may increase.

In its simplest form, *risk* is the product of hazard occurrence probability and consequence magnitude. Thus, *flood risk* results from the potential for physical flood metrics (e.g., spatial extent, depth, duration, and velocity) to produce adverse outcomes to human values with some frequency. The physical metrics associated with a particular flood event result from 1) the quantity and timing of materials delivered (e.g., sediments, wood, and solutes) and 2) the state of receiving area conditions at a given point in time. Differential feedbacks and lagging by system components (e.g. water, sediment, and vegetation) often vary asynchronously on timescales far greater than a flood (or other disturbance) event itself (cf. Fryirs and Brierley, 2012, ch.2). Incremental and punctuated changes to site, catchment, weather and/or climate conditions during and between floods create an infinite number of interactions such that any given location within a riverscape is unique or "perfect" (sensu Phillips, 2007). Consequently, similar water discharge can result in two (or more) very different expressions of flooding depending on the state of a system at time of receipt (e.g., Stover and Montgomery, 2001; Slater, 2016). Inundation and morphological effects are the first-order outcomes that typically receive the greatest focus. As preconditioned by interim processes, the complex and variable spatial relationships through time form a riverscape (e.g. Carbonneau et al., 2012). This complex array of riverscape responses and biophysical feedbacks in space and time encapsulates *riverscape dynamics*, which lie at the heart of this thesis.

1.1 Background

Throughout this thesis, *hazard* indicates a process, phenomenon, or activity capable of adversely affecting human values, the consequences of which may include death, health, property, environmental or socioeconomic degradation and/or disruption. In establishing the relevance of this thesis, consideration of present flood hazard assessment and protection practice frames the

importance of understanding riverscape dynamics which, ultimately, drives the need for this research.

1.1.1 Flood hazard: protection and assessment uncertainties

Global efforts to prevent flood losses over the last century have emphasised flood protection infrastructure (FPI) to moderate rates of water delivery (e.g., flood control reservoirs) and/or physically isolate rivers (e.g., levees, channelisation, etc.) in proximity to tangible human interests. However, dramatic increases in flood related losses since 1980 have co-occurred with increased structural flood protection investment and increasingly raised questions of efficacy (Pielke, 1999; European Environment Agency et al., 2008; de Moel et al., 2009). Early research identified one-third of flood-disasters in the U.S. resulted from levee (i.e. stop bank) failures (National Research Council, 1982). Further, documentation that structural approaches may perversely incentivise development into flood-prone areas (e.g. Pinter, 2005) via "The Levee Effect" (Tobin, 1995) indicates overall exposure increases when a flow event exceeding the protection design standard eventually occurs. *Exposure* is considered the situation of tangible human interests located in hazard-prone areas such as the number of people, types of infrastructure assets, or production capacities (United Nations Office for Disaster Risk Reduction and International Science Council, 2020).

Socioeconomic factors like wealth, population, and human expansion into vulnerable areas are routinely identified as the main contributors of increased losses (Downton and Pielke, 2005; Barredo, 2009; Smart and McKerchar, 2010; Bouwer, 2011; Mohleji and Pielke, 2014) though backwatering, velocity redistribution and reduced sediment transport capacity directly caused by FPI have also been implicated (Tobin, 1995; Syvitski and Brakenridge, 2013). While there is concern regarding the potential effects of climate change on flood frequencies and magnitudes, definitive evidence of present occurrence is slow to emerge. Two studies have suggested that damages, when normalised by exposed population and gross domestic product, may have declined since the mid-2000s (Jongman et al., 2015; Tanoue et al., 2016) implying some potential effectiveness of broader flood risk management than previous purely FPI-based regimes. Human decision-making and spatial distribution of human population density were implicated as primary drivers of losses and exposures in both studies.

Increased awareness of FPI limitations has driven increased interest in risk-based based approaches that incorporate complimentary non-structural measures and/or adaptation (Faisal et al., 1999; Flood Risk Management and River Control Review Steering Group, 2008; Liao, 2014; Kreibich et al., 2015; Hutchings et al., 2019). Application of adaptive and non-structural approaches such as zoning ordinances, sealing and shielding buildings, detection and notification systems, mobile protection devices and use of floodplain and off-channel storage has gained support in recent decades (International Commission for the Protection of the Rhine, 2002; Bouwer et al., 2007; Bouwer et al., 2010; Liao, 2014; Kreibich et al., 2015; Bubeck et al., 2017; Mai et al., 2020) including consideration in law (e.g. 103rd Congress of the United States, 1994; European Parliament and the Council of the European Union, 2007) and national standards (Standards New Zealand, 2008). Despite this, international spending on proactive elements (prevention and preparedness) is about $1/20^{th}$ of reactive expenditures (emergency response, reconstruction, relief and rehabilitation) (United Nations Office for Disaster Risk Reduction, 2019a). New Zealand Central Government expenditures track similarly, with the majority spent on response and recovery phases. Regardless of approach and distribution of expenditures, expert opinion has long been clear (e.g. National Research Council, 1982) that flood prone areas never become safe or risk-free.

Flood ordinances and zoning may be effective in slowing human exposure increases but have had far less success actually reducing exposure (Patterson and Doyle, 2009) and areas immediately adjacent to regulated floodway boundaries experience faster rates of development than distal areas (Patterson and Doyle, 2009; Ferguson and Ashley, 2017). Standard flood mapping and mitigation practices assume stationary (i.e., mean and variation are static through time) boundary conditions and most continue to treat regimes as deterministic despite increasing scientific recognition that conditions are generally non-stationary (Slater et al., 2015; Call et al., 2017). Nonstationary boundary conditions add nonlinear uncertainty to hydraulic parameter estimates (Call et al., 2017) and may contribute to significant underestimates of flood hazard exposure (Lane et al., 2007) with inundation probabilities for areas outside of official floodways estimated up to 80% (Stephens and Bledsoe, 2020). Realisation that topographic complexity is a greater driver of inundation than process representation in hydraulic models (Hunter et al., 2007) has been slow to enter flood management practice. Similarly, 2-dimensional hydraulic models have only entered more regular management practice in the last 5-10 years and mobile boundary models (i.e., deformable bed and banks) continue to be uncommon outside of research settings. Consequently, the majority of flood maps and, by extension, floodway zoning and regulations are based on 1-dimensional fixed-boundary hydraulic models that do not accommodate fluvial morphodynamics increasingly recognised as important to flood inundation (Slater et al., 2015; Slater, 2016; Call et al., 2017; Naylor et al., 2017) and timing (Staines and Carrivick, 2015) in ways that may exceed climate change effects (Lane et al., 2007).

Geomorphic (sensu Croke et al., 2016; Naylor et al., 2017) and probabilistic (e.g. Stephens and Bledsoe, 2020) approaches have been shown to improve characterisation of flood risk, though uptake has been slow in many parts of the world. Overall limitations and fallibility of current flood hazard practice can be tied to the socio-political contexts that ultimately frame them (sensu Baker, 2007) with predisposition favouring floodplain development in some form and generally reactive infrastructure-based approaches in response to stakeholder pressure (O'Connell and O'Donnell, 2014). As improved data and methods become available, there is no trigger to revisit existing flood maps (i.e., developed via traditional, deterministic methods) beyond regularly scheduled intervals that may be decades in the future. Loss-projections for instances where flood hazards and exposures are well-characterised may still ignore societal vulnerability for which spatiotemporal patterns are often lacking (Jongman et al., 2015).

A recently developed national-scale flood model (FSF-FM; First Street Foundation, 2020b) for the entire United States couples data sourced across levels of government, expert modelers, and third party sources. The FSF-FM considers a spectrum of flood mechanisms and identified approximately 1.7 times as many properties at risk than designated within Special Flood Hazard Areas (SFHAs; First Street Foundation, 2020a). Though SFHAs are the present U.S. legal standard used for insurance pricing and disaster planning, they have mostly been designated in populated areas, focus purely on fluvial flooding, and large portions of the country are unassessed. The integrated approach of the FSF-FM identifies 14.6 million properties at substantial risk, approximately 40% (5.9 million) of which are not officially identified within SFHAs. Accounting for climate change and human population expansion (but not morphological changes), the FSF-FM projects an 11% increase in properties at substantial risk by 2050. Given global socio-political pressures driving floodplain development, such an under-assessment of risk seems to be a global problem.

1.1.2 River Dynamics

Broadly, dynamics are “a pattern or process of change, growth, or activity” (Merriam-Webster, 2020). *River dynamics* are changes to rivers through space and time resulting from the interaction of

ecological, chemical, and physical processes. As a field of study, *morphodynamics* investigates process interactions and outcomes related to sediment transfer and the shaping of landforms, often referred to as process-form linkages (*sensu* Tunnicliffe and Brierley, 2016). The morphodynamics of gravel bed rivers pose a particularly challenging range of hazards to human life and property that vary through space and time by event-scale (e.g., individual storm or dam-breach) to millennial-scale (e.g., tectonic, climatic, or volcanic) processes. The nature of event magnitude distribution through time, as well as the very definition of risk, necessitates statistical treatment and/or parameterisation. However, lack of incorporation of 'extreme' events into statistical contexts compounds under-estimates of dynamics and adds to uncertainty (Macklin and Lewin, 2008). Further, statistics overlook the individuality of a given event and, in particular, the role of dynamics between events in conditioning channels (Naylor et al., 2017).

Human memories are short regarding effects on post-disaster decision-making and societal pressure to address routine / nuisance issues often drive subsequent actions without regard for adversely pre-conditioning the next disaster. As land uses intensify between disasters, incremental river changes such as bank erosion associated with more routine (non-disaster) flow events generate pressure from stakeholders for government action favouring stability. Human conditioning of channels results from the cumulative effects of infrastructure (FPI, transportation, buildings, etc.) and more distributed manipulations of channel and/or floodplain hydraulics, such as vegetation removal/planting, gravel extraction/augmentation, bar grading, large wood removal/placement, et al.

Unconfined rivers on alluvial fans maintain sediment transport capacity via lateral migration. Those fixed in place laterally (e.g., by FPI), must steepen and by extension, aggrade, to maintain transport capacity (Davies et al., 2003; Davies and McSaveney, 2006). As such, FPI can amplify aggradation (e.g. Beagley et al., 2020b), and accelerate the rate at which bed rise encroaches on a stopbank's (i.e. levee) capacity to contain a specific water flow for a designed AEP. While inundation is the more frequent focus of flood risk mitigation, channel movements inclusive of avulsions may be more consequential. This is especially important as bed-slope is a key component of the relationship between sediment supply and avulsion frequency (Ashworth et al., 2004).

The configuration and connectivity of a river system at any point in time establishes a domain of possible future trajectories. These are based on interactions of perturbation type, magnitude, and frequency as well as the degree to which such forcings are in-phase (sensu Schumm and Lichty, 1965; Fryirs and Brierley, 2012). For example, location within a riverscape (e.g. Ashworth et al., 2004), lithology (Keen-Zebert et al., 2013), floodplain morphodynamics (Hajek and Edmonds, 2014) and channel morphology (Valenza et al., 2020) are recognised in determination of avulsion frequency and style. Consideration of scale is critical for capturing form-process and/or process-response linkages, particularly at fine-scales and where behaviours are non-linear (Lane and Richards, 1997). In the case of avulsions, this becomes complicated when some researchers classify spatially in a network context (i.e. local vs. regional, sensu Heller and Paola (1996)) while others differentiate between processes (e.g. progradational vs. incisional, sensu Hajek and Edmonds (2014)). While significant commonalities to both approaches exist (i.e., tendency to re-occupy existing channels or not), they are not mutually-inclusive. To a degree, this can be addressed by taking a step back and considering time, space, and process through the lens of "behaviour".

Behaviour is a useful concept for thinking about changes through time and has been defined as how a landscape "adjusts over time to various impulses for change" (Fryirs and Brierley, 2012, p. 26). For this thesis, I refine a working definition of *change* as the suite of adjustments resulting from the interactions of energy impulses through time. My application of "change" in this thesis is purely

functional and can be considered *spatially explicit change*: a detectable difference for a given spatial unit between points in time. By tradition, behaviour is characterised descriptively, though I supplement with spatially explicit metrics of statistical variability. I do not constrain "behaviour" by partitioning natural from non-natural adjustments nor do I differentiate "change" as a wholesale change in river type (sensu Fryirs and Brierley, 2012). My streamlined usage is intended to maintain up-front, quantitative clarity while still accommodating (but not requiring) differentiation of change mechanisms or origins. Further, it maintains consistency with standard usage related to key driving factors of geomorphic change, water, and sediment transfer, which are the critical elements in two fundamental geomorphic processes: deposition and erosion. In terms of dynamics, deposition-dominated spatial units tend to be more laterally active and over extended time periods may be considered aggradational (sensu Mackin, 1948). Such systems are typically associated with more dynamic behaviours.

1.2 Study significance and rationale

Many of the world's great civilisations developed in association with aggrading river systems and demonstrated patterns of development both affected by and adaptive to river channel changes (Macklin and Lewin, 2015). If ancient cultures could persist for thousands of years in aggrading environments without modern technologies, why are humans so challenged today?

The answers, of course, are well beyond the scope of this thesis. However, put simply, many ancient cultural systems valued and even depended on natural dynamics differently than contemporary cultures. They were also constrained by the limits of their respective technologies to affect change. By contrast, contemporary land-uses are globally implemented with aspirations of permanence and generally threatened by natural system dynamics. More people are in harm's way than ever before, with socioeconomic decision-making focused on short-term profitability that externalises costs to future owners and inhabitants, and a general over-confidence in technology-driven mitigation processes that are often poorly parameterised. Given contemporary socioeconomic trends are unlikely to abate, the need to better understand river dynamics becomes even greater to sort-out where on a continuum of necessity accommodating dynamics sits.

The logical chain that flows through the above sections is: A) rivers are fundamentally dynamic entities, B) human understanding of river dynamics is incomplete and C) failure to accommodate what is known of dynamics leads to problems (sensu Brierley et al., 2021). These premises become particularly problematic when 1) current risks are underestimated and/or 2) there is good reason to expect future risks to increase, particularly as modern human developments are increasingly intended as semi-permanent in locations that are geomorphically transient. If the movement of riverbeds and banks is the simplest conception of dynamics, then it can be said that societal tolerance of such behaviour is generally low. In the present period of increasing climate non-stationarity, humans are learning just how much isn't known as the cumulative limitations of methodology and data to predict future outcomes continue to become known. Thus, a counterintuitive relationship exists: the demand for stability of flood-prone areas increases despite greater understanding of the uncertain, hazardous, and costly nature of constraining riverscape dynamics.

Effectiveness of catchment management in general depends on knowing the spatiotemporal scales of river-system adjustments (Macklin and Lewin, 1997). The need to consider disaster risk across scales is increasingly recognised and integrated in the UN's biennial Global Assessment Report (GAR) for the first time in 2019 (United Nations Office for Disaster Risk Reduction, 2019a). Planning frameworks that anticipate uncertainty are essential for dealing with non-linear changes in risk and

maintain buffers (conceptual and real) to avoid creation of new risks while reducing existing ones. Between 2005 and 2017, global humanitarian financing in repeated cycles of disaster-response-repair was roughly $137 billion versus $5 billion for prevention in the same period (United Nations Office for Disaster Risk Reduction, 2019b). The transition from present emphases on disaster management and response to regimes that emphasise risk prevention and uncertainty adaptability require integrated, transdisciplinary systems-based approaches (United Nations Office for Disaster Risk Reduction, 2019a) whose success requires robust hazard and risk information (United Nations Office for Disaster Risk Reduction and International Science Council, 2020).

The comfort provided by familiarity of traditional methods is not commensurate with their often (in)accurate representation of known real-world complexities and uncertainties. The first heading in the executive summary of the 2019 Global Assessment Report (2019 GAR) on Disaster Risk Reduction (United Nations Office for Disaster Risk Reduction, 2019a, p. iv) states, "Surprise is the new normal". The need for risk assessments to shift to transdisciplinary multisectoral approaches and consider interrelated causes and vulnerabilities has been identified by the insurance industry (Mills, 2005) and government (United Nations Office for Disaster Risk Reduction, 2019a). While data quality is recognised as a key component throughout risk assessment and management processes (United Nations Office for Disaster Risk Reduction, 2019a), data of poor or otherwise uncertain quality only compounds the frequency potential and consequence magnitude of 'surprises'.

Resilience concepts are useful for minimising potentially adverse effects of 'surprise' disturbances. Their convergence with scale and hierarchy concepts at the core of geomorphology has important applications (Thoms et al., 2018). Resilience is the sum of resistance and recovery and, using response amplitude, recovery rate, and disturbance frequency can be used to frame dynamics (Fuller et al., 2019a). Intuitively, both real and conceptual 'space' (e.g., in decision processes) as well as a tolerance for change are important for implementing resilience. Given allowable space is often not the present risk management model employed in a locality, adaptation is required.

Adaptive human behaviour has potential to largely contain future flood losses (Jongman et al., 2015). However, to be adaptive, one must first be aware. My multidisciplinary investigations in this thesis increase awareness of riverscape dynamics across spatiotemporal scales and address both methodological and knowledge gaps. An emphasis is placed on spatially explicit geomorphic change detection, that is, changes to the Earth's surface through time that can be assigned to discrete locations. Spatially-explicit understanding of natural hazards can aid decision-makers' and first-responders' perceptions of vulnerability to better target preparedness and outreach (Keller et al., 2019). It is hoped this thesis enriches the foundation of data and information upon which more resilient decision-making regarding river channel dynamics will be made.

1.3 Thesis Aims and Objectives

The intent of this thesis is to advance global knowledge of multiscale morphodynamics and provide a foundation for more effective and sustainable flood and erosion hazards decision-making in the Ruamāhanga catchment. The Ruamāhanga catchment is in New Zealand's Wairarapa region at the southern end of the North Island (Figure 1-1), approximately 100 km west of the Hikurangi Margin where the Pacific Plate is actively subducted under the Australian Plate. Coupled with the high density of active geologic structures (folds and faults) produced by the plate setting, ninety-three percent of buildings in the catchment occur on river deposits. Twenty-six percent of all buildings sit on ground that has been fluvially active during the Holocene (Chapter 3, this thesis). Thus, the Ruamāhanga catchment provides an excellent opportunity to explore a wide range of river and landscape dynamics of high relevance to human values within a very modest area (<3,500 km^2).

The importance of scale-integrated analyses is increasingly recognised and made possible by recent, combined advances in spatially continuous, high-resolution geospatial data and modern computing power. In this thesis I employ a blend of field and remotely sensed data to explore multiscale fluvial relationships and interactions with non-fluvial forcing associated with tectonic and anthropogenic disturbance. This research also furthers methodological developments in the alluvial change detection and remote-sensing sub-field by developing and refining procedures that improve data characterisation and quality control. Taken as a whole, this work intends to provide novel insights into river morphodynamics within and across scales, enhance communication of research confidence and facilitate robust data-driven decision-making for river managers. In so doing, my thesis addresses three of four trajectories in the field of geomorphology identified by Church (2010), specifically: 1) reconciling representations across spatiotemporal scales, 2) comprehending historic process and landform complexity, and 3) recognising anthropogenic dominance in modifying terrestrial surfaces.

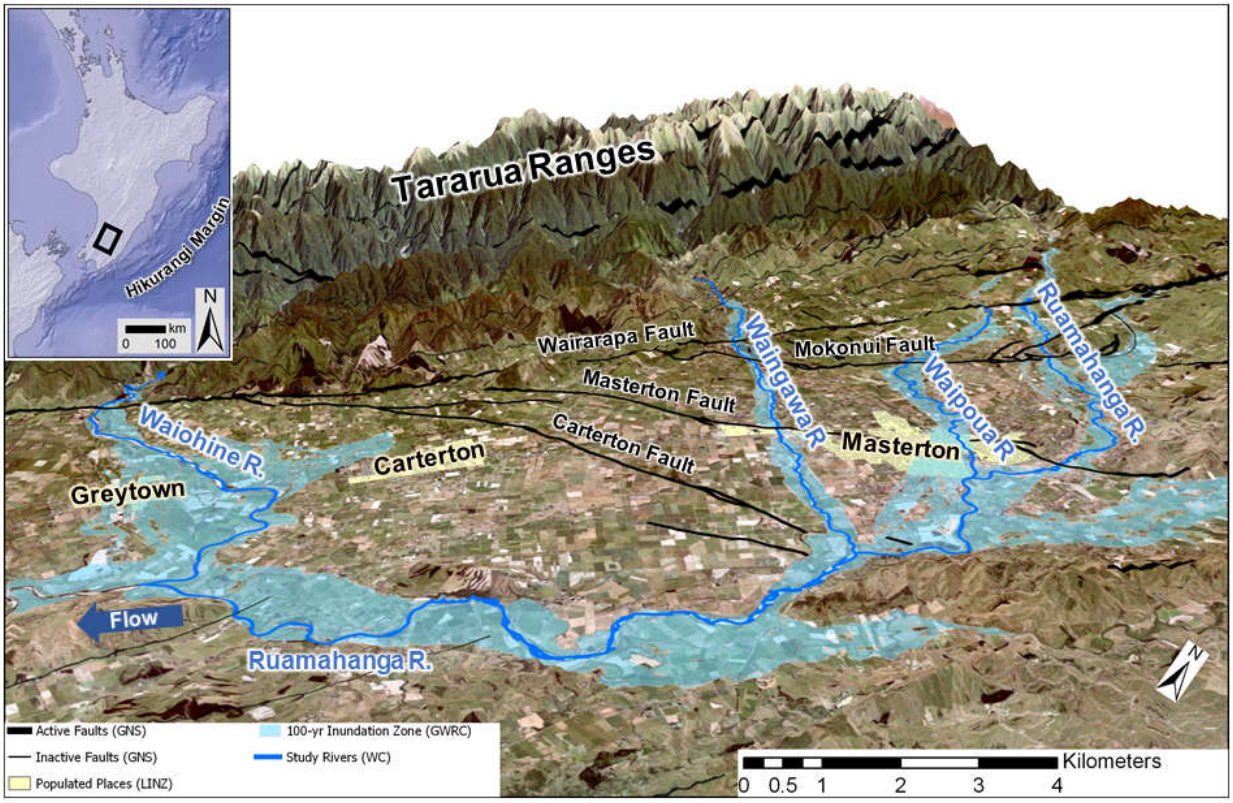

Figure 1-1. Upper Ruamāhanga catchment study area (adapted from Conley et al. (2017a)).

The overarching aim of this thesis is to deepen understanding of gravel bed river dynamics in New Zealand's upper Ruamāhanga River catchment across spatiotemporal scales in a manner that is both scientifically novel and fills management-relevant information gaps, particularly related to river sensitivity and hazards.

Specific thesis objectives are:

i. Highlight the need for formal data quality assessment of spatially referenced time-series, e.g., archival aerial imagery, and contribute methodology to improve confidence and communication of fitness-for-purpose in geomorphic change detection practice.
ii. Develop a landscape-scale screening framework to address and streamline river avulsion hazard identification and prioritisation across geomorphic settings.

iii. Evaluate detectability, persistence, and spatial partitioning of unconfined vertical bed dynamics by active geologic structures during an interseismic period.
iv. Juxtapose multidecadal, riverscape trends to within-season morphodynamics across common runoff events to identify and explore an anti-pattern resulting from competing river management aims.

1.4 Thesis Organisation

This thesis is prepared in a "with-papers" format that includes a broad literature review (Chapter 2), a study area description (Chapter 3), four chapters (Chapters 4-7) contributing original research, and a coherent synthesis and conclusion for the collective body of work (Chapter 8). Chapters 4- 7 are presented in-preparation for journal submission but have been partially reformatted to improve flow using continuous page, figure and table numbering as well as a single, aggregated references cited. Some content, such as area maps and study area descriptions, is necessarily duplicated across journal manuscript chapters, though chapter-specific introductions and summaries have been added to further aid flow and overall thesis cohesion. The general flow across scales is from data quality applicable to all spatiotemporal scales (Chapter 4) to long-term (multidecadal to millennial), landscape-scale (Chapter 5), to persistent interseismic partitioning of bed dynamics at decadal riverscape scale by active tectonics (Chapter 6), to multiscale morphodynamic response to human-scale forcing (Chapters 7). Figure 1-2 provides a visual reference of thematic interrelationships between chapters along spatial and temporal axes.

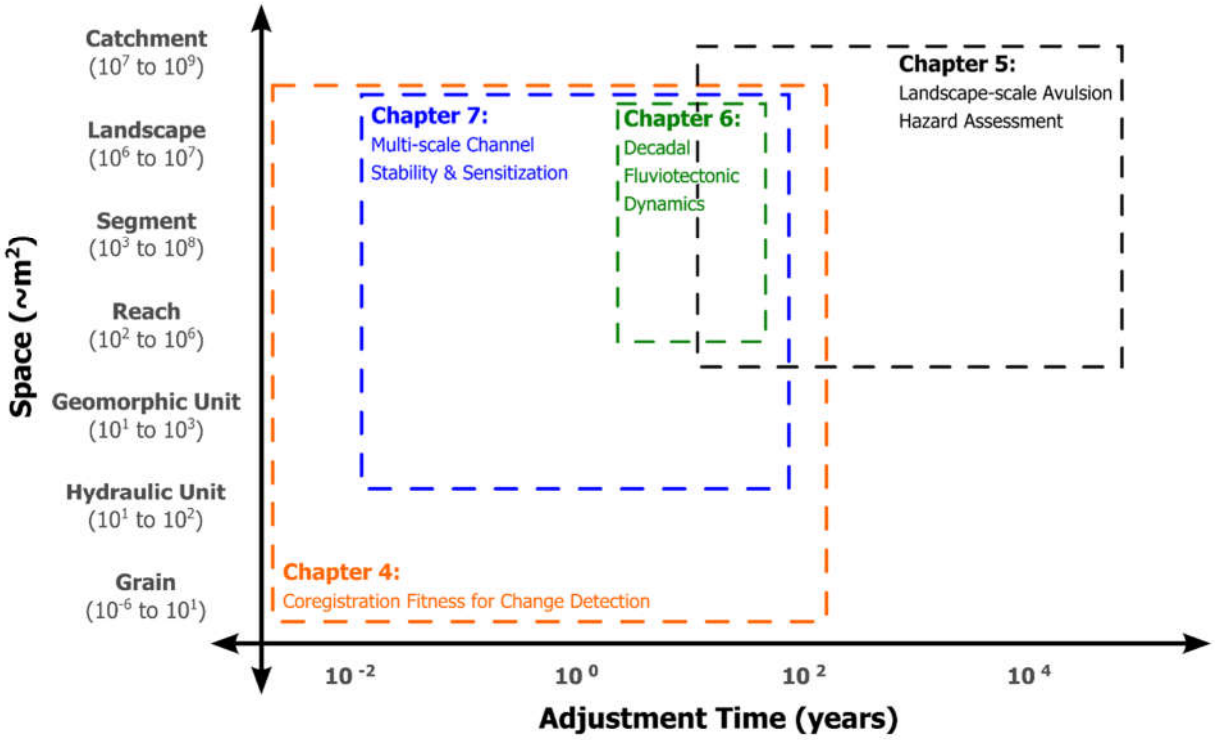

Figure 1-2. Conceptual spatiotemporal scaling of the research chapters in this thesis.

Chapter 2 The thesis opens with a high-level review of spatiotemporal concepts and morphodynamic controls to frame core chapters (4-7). Given the multidisciplinary nature of this thesis and "with papers" format, I reserve detailed subject matter review for the respective core chapters to minimise redundancy. Thus, this chapter ought not be conceptualised by reviewers as a comprehensive review for all subjects addressed subsequently.

Chapter 3 In Chapter 3, I introduce the Wairarapa region and upper Ruamāhanga study area. The geologic and geomorphic setting, rivers, hazards, and management are described based on local and regional literature supplemented with first-hand observation and findings.

Chapter 4 The overall theme of Chapter 4 is certainty in change detection analyses as it relates to positional accuracy and ensuring the same spatial unit(s) is compared through time. I explain that the relevance and confidence of spatially explicit change analyses are inherently related to the positional quality of input data. In practice, evaluation of input data fitness for change detection is study-specific and ranges across a gradient from rigorous statistical approaches to assumed fitness. In this chapter I also present an assessment hierarchy that groups and screens key data quality attributes by study aims and scale. I include a comprehensive review of the development of the spatially explicit change detection sub-field. It emphasises fluvial change due to the disproportionately high representation in the literature, significance in historical development, and relevance to this thesis. I employ a combination of numerical modelling and case studies to identify and illustrate key areas of uncertainty, which are then addressed by a proposed process and framework to evaluate quality and screen suitability of positional data. My quantitative approach builds upon empirical error evaluation presented by Hughes et al. (2006) and emphasises graphical evaluation of spatial distribution of positional errors. This approach underpins all subsequent thesis chapters, particularly chapter seven. Chapter 4 is 'in-preparation' for *Geomorphology* as: Conley, W.C., S.T. McColl, I.C. Fuller, J.F. Tunnicliffe, and M.G. Macklin. Framing coregistration fitness for geomorphic change detection.

Chapter 5 I build on the previous chapter in Chapter 5 by taking a landscape view of avulsion-based flood hazard for a variety of low-relief, alluvial settings in the Ruamāhanga catchment. Flood hazard assessment in the Ruamāhanga catchment mirrors global practice with hydrologically-oriented modelling based on short time-series and expectations of systematic responses to design events and without regard for geomorphic non-linearity (sensu Sinha, 2008; Croke et al., 2016). Despite general recognition as a hazard, avulsion often escapes explicit consideration in global (e.g. Gill and Malamud, 2014) and New Zealand-based (e.g. Grant, 2005; Spector et al., 2019) reviews of hazards and/or resiliency. Technical treatment of avulsions tends to be fragmented by sub-fields (e.g., fans/sedimentary basins, braided rivers, deltas, and lowland rivers). Chapter 5 partly addresses the collective need for consideration across geomorphic settings, explicitly includes active tectonics while integrating mechanisms across a sensitivity spectrum of preparation, preconditioning and triggers. A DEM-based approach is used to localise potential geomorphic hotspots (sensu Czuba and Foufoula-Georgiou, 2015) and prioritise system components approaching or near thresholds or that may otherwise be susceptible to significant morphological responses (sensu Phillips, 2003). Thus, my results can assist land-use and emergency planning prioritisation of these infrequent, but consequential channel behaviours. Chapter 5 is 'in-preparation' for submission to *Natural Hazards* as: Conley, W.C., I.C. Fuller, S.T. McColl, and J.F. Tunnicliffe. Landscape-scale river avulsion sensitivity in a low-relief, active tectonic setting: streamlined hazard screening.

Chapter 6 In Chapter 6, I refine the spatial and temporal scales of Chapter 5 by exploring decadal active channel dynamics along a 15-kilometre unconfined segment of the Waingawa River. I build upon modelling results of Heller and Paola (1996) and use six repeat surveys of thirty benchmarked cross-sections over a 22-year period to evaluate detection, persistence and partitioning of vertical bed changes by intersecting tectonic structures. A conceptual model is presented to expand global conceptions of how rivers may adjust to vertical deformation beyond simple planar offset to consider effects of tectonic back-tilt. Chapter 6 is 'in-preparation' for submission to *Nature Communications: Earth and Environment* as: Conley, W.C., S.T. McColl, I.C. Fuller, J.F. Tunnicliffe, T.

Stahl, and M.G. Macklin. Persistent control of vertical bed dynamics by active faults in unconfined gravel-bed rivers.

Chapter 7 I take a multiscale, spatially continuous approach in Chapter 7 to characterise and contrast the morphodynamic end-members of human-scale management. Trends in geographic and statistical distributions of active belt width are examined at riverscape scale based on a 69-year aerial photographic record that begins prior to the onset of widespread in-channel earthworks. I also empirically establish a magnitude-frequency context for geomorphic change in support of a spatially-nested, high-resolution segment-scale investigation of differential reach-scale stability associated with contemporary runoff events. Planimetric and volumetric geomorphic changes are evaluated using ultra-high resolution orthophotography and terrain models derived from repeat UAS surveys. Spatiotemporal proximity to physical disturbance from flood protection actions and mechanisms for increased channel sensitisation are identified and discussed related to flood protection operations and concurrent management aims of channel stability and reducing flood extent. The combination of sensitivity with connectivity concepts adds utility to assessing scenarios of reach-scale adjustments (sensu Lisenby et al., 2020). Chapter 7 is 'in preparation' for submission to *Science of Total Environment* as: Conley, W.C., I.C. Fuller, and S.T. McColl. Scale-dependent morphodynamic patterns of channel stability and sensitisation in managed rivers.

Chapter 8 I conclude the thesis with the synthesises of chapter-based content within the overall context of multiscale alluvial channel dynamics and river management of gravel bed rivers in the Ruamāhanga catchment. Conclusions are provided within the context of thesis aims and objectives and follow-on research opportunities are identified.

Chapter 2

Literature Review

Morphodynamic investigation relates changes in shape or form (*where, when, and what*) to more pertinent questions of geomorphic process (*how* and/or *why*). Thus, detection, description, and understanding of morphodynamics depends on multiple observations through time. Fundamental questions of *when* and *where* must be determined with some degree of certainty before characterisation or inference of *what*, *how* and/or *why* can be confidently assessed. Along such a spectrum, this chapter provides a high-level review of core morphodynamic concepts that frames my original research presented in chapters four through seven. This thesis incorporates the fields and subfields of fluvial geomorphology, tectonic geomorphology, geoinformatics, geoanalytics, remote sensing, photogrammetry, geomorphic change detection, sediment budgeting, and sediment transfer. Given its multidisciplinary nature and "with papers" format, I present detailed subject matter review within the relevant research chapters to minimise overall redundancy. Thus, this chapter presents a high-level overview of key morphodynamic concepts to broadly frame the thesis and should not be considered a comprehensive review. Subheadings generally have a chronological flow to give a sense of origins and trends through time.

2.1 Spatiotemporal Scaling

Concepts of space and time are central to all morphodynamic enquiry because related processes are inherently multidimensional. However, dependent and controlling factors shift with spatiotemporal scale. Historically, these were organised by conceptual typologies (e.g. Schumm and Lichty, 1965). To reflect that some variables may act to independently control other variables (and related processes) at some scales but respond dependently at other scales (Figure 2-1). In general, *controls* can be grouped as: 1) regional history, inclusive of lithology, tectonism, and geomorphology, 2) base-level, and 3) elements that control runoff and sediment generation, such as climate and land cover (cf. Schumm and Lichty, 1965; Bull, 1979; Harvey, 2002).

Variables	Long timescale $>10^5$ years	Medium timescale 10^3–10^4 years	Short timescale 10^1–10^2 years	Instantaneous time $<10^{-1}$ years
Geology	E	E	E	E
Climate	E	E	E	E
Regional relief	D	E	E	E
Slope morphology	D	D	E	E
Soil properties	D	D	E	E
Vegetation properties	D	D	E	E
Mean water and sediment discharge	I	D	E	E
Channel morphology	I	D	D	E
Instantaneous flow characteristics	I	I	I	D

E, environmental or independent variable; D, dependent variable; I, indeterminate or irrelevant variable.

Figure 2-1. The conceptual typology of Schumm and Lichty (1965) relates how variables that exert control on fluvial systems act as independent or dependent variables depending on the time scale considered (reprinted from Knighton, 1998). As temporal scale increases, controls generally become dependent. It is also noteworthy that indeterminacy increases with time, especially for key management variables like channel morphology and water and sediment discharge. Underscores ("D") indicate variables that may be dependent or indeterminate.

Scale-dependent shifts have been organised to represent geographic groupings (Figure 2-2) and morphological forms (Figure 2-3) along axes of space and time. However, these models originate from an era of geomorphology dominated by single-path single-outcome frameworks (sensu Phillips, 2009). Further, they are predicated on time-averaged steady-states and informed by morphological variables (e.g. channel width) as surrogates for processes (Lane and Richards, 1997). While models such as Figure 2-4 are still largely based on form proxies, their representation of variable spatiotemporal directionality affords multiple pathways while consideration of 'bed configuration' implicitly captures processes in a way that begins to address Lane and Richards (1997) call to focus on form-process relationships.

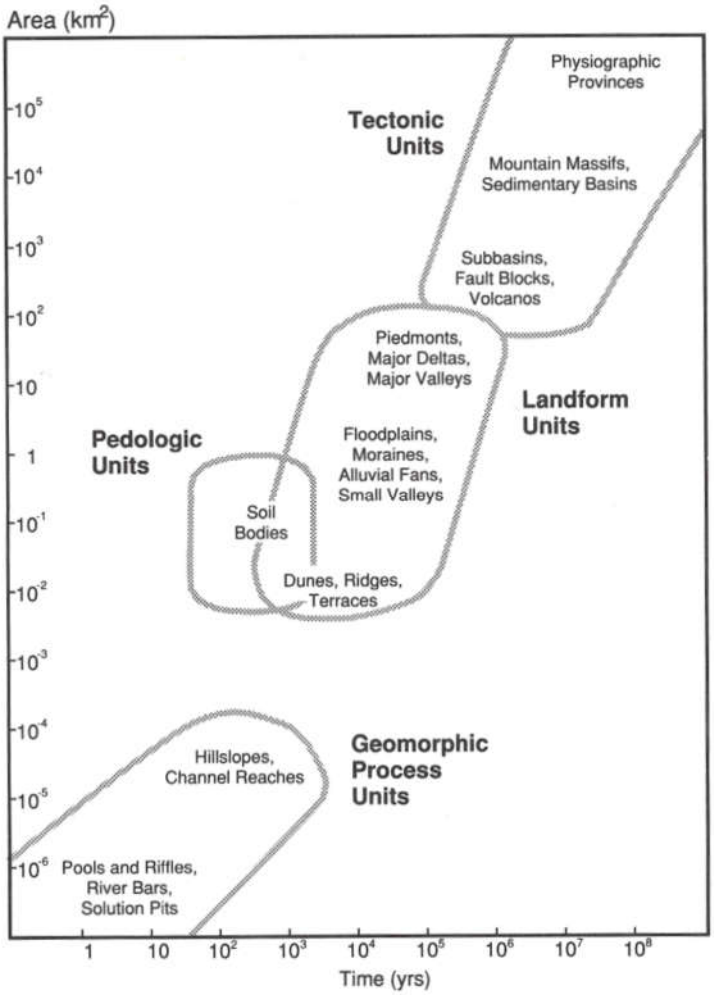

Figure 2-2. Organisation of landscape features along spatiotemporal gradients (reprinted from McDowell et al., 1990).

As the importance of form-process investigations has been increasingly recognised over the past twenty years, awareness of the importance of scale has only increased, including: catchment-scale disequilibria in response to forcing shifts (Tunnicliffe and Church, 2011), sediment supply and bedrock erosion for sub-grain and bed scales (Inoue et al., 2014), feedbacks between vegetation and geomorphic forms and processes (Corenblit et al., 2015), co-evolution of channel bifurcations relative to flood duration and bar migration (Bertoldi, 2012), bedload transport prediction (Recking et al., 2012; Anderson and Pitlick, 2014; Ancey and Pascal, 2020), sediment transport pathways and effectiveness (Milan et al., 2002; Wester et al., 2014), and habitats for aquatic organisms (Wheaton

et al., 2010a; Stoll et al., 2016; Wheaton et al., 2018). Consequently, more nuanced, multi-path, and multi-scale models (e.g., Figure 2-5) have arisen.

Figure 2-3. Controls, responses and spatiotemporal scales for sediment flux in a basin (reprinted from Frostick

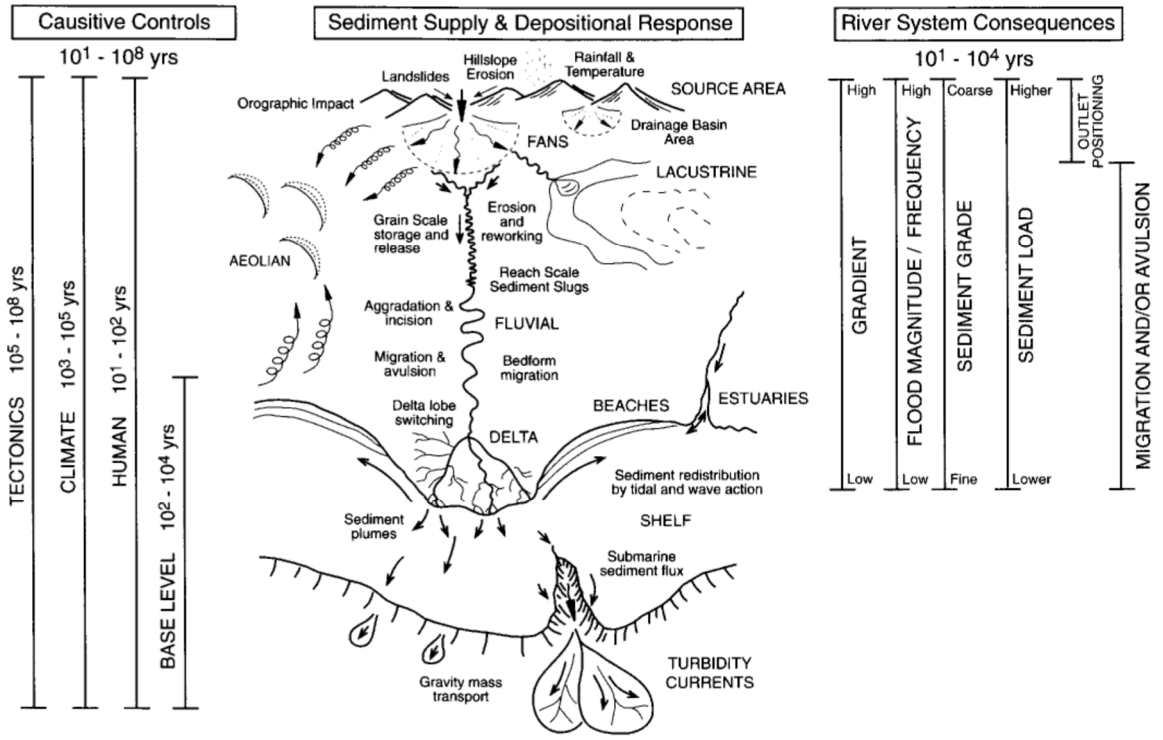

and Jones, 2002). Conceptual location of study area in hashed box.

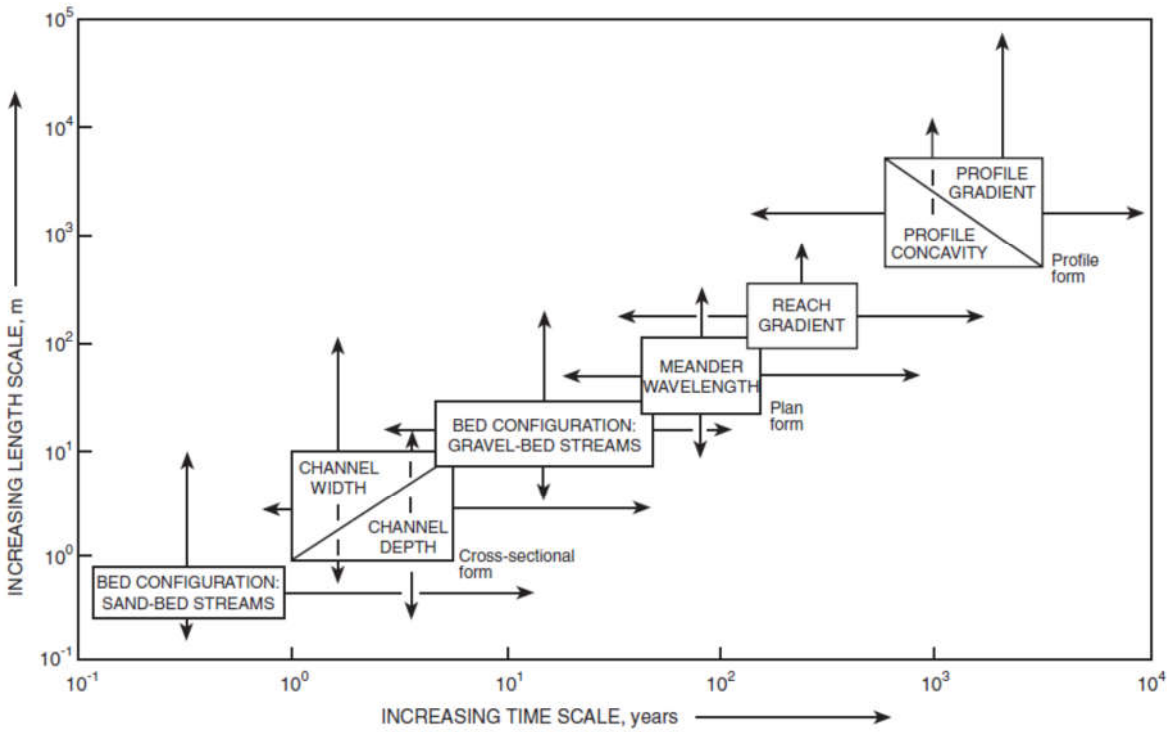

Figure 2-4. Spatial and temporal scales of adjustment for channel boundary conditions (reprinted from Knighton, 1998).

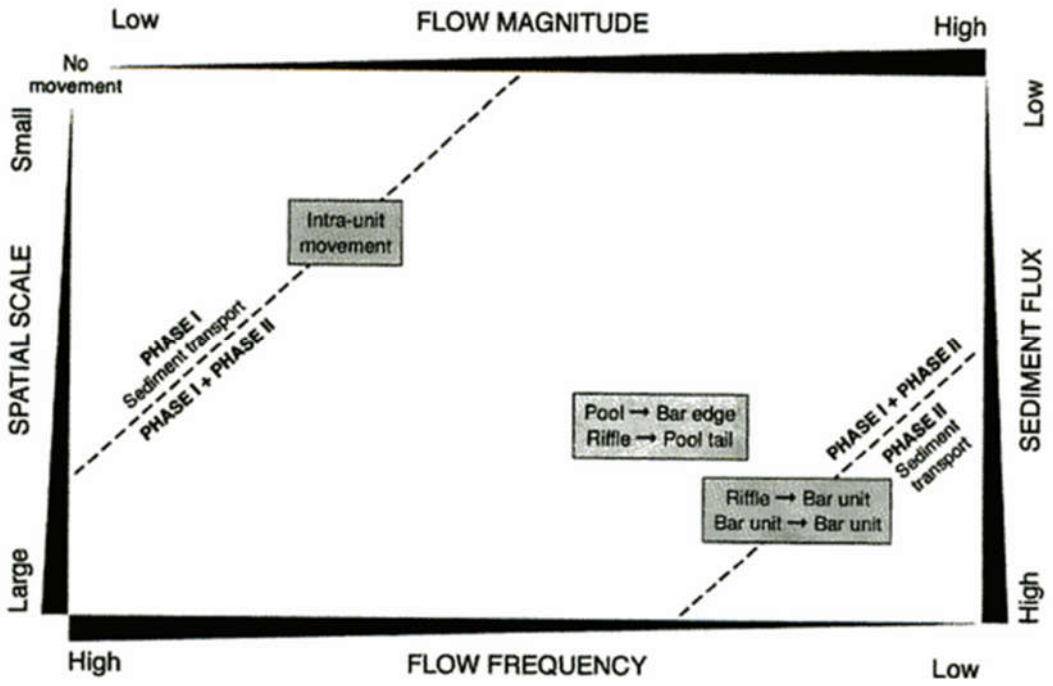

Figure 2-5. Relation and scale of sediment flux to flow frequency and magnitude in a pool-riffle stream (reprinted from Milan et al., 2002).

While the earlier "functional approach" (e.g. Chorley, 1978) era of geomorphology effectively used form-inversion to characterise systems, more recent models (Figure 2-6) better contextualise morphological variables (e.g. channel width) as responding to drivers of sediment transfer, including anthropogenic influences (cf. Raven et al., 2010). Greater understanding of sediment scaling relationships combined with refinements in sampling techniques enable organisation of methodological suitability along spatiotemporal axes (Figure 2-7, cf. Wainwright et al. (2015)). These more recent models address the need for study designs that identify and emphasise scale-appropriate linkages relevant to elements of interest (sensu Phillips, 2016).

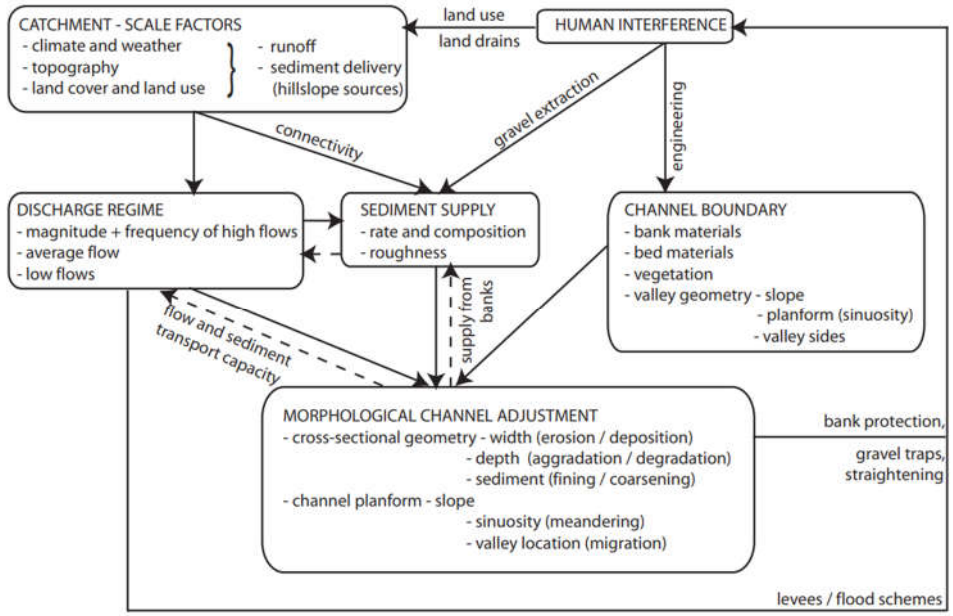

Figure 2-6. Relationships between factors that influence channel morphology (Raven et al., 2010).

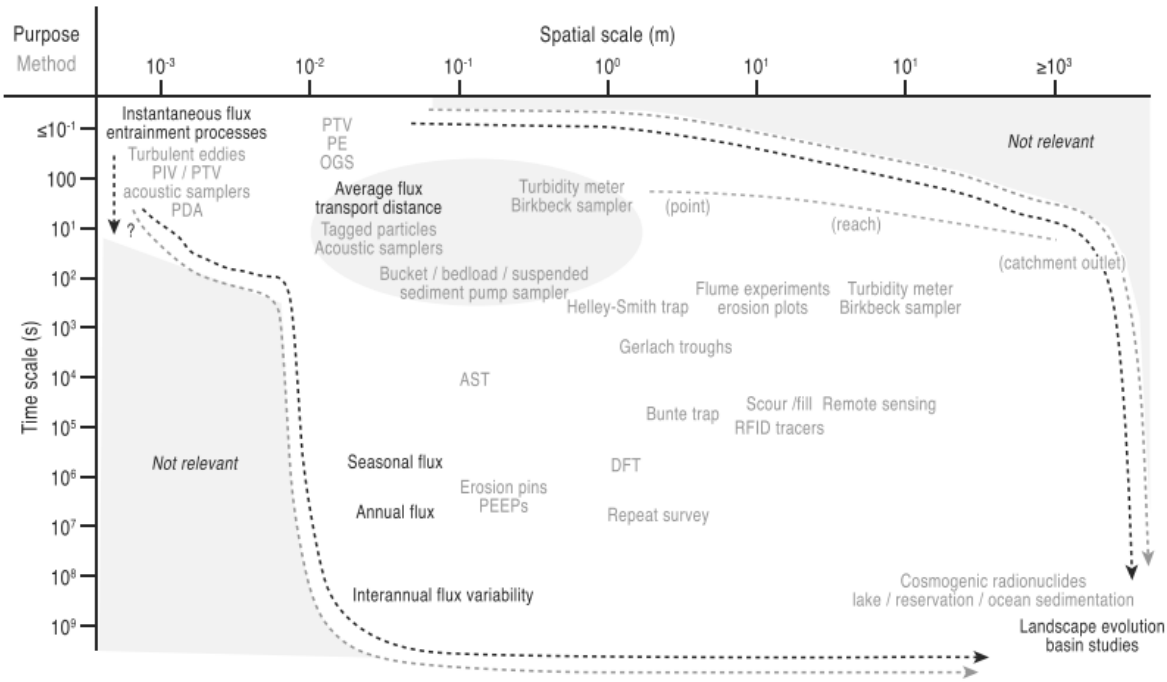

Figure 2-7. Spatiotemporal scaling of sediment transport measurement and relevant applications (reprinted from Wainwright et al., 2015).

Nested spatial hierarchies (Figure 2-8) provide a framework for contextualising landscape positions and scale linkages and build off the concepts of spatial zonation (cf. Schumm, 1977) and process domains (cf. Montgomery, 1999). Though location within a drainage network is important, clear longitudinal patterns of morphological change may be lacking (Marchese et al., 2017) and/or disrupted by antecedent controls, such as buried terraces and/or bedrock (Hoyle et al., 2008). Further, locally contingent responses such as differential fluvial response magnitude to catchment scale disturbance by landscape position occur (e.g. Nelson and Dubé, 2016). Setting-specific inversions of process-response may also occur, such as where elevated erosion is associated with lower sediment supply in an unconfined braided stream (Bakker et al., 2019) but greater sediment supply in an experimental confined bedrock channel (Fuller et al., 2016b). Nested hierarchies can accommodate such irregularities of process roles and rates within and between system components (cf. Fryirs and Brierley, 2012) and, thus, provide robust conceptual framing for this thesis.

Though management-relevant timescales often lie within medium scales (e.g. reach, annual), much of the knowledge base is either longer term (e.g. from the sedimentary record) or shorter term, finer scale derived from physical and numerical modelling as well as field studies (Brasington and Richards, 2007). At grain-scale and very short (~instantaneous) time scales, the magnitude and duration of turbulent forces as well as their product (impulse) is very important for thresholds of motion (Diplas et al., 2008). At basin-scale over long time periods, such turbulence tends to average-out stochastically and stream power models can reasonably predict longitudinal profiles (Gilbert, 1877). However, the reach scale is a bottleneck where problems of up-scaling mechanistic-based predictions and down-scaling parameterised power models converge (sensu Venditti et al., 2019). The common focus of river management and gaps in process-form relationships makes the reach-scale a particularly relevant area of investigation.

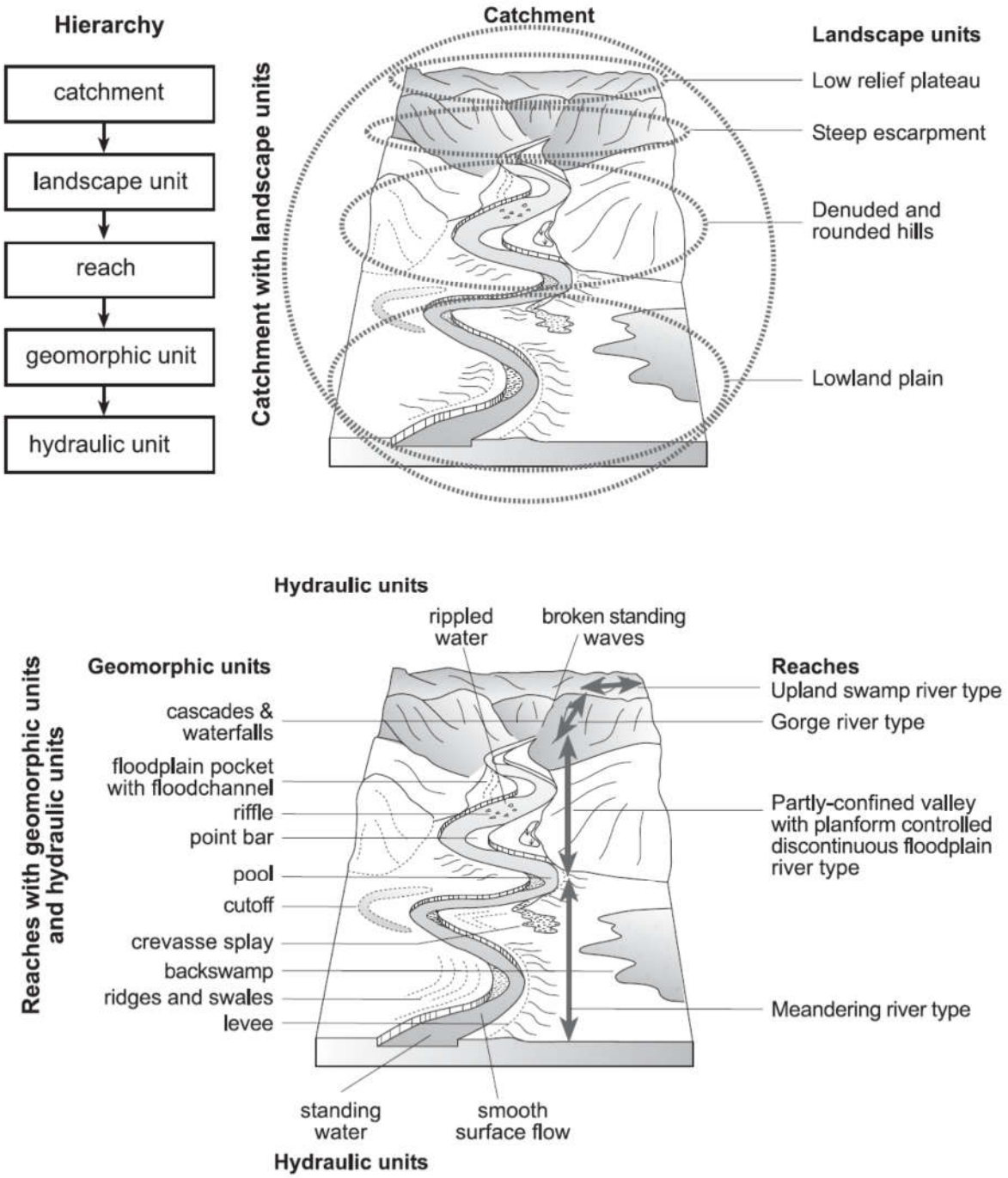

Figure 2-8. Nested spatial hierarchies in fluvial structure (reprinted from Fryirs and Brierley, 2012).

Variable sediment connectivity between the fluvial system and catchment sources (Figure 2-9, Bracken et al. (2015)) underscores the need to move beyond steady-state representations. Those that accommodate disturbance episodes followed by recovery where the interplay of discontinuous and continuous processes contribute to fluvial and landscape evolution should be favoured (cf. Grant et al., 2017). Recognition that controls like large-scale sediment supply events (LSEs), coseismic tilt and displacement, base-level shifts, climate changes recur, and human influences interact underlies this thesis. Review of key concepts related to morphological response follows, organised by themes of continuity, magnitude-frequency, complex response, non-linearity, temporal variability, and cross-scale geomorphic effectiveness.

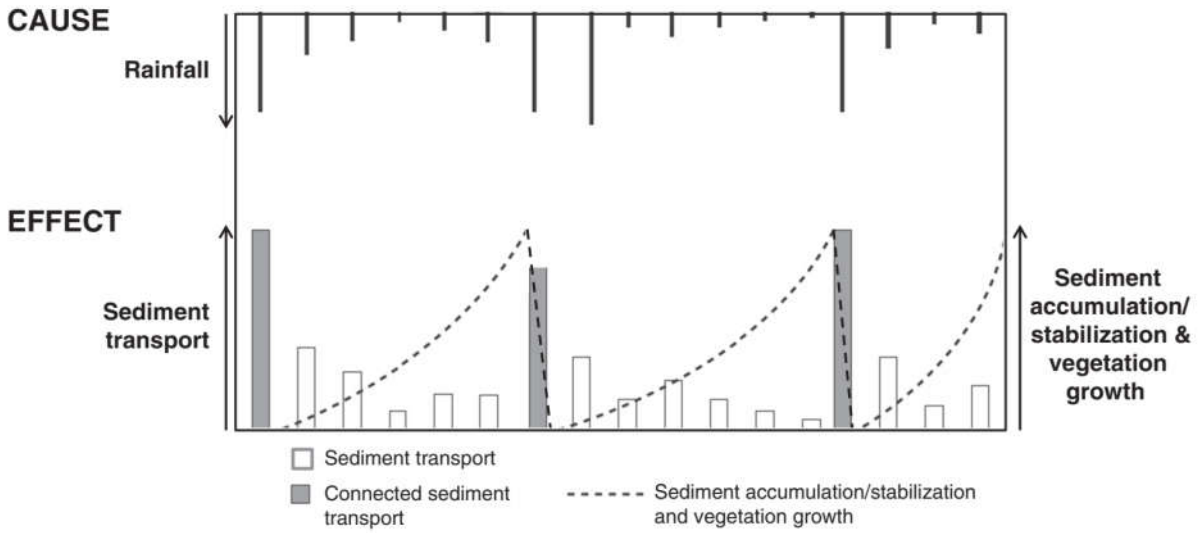

Figure 2-9. Conceptual time-series of catchment-scale mobilisation events showing variable connectivity to the fluvial system as influenced by vegetation stabilisation of hillslopes and river banks (reprinted from Bracken et al., 2015).

2.2 Morphological response

The response of a geomorphic system (or other spatial unit of interest) usually lags behind a change in the intensity of a process (*disturbance*; cf. Fryirs and Brierley (2012)). The elapsed time from when intensity of a control process changes until the system begins to change is known as *reaction time* (Allen, 1974; Fryirs and Brierley, 2012). *Relaxation time* is the elapsed time from when system change begins until system change no longer keeps pace with the process change (Allen, 1974) or otherwise takes on a characteristic state, which may or may be the pre-disturbance state (Fryirs and Brierley, 2012). *Recovery time* is the sum of the reaction and relaxation times (Fryirs and Brierley, 2012). *Propagation time* (Harvey, 2002) recognizes lags in reaction, relaxation, and recovery vary between system components by landscape position and with differential transmission of up- versus down-catchment signals.

Coarse-bedded rivers are well-known for having variable bed transport and channel behaviours generally recognized as cyclical and highly responsive to changes in the balance between sediment supply and transport capacity (Brewer and Passmore, 2002; Church, 2006; Inoue et al., 2014; Church and Ferguson, 2015). Sediment flux is often conceptually attributed to changes in supply and/or variability in transport capacity and/or competence (Frostick and Jones, 2002) and can have substantially different effects on bed characteristics and channel processes such as observed by Salant et al. (2006). In their study of two rivers with equal dam-related reductions in water discharge, the river where impoundment also limited sediment supply experienced rapid incision and armouring. In contrast, the river with constant sediment supply exhibited decadal aggradation and embeddedness. These contrasting trajectories underscore the importance (and independence) of sediment flux as a control of morphological response.

Large-scale sediment supply events (LSEs) are particularly noteworthy disturbances that involve a punctuated increase in sediment delivery to a river or channel network and typically result from landslides associated with large earthquakes or intense storms. Substantial and persistent riverscape changes have been documented related to single atmospheric (e.g. Tseng et al., 2015; Yellen et al., 2016; Tunnicliffe et al., 2017), tectonic (e.g. Yanites et al., 2010; Li et al., 2016a; Croissant et al., 2019), and wildfire (e.g. Moody, 2017; Brogan et al., 2019) events. Reaction and relaxation times

following LSEs are system-specific with rigorous empirical study generally limited to smaller catchments. For steep Japanese eight catchments between 18.8 and 487 km^2 in size, Izumiyama et al. (2020) found the period over which the effect of an LSE persisted between <1 and 19 years with recovery time for annual sediment yield to be shorter than *residence time* (time that sediments were retained). A rare case from a larger catchment (1,734 km^2) in New Zealand found immediate reaction times and 17-20 year peak aggradation propagation times for headwater and intermediate reaches while a morphologic reaction signal in the lowest reach had not appeared 28-years post-cyclone (Tunnicliffe et al., 2017). Based on modelling from an adjacent catchment (Herzig et al., 2011), they estimated a 60 year relaxation time for upper reaches assuming existing gully complexes stabilised and no new gullies formed.

While LSEs are not a specific focus of this thesis, the tectonic and climatic setting of the study area makes LSEs a critical, implicit driver of periodic shifts in fluvial behaviour and threat to any infrastructure failing to plan for such shifts. The amount of time to transition states and, ultimately, capacity for morphodynamic response of any system is largely dependent on the rate at which matter and energy move (or do not move) between system components.

2.2.1 Transfer, Continuity, Coupling, and Connectivity

Transfer is simply the movement of matter and/or energy from one place to another that can be visualised (e.g. Figure 2-10) in a four-dimensional framework (Ward, 1989). *Continuity* is a fundamental scientific principle that governs physical, biological, and chemical relationships and ensures matter and energy are conserved consistent with the laws of thermodynamics. In its simplest form,

$$I = O \pm \Delta S$$

Where *I* is an input, *O* is an output and ΔS is the change in storage. The transfer of matter and/or energy between system components indicates those components are *coupled* (Chorley and Kennedy, 1971; Brunsden and Thornes, 1979). For example, if a large proportion of a landslide is recruited into a stream over some time period, then a high degree of coupling exists for that window of time. In such cases, *I* and *O* will be of similar magnitude and ΔS will be small. Conversely, if the slide terminates on a terrace tread and little material is transferred to the stream, then ΔS is large and the two may be considered *de-coupled*. Morphological response in well-coupled landscapes tends to be rapid (Brunsden, 2001; Fuller and Marden, 2011).

Harvey (2002) presents a conceptual model that differentiates between local and larger scale coupling. *Local transfers* are primarily down-system where magnitude-frequency and recovery time are of particular significance and occur through sequential space: within-hillslope, hillslope-to-channel, within-channel, tributary junction, and reach-to-reach. Large scale coupling can be down-system or up-system (e.g. base level change) and divided into zonal and regional where propagation time becomes increasingly important. At a given spatial scale, the time scale for sediment transfer between coupling zones may increase or decrease disproportionately (Schwendel and Fuller, 2011). In practice, coupled/decoupled tends to be treated in a binary fashion, while matters of degree are addressed as issues of connectivity.

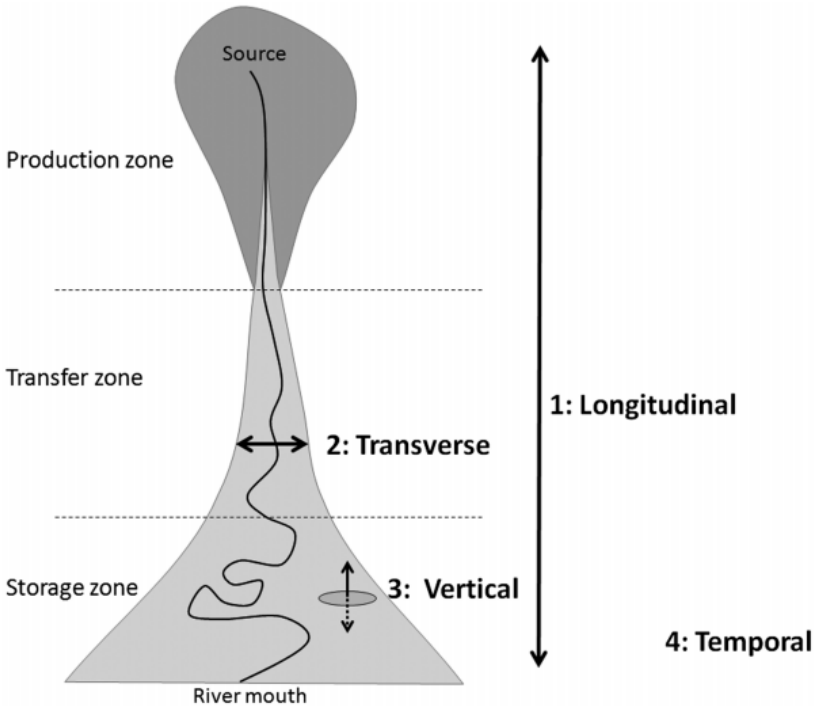

Figure 2-10. Schematic of matter and energy dimensional flux (reprinted from Corenblit et al., 2015). 'Transverse' and 'lateral' are used interchangeably in this chapter.

Over the last two decades or so, the status and nature of coupling is increasingly referred to and described as *connectivity* and/or *(dis)connectivity*. It has been suggested that connectivity and (dis)connectivity (cf. Fryirs, 2013) are better considered as states while continuity and discontinuity refer to processes (Grant et al., 2017). I consider continuity to be the more fundamental as it is compulsory (related to laws of conservation) while connectivity is optional, or at least contingent. Considering that 1) connectivity investigations usually consider finite spatiotemporal constraints and 2) have broad acceptance in geomorphology as a conceptual framework connectivity provides sound framing to quantify transfers within and between through space and time (cf. Wohl et al., 2019). Within geomorphology, connectivity is often grouped into landscape, hydrologic, and sediment groupings (Wohl, 2010), though in practice, there is much interrelation. Heckmann et al. (2018) divide connectivity approaches into two classes with *structural* consisting of point-in-time physical forms, materials, and topological relationships while *functional* represents the outcome(s) (e.g. precipitation type, flow velocity, or transport capacity) of spatial interactions between structural and functional properties with external controls. Turley et al. (2021) evaluate index-based methods for quantifying structural and functional connectivity.

The degree of relation between elements within hierarchical spatiotemporal networks decreases with increased differences in scale and respective controls often vary (cf. Phillips, 2016). For example, morphology and channel dynamics produce alluvial units/packages in the short-term while stratal patterns are developed in the long-term by basin-scale controls (cf. Ashworth et al., 2007). In other words, while a given bedform and bar may be directly linked, the relationship between that same bedform and its catchment will not be as strong by virtue of intermediately-linked units and processes (Figure 2-11). Graphs are useful for modelling how a channel network's spatial structure may impose morphological controls by regulating how stochastic watershed disturbances are expressed at any given point in the system (Benda et al., 2004) or sediment cascades are transferred to and through the fluvial system (Heckmann and Schwanghart, 2013; Walley et al., 2017). Within such mathematical networks, analysis of sediment entrainment, transport and deposition has been

used to reveal differential scaling of spatially-explicit connectivity (Schmitt et al., 2016) including accurate representation of morphological response given historic sequences of anthropogenic forcing (Tangi et al., 2022).

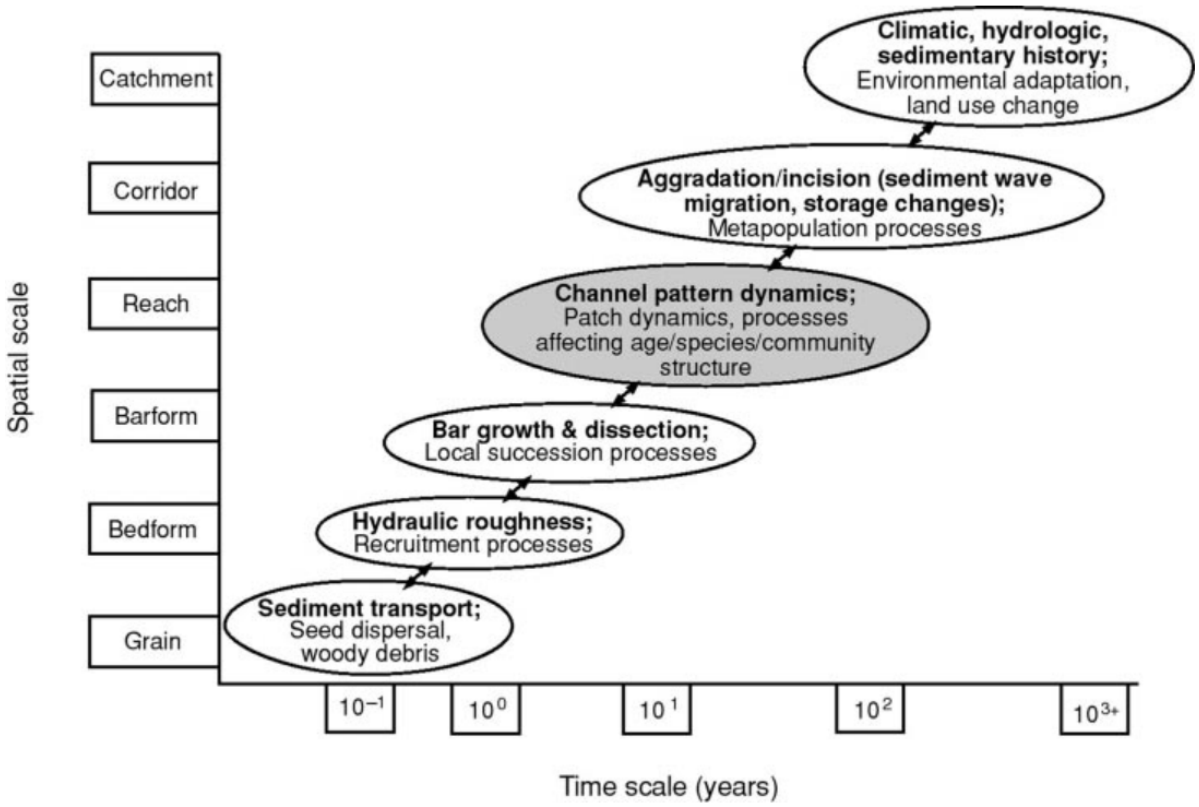

Figure 2-11. Conceptual hierarchy of linked fluvial and ecological processes ordered in space and time (reprinted from Richards et al., 2002).

Distributed anthropogenic effects commonly accelerate down-catchment connectivity. Roads increase hydrologic connectivity by extending the drainage network (e.g., Wemple et al., 1996; Wemple and Jones, 2003) and slope-channel coupling (Wemple et al., 2001). Sediment connectivity increases as well (Reid and Dunne, 1984; Luce and Black, 1999, 2001) with as much as 2863% to 860% greater total suspended sediment concentration (SSC) for second and third order streams (respectively; Thomaz and Peretto (2016)). In terms of sediment provenance, Thomaz and Peretto (2016) found 4-8% of SSC related to headwater sources in unroaded catchments and 70 to 87% attributable to headwaters at the outlet of roaded catchments where filtration by riparian vegetation was also considered ineffective. Conversely, slope-channel coupling may become less connected following abandonment of human settlement (Madej, 2001; Latocha, 2014). At more refined spatial scales, connectivity between channel units can be expected to increase given typical river corridor responses to anthropogenic forcing include straighter, steeper and fewer channels; increased eroding bank abundance and channel migration; and lower resistance associated with lower riparian vegetation and large wood abundance (Brooks et al., 2003; Hoffmann et al., 2010; Fuller et al., 2011; Beckman and Wohl, 2014).

2.2.2 Non-linearity and temporal variability

Nonlinearity exists when the difference between input and response varies across the range of inputs (Phillips, 2003). Issues of non-linearity in geomorphology are generally considered as driver-response relationships. For the purposes of this thesis, nonlinear trends over time are treated as

temporal variability. Conceptually, much of the discipline arose from linear concepts, particularly with regard to evolutionary progressions such as Davis' erosion cycle (Davis, 1899). Such concepts require sequential progressions of change and are sometimes referred to as single-pathway, single-outcome models, though are generally now recognised to be exceptional cases (Phillips, 2009). Non-linearity generally relates to "contingency" or "spatially-explicit" response and/or processes which now have a fifty-year empirical foundation (e.g. Knox, 1972; Church, 1983; Magilligan, 1992; Stock and Montgomery, 1999; Fuller, 2008; Tunnicliffe and Church, 2011; Kuo and Brierley, 2014; Nelson and Dubé, 2016; Valenza et al., 2020).

Temporal variability is possibly the most challenging as it is subject to issues of perception and framing. The classic example is sediment discharge which varies sub-annually, but may appear steady when averaged over millennia (Schumm, 1973). Perceptions of this variability tend to be a bit trickier as they are strongly shaped by the nature of data collection. While variable in reality, limited empirical data influences interpretations of variability, steadiness, and trend (cf. Ferguson, 1977), particularly due to density and timing of sampling (Lawler, 1993) as shown in Figure 2-12. Temporally-dense data sets can provide richer spatiotemporal insights into directional processes, such as channel migration (Figure 2-13).

Water and sediment discharge are frequently out-of-phase (Nash, 1994) which contributes to variable morphologic effects. Making sense of the variability is further complicated by feedbacks of morphologic changes on bed transport. The simplest and most elegant form of this is easily visualised in Dust and Wohl (2012) revised version of "Lane's Balance" that relates to width/depth (in lieu of the original "aggradation" and "degradation"). The nature of morphologic effects on bedload transport differ by form, grain size, and in relation to flume studies with increasing deviation for larger rivers (Recking et al., 2016). Conversely, bank stratigraphy and provenance (Knox, 1972; Dow et al., 2020) as well as catchment lithology (Stock and Montgomery, 1999) affect rates and processes of morphologic change. Assessing the morphologic effects in braided rivers becomes even more challenging because width is often considered a dependent variable of sediment supply rate (e.g. Pfeiffer et al., 2017). However, Dunne and Jerolmack (2020) suggest that grain size changes to sediment supply will have a more immediate impact on channel geometry than changes in critical shear stress.

In the vertical dimension, experimental and computational modelling suggest bedform height and wavelength increase rapidly with the onset of effective discharge (where sediment motion is induced), but wavelength decreases much slower than height once flows return to initial discharge (Nelson et al., 2011). Hydrologic variability is recognised for influencing forms and behaviours across seasonal (Leier et al., 2005; Hansford and Plink-Björklund, 2020) and annual (Bledsoe and Watson, 2001; Welber et al., 2012; Kidová et al., 2016; Call et al., 2017) timeframes which may shift over still longer periods (e.g. decades) given longer-term controls such as flood-rich and flood-poor period (Macklin et al., 2006; Toone et al., 2014; Kidová et al., 2016). At late-Pleistocene to Holocene scales, lagged responses to climate change affect sediment supply (Knox, 1972) such as at transitions from cold, dry periods where lower vegetation cover may persist as wetter atmospheric regimes commence and may result in extensive aggradation surfaces (Formento-Trigilio et al., 2003; Clement and Fuller, 2007).

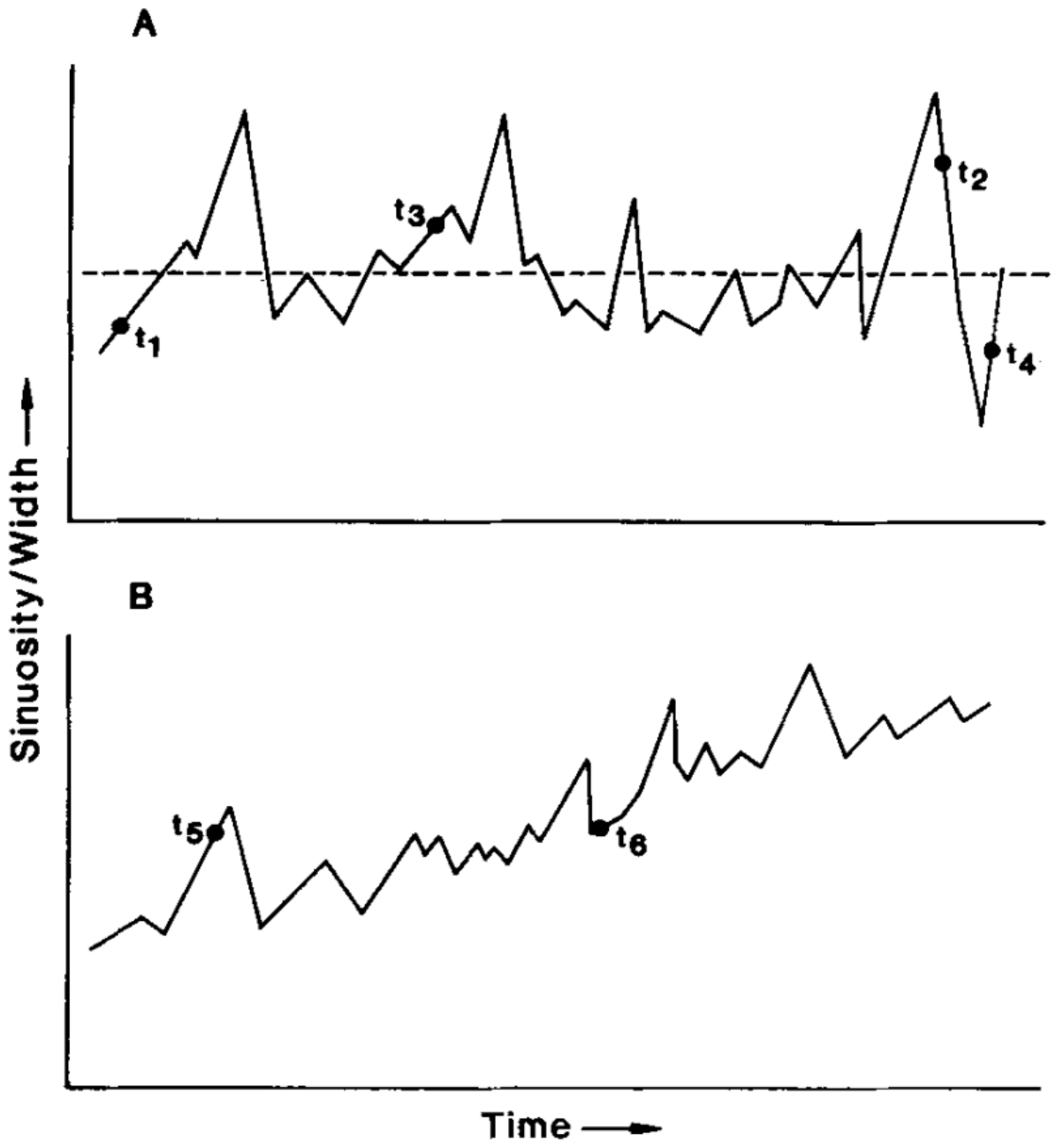

Figure 2-12. Timing and density of data sampling (points) influence perception and identification of trends in actual change (solid lines; reprinted from Lawler (1993)). (A) If all points are sampled, one may conclude no trend in the data (hashed line); if t_1 and t_2 only are sampled, then an increasing trend is incorrectly inferred; if only t_3 and t_4 are sampled, then a decreasing trend is incorrectly identified. (B) By contrast, a true increasing trend may be missed if only t_5 and t_6 are sampled.

Non-linear responses and temporal variability include themes of thresholds, storage effects, feedbacks, hysteresis, and initial properties (Phillips, 2003; Coulthard and Van De Wiel, 2007; Temme et al., 2015). Collectively, these occur across a range of scales that, for example, represent geologic and climatic variability at regional scales (Marchese et al., 2017), event-based reach-scale reversals of erosion and sedimentation with upstream sediment supply (Bakker et al., 2019), or sub-event bed-scale hysteresis (Roth et al., 2014). Discussion of end-members follows to illustrate the spectrum along which non-linearity occurs.

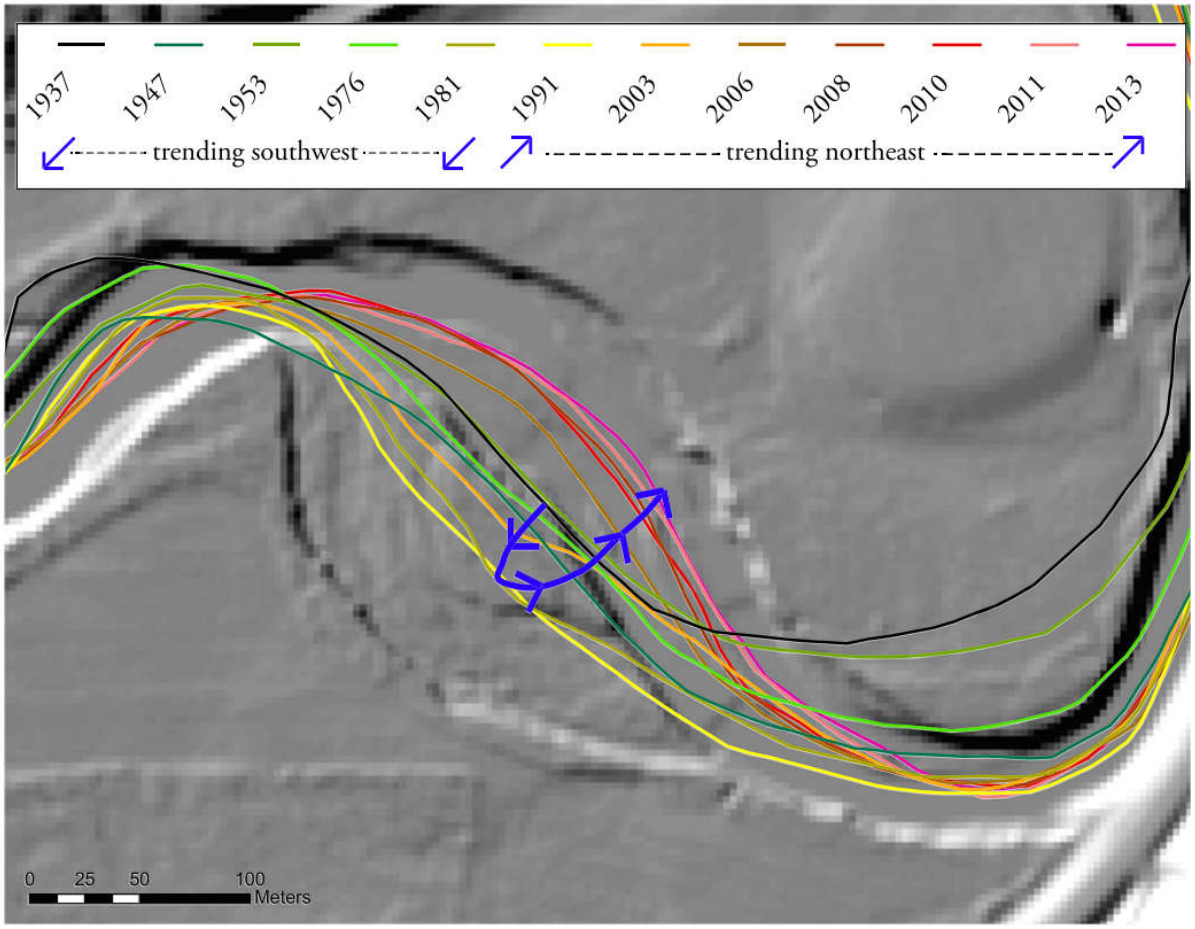

Figure 2-13. Direction reversal of channel migration made possible by numerous samples over time (reprinted from Donovan and Belmont, 2019).

2.2.2.1 Deep time

The suite of channel behaviours and related patterns we know globally today developed during the Palaeozoic Era co-incident with plant evolution (Gibling and Davies, 2012; Corenblit et al., 2015). In particular, evidence of meandering channels appears suddenly in the stratigraphic record at the end of the Silurian Period coincident with evidence of root reinforcement and charcoal (Figure 2-14). Similarly, anastomosing channel forms appear in temporal proximity to concentrations of logs (large wood). The effect on longitudinal distribution of channel forms can be visualized in Figure 2-15 which shows more stable river forms co-evolving with vegetation beginning in the Devonian (Corenblit et al., 2015) though most characteristic fluvial forms we observe today had developed by the end of Carboniferous (Gibling et al., 2014). Inversely, increased sedimentation and the dramatic disappearance of meandering channel forms (shifting to braided forms) at basin-scale coincident with catastrophic terrestrial plant die-off during the Permian-Triassic (Ward et al., 2000) underscores long-term perspectives of the importance of flowering plants to form-process relationships.

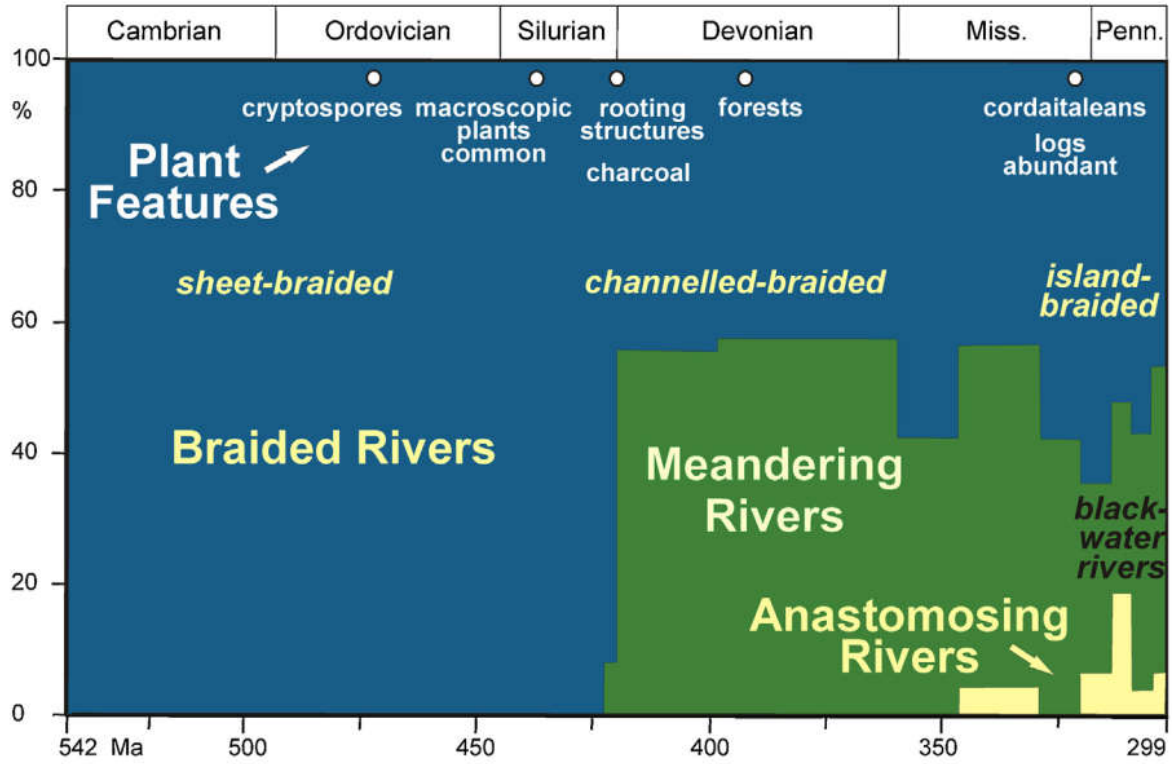

Figure 2-14. Relative abundance of major channel forms during the Palaeozoic Era. The sudden appearance of meandering rivers correlates with the evolution of flowering plants (reprinted from Gibling et al., 2014).

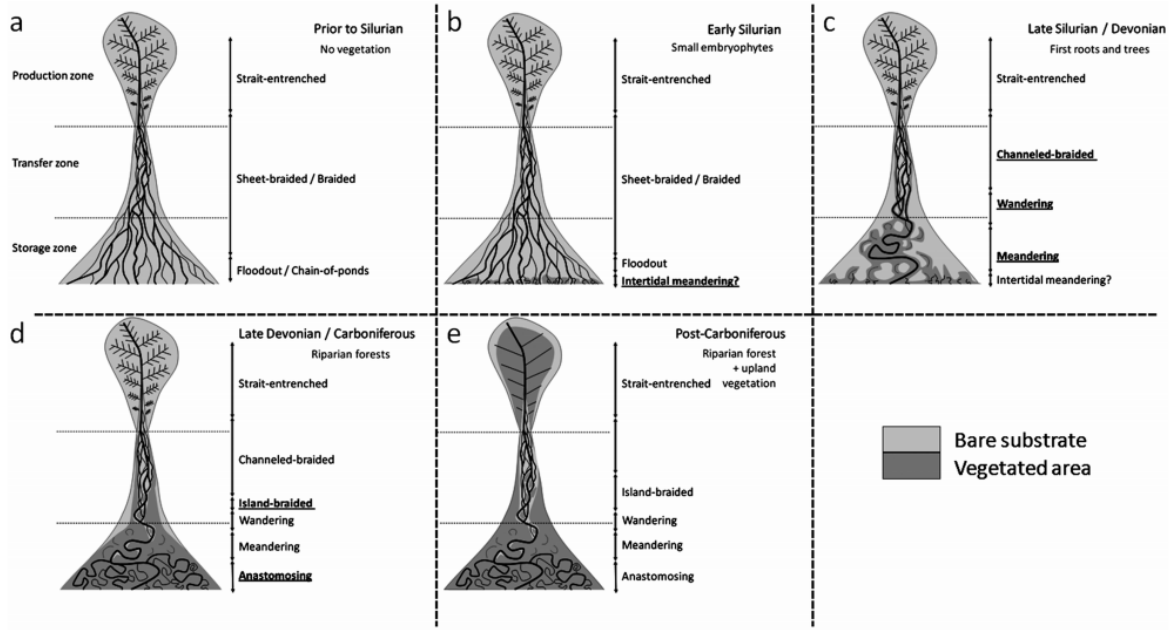

Figure 2-15. Conceptual fluvial zonation of fluvial forms before, during and after appearance of flowering plants during the Silurian Period (reprinted from Corenblit et al., 2015).

2.2.2.2 Sub-event

At the opposite end of the temporal spectrum, sediment transport may change relative to hydrograph peak within a single event. Hysteresis has been recognised in sediment transport relationships for many decades (e.g. Klingeman and Emmett, 1982) and are non-linear by their very

nature such as where re-organization of surface grains during an event produces differential transport conditions. Rising-limb scour is implicated as a transport control in hydrologically flashy streams (Schick et al., 1987) while lag in the formation of bed roughness elements (structure) was suggested for greater transport rates associated with rising limb samples from two small streams (Kuhnle, 1992). In field settings, hysteresis where a given discharge on the rising limb produces greater transport than the same discharge magnitude on the falling limb suggests time-dependent bed evolution at event scale (Roth et al., 2014). Greater rising limb sediment transport in a flume study was attributed to lower vertical roughness during the falling limb associated with clast rearrangement (Mao, 2012). Using a combination of flume and numerical modelling, Johnson (2016) proposed net entrainment as a negative morphologic feedback to explain within-event increases and decreases in shear-based mobility thresholds where, for example, net erosion leaves progressively more stable particles behind resulting in reduced transport rates. Differential growth and decay of bedforms and temporal lagging of adjustment post-peak can add further complexity (Martin and Jerolmack, 2013). Thus, within a single event, grain- and bed-scale re-arrangement produce degrees of imbrication, protrusion, shadowing, and/or orientation that are often progressively less favourable to transport.

2.2.3 Complex response and behaviour

Complex response (cf. Schumm, 1973) is the premise that disturbance of a given magnitude may generate different outcomes in space and/or time. Traditionally, complex response entails different outcomes for the same spatial unit resulting from multiple, comparable events. However, application to spatially differential response by sub-components to a single event is also reasonable. The core elements of *nonlinear complex behaviour* are 1) rapid change driven by threshold crossing, 2) spatially asynchronous change, and 3) process zonation (cf. Wohl, 2013) which I suggest underlie both applications. For the remainder of this section, I use *complex behaviour* to encapsulate both applications.

Spatiotemporal expressions of complex behaviour occur and vary across all scales. Infrequent, large magnitude events are capable of system-scale reorganization, but within-system responses are not uniform, particularly as it relates to valley floor and channel configuration. At the riverscape scale, such behaviour has been documented during (Magilligan, 1992; Miller, 1995) and following (Moody, 2008; Nelson and Dubé, 2016) high-magnitude, low-frequency events. Similar external forcings by humans and/or climate to rivers of similar form may produce different trajectories of metamorphosis (Nadler and Schumm, 1981). Lithology and valley form have been implicated in producing dissimilar geomorphic effects by events of similar magnitude or frequency (Magilligan, 1992; Fuller, 2008). Macklin et al. (1998) found valley floor morphology as the principal basin-scale control on unstable reaches while cyclical patterns (decades to centuries) of instability were climate-driven. While multi-thread channel forms are frequently expected to increase during *expansion* (alluvial widening) and diminish during *contraction* phases (Piégay et al., 2006) such shifts are not always linked (Marchese et al., 2017). Further, channel response may differ during peak passage of a sediment pulse than earlier or later (East et al., 2018), though such signals may not be preserved due to (Jerolmack and Paola, 2010; Straub et al., 2020). Floodplain and valley controls have also been strongly implicated in frequency and timing of sediment transport (Reid et al., 2007a) differential response/recovery to large magnitude events (Fuller, 2007; Fryirs and Brierley, 2010). Landforms and flow engagement have been correlated with transfer directionality, with large floods exhibiting longitudinal and periods of modest floods associated with lateral sediment redistributions (Weber and Pasternack, 2017). Adjacency is also important, such as proximity to a meander cut-off (i.e.

threshold breach) supplies sediment that may promote equilibrium behaviour in the downstream reach (Biedenharn et al., 2000).

While greater amounts of geomorphic work may occur during episodes of high shear, concepts of particle motion and/or geomorphic change should not be constrained solely to higher discharges and/or velocities. Incipient motion-based approaches related particles of a particular size to some physical value (e.g., tractive force or power) such that transport is assumed to occur at all values greater and not occur during periods less than the threshold value. However, shear stress cannot be assumed to vary by average downstream hydraulic geometry (Magilligan, 1992) and motion thresholds are sensitive to bed slope, morphology, and flood history (cf. Rickenmann, 2020). Further, bank erosion may occur in areas of low shear when a high degree of turbulence is present (Rennie and Church, 2010). Longitudinal position within a riverscape relative to flow constrictions controls specific stream power and bed scour (Miller, 1995; Venditti et al., 2019).

2.2.3.1 Geomorphic effectiveness and magnitude-frequency relationships

Most morphological responses may be framed and/or quantified as a matter of the *geomorphic effectiveness* (effectiveness) of the event or force that was applied. The cumulative effects of forcing processes that contribute to the morphologic response are often conceived as the amount of *geomorphic work* performed and often constrained to a discharge event (cf. Fryirs and Brierley, 2012). Magnitude-frequency relationships relate the size or intensity (*magnitude*) of an event to the statistical probability in which it recurs (*frequency*). These are largely of interest for establishing temporal contexts of effectiveness that enables future forecasts: how often might that degree of change be expected?

Wolman and Miller (1960) introduced the notion that most geomorphic work is performed by relatively common water discharges (generally occurring between several times a year and once every other year) of moderate magnitude that correlate to the point at which a channel is filled to the top of its banks (*bankfull*). The authors recognised potential for different features to be formed by different magnitude-frequency relationships and noted that nearly all landforms they discussed were depositional. Evidence from catchments where strongly right-skewed flow-frequency distributions concentrate work into fewer, high-magnitude events (e.g. Baker, 1977) and regional contrasts where the same morphometric parameters indicated flow-recurrence as starkly different as mean annual and maximum-of-record (Patton and Baker, 1976) casts doubt on broad application of the bankfull premise. Further, model (Pickup and Rieger, 1979) and field-based (Williams, 1978; Gupta, 1983; Phillips, 2002; Lenzi et al., 2006; Surian et al., 2009; Galia and Škarpich, 2016; Rainato et al., 2020) evidence suggests neither channel morphology and/or bed transport are necessarily linked to bankfull or 1-2 year recurrence discharge and may in fact be a function of a range of discharges. Nonetheless, “bankfull” as an indicator (or predictor) of channel-forming discharge and/or change frequency persists as dogma, especially where fluvial geomorphology is practised by non-geomorphologists.

Within geomorphology, the need to understand time-dependent morphodynamic responses to event-based processes spawned the concept of *geomorphic effectiveness* by Wolman and Gerson (1978) who initially proposed characterising relative measures of event flow magnitude scaled to recurrence frequency. While conventional wisdom expects high-magnitude events to generate change, large infrequent floods do not always produce major or persistent landscape change (Wolman and Eiler, 1958; Gupta and Fox, 1974; Magilligan et al., 1998). Conversely, infrequent large-magnitude events much larger than bankfull may be necessary to generate live-bed conditions (Baker, 1977; Phillips, 2002) generally expected from more routine flow peaks. Because overbank

frequency can change as a function of channel changes when hydrologic variability is controlled (Stover and Montgomery, 2001; Hooke, 2015; Slater et al., 2015) and water and sediment discharge are frequently out-of-phase (Nash, 1994), there is often poor agreement between flood probability and geomorphic adjustment frequency (Baker and Costa, 1987; Magilligan, 1992; Nash, 1994).

The inability of discharge magnitude-frequency relationships to consistently explain morphological responses (e.g. Newson, 1980), motivated Baker and Costa (1987) to reframe effectiveness as a hydraulic matter of balancing impelling and resisting forces along a unit of a channel boundary, specifically as shear stress and specific stream power (W/m^2). Though such an approach still allows magnitude-frequency linkage, not requiring it increased applicability of the concept. This was affirmed by Magilligan (1992) who found the range of recurrence for a given reach to attain a specific formative flood power (e.g. 300 W/m^2) varied within a basin between two and eighteen times the 100-year flood with reaches exceeding critical thresholds less frequently more likely to become sediment sinks. Miller (1995) was unable to replicate explicit correlation of flood damage and stream power, instead emphasising the role of longitudinal variation in cross-sectional valley morphology as he found substantial spatial correlation downstream of flow constrictions. Kuo and Brierley (2014) subsequently linked longitudinally-variable stream power, geomorphic mapping, and a 30-year time-series of catchment-scale sediment flux to identify controlling processes varied by system component with spatially- variable magnitude-frequency relationships.

The variability of event-based effectiveness across space, time, and process begs a need for consistent comparison of geomorphic work as a standardized indicator of change. Generally, effectiveness response has been framed in terms of sediment movement or volumetric change. Hassan et al. (1992) found weak correlation between particle movement distance and excess stream power, with somewhat better results when comparison with virtual travel rate was constrained to the first flow event only. Observed and predicted recurrence intervals of discharge generating sediment transport (i.e. effective flow) may be in poor agreement, mainly due to the respective magnitude-frequency relationships of water and sediment being out-of-phase (Nash, 1994). Similarly, excess peak stream power (i.e. the component that exceeds threshold of motion) correlates only weakly to mean particle transport length and virtual rate of travel (Hassan et al., 1992).

The most promising approaches integrate force (either implicitly or explicitly) over time. Costa and O'Connor (1995) used time-integration of event-based stream power to emphasise the importance of both flow magnitude (in excess of a mobilisation threshold, e.g. Rainato et al. (2020)) and duration in explaining geomorphic change or its absence (Figure 2-16). Phillips and Jerolmack (2014) use time-integrated dimensionless shear stress (which they refer to as dimensionless impulse) to compare number of tracer particles mobilised and distance transported across events of different duration and magnitude. Gilet et al. (2020) use a similar stream impulse-based approach for evaluating tracer transport distances across multiple flow peaks. However, both of these field-based investigations involved single thread mountain channels with banks that were relatively immobile. In a thorough review of geomorphic effectiveness, Lisenby et al. (2017) conclude that combination of total energy (joules; after Costa and O'Connor (1995)) and total volumetric change is the only combination of driving and response metrics (respectively) that facilitates comparison across all settings and scales.

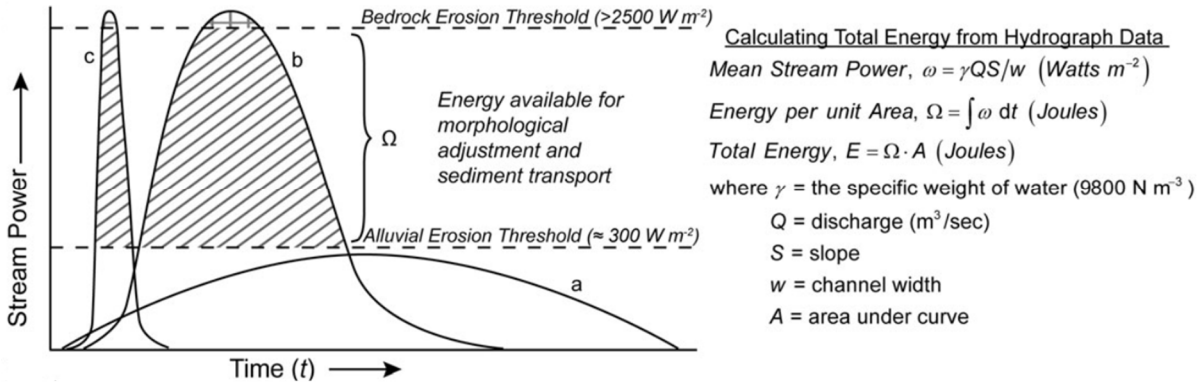

Figure 2-16. The ability to do geomorphic work rests on intensity (e.g. stream power magnitude) over some duration of time (Costa and O'Connor (1995) adapted by Lisenby et al. (2017)).

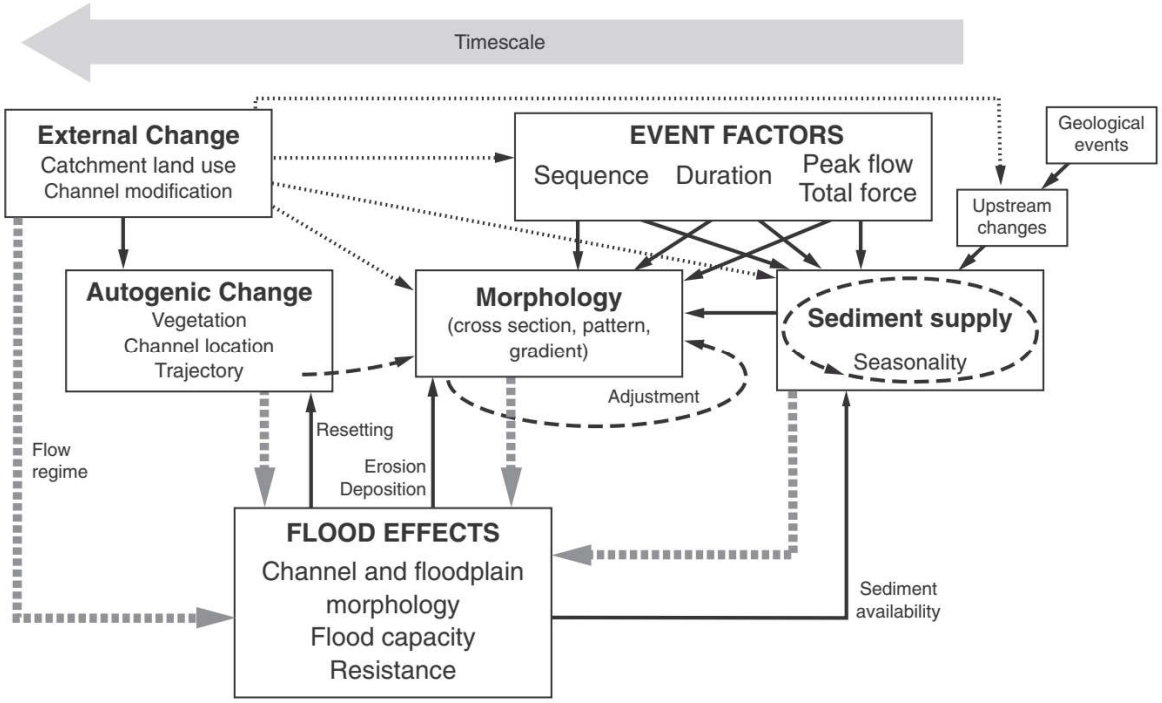

Figure 2-17. Conceptual model reflecting scaling of processes and feedbacks along a temporal axis to represent relational controls on variable morphological response to flooding (reprinted from Hooke, 2015).

2.2.3.2 Sensitivity

Landscape *sensitivity* is the degree of morphological change that may be expected of a spatial unit given a disturbance of some magnitude and was first detailed as a landform evolution concept by Brunsden and Thornes (1979). Their recognition of non-linear sensitivity aspects includes transient behaviours, threshold relations, complex response and remains highly relevant. Perhaps most interesting are discussion points regarding linkage to coupling and potential for threshold change. To evolve sensitivity from concept to operational utility, Downs and Gregory (1995) recognised a need to standardise usage and identify metrics (Figure 2-18). They organised sensitivity applications into four groups (each linked to units for evaluation): 1) ratio of disturbing to resisting forces (dimensionless), 2) proximity to threshold based on force imbalance (force), 3) ability to recover from force balance change (recovery time OR dimensionless ratio of recurrence interval to recovery time), and 4) rate of time-dependent system response (morphological change quantity per unit

change of input). They keenly recognised that the challenge lies in the rigour and resources needed to quantitatively characterise force and resistance. As such, their ordering facilitates structured evaluations of the ways in which changes to factors that influence force and resistance may shift in relation to a threshold (e.g. Figure 2-19).

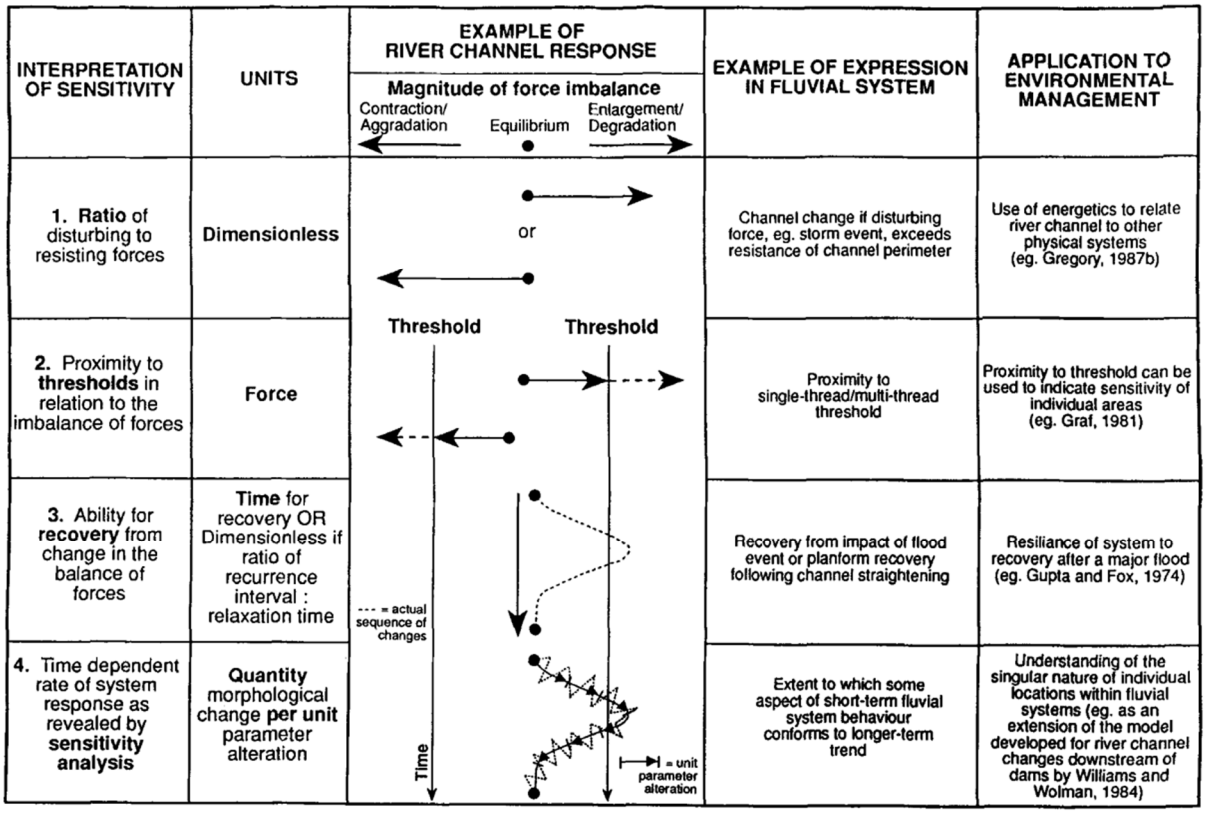

Figure 2-18. Investigative applications of sensitivity with metrics and examples (reprinted from Downs and Gregory, 1995).

Though the concept lay largely dormant for an extended period, it has enjoyed something of a renaissance in recent years. Fryirs (2017) relates sensitivity to and defines 19 different applications to highlight how interwoven it is throughout geomorphology. On a more general level, landscape sensitivity can be addressed by characterising sensitivity within- and between-compartments (Fryirs et al., 2007) by considering force and resistance, disturbance frequency relative to relaxation time, resilience to perturbation, and historic and spatial contingency (Phillips, 2009). As with all other concepts in this chapter, scaling is important (Figure 2-20) particularly in considering how sensitivities pass between scales and the potential for lags and feedbacks. Although sensitivity is generally treated on human scales (e.g. decade to centuries at reach to catchment scales), it is equally applicable to geologic scales, such as differentiating palaeo-mean annual precipitation from active tectonic influence on longitudinal stream profile adjustment (D'Arcy and Whittaker, 2014).

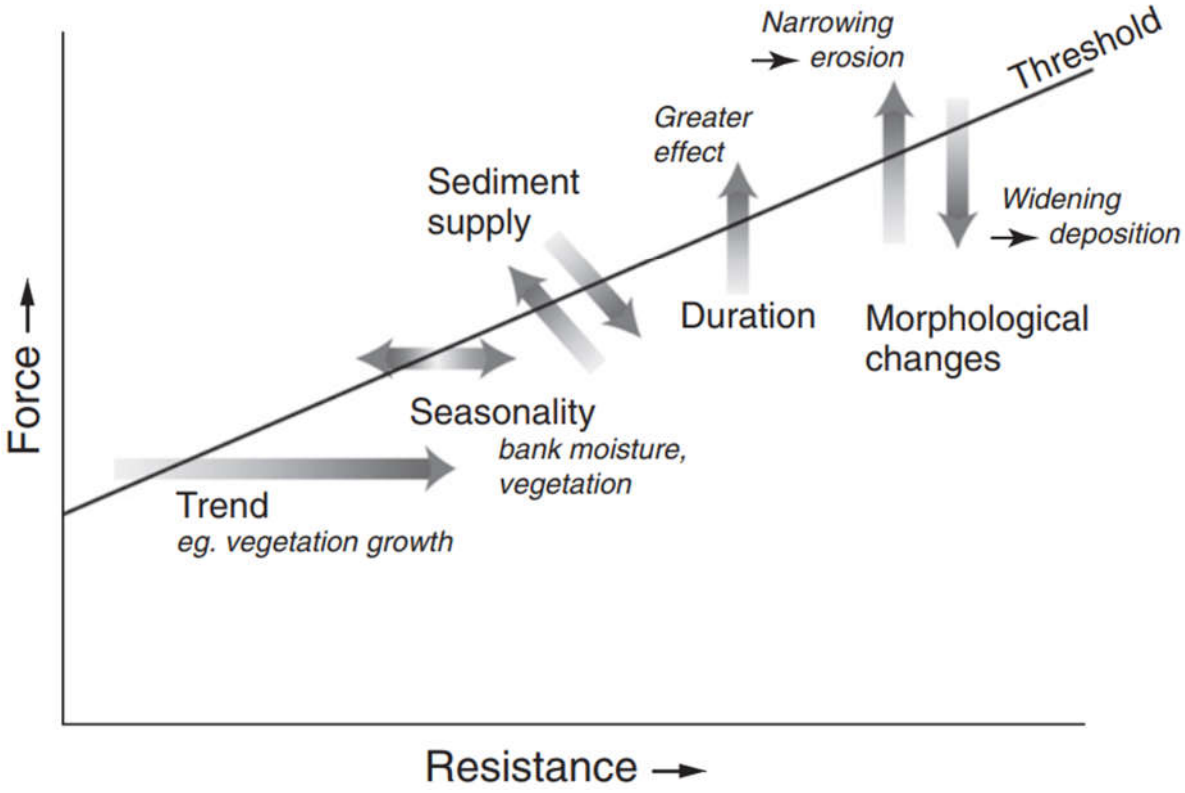

Figure 2-19. Example of changes in factors that affect force:resistance balance relative to an arbitrary flood impact threshold (reprinted from Hooke, 2015).

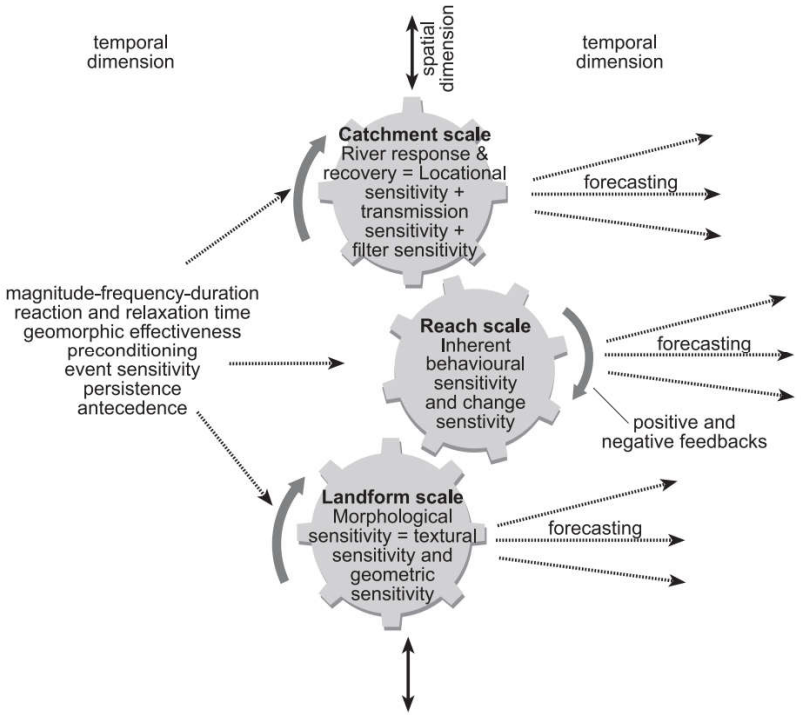

Figure 2-20. Conceptual representation of river sensitivity assessment across space and time (reprinted from Fryirs, 2017). Paths indicating potential for multiple outcomes (non-determinism) is of particular importance.

The utility of application on river management scales is aided by using standardised physical quantities. Measures of stream power, energy, and volumetric channel change have been used to indicate erosion/deposition sensitivity (Fuller, 2007; Bizzi and Lerner, 2015). Network modelling has

become increasingly popular for identifying local imbalances of sediment flux that may selectively predispose network component sensitivity as *hotspots* that are more prone to morphological response (e.g. Czuba and Foufoula-Georgiou, 2015). Recent advances in modelling show promise for identifying and exploring hotspots relative to sediment transfer and connectivity (Khan et al., 2021; Tangi et al., 2022). The benefits of such network modelling exercises may be enhanced by inclusion of behavioural expectations of the system and/or site (Lisenby et al., 2020). While non-linearity and complex behaviour preclude deterministic forecasting of form with any certainty, behaviour (and sideboards of behaviour) are better informed when the nature of component conditioning and sequencing are assessed.

2.2.3.3 Conditioning

Conditioning as a concept does not reside within geomorphology's lexicon with the same emphasis or refinement as the other concepts in this chapter. While multiple review papers, journal special issues, and books have been published on preceding concepts, conditioning per se does not even rate mention as an item in textbook indices. Nonetheless, I believe it is an important element of morphodynamics and its relevance will only grow in the future as the capacity to collect and analyse detailed time-series data. The more relevant dictionary definition from (Merriam-Webster, 2020) is: "a simple form of learning involving the formation, strengthening, or weakening of an association between a stimulus and a response". Conditioning in morphodynamics seems to be a latent premise: its sporadic appearance in text (cf. Lane and Richards, 1997; Fuller, 2014) belies its real-world prevalence.

I adapt Webster's definition of *conditioning* to: changes in one or more system components, often incremental, that alter subsequent component or system-level behaviour(s). Examples include increases in boundary resistance associated with riparian vegetation encroachment (e.g. Manners et al., 2014) or channel sedimentation effects on overbank flow frequency (e.g. Slater et al., 2015). While longer-term forcings such as glacial history (Tunnicliffe and Church, 2011; Curran et al., 2017) also reflect conditioning, they are encapsulated within the existing notion of *memory* (cf. Brierley, 2010) where lags from historic or prehistoric system controls may continue to influence contemporary forms and processes. Thus, processes or states related to memory are a subset of conditioning processes and states differentiated by signal persistence: conditioning effects may or may not persist; ones that do may be considered to impart memory, such as armouring associated with a palaeoflood.

Though broad explicit mention is uncommon, the premise of conditioning is well-established within subfields such a slope stability (Glade and Crozier, 2005) and avulsions (Jones and Schumm, 1999; Slingerland and Smith, 2004) which are both threshold-driven. Each has well-established factors/phases of "preconditioning", "preparation", and "set-up" in advance of a critical instance or trigger. Avulsions are commonly conceptualised as occurring in two phases, where incremental changes at a site may accumulate over decades to millennia to condition the site's susceptibility to a triggering event that is usually more concentrated in time (Slingerland and Smith, 2004; Aslan et al., 2005). The classic representation as applied to avulsions is adapted from Schumm's (1973) paper where the system state is a sub-horizontal line with conditioning represented by slope (Figure 2-21). Disturbance events (vertical lines) of varying magnitudes are imposed through time on the conditioned system, which eventually breaches the threshold. As with other concepts in this chapter, conditioning can occur across a wide range of scales and processes.

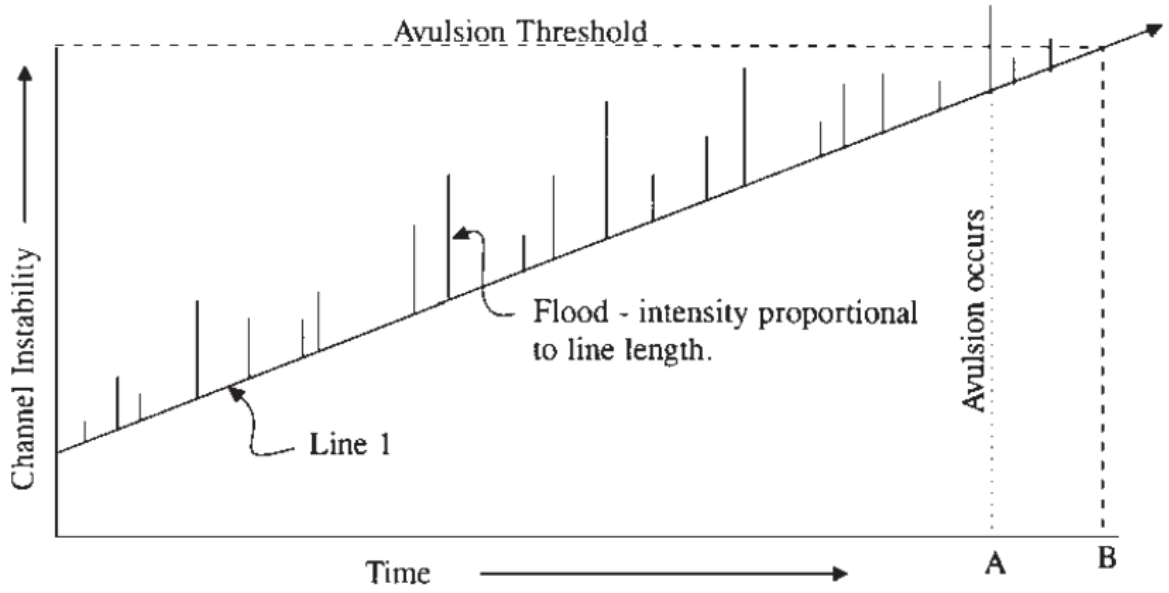

Figure 2-21. System conditioning toward a critical threshold. Events (vertical lines) super-imposed on a linearly-conditioned system through time (sloping line, "Line 1") relative to a behavioural threshold, in this case an avulsion (reprinted from Jones and Schumm, 1999).

Conditioning of bed mobility

The combination of bed structure, seepage and turbulence have greater influence on particle mobility than more common hydraulic variables like discharge and mean velocity (cf. Neverman, 2018). Sediment transport can be orders of magnitude lower in the presence of bed forms like ribs and clusters (Church et al., 1998) and well-armored beds have shown little mixing and large single-event path lengths (results of Tacconi et al. (1990) noted in Hassan et al. (1992)). Variation in bed structure can result from magnitude of previous high flows (Masteller et al., 2019), upstream supply rate (Recking, 2012; Rickenmann, 2020), and time-lag in bedform development (Martin and Jerolmack, 2013). Structure conditions transport via an array of changes including grain protrusion (Yager et al., 2012), bed surface stabilisation during low-flow periods (Masteller and Finnegan, 2017), shifts in particle interlocking (Turowski et al., 2009), dominant bed morphology (Recking et al., 2016), near-bed seepage (Neverman, 2018), and active layer thickness (Rickenmann, 2020). Vertical sediment exchange is well-established in gravel bed rivers (Haschenburger, 2013; Houbrechts et al., 2015; Gilet et al., 2020) and mixing reduction does not occur until sediment dispersion has matured (Haschenburger, 2013; Houbrechts et al., 2015) such as with development of an armor layer. Disruption of the armor layer and increased bed supply have been linked to within and between-event non-linearity of sediment transport in meandering (Downs et al., 2016) and mountain streams (Lenzi et al., 2004). Changes in texture, such as where an event that fills voids between clasts with sand (Ferguson et al., 1989) or finer clasts (Venditti et al., 2010) effectively decreases bed roughness and critical shear stress. Stream power at the threshold of motion in coarse-grained channels may vary by many times from one event to the next depending on the state of the bed at time of discharge (Reid et al., 1985). Lowering of critical shear stress associated with filling may condition a channel-scale erosion response by a subsequent event (Johnson, 2016). Coarse particle transport rates (Wilcock et al. 2001) and distance travelled (Hassan et al., 1992) can increase by one or more orders of magnitude as sand content increases. Within-event coarsening can occur as proportionately greater removal of mobile particles occurs and leaves an increasing proportion of stable grains behind (Dietrich et al., 1989; Johnson, 2016). However bed topography has been shown to be more responsive to flow strength than bed material size (Bertin and Friedrich,

2018) suggesting perhaps that quantification of coarsening is scale-dependent. Accounting for bed state (e.g. structure) between sequential events has been shown to improve bedload transport prediction (Rickenmann, 2020), thus, reinforcing the importance of bed conditioning.

Conditioning reach and catchment behaviour

Thicker active-bed layers at reach scales have been implicated in longer duration disequilibrium cycles (Rickenmann, 2020). Progressive sedimentation has important implications for flood inundation (Hooke, 2015; Slater et al., 2015; Slater, 2016; Call et al., 2017; Collins et al., 2019). Sedimentation may result from translocation of sediments from upstream channel incision and/or coupling to other sources. Sediments from slopes and reworking of valley bottom fills are especially important sources that can cause not only morphological response, but substantial behavioural shifts (Nelson and Dubé, 2016; Tunnicliffe et al., 2017). Such responses are often conditioned by floodplain connectivity (e.g. Magilligan et al., 1998; Reid et al., 2007a) and/or floodplain resistance (Toone et al., 2014). Channel bottom deposits left by large floods may condition subsequent flushing events (Gupta and Fox, 1974) or moderate sediment recruitment by smothering other landforms (Fryirs et al., 2007). Event-based conditioning can be an important source for complex response in small catchments, such as where an initial event may be disproportionately effective on slopes and a following event of similar magnitude-frequency may be more effective within channels as sediments introduced by the initial event are reworked (Newson, 1980).

Biogenic conditioning

Awareness of the roles of plants and animals in conditioning morphological response has grown in recent decades, including frequent use of the phrase “ecosystem engineers” (cf. Gurnell, 2014; Atkinson et al., 2018; Butler, 2019; Harvey et al., 2019; Brazier et al., 2021). Climatically-forced vegetation shifts have been implicated in variable supply in the Holocene and late-Pleistocene and linked to shifts in fluvial form and behaviours (Knox, 1972; Formento-Trigilio et al., 2003; Clement and Fuller, 2007). This effect may be observed in a space-for-time substitution along a contemporary gradient described in the headwaters of the Yangtze and Yellow rivers by Yu et al. (2014) where differing regional climates and hydrographs drive vegetation patterns and, by extension, channel forms. Anthropogenic deforestation increased erosion rates by an order of magnitude over long-term (>Holocene) background in a small New Zealand catchment (Cerovski-Darriau and Roering, 2016). While floodplain trees and forest with suitable density can reduce velocities (Harwood and Brown, 1993; Rodrigues et al., 2007), diminished floodplain cover has been implicated in conditioning erosional overbank responses to floods (Toone et al., 2014).

Zoogeomorphic conditioning can act either to reinforce resistance to change or encourage change (Butler et al., 2018). Changes to bed structure by crayfish (*Pacifastacus leniusculus*) and Pacific salmon (*Oncorhynchus* spp.) nearly double grain transport in a flume study (Johnson et al., 2011) and account for almost half of reach-scale annual bed-load yield (Hassan et al., 2008), respectively. Catchment-scale effects have been suggested by modelling that increased sediment transport efficiency resulting from salmon spawning may alter longitudinal profile concavity (Fremier et al., 2018). Bank burrowing by signal crayfish has also been shown to accelerate bank retreat and increase sediment supply at bank and reach scales by 29.8% and 12.2%, respectively (Sanders et al., 2021). Burrowing by nutria (*Myocastor coypus*) has been recognised as a problem in grey literature for decades (Sofia et al., 2017) and emerged into global literature more recently as awareness of the collective extent and intensity of alterations by invasive burrowing animals is raised (Atkinson et al., 2018).

While the body of literature pointing to animals as accelerators of geomorphic processes is possibly developing more rapidly, there are numerous instances where they are also shown to reduce transport rates, retain matter and/energy, and condition ecosystem-level responses. A patch-scale study of river-deployed trays showed fine gravels colonised by net-spinning caddisfly larvae (*Hydropschidae* spp.) have significantly greater critical shear stress than uncolonised gravels (Johnson et al., 2009). Given the global distribution of hydropsychid caddisflies, the authors suggest extensive spatial implications. Perhaps the best documented examples of biogenic conditioning in favour of retention and complex response across scales are associated with beaver (*Castor* spp.) throughout the northern hemisphere (cf. Gurnell, 1998; Brazier et al., 2021). Beaver dams create slope inflections that conditions sediment, carbon, and nitrogen retention (Puttock et al., 2018) and generally encourages lateral connectivity (Hood and Larson, 2015). In turn, these conditions promote, for example, unconfined aquifer recharge (Westbrook et al., 2006) and more complex channel forms (Polvi and Wohl, 2012). The high effectiveness of beaver in conditioning generally desirable and self-maintaining ecosystem services has led to substantial interest in their application for river and stream restoration (e.g. Pollock et al., 2007; Pollock et al., 2014) with implications for regional (Macfarlane et al., 2017) to hemispheric (Brazier et al., 2021) scales.

The large extent and intensive nature of humans as biotic conditioning agents of morphological response is increasingly recognised over the last twenty years and is now well-established, potentially on the scale of plant evolution during the Silurian (Williams et al., 2014). In reviewing alteration of human effects on fluvial sediment, Wohl (2015) establishes three groups of mechanisms: reduced sediment supply, increased sedimentation, and contamination. Here, I focus on direct conditioning of sediment supply within river corridors. Of various direct forms of human disturbance to rivers, riparian vegetation clearance and removal of large wood (LW) are potentially the most widespread (Brierley et al., 2005). Extensive deforestation and removal of LW has been correlated with increased lateral channel migration rates up to 150 times greater than pre-clearance and considered a first-order control on channel metamorphosis (Brooks et al., 2003). Common responses conditioned by large wood removal include enhanced scour and bed coarsening (Lisle, 1995), increased transport of bed and bank sediments (Smith et al., 1993a), and channel widening (Smith et al., 1993b). Further, once key pieces have been removed, remaining or subsequent wood is less likely to be retained due to the loss of key pieces (cf. Wohl, 2013) and/or morphological response changing requisite key piece size (Brooks et al., 2003), potentially extending the duration of the conditioning effect. Because of lags in sedimentary system components, human conditioning of contemporary channel forms and processes may persist from decades to over a century following cessation of the perturbing management regime (e.g., James, 1999; Dow et al., 2020; Cienciala et al., 2022). Human enrichment of the cohesive component of suspended sediment can condition braided river metamorphosis to single-thread forms (Richards, 1979; Nadler and Schumm, 1981). Mining of bed materials from coarse-bedded rivers can condition continuity interruption by trapping (Reid et al., 2007b) or enhance channel-channel coupling via headward incision migration (Kondolf, 1994). It is a well-established view that increased bed response can be expected with restriction of lateral 1) channel movement and 2) sediment transfer imposed by river management (Schumm, 1979; Harvey, 2001; Hooke, 2003; Davies and McSaveney, 2006). Disconnection of the potential to deposit and store sediment on floodplains increases in-channel deposition which exacerbates flood risk by reducing flow capacity, accelerates bank erosion (Reid et al., 2007a) and accelerates reach-scale aggradation rates (Beagley et al., 2020b).

2.2.3.4 Sequencing

The sequencing of flood events can be significant to bedload transport volumes with recently disturbed beds more likely to be mobilised on the rising limb and, hence, acted upon for a longer duration of an event (Reid et al., 1985). In a flume study, an event preceding a second event of similar magnitude was found to reduce transport rates of the second event with greater relative (%) reductions generated with low-magnitude sequences (Mao, 2018). In the same study, events of differing magnitudes produced differing outcomes where a high magnitude event preceding a low-magnitude event reduced the sediment transported by the low-magnitude discharge as a standalone event; a smaller flood in advance of a large one did not change transport (Mao, 2018). Within a runoff season at field scale, a given flow may become less geomorphically effective and coincide with morphological shifts to less concentrated flow forms (Misset et al., 2020). Intra-annual shifts in transport thresholds may occur due to accumulation of in-channel materials during lower flow periods (Moog and Whiting, 1998; Martin and Conklin, 2018).

Across multiple years in a strongly bi-modal bed, transport distances associated with each of three sub-bankfull discharge categories decreased as particles found stable locations (Rainato et al., 2020). Intra-annual shifts in transport thresholds may occur due to accumulation of in-channel materials during lower flow periods (Moog and Whiting, 1998; Martin and Conklin, 2018). Within a runoff season at field scale, a given flow may become less geomorphically effective and coincide with morphological shifts to less concentrated flow forms (Misset et al., 2020).

In terms of morphologic implications, sequencing of event magnitudes has been identified as a control on mechanism dominance in braided systems (Wheaton et al., 2013) and the magnitude of the most recent major storm a better determinant of active channel width than time in flashy systems (Graf, 2000). In the vertical dimension, experimental and computational modelling suggest bedform height and wavelength increase rapidly with the onset of effective discharge, but wavelength decreases much slower than height once flows return to initial discharge (Nelson et al., 2011). Over longer periods (years), hydrologic variability is recognised for influencing forms and behaviours (Bledsoe and Watson, 2001; Welber et al., 2012; Kidová et al., 2016) which may shift over still longer timeframes (decades) given longer-term controls such as flood-rich and flood-poor periods (Macklin et al., 2006; Toone et al., 2014; Kidová et al., 2016).

2.3 Summary

The upshot of this chapter is that scaling and highly variable transfer pathways produce complex morphological behaviours that vary in space and time. Even the interaction of linear system components may still produce non-linear outcomes which become increasingly complex as stochastic, extrinsic controls are imposed. Because it's not possible to model the diversity of complex outcomes with certainty, well-informed management requires field data for robust understanding and proper contextualisation. As noted by Wohl (2013, p. 57):

> *"…a one-size-fits-all approach is inadequate. Spatial and temporal proximity to thresholds, the potential for diverse outcomes from a single external perturbation, and the likelihood of different responses to management actions through time and space across a river network indicate the need to be aware of the process domain in which the river reach is located and how the details of that process domain will influence likely behavior of that reach of river."*

The research community now recognises that complex effects condition variable flood inundation responses (Stover and Montgomery, 2001; Hooke, 2015; Slater et al., 2015; Slater, 2016; Call et al.,

2017). However, this has generally not materialised into management settings which are still often locked into regime-based approaches dependent on broad assumptions of spatial and temporal averaging. Persistent belief that classical notions of equilibrium or dynamic-equilibrium must eventually prevail is at odds with recognition that equilibrium, disequilibrium, and nonequilibrium forms can occupy a landscape concurrently (Nanson, 1986; Renwick, 1992) and sedimentary lags persist for decades to millennia (e.g. James, 1999; Tunnicliffe and Church, 2011; Cienciala et al., 2022). In short, as stated by Phillips (2009), steady-states are a "convenient fiction".

There is a significant need to recognise contemporary systems are the product of spatial and historical contingency (Phillips, 2006). That is, the suite of forms and processes that have interacted to create the systems we observe are unique for each point within a system and for each time step at which an observation exists. Revising management regimes to include understanding of dynamics will better inform flood management to accommodate variability of flood impact and complex response (sensu Hooke, 2015).

In the interest of producing not only robust and accurate, but useful results, the following chapters proceed on the basis that place-based understanding of river behaviours is critical, as advocated by Brierley et al. (2013). In tune with those authors, this thesis provides a "basis for scientifically informed management efforts that respect and work with the inherent diversity and dynamics of any given river system" (Brierley et al., 2013, p 602) by developing understanding of a spectrum of diversity and dynamics at multiple spatial and temporal scales within the Ruamahanga catchment.

Chapter 3

Study Area

The 3,435 km^2 Ruamāhanga River catchment is located at the southern end of New Zealand's North Island (Figure 3-1). It drains in a west-southwest direction generally aligned with major faults and is the largest catchment in a geographic region known as the Wairarapa. A thorough inventory and discussion of catchment-scale character, data, and related research can be found in (Dykes et al., 2015). The intent of this chapter is to provide general overview of environmental conditions relevant and specific to the scope of this thesis.

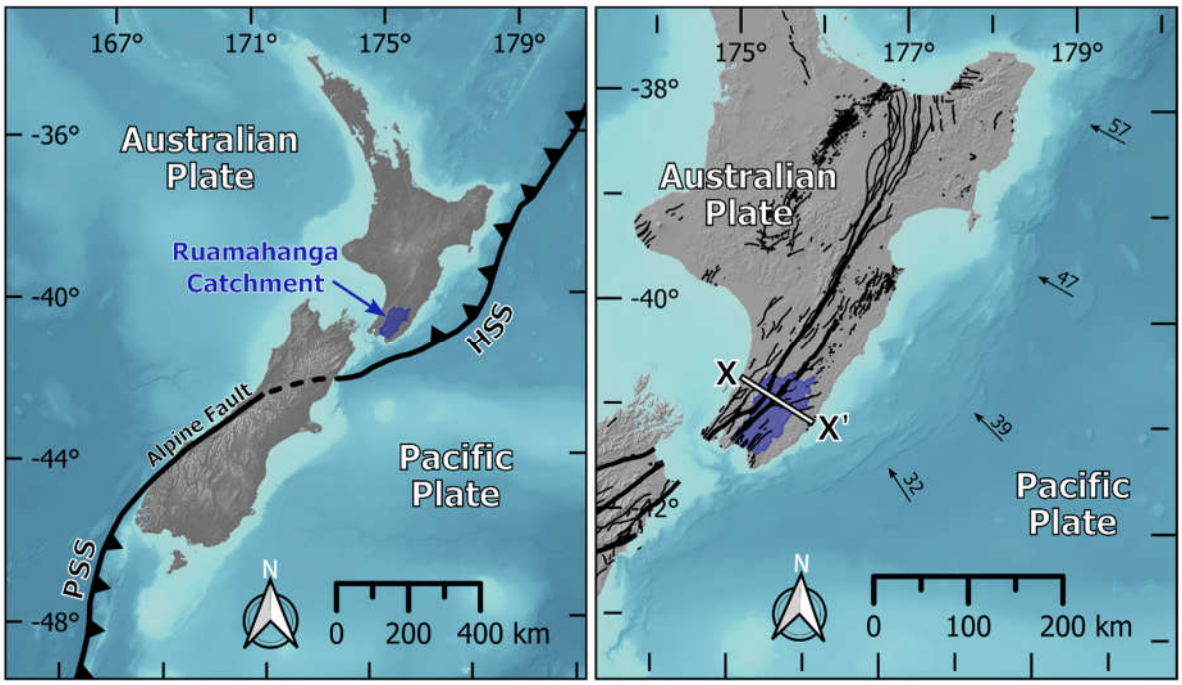

Figure 3-1. Left: The Ruamāhanga Catchment is located at the southern end of North Island near where the Pacific Plate (PP) / Australian Plate (AP) boundary crosses from New Zealand's east coast to west coast and subduction in the Hikurangi Subduction System (HSS) reverses to the Puysegur Subduction System (PSS) (after Anderson and Webb, 1994). Right: The PP is subducted under the AP at different rates (arrows, mm/year, after Clark et al., 2019) along the HSS with slower rates in proximity of the study area; black lines are active terrestrial faults (Langridge et al., 2016; accessed January 2021) with heavy lines representing major axial faults.

3.1 Geology

3.1.1 Plate Setting

New Zealand straddles a major plate boundary with the North Island occupying the Australian Plate and the South Island mainly sitting on the Pacific Plate (Figure 3-1). Opposing net northeast motion of the Australian Plate and southwest motion of the Pacific Plate result in net convergence rates that are highest along the East Cape region and gradually diminish toward the south (Figure 3-1, right). The North Island lies on the eastern margin of the Australian Plate which is overriding the Pacific

Plate off-shore along the Hikurangi Subduction System (HSS). The study area is located approximately 80 km northwest of the trough, within a forearc basin. The tectonic strain produces a planform inflection that crosses the primary axis of New Zealand's landmass effectively creating a giant releasing bend within which the study area lies. The majority of the strain is accommodated on the plate boundary with approximately 3-8 mm/year of upper-plate shortening occurring on the southern North Island (Nicol et al., 2007).

3.1.2 Lithology

Reports accompanying published 1:250,000 scale maps of the Wellington (Begg and Johnston, 2000) and Wairarapa (Lee and Begg, 2002) regions provide an overview of catchment lithology and structural geology. The general layout of the catchment is older (Mesozoic), harder (greywacke) basement rocks compose the core of the Tararua and Aorangi ranges along the northwestern edge and southeastern corner of the catchment, respectively (Figure 3-2). Alluvial sedimentation in the Wairarapa Valley has been occurring for at least 800 ka (Lee and Begg, 2002), though my examination of geologic maps indicates the majority of surface materials by area are <59 ka (Q3 or younger). Softer, younger (Neogene) mudstones dominate the eastern and much of the northern margins of the catchment as well as the Tararua foothills adjacent to the northern Wairarapa Fault. Sandstone and limestone members also occur within these areas.

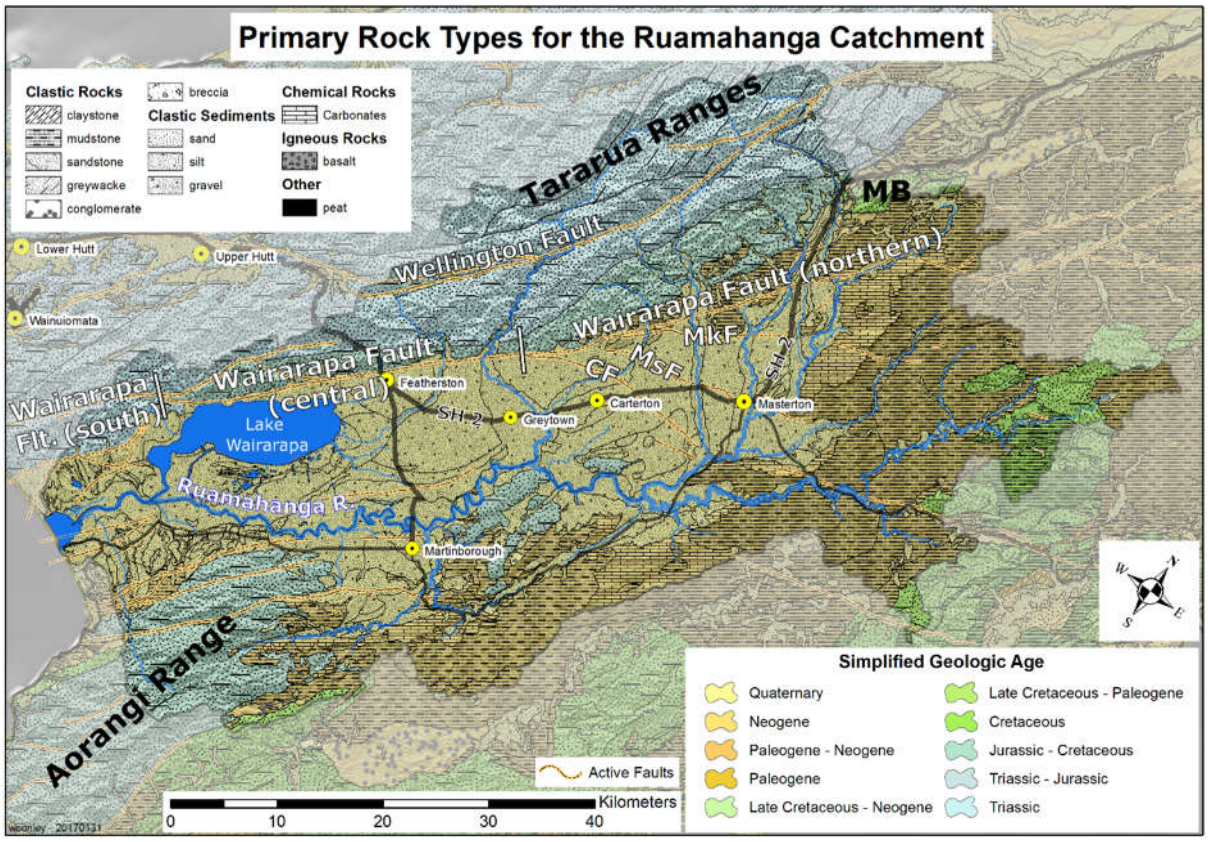

Figure 3-2. Lithology and age of major geologic units in the Ruamāhanga Catchment (GNS Science data after Begg and Johnston (2000) and Lee and Begg (2002)). Note map rotation. Sections of the Wairarapa Fault after Little et al. (2009). CF – Carterton Fault; MsF – Masterton Fault; MkF- Mokonui Fault; MB – Mount Bruce.

3.1.3 Tectonics

Oblique plate convergence produces differential upper-plate strain. Considered along an axis normal to the plate boundary (Figure 3-1, right X-X') manifestation through the study area is primarily

characterised by transpressional faulting (a.k.a. oblique strike-slip; Figure 3-3). Major faults of the study area are mainly characterized by right-lateral (dextral) strike-slip motion and part of the North Island Dextral Fault Belt (NIDFB). Many of the major faults have a secondary dip-slip component (GNS Science, 2020), though direction of motion is undetermined for many of the smaller or inactive faults (Langridge et al., 2016). In New Zealand (outside of the Taupo Volcanic Zone), a fault is considered "active" if it has ruptured and/or caused ground deformation in the last 125,000 years (GNS Science, 2020).

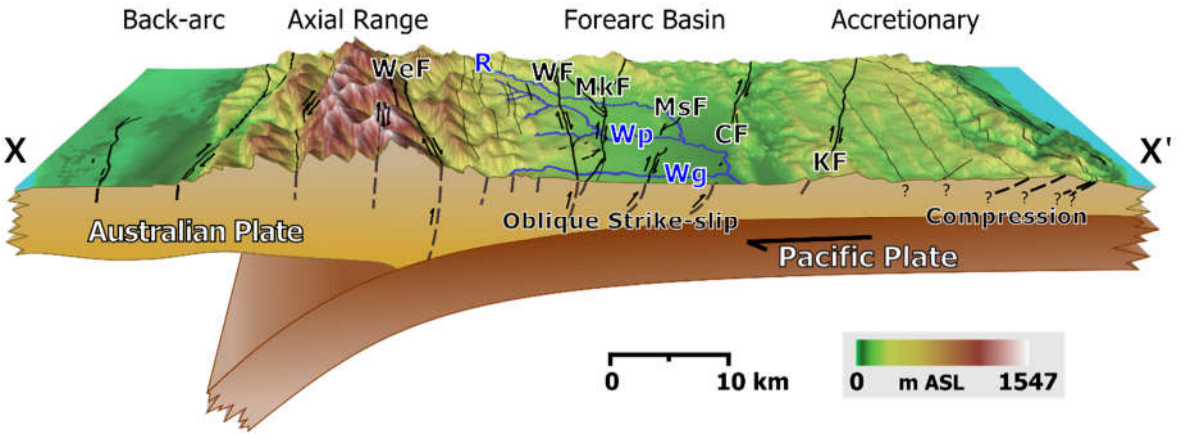

Figure 3-3. Three-dimensional tectonic setting through approximate centre of study area (X-X' in Figure 3-1 and Figure 3-4) after Lee and Begg (2002) and Ballance (2017); WeF – Wellington Fault, WF – Wairarapa Fault, MkF – Mokonui Fault, MsF – Masterton Fault, CF – Carterton Fault, KF – Kaumingi Fault, R – Ruamāhanga River, Wp – Waipōua River, Wg – Waingawa River.

Except for the Wairarapa Fault, slip rates and motion are not well-constrained. The persistence of scarps and observation of other faults in the region indicate co-seismic rupturing behaviour is typical of larger events. Over the last eight ruptures, the Wairarapa Fault has averaged 16.5 m (+/- 2.2) of dextral displacement (Manighetti et al., 2020). The most recent rupture of the Wairarapa Fault produced the largest known terrestrial slip globally (~20 m via high-resolution remote sensing Manighetti et al. (2020); 18.7 m ground investigation Rodgers and Little (2006)). Branching of the Carterton, Masterton, and Mokonui faults from the Wairarapa Fault is a typical fault-splay network which is often indicative of propagating systems (sensu Perrin et al., 2016).

Structural investigation has disproportionately focused on the Southern and Central sections of the Wairarapa Fault (cf. Figure 3-2). However, two studies that considered all sections of the Wairarapa Fault found variable vertical and horizontal deformation with general northward diminution and maximum deformation in the vicinity of the Carterton Fault bifurcation (Grapes, 1991; Manighetti et al., 2020). This suggests broader surficial diffusion of tectonic strain northward across the landscape.

3.1.4 Regional uplift and coastline shifts

Exhumation rates for the southeast North Island have been greatest during the last 5 Ma and generally linked to increased plate convergence rates (Jiao et al., 2017) with prevailing sub-aerial exposure of the study area above sea level occurring approximately 1 Ma (cf. Lee and Begg, 2002; Trewick and Bland, 2011; Ballance, 2017). Uplift in the vicinity of Mt. Bruce (Figure 3-4, top-centre) approximately 1.5 Ma disconnected an inland seaway and began differentiation of the Ruamāhanga catchment from the Manawatū (Trewick and Bland, 2011). Projection of interglacial benches relative to summit heights suggests a disproportionate amount of uplift may have occurred in the last 200 ka (Ghani, 1978). Marine highstand during the Holocene likely commenced ca. 8,300 BP, crested ca.

7,000 BP ~2.5 m above contemporary sea level and receded to present levels ca 4,000 BP (Clement et al., 2016). Litchfield and Berryman (2005) reported maximum highstand shoreline position 47 km inland based on intercalation of post-LGM fluvial terrace and marine sediments in eight East Coast catchments that included the Ruamāhanga. My interpretation of floodplain scarring patterns and valley slope in the study area suggests high-stand base level control was in the vicinity of the contemporary confluence of the Ruamāhanga and Waiohine rivers (47 +/- 3 km from the contemporary coastline).

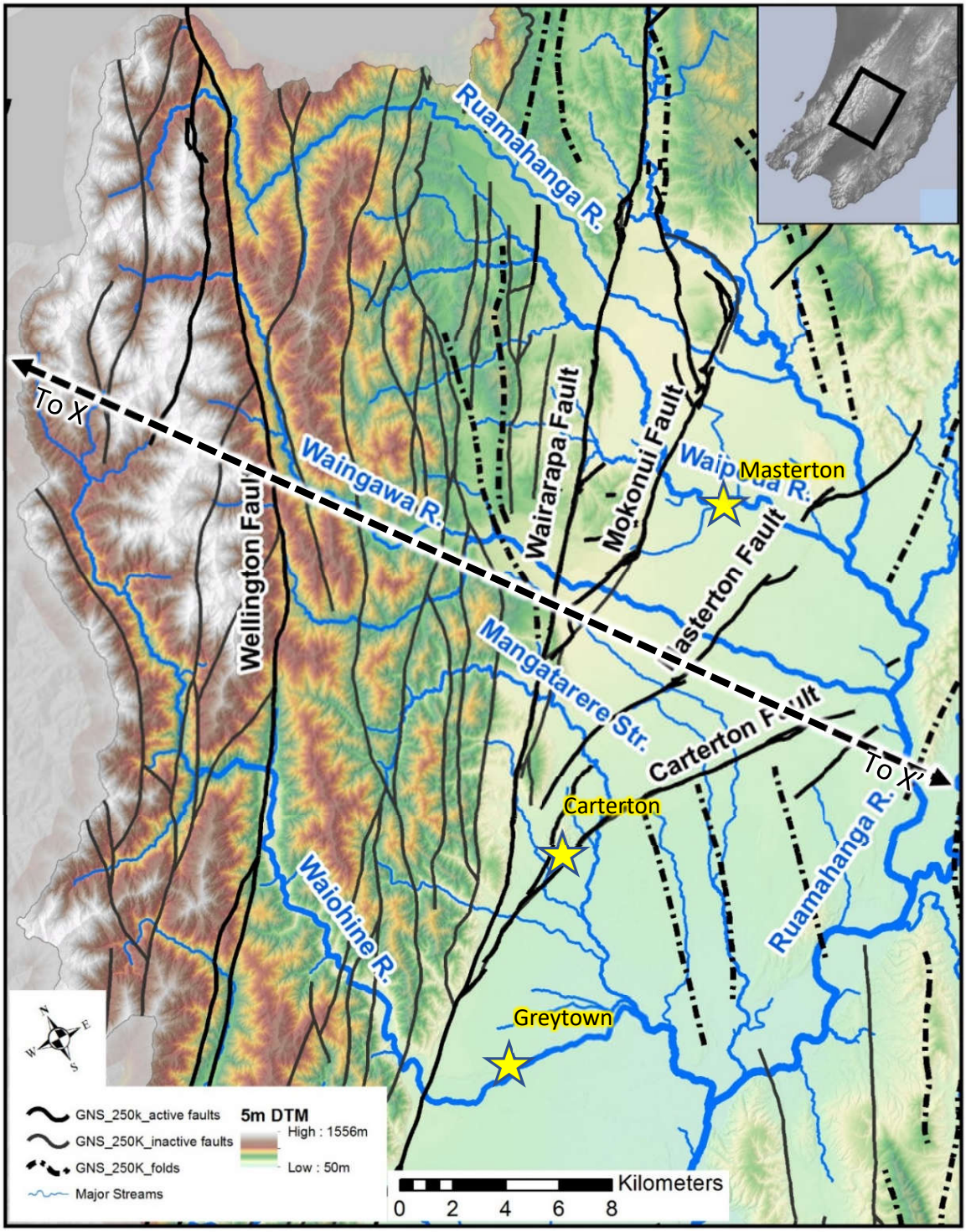

Figure 3-4. Relief map of the study area with towns, major rivers, and published faults. See Figure 3-3 for cross-section (X-X').

3.2 Weather and Climate

As an island nation in the southern Pacific Ocean, New Zealand has a generally humid climate with a moderate temperature regime. However, this same mid-latitude position in the 'roaring forties' exposes NZ to a wide range of often intense weather patterns inclusive of cyclones that stray from the tropics and polar systems from the Southern Ocean. Prevailing winds are westerly, though weather systems may approach from any direction. Kidson (2000) summarized three major national-scale regimes as: 1) zonal, 2) trough, and 3) blocking. Zonal tends to produce drier conditions for the Wairarapa while trough and blocking tend toward wetter Wairarapa conditions (Figure 3-5).

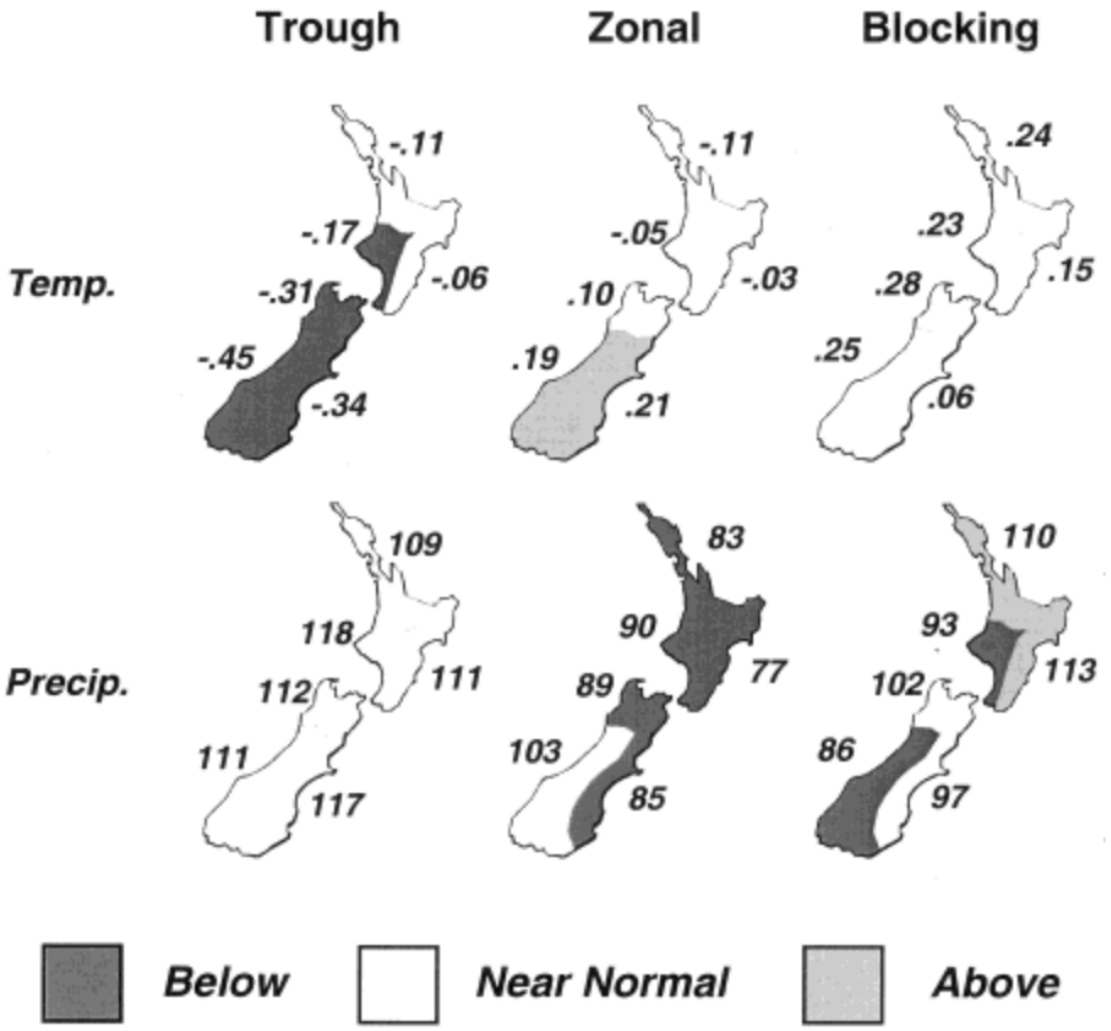

Figure 3-5. NZ weather regimes reprinted from Kidson (2000). Temperature and precipitation departures from normal are expressed in °C and % of normal, respectively. Shading indicates 95% confidence.

Weather and climate of the Wellington Region are summarized in Chappell (2014). Weather and river flows within the Study Area are controlled by orographic effects and storm direction. Mean annual precipitation within the catchment is closely tied to elevation and varies from >5,000 mm along the crest of the Tararuas to <1000 mm on the Wairarapa valley floor (Figure 3-6). Median annual air temperature is roughly 13° C in Masterton (Table 3-1) but less than 10° C in the Tararua Ranges (Chappell, 2014). Snow at upper elevations in the ranges is not uncommon and may persist for days to a week or so, while snow is very rare on the valley floor. Westerly and north-westerly storms typically produce disproportionately greater rainfall within the western and central Tararua

Ranges (Thompson, 1982; Council, 2014) and generate the largest discharges for rivers draining the Tararuas (Gordon, 2012). Lower elevation areas to the east and south will often experience warmer and drier weather during such weather events due to a rain shadow effect. By contrast, southerly and easterly storms can result in higher catchment-wide rainfall (Thompson, 1982) and greater total discharges in the mainstem Ruamāhanga River (Council, 2014).

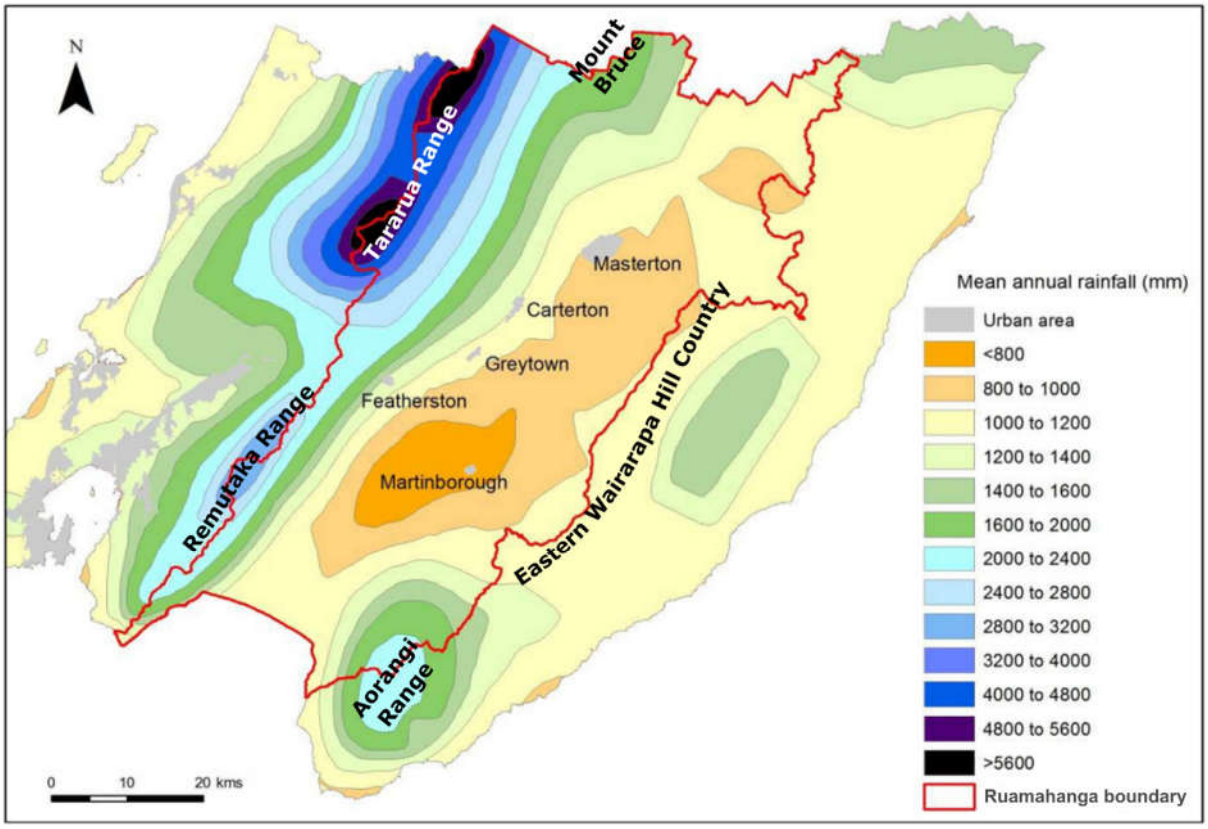

Figure 3-6. Mean annual rainfall for the Wellington Region for 1981-2010 (base map reprinted from Dykes et al., 2015).

Table 3-1. Annual climate summary statistics (1981-2010) for Masterton (data: NIWA, 2021).

Rainfall (mm)	Days ≥ 1.0 mm rain	Sunshine (hrs)	Temperature			Ground frost (days)	Mean wind speed (km/hr)
			Mean (°C)	Max (°C)	Min (°C)		
979	130	1915	12.7	35.2	-6.9	60	11

Though yet to be thoroughly explored in the Wairarapa, Holocene climate fluctuations have been correlated with river dynamics in other regions of the North Island (Richardson et al., 2013; Fuller et al., 2019b). A review of 44 North Island catchments (Clement and Fuller, 2007) noted that fluvial sensitivity (as determined from terrace records) increased during the Holocene with Wairarapa rivers (as evidenced by terrace formation/preservation) particularly sensitive to variable sediment supply.

Over much shorter periods (~decadal or less) within the Holocene, discrete sedimentation phases and above-average flood activity have been linked with El Niño Southern Oscillation (ENSO) (Fuller et al., 2019b). ENSO (El Niño/La Niña) cycles have been linked to seasonal rainfall changes within the Ruamāhanga (Tait et al., 2002; Mullan et al., 2005). While ENSO effects in New Zealand are known to modulate by IPO phase (Salinger et al., 2001), specific effects in the Ruamāhanga are unclear. Annual discharges of rivers in the Ruamāhanga catchment co-plotted with SAM, IPO, and SOI (Dykes et al.,

2015) doesn't yield any clear relationships, though further refinement seems warranted. Richardson (2013) broadly correlated ENSO and Southern Annual Mode (SAM) phases with the Kidson regimes and found more frequent blocking conditions during La Niña and more frequent zonal conditions during El Niño phases. Trough frequency increases during negative SAM while blocking and zonal regimes increase during positive SAM phases. Dykes et al. (2015) note that while extended dry periods are more common for the Wairarapa during La Niña (blocking) conditions, prevailing northerly/easterly winds increase likelihood of landfall by ex-tropical cyclones. On average, a cyclone passes close to or over the Wairarapa every three years, with 10 passing within 300 km between 1960 and 1989 and only one of which directly crossed (Else, January 1976) (NIWA, 1999-2000). In terms of precipitation, analysis in NIWA (1999-2000) found rainfall for these ten storms no more significant that typical storms. Single-day maximum rainfall ranged from 17 to 136 mm which is considerably less that other storms the Wairarapa has experienced (cf. Table 3-3).

3.3 Physiography

Three broad groupings for landforms of the Ruamāhanga catchment have been recognized by multiple authors (e.g. Kamp, 1992; Begg et al., 2005). These roughly align along the primary axis of the catchment and have strong spatial correspondence with parent material. They also reflect elevational, relief and weathering/curvature characteristics. For simplicity, I use the nomenclature of (Begg et al., 2005) who grouped as 'western', 'central', and 'eastern' (Figure 3-7 and Figure 3-8). The 'western' unit (Figure 3-8, top) is the hard, high-relief Tararua and Remutaka ranges which are the major axial ranges of the southern North Island. They are composed of greywacke basement rocks, are mostly forested, have thin soils, and very little hydraulic storage.

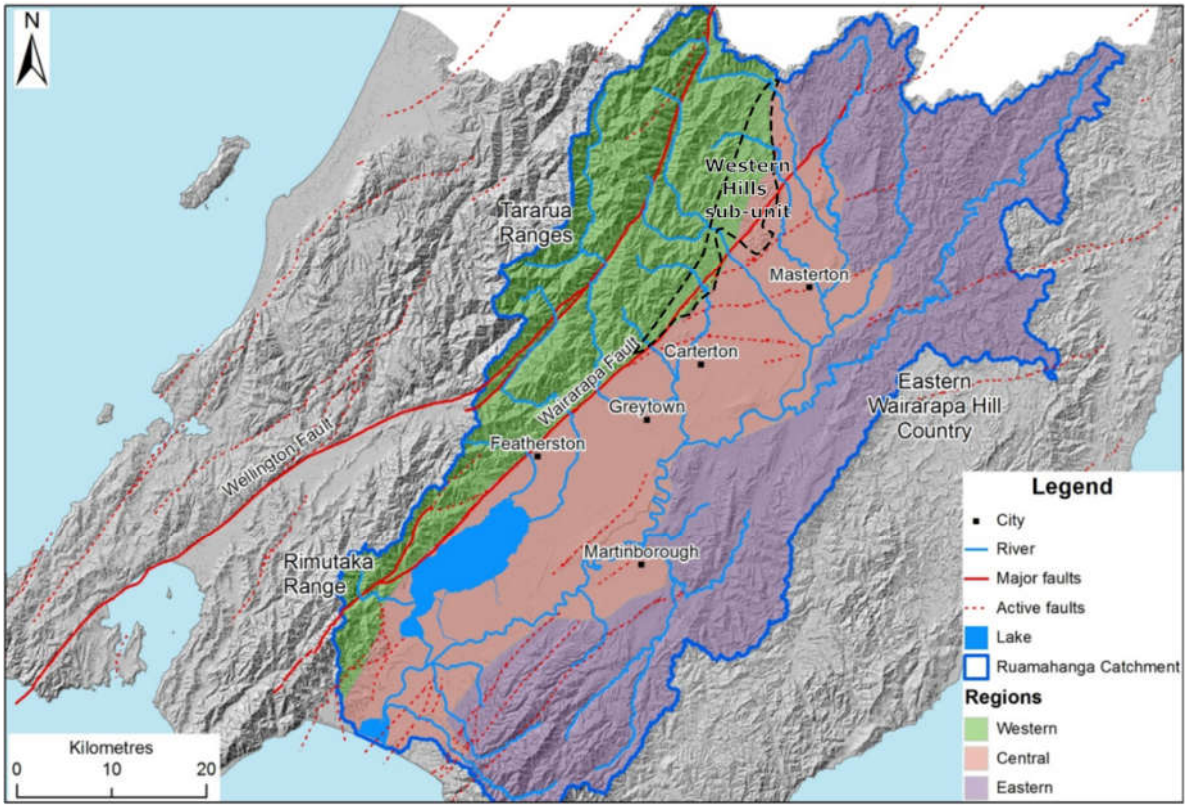

Figure 3-7. Major topographic zones within the Ruamāhanga catchment after Begg et al. (2005) (map reprinted from Dykes et al., 2015). The 'Western Hills' sub-unit has been added to delineate an area that is more physiographically like the Eastern Hill Country, than the proper Tararuas.

I've delineated a supplemental 'western hills' sub-unit (Figure 3-7, top) to indicate a sizeable area of softer lithology and moderate relief than the 'western' unit proper and more typical of the 'eastern' unit though the moderately resistant sandstones and limestones comprise a greater relative proportion by area. The 'central' unit (Figure 3-8, middle) is the very low-relief Wairarapa valley floor dominated by clastic alluvial materials exported from the 'western' unit. The 'eastern' unit is defined by generally modest relief with soft to moderately resistant lithologies (mudstones, sandstones, and limestones) and pastoral land cover (Figure 3-8, bottom). Landslides and cohesive alluvial fills are common in the 'eastern' unit.

Figure 3-8. Photographic examples of the three general physiographic areas in the Ruamāhanga catchment. Top: Looking west from the Ruamāhanga River across the valley floor at more rugged forms (background) of the Tararua Ranges ('western'); rounded hills in mid-ground are composed of similar materials as Eastern Hill Country but not differentiated. Middle: Typical low-relief, alluvial landscape of the valley floor ('central') on either side of the Waingawa River (eastern hills in background). Bottom: Looking east from the Ruamāhanga River across valley floor ('central') at the rounded forms of the Eastern Hill Country ('eastern').

3.4 Study Rivers

River character in the Ruamāhanga catchment tends to group similarly to physiography. Within the 'western' unit, rivers tend to be steep, bedload dominated, confined to highly confined with frequent bedrock controls, and have deeper valley incision with fewer/thinner alluvial covers. In the 'eastern' unit, landslides are common, and rivers appear to be washload dominated. Compared to the 'western' unit, alluvial valley bottom covers are more common and thicker, although rivers and streams have generally incised into them and are not well-connected to floodplains. River segments

within the 'central' unit are low relief and occur on a spectrum of forms that reflects their sediment source. Generally speaking, upstream of the Huangarua confluence, rivers that join the mainstem Ruamāhanga from the left bank are sinuous with cohesive banks. Rivers joining from the right-bank (that drain the Tararuas) have beds and banks composed granular materials and commonly have multithread, wandering forms. By area, these rivers (or their ancestors) appear disproportionately responsible for construction of the Wairarapa's valley floor.

This thesis focuses on coarse-bedded rivers within the 'central' unit that drain the Tararuas. This includes unconfined reaches of the Tauherenikau, Waiohine, Waingawa, Waipōua, and upper Ruamāhanga rivers. Rivers draining the Tararuas are short with only one (Waiohine) longer than 25 km to where they exit the range. The Ruamāhanga, Waingawa, and Waiohine head along the crest of the range and drop approximately 1,200 m by the time they leave the range front where they exhibit multi-thread forms as they traverse their alluvial fans and floor of the axial valley. The Waipōua has its headwaters in the Blue Range, descends approximately 800 m by the time it exits the range front, and primarily exhibits wandering behaviour as it transits the Wairarapa valley. Bed slopes of the four rivers vary between 0.001 and 0.01 m/m and all have coarse (gravel or larger) beds. Bed surface material data (Christensen, 2013, Appendix C) for the Waipōua, Waingawa, and upper Ruamāhanga (upstream of the Waiohine confluence), indicates the d_{84} varies between 80 and 350 mm. Channel forms are multi-threaded with early aerial imagery typical of an island-braided or wandering rivers while imagery from the last forty years suggesting braid-like behaviours are common. All pass through or in proximity to major population centres (Figure 3-2, Figure 3-4, Figure 3-7) though the density of persistent channel-spanning infrastructure is modest. In approximately 170 km of total river length, there are 30 subaerial crossings (29 bridges and 1 pipeline), with half of those occurring on 30 km of the Waipōua. Hydrology is unregulated, rain-driven and flashy with very steep rising and falling limbs (Figure 3-9, top). In general, storm frequency is greater during winter and early-spring and decreases during summer and autumn, though large magnitude events can happen at any time (Figure 3-9, bottom). More detail specific to each river is found in Dykes et al. (2015).

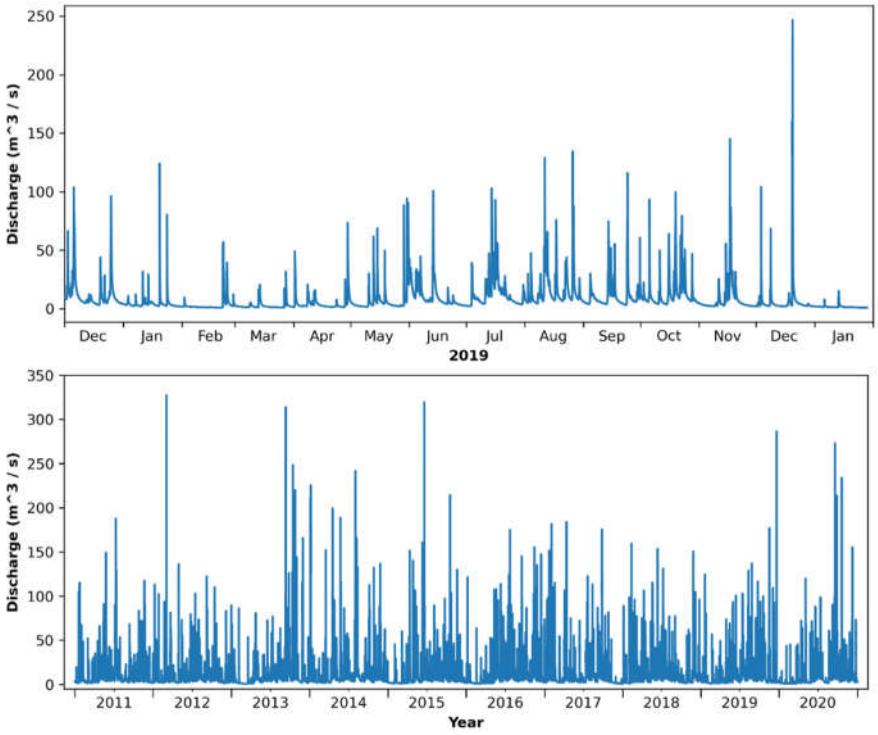

Figure 3-9. Five-minute (top) and fifteen-minute (bottom) hydrographs for the Waingawa River at Kaituna (data: GWRC) for 2019 and 2011-2020, respectively.

Adjacent floodplains and terraces are almost entirely composed of Holocene and Late Pleistocene alluvium overlying Neogene mudstones. Field observations indicate lithic channel contacts are generally mudstone, though these locally recruited clasts deteriorate to finer fractions (<2 mm) rapidly, usually within 100s of meters. Even within close proximity of lithic contacts, bed clast provenance still appears to be of >99% from greywacke units. Field observations and GIS exploration indicate late-Quaternary fluvial terraces generally define the margins of the 100-year floodplains. Active channel contacts are generally rare though become more common along the Ruamāhanga mainstem.

Coarse-bedded rivers are generally known for having temporally variable bed material transport and channel behaviour that are often cyclical and highly responsive to changes in sediment supply and transport capacity. Piégay et al. (2006) proposed a conceptual model with 'expansion' phases characterized by frequent lateral shifts during periods of high sediment supply and 'contraction' phases where low supply is associated with narrowing and incision. Management anecdotes suggest study area streams experienced an expansion phase from the 1940s into the 1980s, then a contraction phase from the 1980s to the present. However, Fuller (2010) found no evidence of expansion and documented a 32% reduction in active channel area occurring between 1943 and 1966 followed by slower, but steady narrowing of the active corridor. This narrowing is generally consistent with prevailing land-use of the day that emphasized "farming all available land to the river edge" noted by Heslop (1996, p. 2) and large quantities of gravel extraction (e.g. 519,000 m^3 removed from the Waingawa River alone between 1977 and 1990 (Williams, 1990)).

3.5 Selected Hazards

Local and regional governments responsible for identifying natural hazards under the Civil Defence Emergency Management Act (Parliament, 2002). Natural hazard have been discussed at both the Wellington region (e.g. Grant, 2005; Dawe, 2007) and Wairarapa (WELA, 2003) scales across a broad spectrum of hazard types. The two most relevant to this thesis are floods and earthquakes (inclusive of coseismic landsliding).

3.5.1 Human Values

Hazards by definition are intrinsically linked to human values and, thus, do not exist in the absence of humans. While floodprone human values is far too broad a subject to be addressed here, buildings provide a discrete and indicative proxy for framing alluvial hazards. Building outlines acquired from LINZ Data Service indicate there are 50,084 total buildings in the Ruamahanga catchment. The vast majority of buildings lack attribution for use and occupancy so deeper analysis was not performed. Generally, most buildings occur in the low-relief "Central" physiographic unit (Figure 3-7 and Figure 3-8) and similarly associated with Quaternary gravels shown in Figure 3-2. Converting the building polygons to point features and querying QMAP geologic unit polygons (Lee and Begg (2002), Begg and Johnston (2000)) indicates that 46,466 buildings (92.8%) occur on alluvial deposits. This includes 100% of buildings in all five towns (Figure 3-10). Of particular note is the substantial number (n=12,943, 25.8%) on Holocene alluvial deposits (Table 3-2) including 31% (4584 of 14,766) of buildings in Masterton and 100% in Greytown (Figure 3-10). Such a high proportion of human investment on ground constructed and occupied by rivers within the recent geologic past warrants greater consideration of river dynamics than has historically been given.

Table 3-2. Number of buildings occurring by geologic age of surface.

Geologic Age and Type of Surface	Absolute Range (x 1,000 years)	Number of Buildings
Early Pleistocene alluvium	524 – 1,830	475
Middle Pleistocene alluvium	128 – 524	818
Late Pleistocene alluvium	14 – 128	31,980
Holocene alluvium	< 14	12,943
Undifferentiated (Holocene to Pleistocene) alluvium	0 – 524	250
Non-alluvial (all ages)	n/a	3,618

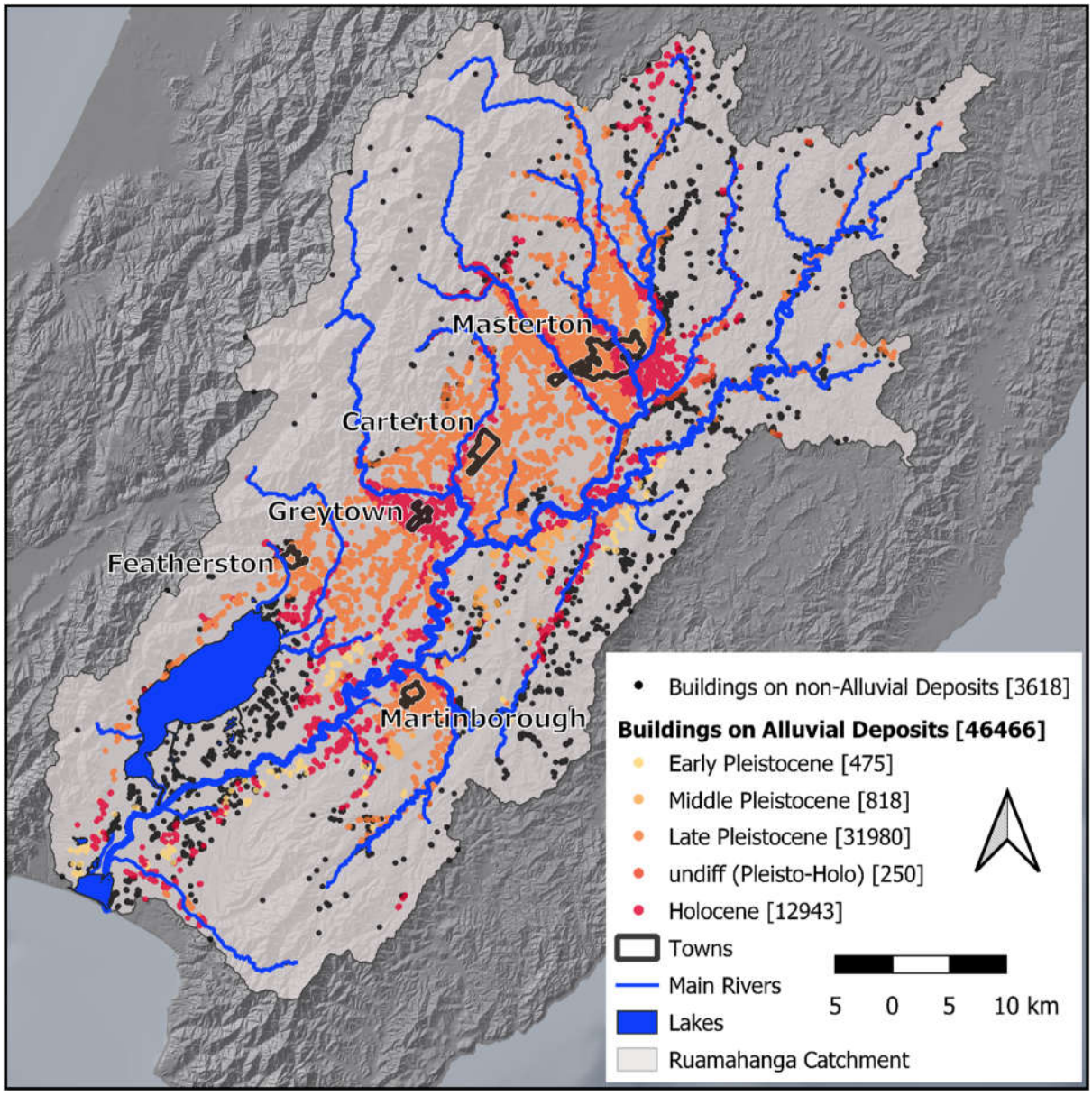

Figure 3-10. Ninety-three percent of buildings in the Ruamahanga catchment occur on alluvial surfaces. Twenty-six percent sit on Holocene alluvial deposits (Table 3-2) including 31% of Masterton and 100% of Greytown buildings. (source data: author, NIWA, LINZ and GNS Science).

3.5.2 River Floods

Floods are the most frequent natural hazard in the Wellington region (Dawe, 2007). Though broad, multi-disciplinary hazard assessments acknowledge potential for "change of course" (i.e., avulsion) and erosion, most assessments focus on flood inundation. Studies specifically focused on study area rivers (e.g., Heslop, 1995; Allan, 2014) also clearly identify erosion hazard as a key concern. In that regard, erosion is treated in the sense of lateral migration of the contemporary channel and aside from a couple of descriptive reports specific to the Waingawa River (Williams, 1990, 2010), avulsion hazards have not been investigated. Gravel bed river behaviour in the Wairarapa can be dramatic and have particularly challenged European-based development styles over the last 160+ years. High relief headwaters with shallow soils and little hydraulic storage translate to rivers that respond very quickly to frequent rain events (e.g., Figure 3-9). A long-standing awareness of potential dynamics is reflected in the Māori name of the Waingawa River, 'Waiawangawanga', which translates to troubled or uncertain waters (Allan and Girvan, 2015).

Given that alluvial river morphologies and behaviours are fundamental products of sediment flux (Brewer and Passmore, 2002; Church, 2006; Davies and McSaveney, 2006; Church and Ferguson, 2015), general conditions in the Ruamāhanga catchment are prime to produce sediment pulses that create small and local bed elevation changes to which wandering and braided rivers are well-known to be sensitive. Large earthquakes can generate large numbers of coseismic landslides in high-relief areas and tectonically active mountain belts are considered well-connected landscapes (Kuo and Brierley, 2013) for downstream transmission of sediment. A study from the nearby Ruahine Range identified a high-degree (78%) of slope-channel connectivity (Fuller et al., 2016a). The effects of these transfers to the fluvial system may manifest rapidly such as proximal failure of landslide dams or may occur over decades or longer. For example, the Waiohine river is known to have aggraded and dramatically increase its lateral activity near Greytown starting approximately 11 years after the 1855 Wairarapa earthquake and persisting for 11 years before restabilizing roughly 23-25 years post-earthquake (Stubbe, 1981). This period is concurrent with historic accounts synthesised in the Foreword of this thesis that note geographically extensive effects and at least two avulsion instances (1884c; 1884a; 1884b; Correspondence, 1884), one of which occurred in the area described by (Williams, 1990). Multiple accounts of the 1884 event specifically implicate (then) recently engineered works having magnified the effect of the flood.

In terms of establishing local flood histories, it is especially valuable to know that given the death, destruction, and disruption of the 1884 flood, more extensive floods had occurred at least three times within the prior 26 years (Foreword, this thesis). Occurrence of a nodal (a.k.a. regional) avulsion of the Waingawa River into the Waipōua River in the late-1860s is consistent with poorly developed soils observed in the field as well as online soils data (https://soils-maps.landcareresearch.co.nz/). Though the personal account does not indicate if a total avulsion occurred, it seems to be implied. Considering rapid hydrologic recession and assuming present-day stage-discharge relationships and settlers working in knee-deep water (to construct their "break-water"), it seems highly likely that the primary channel shifted at the least. Beyond avulsions, there is a more general history of serious, often widespread flooding of study area rivers; key examples found in reviewing various reports and records are compiled in Table 3-3 with maximum observed discharges by rivers presented in Table 3-4.

Table 3-3. Significant historic floods associated with study area rivers based on damage and/or media coverage (compiled from WELA (2003), (Dawe, 2007), and https://hwe.niwa.co.nz/).

Event Start Date	Rivers	Comment
1856 – 1868	all	See Foreword, this thesis
1875-12-06	Waiohine	A bridge between Greytown and Carterton gave way. Northern end of Greytown under water from town bridge to near the Rising Sun Hotel.
1880-03-23	Ruamāhanga	Peakflow = 2830 m^3/s
1884-09-02	Ruamāhanga et al.	See Foreword, this thesis
1892-10-13	Waingawa et al.	Great rise in all the Wairarapa rivers. Considerable damage to roads occurred in some parts. All low lying country was flooded. Approach to the bridge over Waingawa River was washed away.
1912-07-15	Waiohine	Heaviest flood for 20 years at Carterton. Water running over roadways and transforming them into rivers. Many houses were flooded, though only to a depth of a few inches. The approaches to four bridges, on the Dalefield, Belvedere and Mannings roads washed out. Extensive damage to roads. Worst flood for years in Greytown; country covered with water as far towards Woodside as one could see. All streets and paddocks flooded.
1928-11-01	Ruamāhanga et al.	Serious floods all over the district. Rivers overflowed their stopbanks and the whole country was inundated. Kokotau Bridge approaches washed-out.
1931-04-02	Waiohine	Waiohine River overflowed its banks around Matarawa. Water flowed across the road (SH2?) and into the saleyards and the houses in the vicinity.
1932-08-27	Waiohine Ruamāhanga	Waiohine River broke its banks and inundated an extensive area. Carterton had its worst flood since 1924. The rivers round Carterton rapidly filled and overflowed their stop banks. Waiohine River inundated the whole countryside. Ruamāhanga River had a peak discharge estimated of 1841 cumecs
1935-05-22	Waiohine	Carterton recorded 2.61 in (6.63 cm) of rain in 24 hours. Water running across the road between Carterton and Greytown.
1939-12-10	Waiohine	Water over the road at Waiohine Bridge between Greytown and Carterton.
1941-05-04	Ruamāhanga Eastern tributaries	Wairarapa district received 10 in (25.4 cm) of rain in 30 hours. Upper Ruamāhanga River broke its banks. Severe stock losses. Several bridges washed away. Areas around Te Whiti isolated.
1947-06-27	Ruamāhanga	20,000 hectares inundated for many days. Severe stock and production losses. Many homes isolated and/or evacuated. “100-year” Ruamāhanga at Waihenga peak = 2044 m^3/s
1948-05-22	Ruamāhanga Waiohine	flooding throughout the Wairarapa. Some rivers broke their banks and large areas of low-lying land flooded. In some parts it was the worst flood for many years. Waiohine crossed the road near Greytown. Extensive flooding near Carterton.
1981-05-21	Waipōua Ruamāhanga	Queen Street shops in Masterton were flooded. Ruamāhanga River peaked at 4.8 m at Waihenga.
1988-09-13	Waingawa	Wairarapa received 250 mm (25.0 cm) of rain in 12 hours; A pier of the Waingawa bridge subsided 7.5 cm, and State Highway 2 was closed.
1990-01-	Waiohine Ruamāhanga	268 mm of rain in 6 hours at the Angle Knob station (Tararuas, Waingawa catchment); Waihenga bridge closed
1994-11-05	Ruamāhanga	Highest stage (15.15 m) to date for Waiohine River. Many Greytown residents evacuated. “50-year” flow; Ruamāhanga at Waihenga peak = 1819 m^3/s
1997-10-03	Waiohine Ruamāhanga	Tararua Range recorded 323.5 mm (32.35 cm) of rain; Ruamahanga at Waihenga stage was 4.7 m for 22 hours
1998-10-20	Waipōua Ruamāhanga	Waipōua River stopbank breach, extensive damage to campground. Roads closed in the Wairarapa

2000-10-02	Ruamāhanga	850mm over 72 hours recorded in the Tararua Range. Ruamāhanga River flooded large areas, homes isolated, and roads closed
2000-10-08	Ruamāhanga et al.	~300mm of rain in the Tararua Range in 24 hours. Roads and bridges damaged, stock losses
2003-10-03	Ruamāhanga	Heavy rain in the Tararua, Akatarawa and Remutaka ranges. Unspecified damages.
2004-02-14	Ruamāhanga et al.	Ruamāhanga River "50-year" flood; pea harvest wiped out. 31 roads closed.
2005-03-29	unspecified	Masterton recorded 148 mm (14.8 cm) of rain in 24 hours (which has a return period of 90 years

Table 3-4. Largest recorded floods for major rivers in the study area (adapted from WELA (2003) and Oxenham (1993)). Floods occurring since 2003 have not exceeded values listed below.

River	Gage	Drainage Area (km^2) [a]	Max. Recorded Discharge (m^3/s) [b]	Year
Ruamāhanga	Mt. Bruce	78	467	1982
	Wardells	637	1,024	1998
	Waihenga	2340	2,044	1947
	Onoke Spit	3365	n/a	-
Waipōua	not specified	149	355 [c]	1994
Waingawa	Kaituna	139	426	1980
Waiohine	Gorge	378	1558 [d]	1982
Tauherenikau	not specified	140	670	1994

[a] at gage or mouth (tributaries) [b] at gage [c] GWRC (2021b) [d] landslide dam failure outburst

3.5.3 Earthquakes

Major active faults in the study area are generally transpressional with primary dextral motion, often with secondary dip-slip (GNS Science, 2020). In the Wellington region (inclusive of the study area), mean lateral slip rates range between 1 and 10 mm per year and meter-scale rupture recurrence varies between 500 and 5000 years (Van Dissen and Berryman, 1996). The five major active faults that intersect study area rivers are summarised in Table 3-5. There have been three surface rupturing events on faults intersecting the study area in the last 1000 years: two on the Wellington Fault (~350 & ~750 B.P.) and one on the Wairarapa fault (1855) (Dawe, 2007). The 1855 Wairarapa quake is the largest magnitude earthquake in New Zealand's recorded history and generated the largest known maximum terrestrial slip globally (~20 m via high-resolution remote sensing Manighetti et al. (2020); 18.7 m ground investigation Rodgers and Little (2006)).

Table 3-5. Earthquake recurrence for major active faults intersecting study area rivers (after Grant (2005), Dawe (2007), and WELA (2003)); maximum magnitude is an estimate for a penultimate rupture.

Fault	Recurrence Interval (years)	Time elapsed since last event (years)	Maximum Magnitude	Mean Single Event Lateral Displacement (m)	Single Event Vertical Displacement (m)
Wellington	~900	~300	7.6	4	1 - 2*
Wairarapa	1200-1600	166	8.1-8.3	12	3
Mokonui	1300-2000	1100-2600	6.7	2	-
Masterton	~1000	unknown	6.7	0.3 - 0.7	-
Carterton	700-1000	unknown	7.0	2	-

As the fault which generated the largest magnitude earthquake in NZ recorded history, the Wairarapa fault has received the greatest attention within the study area including its own

conference in 2005 (The 1855 Wairarapa Earthquake Symposium). The 1855 event ruptured along 75 km, including through the length of the study area, and uplifted over 5,000 km^2 of land west of the fault (Grapes and Downes, 1997). Over the last eight ruptures, the Wairarapa Fault has averaged 16.5 m (+/- 2.2) of dextral displacement (Manighetti et al., 2020). Along the fault's strike, Grapes (1991) observed segmented fault behaviour such as throw-reversals and spatially variable displacement of the Last Glacial Maximum (LGM) surface, regionally known as the 'Waiohine' surface (c. 10-12 ka Formento-Trigilio et al. (2003); Wang and Grapes (2008); Little et al. (2009)). His general data trends indicate maximum cumulative horizontal (125 ± 5 m) and vertical (20 m) displacement occur between the Waiohine River and Mangatarere Stream with strong diminution northward through the study area (e.g. < 5 m where it crosses the Ruamāhanga River). Carne and Little (2012) further differentiated segmentation into deformation types with nested scaling (kilometres and hundreds of metres) within a zone up to 350 m wide. In sum, these studies indicate persistent and complex tectonically-forced topography in proximity to the Wairarapa Fault.

The persistence of scarps along the Carterton, Masterton, and Mokonui faults indicate co-seismic rupturing behaviour, though these have received far less attention than the Wairarapa Fault (R. Langridge, pers. comm. May 2019). Two late-Holocene events were differentiated within the trench on the Carterton Fault producing a single event, dextral displacement estimate of 2 metres with a return period of 1,000 years (Begg et al., 2001) with normal sense of vertical motion. The trench on the Masterton Fault did not yield dateable material and discrete events were not distinguished, thus Begg et al. (2001) estimated 0.3-0.7 m single-event, dextral displacement, normal dip-slip, and ~1,000 year recurrence interval based on proximity to the Carterton Fault. Townsend et al. (2002) suggest an undetermined rate of dextral motion with a 0.1-0.8 mm/year vertical slip rate of undetermined direction for the Mokonui Fault, though they report back-tilting of older terrace gravels. Though the follow-up trench was inconclusive, authors inferred likely strike slip which, given a lack of horizontally-displaced late-Holocene geomorphic features, they concluded multi-meter displacements were unlikely (Langridge et al., 2003). They determined dip-slip motion based on Quaternary topographic offset but were unable to differentiate between normal or reverse motion. Based on available data, they concluded that the segment of the Mokonui Fault they studied (between the Waipōua and Ruamāhanga rivers) is purely oblique (H:V displacement = 1). With one variably conclusive trench for each of three segmented faults, it is fair to say the kinematics of the major splay faults are not well-constrained.

Though considerable uncertainty remains about specific behaviour of the area's faults, considerable effort has gone into documenting the effects and reconstructing past earthquakes. A range of first-hand accounts associated with the area's major earthquakes (Table 3-6) were recorded and have been published in both general interest (e.g. Bannister, 1940; McLaren, 2002) and technical publications (Grapes and Downes, 1997; Downes et al., 1999b; Downes et al., 2001; Downes, 2006). Recognising the considerable damage and human strife caused by these events, this thesis focuses only on the geomorphic effects.

The earliest recorded human account of earthquake-related river hazard is an oral Māori history recorded by Bannister (1940) that documents an instance where the Ruamāhanga River's flow temporarily ceased immediately following an earthquake, then returned abruptly when a wall of water raced downstream. Though the duration of the dam is not noted, Māori were harvesting live eels from the dewatered channel at the time of the outburst. Thus, I interpret the dam as having been short-lived. Bannister (1940), an early colonist, constrains the timing of occurrence to approximately 1838, which pre-dates formal European colonisation of NZ (1840). However, he seems to conflate the location with the site of a slide and failure that is known to have occurred in

1855 (Grapes and Downes, 1997). Bannister's recounting indicates earthquake shaking propagated from Wairoa toward the South Island. This is opposite of the 1855 earthquake which originated in the southern Wairarapa and ruptured northward. Thus, there seems good potential to have been two different events. A second-hand account of the same outburst recorded by Bannister was from a pioneer who had arrived in the Wairarapa in 1846 and been told of the event and noted a water depth [on the floodplain] of eight feet, which was consistent with traces of a debris line eight to nine feet (2.4-2.7 m) high in the trees later observed by Bannister.

Table 3-6. Earthquakes that have generated shaking ≥ MM VII (i.e. where small slides and rock falls begin to occur) within the study area interpreted from isoseismal maps in (Downes, 1995)..

Date	Name	Magnitude	Depth	Time (UTC)	Max. Shaking Severity (MM) in Study Area
1848-10-15	Marlborough	7.1 M(I)	shallow	14:10	VII – VIII
1855-01-23	Wairarapa	8.1-8.2 M(I)	shallow	09:32	IX – X
1904-08-08	Cape Turnagain	6.7 Ms Mw 7.2 [a]	lower crust	22:50	VII – VIII
1917-08-05	Tinui [b]	6.8 Mw	12 km	15:12	-
1934-03-05	Pahiatua	7.6 Ms	lower crust	11:46	VII+
1942-06-24	Wairarapa I	7.2 Ms	15 km	11:16	VIII
1942-08-01	Wairarapa II	7.0 Ms	43 km	12:34	VII+

[a] Downes (2006) [b] inferred from news articles (GNS Science, 2021)

In 1904, NZ seismic instrumentation was primitive and located only in Wellington and Christchurch (Downes, 2006). The epicentre of the Cape Turnagain quake was approximately 120 km ENE with the closest ground damage on the periphery of the study area. Bridge subsidence at Tauweru (~10 km east of Masterton) was noted and the largest inland landslide produced by the event originated from a high eroded terrace (cf. Downes et al., 2001) near Gladstone (~15 km south of Masterton). The slide sloshed water, eels and trout overbank from a tributary of the Tauweru River and the nearby river (unclear if Tauweru or Ruamāhanga) was observed to rise and fall from its bed (McLaren, 2002). Isoseismal maps for the Tinui earthquake were not found, but the GNS Science Earthquake Catalogue (2021) indicates the epicentre was located in the headwaters of the Tauweru River, approximately 30 km NE of Masterton. Contemporary news articles indicates strong shaking with minor ground cracks (Manawatu Times, 1917) and subsequent closures and load restrictions of bridges in the hill country immediately east of the study area (Wairarapa Daily Times, 1917). The Pahiatua earthquake is somewhat better constrained as the NZ seismic network had grown to 12 stations with the epicentre located approximately 60 km NE of the study area (cf. GNS Science, 2021) and though extensive building damage occurred as close as Eketahuna, documented ground damage in the study area was negligible. Bad cracking of stopbanks (levees) at Kahutara (near Lake Wairarapa) was the only noteworthy instance in the study area (cf. Downes et al., 1999a). Three aftershocks between M4.2 and 4.9 had epicentres in the Ruamāhanga and Waingawa catchments within two months of the mainshock.

As expected, large earthquakes with epicentres within or very close proximity to the study area have generated the greatest ground damage. The 1855 Wairarapa quake is the largest magnitude earthquake in New Zealand's recorded history and generated the largest known maximum terrestrial slip globally (~20 m via high-resolution remote sensing Manighetti et al. (2020); 18.7 m ground investigation Rodgers and Little (2006)). Vertical throw diminished northeasterly from roughly 6 m at Turikarae Head at the to 0.3 m at Mauriceville (~5 km NE of study area) (Grapes and Downes, 1997). The epicentre was shallow (33 km) and approximately 16 km SW of the study area (cf. GNS Science, 2021) and ruptured along at least 140 km of the fault (Grapes and Downes, 1997). Ground damage

was reported over 135,000 km^2, well beyond the Wairarapa region, with the maximum area of severe damage estimated at 52,000 km^2.Though the Wairarapa was very lightly populated, and no bridges or railroads had yet been constructed, widespread ground damage was noted. At least five aftershocks between M 6.5 and 7.0 occurred, with hundreds between M 5.0 and 6.4 over several months following the mainshock (Grapes and Downes, 1997). High-frequency fissuring and cracking was widely distributed, with individual cracks up to 9 feet wide (≤3 m), 15-20 feet (~5-6 m) deep, and hundreds of yards long (Grapes and Downes, 1997; McLaren, 2002). Liquefaction effects including sand/mud volcanoes were observed and ridges up to 2 feet (0.6 m) high formed in some ploughed ground and wet areas. Water emanating from floodplain cracks in the vicinity of the confluence of the Ruamāhanga and Waiohine rivers splashed over adjacent bushes despite being half a mile (~0.8 km) from wither river (Grapes and Downes, 1997). A landslide blocked the Ruamāhanga River roughly 1-2 km upstream of its intersection with the Wairarapa Fault (Grapes, 1988) creating planform displacement toward the west greater than channel alignments shown on prior maps or later aerial photos (1943) (Grapes and Downes, 1997). The Tararuas were in native vegetation cover with almost no human presence, so no direct landslide observation occurred. However, the many landslides noted in the Remutakas (Grapes and Downes, 1997; McLaren, 2002) and shifts in channel morphologies of the Waiohine River over subsequent decades (Stubbe, 1981) suggest that study area catchments likely experienced substantial landsliding.

The Masterton earthquakes of 1942 were the most severe quakes since 1855 and also the most recent strong ground motion within the study area. The three epicentres all occurred below the Wairarapa valley floor on 24-June (M_w 7.2, near Masterton), 1-August (M_w 6.8, near Carterton) and 2-December (M_w 6.0, near Gladstone) at depths of 12, 40, and 20 km, respectively. Through December 1941, eight aftershocks M 3.9 – 5.0 occurred in the Waingawa, Waiohine, and Tauherenikau catchments (cf. GNS Science, 2021). The most extensive and, generally, most intense damage occurred associated with the initial quake in June where the heaviest road damage occurred over a ~4,000 km^2 area with widespread damage to bridges and roads. Bridge damage included sunken approaches included Wardell's (Ruamāhanga R., unspecified magnitude), Kahutara (Ruamāhanga R., 1 m) and Waiohine (0.5 m) bridges (cf. McLaren, 2002). Most roads east and south of Masterton were closed due to landslides and/or cracks with the heaviest road cracking ~15 km east of Greytown (Downes et al., 2001). Landslide damage occurred over about a 6,500 km^2 area (Downes et al., 2001) with the worst near Tauweru where there was much debris noted on the riverbanks from hills that had been 'blown apart' (McLaren, 2002). Overall the heaviest landslide damage occurred in a 60 km long belt along the eastern periphery of the study area from Hinahura to Bideford (Downes et al., 2001; McLaren, 2002). Of greatest significance to study area catchments, rock falls, cracking and subsidence were noted on Remutaka Hill Road and moderate to large slides were noted in greywacke terranes SE of Otaki (Downes et al., 2001). These areas border study catchments to the south and west, respectively, with Otaki located on the opposite side of the Tararuas from Masterton. Given the general inaccessibility of the catchments in 1942, these reports indicate good potential for undocumented coseismic sediment recruitment. Liquefaction effects occurred over 11,500 km^2 and badly affected stopbanks and river banks near Gladstone and Greytown (Downes et al., 2001).

Damage from the August 1942 quake was generally less than the June quake, though local subsidence affected approaches at four of the five major bridges in the Wairarapa (Downes et al., 2001; McLaren, 2002). However, human structures damaged in the June quake did experience extensive damage and landslides were observed to generally occur in areas similar to June as well (Downes et al., 2001). The area of landsliding, cracking and liquefaction was smaller (5,600 km^2), though small landslides were again reported in Otaki Gorge. McLaren (2002) notes that more

damage occurred in the Matarawa vicinity (NW of Greytown) than in the June quake and that both ends of the Waiohine bridge subsided along with fresh road cracks between the bridge and Greytown. Overall, Downes et al. (2001) found observed ground damage correlated well with shaking maps using the Modified Mercalli scale large reconstructed based on damage to human structures.

The Modified Mercalli (MM) scale is a descriptive index for characterising seismic intensity (Wood and Neuman, 1931; Dowrick, 1996) based on felt/observed effect severity (Table 3-7). It is particularly useful for standardising comparisons of earthquake histories and aids reconstruction of pre-instrumentation events from historic accounts. Minor surficial geomorphic expression occurs at MM VI with increasingly significant effects at higher index values. Despite considerable effort documenting historic accounts of broad landscape effects (e.g., Grapes and Downes, 1997; Downes, 2006) and localised case study of one coseismic landslide dam (Grapes, 1988), relatively little work has been done to anticipate future effects on study area rivers. One key exception is Kritikos and Robinson (2014) whose modelling of a M7.4 earthquake on the Wellington Fault suggests 2,000 landslides in the Waiohine catchment alone could occur and deliver 35-40 million m^3 of sediment. This sediment could take a decade to arrive at Greytown with fluvial effects persisting for over a decade (Davies et al., 2014).

Table 3-7. Abridged version of the Modified Mercalli Scale for values MM VI and greater (adapted from Wood and Neuman (1931), Dowrick (1996), and WELA (2003)) with an emphasis on environmental effects.

VI	Generally felt by everyone, many frightened and run outdoors. Furniture moves, objects fall from shelves. Some instances of fallen/cracked plaster. Minor chimney damage. Overall damage slight. Trees and bushes shake or rustle. Loose material may be dislodged from sloping ground (e.g. existing slides, talus).
VII	General alarm, difficult to stand up, noticed by drivers of moving vehicles. Damage negligible to well-designed and constructed buildings. Damage to weak masonry buildings. Small slides and rock-falls. Waters becomes turbid by mud agitation. Small slides along gravel banks and rock-falls from steep slopes. Some settlement of unconsolidated, wet, or weak soils with a few instances of liquefaction (small water and sand ejections).
VIII	General alarm approaching panic. Disturbance to moving vehicles makes sterring difficult. Non-reinforced chimneys/stacks and walls damaged or fall. Heavy furniture overturned. Cracks on steep slopes and wet ground. Small to moderate slides in unreinforced excavations (e.g. roadcuts). Small water and sand ejections related to liquefaction and localised lateral spreading adjacent to water bodies.
IX	Panic. Permanent damage to buildings and structures built before 1970 with. Serious damage to masonry buildings, some destroyed, many partially collapse Some buildings shift off their foundations. Conspicuous ground cracking and breakage of buried, non-ductile pipes. General landslide occurrence on steep slopes. Liquefaction more intense and widespread, with large lateral spreading and flow sliding adjacent to water bodies.
X	General panic. Masonry buildings destroyed, wooden buildings seriously damaged, moderate damage to buildings and structures built after 1970. Some damage to seismically designed buildings (built after 1980). Ground badly cracked. Landsliding very widespread in susceptible terrain with very large rock masses displaced on steep slopes and river banks. Water splashes over banks. Possible formation of landslide dams. Liquefaction effects widespread and severe.
XI	General panic. Few masonry structures remain standing. Partial collapse of buildings and structures built after 1970, minor to moderate damage to seismically designed buildings (built after 1980). Broad fissures in ground. Buried pipelines completely out of service. Soil slumps and landslips common in soft ground.
XII	General panic. Objects thrown up in the air and waves observed on ground surface. Total destruction of most buildings, moderate damage to seismically designed buildings (built after 1980).

Though streams have factored into several studies of active tectonics along the southern and central sections of the Wairarapa Fault, it has been purely at site-scale from the fault's perspective for establishing slip rates (from channel displacement) and/or refining models of terrace deformation (e.g., Rodgers and Little, 2006; Little et al., 2009; Carne et al., 2011). Linkage between the Modified Mercalli and actual physical ground acceleration have been made (e.g. Wald et al., 1999) and provide a foundation for using physics-based models (e.g. Figure 3-11) to predict felt effects (e.g.

Figure 3-12). Current models for 10% in 50-year event predict 0.4-0.6 g (3.9 – 5.9 m/s^2) peak ground acceleration within the study area and place the region within the most intense belt of shaking that correlates roughly with proximity to the plate boundary.

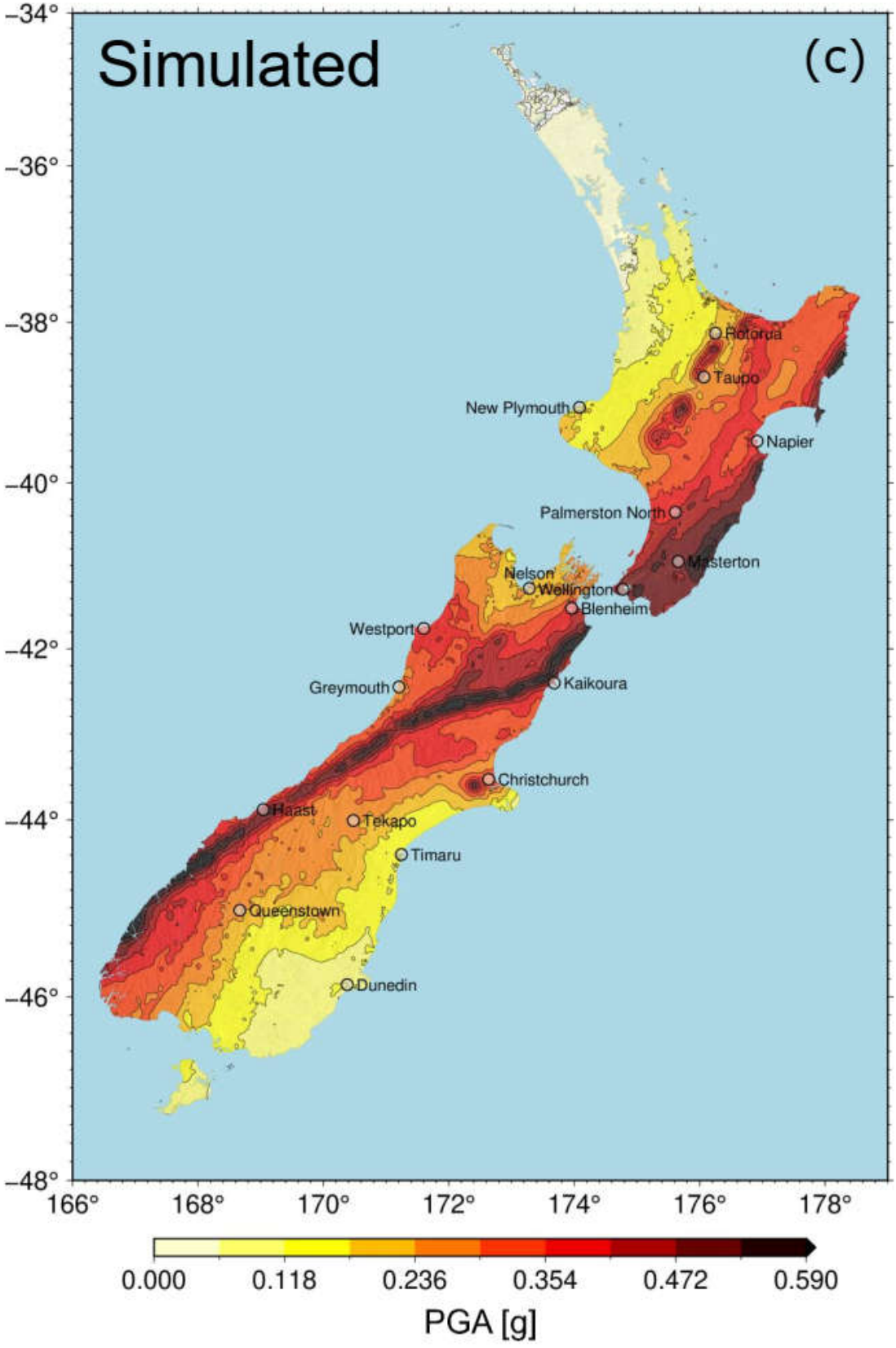

Figure 3-11. Probabilistic (10% in 50-year) seismic hazard for New Zealand (reprinted from Motha et al., 2020).

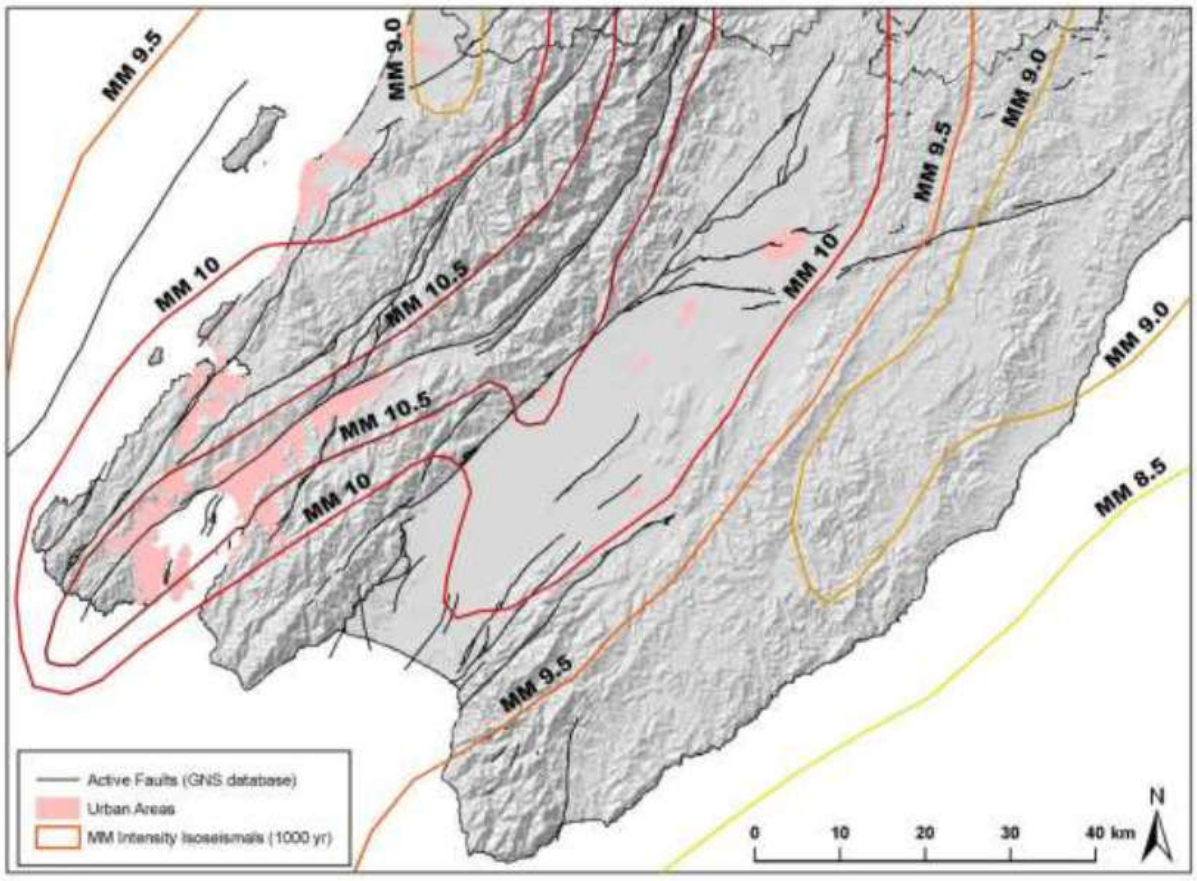

Figure 3-12. Isoseismal (Modified Mercalli) map of a modelled event with 1,000 year recurrence in the Wellington region. Reprinted from Dawe (2007).

Collectively, the 1942 earthquakes were the final two of a series of eight shallow (<45 km) earthquakes ≥ M_s6.9 that occurred in NZ within the prior thirteen years (Downes et al., 2001) in a zone from approximately 350 km southwest to 250 km northeast of the study area (GNS Science, 2021). In terms of seismicity, the study area has been quiescent since, although it has been proposed that a landslide discovered in March 2017 which created a small pond on the Tauherenikau River may have been related to the November 2016 Kaikoura earthquake (Hendery, 2017). The seismic signal of the Kaikoura earthquake propagated from south-to-north so would have diminished into the study area with minimal landsliding expected. Nonetheless, given the Wairarapa's tectonic setting, it is certain that study area rivers and catchments will experience coseismic effects (displacement and sedimentary) again. Because an area can experience shaking-induced ground damage from an earthquake originating outside of that area, recurrence of geomorphically-significant shaking is more frequent than local rupturing. It is estimated the Wellington Region experiences very strong to extreme shaking approximately once every 150 years (GNS Science, 2017).

Despite considerable effort documenting historic accounts of broad landscape effects (e.g. Grapes and Downes, 1997; Downes, 2006) and localised case study of one coseismic landslide dam (Grapes, 1988), relatively little work has been done to anticipate future effects on study area rivers. One key exception is Kritikos and Robinson (2014) whose modelling of a M7.4 earthquake on the Wellington Fault suggests 2,000 landslides in the Waiohine catchment alone could occur and deliver 35-40 million m^3 of sediment. This sediment could take a decade to arrive at Greytown with fluvial effects persisting for over a decade (Davies et al., 2014). Though streams have factored into several studies of active tectonics along the southern and central sections of the Wairarapa Fault, it has been purely

at site-scale from the fault's perspective for establishing slip rates (from channel displacement) and/or refining models of terrace deformation (e.g. Rodgers and Little, 2006; Little et al., 2009; Carne et al., 2011).

3.6 Morphotectonic forcing of rivers

The traditional view of the study area's landscape morphology is reflected by Kamp (1992, p. 374-375), specifically:

> *"To the west of the Ruamahanga River, younger and undeformed, large coalescing gravel fans have been constructed by the Tauherenikau, Waiohine, and Waingawa Rivers. The outward and upward growth of these has forced the Ruamahanga River against the hilly topography of the older, now deformed fans* [on the eastern valley margin]*."*

Subsequent work recognised some generic deformation (Lee and Begg, 2002), particularly in proximity to the major named faults (Zachariasen et al., 2000; Begg et al., 2001). However, at the outset of my research, there was generally little awareness of the degree, extent, or persistence of tectonic control on water courses in the study area.

While I concur with the inference of coalescing fans, there is abundant field and DEM-based evidence of significant deformation of the younger fans along the western valley margin (Figure 3-13 and Figure 3-14). There is also reason to suspect that relative subsidence of the Ruamāhanga River valley segment upstream of the Waiohine confluence and inclusive of the lower Taueru River control mid-scale base level may encourage tributary alignments and persistent fan growth toward the eastern margin of the study area. Considering the extensiveness and variety of landscape-scale tectonic deformation (Figure 3-13, Figure 3-14, Figure 3-15), exploration of controls on fluvial processes at more refined scales was warranted.

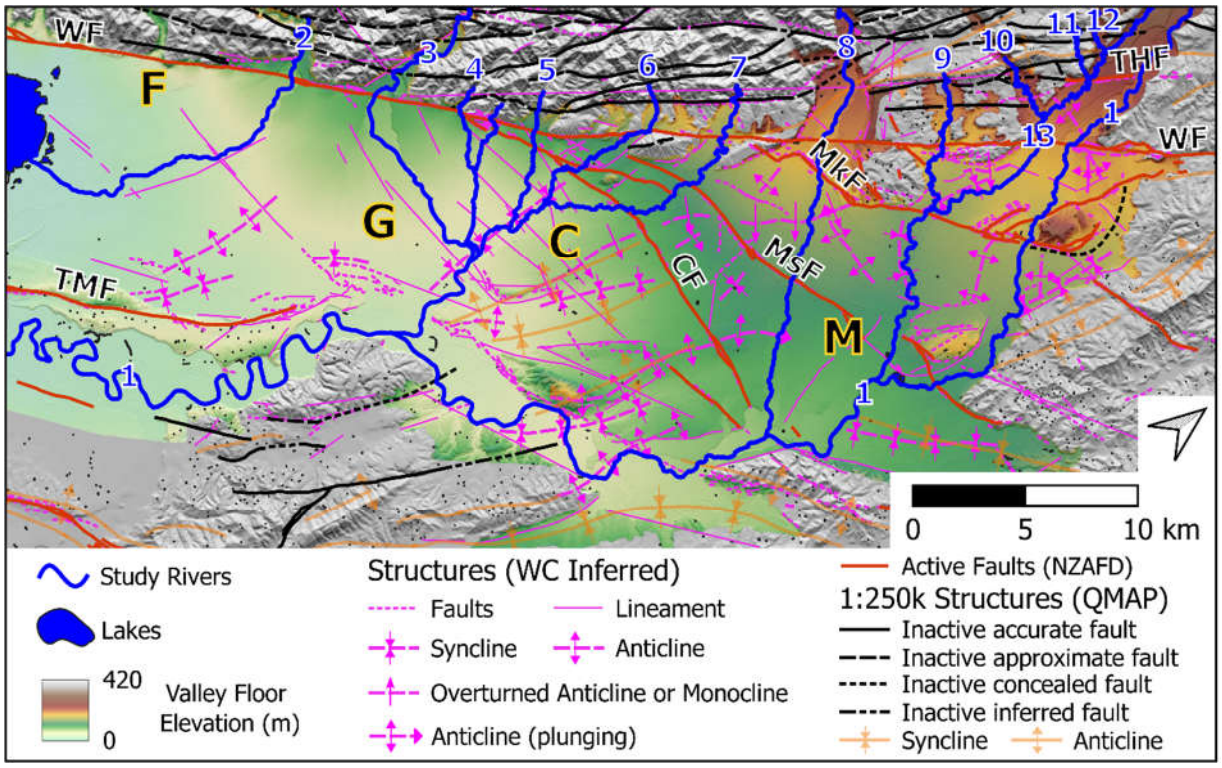

Figure 3-13. Colorshade of Ruamāhanga valley floor with emphasising geologic structures and lineaments (GNS Science and LiDAR interpretation by author) deforming Quaternary alluvium units. Even at this coarse

scale of presentation (~1:300,000), my interpretation of LiDAR terrain suggests a much greater degree of deformation than previously recognised. Rivers: 1 - Ruamāhanga River, 2 - Tauherenikau River, 3 - Waiohine River, 4 - Beef Creek, 5 – Kaipaitangata Creek, 6 – Enaki Stream, 7 – Mangatarere Stream, 8 – Waingawa River, 9 – Wakamoekau Creek, 10 – Mikimiki Stream, 11 - Kiriwhakapapa Stream, 12 – Te Mara Stream, 13 – Waipōua River; Faults: WF – Wairarapa Fault, WeF – Wellington Fault, CF =- Carterton Fault, MsF – Masterton Fault, MkF – Mokonui Fault, THF – Te Hau Fault, TMF - Te Maire Fault; Towns: F – Featherston, G – Greytown, C – Carterton, M – Masterton.

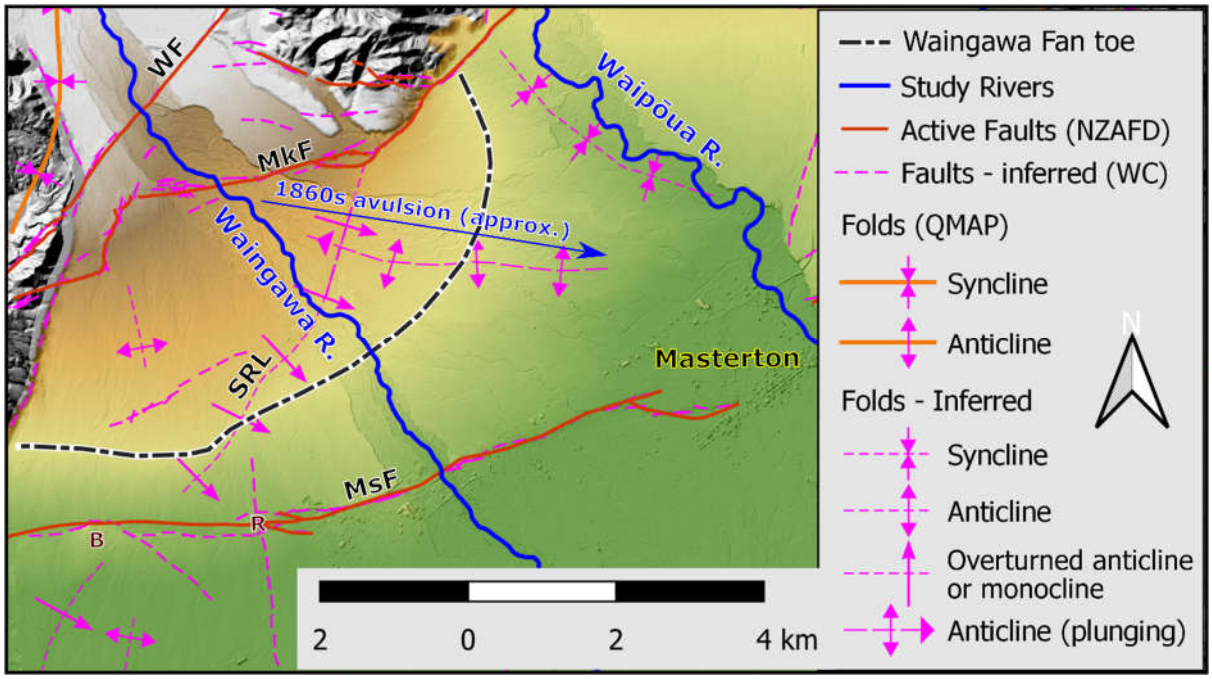

Figure 3-14. Tectonic deformation of the Waingawa River's alluvial fan (after Conley, 2017). WF – Wairarapa Fault, MkF – Mokonui Fault, MsF – Masterton Fault, SRL – Skeets Road Lineament. The study area's major faults (e.g., WF, MkF, and MSf) exhibit segmentation with throw reversals (e.g., 'R') and bulges (e.g., 'B') frequent at intersections with other faults and uplifted folds, respectively. The SRL is a subtle topographic feature and interpreted as a fold (monocline or overturned anticline, perhaps) with possible surface rupture near the intersection with an inferred anticline (vicinity of Skeets Road and West Manaia Road intersection). The diversion point for the late-1860s avulsion of the Waingawa River into the Waipōua River occurred between MkF and SRL and caused significant flooding in Masterton. While fan deposits of the Waingawa River occur over a broader area, the toe delineated in this figure appears to have a fairly continuous topographic break with delineation of the left-half aided by the location of sapping heads where shallow groundwater becomes expressed in channels.

3.6.1 Prior work in the Ruamāhanga catchment

Surficial materials of the basin's valley floor are largely late-Pleistocene and Holocene alluvial gravels exported from the Tararuas and deposited into coalescing fans by the main study area rivers (Grapes, 1991; Kamp, 1992; Begg and Johnston, 2000). While alluvial sediment dynamics are a focal point of river management concerns, there has only been very generic mention of the roles of major faults regarding channel gradient and alignment (e.g. Williams, 1990; Stojmirovic, 1998; Williams, 2010). Recognition by Williams (1990) of the proximity of a major palaeo-belt bifurcation of the Waingawa River near the Mokonui Fault is the only report to suggest potential linkage, though without mechanism or process.

Site-scale changes of sequential ruptures along the southern section of the Wairarapa Fault have translocated low-order streams channel outlets from the Remutaka range-front and beheaded

valley-floor channels (Rodgers and Little, 2006) approximately 20 km south of the study area. Multiple site-scale investigations have occurred at the intersection of the central Wairarapa Fault and Waiohine River (Lensen and Vella, 1971; Carne et al., 2011) using terrace displacements to infer slip rates and refine models of tectonic terrace abandonment.

Riverscape-scale fluviotectonic work has been conducted along the Huangarua River, a tributary of the Ruamāhanga River approximately 10 km south of the study area by Formento-Trigilio et al. (2003). They found significant terrace deformation with shifts in the locus of fold growth through time and rates during the Holocene roughly double than those between 10 and 80 ka. They also found five periods of terrace cutting separated by 5 to 65 ka intervals. All cutting episodes were independent of tectonic deformation and base level lowering and they concluded that sediment influxes associated with recurrent climate shifts was the main driver. Their model, where sediment supply exceeded transport capacity through valleys during cooler glacial periods is generally consistent with other models, particularly that prevailing alluvial surfaces of the Wairarapa valley floor in the study area are aggradation surfaces with inset contemporary river belts cut during the Holocene (cf. Vella, 1963b; Kamp, 1992).

3.6.2 Exploratory data analysis

My initial, exploratory analysis of high resolution topographic data identified substantial spatial correlation between transitional fluvial signatures and geologic structures (published by others and those I've inferred) suggesting widespread tectonic control at multiple scales (Conley et al., 2017a; Conley et al., 2017b). I present examples of my findings here as background and descriptive context for later chapters, particularly Chapters 5 and 6.

3.6.2.1 Landscape scale

Aside from the noted fan deformation (Figure 3-13 and Figure 3-14), widespread signatures of misfit valleys and palaeochannel belts provide further evidence of tectonic control. These tend to cluster in proximity of the distal zones of major splay faults within the valley. Thrusting oblique to the prevailing valley alignment and segmentation of transpressional faults create particularly complex local relief in these areas. One such area is northeastern portion of the study area between the Wairarapa and Mokonui faults where the Kopuaranga, Ruamāhanga, and Waipōua rivers flow (Figure 3-15 and Figure 3-16, left). Notably, the contemporary Ruamāhanga River has the largest drainage area (113 km^2) and experiences the greatest discharges (GWRC data) but occupies the narrowest valley of the three rivers that cross the axis on the Mokonui Fault. The most striking contrast is with the Waipōua River (86 km^2) which has 31% less drainage area, but a substantially wider valley and active floodplain (Figure 3-17, particularly cross-sections C-C' and C-C'').

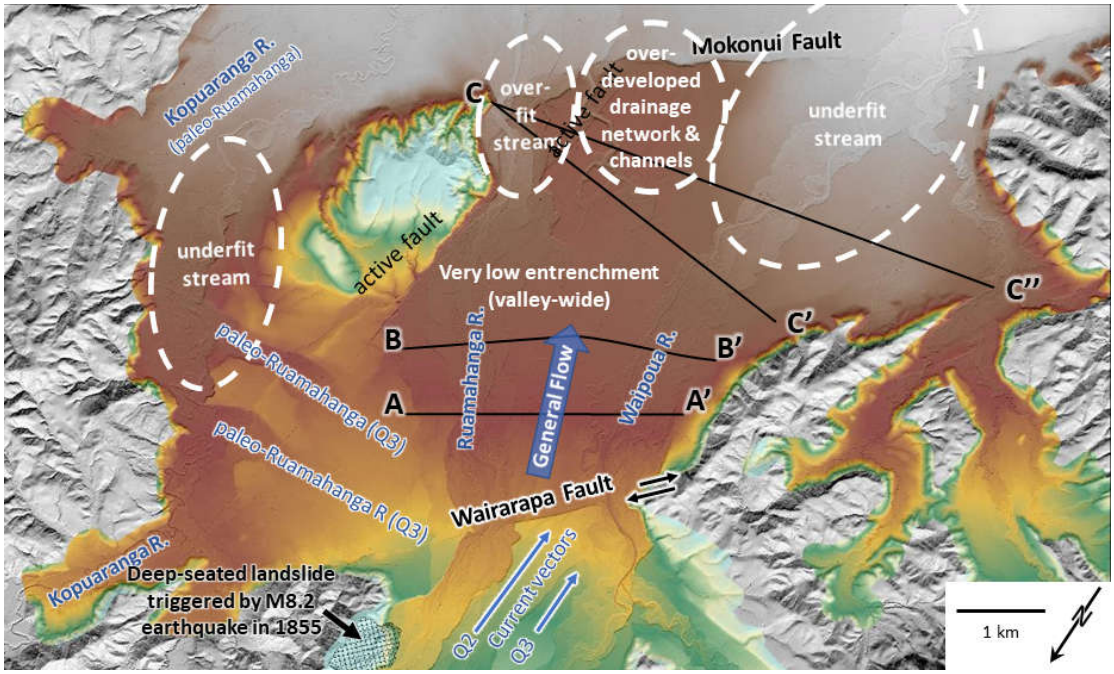

Figure 3-15. Example of valley forms out-of-phase with modern fluvial processes and driving forces. Named/active faults and palaeochannel ages per NZAFDB (GNS Science, 2020) and QMAP (Lee and Begg, 2002), respectively (reprinted from Conley, 2017a). Valley cross-sections are presented in Figure 3-17.

Palaeochannel alignments exist in this same valley segment that diverge wildly from contemporary courses. Most notable are two cuts near the eastern margin that join the contemporary Kopuaranga floodplain (Figure 3-15, near 'A') from the west within a larger geologic unit mapped as Q3 (24-59 ka, Lee and Begg, 2002). Given their presence along an uplifted boundary, their width corresponds roughly to that of the contemporary Ruamāhanga where it crosses the Mokonui Fault. However, their planimetric alignment diverge at roughly 90-degrees to A) inferred current vectors on Q2 (12-24 ka, Lee and Begg, 2002) and Q3 terraces upstream of the Wairarapa Fault and B) contemporary alignments of the Ruamāhanga and Waipōua rivers (Figure 3-15). The cupped form of the Q2 inset terrace (~ STA 50-400) in cross-section A-A' (Figure 3-17), suggests that abandonment was potentially rapid.

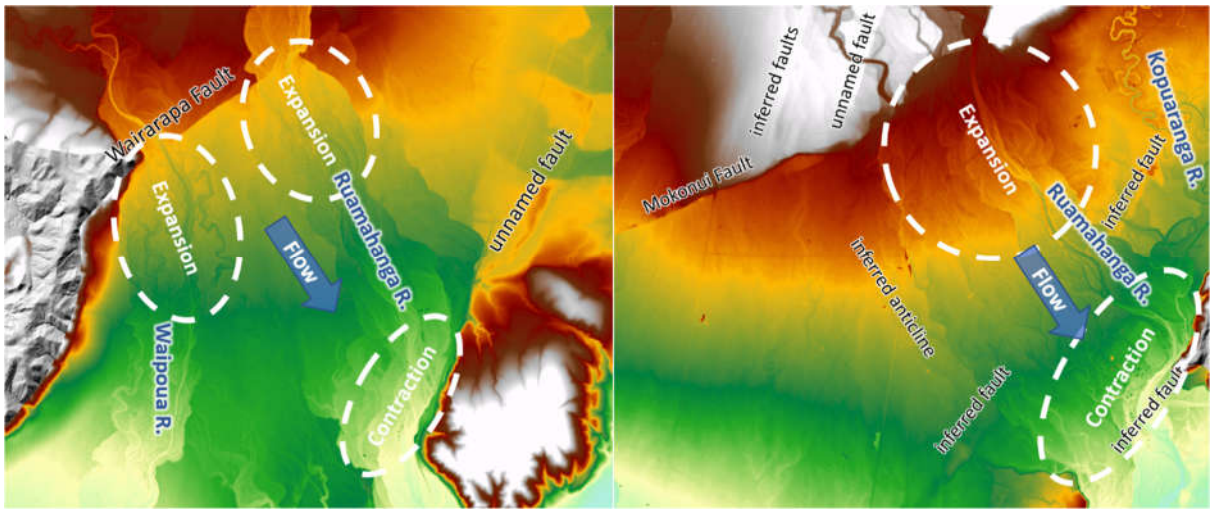

Figure 3-16. Uplifted zones, particularly along the major active faults, promote incision and relative confinement for the alluvial rivers. Fluvial sculpting suggests the gravel bed rivers tend to be most laterally active in expansion zones downstrean of these structural nozzles and at the upsptream end of contraction zones where increased width and backwater effects (respectively) reduce sediment transport capacity. Left: Expansion and contraction process zones on the Ruamāhanga River between the Wairarapa and Mokonui faults. The Waipōua River also has an expansion zone downstream of the Wairapa Fault, but with different channel forms related to lithology and sediment character. Right: Expansion and contraction zones of the Ruamāhanga River repeat (downstream of left panel) at the Mokonui fault and an inferred fault that bounds the Kopuaranga valley and adjacent hills (after Conley, 2017a).

3.6.2.2 Riverscape scale

Review of profiles extracted from the 1 m regional DEM (GWRC data) reveals numerous convexities and concavities (Figure 3-18). The lack of correlation of such inflections with tributary confluences implicates extrinsic control such as tectonic deformation, evidence of which exists in partial spatial correlation with intersections of active faults. However, there are at least as many inflections that do not correlate to active faults (Figure 3-18) suggesting other active tectonic structures or persistent long-term tectonic (LTT) control. I inferred a substantial number of faults, folds, and lineaments during a fine-scale (1:1,000) interrogation of the 1 m DEM and derivative models (e.g., rDEMs, see Chapter 5). When the intersections of these probable structures are projected onto river profiles, an even richer case for tectonic control develops (Figure 3-19).

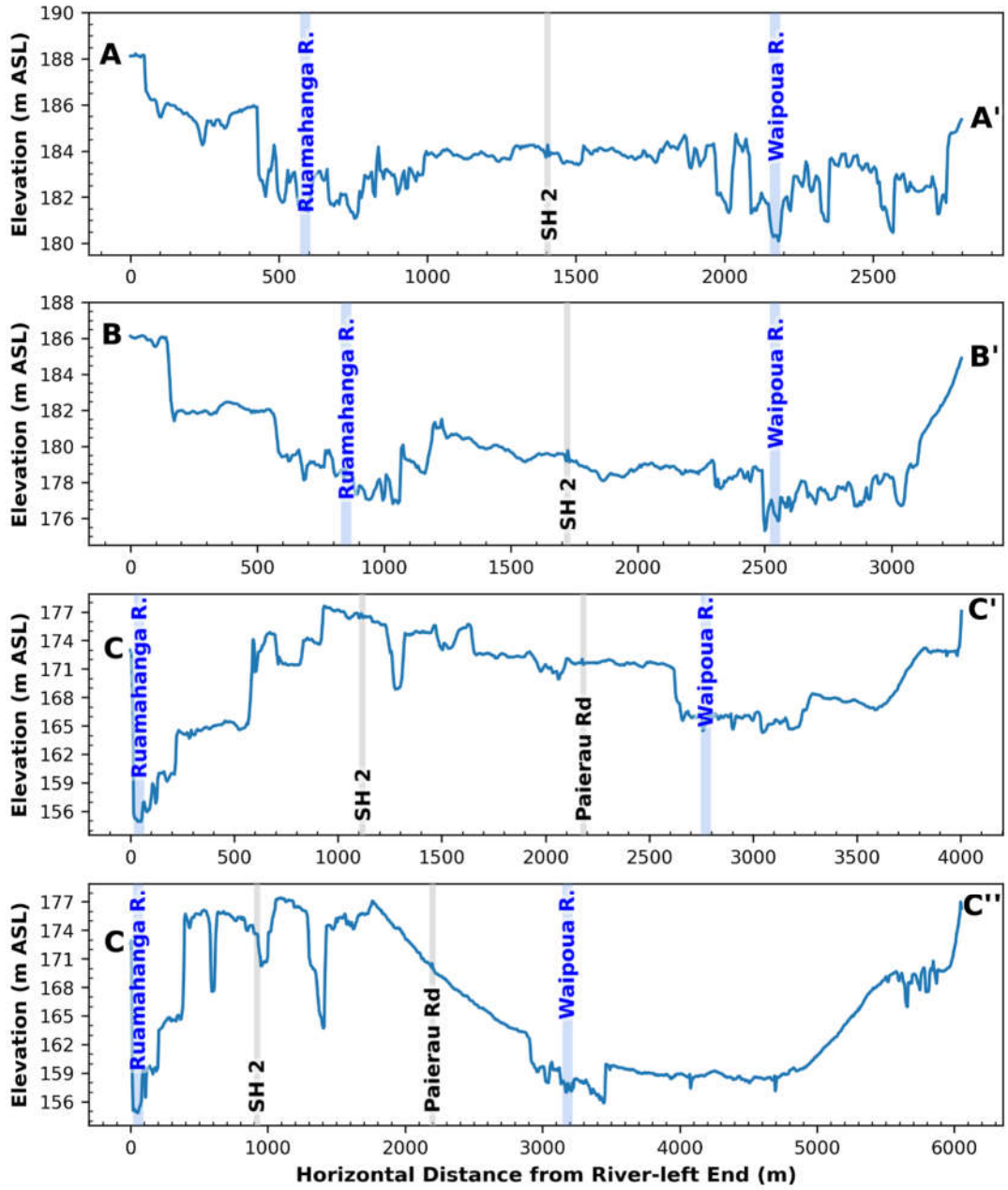

Figure 3-17. Valley cross-sections across the upper Ruamāhanga and Waipōua rivers between the Wairarapa and Mokonui faults. A-A' and B-B': Cross-sections approximately 0.9 and 1.6 km downstream of the Wairarapa Fault, respectively, suggest, multiple palaeoalignments with distinct interfluves suggest rapid abandonment (avulsion). C-C' and C-C'': Differential tectonic forcing produces mis-fit valleys for the Ruamāhanga (113 km2 drainage area) and Waipōua (86 km2 drainage area) rivers. C-C' Section is perpendicular to an axis of inferred back-tilt; back-tilted zone from approximately STA 900 to STA 2100. C-C'' Section is roughly perpendicular to axis of inferred syncline (or, possibly, half-graben); note curved projection of terraces adjacent to the Waipōua River and that channel is off-centre (to left) from probable fold axis and oblique to back-tilt axis. Contemporary channel belt location of the Waipōua River is likely a matter of superposition on an antecedent topographic low and long-term clock-wise rotation (relative to down-valley view). Ongoing rotation creates long-term forcing of the right channel margin and precondition for possible avulsion. Review of archival aerial imagery indicates river management activities re-trained to the location shown from prior migration to the low position (~STA 3450).

Looking across the five profiles, a couple of landscape-scale trends emerge: 1) profiles have more gradient inflections as one moves north (top-to-bottom in Figure 3-19) and 2) intersections of the

major active faults seem to correlate with profile concavities rather than convexities. The presence of more graded profiles toward the south reflects greater proportional alluvial influence which may be related to one or more of: A) concentration of vertical deformation along fewer structures, B) greater unit production of clastic sediment by southern catchments, C) closer proximity of greywacke terrains to the mountain front, D) greater distance from the head of Wairarapa Fault propagation (i.e., longer response and/or relaxation times for southern rivers). Greater stream power likely contributes to lower profile complexity for the Waiohine River. By contrast, the river with the lowest stream power (Waipōua) appears to be the most strongly tectonically-controlled.

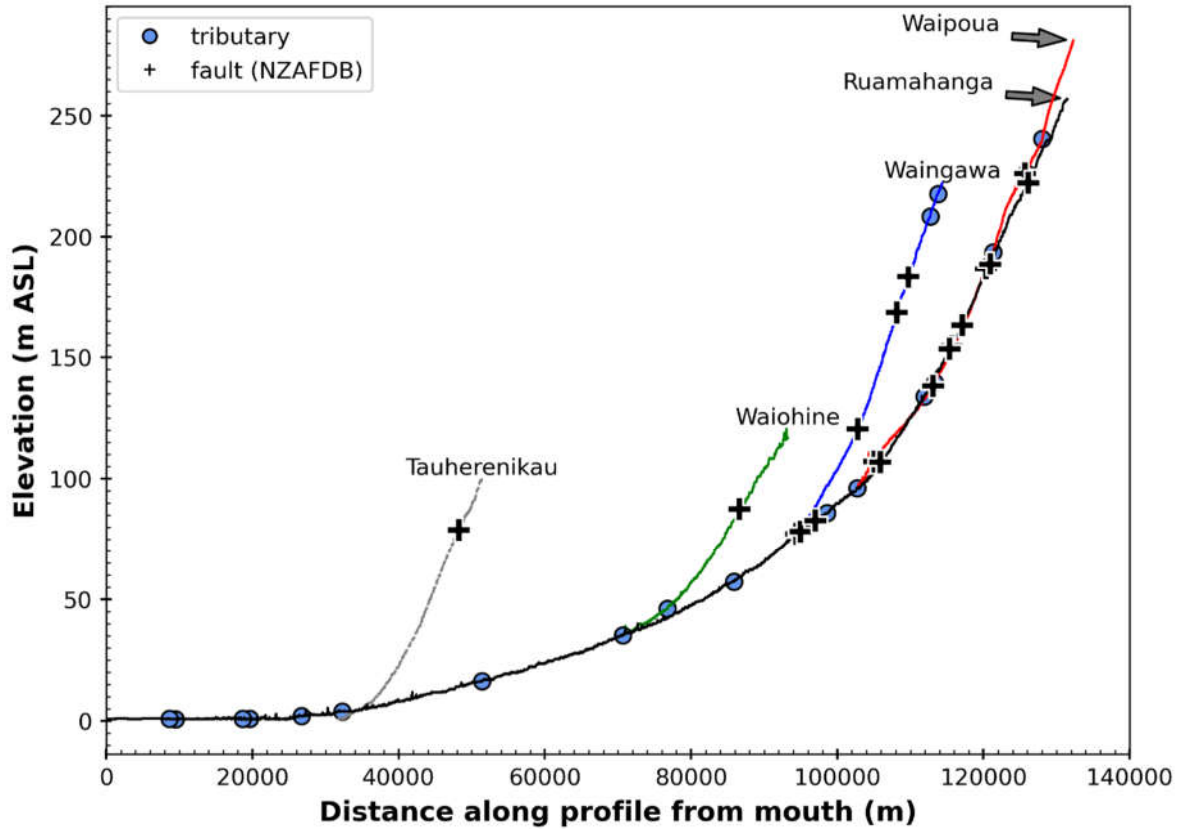

Figure 3-18. Channel profiles of the five large rivers draining the east flank of the Tararuas to the Wairarapa valley. Few tributary junctions correlate with profile inflections. Active fault intersections co-occur with some but not all inflections. More detailed profiles are presented individually in Figure 3-19. The Tauherenikau River drains directly to Lake Wairarapa which drains to the Ruamāhanga approximately 9 km from the ocean.

While discussing the details of each profile inflection is beyond my scope here, there are several key locations worth specifically noting. The most prominent profile irregularity (a convexity) in proximity of the Wairarapa Fault occurs along the Tauherenikau River (Figure 3-19, top). Specific to the Tauherenikau River though, an inferred range-front fault ~STA 17,500 occurs closer to the inflection and, in combination with an unnamed fault (~STA 18,500) is associated with a sigmoidal sub-profile in proximity to the fan head. On the Waiohine River, the convexity in the vicinity of STA 18,500 is at a transition in hydraulic confinement that co-occurs in proximity of several inferred faults. The prominent concavity of the Waiohine River (Figure 3-19, second row) is at the distal end of the contemporary (telescoping) alluvial fan where river enters an inferred synclinal axis at approximately STA 6,000.

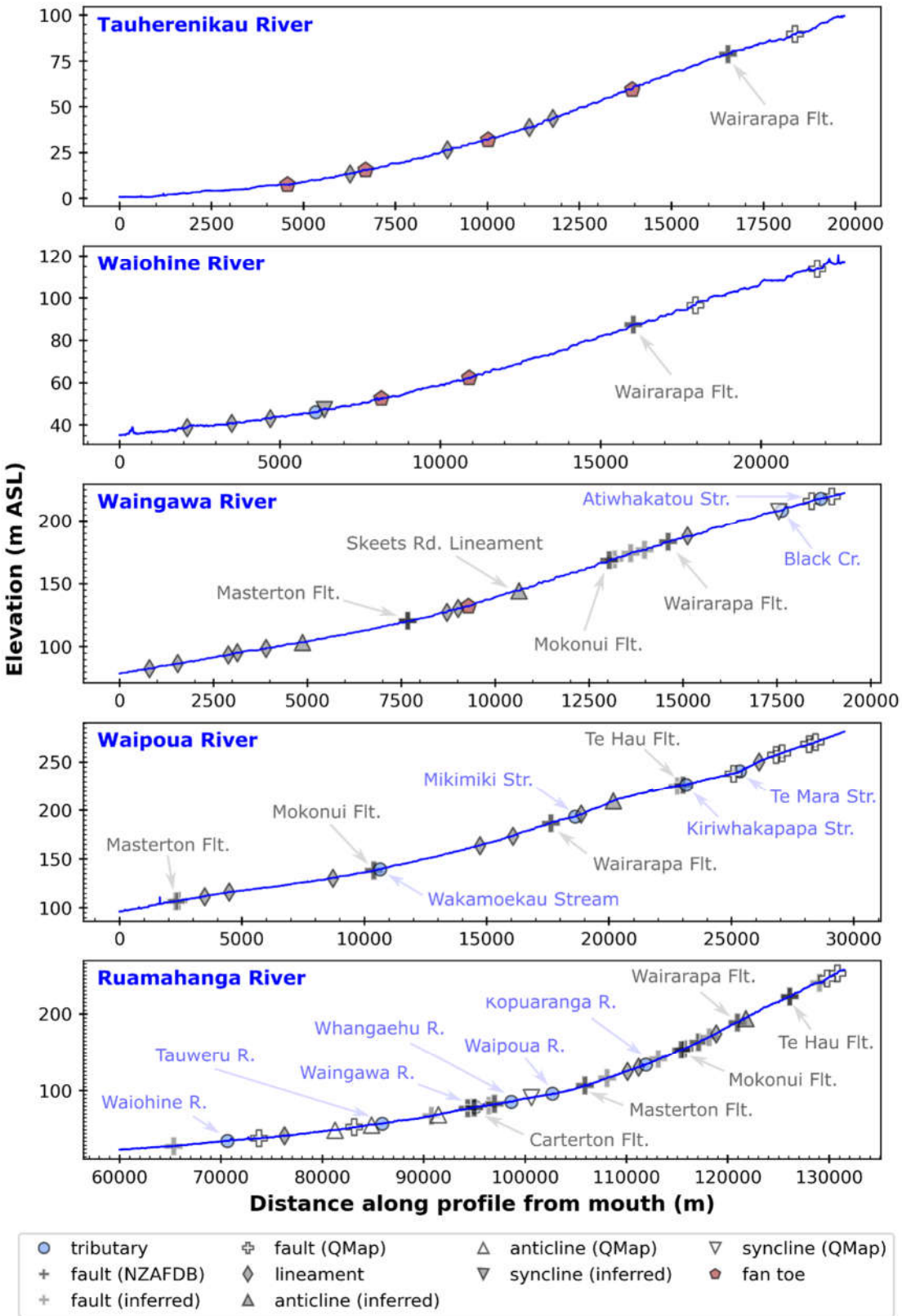

Figure 3-19. Individual profiles for each of the major rivers in the study area. Top-to-bottom ordering of subplots reflects south-to-north order in which each river crosses the Wairarapa Fault. Points indicate tributary confluences, intersections with geologic structures, and approximate location of distil margins of alluvial fans (where present). Multiple fan points on a stream indicate proximity of prevailing, inset, and/or telescoping fan toes. NZAFDB markers indicate faults officially considered "active" based on published palaeoseismic field investigation.

The Waingawa River (Figure 3-19, middle) has a pronounced concavity at approximately STA 8,200, upstream of the Masterton Fault. The highly faulted zone between the Mokonui and Wairarapa faults co-occurs with the main profile convexity along the Waingawa River. The Waipōua River (Figure 3-19, second from bottom) has the most irregular profile of the five rivers with the most pronounced convexities occurring at inferred structures/lineaments between STA 2,500 and 4,500 (immediately upstream of Masterton) and approximately STA 20,000 in the vicinity of an inferred anticline. Notable Waipōua River concavities occur in vicinity of the Mokonui Fault where the river enters and aligns with an inferred syncline and at an unnamed fault near the Te Mara stream confluence.

By virtue of its status as the trunk river, the greater length of the Ruamāhanga River mutes profile expression on a single subplot (Figure 3-19, bottom). However, major concavities occur in proximity of the Masterton and Mokonui faults. Fluvial entrenchment occurring where the Ruamāhanga cuts along/through thrusting of the respective fault blocks provides a degree of natural 'training' of river position by comparison to the broad, alluvial wanderings immediately upstream of each. Convexities occur at an anticline I field-confirmed immediately upstream of the Wairarapa Fault and where the Carterton Fault / Waingawa River converge. The reach downstream (STA 91,000 to 95,000) of the latter is particularly notable for the apparent interplay of tectonic and fluvial control and marks, in my opinion a key location in fluvial processes in the catchment. The profile steepens where the southeastern trace of the Carterton Fault crosses downstream to a fault I've inferred near STA 91,000 at which point the Ruamāhanga River enters a valley segment that appears to be experiencing relative subsidence. Though further enquiry is beyond the scope of this thesis, this is a key location for understanding catchment-scale controls.

3.6.2.3 Local / reach scale

Signs of tectonic forcing also manifest at refined scales. My exploration of a 1 m LiDAR-derived elevation model indicates active faults (particularly the Carterton, Masterton, and Northern section of the Wairarapa Fault) crossed by the Waingawa River exhibit segmentation features including overlapping step-overs, bulges and rents within similarly narrow bands (~350 m) similar to those in the Central section of the Wairarapa Fault documented by Carne and Little (2012). Given this, major structures may be better considered as zones rather than discrete lines. The topographic complexity of these zones, coupled with varied horizontal and vertical displacements, contributes to highly complex channel and floodplain forms (Figure 3-20). Though largely alluvial in nature over shorter time periods, their broader form is not alluvial in the self-organised sense. Thus, temporal variations in control mechanisms and spatial variation along the profile mean these reaches should be expected to behave in highly non-linear fashion.

In summary, fluviotectonic relationships have been poorly documented, but have promise for assisting understanding river dynamics in the study area. Geologic structures appear to be influential on the Ruamāhanga catchment's gravel bed rivers at all scales examined. The notion that fans along the Tararua range front are undeformed should be discarded. There appears to be a gradient along the Wairarapa Fault at which the relative contributions fluvial and tectonic processes shift with increasing tectonic influence to the north (toward the head of Wairarapa Fault propagation). Given the plate setting, influence on river profiles, and deformation of active floodplain surfaces, it seems highly likely that many of the inferred structures are active, though not yet properly documented as such.

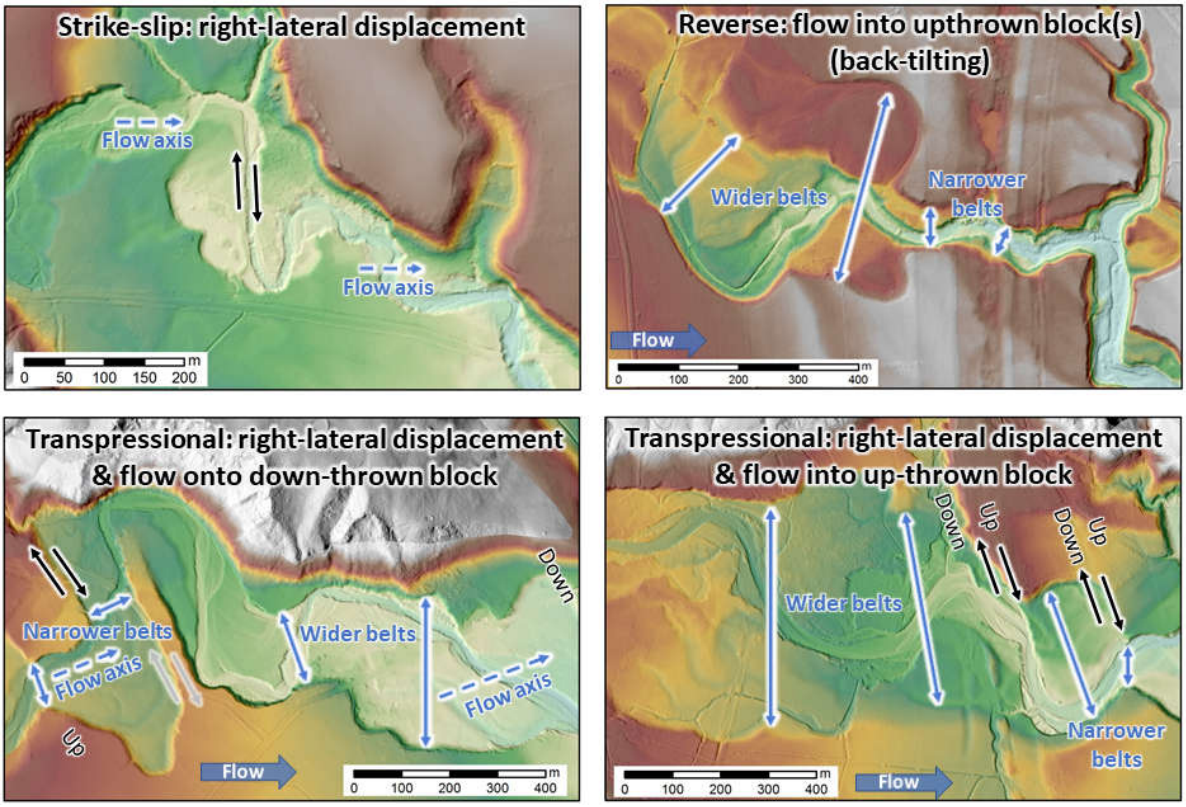

Figure 3-20. Examples of reach-scale tectonic forcing. In addition to channel offsets, degree of terrace re-working can indicate local slope adjustment to inform deformation trend. Inferred tectonic deformation is noted at the top of each panel (from Conley et al., 2017b).

3.7 Management Context

The study area is within the jurisdiction of the Greater Wellington Regional Council (GWRC) which has statutory responsibility to protect people, property, infrastructure, and productive rural lands. The study area encompasses portions of three District Councils (Masterton, Carterton, and South Wairarapa) and three of the five major human population centres. Collectively, Masterton Carterton, and Greytown all experience varying degrees of flooding and are home to approximately about 85% of the total urban population (30,000 people) within the three districts.

Prior to human occupation most of the Wellington Region from sea to upper treeline was forested (Singers et al., 2018). Characterisation of historic accounts suggests 17th century fires initiated a major conversion of cover type (cf. Stewart, 2014). A patchwork-style landscape of grasslands, swamps, forest and scrub is described in archival accounts at the onset of European settlement in 1843, with denser bush extending to the valley floor on the periphery of the ranges (Hill, 1963). At the same time lands along the Ruamāhanga River were in dense bush often fringed by swamp (Hill, 1963). The onset of European settlement in 1840 initiated even more intense and geographically extensive land clearance that persists today.

Presently, land-use surrounding study area rivers is typically agricultural with increasing subdivision for rural lifestyle residences. A mid-1990s report on the nearby Ruamāhanga River notes an "emphasis on farming all available land to the river edge, leaving no margin for natural river erosion/accretion processes" (Heslop, 1996, p. 2) and a general intolerance of even minor amounts of erosion. Around the same time a unification of flood protection areas under a common *scheme*

funded by rate payers and managed by GWRC brought a coordination for over 130 km (collectively) of managed channels under a single entity.

3.7.1 River Management

The three main forms of direct anthropogenic river manipulation in the Ruamāhanga catchment are water abstraction, gravel extraction and river-training. Water abstraction from surface water and tributary groundwater occurs throughout the study area and is mainly used for irrigation of crops/paddocks, stock water races, and municipal supply. More information related to abstraction in the Ruamāhanga catchment can be found in Royal (2011), Keenan (2012), and Bunny et al. (2014). Latent effects are expected to mainly impact low-flow hydroperiod and related ecology (including plant dynamics) though further consideration of abstraction effects is beyond the scope of this thesis.

Gravel extraction from active channels is and has been used to increase channel capacity and has occurred in all major gravel bed rivers in the study area (Figure 3-21). The annual volume of gravel extracted from study area rivers peaked in the 1980s and has generally been decreasing for roughly 25 years (GWRC data). Reduction was initiated as bed degradation effects were observed and concern grew regarding stability of bridge foundations and stopbanks. Historically annual gravel extraction volumes were reported in bulk by river (Williams, 2000; Williams, 2010; Harley, 2014), but record-keeping since 2001 facilitates more localised analysis (Figure 3-21). Gravel extraction is also discussed in river management scheme reviews (e.g., Williams, 1990; Heslop, 1993; Williams, 2010b, 2010a) and as a component of river sediment budget calculations (Christensen, 2013a).

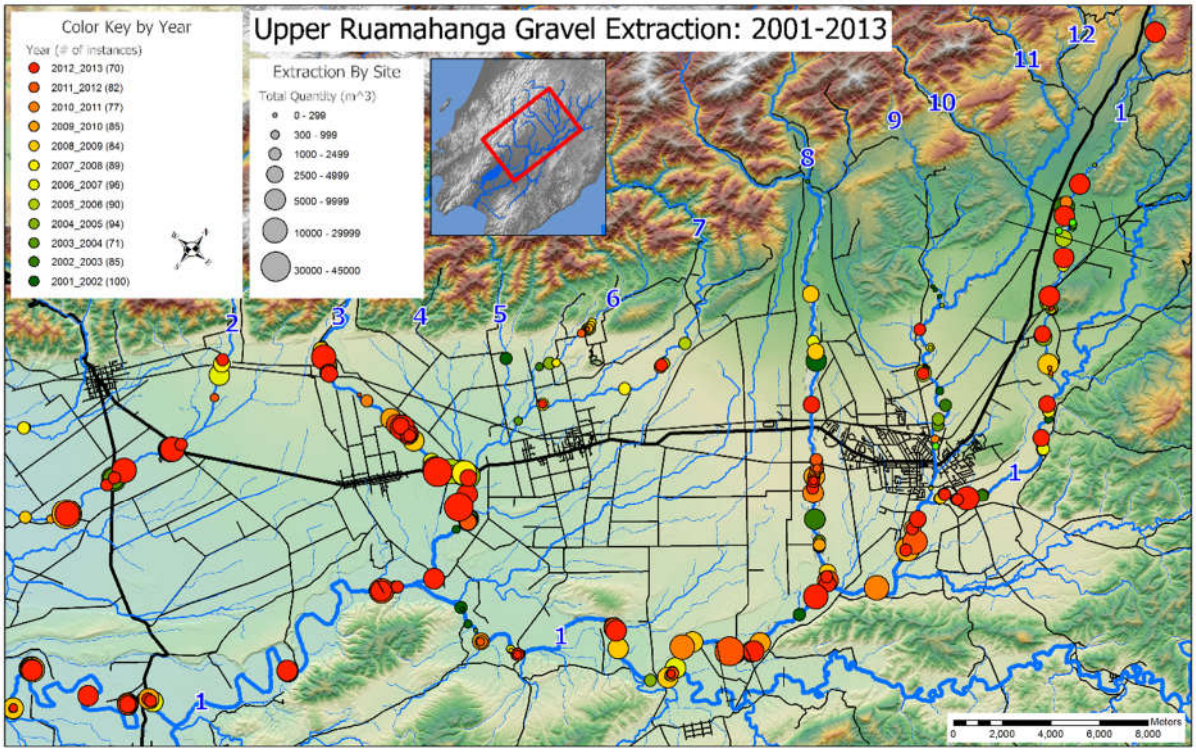

Figure 3-21. Gravel extraction volume by site and year 2001-2013 (GWRC data).

To date, sediment budgeting exercises in the catchment have taken an end-area approach based on benchmarked cross-sections. However, the coarse nature of cross-sections in space (hundreds of metres apart) and time (three to seven year re-survey intervals) precludes much morphodynamic insight given high frequency of motion and the diversity of effects that gravel extraction is known to

cause (Kondolf, 1997b; Wishart et al., 2008; Zawiejska et al., 2015; Sims and Rutherfurd, 2017). The draft flood protection management plan for the upper Ruamāhanga (Allan, 2014; Allan and Girvan, 2015) notes interest in adaptive management and monitoring effects of gravel extraction. However, the spatiotemporal resolution of data reviewed for this thesis were not fit-for-purpose in this regard and no specific outline is discussed in the plan. This is a key need and Chapter 7 provides insight to mobilisation thresholds and geomorphic effectiveness.

While there should be little doubt that water abstraction and gravel extraction affect dynamics of study area rivers, many hundreds of hours of aerial photo review and many more hundreds of hours in the field, indicated all gravel-bed reaches within management schemes in the study area are influenced by physical human modification. In terms of anthropogenic influence, this thesis focuses on the latter given no prior work has been done to characterise or unwind the morphodynamic effects direct physical alteration by humans in the study area. Interestingly, the term 'natural' occurs frequently in reports to describe study area channels. While the vast majority of channel boundaries are composed of natural materials (e.g., rocks and plants), I found no evidence of any reaches behaving naturally (i.e., as it would be expected without recent or historic physical manipulation) in terms of geomorphic processes. Thus, I make effort to generally refrain from using the value-laden term in this thesis.

GWRC's primary aim for study area rivers is to, "establish a stable channel alignment through the adoption of design channel fairways with vegetative buffer on either side of the river" (Harley, 2014). Since the early- to mid-1990s, rivers have been managed using a *fairway* strategy to achieve this aim (Figure 3-22). This strategy involves an inner planform zone ("fairway") which is actively managed for low hydraulic resistance. An outer, vegetated "buffer", zone borders both sides of the fairway. Planimetric fairway boundaries are delineated by professional opinion informed by a mix of qualitative aerial photo review, benchmarked cross-sections, and regime equations. During the study, physical manipulations of channel form, location, and floodplain vegetation (e.g., groynes, channel 'blocks', cross-blading, and bar scraping) were observed to "train" the river within the fairway. Willow plantings are commonly used to reinforce rock barbs/groynes composed of native alluvium on the margins as well as roughened secondary channels outside the fairway. Within the fairway, vegetation is maintained in an early seral state with blading of floodplain vegetation occurring approximately annually. Periodic local realignments are performed mechanically, often with the use of cross-blading.

3.8 Need / Thesis Relevance

In their catchment-scale review, Dykes et al. (2015) identified four general research themes for the Ruamāhanga: 1) sediment supply, 2) Holocene river response to changes in climate and sediment supply, 3) contemporary river response and the impacts of anthropogenic activities, and 4) future river response to changes in climate and sediment supplies. These themes all centre on recognition that interaction between sediment and flow regimes is the central driver of river morphology (Brierley and Fryirs, 2005) and understanding the influence of external (e.g. land-use change, climate change) and internal (e.g., internal morphodynamics) controls provides more robust understanding of historic and future river response in the Ruamāhanga catchment.

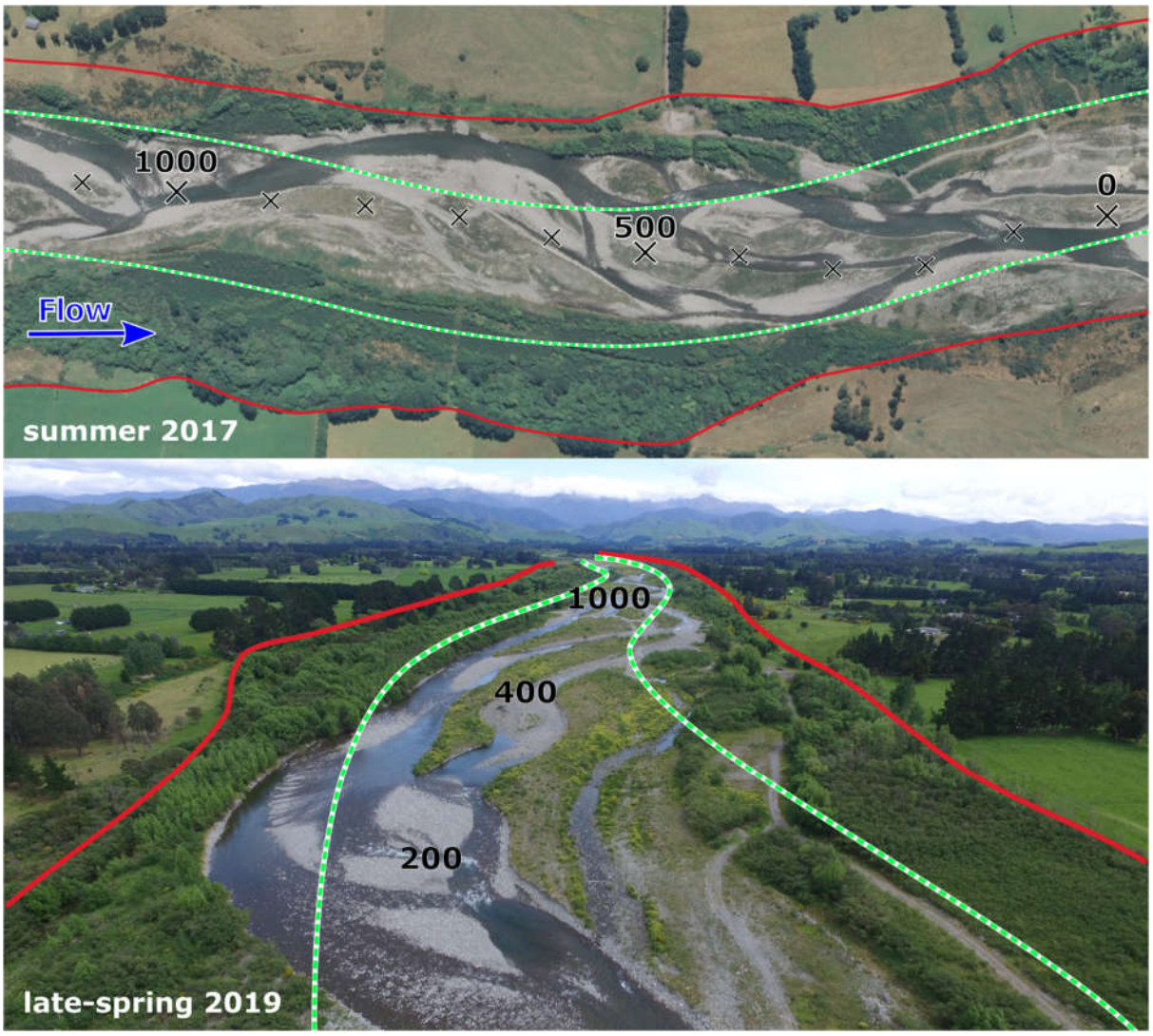

Figure 3-22. Since the 1990s, the management strategy for study area rivers has involved an inner zone managed for low hydraulic resistance ("fairway", green and white lines) and a rougher, outer zone ("buffer", red lines) to temporarily accommodate shifts until it is re-trained to the fairway.

While I expect climate to be highly important, especially over longer time scales, the potential to extract signals without a budget for subsurface exploration or dating was highly limited and not the focus of this work. On shorter timeframes, the pervasiveness of human effects on morphology in the Ruamāhanga catchment are entangled with those from climate or weather and the lack of spatially-explicit records (e.g., as-built surveys) prevents partitioning of signals on decadal scales. Unexplored tectonic and anthropogenic forcing of river channels presumed to occur on shorter timeframes than climate with more acute effects appeared more relevant to management timeframes as well as important to resolve in advance of attempting to distil climate signals. Further, the fault-splay network of the study area is commonly associated with fault-propagation systems (sensu Perrin et al., 2016), thus, future geomorphic responses (including rivers) to tectonic forcing can be expected to be non-linear. In other words, specific system responses will differ through time. However, trajectories can be established and are important for anticipating future adjustments and hazards. Consequently, tectonics and anthropogenic forcing are the two key themes within the thesis.

Chapter 4

Framing coregistration fitness for geomorphic change detection

Introduction to Chapter 4 of Thesis

Chapters 2 and 3 review core themes and processes of fluvial morphodynamics, a subfield of geomorphology that is fundamentally about change in time. Here, Chapter 4 is concerned with establishing certainty that perceived changes are real, and specifically addresses thesis objective 'i', by describing a coregistration quality assessment workflow and linking to a proposed hierarchical classification based on change detection aims. This is increasingly important for increasing certainty of spatially explicit change detection, particularly as collection, creation and processing become decentralised and performed by non-specialists. Within the scope of this thesis, the local need became apparent during initial visual review of existing GIS data sets which revealed registration errors many times the widths of river channels indicating high unsuitability for channel migration analysis. In trying to frame and communicate the (lack of) suitability, a global gap also became apparent. Thus, Chapter 4 facilitates data suitability evaluation for spatially-explicit change detection that addresses global (United Nations Office for Disaster Risk Reduction, 2019a), field-specific (Thorne, 2002; Hooke, 2019), and local data quality needs.

This chapter is in preparation as a manuscript for Geomorphology as:

Conley, W.C., McColl, S.T., Fuller, I.C., Tunnicliffe, J.F., Macklin, M.G. (In Prep). Framing coregistration fitness for geomorphic change detection.

4.1 Abstract

Geospatially referenced images are a foundation upon which many geomorphic and landscape change investigations are based. Historically, raw and processed imagery originated from a limited number of sources, typically involving cartographic and/or photogrammetric experts at larger governmental organisations, research institutions, and specialty firms. This enabled end-user confidence through adherence to explicit methodologies as well as by implicitly ensuring measures of consistency. Advances in desktop processing (e.g., GIS) and acquisition platform (e.g., UAS) accessibility over the last two decades have enabled acquisition and/or processing at increasingly localised levels across academic, business, and government sectors. Gains in data quantity have been accompanied by diversification of quality which, in practice, often lack documentation such as metadata that commonly accompany state, provincial or nationally generated data. Nonetheless, pre-existing data, (independent of origin and documentation) are frequently incorporated into investigations by default and their suitability is commonly assumed. This can be problematic when inherited by an analyst who lacks knowledge of data history and/or geographic area. Even where the end-user has cradle-to-grave control over their data supply chain, it may have passed through black-box processes such as on-the-fly GIS reprojection or Structure-from-Motion. Thus, assessing fitness-for-purpose (with regard to positional errors) is increasingly paramount as the decision to use or not use is the point in the data life cycle where the end-user has the greatest control. However, my meta-analysis of the academic literature involving geomorphic change suggests a persistent and possibly widening gap of communicating uncertainty, accuracy, or error in abstracts. Where error(s) is/are characterised, spatially-averaged (e.g., RMSE) metrics to a common reference are customary despite long-running recognition of the practical importance of spatially variable error. I present a numerical model that shows median and 95th percentile RMSE values resulting from intercomparison of randomly varied datasets to be 41% and 73% greater (respectively) than the RMSE compared to a common reference; datasets with systematic bias exhibited even greater errors. I demonstrate error structure visualisation with a case study of archival aerial photomosaics (n = 5) that shows, across a wide quality spectrum, RMSE consistently represents only 65-75% of error frequency and 30-36% of the maximum observed error magnitude based on empirical cumulative distribution functions (ECDF) and residuals are not normally-distributed. Finally, I present a conceptual framework that links positional quality elements to analytical intent to aid fitness-for-purpose determination.

4.2 Introduction

Remote sensing has, with field work and data analysis, been considered one of three core elements of geomorphic investigation for at least two decades (Church, 2013). Contemporaneously, technological advances have enhanced data collection and analysis and brought geoscientific investigation into a new era (Legleiter and Marston, 2013; Viles, 2016). Unprecedented end-user access to remote sensing collection platforms (e.g., UAS) and digital processing of archival sources (e.g., photos and maps) using a variety of emergent procedures (e.g., Structure-from-Motion) have fuelled a dramatic rise in the quantity of spatially-continuous data at high spatiotemporal resolutions, especially aerial- and spaceborne data. Greater numbers of individuals from an increasingly diverse array of training backgrounds participating in collection and processing (sensu Devillers et al., 2010; Marcus and Fonstad, 2010; James et al., 2019) heightens the importance of addressing longer-term issues of reproducibility and communicating uncertainty so data quality does not suffer (sensu Unwin, 1995; Devillers et al., 2010; Hsu et al., 2015).

The concept of *uncertainty* is generally approached as a matter of data quality (Unwin, 1995). Positional accuracy, the focus of this paper, is a critical consideration for sequential comparisons that are fundamentally dependent on determinations that the same location is being compared

through time. While lexiconical creep over the last decade often implicitly equates geomorphic change with volumetric change, I employ a broader usage in this paper: any spatially explicit characterisation of landscape change through time. As such, this paper is relevant to questions of presence/absence, abundance, linear extension/contraction or displacement, and areal and volumetric deformation or displacement of landscape features and/or surfaces at specific location(s) through time. The difference in horizontal spatial alignment is traditionally characterised by the root mean squared error (RMSE) of a selection of comparison points. The RMSE continues in common usage as a minimum change detection threshold (Grabowski and Gurnell, 2016) although the inability of a single, spatially-averaged metric to characterise the spatial distribution of error has been repeatedly noted (e.g. Hunter and Goodchild, 1993; Unwin, 1995; Fisher and Tate, 2006; James et al., 2012; James et al., 2019). While the importance of spatially-variable error accounting has been promoted (Schaffrath et al., 2015; Lea and Legleiter, 2016b; James et al., 2019), its reporting has not been widespread. Positional error and accuracy are fundamental components of fitness-for-purpose (i.e., suitability of a specific data set for a specific use) which is customarily determined by investigators (Chrisman, 1982; Hunter and Goodchild, 1993; Lillesand et al., 2015). However, common practices to ensure fitness is similarly assessed across studies have not matched the pace of innovation in data production and application.

As geomorphic practice is increasingly applied across scientific disciplines and within administratively or legally regulated contexts (Wohl, 2014; Hooke, 2019), the need for communicating data quality and defending conclusions only grows (sensu Thorne, 2002), thus placing ever greater demand on ensuring data are fit-for-purpose. In this paper of three parts I 1) discuss factors driving the need to assess and communicate positional uncertainty in geospatial datasets related to geomorphic change detection and illustrate with a numerical model; 2) aid characterisation and expression of errors within geospatial data, using digital aerial photo datasets as an example; and 3) present a conceptual framework to assist data fitness-for-purpose determinations. Part 1 (section 4.3) provides a foundation by discussing concepts of uncertainty and fitness as well as providing a review of developments in aerial image use in geomorphic change investigation that contribute to the present need. Part 2 (section 4.4) starts with a cautionary example of contrasting geomorphic interpretations depending on registration then provides a granular, systematic walk-through of error characterisation for each photomosaic of a historic aerial image time-series that illustrates the serious limitations with sole reliance on RMSE. My case study uses inherited photomosaics which makes my assessment much more typical of applied settings where data are frequently provided by an institution, agency or client without metadata or connection to the original producer or knowledge of original acquisition/generation purpose. However, the workflow is applicable to any geospatial data (e.g., archival maps, spaceborne imagery, road vectors). Finally, Part 3 (section 4.5) provides a conceptual framework that resolves error type and magnitude with analytical intent dimensionality to assist fitness-for-purpose data assessments for geomorphic change investigations.

4.3 Uncertainty, imagery in change detection, and data fitness

4.3.1 Long-standing Issues in Positional Data Quality as a form of Uncertainty

"We demand rigidly defined areas of doubt and uncertainty!" – Hitchhikers Guide to the Galaxy (Adams, 2005)

Uncertainty, or doubt in one's data or results, is a concept generally approached as a matter of *data quality* which ultimately addresses fitness-for-purpose considerations (Unwin, 1995) and includes my focus in this chapter: *positional accuracy*. Spatially-averaged metrics like root-mean-squared-error (RMSE) are well-established (Fisher and Tate, 2006) and firmly grounded in formal standards

(e.g. FDGC, 1998) for characterising and screening positional accuracy. The importance of understanding positional error structure (i.e. variation) and the inability of RMSE and similar metrics for doing so has been discussed within geoinformatics literature for thirty years (e.g. Hunter and Goodchild, 1993; Unwin, 1995; Fisher and Tate, 2006) and, increasingly, within geomorphology (e.g. James et al., 2012; Schaffrath et al., 2015; Lea and Legleiter, 2016b; James et al., 2019). However, legacy effects from early single-metric standards (e.g. ASPRS1989) persist and RMSE remains the most popular metric for representing positional error within geomorphology and is commonly used as a minimum change detection threshold (Grabowski and Gurnell, 2016). Regarding development of ASPRS standards during the 1980s, Chrisman (1991) notes, "that certain government agencies wish to have a simple standard does not mean that problem is simple." And so, like the representatives of the "Amalgamated Union of Philosophers, Sages, Luminaries and Other Professional Thinking Persons" (Adams, 2005) the rigidity with which uncertainty is commonly simplified adds constraint, ironically contrary to the amorphous nature of uncertainty itself. In the process, I may also diminish, misdirect, or otherwise oversimplify the complex systems and processes I explore.

James et al. (2012) provide a rich discussion of positional accuracy including the importance of image co-registration and the limitations of standard GIS applications for evaluating error. Tabular presentation of multiple metrics common in the photogrammetric literature (e.g. Turner et al., 2012) characterise statistical distributions called for in geoinformatics (e.g. Chrisman, 1991), but still fall short of communicating spatial relationships of errors. Hunter and Goodchild (1993) noted error propagation, data fitness determination and error comprehension across skill levels as key challenges given that single metrics don't adequately represent complex concepts. They amongst others specifically recognised the value of supplemental error surfaces (Lowell, 1992), propagated scenarios (Fisher, 1991) and probabilistic representation (e.g. Brunsdon, 1995).

Reproducibility and formal propagation of positional errors in geomorphology tends to be a latent subject, though has been treated more frequently and formally within the volumetric change detection sub-field (e.g. Lane et al., 2003; Wheaton et al., 2010b; Clapuyt et al., 2016; James, 2017; Anderson, 2019). Within planimetric change detection, it is more customary to simply consider RMSE as a threshold above which any measurement quantity is considered real. Notable examples of planimetric error propagation include Mount and Louis (2005), Hughes et al. (2006), Toone et al. (2014) and Lea and Legleiter (2016b) however, uptake has not been broad. Wholesale exploration (including probabilistic reproducibility) and reporting of data life-cycle errors, including those resulting from digitisation and/or vector-raster conversion (e.g. Gurnell et al., 1994) or spatial variations of errors associated with source data, processing, or finished maps (James et al., 2012) are similarly rare.

To demonstrate how RMSE oversimplifies the spatial structure of errors I created a numerical model with six hypothetical datasets, each representing a data quality scenario (Table 4-1). Each dataset may be considered a time-series member, each having six points representing the same six features (e.g., road intersections). The *refpts* dataset represents the "true" positional coordinates of each feature which are stationary through time (Table 4-1, Figure 4-1A). The other five datasets represent check-points of the same features derived from hypothetical imagery referenced to *refpts*. The check-point datasets have identical RMSE values (by comparison to *refpts*) that result from different types and/or combinations of error. Each subplot in (Figure 4-1) can be thought of as a "map" where each of the six point clusters represents the same six features at different times. For example, the "+" symbols in Figure 4-1A could be the real-world position of fire hydrants whose interpreted position changes through the time series because of errors associated with image acquisition (e.g., lens distortion, scanning stretch), processing (e.g., datum registration), and/or interpretation.

Table 4-1. Six data quality scenarios modelled to evaluate how RMSE characterises error associated with intercomparisons.

Layer	Displacement		Quality Scenario
	Magnitude	**Direction**	
Refpts	None	None	"true" location of coregistration feature
Chkpts1	Random	Random	Ideal (no systematic errors or have been removed)
Chkpts2	Random	Random	Ideal (no systematic errors or have been removed)
Chkpts3	Variable, increasing along x-axis	Random	Paper stretch from sheet-fed scan with digitising occurring at too coarse a scale
Chkpts4	Constant	Constant	Oblique-slip tectonic displacement; also, approximates effect of a datum offset
Chkpts5	Variable, increasing along x-axis	Constant	Paper stretch resulting from sheet-fed scanning

The direction and magnitude of the displacement errors are randomly distributed for *chkpts1* and *chkpts2* (Table 4-1, Figure 4-1B) and represent "ideal" datasets where all systematic bias has been removed. *Chkpts3* has random directional error and a geographic bias where displacement magnitude increases along the x-axis (Table 4-1, Figure 4-1C), such as might arise from paper stretch associated with sheet-fed scanning and on-screen digitising at too coarse a scale (i.e. zoomed-out too far). *Chkpts4* has directional bias (±10° from 90°) and fixed displacement magnitude, such as might arise from oblique-slip tectonic displacement with primary strike-slip and secondary dip-slip motion. It also approximates the result of a map projection change or datum shift. *Chkpts5* has directional bias roughly opposite *chkpts4* (±10° from 270°) and variable displacement magnitude that increases along the x-axis, such as might arise from sheet-fed scanning (in the opposite direction of *chkpts3*). I generated 10,000 coordinate replicates for each of the five check-point datasets while maintaining a constant RMSE value of 7.0 in comparison to *refpts*. Each of the four subplots (A-D) in Figure 4-1 visualises one iteration of the simulation.

The probability distributions (Figure 4-1, E - G) for all dataset intercomparisons are all slightly left-skewed (-0.37 to -0.45) with median values of 9.90 ±0.04 (SD = 1.47 ±0.02) except for those where both datasets have a geographic (*chkpts3* to *chkpts5* median RMSE is 9.90 with SD=1.92) and/or directional bias (*chkpts4* to *chkpts5* median RMSE is 13.7 with SD=0.18). Except where both datasets have opposite directional bias, median and 95th percentile magnitudes of RMSE from intercomparisons of checkpoints are consistently 41% and 73% (respectively) greater than those involving the reference points. The most significant result from a practical perspective is the comparison of the two "ideal" check-point datasets (*chkpts1* and *chkpts2*). Though each is coregistered to *refpts* with an RMSE of 7.0 units, the statistical distribution indicates the 5th percentile value is 7.2 units (Figure 4-1B and Figure 4-1E). In other words, intercomparison of the two ideal (no residual systematic errors) check-points datasets exceeded the 7.0 RMSE value over 95% of the time despite being coregistered to the same reference layer. Interestingly, similar results occurred for intercomparison *chkpts2* and *chkpts3* (Figure 4-1C) that includes increasing systematic error in *chkpts3*, although the lack of a noticeable difference from intercomparison of *chkpts1* and *chkpts2* could be the result of a small range of x-axis values over which the effect was simulated for *chkpts3*.

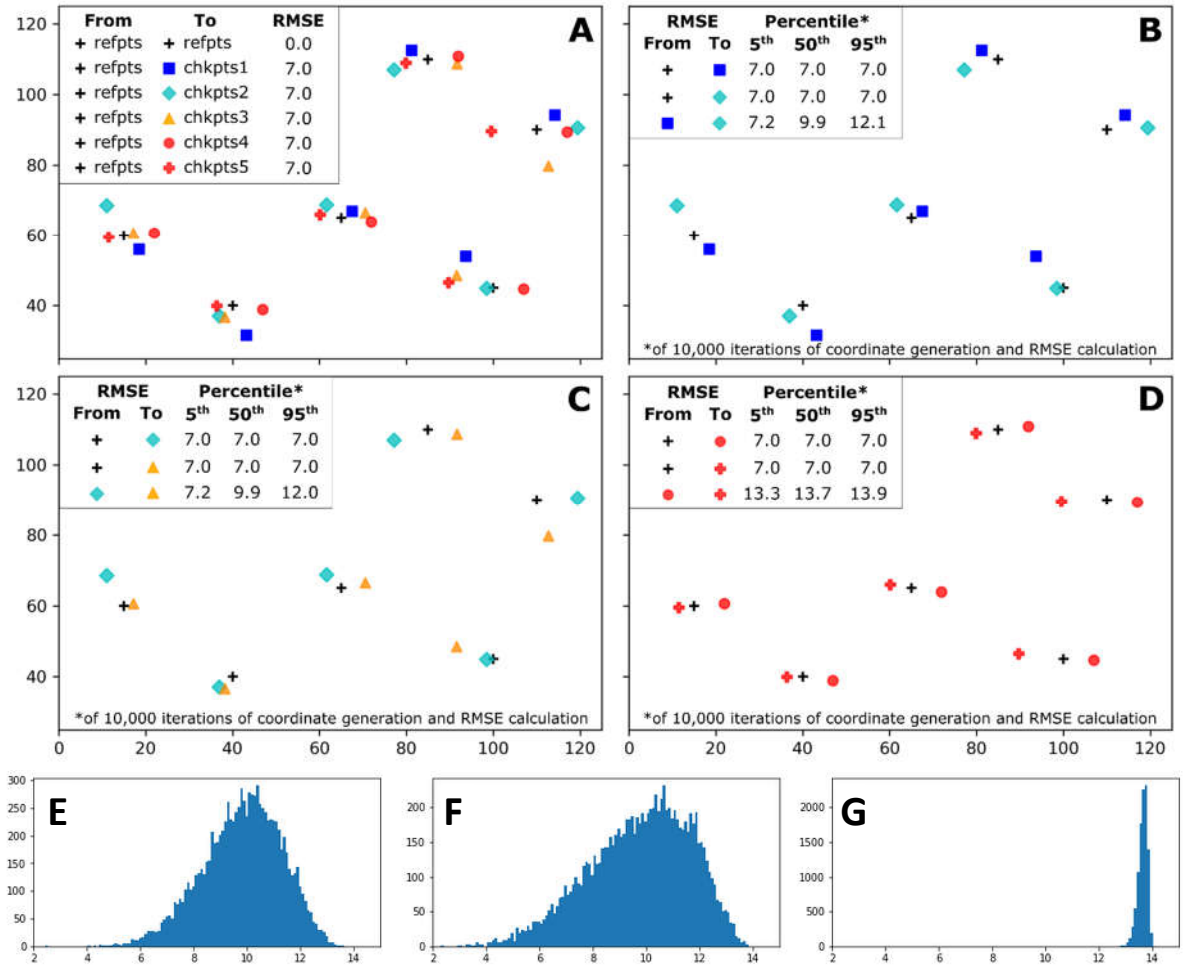

Figure 4-1. Simulation results for comparison of experimental datasetshaving identical RMSE, but different sources of error (i.e. that underlies error structure). A) all datasets plotted with RMSE values compared to reference dataset (refpts). B) Comparison of the two "ideal" check-point datasets (chkpts1 and chkpts2) where systematic errors have been removed and residual error results from random displacement magnitude and direction with each other and the reference dataset. C) Comparison of an "ideal" dataset (i.e. with random displacement magnitude and direction) with a dataset having random directional, but systematic displacement bias, this case that increases along the x-axis (chkpts3). D) Comparison of dataset with fixed displacement and direction bias (chkpts4) with dataset that has fixed directional bias in opposite direction whose displacement magnitude increases along the x-axis (chkpts5). E-G) histograms for 10,000 RMSE iterations of chkpts3 vs. chkpts5 (F), chkpts4 vs. chkpts5 (G), and typical histogram for all other intercomparisons (E).

Thus, 1) using RMSE based on comparison to a single reference to characterise error magnitude of intercomparisons provides highly optimistic representation where displacement magnitude that exceeds RMSE magnitude >95% of the time and 2) RMSE magnitude based on intercomparisons is insensitive to differences in the spatial error structure except in special cases (i.e., where both datasets have a directional and/or geographic bias). The skewed distributions also call into question routine assumptions of normality. Thus, I concur with earlier workers, that RMSE as a single metric does not adequately account for error.

Despite recognition of the need to better communicate uncertainty, uptake into geomorphic practice has been limited (Devillers et al., 2010). While focused effort in geomorphology has been similarly limited, the convergence of disciplines and increased use of images in volumetric change detection over the last decade has recently produced calls for greater general attention to accuracy, precision, and uncertainty (Piégay et al., 2015; Anderson, 2019) and improved metadata reporting

related to experimental modelling (Hsu et al., 2015), image capture (O'Connor et al., 2017), and structure-from-motion (James et al., 2019). Collectively, there continues to be a broad need for characterising and communicating uncertainty, particularly as it relates to suitability and consequences of data interrelationships (sensu Goodchild, 2008) not addressed by current standards and practices. Anderson (2019) identifies reduction and characterisation of uncertainty as keys to data understanding and application of the array of analytical tools now available. These needs flow beneath and throughout the evolution of geospatial data use in geomorphic change detection over the last fifty years, which I liken in Table 4-2 to the "forming" and "storming" phases of Tuckman's (1965) group development model.

Table 4-2. Decadal synopsis of aerial photograph application and development in geomorphology informed by the authors' collective experience, supplemented by literature (Smith and Pain, 2009; Church, 2010; Devillers et al., 2010; Church, 2013; Wohl, 2014; Hooke, 2019; Viles, 2019), and framed in adapted nomenclature from Tuckman's (1965) stages of group development.

Stage	Decade	Synopsis of Geomorphic Aerial Photographic Application & Development
Forming	Novelty, early methodological development, and application	
	1950s	Early purpose-driven field applications in grey literature; governmental use in development of topographic maps
	1960s	Appearance in peer reviewed literature across the spectrum of geomorphic disciplines
	1970s	Increased use for one-off mapping and evaluations; pioneering work in channel migration and integration with archival maps
	1980s	Increased use of repeat photographic time-series for evaluating pattern and planform changes; growth of desktop computing
	1990s	Transition to digital processing and growth of GIS; widespread desktop computing; growth of digital networks; increased comparison of time-series data raised importance of positional accuracy (control); widening public availability of government photographic collections
Storming	Explosion of end-user processing and collection due to software and hardware developments and increased accessibility	
	2000s	GUI-driven desktop GIS; initial self-deployed UAS; early self-deployed desktop photogrammetric processing; widespread availability of high-resolution digital imagery; increasing non-technical user-base of geospatial data; increasing cross-disciplinary integration concurrent with increased within-field specialisation
	2010s	Widespread availability of UAS and desktop processing software; proliferation of aerial acquisition and photogrammetric processing by end-users; dramatic increase in availability and quality of digital historic archives
Norming	Need for best practices	

4.3.2 Forming: Evolution of Image Application for Geomorphic Change Detection

Analysis of aerial photographs, archival maps, and spaceborne imagery has been recognized as a key method in geomorphology for over fifty years (e.g. Cooke and Doornkamp, 1990; Trimble and Cooke, 1991) with remote sensing considered a standard component of geomorphic investigations by the close of the 20th century (Church, 2013) (Table 4-2). While pioneering work began in the 1940s and 1950s, airborne applications in geomorphology and landscape investigation emerged from grey literature and appeared across academic subdisciplines including fluvial (Schumm and Lichty, 1963),

coastal (El Ashrey, 1967), hillslope (Norman, 1969), and glacial (LaChapelle, 1962) in the 1960s. Chorley's (1972) seminal paper characterised the 1960s as the initial decade of geomorphic spatial analyses (where formal linkage between quantitative data attributes and spatial coordinates are maintained) with 1971 as the coming-of-age as statistical applications took hold. Early applications of aerial photography often used analogue planimetry of raw prints such as for comparing change in channel area (e.g. O'Loughlin, 1969). Application of photogrammetric tools to large-scale (1:5,000 to 1:7,500) three-dimensional and floodplain mapping revealed detail and spatial relationships that expanded awareness beyond the prevailing notion of a single discharge-related flood stage (Lewin and Manton, 1975). Coupling field work with a time-series of aerial photographs and archival maps facilitated differentiation of form-change thresholds with discharge (Thorne and Lewin, 1979) as well as dispersal and redistribution of toxic materials (Lewin et al., 1977). While techniques and applications progressed through all sub-fields, the fluvial subfield, as the largest subfield within geomorphology (Wohl, 2014), has accounted for much of the work and hence most of the examples in this paper.

By the late 1970s compilations and syntheses across studies of geomorphic change began to appear (e.g. Lewin, 1977; Gregory, 1979) including many involving use of aerial photographs. Thornes and Brunsden (1977) recognised the value of (then) recent availability of repeat aerial photograph coverage and Church (1980) specifically noted the potential for extracting high resolution measurements. Werritty and Ferguson (1980) were one of the first to describe materials and methods for image handling and co-registration and integration with maps to enable large-scale mapping of decadal and century-scale channel patterns. In particular, the spatial continuity inclusive of vegetated floodplains enabled them to assess river channel changes not directly captured by their time-series. Planimetric time-series assessment increased and in 1983 a review Hickin (1983) noted that most river channel migration measurements were obtained via aerial photography and serial cartography, though he also noted constraints associated with temporal and geographic availability. Photogrammetric techniques enabled identification of process translocation (e.g. Church, 1983) and volumetric bank flux (e.g. Nanson and Hickin, 1986) at landscape scales (1:40,000 to 1:50,000) as well as glacier movement rates (Brecher, 1986) and slope stability (Chandler and Cooper, 1989) at larger scales. Combined applications of photo- and cartographic time-series paired with environmental data facilitated process-based identification of sediment transfer dynamics (e.g. Macklin and Lewin, 1989). However, image acquisition often remained difficult (Cooke and Doornkamp, 1990) and constrained application frequency along with labour and technological rigour.

Photogrammetrically-based change detection work in the 1990s shifted from descriptions of form and pattern to quantitative detection at large scales (better than 1:12,000). Lawler (1993) and Lane et al. (1993) provided reviews on channel change measurement and photogrammetric developments that recognised and discussed further applications in geomorphology. Airborne digital photogrammetric mapping using scanned prints for performing change detection in GIS environments gained hold and quantitative error reporting became customary (Gurnell et al., 1994; Gilvear et al., 1995; Lane et al., 1996; Winterbottom and Gilvear, 1997; Westaway et al., 2000). As quantitative change analysis progressed to ever-finer scales, positional accuracy became recognised as the primary limitation (Gurnell, 1997; Winterbottom, 2000).

During this time, Digital Elevation Model (DEM) creation, visualisation, and comparison became easier with increased availability of GIS software. Ground-based photography was used to develop a DEM that enabled high-resolution characterisation of morphodynamics and calculation of sediment transport rates (Lane et al., 1995, 1996) as well as grain-scale characterisation (Kirby, 1991; Heritage et al., 1998) at reach, bar, and patch scales. The prospects of photogrammetrically-derived DEMs

from aerial photography (Lane et al., 2000) was a natural extension and recognition of the utility of photos to integrate spatiotemporal scales (Brasington et al., 2002) grew at the beginning of this century. The traditional division of labour between data producers and data analysts (Chrisman, 1991) began to subside as end-users increasingly supplemented data from centralised governmental and specialty firms and data quality checks became more decentralised. Aside from the ease and generally low cost of data acquisition, software developments enabled end-users to produce their own DEMs and orthophotos without formal knowledge of photogrammetric principles of which Lane (2000) expressed anecdotal concern.

4.3.3 Storming: Rapid Technological Growth and Multi-Disciplinary Convergence

The term "democratisation" has been used (e.g. Butler, 2006; Devillers et al., 2010; Gomez et al., 2015) to characterise the dramatic shift to end-user-driven data acquisition, processing, and analysis that has made cradle-to-grave remote sensing and analysis increasingly common in geoscientific investigations. Georeferencing, rectification, and other processing techniques, formerly the domain of specialists, became ubiquitous as graphically-driven desktop GIS became widely available and photo archives were digitised. Uptake of three dimensional photogrammetric collection and processing by end-users grew considerably, including fluvial (e.g. Brasington et al., 2003; Lane et al., 2003; Fonstad and Marcus, 2005; Marcus and Fonstad, 2008; Rumsby et al., 2008; Bird et al., 2010), glacial (e.g. Barrand et al., 2009), coastal (e.g. James and Robson, 2012), and hillslope (e.g. Gessesse et al., 2010) settings facilitating reasonably precise change detection from sub-annual to hourly (e.g. James et al., 2007) timescales.

Interest in highly detailed and spatially continuous datasets afforded by photogrammetry grew for archival data as digital conversion became more common and enabled more precise quantification and linkages between driving processes and fluvial change (Ham and Church, 2000; Westaway et al., 2000), landslide activity (Walstra et al., 2007; Mackey et al., 2009), cliff erosion (De Rose and Basher, 2011) and aeolian change (Hugenholtz et al., 2013). Concurrent advances and wider availability of spaceborne imagery in the 2000s enabled development of sub-fields such as fluvial remote sensing (Marcus and Fonstad, 2010; Carbonneau and Piegay, 2012). By 2010, it was noted that noted a most papers published in the Earth sciences literature were by "people on the fringes of remote sensing" (Marcus and Fonstad, 2010).

Experimentation with a wide variety of low-cost, self-deployed, mobile, low-elevation collection platforms including lighter-than-air (Vericat et al., 2009), parafoil (Smith et al., 2009), pole (Bird et al., 2010) and untethered UAS (Hugenholtz et al., 2013) further stimulated interest and primed the supply chain for major processing advancements. Refinements in image-matching algorithms (i.e. Structure-from-Motion, a.k.a. SfM) delivered resolution and data quality comparable to classic stereo-pair photogrammetry and LiDAR, but at lower cost and with greater ease of use (James and Robson, 2012; Westoby et al., 2012; Fonstad et al., 2013). SfM applied to archival imagery with detailed attention to image quality and topology can achieve comparable results to traditional photogrammetric techniques, including decimetric or better accuracy (Bakker and Lane, 2017). Coupled with a range of software developments for managing and interrogating 3D point clouds, these advances provided unprecedented cradle-to-grave control and drove proliferation of collection, processing, and analysis by end-users over the past decade. Thus, in a little over a decade, the scenario Lane (2000) forecasted concern came about as data generation shifted from specialists to non-specialists across a wide variety of disciplines

As the number of investigators generating high resolution photogrammetric time-series has grown, so too has variation in methodological descriptions. Having read a great many papers in preparing this chapter (including many not cited), there appears to be a trend where many earlier papers made

effort to detail methods and characterise their error, while papers since about 2010 seem to increasingly rely on referential methodologies and provide little detail on positional control, accuracy, or error other than RMSE.

To provide an indication of trends in geomorphic change detection and general indication of attitudes toward communicating uncertainty, I conducted a semi-automated literature meta-analysis using the Web of Science Core Catalogue (WOSCC) in September 2019. A generic topical search (section 4.9) for geomorphic change produced 290 results with 94% (n=273) occurring since 2000 and a major uptick since 2012 (Figure 4-2A). Of the 460 results for combined terms related to topography and aerial imagery (*Figure 4-2*B), 310 had abstracts of which 86% (n=268) included at least one text string (see Appendix A) explicitly or implicitly suggesting temporal change. Of those 268 abstracts, 61% of the abstracts (n=163) contained at least one terminological instance associated with error (see Appendix A). Most interestingly, variation in occurrence generally tracked titles published until approximately 2010 when a distinct and persistent (and possibly growing) reduction of error expression in abstracts is identified (*Figure 4-2*C). In other words, since 2010 there is a noticeable decline in communication of uncertainty within abstracts. Thus, during a time of rapid growth in geomorphic change detection publications by an ever-broadening user-base, explicit acknowledgement of uncertainty in research summaries seems to be decreasing.

Deemphasised accuracy communication in abstracts over the last decade seems odd for a field that is increasingly called upon to inform decisions related to land-use and public safety. Considering general blunder frequency increase in geo-spatial data products from non-commercial sources (Fisher and Tate, 2006), recognition that the standard geospatial data user is no longer a GIS expert (Devillers et al., 2010) and the importance of experience identifying data suitability and limitations (Hunter and Goodchild, 1993), there is increased potential for unaccounted errors to propagate and/or data to be used mis-fit to purpose (e.g. section 4.4.1) . Calls and examples raising the profile of QA (James and Robson, 2012; James, 2017; James et al., 2017; O'Connor et al., 2017) and refined research manuscript submission requirements (James et al., 2019) are important but may not effectively reverse the trend depending on the underlying problem. I suggest the tendency to overlook uncertainty and its implications could result from 1) carry-over customs from days when production was centralised and QA performed by specialists separate from analysts (sensu Chrisman, 1991); 2) assumptions that high-resolution data are inherently more accurate; 3) an increase in the proportion of practitioners from backgrounds that lack even basic familiarity with statistics, geoinformatics, and/or photogrammetric principles and/or; 4) tools for uncertainty characterisation have not developed as rapidly as methods of data generation.

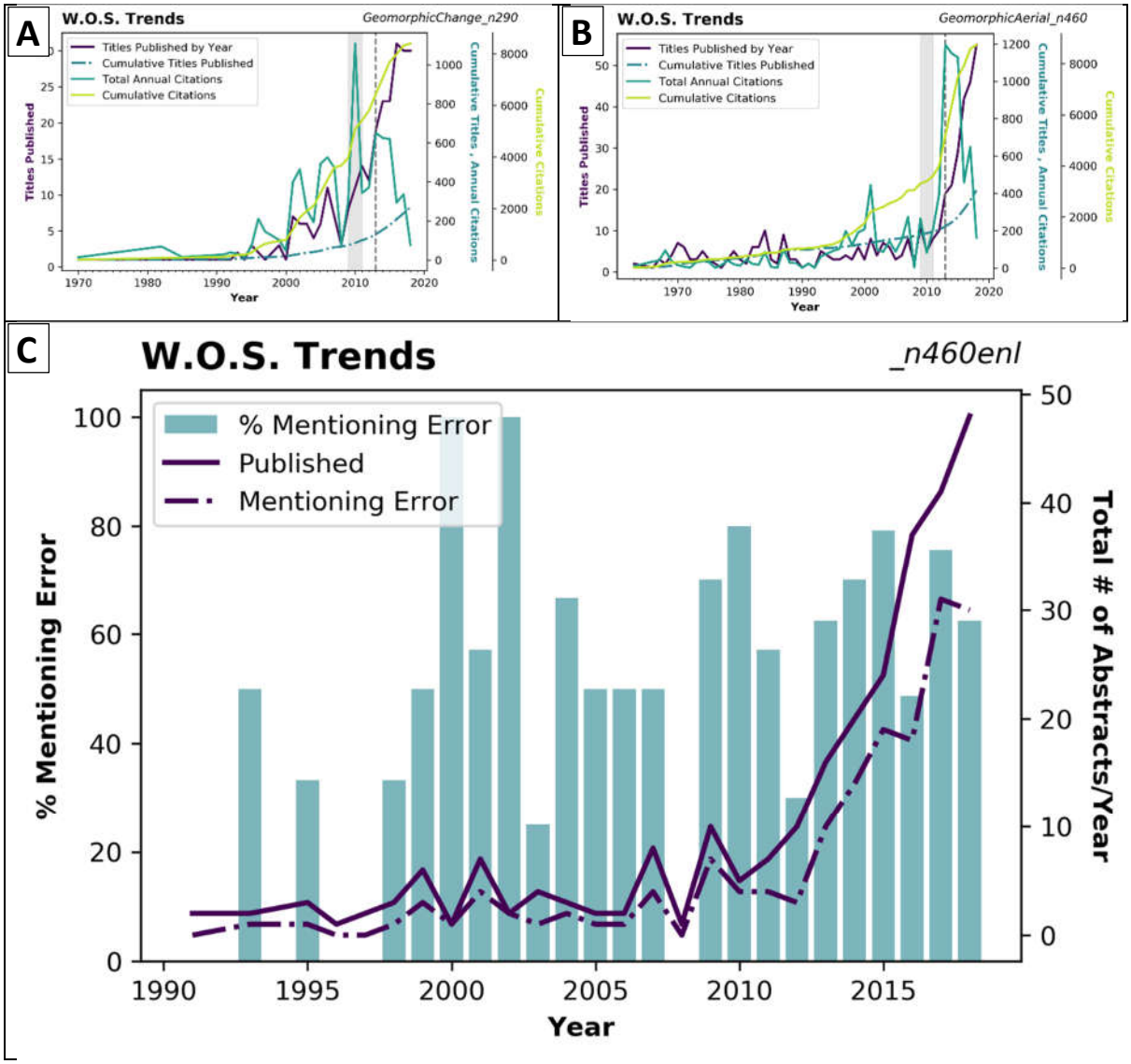

Figure 4-2. Top: Trends in the peer-reviewed literature in Web of Science (WoS) for publications involving geomorphic change (A) and use of aerial imagery in geomorphology (B). Grey bar indicates 2009-2011 and black hashed line indicates 2013 in both images. Bottom (C): Relation between titles from Figure 4-2B and specific mention of an error-related term in the abstract.

A review of geomorphology reference books indicates infrequent and shallow treatment of aerial photograph use with no discussion of how inaccuracy could lead to misinterpetations of geomorphic form or process. Many foundational books published prior to ca. 2000 (Cotton, 1945; Leopold et al., 1964; Knighton, 1998) whose use classroom use persisted for decades make no mention of aerial photographs as tools for landscape analysis. Notable exceptions include more specialised texts such as Thornes and Brunsden (1977) who frame an example of incidental measurement and specifically note this has "value now that repetitive cover is available" (p. 54). Hooke and Kain (1983) addressed measurement error in historical data sources though, in a review of the book, Richards (1984) noted the need to resolve "serious, specific methodological issues". Cooke and Doornkamp (1990) discussed applications and included specific guidance to specialised photogrammetric source publications with no treatment of positional evaluation. Mention of aerial photographic applications occurs more frequently in books published after 2000 (e.g., Sear et al., 2010; Fryirs and Brierley, 2012; Bierman and Montgomery, 2014) though generally without discussion of suitability and without mention of error handling. Gilvear and Bryant (2003; 2016) summarised conceptual

approaches and noted the need for rectification for geometric accuracy and co-registration when using time-series for change detection. Grabowski and Gurnell (2003, 2016) addressed a range of archival data types (including photos) and explicitly discussed positional accuracy, mainly related to cartographic representation but also outlined conceptual approaches for assessing accuracy. While Jensen (2000) provided excellent discussion of principles as well as specific application to water, soils, minerals, and geomorphology, like other remote sensing texts (e.g. Lillesand et al., 2015), change detection discussion emphasised radiometric differencing and accuracy assessment coverage focusing on classification and segmentation effectiveness. Of the texts reviewed, Lillesand et al. (2015, p. 293-295) provided the most granular treatment of positional error and accuracy, including equations and assumptions. However, no texts provided specific guidance for evaluating suitability and, overall, treatment of positional accuracy is very limited. Thus, I conclude that a more granular level of subject treatment is needed to understand how to characterise and communicate uncertainty, and to explore how to assess fitness-for-purpose for time-series analysis.

4.3.4 Norming: Positional uncertainty and fitness-for-purpose

It is customary across all fields for investigators to determine data fitness-for-purpose (a.k.a. suitability) (Chrisman, 1982; Hunter and Goodchild, 1993; Lillesand et al., 2015), but differential treatment of spatial error is particularly common for multi-disciplinary fields (Chrisman, 1991). While metadata can be of great assistance, Ureña-Cámara et al. (2019) note considerable variability in both metadata producers and standards, for which positional accuracy is optional and usually based on spatial extent (e.g. bounding box as opposed to correctness of feature-specific geometry). Validation testing for compliance with standards is often automated and limited to format interoperability and completeness as opposed to factual correctness (Ureña-Cámara et al., 2019) such that even ISO- or FDGC-complaint metadata may not provide sufficient information to determine positional suitability. Of course, this assumes that spatial data have companion metadata in the first place.

It is critically important to note a fundamental dichotomy between customary approaches to academic versus applied professional investigation. With some supplementation of commercial products, nearly all the academic investigators in the studies involving primary research cited in this paper performed their own data processing prior to analysis. This level of control and familiarity with one's data stands in punctuated contrast to applied settings like consulting and river management where the default approach usually involves analysis of pre-existing (usually generated by others) data. However, formal positional accuracy assessments are not customary, and budgets (often developed without explicit scoping of error propagation) often constrain pre-analysis assessment to informal spot-checking.

Whether produced by specialists or non-specialists, the growing volume of data will collectively be called upon for analysis. I suggest that increasingly decentralised data production and related quality control and assurance (QA/QC) in the absence of formal best practices by investigators from increasingly diverse backgrounds is unlikely to improve long-standing issues of data quality and is more likely to create new ones. As semiautomated and automated data mining processes advance, the importance of conducting and documenting data-checking in a matter that can differentiate the quality spectrum will similarly increase. Full error accounting relative to results associated with low-quality, low-precision data can yield higher certainty than complex, poorly-documented handling and analysis of good-quality, high-precision data (Hunter and Goodchild, 1993). Though presented within the context of river restoration, Graf's (2008) juxtaposition of uncertainty handling strategies has broad application and presents the decision more starkly: 1) incorporate uncertainty as a part of the study or 2) ignore uncertainty and hope for no adverse effects.

While methods of data acquisition by non-specialist end-users have become much more accessible, methods for assessing and characterising error have not kept pace. Regardless of the quality spectrum in an absolute sense, uncertainty is data-, context-, and user-dependent (Deitrick and Edsall, 2008). There is a fundamental need to raise awareness of the need and means of characterising error and/or accuracy. Deeper analyses of statistical (Hughes et al., 2006; James et al., 2019) and geographic distributions (Lea and Legleiter, 2016b) provides the greatest promise for addressing the substantial and growing need to inform positional uncertainty.

4.3.5 Terminology

Conflation of terminology related to spatial data quality has been noted through time (Unwin, 1995; Devillers et al., 2010) and different meanings of terms in different fields is a potential obstruction to cross-disciplinary solutions (Devillers et al., 2019). I generally follow Table 14.1 in Deitrick and Edsall (2008) where *error* is "the difference between a measured or reported value and the 'true' (includes both precision and accuracy). *Precision* is used to mean repeatability or reproducibility. For *accuracy* I specifically mean positional accuracy or the closeness of a feature's location value to the value of a reference location for that feature (absolute or relative). *Internal quality* is the similarity between data and the real world at time of capture and e*xternal quality* is data fitness for a specific (user-defined) purpose (after Devillers et al., 2019).

4.4 Error characterisation and assessment

Whether historic or newly collected data, fitness-for-purpose is often assumed. This section examines error detection and explains the consequences of using a combined graphical and statistical approach as a precursor for informing data suitability decisions.

4.4.1 A cautionary tale: co-registration error consequences at large-scale

To promote attention to data quality and suitability, Devillers et al. (2010) suggest the need for examples to draw attention to the consequences of using unfit data. To underscore the importance of the subsequent case study, I compare two photomosaics of the Waingawa River in the vicinity of the municipal water intake for the town of Masterton, New Zealand. Evaluation of large-scale (approximately 1:6,700) channel migration maps from a previous study (Christensen, 2013) suggested the active channel shifted about half a channel width away from the intake (Figure 4-3, top panel) between 1944 and 1963. However, reexamination of these data shows that the apparent 34 metre average of horizontal accretion along 350 m of bank (A to B) is a function of source image registration error. After re-registering 1944 and 1963 imagery to a common, high-quality base (0.6 metre resolution orthophoto of the 1963 imagery derived by SfM with ground control by 2012/2013 orthoimage and 2012 LiDAR), average displacement along the bank is 2 metres, which is within the margin of error of the corrected image (1.2 metre RMSE and 2.1 metre maximum displacement based on co-registration error to the high-quality orthomosaic from 2012/2013). While outside the scope of the present paper, I direct readers to Bakker and Lane (2017) for discussion of additional quality control metrics and measures associated with archival imagery analysis including output mosaic texture, extent of input frame overlap, and inclusion of Ground Control Points (GCPs) in bundle adjustment.

Specific to whether channel migration potentially disturbed water intake infrastructure, the geomorphic trajectory of the original false-positive (change "detected" that didn't occur) is arguably better than a false-negative (where real change went undetected). Independent of relative desirability in this instance, the original relationship was incorrect, and the verity of geomorphic trajectory is purely coincidental. For example, there is no reason to believe registration errors

consistently produce one type of error. Given the common practice of using base data "as-is", it is likely that errors and spurious changes often go undetected. To help address this, I propose a standardised workflow, and have developed a Python tool to aid characterisation of registration error.

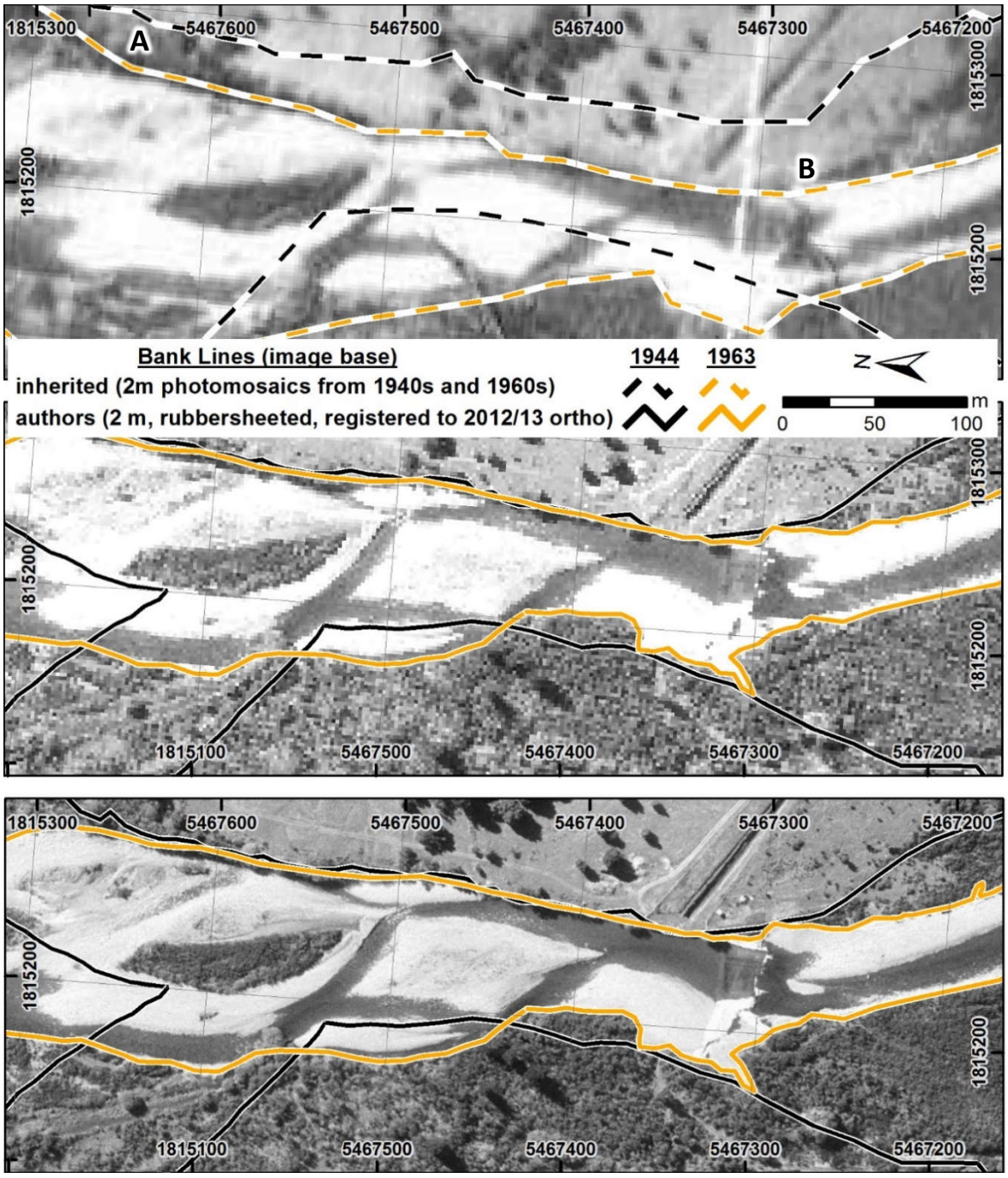

Figure 4-3. Images (1:3,400 scale) originating from same flight in 1963 with different processing lineages. Top: 1963 photomosaic (2 metre pixels, presumed scanned from prints then mosaiced and georeferenced via unknown process) and channel margin polylines inherited from a prior study suggest 34 metre average bank ('A' to 'B') migration over a 19-year period at the site of a municipal water intake (data: GWRC). Middle: Georectified image with channel margin polylines derived from single photo frame referenced to a high-quality orthomosaic and down-sampled to 2-meter pixels (data: RetroLens and author). Bottom: Orthomosaic (0.5 metre pixels, created in PhotoScan Pro v.1.4 using co-located control points from 2012/2013 orthomosaic and z-values from 2012 LiDAR; data: author, RetroLens).

4.4.2 Detecting and Characterising Co-registration Error

The ability to detect and accurately characterise a target phenomenon (signal) is fundamentally linked to the ability to differentiate from all other phenomena (noise) not of interest. Understanding the flaws in one's data is essential to filtering signal from noise, though the degree of rigour in characterising noise and/or distilling a signal is often purpose specific. Historically, studies at coarser geographic scales such as landscapes, orogens, or regions tolerate more noise (e.g. +/- tens of meters), while finer scales (grains or depositional units) often require higher degrees of accuracy. However, technological advances make high degrees (metric to sub-metric) of accuracy and precision across landscapes possible and - considering the important implications for hazard studies - necessary. Whether presented with unfamiliar data or assessing one's own data, evaluating error should be a fundamental project step. I provide a case study from New Zealand's Wairarapa region where a multidecadal air photo time-series was evaluated for suitability for channel migration and sediment budgeting. A sequential process of data exploration is described beginning with qualitative visual review and culminating in graphical and statistical characterisation of registration error. My two-step point-based approach is based on traditional practice and straightforward to implement and does not require specialist photogrammetric knowledge. Importantly, it requires only modest GIS proficiency, and can be understood with undergraduate-level knowledge of statistical probability.

4.4.3 Study Area and Data Sourcing

Case study data are from a 22-kilometre X 37-kilometre sub-unit of the Ruamāhanga catchment (*Figure 4-4*) on New Zealand's North Island. Major rivers include the Ruamāhanga, Waiohine, Waingawa, and Waipōua who's wandering to semi-braided gravel-beds have active belts that range from ~22 to 250 m wide. A time-series of five photomosaics (Table 4-3) was provided by Greater Wellington Regional Council (GWRC) to evaluate river channel dynamics, inclusive of sediment budgeting. I collectively named the first three time-steps (1940s, 1960s, and 1989) the "legacy" mosaics as they lacked metadata and were processed in-house by former GWRC staff. They appear to have been scanned from prints to approximately 2 metre ground resolution. Source images for the two earliest time-steps were collected over multiple years, hence are referred to as "1940s" (flights in 1941 and 1944) and "1960s" (1961 and 1963). Subtle, non-orthogonal seams, localised distortion, and patchy, pixelated boundaries suggest some attempt at rectification may have been made for the 1940s and 1960s mosaics. The 1989 orthomosaic has the lowest image quality of the time-series and appears to have been stitched without any attempt at rectification. The fourth (2012/2013) orthomosaic was used as the reference given its high resolution (0.3metre), collection over a single season (the optimal summer collection season spans the calendar year), orthocorrection, and good spatiotemporal correspondence with regional aerial LiDAR acquisition. The fifth (2017) orthomosaic is high-quality, high-resolution (0.3 metre) and was also collected in a single season. Aerial collection and processing of the latter two data sources was by a specialty photogrammetry vendor.

Table 4-3. Attributes of aerial imagery datasets evaluated for suitability to detect geomorphic change.

Photo Year(s)	Scale	Pixel Size (m)	Reported Accuracy	Colour / BW	Rectified?
1941-1944	1:16,000	2.00 x 2.00	None	BW	Partial (geo)
1961-1966	1:17,400	2.07 x 2.09[a]	None	BW	Partial (geo)
1989	1:54,000	1.87 x 1.87	None	BW	No
2012/2013	1:5,000	0.30 x 0.30	±2 m (90%)	RGB / IR	Yes (ortho)
2017	1:5,000	0.30 x 0.30	±2 m (90%)	RGB / IR	Yes (ortho)

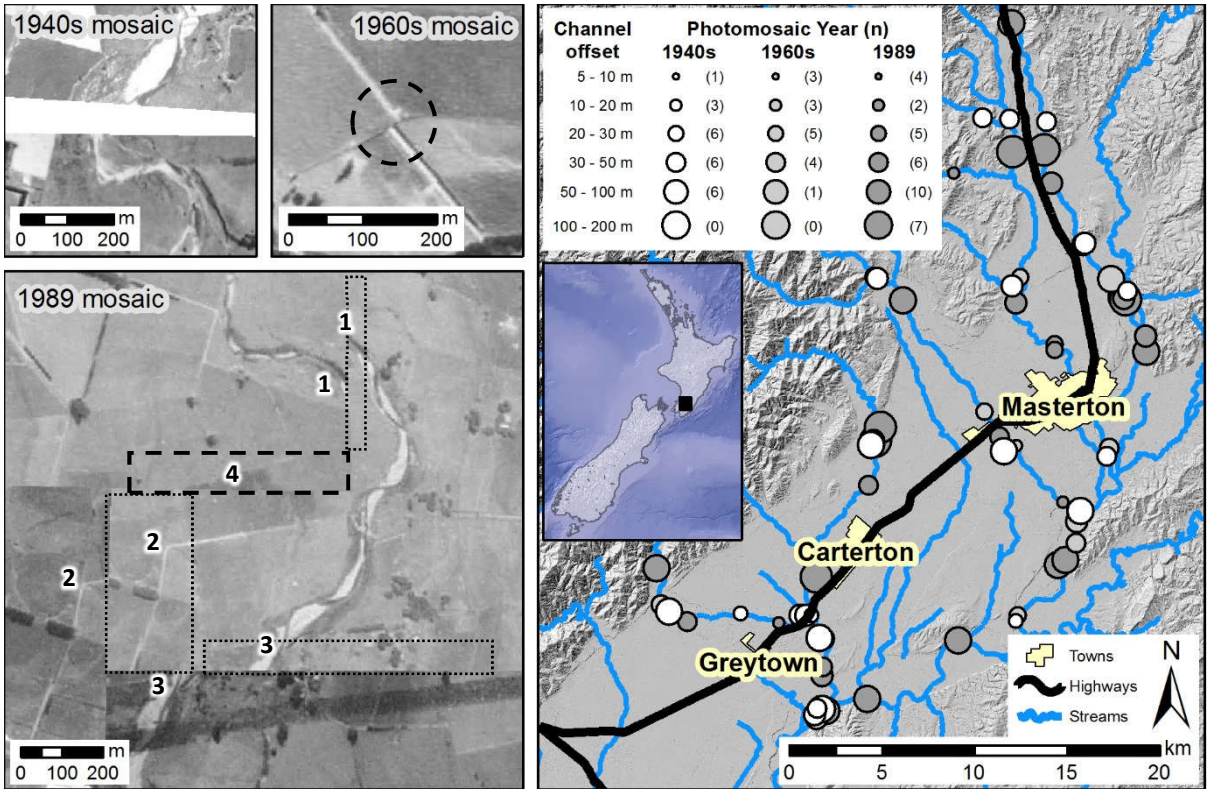

Figure 4-4. Right: Geographic distribution and displacement magnitude categories of stream channel offsets identified during stage 1 evaluation of data fitness (exploratory data analysis (EDA)). Left: Examples of feature displacements found during exploratory data analysis (EDA) indicative of common errors that can constrain study objectives. Top-left: missing data due to gap in flight lines during collection (e.g. 1940s mosaic).Top-right: 16 m offset in road alignment associated with mosaic process (e.g. 1960s mosaic).Bottom-left: A variety of horizontal offsets during processing can create under-lapped areas with duplicate data (dotted perimeters near '1', '2' & '3'; "commission" error) or over-lapped areas (dashed perimeter near '4'; "omission" error) where data is missing (e.g. 1989 mosaic).

4.4.4 Stage 1 - Exploratory Data Analysis (EDA)

Data were explored in a GIS environment (ArcGIS 10.4) to gain familiarity and awareness of capabilities and limitations of each time-step. The key questions considered during this process were: are there any obvious problems, and can the data answer the questions being asked? Specifically, my *a priori* expectation was RMSE of 5 to 6 m or better based on prior work by others (Gurnell et al., 1994; Gilvear et al., 2000; Winterbottom, 2000; Hughes et al., 2006; Nicoll and Hickin, 2010; Michalková et al., 2011; Moretto et al., 2014). Given the size of the river channels being evaluated for changes in form, absolute position, and ground cover I considered such magnitude to be the bare-minimum of suitability. I progressively applied a two-step sub-process of visualisation and mapping to identify and quantify errors and inconsistencies to determine if more thorough investigation was needed.

4.4.4.1 Step 1a: Visualisation & Spot-checking

Unwin (1995) suggested the frequency of blunders in GIS is much higher than generally recognised or what would be tolerated if awareness of such errors existed. Barrand et al. (2009) specifically called for the manual checking of models as part of their quality assurance process. Upon receipt, I checked each mosaic for internal consistency (i.e., within a single time-step) for issues of alignment, gaps, and/or displacement (*Figure 4-4*, left side) by zooming and panning around each mosaic. During this step I also assessed whether the image was a georectified image, an orthomosaic or simply a

photomosaic. A *photomosaic* is any aggregated image where multiple photographs are merged, stitched, or otherwise compiled into a single image. A *georectifed* image is an image that has experienced some level of mathematical transformation to correct distortions and better approximate a plane, usually based on an accepted planimetrically-correct map, photo, or similar base layer. An *orthomosaic* is a special type of rectified image that is compiled from multiple overlapping images subjected to special photogrammetric or matching treatment that planarises the resulting image so straight features appear straight, vertical objects have minimal or no lean and boundaries between individual frames are either undetectable or less-sharp.

All three legacy mosaics showed some signs of linear feature curvature and seam misalignment suggesting they were better considered as "photomosaics" than "orthomosaics". The 2012 and 2017 images were excellent quality and had clearly been orthocorrected. Spot-checking performed during this step involved measurement of linear feature offsets (roads, rivers, fence lines, buildings, logs, et al.) to approximate potential horizontal errors.

4.4.4.2 Step 1b: Mapping / Semi-quantitative

Step 1a raised concerns about legacy mosaic suitability so I conducted a systematic GIS-based inventory along each of the features of interest. Each of the five mosaics was evaluated in an upstream direction by panning continuously along each of the four rivers and major tributaries (~180 kilometres cumulative) at approximately 1:2,000 scale. A point was digitised at each discrete location where a linear channel and/or floodplain offset was observed, and the linear offset measurement and descriptive comments were attributed for each point. Offsets in roads, fences, or hedges were measured in proximity to channel offsets at temporal boundaries in lieu of channel measurements that may also have been affected by channel migration.

Step 1b review found no discrete channel offsets within the 2012/2013 or 2017 mosaics, though each of the legacy mosaics had large (10s of meters) offsets distributed throughout the study area. Seventy-two total channel offsets associated with data processing were identified for the 1940s, 1960s, and 1989 mosaics (*Figure 4-4*), 56 of which were 20 metres or larger. Only eight were less than 10 metres. Image over-lapping (where some amount of real-world area is not represented due to one image obscuring data unique to an underlying image) and under-lapping (where identical features are present on both sides of an offset) were found (e.g., *Figure 4-4*, 1989 mosaic). While under-lapping of images is conceivably correctable, over-lapping is not. A gap in the photographic coverage was also identified in the 1940s mosaic. Distortion effects (from the camera and/or registration transformation) were also evident for the legacy mosaics and most easily observed when straight road segments were compared to the 2012/2013 and 2017 mosaics.

While it was clear at this point the 1989 mosaic was unfit, the two older mosaics were still considered as potentially correctable. However, because multiple types of error were present, a more thorough assessment was implemented to determine if correction was actually possible and what sort of re-processing might be required.

4.4.5 Stage 2 – Quantitative Screening

While Stage 1 is about data familiarisation, Stage 2 is about understanding error structure and quantitatively determining reasonable data applications. The indication of internal mosaic quality provided by Stage 1 does not quantitatively set reasonable expectations of accuracy within or between time-steps. I use the term *correspondence* for the latter concept which is particularly important for detecting real change and avoiding non-true results such as that illustrated by this cautionary tale (*Figure 4-3*). Two perfectly corresponding images would have equal distances between features that have not moved (or otherwise changed in orientation or dimension).

Differences in horizontal distances between otherwise static features provides an indication of the noise from which a true change signal must be differentiated. Effectively, it is the spatial consistency between time-steps. Here, I build upon Hughes et al. (2006) who recommend error characterisation for measurements involving temporal change be based on empirical probability functions from test points independent of ground control points (GCPs).

4.4.5.1 Step 2a: Check-point creation

Point-based approaches have been a foundation of positional accuracy assessment for at least three decades (Chrisman, 1991) because there is neither dimensional (i.e. no length, so can't be distorted) nor attribute (a point only represents one real-world feature) ambiguity. I use a typical approach based on comparing a set of points associated with common, unmodified ground features through time to a set of points from a single reference orthophoto (e.g. Gurnell, 1997; Fisher and Tate, 2006; Hughes et al., 2006; James et al., 2012; Lea and Legleiter, 2016b; Lallias-Tacon et al., 2017). For this investigation, I consider the points digitised from the 2012/2013 orthomosaic as "true" and refer to them as *reference points*. I collectively refer to points digitised from the other four mosaics as *check-points* and the real-world feature represented by each five-point cluster as a *location*. The displacement between any check point and its companion reference point is the *residual*. Well-defined features that were positively identifiable on all five mosaics (*Figure 4-5*) were digitised into an ArcGIS 10.4.1 file geodatabase such that each location has one reference point and four check-points. A total of eighty-four reference points and 336 check points were generated for 84 locations across the study area (*Figure 4-5*).

Unlike Stage 1 (which sought to identify and measure offsets), reference point locations were selected to be well-distributed through the study area and to have experienced minimal alteration over the study period. Though precision between time-steps can be improved by an order of magnitude when check-points are from locations other than the original ground control points (GCPs) used for image rectification (Clapuyt et al., 2016), I had no knowledge of GCP locations for any of the mosaics so I focused more on geographic distribution and location identifiability. Average reference point spacing is approximately 3.1 kilometres which approximates the smallest ground footprint of tiles from the largest-scale (1:16,000) source photos used to create legacy mosaics. Point distribution tends to be denser near target rivers and edges of the study area.

Common point identification was the most time-consuming part of the process. While I initially started by comparing the oldest mosaic with the newest, it became apparent that the low image quality of the 1989 mosaic was the greatest limiting factor. Cell resolution and dark and blurry image patches limited the types of features that could be used, generally excluding higher precision options like fence or roof corners, and frequently resulted in use of roadways in some form. Primary roads and major bridges were frequently found to have experienced improvements and/or alignment changes and were generally avoided. Secondary, tertiary, and private access roads were selected with higher frequency as they seemed to experience the least amount of alteration. Centrelines were often digitised and projected to intersections to assist more precise point placement. Water-race (irrigation ditch) crossings at roads tended to be reliably distinct and unaltered through time.

Data structure is an essential element of the process with one-to-many relationships occurring within a 'flat' attribute table (Table 4-4). Each table record relates to a single point and has a unique identifier, in this case *PtID* is an integer field. *PtID2012* contains *PtID* values of the reference points to which any point is to be compared. Thus, for each unique value of *PtID2012* there are five records with unique *PtID* values (one of which will equal the *PtID2012* value). Northing (Y_NZTM) and Easting (X_NZTM) grid coordinate fields (New Zealand Transverse Mercator 2000) were calculated for each point within the GIS environment. *PhotoYear* is important as a grouping variable (across

locations) and is also used for labelling. Once all reference and checkpoints were digitised and attributed, the table was exported from GIS to a text file (*.csv).

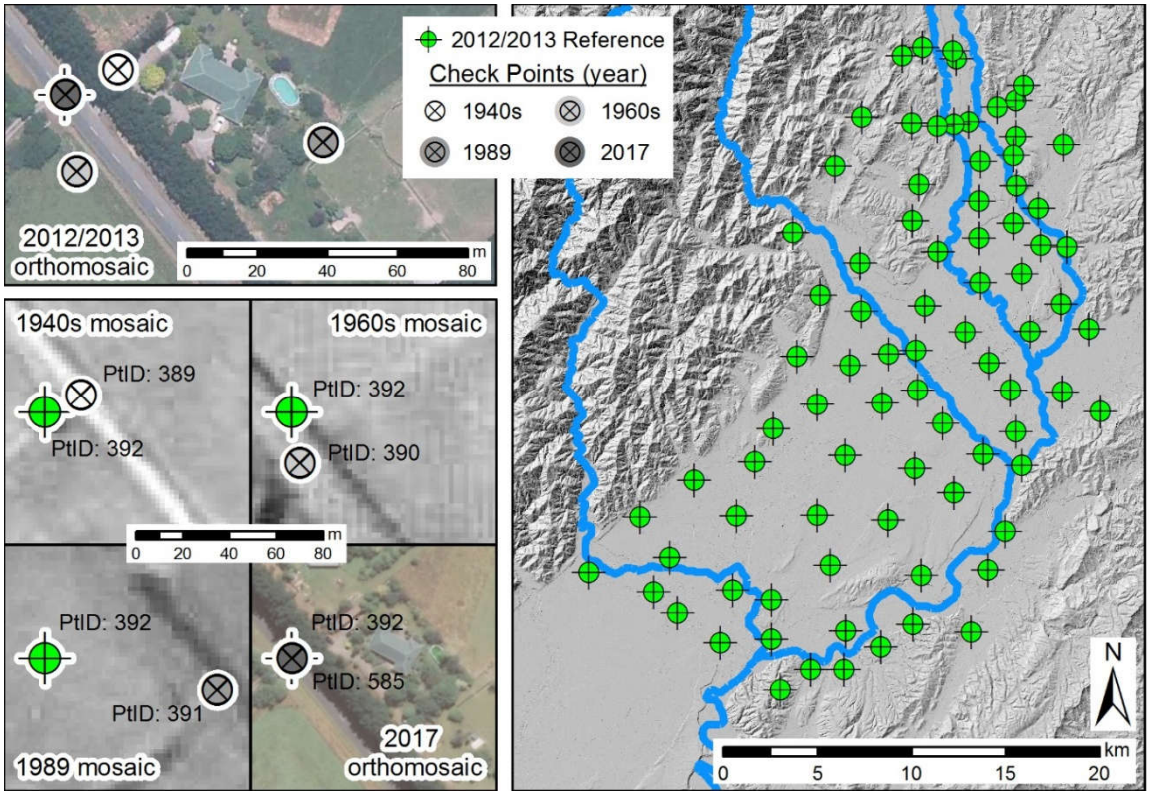

Figure 4-5. Right): Points used to evaluate image co-registration are distributed throughout study area mark ground features in-common and unmodified between time series members. Lower-left: Detail maps of a single co-registration evaluation site location detail reference and check-point placement for a common feature (in this case, a road intersection) for each of four time-steps. Point attributes are presented in Table 4-4. Top-left: Co-plotting of reference and check-points points onto the reference year2012/2013) base image to visualise scatter and contrast variation by time series member.

Table 4-4. Example attribute table structure for reference and check-points; spatial distribution of records with PtID2012 = 392 are presented in Figure 4-5.

PtID2012	PtID	PhotoYear	FeatureType	X_NZTM	Y_NZTM
392	389	1941/1944	road intersection	1817615.658	5463029.663
392	390	1961/1966	road intersection	1817603.964	5463000.599
392	391	1989	road intersection	1817673.973	5463008.978
392	392	2012/2013	road intersection	1817600.352	5463022.447
392	585	2017	road intersection	1817600.741	5463022.457
396	393	1941/1944	road intersection	1822649.446	5457660.962
396	394	1961/1966	road intersection	1822611.743	5457694.300
396	395	1989	road intersection	1822622.458	5457673.265
396	396	2012/2013	road intersection	1822628.861	5457684.206
396	528	2017	road intersection	1822628.743	5457684.509

4.4.5.2 Step 2b: Processing Point Comparisons

After Lillesand et al. (2015), the x and y error components are calculated as:

$$RMSE_x = \sqrt{\frac{\sum\left(x_{chk,i} - x_{ref,i}\right)^2}{n}} \quad \text{(Eq. 1)}$$

$$RMSE_y = \sqrt{\frac{\sum\left(y_{chk,i} - y_{ref,i}\right)^2}{n}} \quad \text{(Eq. 2)}$$

The horizontal RMSE is:

$$RMSE_{horiz} = \sqrt{RMSE_x^2 + RMSE_y^2} \quad \text{(Eq. 3)}$$

If systematic errors are eliminated, x and y errors are independent and normally distributed, and $RMSE_x = RMSE_y$, the 95% confidence horizontal accuracy is:

$$HA_{95} = 1.7308\ X\ RMSE_{horiz} \quad \text{(Eq. 4)}$$

Else, the 95% confidence horizontal accuracy is:

$$HA_{95} = 1.2239\ X\ (RMSE_x + RMSE_y) \quad \text{(Eq. 5)}$$

Point computations were conducted in Python 3.4 in a Jupyter Notebook environment using *matplotlib*, *numpy*, *pandas*, *csv*, *math*, and *os* package dependencies. A text file with coordinate values and point identification fields (e.g., Table 4-4) is imported into a Pandas dataframe, displacement vectors computed, statistics calculated, and plotting is performed. Non-zero displacements between reference points and checkpoints are considered coregistration error.

4.4.5.3 Step 2c: Coregistration Results and Evaluation

To provide a quantitative basis for data suitability determination, Stage 2 results address three key considerations: error magnitude, geographic distribution or error, and directional bias. First, I consider the adequacy of the sample size. A key recommendation of Hughes et al. (2006, Fig. 7) is the generation of probability functions from independent check-points (i.e. not the GCPs used for registration/rectification) for which they present a series of curves whose shape changes from linear to sigmoidal as the number of check points increases. Such plots are sometimes known as cumulative-frequency or empirical cumulative distribution function (ECDF) curves and are populated by study-specific data, as opposed to being based on theoretical statistical distributions. I interpret the general sigmoid shapes of my ECDF curves (*Figure 4-6*) to be indicative of adequate sample size. While I suspect the "steps" in my ECDF curves and shape differences between years may indicate differential influences of different types or subpopulations of errors, detailing such differences is beyond the scope of this paper.

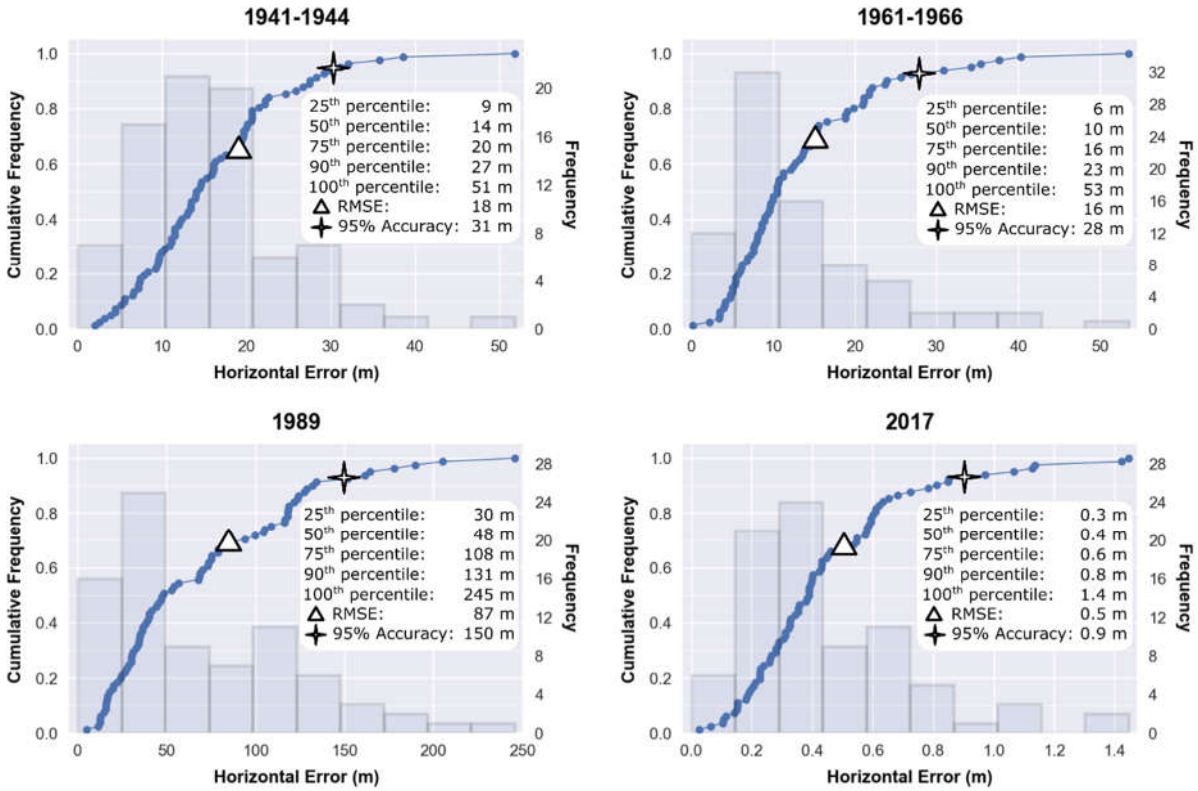

Figure 4-6. Empirical cumulative (line) and probability (bars) distribution functions for co-registration check-points show non-linearity and non-normality. RMSE and 95% Accuracy are calculated per Equations 3 and 5, respectively. RMSE values represent only 30-36% of the maximum observed error magnitude. Equation-based 95% accuracies generally underrepresent the empirically determined values.

4.4.5.3.1 Error magnitude

To a degree, this is the one element of positional uncertainty that RMSE can address, albeit as noted in Part 1, imperfectly. At the coarsest level (spatially-averaged) only the 2017 mosaic met my desired 5 metre criterion (Table 4-5) with very good coherence with the reference mosaic. The legacy mosaics (1940s, 1960s, 1989) generally have large average errors (Table 4-5), many times larger than my criterion. Perhaps most interesting is that for all four datasets (including the high-quality 2017 mosaic), 1) displacement magnitude is not normally distributed (*Figure 4-6*) and 2) the plotting position of RMSE is consistently between 65 and 75% of cumulative probability. Importantly, RMSE magnitude represents only 30-36% of each dataset's maximum observed error. In other words, there's a good chance of 30 m error hot-spots lurking within a dataset that has an RMSE of 10 m. Such error hot-spots can be expected to have a greater effect on mean error (e.g., RMSE) than other statistical measures of central tendency (e.g., median).

While budgeting contributions of different error sources is beyond the scope of this paper, it is worth noting that if error magnitude were simply related to pixel effects, I might expect a 4-6 metre error (2-3 × the pixel size). However, RMSE for the 1940s and 1960s is three to four times greater and the RMSE value of the 1989 mosaic is eight to fourteen times greater, suggesting the influence of other errors. Judging by the empirical cumulative distribution functions (ECDFs), approximately 95% of control points for the legacy mosaics had error magnitudes larger than what might be attributed to pixel-scale effects. By contrast, the accuracy of the 2017 mosaic is three times the pixel size with 90% of checkpoints occurring within a 2-pixel (0.6 metre) radius of reference points.

Table 4-5. Spot-checking estimates (from Stage 1) and summary statistics (from Stage 2) for horizontal co-registration check points (n = 84) for four mosaics compared to 2012/2013 reference orthomosaic.

Mosaic	Spot-Checking (Stage 1)	Quantitative Screening (Stage 2)					95% Accuracy	
		Min.	Max.	$RMSE_x$	$RMSE_y$	$RMSE_h$	Eq. 5.2[a]	Eq. 5.3[b]
1940s	6-31 m	2	51	13.3	12.5	18.2	31	31
1960s	4-10 m	0	53	10.1	12.9	16.4	28	28
1989	>= 122 m	4	245	62.9	59.8	86.8	147	150
2017	<=1 m	0.0	1.4	0.4	0.3	0.5	0.9	0.9

[a] *per Eq. 4* [b] *per Eq. 5*

4.4.5.3.2 Geographic distribution

The spatial arrangement of errors can help identify areas of bias, potential error sources and/or assist triage of areas less critical to study objectives. All four mosaics exhibit spatially-explicit variability (hot spots) in error magnitude (Figure 4-7), although the geographic distribution for the 2017 mosaic is reasonable, considering the small displacement magnitudes (Table 4-5) that are all within the 2 metre published accuracy (LINZ2018). By contrast, the arrangement of errors in the 1989 mosaic is very patchy, with errors whose spatial distribution would likely render most change detection unreliable. Geographic error distributions for the 1940s and 1960s mosaics tend to transition less sharply than the 1989 mosaic but are still sufficiently large and variable that they could be a significant source of interpretative error at the landscape scale, though small-scale (1:50,000) visualisation and/or length measurements in the lower two-thirds of the study area may be acceptable. The legacy mosaics seem to exhibit a general trend of smaller error magnitudes in proximity to major roads and denser human habitation, likely due to the originally intended application of the dataset (tax parcel classification).

4.4.5.3.3 Directional consistency

Vector maps (*Figure 4-8*) indicate angular orientation of errors relative to reference points. This is variable for all four mosaics, supporting a conclusion that observed errors are not due to mathematical artefacts from differing coordinate systems or datums (which would be expected to give rise to more uniform vector distribution). Polar plots (*Figure 4-9*) standardise all reference points to the same coordinate value (e.g., 0, 0) at the centre of the plot, with each checkpoint displacement represented as a residual whose distance and direction from the centre of the target indicates the orientation and magnitude of displacement of a check point from a reference point. These can be helpful in detecting directional bias. The 2017 mosaic has a well-distributed polar plot (with only slight directional bias) and small error magnitudes, making it highly suitable for the purpose of measuring channel changes and sediment budgeting. However, for the legacy mosaics, the polar distributions indicate an average bias to the northeast, north, and south for the 1940s, 1960s and 1989 mosaics, respectively. The scatter distribution indicates that bias cannot be easily corrected (*Figure 4-8*), such as by simply shifting in a particular direction (e.g., a horizontal datum offset).

The landscape scale of my investigative purpose also means that errors cannot be locally ignored and creates a decision point to either use as-is or reprocess from the raw digital image tiles. Instead of investing time trying to refit already altered imagery, I started over with high quality scans and good-quality control points based on a vetted reference layer (e.g., *Figure 4-3*, bottom). Aside from time savings specific to my use-case, this approach of starting with the raw data increases certainty in the outcome by pre-empting GIS blunders present from earlier processing (section 4.4.4.1) and is consistent with the fundamental scientific principle of reproducibility.

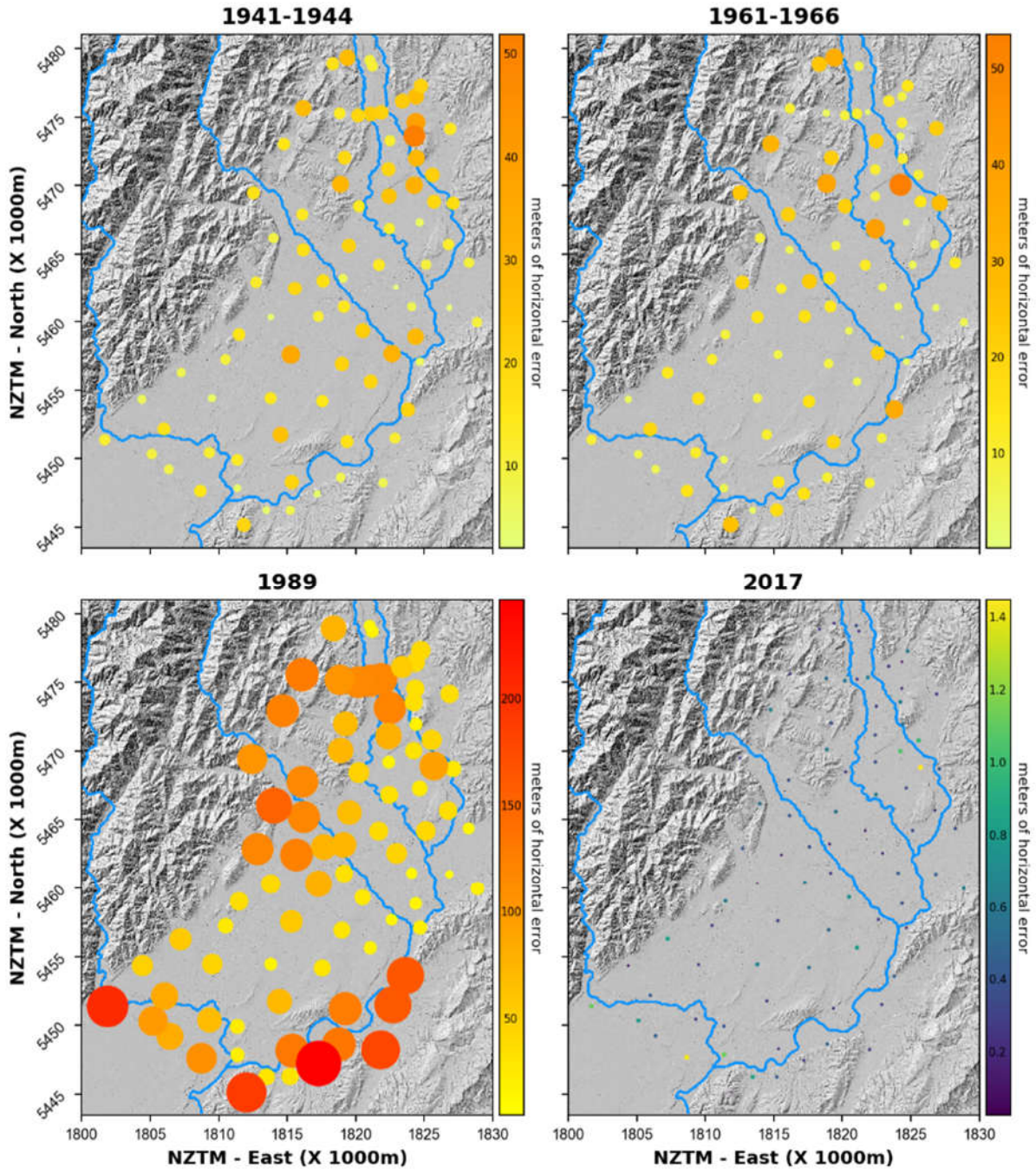

Figure 4-7. Geographic distribution and horizontal displacement magnitude for 84 check-points for each of four mosaics compared to 2012/2013 baseline.

The sequential application of Stage 1 and Stage 2 tells the same story, with Stage 2 providing hard numbers supporting trends suggested by Stage 1. The large range of error magnitudes and varied spatial distribution through time necessitate caution in proceeding into geomorphic analyses and should prompt the operator to consider the purpose(s) for which each individual dataset is suited prior to making any intercomparisons. While Stage 1 was sufficient to determine that the legacy mosaics were unfit for this study, the Stage 2 process provides a quantitative foundation to justify alternate effort (e.g., reprocessing raw source imagery) and enables creation of error surfaces. Where analysing datasets with such a wide spread of coregistration error and skewed statistical distributions, it is more appropriate to use the empirically determined 95% confidence interval (Eq. 5) rather than the RMSE (Eq. 3) which assumes a normal distribution.

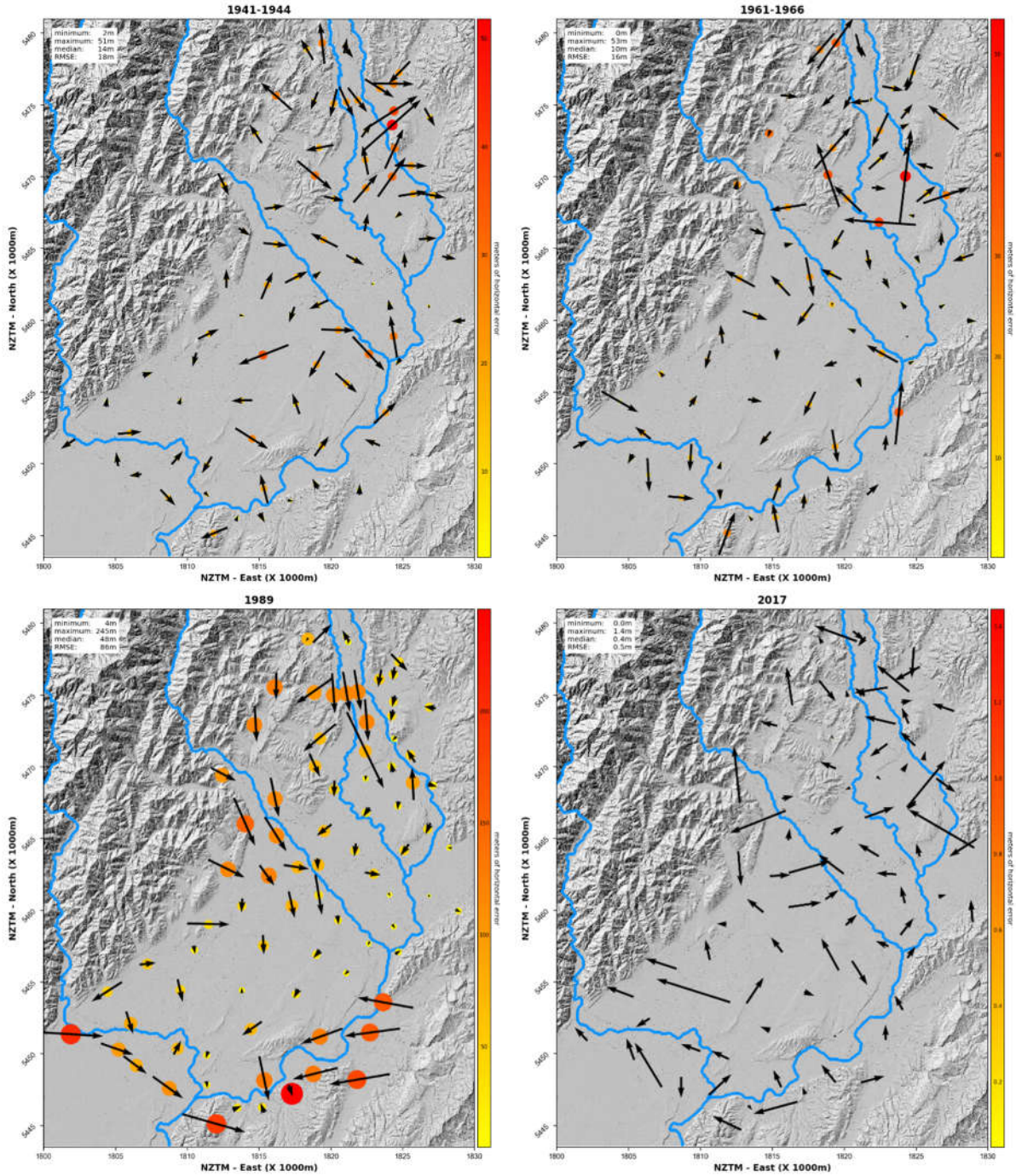

Figure 4-8. Geographic distribution of check point displacement direction (arrows) and magnitude (point radius & colour) for each of four mosaics compared to 2012/2013 baseline.

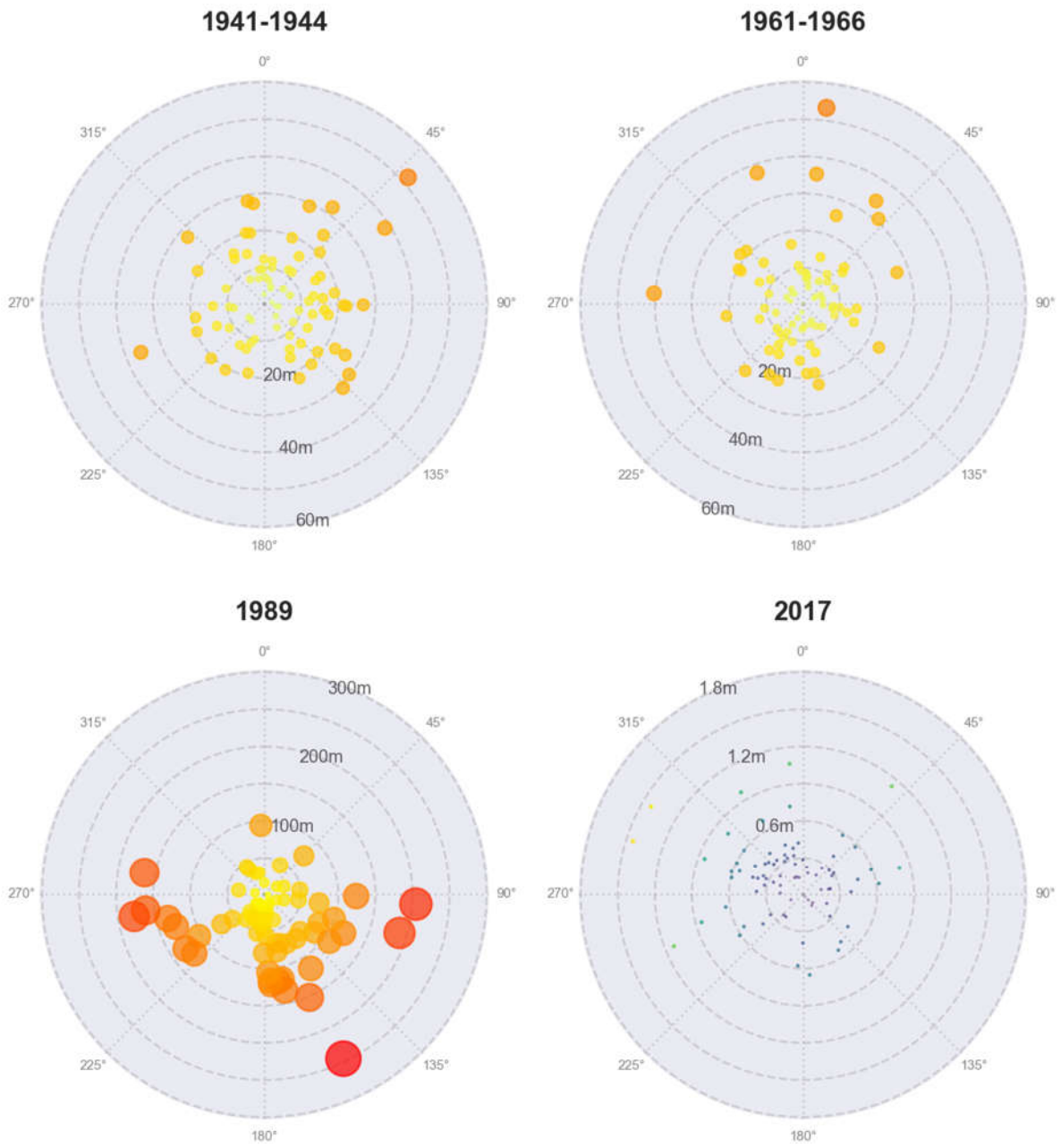

Figure 4-9. Polar plots show angular distribution of check points displacement relative to reference points. If plotted, all reference points would be located at the origin.

4.5 Data suitability framework and change detection hierarchies

The features, processes, and/or relationships of interest collectively across studies are vast and study-specific. Hence, it is customary that data suitability determinations are specific to each study (Chrisman, 1982; Hunter and Goodchild, 1993; Lillesand et al., 2015) and should remain so given that uncertainty depends on intrinsic data properties and context of use (Deitrick and Edsall, 2008). The preceding section provides quantitative and descriptive means to characterise individual data sets by comparison with a common reference. However, geomorphic time-series analyses usually evaluate change between each step. Because uncertainty also depends upon considerations such as training and experience of personnel involved (Hunter and Goodchild, 1993; Deitrick and Edsall, 2008), decision frameworks offer a means of consistency. Given the increasing breadth and depth of users' skills in generating and employing geospatial data to evaluate geomorphic changes, I propose a

typology for assessing data suitability (*Table 4-6*, Figure 4-10). My hierarchy links the three Stage 2 positional quality questions with analytical intent to aid visualisation of alignment (or misalignment) of data capability.

Table 4-6. Hierarchies, dimensionality, and correspondence needs for spatiotemporal change detection using aerial imagery. Accuracy and precision ranges in the table are qualitative and intentionally broad as they are ultimately case-specific, depend on investigative purpose and scale to the change magnitude intended for detection.

<table>
<tr><th rowspan="3">Change Type</th><th colspan="3">Analytical Intent</th><th colspan="3" rowspan="2">Minimum Positional Quality Needs</th></tr>
<tr><th rowspan="2">Comparison</th><th colspan="2">Changes of Interest</th></tr>
<tr><th>Displacement or deformation</th><th>Physical Dimension</th><th>Spatial Reference</th><th>Co-registration Accuracy</th><th>Positional Precision</th></tr>
<tr><td>0</td><td>Qualitative</td><td rowspan="3">No / Qualitative/ scalar</td><td>None (Presence-Absence)</td><td rowspan="2">Relative</td><td>Low</td><td>Low</td></tr>
<tr><td>1</td><td rowspan="3">Quantitative</td><td>None (Feature abundance)</td><td rowspan="2">Low to medium</td><td rowspan="2">Medium to high</td></tr>
<tr><td>2</td><td>Length</td><td>Common coordinate (relative OK)</td></tr>
<tr><td>3</td><td rowspan="2">Yes / Quantitative/ vector</td><td>Area, length</td><td rowspan="2">Common coordinate (absolute preferable)</td><td rowspan="2">Medium to very high</td><td>High</td></tr>
<tr><td>4</td><td>Volume, area, length</td><td>Very high</td></tr>
</table>

Base imagery can be used for purposes ranging from qualitative observations requiring no spatial reference through to quantitative observations and measurements in which positional accuracy and spatial reference needs change depending on intent. Spatially explicit change characterisation may include questions of A) presence/absence, B) abundance, C) linear extension/contraction or displacement and/or D) areal and volumetric deformation or displacement of features or surfaces which, combined with scale, ultimately dictate minimum positional quality needs. These needs can be represented as a hierarchy from Type 0 (minimum) to Type 4 (maximum) change detection (Table 4-6). For example, the legacy mosaics in this case study may be suitable for Type 0, Type 1, or possibly Type 2 change detection. Data quality may also inversely dictate the type of change detection that is feasible.

I suggest that analytical intent for most geomorphic change detection studies can be differentiated based on 1) dimensionality and 2) relationships (e.g., displacement and/or deformation). Their combination determines a change "type", which in its least intensive form (Type 0) might be as simple as looking at two images and seeing that a particular hillside is forested in one image but not in another (general character or presence-absence). In Type 1 change detection, abundance is the analytical focus such as the number of unvegetated river bars on a river reach. Measurement comes into Type 2 detection but mainly to characterise features (e.g., total length of unvegetated bars on a river reach) though the change in distance between a static feature and a spatially variable feature (e.g., terminus of a glacier) could be considered Type 2. Type 3 and 4 change detections address feature movement or other displacement and are differentiated based on whether the interest is two- or three-dimensional change, respectively. While purpose will generally be the primary interest, typing should be thought of as quality-driven or enabled. For example, a dataset suitable for Type 4 change detection is suitable for all other types because of its quality and isn't downgraded to Type 3 quality if only used for planimetric analysis.

Investigative purpose, and hence differential accuracy and precision needs, can be expected to vary by sector. For example, the importance of detecting small changes in channel position in time is a

more typical investigative purpose for management. By contrast, geomorphic research tends to focus on thresholds, changes in pattern and other signs of altered dynamics that may be detectable without a high degree of absolute accuracy. Thus, contrary to common stereotypes, greater data rigour and coregistration accuracy will likely be required of river management applications.

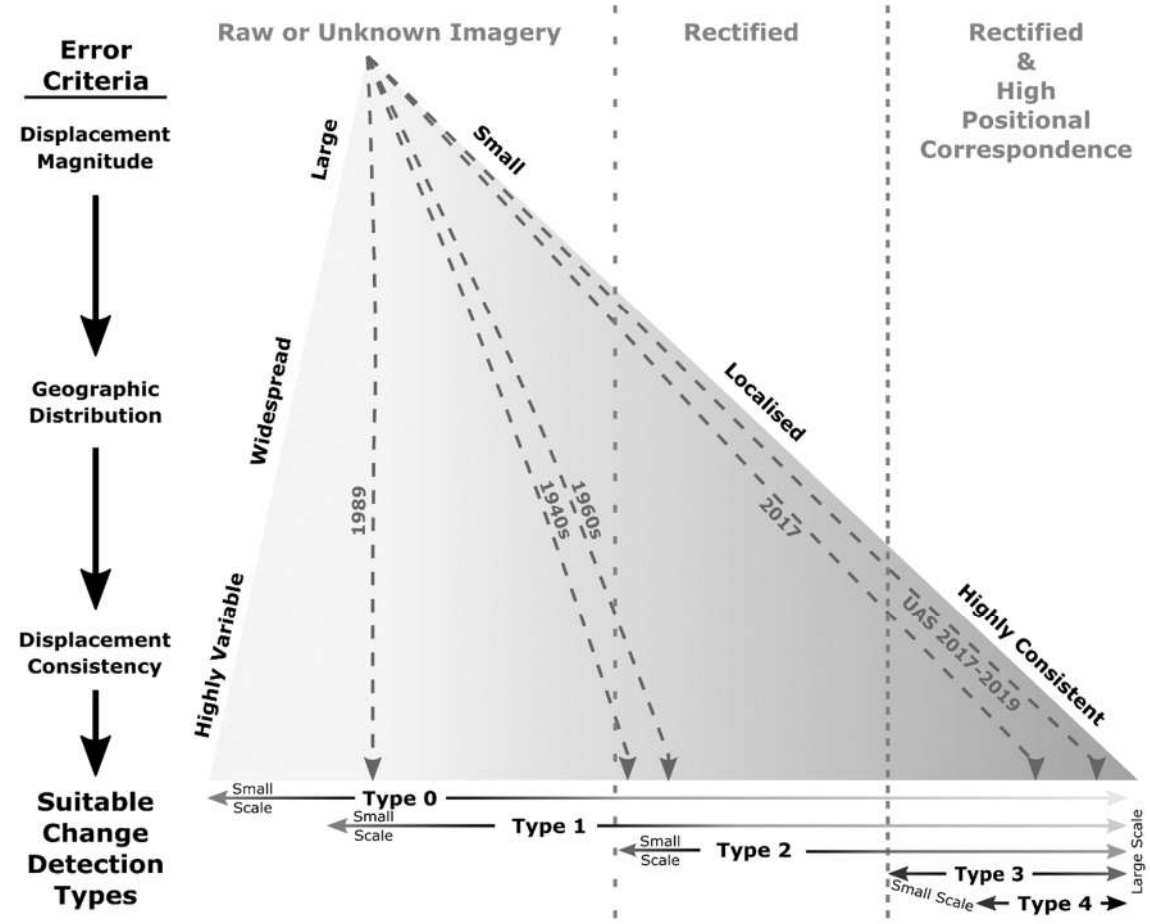

Figure 4-10. Graphical framework for Phase 2 suitability screening where the triangle represents the data domain and typing (bottom) relates to Table 4-6. Location of the triangle's tip indicates assumed data fitness is only suited to more rudimentary (lower numbered) change analysis type. Intensity of areal shading is proportional to data processing rigour; area of sub-domains created by quality thresholds (vertical lines) are symbolically representative of the proportionality of data suited to a particular type. Detailed discussion of error criteria (left margin and side of triangle) occurs in "Stage 2 – Quantitative Screening". Sloping, hashed trajectories represent the case-study mosaics and are supplemented with the UAS SfM imagery generated with a high density of RTK ground control. Pathways through the triangle are not necessarily linear, though are likely in practice.

Type 0 and 1 comparison can be expeditiously performed on hard copies or digitally where the spatial referencing is simply notional (i.e., occurs in the mind of the observer). Type 0 merely requires the observer to know that they are looking at the same spatial unit whether it be by vegetation, infrastructure, or visual matching of other landscape patterns. Type 1 and 2 change require more specific control to ensure consistent spatial unit boundaries such as provided by bridge crossings, stone walls, valley confluences, and the like. Minimum data requirements and handling rigor increases as spatially explicit dimensional change becomes the analytical interest. Time series for Type 3 and 4 change detection must share a common spatial reference with a degree of coregistration (accuracy and precision) suitable to meet study objectives.

The boundary between Type 2 and Type 3 detections can be difficult to appreciate but is very important and lies at the heart of how photogrammetric practice addresses the myriad of things

(which many of us prefer not to think about) that cause the raw detection of the things I care about as a geomorphologist to be distorted. In the absence of orthocorrection, length can be reasonably estimated by calibrating to known dimensions within the same photo frame. For example, known values (e.g., width of a roadway or wall length of a building) may be used to create a scaling or correction factor. Hence, Type 2 analysis can be done without rectification (correction to a planimetrically-correct base). However, once Type 3 (area) change detection is desired, imagery should be rectified (orthocorrection is one form). As noted by Jensen (2000, p. 178), "it is not good practice to digitize polygons from unrectified…photomaps", a sentiment that is as true today as it was when written twenty years ago.

To further help to evaluate fitness for purpose and to narrow the permissible types of change detection for a given dataset, a visual integration of Table 4-6 with framework components, key data conditions, and key error criteria is presented (Figure 4-10). The top of the graphic provides a coarse metadata categorisation related to data needs in Table 4-6. The three error criteria on the left margin relate directly to the questions addressed in Step 2c: Coregistration Results, though the figure treats them on a conceptual level. The vertical hashed lines represent data screening thresholds and divide the triangle into subunits whose areas provide symbolic scaling of the proportion of the data domain that might be satisfactory for given analysis types. Shading within the triangle represents a hypothetical gradient of collection, processing, and analytical intensity with darker regions indicating greater rigour (and cost). Areal shading can also be thought of as the burden-of-proof necessary to assert a dataset is suitable for a particular analysis. Lines across the bottom of the graphic indicate the typing spectrum and scale-dependency for which data passing vertically out of the triangle are suitable with more intense shading indicating ranges where cost/benefit may be optimised. While data suitable for Type 3 or 4 detection are also suitable for types 0, 1, and 2, costs of acquisition/production may be unwarranted if, for example, the sole intent is determining presence/absence (unless trying to detect very small features).

The top-down workflow is oriented from the perspective of an end-user who has received data and needs to determine what it can reasonably be used for. Specific knowledge of data origin is not required, though it is possible they have collected the data themselves. My experience, illustrated by the preceding case study, promotes caution, and suggests the default position when initiating an investigation should be to assume, until proven otherwise, that legacy data are suitable for only Type 0 or Type 1 change detection. Something akin to my Stage 1 process (though not necessarily requiring formalised mapping) should be a minimum for proceeding to Type 2 analysis. Type 3 or 4 analyses should require formal quantitative documentation (metadata by others is acceptable).

The annotated diagonal dashed lines on Figure 4-10 offer some examples of the top-down utility of *Figure 4-8*, from my case study mosaics evaluated in Part 2 and an additional UAS dataset. All five datasets initially begin at the top of the triangle as "unknown" until they have been scrutinised using the two-stage approach presented in Part 2. Generally, the three legacy mosaics (1940s, 1960s, and 1989) are only suitable for medium- to small-scale analyses (e.g., coarser than 1:20,000). The large, widespread, and patchy errors of the 1989 mosaic may be tolerable for Type 0 and Type 1 studies at small scales (e.g., 1:50,000). However, the evaluator would still need to consider if study objectives could be met given discontinuities in curvilinear features (e.g., streams and roads) and areas of missing data (*Figure 4-4*). The 1940s and 1960s mosaics appear to have had some rectification applied which, makes them potentially suitable for Type 2 analysis, though feature discontinuities would still need consideration. While they are likely fine for Type 0 and 1 analyses at larger scales (e.g., 1:10,000), high coregistration errors limit Type 2 use to smaller scales (e.g., no better than 1:20,000). The high quality of the 2017 orthomosaic is very well-suited to Type 3 analyses at most scales (e.g., 1:1,000) and, though not explicitly evaluated, the raw imagery with control elevations from the

LiDAR could likely generate an elevation model worthy of smaller scale volumetric studies (1:10,000 to 1:20,000). The UAS 2017-2019 example relates to multitemporal surveys I have conducted within part of the spatial extent of the case-study mosaics. The dataset has a 3 cm nominal image resolution and RTK GPS ground-control with independent coregistration better than 0.15 metres across eight field collections. This makes it highly suitable for planimetric or volumetric (e.g. SfM) Type 4 change detection at better than 1:1,000 scale. Table 6.5 in Gilvear and Bryant (2016) may be useful to consult regarding mapping scale relative to project intent.

While Figure 4-10 favours top-down flow, it may also be used top-up when planning a study. For example, at the outset of a study to characterise sub-reach river channel dynamics by measuring spatially-explicit changes in volume, Table 4-6 indicates a Type 4 change detection and Figure 4-10 (entering from the bottom) identifies data needs including spatial-correspondence. Because the study scope is sub-reach, the data needs occur toward the more rigorous end (larger scale) of the Type 4 spectrum.

From the resource manager's point of view, the framework can be used for tailoring data collection to better address management triggers or thresholds. For example, if control treatments are implemented based on a response trigger of 1 metre bank erosion for a 50-metre-wide active corridor, then attempting Type 3 analyses based on images with 25 metre of registration error are likely of little value. By contrast, the same images may be perfectly acceptable for classifying ground cover types (Type 0 or Type 1) for large tax parcels (many dozens to hundreds of acres) in rural areas at regional extent.

4.6 Discussion

The large- and small-scale scale case studies presented in this chapter provide caution for customary "as-is" or assumed data analysis without a proper assessment. Based on decades of experience analysing archival data, it is common for fitness to vary differentially, though some of the displacement magnitudes (> 200 metres) within the example time-series are extraordinarily large. Poor documentation often foreshadows the presence of latent quality issues. The importance of metadata increases proportionally with the diversity of collection platforms, producers, and rectification methods. The diversity of data provenance in the example time-series makes this case study highly typical of real-world situations experienced by managers, consultants, and some researchers and begs the need for proper uncertainty characterisation

4.6.1 Characterising Uncertainty

Valid application of common metrics (e.g. RMSE and 95% Accuracy) require normally distributed and/or random errors (Lillesand et al., 2015). However, the case-study and experimental data call into question the customary assumption of normally distributed data. Specific to error magnitude, even the best-case comparison of the highest quality mosaics (2012/2013 and 2017) produced a skewed statistical distribution suggesting traditional means of evaluation predicated on normality are probably not as safe as first thought. The maximum residual was approximately three times the RMSE for each of the four mosaics indicating a lack of accounting of, in some cases, very sizable errors. Further, when considered within the intercomparisons of the experimental data, the errors in the case study data grow even larger in a change detection context.

Approaches based on the empirical distributions of individual data sets (Hughes et al., 2006) seem quite robust in terms of magnitude and compared to averaging errors. If I must select a single measure of magnitude, then a value at the inflection of the ECDF curve's upper shoulder, 95^{th} percentile or similar is more appropriate than a measure of central tendency like RMSE. Coupled with characterising the distribution's spread (e.g., n^{th} to i^{th} percentiles) would reflect uncertainty for

any single measure. As an analogy, consider that grain-size distributions have been expressed as such (e.g. D_{16} : D_{84}, etc.) for at least sixty years. Just as an average particle size is inadequate for characterising sediment populations (much less estimating transport), so is RMSE a crude approximation of spatial error.

Moreover, characterising the distribution of the error magnitude still only provides a glimpse of the error picture. To continue with a sedimentary analogy, I should be wary of using methods that 'bulk' grain-size distributions across hydraulic environments (e.g. Kondolf, 1997a), but do not practice the same effort representing error variation in more routine use of maps and aerial photographs. The importance of identifying and, if possible, filtering, correcting, and/or propagating spatially-explicit errors is well-recognised in the 3D literature (e.g. Monckton, 1994; Lane and Chandler, 2003; Carbonneau et al., 2006; Wheaton et al., 2010b; Carley et al., 2012; Schaffrath et al., 2015; James et al., 2017; Anderson, 2019) and seems to have gained ground in practice due to improved user accessibility of software products like 'GCD' (Wheaton et al., 2010b) By contrast, the frequency with which RMSE is used as a change detection threshold for planimetric studies reflects less consideration. Though viable methods of accounting for planform error exist (e.g. Brunsdon, 1995; Lea and Legleiter, 2016a) specifics of implementation require a greater degree of expertise and/or are associated with proprietary software (e.g. MATLAB, SAS) to which relatively few practitioners have access. While means for quantifying exist, the most intuitive and, I believe, first-order approach to spatial uncertainty should be visualisation (sensu Hunter and Goodchild, 1993) and I suggest the combination of plots and maps I have generated (*Figure 4-5* through *Figure 4-9*) fully satisfy characterisation of planimetric spatial error.

4.6.2 Implications for Change Detection Suitability

The framework described here is oriented toward screening individual datasets and aid the portion of a project where an investigator wrestles with the question, "Even though the GIS will let me use it, should I?" Once suitable datasets are determined, there is still a need to account for error and uncertainty. As indicated by my experimental data (Figure 4-1) and vividly demonstrated in the large-scale case study (*Figure 4-3*) it is necessary to explore the relative error between any two time-steps when assessing fitness for change detection, and not simply assume the error (or accuracy) of any individual dataset to a common reference is representative. Effects at the study area scale can be visualised by comparing error distribution maps (*Figure 4-5* and *Figure 4-7*). Patchy geographic distribution of displacement magnitude is compounded by geographic shifts of directional displacement through time for many locations. The importance of awareness of directional effects becomes greater as displacement magnitude increases. As a result, there are very few geographic subunits within the study area where the time-series analysis could be focused using the imagery as-is. That said, it is unclear how robust exclusion of unsuitable areas would be given standard accuracy calculations don't adequately encapsulate error between time-steps. Considering the false-positive (detected change that didn't happen) scenario of the large-scale case study, the 34 m of apparent change is nowhere near the maximum displacement magnitude (51 and 53 metres for 1940s and 1960s, respectively) identified for either dataset , yet still exceeds the calculated 95% accuracy of both the 1940s (31 m) and 1960s (28 m) mosaics (Table 4-5, Equations 4 and 5).

In terms of setting change detection thresholds, the spatially-averaged approach that Hugenholtz et al. (2013) applied to calculate a vertical threshold (T) based on extreme tails of a normal distribution is:

$$T = \pm 3 \times \sqrt{{RMSE_1}^2 + {RMSE_2}^2} \quad \text{(Eq. 6)}$$

Where $RMSE_1$ and $RMSE_2$ are the is the root mean squared error of control point displacement for images 1 and 2, respectively, compared to some reference. When adapted to my planimetric data, it captures the worst (1989 vs. 1940s) case-study comparison, though the multiplier of three seems overly conservative for data generated in my numerical model. The fixed-dimension buffer approach (e.g. 5 m either side of river channel) of Hughes et al. (2006) is another option. They determined a buffer 1.25 times the RMSE of their best rectification model (second order polynomial with 30 GCPs) mitigated 90% of the georectification error. However, they also found that calculated rates of channel movement in areas with relatively little change might reflect buffer size more than actual channel change. The at-a-station approach of Mount and Louis (2005) scales calculations of 'real' change (e.g. in channel midpoint) depending on assumptions (e.g. independence of directional and/or temporal errors, homogeneity of random error). While their specific method is potentially quite labour-intensive if continuous, high-resolution measurements are needed, their assertion – that favourable assumptions should not be made unless there is clear evidence for doing so – is universal. Given modern computing power and software, using a continuous, spatially explicit error surface probably works-out better in terms of cost:benefit. Using an interpolated error surface, Lea and Legleiter (2016b) leveraged spatially-explicit errors to both reduce local detection thresholds (i.e. increased ability to detect change) and similarly reduce both false-positive and false-negative results. While desirable, application of this approach depends on having enough suitable points across the study area to create a representative error surface. Overall, while co-registration sameness of one dataset to another is critical for change detection analyses, it could be argued that knowledge of wrongness continuously and at any point in space is better than summarising sameness across space. However, one must be careful in interpreting how continuous uncertainty estimates are computed and applied, particularly if derived from point-based measurements used for thresholding (Anderson, 2019) to generate net estimates of volumetric change.

4.6.3 Changing Perceptions and Influence of Scale

Mapping scale has traditionally been a suitable correlative consideration for what an investigation was feasibly able to accomplish based on resource availability. Due largely to limitations of data access and rigors of compilation, small and very small-scale (e.g., 1:1,000,000) studies have traditionally been performed with data of coarse resolution. This has shaped the development and continued acceptance of linkages between variable dependence/independence and spatiotemporal scales identified by (Schumm and Lichty, 1965). Modern desktop computing, web-based data storage and sharing, a plethora of high-resolution aerial and space platforms, and automated and semi-automated segmentation processes now make it possible to accurately and precisely quantify phenomena that were historically treated at larger scales (e.g., <1:20,000).

Eventually, researchers will seek to complement sub-continental empirical models (e.g. Hicks et al., 2011) by assigning processes (e.g. bank erosion). There will be great temptation to assume that higher resolution and broader spatial extent translate to robust inputs, but it is important to recognise that modern GIS facilitates work at precisions "much, much higher than the accuracy of the data themselves" (Unwin, 1995). Cucchiaro et al. (2020) demonstrate the risk of assumed co-registration with a 95% reduction in net sediment transfer volume detected once LiDAR-derived DTMs are properly aligned. Despite the sophistication of modern data products and computing, user-discretion is still the fundamental check on whether numerical results are an academic exercise or have applicable meaning. For my case study, higher-resolution, but similarly-registered legacy base images will produce results that are more visually pleasing, though bank locations will be every bit as incorrect.

4.6.4 Data Lineage

The lack of fitness of the legacy mosaics for my purpose (1:1,000 mapping) is less a function of old vs. new and more about how data were processed. Aside from differences in positional accuracy, *Figure 4-3* illustrates the gain or loss in image quality that can result from different handling and/or processing pathways. All three images originated from the same negative frame on the same roll of film on the same flight. However, source imagery for the top mosaic was likely scanned from prints and its blurry and dark character makes resolving features less certain. The middle panel is sourced from a scan of the negative and down-sampled to the same (2 m) pixel resolution as the top panel though with more favourable colour balance and contrast for differentiating individual features and their shadows. Because of the low-relief setting, the high-quality orthomosaic of the bottom panel (sourced from multiple frames scanned from negatives) effectively tells the same (lack of) bank migration story as the middle panel (single frame with second order rectification). As more and more data are collected by an increasing number of individuals across growing spectrums of training, expertise, and inclinations towards data processing and documentation rigour, lineage will remain a growing issue into the future, and likely increase the need for a suitability grading system (such as my typology).

4.6.5 Advancing Practice

Considering Marcus and Fonstad's (2010) call for development of software products to accommodate non-expert users, there has been tremendous growth in the availability of analytical tools over the last decade. Repositories and toolsets such as CSDMS, CUAHSI, OrfeoToolbox, Riverscapes, WhiteboxTools, etc. provide an almost overwhelming variety of analytical tools, including many non-proprietary options (e.g., without MATLAB, SAS or ESRI dependencies). However, I suggest that with a few exceptions (e.g. 'GCD' by Wheaton et al., 2010b), most do not facilitate non-expert uncertainty characterisation or propagation. Similarly, there are no easily implemented native functions within popular GIS software (e.g., ArcGIS or QGIS) for evaluating or presenting such distribution functions. To partially address this void and promote methodological uptake, I have developed a Python-based tool, GeoDisPy ("Geospatial Displacement Python"), that facilitates the Stage 2 analysis I have presented. While the tool requires some *a priori* knowledge of Python, the approach provides graphical outputs that are easily and rapidly understood to increase certainty and strengthen results.

Despite the inadequacy of RMSE for thresholding or characterising coregistration fitness, I concur with Hughes et al. (2006) that it is an acceptable estimate of average error magnitude when input points are independent from points used in transforming imagery. Combined with ease of calculation and widespread familiarity, RMSE has persistent value in preliminary error structure evaluation. More specific to volumetric change detection (Type 4) uncertainty, increased awareness that thresholding is not necessarily the same as error propagation and retains uncharacterised uncertainty will become increasingly important.

Anderson (2019) provides thorough discussion of volumetric error propagation to quantify systematic error remaining in a DEM-of-Difference after coregistration and thresholding. One of his key premises is that systematic errors are still present within thresholded measurements considered to be "real". However, such latent errors go unquantified in the absence of propagation analysis and accumulate when integrated over large areas. Further, thresholding treats real, but sub-threshold changes as zero even though they may aggregate to be statistically significant. Awareness of such uncertainty is important to all analysis, though effort made to reduce and quantify errors should be scaled to analytical goals (Anderson, 2019). In a thorough review of uncertainty concepts and linkages in river restoration, Wheaton et al. (2008) present a broadly applicable (and adaptable)

framework that fundamentally differentiates between uncertainty caused by variability and uncertainty caused by lack of knowledge. Applied to my scope of coregistration of remotely-sensed data for spatially-explicit change detection, practices that ignore or express uncertainty as single, spatially-averaged metrics keep both pathways in-play. I propose that application of work presented and referenced in this paper that explicitly recognises and characterises spatial structure of positional errors enables uncertainty-related decision-making to focus resources addressing variability side of Wheaton et al.'s (2008) framework.

4.7 Conclusion

Scientific process is often a balance of the exhilarating and the mundane. While coregistration assessment of base imagery clearly falls into the latter and the amorphous nature of uncertainty creates discomfort, the quality of change detection interpretation and derived results are fundamentally linked to input quality. Though formal data suitability evaluations may be viewed as a nuisance that slow down and/or increase cost of investigative processes, they occur along a spectrum of rigour and, depending on investigative purpose, may be addressed by qualitative review. It is not my position that all data be made absolutely accurate. Nor do I suggest the need for forensic error reconstructions or exhaustive error budgeting as I believe treating sources of positional error in composite is adequate for the need and scope of most geomorphologic investigations. That said, some form of explicit consideration of data quality fitness-for-purpose should be a requisite step to ensure verity of the more exciting parts of geomorphic investigation. Moreso, the need for rigour increases when investigative purpose includes legal, financial, and/or land-use issues. There is a strong case for raising the standard for uncertainty awareness and understanding its effects on change detection, interpretation, and communication. The fitness framework presented in this chapter provides an implicit means of scaling uncertainty (and rigours of characterisation) to analytical purpose.

Evidentiary documentation and rationale communication remain important challenges to applied geomorphology in general (Hooke, 2019) and increased frequency of geomorphic investigations within administratively or legally regulated contexts (Wohl, 2014) reinforce more specific calls for greater quality assurance (sensu Thorne, 2002). While it is good practice to understand the precision (or otherwise) of one's data, the veracity of data becomes increasingly important when dealing with hazards such as flood protection or slope instability. The results of the experimental and case-study presented in this thesis clearly demonstrate limitations of single, spatially averaged metrics for characterising error and accuracy, and reinforce the previously identified inadequacy of metrics such as RMSE for characterising individual datasets. More importantly, using a single RMSE value for a time series referenced to a common source for a change detection threshold represents a statistically improbable (fifth percentile) condition and is unwarranted. I hope to stimulate "rationale scepticism" at the heart of scientific inquiry (sensu Osborne, 2010) and have demonstrated a constructive approach for doing so.

As remotely sensed datasets become increasingly abundant from increasingly diverse sources, positional quality will need to be approached less casually than in the past for documenting spatially explicit change. End-users will increasingly need to conduct (and funders to fund) formal data screening as a standard workflow component. This is particularly important for projects with public safety implications, such as flood protection and other hazard-related investigations. When applying my framework to such consequential projects, it may be appropriate to adjust "type" up a level as a data quality factor-of-safety (i.e., an error buffer). The default assumption should be that photomosaics are not fit for anything more rigorous than Type 1 change detection unless documentation exists confirming otherwise.

While RMSE provides a reasonable estimate of average error magnitude, it should be viewed as a best-case metric for thresholding change. Its ease of calculation and well-entrenched use make it highly relatable, though users should proceed with the awareness that it may only provide roughly 5th percentile error confidence (i.e., equalled or exceeded 95%). However, the traditional dependence on RMSE should consider the 200+ year wisdom of Robert Burns; "There is no such uncertainty as a sure thing". Accuracy calculations and/or other documentation based on assumptions of normally-distributed error should be viewed cautiously and, ideally, cross-validated by reviewing a dataset's empirical distribution derived from independent check-points (e.g. Hughes et al., 2006). Thus, where analysing datasets with wide coregistration error spreads and/or skewed statistical distributions, it is more appropriate to use the empirically determined 95% confidence interval (Eq. 5) rather than the RMSE (Eq. 3).

It is an interesting contrast that spatially stratified sampling and reporting of statistical distributions to characterise substrate uncertainty has been standard for six decades, yet standard treatment of geospatial data rigidly clings to spatially-averaged metrics and assumed data fitness. Given remote sensing is as much (or more) of the modern geomorphologist's toolbox as grain-size analysis, an un-rigid, more wholistic approach inclusive of empirical characterisations of geographic and statistical error distributions will increase awareness and ultimately enhance understanding uncertainty's role in spatially-explicit change interpretation.

4.8 Acknowledgements

This work was funded in-part by Greater Wellington Regional Council and Massey University.

4.9 Appendix A

"Search 1" – Geomorphic Change

"Search 1" (Appendix A) is a generic topical search for geomorphic change and produced 290 results with 94% (n=273) occurring since 2000 and a major uptick since 2012 (*Figure 4-2*).

WOSCC query string:

TS= ("Geomorphic Change") NOT WC = ASTRONOMY ASTROPHYSICS
Timespan: All years. Indexes: SCI-EXPANDED

"Search 2" – topography/morphology and aerial (but not change)

Combining topographic-related terms with aerial imagery (Appendix A, "Search 2") combined terms relted to topography and aerial imagery and yielded 460 results. Of 310 records with abstracts, 86% (n=268) included at least one text string explicitly or implicitly suggesting temporal change ('change'| 'adjust' | 'migrat' | 'budget' | 'response' | 'repeat' | 'dyn' | 'shift' | 'perturb' | 'tempo' | 'thresh' | 'sequen' | 'chron' | 'rate' | 'resilien' | 'coarsen' | 'fining' | 'enlarg' | 'shorten' | 'exten' | 'sensiti' | '4D' | '4-d' | 'conversion' | 'convert' | 'adapt' | 'transform' | 'modif').

WOSCC query string:

TI = (*morph* OR surface OR bathymet* OR topo*) AND TI=(aerial near/1 photo* OR photog* OR UAS or UAV OR RPAS OR sfm OR structure near/2 motion) NOT TI = ((video AND stream*) OR (image AND stream) OR molecular OR gelatin OR agent OR elastic) AND WC=(GEOSCIENCES MULTIDISCIPLINARY OR PHYSICS MULTIDISCIPLINARY OR ENGINEERING OCEAN OR GEOGRAPHY PHYSICAL OR PLANT SCIENCES OR SOIL SCIENCE OR FISHERIES OR ENVIRONMENTAL SCIENCES OR ARCHAEOLOGY OR FORESTRY OR IMAGING SCIENCE PHOTOGRAPHIC TECHNOLOGY OR REMOTE SENSING OR BIODIVERSITY CONSERVATION OR COMPUTER SCIENCE INFORMATION SYSTEMS OR COMPUTER SCIENCE INTERDISCIPLINARY

APPLICATIONS OR MULTIDISCIPLINARY SCIENCES OR WATER RESOURCES OR ECOLOGY OR OCEANOGRAPHY OR ENGINEERING AEROSPACE OR PHYSICS APPLIED OR ENGINEERING CIVIL OR ENGINEERING ENVIRONMENTAL OR ENGINEERING GEOLOGICAL OR INSTRUMENTS INSTRUMENTATION OR ENGINEERING MARINE OR MARINE FRESHWATER BIOLOGY) NOT WC =(PHYSICS MULTIDISCIPLINARY OR PLANT SCIENCES OR PHYSICS APPLIED OR SPECTROSCOPY OR TELECOMMUNICATIONS) NOT SU= (MATERIALS SCIENCE OR CHEMISTRY OR ELECTROCHEMISTRY OR MATHEMATICS OR ASTRONOMY ASTROPHYSICS OR LIFE SCIENCES BIOMEDICINE OTHER TOPICS OR MICROSCOPY OR NUCLEAR SCIENCE TECHNOLOGY OR AUTOMATION CONTROL SYSTEMS OR GENERAL INTERNAL MEDICINE OR INFORMATION SCIENCE LIBRARY SCIENCE OR MEDICAL INFORMATICS OR OPTICS OR TOXICOLOGY)
Timespan: 1900-2019. Indexes: SCI-EXPANDED.

Summary of Thesis Chapter 4

This chapter provides a historic perspective on spatially-explicit time-series analysis. A numeric model was developed and presented to illustrate the shortcomings of RMSE for error characterization. A case study of catchment-scale photomosaics from the Ruamāhanga across a spectrum of coregistration quality from very good to very poor is used for visualizing three key elements of suitability: displacement magnitude, geographic distribution, and displacement consistency. These elements in combination with a hierarchical classification based on analytical intent and dimensionality serve as the axes for a suitability workflow that can be applied to data at any scale. The approach described in Chapter 4 can be applied at any scale and underpins all subsequent thesis chapters, with the results of the photomosaic case study explicitly for the decadal analysis in Chapter 7.

Chapter 5

Landscape-scale screening of river avulsion sensitivity in a low-relief, active tectonic setting

Introduction to Chapter 5 of Thesis

Chapter 5 considers the infrequent, but consequential morphodynamic phenomenon of river avulsions. Causal factors of avulsions vary by geomorphic setting, result from a mix of spatial scales, and often accumulate over timespans much greater than the actuation of actual channel realignment. The generally low frequency of avulsion occurrence makes empirical study particularly difficult, thus much of the peer-reviewed literature is model-based. Further, the literature bodies are fragmented by sub-field linked to specific geomorphic settings as spatiotemporal variation in cause, occurrence, and consequence often depends on landscape position.

Along the multi-scale theme of thesis, this chapter addresses objective 'ii' by consolidating causal factors across settings, refining and generalising conceptual models of avulsions, and presenting a method that ingests landscape-scale data to highlight reach-scale sensitivity. The method creates a relative-elevation DEM based on a specified baseline (e.g., stream alignment) to permit spatially continuous evaluation of topographic advantage. A by-product of the method is enhanced visualisation of geologic structures that intersect selected river courses. Collectively, the approach localises potential geomorphic hot-spots (sensu Czuba and Foufoula-Georgiou, 2015) thereby enabling prioritisation for detailed investigation.

This chapter is in preparation as a manuscript for Natural Hazards as:

Conley, W.C., Fuller, I.C., McColl, S.T., Tunnicliffe, J.F. (In Prep). Landscape-scale screening of river avulsion sensitivity in a low-relief, active tectonic setting.

5.1 Abstract

Field and model-based investigations over the last 45 years have identified a diverse array of factors that contribute to river avulsion. However, partitioning between different subfields closely linked to geomorphic setting challenges comprehensive treatment from a hazard perspective. Topographic advantage, where the present watercourse is elevated above other potential flow paths, is widely recognised as a necessary condition across all settings. Actuation and localisation are often determined by sedimentation rate, relative capacities, and erodibility of potential receiving areas, including existing channels. Research emphasis on basin and coastal settings drives perceptions of causality, which may not fully represent avulsions that happen outside of these domains. Given potential human calamity with many avulsions, there is need for broader view of hazard potential across geomorphic settings to guide resource prioritisation for more intensive assessment and/or mitigation. This paper proposes refinement of the traditional two-phase (setup and trigger) model of avulsions by differentiating preparation (dynamic) and preconditioning (static) factors for consistency with other threshold phenomena, specifically landslides. A rapid GIS-based approach is presented to screen relative channel depth as an indicator of topographic advantage across geomorphic settings with landscape-scale application across a spectrum of site sensitivities within an active New Zealand fore-arc basin. Finally, a simple dichotomous framework is proposed for site characterisation based on sensitivity to preparation factors. Collectively, this chapter provides a more inclusive framework with a single logical entry point for all geomorphic settings upon which more targeted investigations can then be based.

5.2 Introduction

River avulsion (avulsion) is the physical relocation of a channel or channel belt though it is often conceptualised differently amongst geomorphically-related subfields. Sedimentology literature generally considers avulsion as the wholesale abandonment of an active channel or channel belt with varying recognition of partial abandonment (e.g. Allen, 1965; Bridge and Leeder, 1979; Jones and Schumm, 1999; Slingerland and Smith, 2004; Jerolmack and Mohrig, 2007; Hajek et al., 2010) Within this subfield, avulsions are of interest as the primary subaerial mechanism of basin architecture and investigations commonly involve stratigraphy and numerical modelling. In geomorphology, this process has been defined as a first order avulsion (Brierley and Fryirs, 2005). A broader usage generally applied in geomorphology and engineering literature that also encompasses interplay of existing channels within an anastomosed belt (second order avulsion) or active braid (third order avulsion) (e.g. Ferguson and Werritty, 1983; Ashmore, 1991; Ferguson, 1993; Leddy et al., 1993; Wheaton et al., 2013). In these subfields, avulsion as a discrete process and contributor to multi-thread channel forms is largely explored through empirical changes and/or hydraulic modelling of contemporary forms. Some investigators have treated all three orders collectively as *bifurcations* in the course of characterising forming and maintenance processes (Kleinhans et al., 2013). However, from a hazard perspective, third order instances usually relate to matters of more routine stability and erosion hazards by contrast to first order avulsions which can be one of the most dramatic alluvial hazards known (e.g. Soong and Zhao, 1994; Sinha, 2009; Syvitski and Brakenridge, 2013).

As an inherently threshold-based process, avulsion is widely represented by a two-phase conceptual model: 1) a “setup” or “destabilising” phase and 2) a triggering event/phase (e.g., Jones and Schumm, 1999; Smith, 2003; Slingerland and Smith, 2004). Figure 2-21 visualises the cumulative two-phase model for fluvially-driven avulsion inspired by various forms presented by Schumm (Schumm, 1973; Schumm, 1979; Jones and Schumm, 1999). In-lieu of instability (cf. Figure 2-21), I reconsider the y-axis as *magnitude* for both triggering hydraulics and advancement of relative

(conceptual) degrees of adjustment. Other significant changes include a peri-threshold zone that accommodates splays, breaches, and healing (sensu Slingerland and Smith, 1998; Makaske et al., 2012; Nienhuis et al., 2018), non-linearity that accommodates negative feedback (sensu Chen et al., 2012) and disaggregation of the existing channel and receiving area to emphasise their relative nature and varying independence. As with earlier graphical forms, conditions at the time a flow event occurs determine the effective discharge to generate an avulsion such that large flow events are not necessary. The conditions at any given point of Phase 1 accrue as a result of *preparation* (dynamic) factors superimposed on *preconditioning* (static) factors (cf. Glade and Crozier, 2005). Here, I consider *sensitivity* in the sense of threshold proximity described by Downs and Gregory (1995) and define as a landform's inclination to respond to an application of force (cf. Brunsden, 2001). Sensitivity is thus conceptually derived for a point in time as the inverse of the distance (characterised by stream power magnitude) between the condition of preparation of where a channel is compared to where it could be (Figure 5-1).

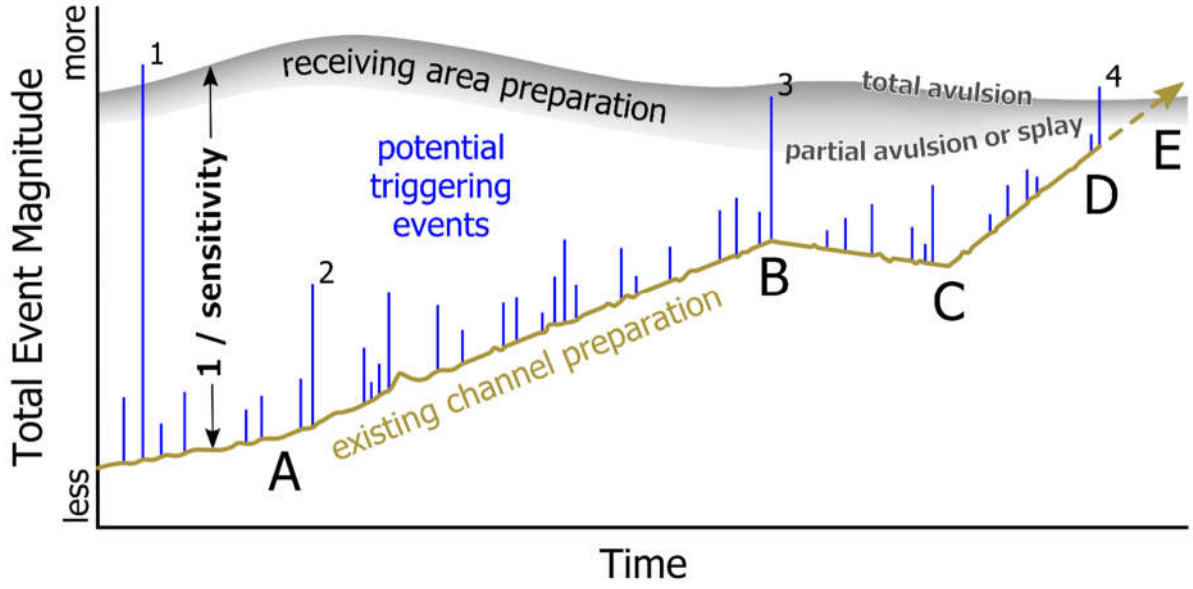

Figure 5-1. Conceptual representation of fluvially-driven avulsion where channel preparation approaches a threshold (adapted from Jones and Schumm, 1999). Different thresholds for partial and total avulsion bound a zone for the potential receiving area (e.g., floodplain) and reflect potential for peri-threshold conditions. Preparation trajectories for the existing channel and receiving area are non-linear and may vary, converge, or diverge with varying degrees of independence. Total event magnitude implicitly accommodates duration of individual flow events and is superimposed on existing channel preparation to provide the potential bridge of the sensitivity gap. Relative trajectories of channel and receiving area preparation govern the magnitude of the "bridge". Inflections in channel preparation may be subtle and reflect incremental catchment changes (A) or acute and reflect local changes or discrete catchment disturbance (B and C). Negative trajectories (e.g., B to C) are accommodated and may result from negative feedbacks such as where persistence of a levee breach (3) provides a measure of channel relief and diminishes overall avulsion potential. In this example, a large, rare discharge event (1) produces an avulsion as expected, however the second largest event (2) does not because the site has low sensitivity at the time it occurs. Preparation of channel and receiving area continue over time, with convergent trajectories such that the system is more sensitive when a repeat of the second largest event (3) occurs and causes a partial avulsion. Eventually, after further channel preparation, a much more routine discharge (4) triggers full avulsion (D). The D-E line segment indicates the potential for routine autogenic processes to advance the system to full avulsion (E) in the absence of a discrete triggering event. Sensitivity is the inverse of the gap magnitude between the total avulsion threshold and channel preparation at any point in time.

A wide range of factors contributing to avulsion has been identified in the literature (Table 5-1), each of which may function in preparation, preconditioning, and/or triggering. Factors are a mix of processes and conditions with the three most widely recognised: 1) relative configuration of channel to valley slope (Mackey and Bridge, 1995; Slingerland and Smith, 1998; Jones and Schumm, 1999; Törnqvist and Bridge, 2002), 2) sedimentation rate (Törnqvist, 1994; Bryant et al., 1995; Mackey and Bridge, 1995; Heller and Paola, 1996) and 3) topographic advantage (a.k.a. super-elevation; Mohrig et al., 2000; Jerolmack and Mohrig, 2007). Channel and floodplain resistance and capacity (independent of bed slope) have also emerged as important underlying factors (cf. Jones and Schumm, 1999; cf. Slingerland and Smith, 2004; cf. Wheaton et al., 2013) as has sediment size distribution (Aslan et al., 2005; Nicholas et al., 2018). Increased awareness of the diversity and complex interactions of factors supports the general conclusion that no single mechanism governs avulsions through space and time (sensu Makaske et al., 2012), although frequent occurrence of topographic advantage in the literature suggests broad agreement as a necessary underlying condition.

Independent of factors, two main avulsion *styles* are widely used to characterise general evolutionary behaviour in lower gradient systems: 1) *incisional* avulsions tend to cut-then-fill and 2) *progradational* avulsions fill-then-cut (cf. Mohrig et al., 2000; cf. Slingerland and Smith, 2004). Reoccupation (a.k.a. annexation) of existing channels is a well-documented behaviour (Richards et al., 1993; Morozova et al., 1999; Mohrig et al., 2000) that is sometimes recognised as a separate style (Slingerland and Smith, 2004), though Hajek and Edmonds (2014) note can occur associated with both progradational and incisional avulsions. By contrast to styles, avulsion *types* indicate topological relationships where *local* avulsions re-join the parent channel and *regional* avulsions remaining separate from the parent channel over long distances or entirely (Heller and Paola, 1996). *Nodal* and *random* avulsions as identified by Leeder (1977) are effectively regional avulsion subtypes where the channel divergence point has a localised affinity versus a more distributed occurrence along the parent channel, respectively, through time. Avulsion frequency, avulsion duration, and interavulsion period have been identified as *parameters* (Törnqvist, 1994; Stouthamer and Berendsen, 2001) though I consider them, along with location (the focus of this paper), to be system-level attributes. The high proportionality of low-gradient, fine-grained systems in the literature has implicitly focused conceptual models on fully alluvial systems potentially at the expense of broader relevance across systems and settings in the process. For example, I suggest general dependency on preparation factors intuitively diminishes for some instances of hillslope, glacial, or tectonically forced avulsions, perhaps indicating need for a more inclusive framework.

Korup (2004) grouped landslide-forced avulsions into 1) damming/backwatering, 2) contact displacement, and 3) downstream sediment loading types with the two former groups generally requiring substantially less preparation to generate an avulsion than sediment loading. A similar asymmetry seems to exist for glacially-forced avulsions with potentially less preparation required to generate an avulsive response during advance (e.g. Kovanen and Slaymaker, 2004) than retreat (e.g. Shugar et al., 2017). Avulsions triggered by fault rupture such as “beheadings” have been documented (Ouchi, 2005; Dumont et al., 2006; Rodgers and Little, 2006) with focus on displacement distance and relatively little attention to outflow of the newly aligned ‘head’ from an avulsion hazard perspective.

Table 5-1. Avulsion factors with example references with my interpretation of engagement along the continuum of precondition to trigger. The most widely recognised contributors are in bold.

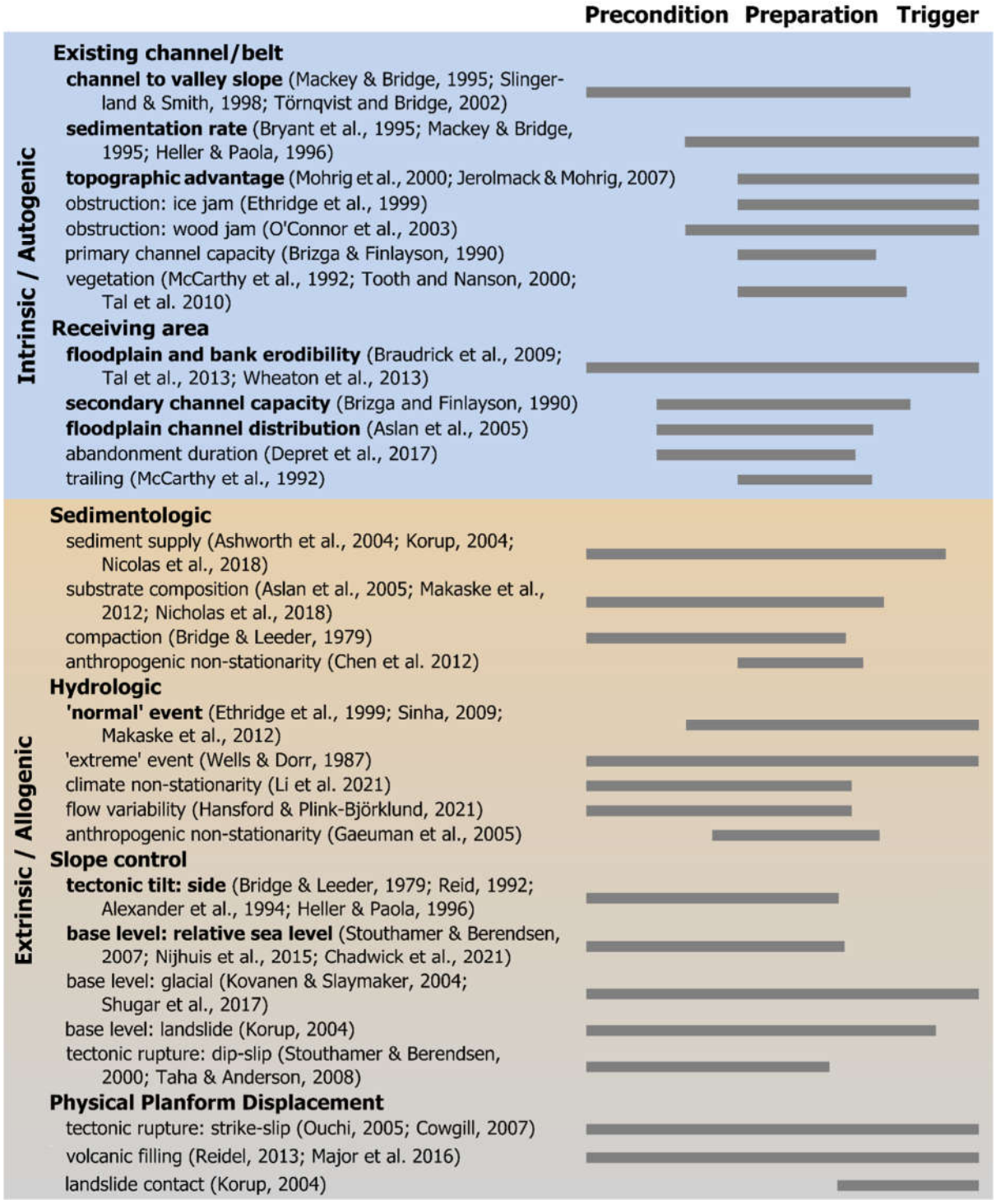

Tectonics have generally been treated as preconditioning factors. Tectonic side-tilt has been related to avulsion behaviours and rates as well as abandonment patterns (Reid, 1992; Alexander et al., 1994), back-tilt has been implicated in increased channel activity (Heller and Paola, 1996) and sediment flux (chapter 6, this thesis). Local tectonics have been implicated in controlling avulsion locations over extended (10^2 - 10^3 years) time on coastal plain and deltaic settings (Stouthamer and Berendsen, 2000; Taha and Anderson, 2008) and range-bounding settings for both strike-slip (Ouchi, 2005; Rodgers and Little, 2006) and dip-slip (Quigley et al., 2010; Stirling et al., 2017) fault rupture

has been associated with avulsion, though the latter only qualitatively. However, the literature has generally explored longer term tectonic displacements as indicators of hydraulic geometry and/or tectonic process (e.g. Replumaz et al., 2001; Walker and Allen, 2012) with exploration as potential avulsion triggers (e.g. Ouchi, 2005) rare. Fault displacements have been considered mostly for establishing slip rates (Sieh and Jahns, 1984; Cowgill, 2007; Carne et al., 2011) and/or terrace reconstruction (Cowgill, 2007; Carne et al., 2011). Regarding hazards, there is a need to assess broader potential across landscapes in terms of current state at human (immediate to decadal) timescales.

Avulsion style can vary by morphology for a single contemporary river (Valenza et al., 2020) and the geologic record suggests that floodplain sedimentation and floodplain architecture can be autogenically dominated with all three styles potentially co-occurring over a range of subsidence rates up to 100 km from sea level control (Flood and Hampson, 2014). Hence, styles may be considered to have some spatial coherence along the river continuum. Given the spatial distribution of river morphologies (and underlying forming processes) is neither uniform, nor random at riverscape scale, overly specific classifications may have restricted geographic applicability. For example, given slope-dependency between avulsion frequency and sediment supply, dynamics on alluvial fans may be very different from unconfined fluvial settings (Ashworth et al., 2004). Recognising this, Kleinhans et al. (2013) grouped channel bifurcations (inclusive of all three avulsion orders) by geomorphic setting (alluvial fans, braided rivers, lowland rivers, and deltas) in a review characterising formative and maintenance processes. Alternatively, descriptive groupings linked to avulsion styles have been used to characterise process sequences for paleostratigraphy (Jones and Hajek, 2007).

This potential for both divergence within factors, styles, and/or type and convergence/equifinality (cf. Schumm, 1991) between styles across the range of process domains, suggests a step back from specific processes (e.g. sedimentation), conditions (e.g. relative slope) or trigger type/origin (e.g. landslide vs. ice lobe) may be needed. The degree of requisite preparation varies not only between, but also within triggering mechanisms as greater degrees of preparation may require progressively lower trigger magnitude (Schumm, 1977; Brizga and Finlayson, 1990). There is no requirement for the triggering mechanism to be the same as the conditioning mechanism(s) (Makaske et al., 2012) and, intuitively, I suggest the potential for multiple forcing mechanisms to interact increases proportionately (but not linearly, sensu Figure 5-1) with response time. To accommodate these various complexities, some reconsideration of framing is warranted.

Since 1) avulsions often happen quickly once a trigger exists in the presence of threshold conditions and 2) trigger mitigation may not be possible, as a matter of hazard I consider degree of preparation to be my critical focus. In other words, triggers requiring less preparation may be more likely to produce avulsions by surprise and, may (balanced by consequences) warrant prioritised resource allocation for more detailed assessment and/or mitigation. Present detection and analytical capabilities, advanced as they may be, cannot yet characterise the likelihood of knowing (or gaging proximity to) site-specific thresholds across landscapes with suitable data tolerance. However, measuring relative channel depth has been recommended as a means of avulsion hazard monitoring on debris fans (de Haas et al., 2019).

This paper presents 1) a landscape-scale GIS interrogation of relative floodplain elevation for rapid screening relative channel depth as an indicator of topographic advantage, 2) interpretive applications for a wide range of cases from an active New Zealand fore-arc basin and 3) a broadened, but refined statement of necessary conditions for an avulsion to occur and conceptual framework to group examples along a sensitivity gradient. Collectively, this provides a more inclusive

framework with a single logical entry point upon which more targeted investigations can then be based. While my framework accommodates all three orders of avulsion, my examples here focus on first order avulsion given generally greater acute consequences.

5.3 Approach: Screening sensitivity

Topographic advantage and/or slope metrics are implicated as either a primary factor or contributor (e.g. transport capacity related effects on sedimentation) throughout the avulsion literature. These topographic parameters can be readily determined from Digital Elevation Models (DEMs) which are widely available and a foundational part of process-based fluvial geomorphic analyses over the last 25 years (e.g. Brasington et al., 2000; Fuller et al., 2003b; Wheaton et al., 2010b). The continuous, spatially-explicit characterisation of topography by DEMs readily accommodates geomorphic relationships that tend to have hierarchical, nested scaling (sensu Fryirs and Brierley, 2012). DEMs are widely utilised in GIS environments, particularly within resource management settings where hazard assessment and mitigation occur. I propose a lightweight, GIS-based top-down screening approach has greater potential utilisation suitable for prioritising investigative resources at river management scales across a broader base.

Detection of local geomorphic relationships over large areas and in complex terrain can be challenging and benefit from enhanced perception of local relief (visually and/or computationally). One approach is to normalise elevation values by using some relevant landscape feature as a datum, such as a stream channel or channel network. Elevation normalisation, also known as *detrending*, generally minimises or even eliminates the slope of the stream or valley profile to reduce the absolute range of values and increase overall contrast. Application of detrended DEMs in fluvial geomorphology has occurred across scales including landscape-scale floodplain complexity (Scown et al., 2015), reach-scale drainage structure (Brasington et al., 2012), reach-scale habitat, bar-scale relief (Hicks et al., 2002), patch-scale grain analysis (Brasington et al., 2012), as well as reach-scale DEM quality control (Javernick et al., 2014).

Detrending based on channel networks, such as Height Above Nearest Drainage (HAND), has gained popularity with use for terrain classification and drainage potential of large regions (Rennó et al., 2008), developing soil water maps (Nobre et al., 2011), and estimating rating curves and flood inundation extent (Zheng et al., 2018; Johnson et al., 2019). However, HAND computes cell values relative to the stream bed cell to which it drains. By contrast, assessing avulsion hazard is fundamentally about where a cell *could* drain. Further, filling or breaching depressions is a standard step in stream network extraction and alters topographic relationships often relevant to topographic advantage between two drainage pathways.

To avoid these potential problems, guided filter approaches emphasising edge detection have been applied at regional scales for paleochannel delineation and migration, but with an intermediate logarithmic transformation (Zhang et al., 2020). However, because avulsion potential is specific to an individual water course, a weighted average approach was selected that uses the target stream as a baseline for detrending (Dilts et al. 2010).

5.4 Study area

The Ruamāhanga River catchment is the largest (~3,500 kilometres^2) on the southern North Island of New Zealand. The catchment's long axis (northeast to southwest) parallels major faults (Figure 5-2) which strike roughly parallel to the plate margin (Hikurangi Margin, Figure 5-2, inset). The Tararua Range ("Tararuas") is the axial mountain range for the southern NI and defines the northwestern margin of the catchment. The highest relief (maximum elevation 1,562 metres) in the catchment

occurs within its greywacke core while foothills composed of mudstones, sandstones and limestones produce more rounded forms. Eastern Hill Country ("Hill Country"; maximum elevation ~500 metres) bounds the catchment along the southeastern (trench) and northeastern margins and is composed of mainly of mudstones and limestones. The Wairarapa Valley Floor ("Valley Floor") is a relatively small (~75 kilometres long and 10-13 kilometres wide) sedimentary basin of low relief (~150 metres to sea level) that lies between the Tararuas and Hill Country.

The study area is characterised by oblique strike-slip tectonic forcing resulting from a giant releasing bend caused by sigmoidal inflection of the plate boundary as net northeast motion of the Australian Plate overrides net southwest motion of the Pacific Plate (Figure 5-2, inset). Though the southern North Island lacks a proper magmatic arc, Hill Country is effectively the middle prism of the outer accretionary wedge and the Valley Floor is generally consistent with Noda's (2016) "neutral accretionary" type of forearc basin. Such basins are associated with oblique strike-slip deformation and tends to lengthen rather than widen as depocentres migrate parallel to the trench. While neutral forearc basins may be weakly deformed in comparison to other accretionary types (compressional and extensional), field observation and LiDAR interrogation indicate the Valley Floor is widely deformed, though surface expression is often subtle.

Tectonic deformation mechanisms and erosion-transport-sedimentation processes are inherently coupled and produce different process-response relationships by setting. As an oblique strike-slip tectonic setting, the study area exhibits landscape behaviours of both compressional and strike-slip settings. As in compressional settings, terrace formation occurs where rivers erode through actively uplifting faults with deposition downstream organised into fan-like features by avulsion while more complex, spatially-distributed morphologies that enhance drainage network interactions result from strike-slip deformation (cf. Graveleau et al., 2015).

Major active faults in the study area are generally transpressional with primary dextral motion, often with secondary dip-slip (GNS Science, 2020). Except for the Wairarapa Fault, which roughly defines the northwest margin of the Valley Floor, slip rates and motion are not well-constrained. The persistence of scarps and observation of other faults in the region indicate co-seismic rupturing behaviour is typical of larger events. Over the last eight ruptures, the Wairarapa Fault has averaged 16.5 metres (+/- 2.2) of dextral displacement (Manighetti et al., 2020) and the largest maximum terrestrial slip globally (~20 m via high-resolution remote sensing Manighetti et al. (2020); 18.7 m ground investigation Rodgers and Little (2006)). The study area exhibits a fault-splay network indicative of propagating systems (*sensu* Perrin et al., 2016).

Marine highstand during the Holocene likely commenced ca. 8,300 BP, crested ca. 7,000 BP ~2.5 m above contemporary sea level and receded to present levels ca 4,000 BP (Clement et al., 2016). Litchfield and Berryman (2005) reported maximum highstand shoreline position 47 kilometres inland based on intercalation of post-LGM fluvial terrace and marine sediments in eight East Coast catchments that included the Ruamāhanga. My interpretation of fluvial scarring and valley slope in the study area suggests high-stand base level control was in the vicinity of the contemporary confluence of the Ruamāhanga and Waiohine rivers (47 +/- 3 kilometres from contemporary coastline).

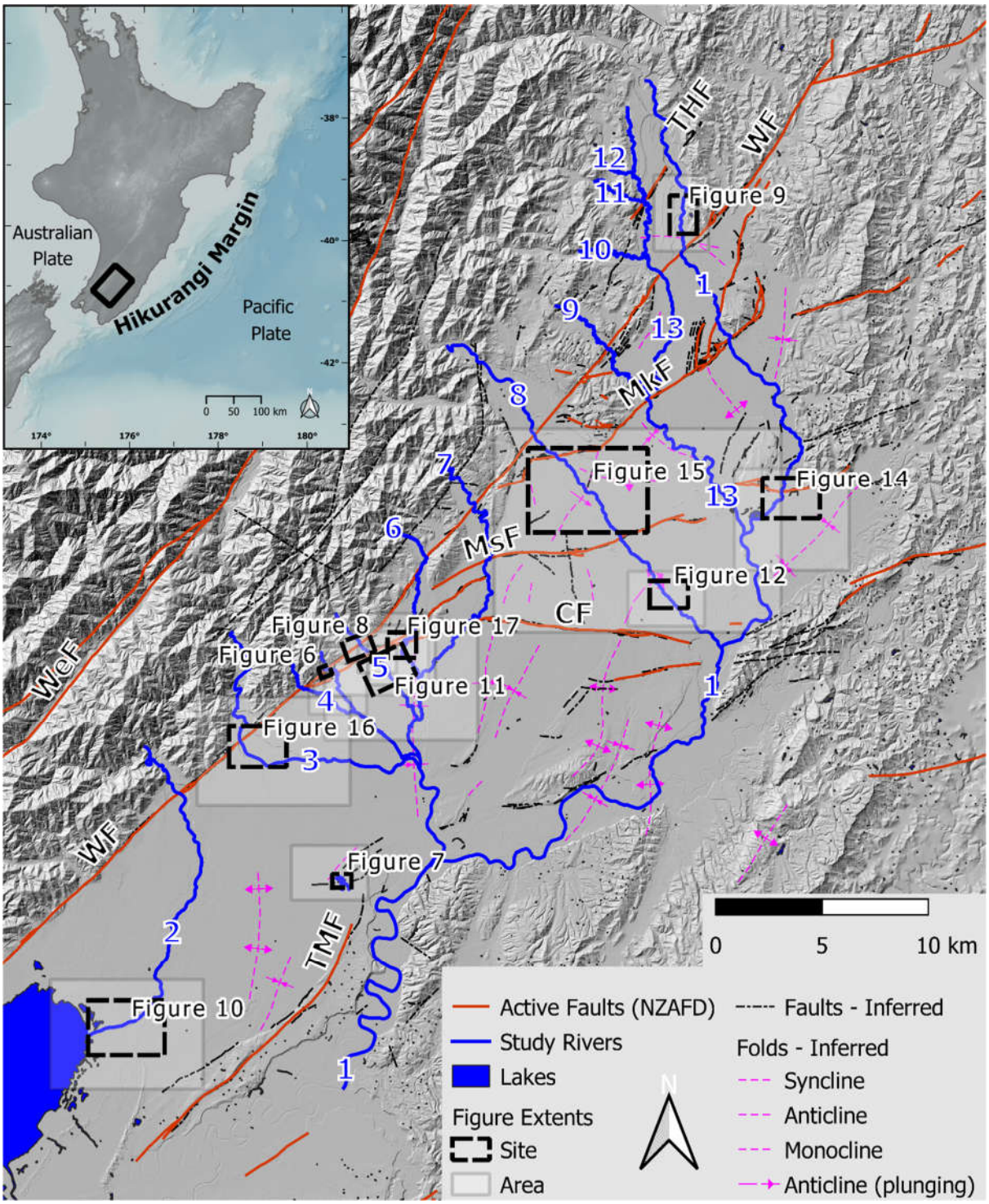

Figure 5-2. Study area and index of example case maps (e,g, "Figure 7"). 1 - Ruamāhanga River, 2 - Tauherenikau River, 3 - Waiohine River, 4 - Beef Creek, 5 – Kaipaitangata Creek, 6 – Enaki Stream, 7 – Mangatarere Stream, 8 – Waingawa River, 9 – Wakamoekau Creek, 10 – Mikimiki Stream, 11 - Kiriwhakapapa Stream, 12 – Te Mara Stream, 13 – Waipōua River, WF – Wairarapa Fault, WeF – Wellington Fault, CF =- Carterton Fault, MsF – Masterton Fault, MkF – Mokonui Fault, THF – Te Hau Fault, TMF - Te Maire Fault

River segments within the Valley Floor are low gradient (≤ 0.01 m/m) and occur on a spectrum of forms that reflect a wide spectrum of sediment sources and geomorphic settings for such a compact amount of space as the study area. Larger, gravel and cobble bedded rivers from the Tararuas are the main source of clastic sediments and have alluvial fans that extend up to approximately 4.5 kilometres from the range front. The contemporary sediment transport regimes of smaller streams

and rivers draining Tararua foothills appear to be mixed-load types as they drain softer lithologies, but often rework antecedent clastic valley fills. Hill Country subcatchments produce rivers and streams that are primarily suspended or washload type sediment regimes. Generally, upstream of the Huangarua River confluence (which drains an isolated area of uplifted greywacke), rivers that join the mainstem Ruamāhanga from the left bank are sinuous with cohesive banks. Rivers joining from the right-bank (that drain the Tararuas) have beds and banks composed granular materials and commonly have multithread, wandering forms. By area, these rivers (or their ancestors) appear disproportionately responsible for construction of the Valley Floor.

5.5 Method

Because avulsion sensitivity and hazard are reach- or stream-specific, DEM detrending was individually processed for each stream using the stream centreline as the baseline following the approach of Dilts et al. (2010). This approach converts a vector polyline of the stream to a raster then a kernel density function is applied in a moving-window along the polyline to generate a weighting grid based on cell proximity to the closest channel cell. The weighting function is then applied to cells with channel elevation values, and subtracted from the original DEM. This process minimises loss or dilution of the local relief signal that might occur due to averaging over larger extents or regional artefacts. This targeted detrending increases the likelihood that slope contrasts other than stream slope that may influence avulsion potential are preserved, particularly outward from the stream. The resulting relative-elevation DEMs (rDEMs) aid identification by highlighting areas of topographic-advantage and enhancing relief contrast. Collectively, this enables more rapid localisation and discretisation of potential hazards as well as interpretation of geomorphic processes.

5.5.1 Data Preprocessing

Six pre-existing stream layers were visually evaluated in GIS for concurrence with channel centreline and considered unsuitable for use as baselines for detrending to generate a relative-elevation DEM (rDEM). To better represent geometry of the channels at the time of LiDAR collection (2013), I ran a standard flow accumulation-based delineation from the source 1 metre DEM and iteratively applied different smoothing. Results were mixed and generally not fit-for-purpose. Ultimately, I determined manual digitisation of the wetted primary channel centreline was necessary and used a 0.3 metre orthomosaic compiled from imagery collected within a year of the LiDAR. The manually-generated polylines were then used as baselines for the detrending process.

Inconsistencies in preliminary results prompted review of the source DEM at large scales (~ 1:500) which revealed numerous non-ground artefacts that raised the apparent baseline elevation by varying magnitudes (Figure 5-3). This can cause the rDEM to suggest adjacent topography is lower than reality. Discussions with data originators and stewards concurred that resolving non-ground artefacts in the source DEM would require manual editing of the original point clouds. Because the data as-delivered was suitable for their purposes and addressing the issues within the source data greatly exceeded my available resources, I adapted the methodology.

I mapped 1,961 artefacts along 218 of 250 stream kilometres that intruded into the wetted channel centrelines. The majority of which involved a distortion less than 2-3 channel widths along the profile with many < 1 channel width. Despite limited spatial extent, vertical distortions of 4-8 metres were not uncommon and with potential influence on channels that are all < 0.01 slope (m/m). Given the general localisation, I attempted a batch “breaching” process in GIS that was unsuccessful. Ultimately, I shifted baseline planform geometry in vicinity of artefacts to positions of lowest

influence that were still within the wetted channel (similar to alignment “LEW” in Figure 5-4) for channels that had already been digitised and adapted my workflow accordingly for remaining channels.

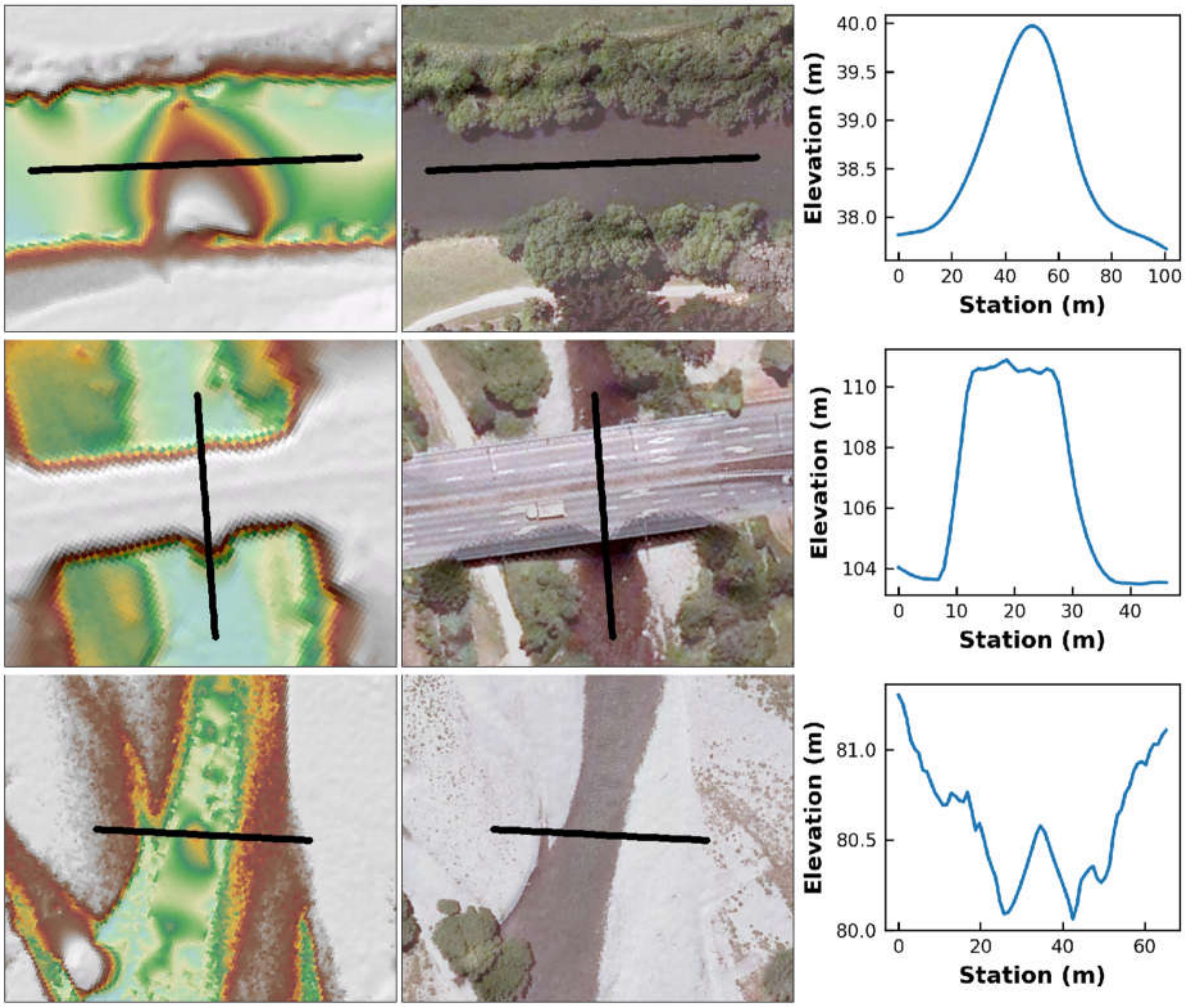

Figure 5-3. Examples of non-ground artefacts in the source DEM that influence perceived channel geometry in profile (top and middle rows) and cross-section (bottom row).

In the interim, another party (LINZ) published a reprocessed version of the data which exhibited fewer outliers/irregularities at small scales (coarser than 1:20,000). However, when compared at large scales (>1:1000) to the original data set, the smoothing that had been applied in the apparent absence of reclassifying/filtering the point cloud was less-suited to the purpose (Figure 5-4). I thus proceeded with the original data set and aggregated to 5 metre resolution using a “minimum” argument. Thus, the value of each output pixel was the smallest value of the 25 related input pixels. This helped minimise not only errors projecting from banks, but also to reduce the effect of roads and small dams (Figure 5-3, middle row) which accounted for only 2% (n=42) of the mapped artefacts but couldn’t be resolved simply by shifting baseline position. Distortions in the resulting DEM were fewer, of less magnitude (generally <0.3 metre or eliminated), and well-within (generally <1-5%) the search radius for the weighted averaging component. The combination of aggregating the elevation data resolution and adjusting baseline geometry improved results and was applied throughout the analysis presented here.

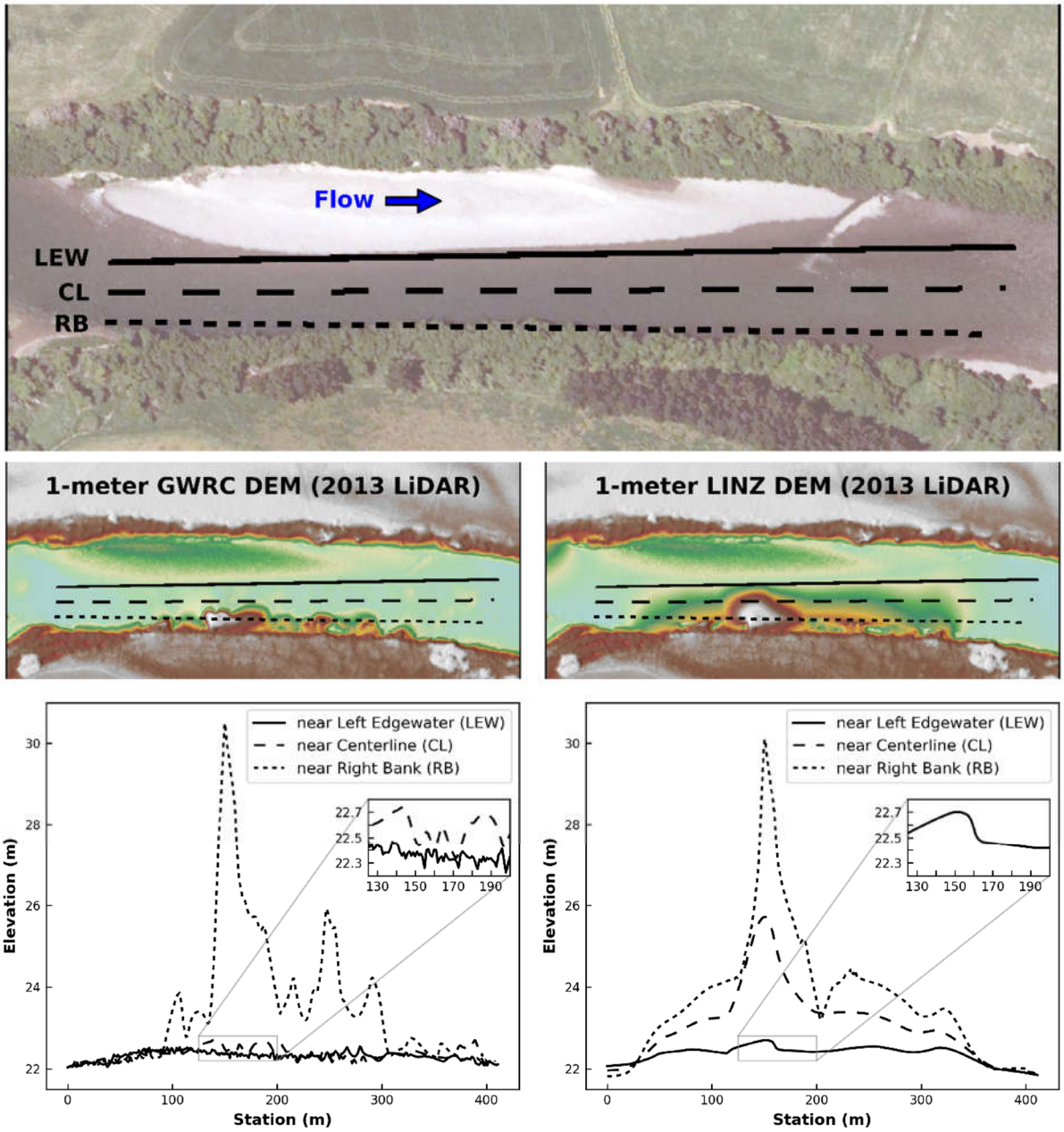

Figure 5-4. Evaluation the effect of baseline position related to elevation extraction for two different source DEMs. Wetted channel centreline (CL) profiles differ strongly (maximum difference > 1.5 metres) between two DEMs sourced from the same data with different processing histories. CL approximates the LEW better in the unsmoothed DEM (bottom, left).

5.5.2 Representation

Setting a maximum value for the rDEM helps optimise feature visualisation by preserving more of a colour ramp for the elevation bands of interest, whereas not doing may mute contrast by overstretching a limited number of colours. I took an iterative approach to finding a maximum value, beginning with 20, reducing to 10 and finally settling on 5 metres which both provides good feature contrast, but is only slightly greater magnitude than where the 1% AEP inundation perimeter intersects the rDEM (typically ~3.5 – 4.8 metres for the subset of water courses that have hydraulic models). In Figure 5-5, these binned values (cells > 5 shown in purple) were retained to enable visualisation of the analysis area.

Visual review of the source DEM, comparison with high resolution orthoimagery and familiarity with ground conditions suggests water depth at the riffle crests at the time of LiDAR acquisition likely ranged from ~0.1 metre for smaller streams to <0.5 metre for larger rivers. I thus consider the lack of bathymetric representation in the LiDAR to be of minor importance and use 5 metres as the minimum value across streams, with larger values used in areas of greater relief. Where more localised spatial extents are of interest (e.g., examples in Results section), I use a variable maximum approach to improve representation of geomorphic context. However, this means that 2 metres is represented with different colours in different places.

5.5.3 Interpretation

Interpretation requires keeping two things in mind: 1) the output makes no representation of the possibility/probability that flow access may occur and 2) averaging effects can mute relief contrasts. Figure 5-5 shows three different rDEMs processed from the same source DEM over an identical spatial extent of valley segments shared by two rivers, using the same search radius (2000 metres), but using different baselines or combinations of baselines.

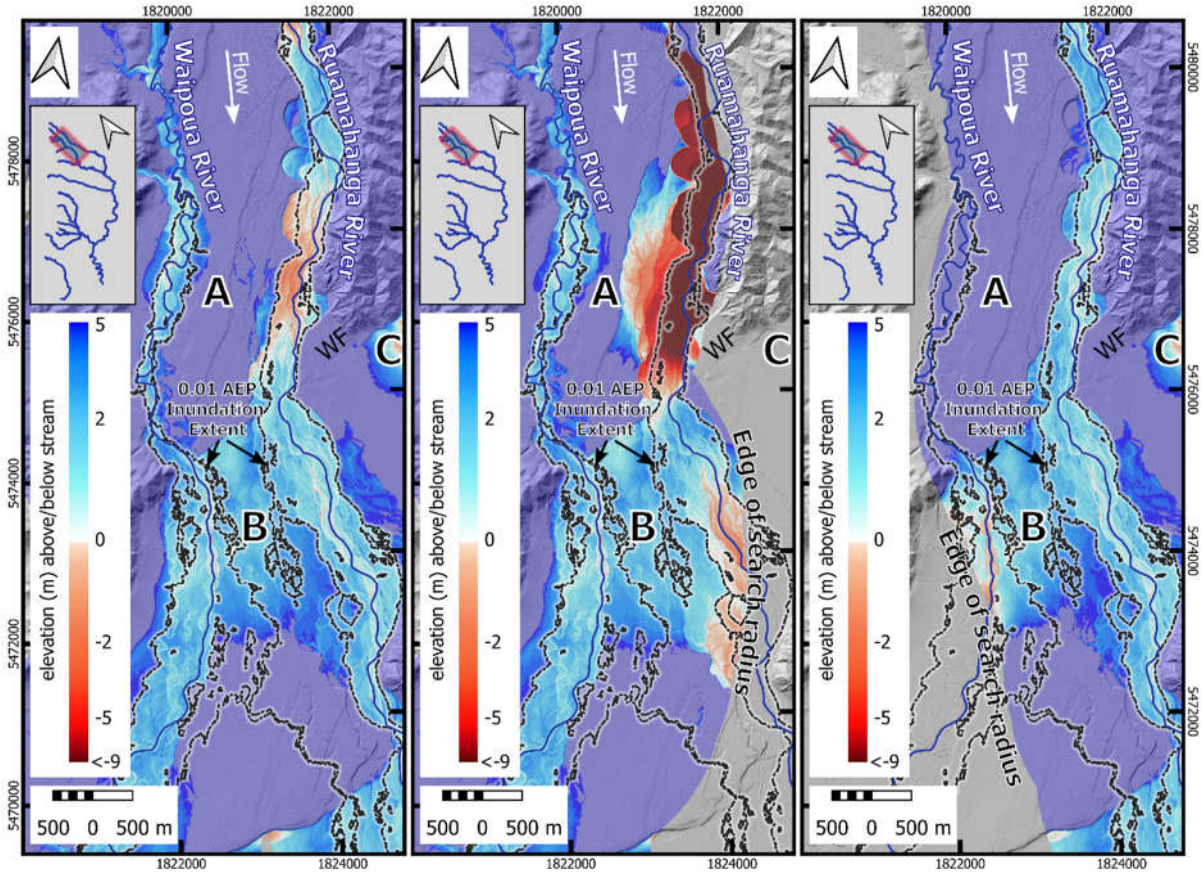

Figure 5-5. Detrended DEMs derived from the same source data for the same valley segment shared by the contemporary Ruamāhanga and Waipōua rivers. Left: baselines processed concurrently. Middle: Waipōua baseline only. Right: Ruamāhanga baseline only. Differences between the three indicate methodological sensitivity and need for both processing and interpretive care. The Wairarapa Fault (WF) crosses approximately mid-segment. Baselines are dark blue and the inundation perimeter of the 1% AEP discharge (by others) is indicated by black and white hashed lines. Purple indicates area within the search radius greater than 5 m above the baseline.

The rDEM in the left panel of Figure 5-5 was processed using baselines for both rivers concurrently and exhibits a smaller footprint for gradient-advantage for the Waipōua over the Ruamāhanga in the valley segment upstream of the Wairarapa Fault ("WF"; vicinity of "A"). A high degree of averaging

has also occurred ("B" vicinity) that diminishes gradient contrast for the valley segment downstream of WF. The rDEM in the middle panel was produced using only the Waipōua River baseline and indicates gradient-advantage over the Ruamāhanga both upstream and downstream of the Wairarapa Fault (WF). Based on the terrace interfluve (>5 m, in purple) coupled with knowledge of catchment characteristics and behaviours, I consider probability of flow access to occur at "A" to be near zero. By contrast, very low relief at "B" coupled with 100-yr inundation perimeters that nearly touch creates a more probable and real avulsion potential, especially once lower frequency discharges, modelling precision, and bed dynamics are considered.

The right panel has a rDEM based solely on the Ruamāhanga baseline the indicates minor, localised gradient advantage within the Ruamāhanga's own 100-year floodplain upstream of WF. It also indicates some gradient-advantage of the Ruamāhanga over the Waipōua downstream of WF (segment "B"). That either river has some gradient advantage over the other within segment "B" suggests increased sensitivity of that area. Coupled with the increasing human floodplain occupancy in the vicinity and downstream along both rivers, makes this segment a higher priority for follow-up investigation. Consulting the source DEM is the quickest and most authoritative check, which in this case, confirms the relationship with topographic advantage of the Ruamāhanga along the upper portion of segment "B" and Waipōua having advantage in the lower portion of the segment. Intermediate topography is more conducive to flow cross-over in the upper half of the segment, so I hypothesised the Ruamāhanga as more likely to augment flows and/or avulse into the Waipōua for framing subsequent investigation (beyond the scope of this paper) to include probabilistic unsteady flow hydraulic modelling supplemented by morphodynamic modelling.

Finally, it is also important to be aware that search radius magnitude has differential averaging effects that can affect perception local relief contrast. Generally, local contrast decreases with increased distance from a baseline and at-a-station relief diminishes similarly. Illustration and discussion of this effect and options for mitigating is provided in Conley (2015, p. 39-42).

5.6 Results

Sensitivity to preparation is a continuum between strongly insensitive and strongly sensitive end members. However, classification can aid manageability when many sites and/or large spatial extents are under consideration.

5.6.1 Low-Sensitivity Cases

A beheading (Figure 5-6, a) of an unnamed tributary of Beef Cr. along the Wairarapa Fault reflects acute tectonic forcing whose outcome is otherwise fairly insensitive of preparation. The contemporary channel (b) is incised into valley fill (c) at least some of which is likely alluvial and accumulated during passage of higher ground (d) across the mouth of the drainage. The horizontal channel offset is 70 metres or less which, assuming average displacement of 16.5 metres (Manighetti et al., 2020) suggests avulsion occurred within the last four or five ruptures (mid-Holocene or younger). The absence of secondary dissection of valley fills except immediately at the fault similarly supports inference of a fairly recent (Holocene) capture.

Though I cannot definitively link the timing of the ultimate realignment explicitly to a seismic event, the allogenic mechanism of the channel displacement was the proximal cause. Topographic elements like shutter ridges may be more important than fault slip rate or maturity (Harbert et al., 2018). I consider the passage of such obstructing terrain to be more an issue of precondition (or inheritance) than preparation. Recognising potential for flow bifurcation or partial alluvial activation to occur and persist for some time in advance of ultimate capture, I do not consider it material in

causing the avulsion. Though I acknowledge the potential for non-rupture contributions (e.g., to timing or rate of capture), I nonetheless consider rupturing as the primary mechanism for both establishing the hydraulic gradient and access of the current alignment in this case. Thus, this site is a good example of preparation-insensitivity.

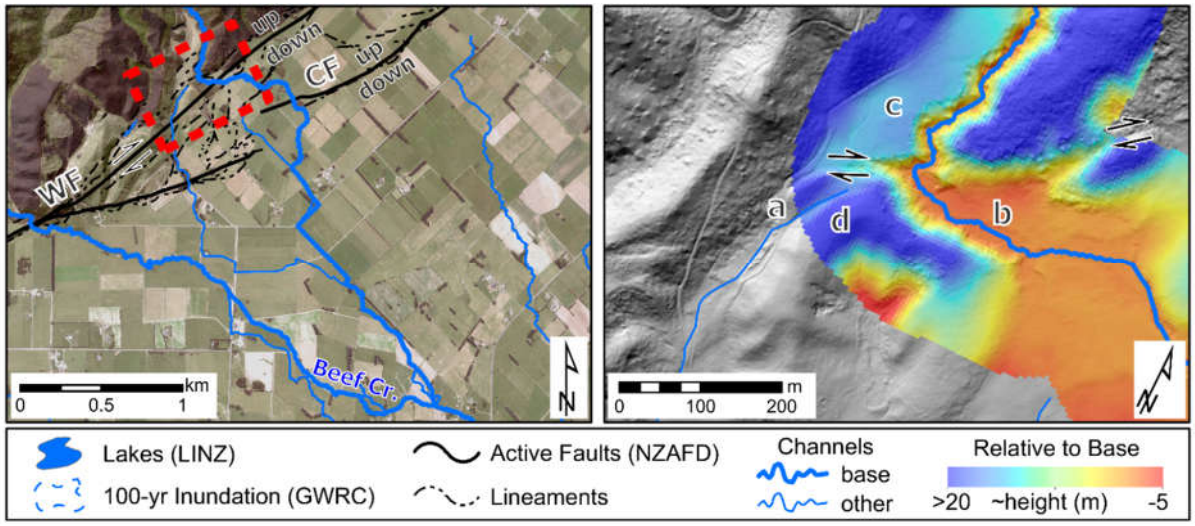

Figure 5-6. Beheading of an unnamed tributary (a) to Beef Creek by oblique strike-slip fault rupturing of the Wairarapa Fault (WF) with downstream capture and avulsion (b) of contributing catchment with the passage of formerly obstructing topographic feature (d). Incised, but undissected valley fill (c) and offset distance suggest relatively recent (Holocene) occurrence.

Vertical rupture (dip-slip) adverse to a stream's flow direction (i.e., where flow orientation is from a downthrown zone to an upthrown zone) may be quite insensitive to preparation. The unnamed drainages in Figure 5-7 presently flow to the northwest. However, the channel structure is suggestive of a branched drainage network oriented to the southeast. Channel segments a-b and w-x seem to indicate a progressive process as the channel alignment may have flattened to the axis of uplift (c-y) over multiple ruptures.

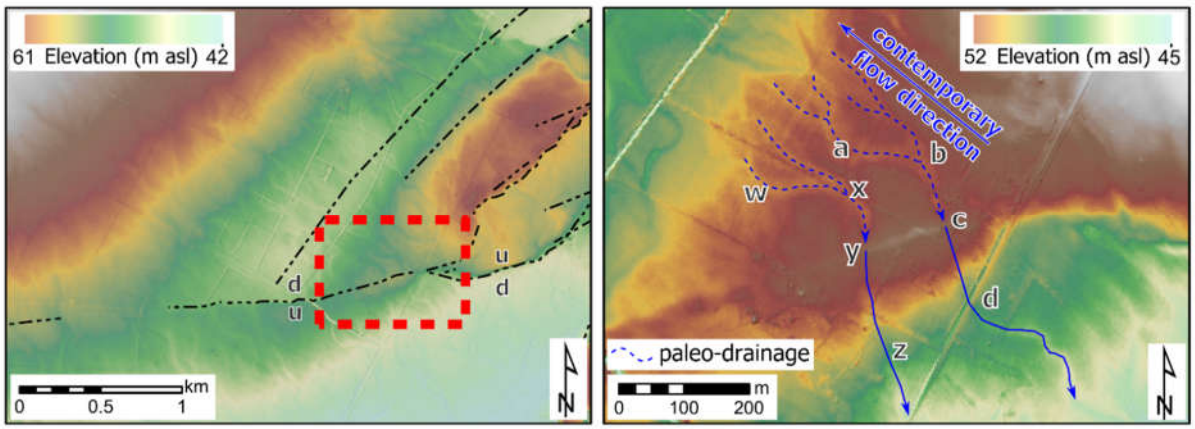

Figure 5-7. Unnamed ephemeral drainages beheaded by dip-slip fault rupture (axis along y-c) with flow-reversal in former headwaters (c-a and y-w).

Though the 'network' could represent incremental abandonment, the directionality likely stands as generating such a network flowing to the northwest with no catchment to speak of to provide discharge or sediment. Eventually, 'd' and 'z' were beheaded, and drainage direction reversed on the downthrown side to b-a and x-w, respectively. This also seems to represent a scenario insensitive to

preparation as whatever may have been happening autogenically does not seem to have mattered because uplift overwhelmed other processes.

Strike-slip displacement can occur without producing channel offset or deflection as illustrated by Kaipaitangata Stream at the Wairarapa Fault (Figure 5-8, 'a'). Others (Ouchi, 2005; Walker and Allen, 2012) have related offset magnitude and frequency to stream size where smaller channels have smaller offsets because they are captured (inverse of beheading) more frequently. In this instance a beheaded alignment is visible at 'b' reflecting approximately 145 metres of cumulative channel displacement (D_c) which is comparable to the aperture of the incised belt (D_a, 152 m) suggestive of approximately 9 ruptures. By comparison the tributary stream at 'c' has a similar channel offset (D_c = 148 metres) while the aperture is only 52 metres, suggesting a more limited potential to rework imposed boundaries, likely related to stream power and/or availability of competent bedload material. Depressions ('d' and 'e') on the down-thrown block to the southwest have been channelled by humans for agricultural drainage but lack obvious signs of alluvial channel occupation. I surmise these reflect near-field tectonic subsidence and though Kaipaitangata Stream has ~2 metre topographic advantage, the hydraulic geometry is unfavorable for avulsion in comparison with the present active belt, a trend that is likely to continue as successive ruptures potential increase the distance between the stream and the subsiding area. Ultimately, I consider the transpressional nature of displacement to be preparation-insensitive where the rapid relocation of the stream with flow from the uplifted block to the down thrown block is notionally the same as moving the end of a hose: the primary driver of where water goes is wherever the nozzle is placed.

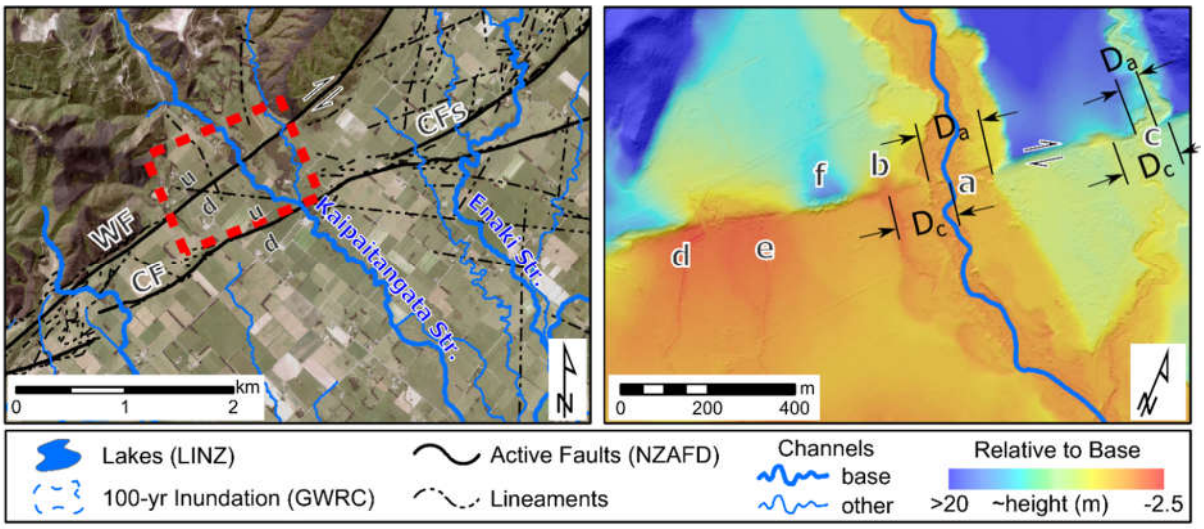

Figure 5-8. Active channel of Kaipaitangata Creek at the Wairarapa Fault (WF, oblique strike-slip) exhibits minimal offset (a) by comparison to terraces and adjacent, smaller tributary (c).

A coseismic landslide occurred during the 1855 Wairarapa Earthquake (M8.2) that temporarily blocked the Ruamāhanga River (Grapes, 1988). The slide originated from the left-bank (Figure 5-9, "a"), the river eventually broke through along the right bank and maps from 1866 indicate the river downstream of the dam was deflected further right than any time since (Grapes, 1988). Contemporary accounts described a large lake upstream of the dam (Grapes and Downes, 1997) with the river drying-up downstream (Grapes, 2000). No specific estimates of dam duration exist, though it has been noted a "short" time after the river dried, fishermen had to climb trees along the bank of the Ruamāhanga when a wave of water arrived (Grapes, 2000). Other scarps and hollows along the left bank (e.g. "b") upstream have been considered as earlier landslides (Vella, 1963a).

Inspection of the LiDAR DEM indicates the ~3-kilometre valley segment up to the crossing of the Mikimiki Fault has an anomalously high degree of terrace re-working along the right valley margin ("c", "d', "e", "f"), with up to 300 metres (horizontal) of penetration normal to the active belt and bend radii smaller than typically observed in the contemporary river. I interpret these scars as evidence of past forcing associated in full or part with past landslides, either due to contact deflection (sensu Korup, 2004) toward the terrace as observed in 1866 (vicinity of 'c') or as a morphological response to more tortuous lateral channel forms resulting from slope reduction associated with persistent local base level increase. In the cases of landslide-forcing, channel preparation would have little or nothing to do with avulsion occurrence nor proximal forms. However, progradational style forcing could also likely occur associated with post-seismic passage/diffusion of sediment slugs.

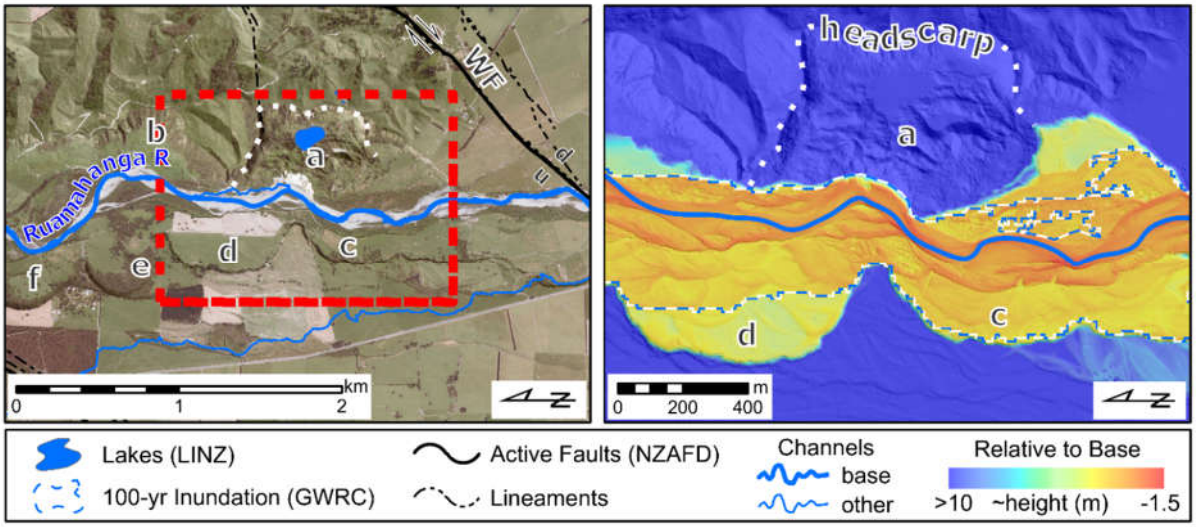

Figure 5-9. Ruamāhanga River at site of coseismic landslide (a) upstream of the Wairarapa Fault (WF) that temporarily dammed the river in 1855 and resulted in persistent channel deflection toward right valley margin (c). Location of prior landslide source area upstream (b) and terrace scalloping on the opposite margin (d, e, f) I interpret resulted from similar processes in previous slope failures.

5.6.2 Sensitive Cases

The contemporary channel of the lower Tauherenikau River has been engineered to a straight alignment confined by stopbanks through its historic delta at the head of Lake Wairarapa (Figure 5-10). The channel invert has aggraded and exhibits considerable (2-4 metres) topographic advantage over much of the historic floodplain except where there is evidence of splay deposits (a) that pre-date stopbank construction in the 1980s. Development of the contemporary river as an alluvial ridge is characteristic of the setting and consistent with historic channels (e.g. b-c-d-e), though the low sinuosity of the alignment and the magnitude of topographic advantage greatly exceed natural analogues preserved in the floodplain. Available information suggests acute forcing by geologic structure is unlikely and, consistent with the setting, I expect sedimentation as the primary mechanism of establishing both hydraulic gradient and access. Access could also be gained by a sapping/geotechnical style of stopbank breach (exterior embankment) or lateral erosion (interior embankment). Routine inspection, gravel extraction, vegetation removal and mechanical reshaping of bedforms are all conducted to delay such occurrences.

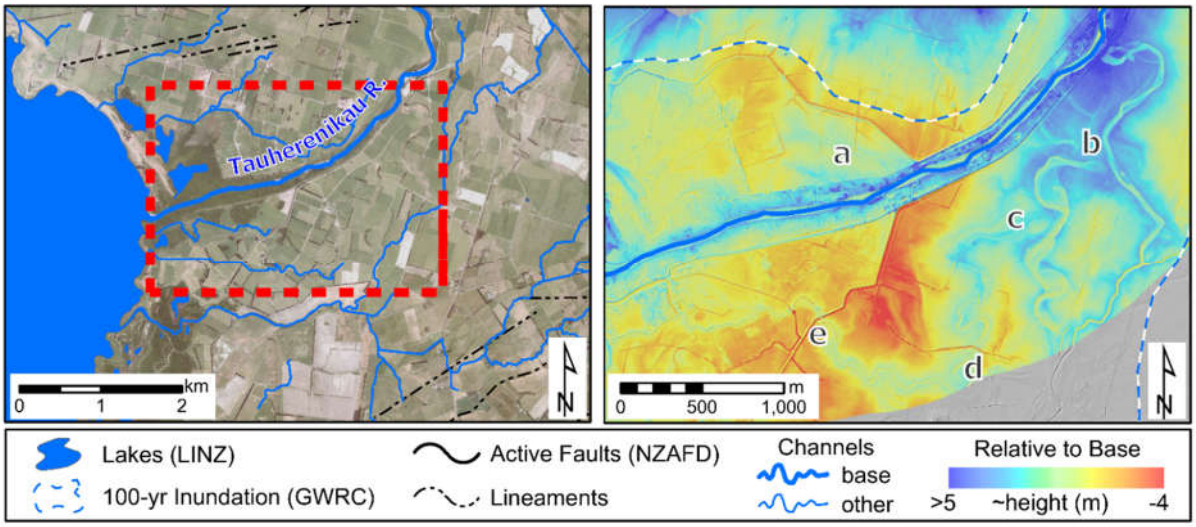

Figure 5-10. The lower Tauherenikau River flows through an engineered channel as it approaches Lake Wairarapa and has formed an alluvial ridge that is super-elevated above the adjacent floodplain. A splay feature (a) pre-dates stopbank construction and provides a measure of hydraulic reinforcement by flattening the local gradient should a breach of the right bank occur immediately adjacent; it will also pond and deflect flow should a breach occur upstream. The alluvial ridge of a paleo-alignment (b-c-d-e) will provide some measure of inundation containment should a breach along the left stopbank occur.

The main alluvial fan of Kaipaitangata Stream is expressed downstream of the Carterton Fault (Figure 5-11). Low areas (a) lie around the fan perimeter while sapping channels upstream (b) and downstream (d) of a road crossing are penetrating the distal fan. Alluvial ridges (dark purple, sinusoidal) are visible throughout, reflecting the fine sediment loading produced by soft lithologies the catchment drains and suggesting high stacking density indicative of active past aggradation. The alluvial ridge of the contemporary channel telescopes downstream of the road crossing (c) well beyond the fan's prevailing footprint which, coupled with the road crossing as the highest point on the distal portion of the fan, makes this area well-primed for avulsion, particularly if the road crossing were to backwater or capacity were otherwise diminished.

Capture of existing channels is a well-established avulsion phenomenon (e.g., Aslan et al., 1999; Morozova et al., 1999; Mohrig et al., 2000; Jerolmack and Paola, 2007; Hajek and Edmonds, 2014) with abundant potential within active belts and floodplains of the study area's larger gravel bed rivers. Both aggradational (fill-then-cut , e.g. Smith et al. (1989); Mohrig et al. (2000); Slingerland and Smith (2004)) and incisional (cut-then-fill, e.g. Mohrig et al. (2000); Fuller et al. (2003b); Slingerland and Smith (2004)) styles may annex or reoccupy such channels. Modelling has differentiated the styles by scaling sediment supply originating from channels to excess shear stress of overland flows and with the potential for both styles to be concurrent on the same floodplain (Hajek and Edmonds, 2014) though the likelihood of knowing input parameters real-world systems may be low and limit differentiation for hazard management purposes. Independent of process and based purely on existing channel density, the floodplain of the lower Waingawa River (Figure 5-12) illustrates abundance of avulsion history and future potential. Interestingly, channel patterns on the left floodplain (e.g., "a", "b", and "c') exhibit a more localised pattern (hundreds of meters) while channels on the right floodplain have potential for diversions exceeding 1 kilometre (e-f-g, h-i and beyond). Generally low-resistance floodplain cover and root strength provided by prevailing graminoid cover also favours avulsion. Such floodplain preparation coupled with highly mobile annual bed flux with local vertical changes on the order of +/- 1 metre (~ 50% of bank height), this reach is a good example of the "sensitive" group.

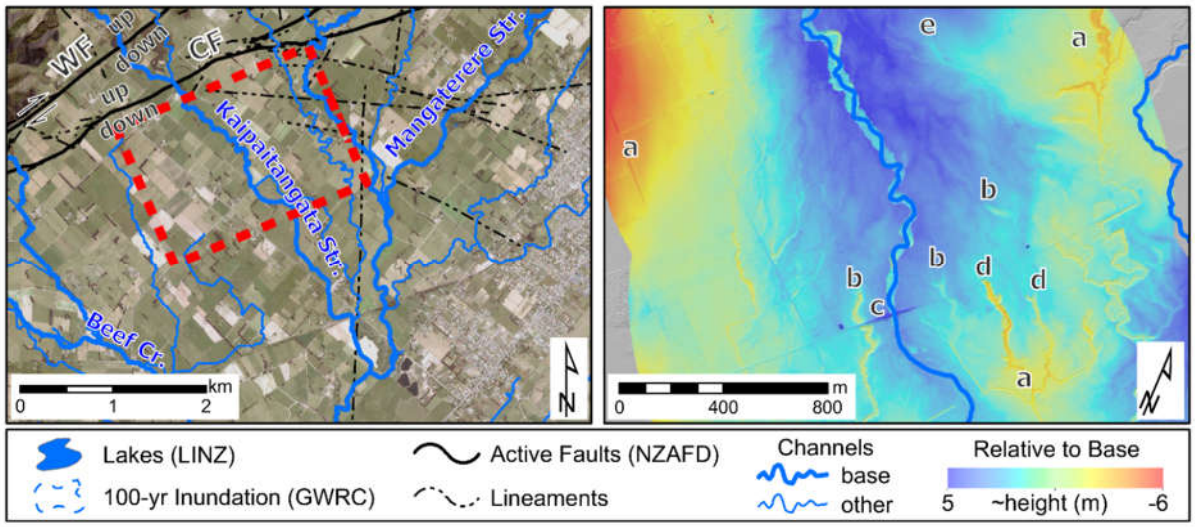

Figure 5-11. Kaipaitangata Stream forms a fan downstream of the Carterton Fault (CF) that is elevated above the adjacent terrain (a) with forms characteristic of cohesive systems including alluvial ridges. The road embankment at (c) is the highest topographic feature on the distal end of the fan where adjacent channels exhibit signs of headward extension and sapping both upstream (b) and downstream (d) of the road. Should the road crossing significantly backwater, these channels become probable capture points. Eastward drainage (e) on the left margin and oblique to the primary fan axis occurs along a lineament that crosses the stream in vicinity of the CF and is a potential nodal avulsion avenue.

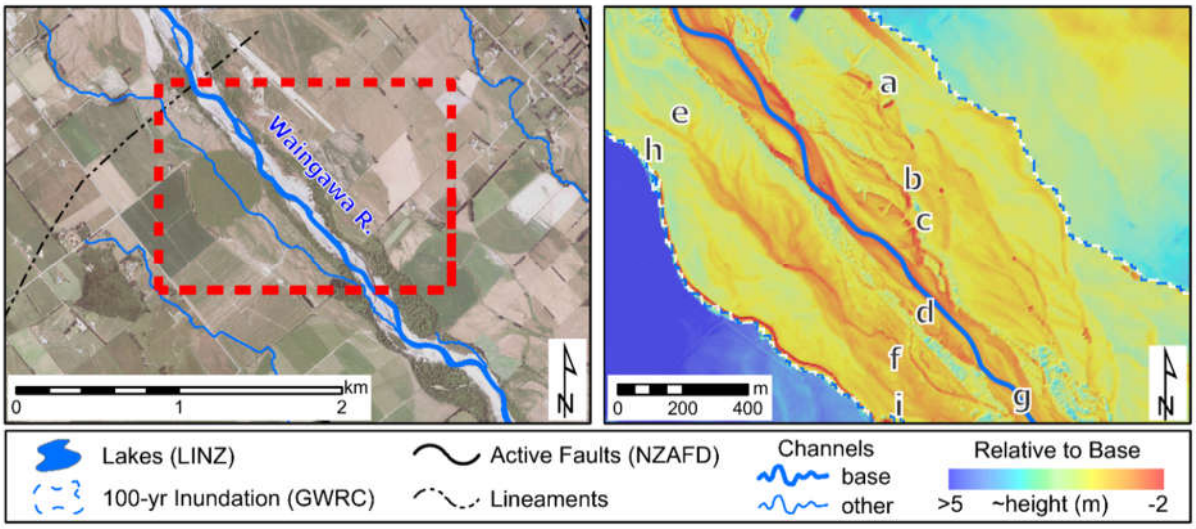

Figure 5-12. Channel scars on the lower Waingawa River suggest general sub-parallel lateral belt shifts (and/or expansion) that produces local, but longer-distance avulsion. Some movements can be temporarily-constrained by morphological signatures of management response which are especially evident at 'a' and 'c'.

Of substantially different size, setting, discharge, sediment, and morphologic regime than the Waingawa, middle Kaipaitangata Stream (in between the prior two examples) also has potential for channel recapture (Figure 5-13). In this case, narrow berms with steep backslopes at the upstream and downstream ends of an abandoned channel are suggestive of construction. Aside from the natural tendency to reoccupy existing channels, there may be an added element of risk here as artificially abandoned channels don't experience the same infilling process of naturally abandoned channels and, consequently, persist longer (Dépret et al., 2017). Such cases effectively extend the duration of avulsion-receptive preparation.

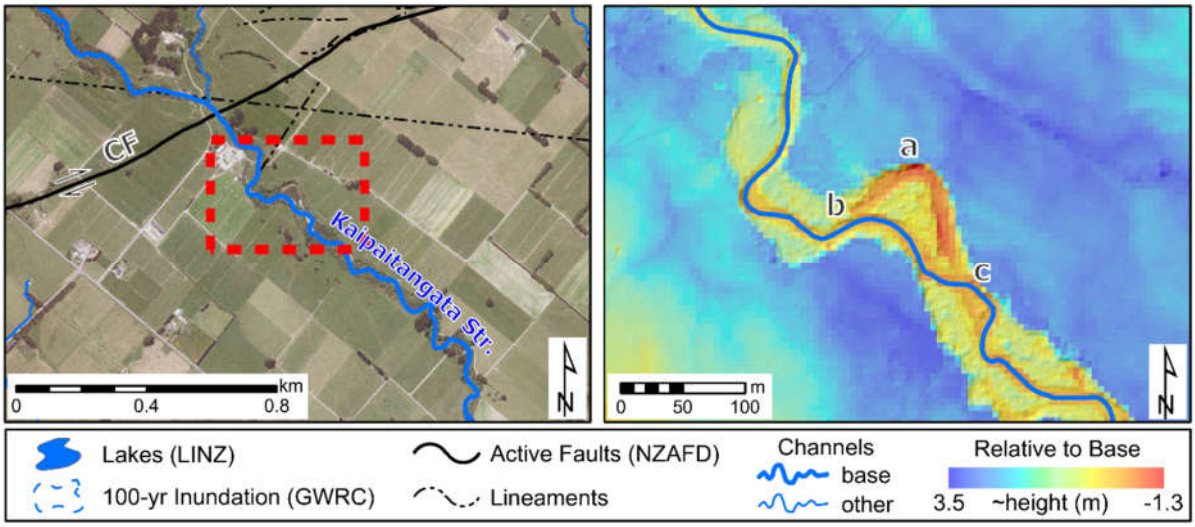

Figure 5-13. Topographic advantage in vicinity of meander cut-off on Kaipaitangata Stream increases sensitivity to preparation factors and increases meander reoccupation (local avulsion) likelihood.

5.6.3 Intermediately Sensitive Cases

Sensitivity to preparation is not always straightforward and some areas will be state-dependent. At the intersection of the Ruamāhanga River and Masterton Fault (Figure 5-14), lies what I infer to be a tectonic pop-up structure ('a') that is hydraulically-engaged at the 1% AEP event and, likely, less. It stands about 2.5 metres higher than the floodplain surface from which it projects and deflects flow to either side, effectively reducing conveyance of higher flows and forces flow to the east side ('e') of the feature where it can access a floodplain channel that re-joins the Ruamāhanga approximately six kilometres downstream via another tributary. In its present incised/contracted state, I consider this site preparation-sensitive as the floodplain channel (b-c) is ~1 metre higher than the Ruamāhanga and approximately 4.5 m WSE is required to access via surface with 'd'). As a result, a good deal of sedimentation and/or increased roughness would be required within the active channel to the west of 'a' (toward 'f') and downstream. If it were discovered that the rupture extended into the active channel causing a backwater that generated either a favourable gradient or increased access (shift in the stage:discharge rating), then I might consider this site more toward the 'preparation insensitive" end of the spectrum. This is because the fault is considered a precondition and the damming effect associated with differential fault uplift while dynamic in the broader sense is effectively the trigger and not a matter of preparation. Nonetheless, as the terrace to the west of 'f' shows little sign of deformation and in the absence of field-based evidence, partial dependence on sedimentation and preparation seems likely.

The Waingawa River is one of the largest and has the steepest channel slope (0.01 m/m between the Mokonui Fault and Skeets Road Lineament) of the Ruamāhanga tributaries. It crosses an area of complex, tectonically-forced terrain downstream of the Wairarapa Fault (Figure 5-15; further discussion in Chapter 6, this thesis) that includes the proximal zone of the Mokonui Fault (MkF, a-b) splay and the Skeets Road lineament (SRL, g-e). Mudstone strath is visible along some bank toes and slopes in the general direction of the contemporary river and is capped by 1-2.5 metres of alluvium indicating dynamic interplay of tectonic and alluvial forcing that, at present, is not well-documented. That said, the contemporary Waingawa River has about a 7-metre topographic advantage over a knickpoint ('e') within its palaeo-braidplain.

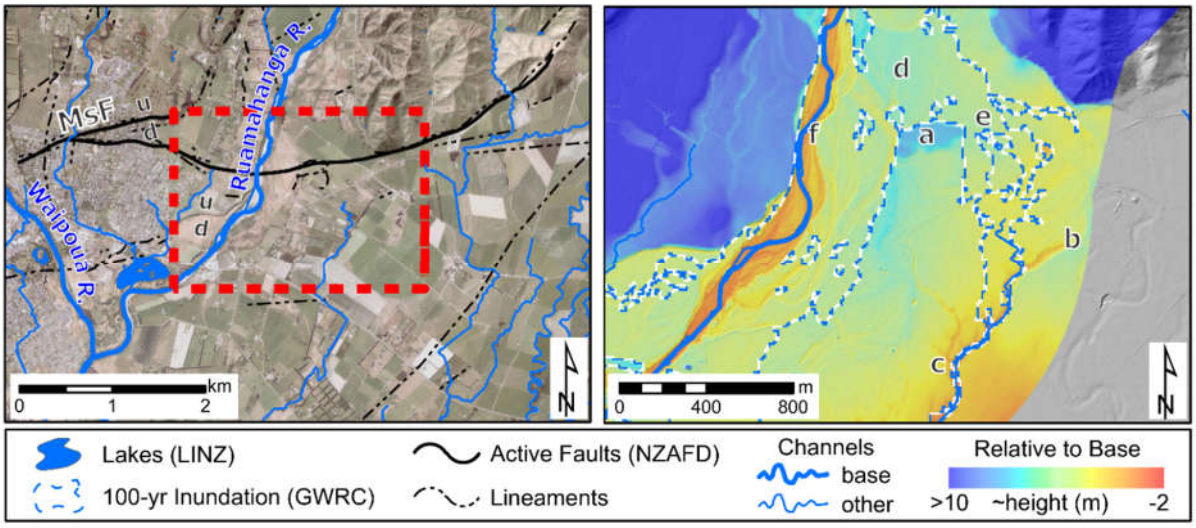

Figure 5-14. Inferred tectonic obstruction (a) in the active floodplain of the Ruamāhanga River near the town of Masterton is hydraulically engaged at 1% AEP event frequency, dividing and localising flow paths.

A newspaper account (Correspondence, 1884) indicates an avulsion reactivated the palaeo-braidplain in 1867 or 1868 channelling flow to the Waipōua River and through Masterton. Given the timing 12-13 years following the 1855 Wairarapa Earthquake, documentation of a shift to a multi-thread form by the Waiohine River during the same period (Stubbe, 1981) and modern knowledge of coseismic sediment transfer and fluvial propagation, I infer that sedimentation was the proximal cause for the 1867/8 event. Complex topography preserved on low terraces (vicinity of 'a') coupled with lithic contacts within the contemporary wetted channel indicate that rupturing across the active channel cannot be ruled-out. The 1885 quake occurred at a time when there were only about 1,400 inhabitants in the entire Wairarapa Region and approximately 15 years before the first local newspaper was founded, so first-hand accounts are few. Undated fluvial sculpting and deposition patterns on the left valley margin (vicinity 'b' and upstream) suggest there has been considerable alluvial forcing in the past. The 1867/8 avulsion was rerouted back to its prior course by early settlers within several days (Correspondence, 1884) to the general alignment of the contemporary belt.

Stopbanks (i.e., levees) at 'b', 'c', and 'd' prevent contemporary discharges to the palaeo-braidplain and a no-defence hydraulic model does not yet exist. However, contact of the 1% AEP perimeter with two of the three structures suggests, in their absence, more frequent flow into the braidplain would occur. These diminish the routine risk of augmented flooding toward Masterton but are untested in terms of alluvial or tectonic forcing. Preservation of intermediate terraces with a relatively linear contact with the contemporary active belt on the right margin contrasts with a more irregular boundary along the toe of the high terrace on the left margin that suggests a forcing bias toward the left side of the margin. On-site observation suggests the improvised nature of the levees are unlikely to withstand persistent alluvial forcing that seems to occur at this location. Further, the northwest end of the levee at 'b' anchors into the trace of the Mokonui Fault and may be compromised during a rupture. Apparent uplift at 'f' with possible back-tilt toward 'd' provides a margin of certainty that flows will occupy the contemporary or left-margin belts as opposed to scrolling in-between. Because of the mixed potential for tectonic and/or alluvial forcing to control access and/or gradient to the paleo-braidplain I consider this site intermediately sensitive to preparation.

By contrast to the episodic, but relative ease with which the Waingawa may be able to exploit topographic advantage along the left margin ('e'), more tortuous planform geometry and the need

for a 3.5 metres WSE to access (even larger to be geomorphically effective) the right side at the SRL, I consider avulsion toward 'g' less likely. Given implications for tectonic back-tilting (Chapter 6, this thesis) in this vicinity, the risk is not zero, but given only 2.5 metres WSE is needed to overtop the left confining margin of the 1% AEP boundary,

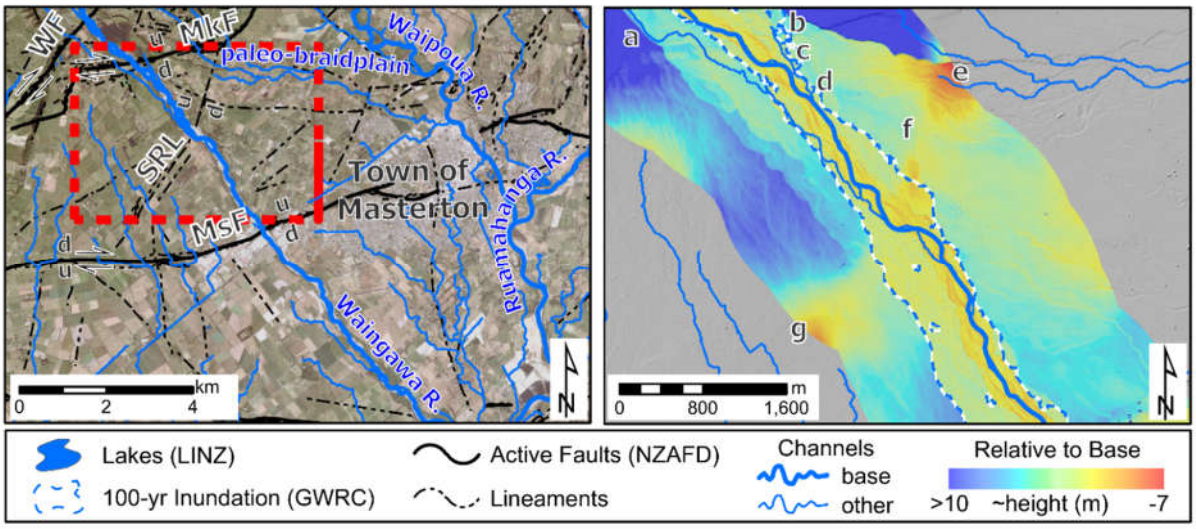

Figure 5-15. The Waingawa River crosses an area of complex tectonic terrain upstream of Masterton with historic (at 'e', ca. 1867) avulsion into the Waipōua River.

The active belt of the Waiohine River has a 3-metre topographic advantage above the left floodplain margin (b) immediately downstream of where it crosses Wairarapa fault (WF, Figure 5-16). This accommodation space could result from differential alluvial filling (in favour of areas to which the river has greater access) and/or tectonic side-tilt. Given the high number of localised topographic depressions in proximity to the segmented faulting, I suspect tectonic is at least partly responsible. Discrete *en echelon* meanders (c, d, and e) indicate past migration attempts whose preservation and symmetry suggest episodic forcing, though the contemporary river is somewhat incised and effective flows in this band may be infrequent.

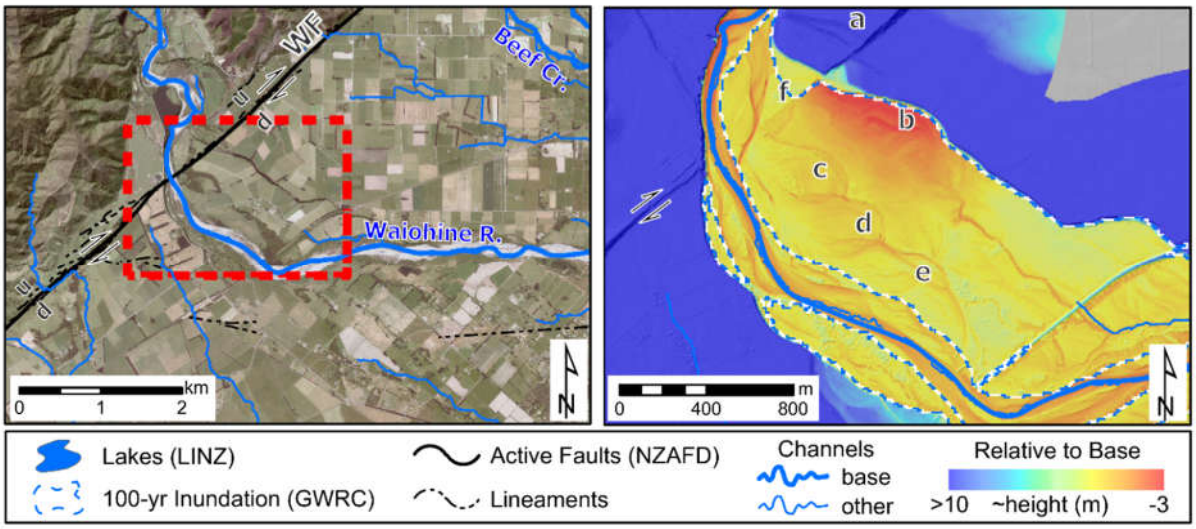

Figure 5-16. Floodplain of the Waiohine River downstream of the Wairarapa Fault (WF) and upstream of the railroad.

Given the displacement along the fault, the low area (b) will come further into play into the future as materials at 'f' get reworked during interseismic periods and coseismic strike-slip improves the

planform geometry for activation. The Waiohine Terraces (a) have been the subject of numerous studies exploring sequences of uplift and channel adjustment over the last 55 years. Given the combination of tectonic and fluvial controls, I consider this to be intermediate in terms of preparation sensitivity as well.

5.6.4 Complex Response Case

As an example, I offer the case of Enaki Stream in the vicinity of the Carterton Fault (Figure 5-17). Though it might be tempting to simply label the mechanism as tectonic forcing, the vectors acting on the stream can be grouped into different processes. The complex structural zone is generally consistent with behaviour of the area's segmented transpressional faults and, in particular, documented on the Wairarapa Fault (e.g., Carne and Little, 2012; Manighetti et al., 2020).

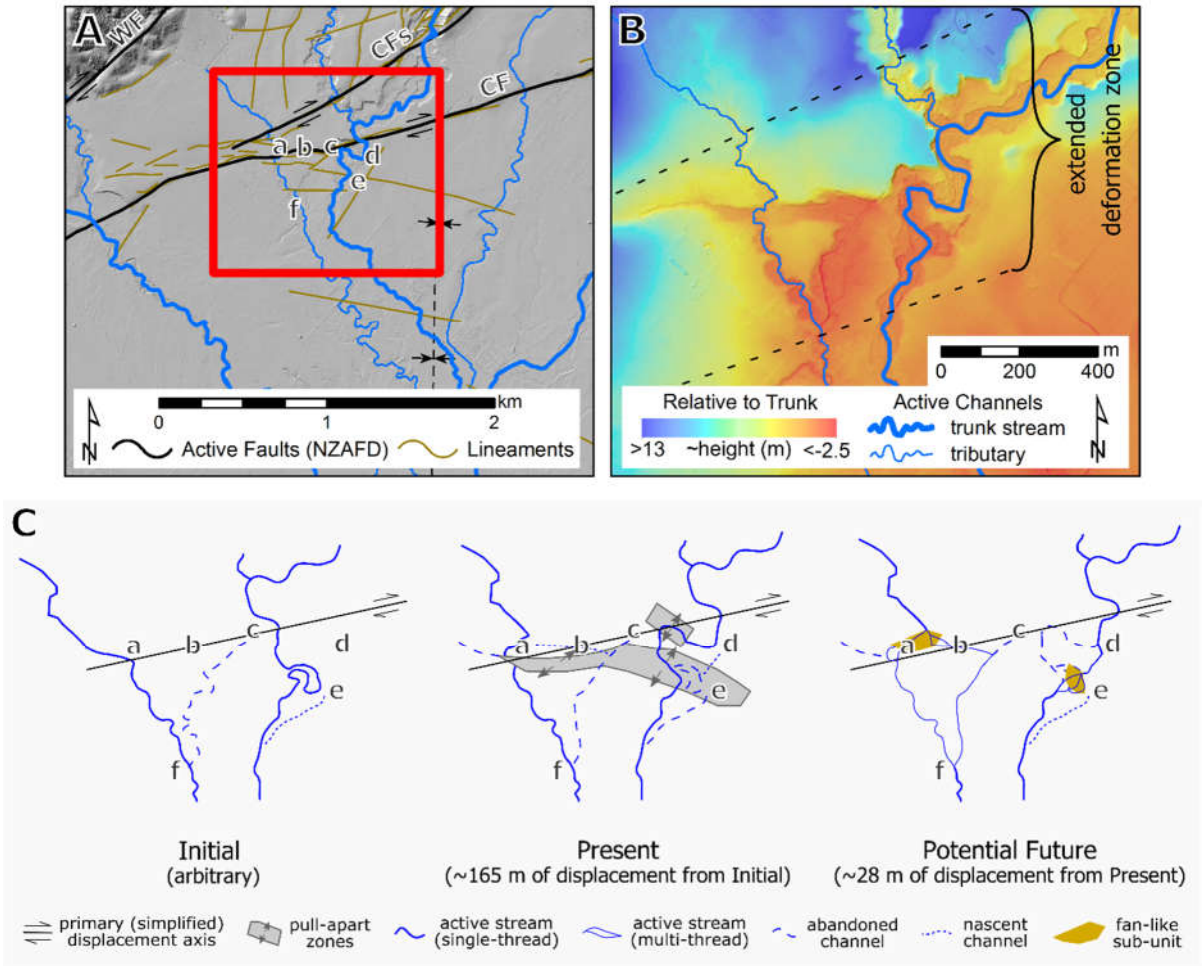

Figure 5-17. Complex response of Enaki Stream and a tributary within a subunit (A) on the Carterton Fault (CF) near divergence of one of its larger secondary traces (CFs) where a pull-apart creates localised subsidence (B). For illustration purposes, a reconstruction along a single, hypothetical slip axis (C) offers a simplified view where the pull-apart deflects Enaki Stream counter to the direction of strike-slip displacement (d-c). Enaki Stream and its tributary abandon channel alignments at different points in time.

I simplify the primary strike-slip displacement to a single axis (along a-b-c) and a somewhat arbitrary starting point where the tributary has a fairly straight alignment (Figure 5-17C, left panel). I hypothesise channel between 'c' and 'f' as an alignment abandoned earlier by Enaki Stream and the channel head at 'e' as developing during overtopping events. The pull-apart may or may not have been present. In the middle panel (representing present conditions), the pull-apart has grown asymmetrically and obliquely to the primary displacement axis creating a small area of local

subsidence downstream of the strike-slip axis. This topographic low provides something of an anchor point for the meander at ‘c’, at least until accommodation space has been filled by sediment. The sinuosity of the meander between ‘d’ and ‘c’ encourages backwater formation during higher peak discharges that periodically spill over the left-bank and initiate channel scour from ‘d’ toward the vicinity of ‘e’.

The tortuous meander of Enaki Stream in the vicinity of ‘e’ has cut-off, due to autogenic processes and/or anthropogenic drainage. Relic channel fills aggrade incrementally, though perhaps very slowly if abandonment was human caused (sensu Dépret et al., 2017), and remains an area of low relative elevation. Pull-apart subsidence enables conveyance of overbank flow (not necessarily channelled) from the tributary (at ‘b’) and the previously-abandoned channel of Enaki Stream. With additional (hypothesised) tectonic displacement and time (right-panel), repeated overtopping incised along the steeper alignment between ‘d’ and ‘e’ captures the main channel of Enaki Stream, partially filling, but also reactivating the relic channel at ‘e’ (sensu Aslan et al., 1999; Morozova et al., 1999; Mohrig et al., 2000). Capture could also be facilitated by lateral erosion of the bank that daylights the cut-off channel closer to river level without the need for overtopping. Displacement of the tributary has made the flow path toward ‘b’ more like ‘a’ and flow bifurcation occurs more regularly with both pathways active.

Despite some fairly acute and localised tectonic influences, I do not consider this site to be “insensitive”, particularly as the hypothetical future scenario incorporates preparation dependencies (i.e., topographic advantage related to reoccupation of abandoned meander), though it is not completely sensitive either. Because strike-slip and the pull-apart effectively create flow access at ‘a’, at a minimum I would consider the tributary “intermediately-sensitive”. By contrast, the Enaki alignment ultimately shifts due to topographically-advantaged incision resulting from backwatering which is behaving in a “sensitive” manner (because preparation accounts for the hydraulic gradient and, to a degree, access). Thus, two connected streams in close proximity, being acted on by multiple, similar tectonic processes can have different sensitivities. Further, there is potential for the main Enaki channel to avulse into the channel draining to ‘f’. In this regard, complex response decouples the *directionality* of where the eventual avulsion will occur (which may be considered sensitive) from the *occurrence* of avulsion (which may be considered intermediately sensitive).

5.7 Discussion

5.7.1 Relative Elevation DEMs (rDEMs)

Relative elevations DEMs maximise local relief/contrast and enable rapid visualisation of localities of topographic advantage, which is a key driver of avulsion hazard. As most avulsions are local and tend to reoccupy existing channels (e.g. Jerolmack and Paola, 2007) methods that enhance identification and relative topographic advantage of those channels are particularly useful. All modelling requires a balance of set-up labour, data cost, and computational demand to meet end-user needs. The empirical, GIS-based nature of this approach using an existing DEM makes it accessible to a much broader user-base and requires less computer performance and very little programming capability than many other approaches. For example, I processed 79.3 kilometres of river with a 1,000-metre search radius at 5 metre resolution in 88.9 seconds on a Windows laptop with a 2.7 GHz i7 processor running standard 32-bit ArcGIS 10.7 with Spatial Analyst.

It is important to be mindful of the effects of input DEM quality which may require an adaptive approach (e.g., to streamline generation) such as I implemented. It is critical to understand the nature of processing in advance of interpretation, particularly the averaging effects that will tend to

diminish apparent topographic advantage and can result in hotspots being overlooked. These become more influential when processing multiple baselines simultaneously (e.g. Figure 5-5) and/or using large search radii (cf. Conley, 2015). Confirmation with the source DEM (m ASL) is always advisable, especially for instances (e.g., low relief drainage reversal, Figure 5-7). This high-level approach can quickly process large extents to direct more intensive and/or specialised resources for target investigation as needed.

Not only does this approach help determine *where* avulsions might occur, but inferences on processes topographic evolution, and/or processes are possible, though this requires specialist knowledge. For example, enhancement of topographic contrasts aids visualisation of potential uplifted and subsiding areas. This, combined with knowledge of directional offset (if strike-slip motion is present) makes enables forecasting of the changes in topographic preconditioning. For example, further dextral motion along the Wairarapa fault effectively moves areas of along-strike negative relief further from the active channel of Kaipaitangata Stream (Figure 5-8) but closer to the active belt of the Waiohine River (Figure 5-16). Thus, the potential for what I consider as *leading depressions* to contribute to avulsion of Kaipaitangata Stream diminishes in time, while *trailing depressions* increases avulsion potential at the Waiohine River. Increased hazard associated with trailing depressions assumes, in part, any subsidence-related component migrates with minimal rebound.

While rDEMs are generally well-suited the aim of this chapter, it is important to be mindful that they are not substitutes for more rigorous hydraulic, hydrodynamic, or morphodynamic modelling. Fundamentally, the screening approach employed aids identification of a necessary condition (topographic advantage) for avulsion to geographically constrain where more intensive efforts should be made. The framework's application and extensibility could be improved by increasing frequency and resolution of geospatial data capture and creating data processing pipelines. For example, a three DEM time-series could become three rDEMs which could, in-turn, be differenced in-sequence to two DEMs-of-Difference (DoDs) to identify trends in bed aggradation and/or overbank relief. Such products would enrich to data underpinning the framework to assure preparation factors like bed level changes and/or relevant hydraulic outputs like depth and excess shear are generated where they are most relevant without unnecessary effort or cost.

5.7.2 Framework

Once localities (e.g., reaches or sites) of existing or anticipated topographic advantage are identified, it becomes important to assess the sensitivity (proximity to threshold) for potentially relevant factors at a given locality. Such sensitivity is a continuum between end members that are strongly sensitive to preparation factors and highly insensitive ones where triggers govern. While the variety of existing styles and classifications all fit their respective purposes, no one of them captures the full spectrum of avulsion examples from the study area, particularly displacements by landslide contact and strike-slip offset. Beyond the study area, it also accommodates other processes not well-captured by traditional avulsion styles include glacial impingement, volcanic filling, flash/outburst flooding, and solution weathering. All but the last of these can be accommodated by addition of a "allogenic displacement" (or similar) style or explicit recognition that existing styles only represent a sub-domain.

Given the limitations of present classifications that generally comingle condition (e.g., topographic advantage) and process (e.g., sedimentation rate) factors (Table 5-1), it seems worthwhile to step-back consider a refined statement of necessary conditions for an avulsion to occur. I propose (Figure 5-18) an avulsion may occur when: 1) boundary conditions capable of producing differentially

optimal hydraulic gradient(s) away from an existing channel AND 2) access by a geomorphically-effective flow to generate those hydraulic gradients.

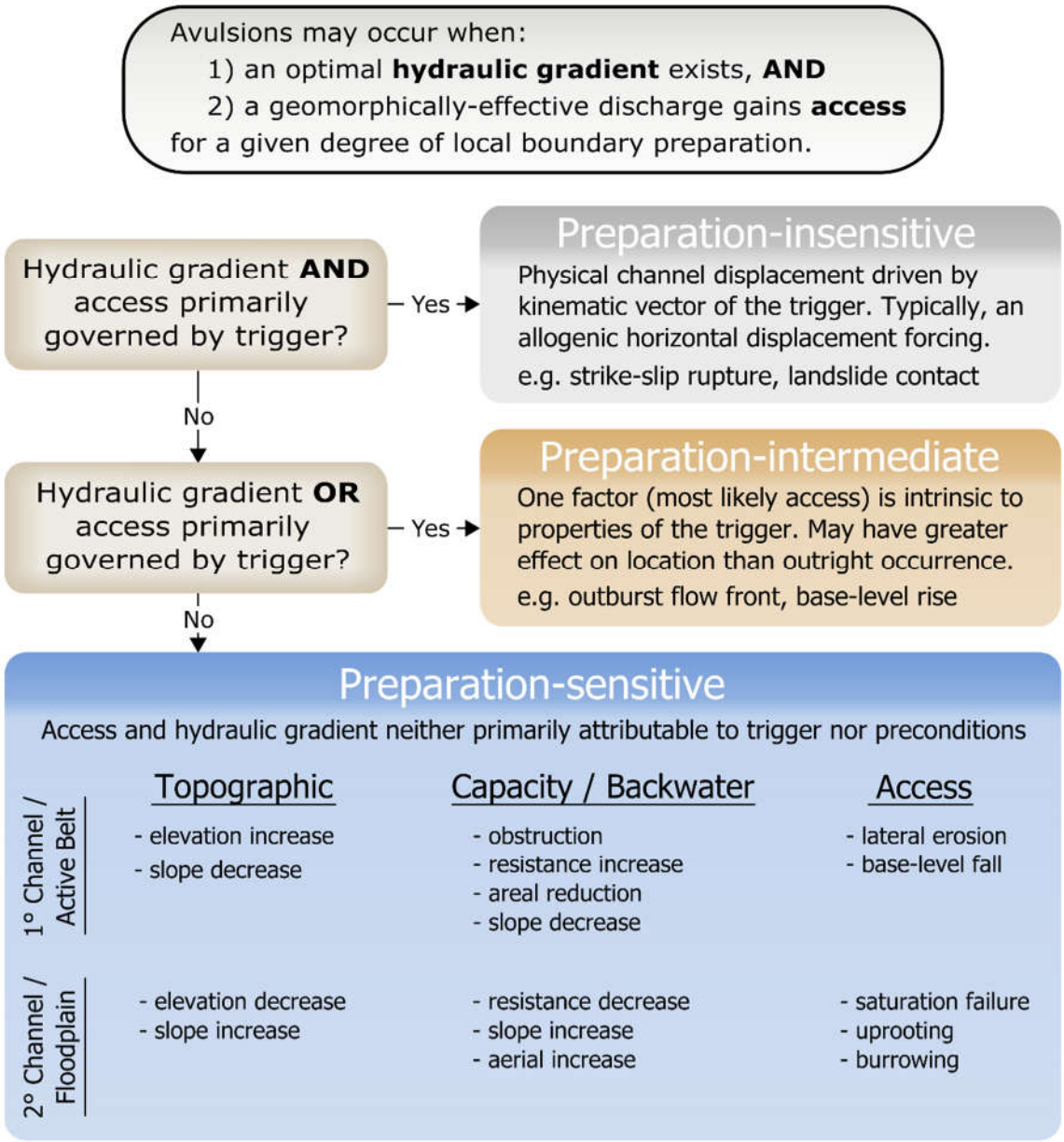

Figure 5-18. A simplified conceptual framing of avulsion causality. These classes can be applied to make processes-based linkages, which can be further screened in terms of occurrence likelihood for a given location, set of boundary conditions, and/or suitable modelling approaches.

This definition seems to be implicit in the work of others (e.g. Jones and Schumm, 1999; Smith, 2003; Jerolmack and Mohrig, 2007; Kleinhans et al., 2013), but lack of a formal, inclusive statement may contribute to differences is usage and perceptions amongst sub-fields. Based on this definition, I can broadly categorise localities based on the sensitivity to preparation which can be resolved inversely by considering dominance (or not) of a given trigger (Figure 5-18).

A locality or system may be considered *preparation-insensitive* if the preferential hydraulic gradient *and* conditions that create flow access are primarily governed by the trigger. Generally, these will be instances of physical channel displacement by an allogenic forcing mechanism such as rupture of a strike-slip fault or contact by a landslide. Instances of preparation insensitivity are where a given trigger vector overwhelms the subject river or stream, such that determination of avulsion vs. no

avulsion is not dependent on preparation. These will be allogenic in nature, driven by wide range of processes including glacial (e.g. Kovanen and Slaymaker, 2004), landslide/earthflow (cf. Korup, 2004) , or tectonic (Ouchi, 2005). In other words, a stream's pre-existing state at the time of avulsion has little to do with whether the avulsion occurs or not (i.e., state-independent). Further, stream state may or may not influence resulting fluvial forms or processes. My suite of "insensitive" examples (Figure 5-6 to Figure 5-9) are biased toward tectonic forcing of smaller channels (fifth-order Strahler or less) that illustrates a spectrum and complexity not presently represented in the literature. I suspect this may be indicative of a general real-world bias, but further work is required to characterise frequency or proportionality. This inferred linkage between small catchment size and disproportionately greater capture frequency are consistent with results of Walker and Allen (2012). Qualitatively, small channels seem to compose a greater portion of the insensitive domain in the study area, however, larger channels are not ruled-out. Modelling by Gupta et al. (2014) suggests very large rivers (e.g. Ganga) can be more acutely sensitive to tectonic subsidence than conditioning factors like gradient advantage or bend migration, though avulsion may only be temporally proximal and direct linkages to coseismic rupture have not been made.

Preparation-intermediate instances occur when a trigger governs either gradient or access such as the flow front of an outburst flood (i.e., where runup or pre-backwatered head establishes access or gradient). Conceptually, the intermediate sensitivity group bridges the gap between endmembers and reflects situations where preparation may not be the determinant of whether or not an avulsion occurs but is a significant contributor to the outcome. This may include instances involving obstruction by large wood (e.g. Abbe and Montgomery, 2003; O'Connor et al., 2003), ice (Ethridge et al., 1999) or tectonic feature (this paper). A drowning-style base-level rise that effectively shifts process zones upstream (sensu Chadwick et al., 2020) would be another example. Instances where access is generated by waves, particularly at the flow front of outburst or flash floods are expected to fall into this group though I did not find documentation of such occurrence. For a given site, the boundary between being sensitive vs. intermediately sensitive may depend on the triggering mechanism and require additional interpretation.

Instances where a trigger is expected to neither independently generate the hydraulic gradient nor access compose the *preparation-sensitive* group. Whether relative slope, relative resistance, and/or sedimentation-driven rise and/or volumetric reduction, channels on the preparation-sensitive end of the spectrum, are simply end-members of capacity-related flood hazard (cf. Slater et al., 2015). Here, hydraulic gradient and access are interrelated (i.e., will almost always involve backwatering) and will include a disproportionate number of avulsions, including those triggered by 'normal' hydrologic flooding. Varying combinations of trigger and preparing factors interactions generally include channels affected by autogenic sedimentation. Sites experiencing backwatering resulting from differential roughness/resistance and/or volumetric capacity gradients (e.g. Brizga and Finlayson, 1990; McCarthy et al., 1992, respectively), shifts in hydrology (Gaeuman et al., 2005) and situations where tectonic influence is a conditioning factor and channel movements are temporally uncorrelated (e.g. Ouchi, 1985; Wells and Dorr, 1987) may also be expected in this group.

The diverse array of potential avulsion factors and sensitivities within my modest sized (600 km^2) but topographically complex study area underscore the spatially-explicit nature of avulsion potential and actuation. The sensitivity-based framing accommodates relational incongruency of common boundary parameters, processes, mechanisms, factors, and styles while providing a grouping that is implicitly relevant to hazard assessment and management. In addition to the way I have discretised grouping, increased repeatability may be gained by having alternate questions or criteria. For

example, if deliberating between “intermediate” and “sensitive”, consider whether avulsion likelihood given the same trigger changes if a channel is incised vs. aggraded.

The fundamental diversity in which complex interactions of contributing factors are expressed across different geomorphic settings means some interpretive flexibility is required. For example, whether a factor is a precondition, preparation or both is likely dependent on the relative timescales on which the variation of the factor occurs relative to the timescale that avulsions occur for a given system. The Ruamāhanga catchment’s avulsion diversity challenges any typology, but with consideration, all instances will fit into one of the three sensitivity classes which can then direct further investigation such as model suitability (Table 5-2).

Table 5-2. Avulsion sensitivity types with order of relevant modelling approaches.

Sensitivity Group	Follow-on Modelling Approaches
Preparation-insensitive (a.k.a. trigger-dominated)	LEM / morphodynamic; ensemble modelling
Preparation-intermediate	Morphodynamic or hydrodynamic; ensemble modelling with hydraulic modelling
Preparation-sensitive	Hydraulic modelling; morphodynamics

5.7.3 Hazard Implications

Avulsions can result in greater mortality, longer-term human displacement, and/or extended interruption of transportation systems than common inundation flooding. Thus, without explicit attention, significant values may unknowingly be at risk (e.g. Chakraborty et al., 2010) with individual instances of first order avulsions potentially affecting millions of people (e.g. Soong and Zhao, 1994; Sinha, 2009; Syvitski and Brakenridge, 2013). The rDEM-based methodological approach is similar to other methods that identify hotspots such as for inundation (Röthlisberger et al., 2017) or geomorphic change (Czuba and Foufoula-Georgiou, 2015). My framework’s sensitivity classes lend themselves to results that are both inclusive and provide unity, though does not eliminate potential ambiguity inherent to classifying the complexity and diversity of any natural system. It is the grey areas that, perhaps most importantly, require extra thought that ultimately enhances understanding of underlying processes and process interactions that involve spatial and temporal complexities.

Complex feedbacks of floodplain morphodynamics including topographic inheritance (Leddy et al., 1993; Hajek and Edmonds, 2014) complicate hazard forecasting, though can aid in constraining hazard. For example, the resulting hazard when a channel eventually avulses off an alluvial ridge is greatly diminished on the opposite side of that same ridge which may constrain subsequent migration and/or inundation flooding (e.g. Soong and Zhao, 1994). Further, the existence of topographic advantage does not obligate avulsion, as size distribution and rheology have been found as complimentary or greater factors in both fine textured, low gradient rivers (e.g. Aslan et al., 2005) and debris fans (Whipple and Dunne, 1992), respectively. In meandering rivers, modelling suggests the balance between bed-forming and floodplain-forming sediment fractions is an important control on channel-floodplain connectivity such that the most super-elevated channel units are not necessarily the most likely to avulse (Nicholas et al., 2018).

Generally, avulsion frequency scales to the time for sedimentation to fill one channel depth (Jerolmack and Mohrig, 2007) though can range between 0.6 (or less, Mohrig et al., 2000) and two (Chen et al., 2015). In real time, this can be generally expected on the order of 10^3 years (Bridge and Leeder, 1979), though varies widely by system from 10^1 to 10^3 years (Jones and Harper, 1998; Stouthamer and Berendsen, 2001; Slingerland and Smith, 2004). Further, only some breaches or break-outs convert to full avulsions as “healing” may occur where long-term (re)occupation as a

primary channel is precluded. On systems exhibiting crevasse behaviour, this intermediate condition may persist or occur over decades (e.g., Slingerland and Smith, 1998; Makaske et al., 2012; Nienhuis et al., 2018). Stratigraphic evidence from the Mississippi River suggests extend periods (10^3 years) of crevassing may act as preparation for avulsion (Aslan et al., 2005). Analyses of the lower Yellow River for the past 2,000 to 4,000 years vary but indicate levee breaches have resulted in avulsion between 0.4 and 11% of the time (computed from data presented in Soong and Zhao, 1994; Chen et al., 2012; Li et al., 2020). The detail and duration of the Yellow River historic data record is quite exceptional, but this avulsion conversion ratio range may be indicative of low-gradient, cohesive systems that develop alluvial ridges. It should also be noted that there were extended subsets of time (e.g. A.D. 1570 to A.D. 1839) where every breach triggered an avulsion and coincided with a period of levee strengthening and repair of all breaches (Chen et al., 2015). By contrast, I would hypothesise much larger proportion of apex breakouts convert to full or partial avulsion at fan-heads. Sedimentary records of the Rhine-Meuse delta suggest autogenic control of avulsion frequency , but allogenic control of location (Stouthamer and Berendsen, 2007). Within coastal plain segments, sea level rise may exert prevailing control during rapid changes, tectonic control emerges under slower periods of rise (Stouthamer and Berendsen, 2007; Taha and Anderson, 2008). Tectonically triggered avulsions have not been sufficiently studied to characterise frequency statistically.

However, insights on relative timing, behaviour, and spatial distribution have been emerging (e.g., Ouchi, 2005; Cowgill, 2007) and are supplemented by this work. The Enaki Stream example raises an interesting point regarding the different timing in which the two streams adjust. That Enaki Stream has been completely captured in the 'future' panel does not necessitate the tributary to have committed to a single channel. Because slip rates are not well-constrained on the Carterton Fault, I do not characterise this sequencing by number of ruptures. However, in principle, it is consistent with examples from Kaipaitangata Stream (whose closest identifiable channel is 8 or 9 ruptures distant) and the Beef Creek tributary (whose closest identifiable channel is 4 or 5 ruptures distant) at the Wairarapa Fault. Put simply, different streams have different sensitivity to rupture and even closely-spaced streams on the same fault (expected to experience comparable slip rates) may be out-of-phase with one another.

In active tectonic settings, consideration of combined events is prudent as rupturing and post-seismic sedimentation can cause complex disaster chains where multiple styles can occur in a single locality and sensitivity can shift (e.g. Zhang et al., 2014). As relationships between sediment supply and avulsion frequency are proportional (Ashworth et al., 2007) any catchment change that alters sediment supply can affect avulsion hazard. Sediment size combined with channel distribution may be more important than topographic advantage in fine-grained systems. Though focus is often on sediment pulses (e.g. from storms or earthquakes), dramatic increases in avulsion frequency have been linked to decadal and century scale land-use shifts (e.g. Chen et al., 2012). While flood risk management in developed countries increasingly considers risks up to 0.2% AEP, flood maps continue to be treated by planners, regulators, and the public as binary and static. Thus, through time, even before non-stationary considerations (such as associated with climate change), many more people are in harm's way than flood maps typically represent. Given sedimentation rate as the most widely recognised proximal causal factor (Slingerland and Smith, 2004) and the stochastic nature of triggers, the two greatest potential avenues for effective management seem to be: 1) pre-emptive catchment and channel strategies that constrain (or reduce amplification of) sediment transfer and mobility dynamics and 2) appropriate land-use planning for areas where movements can be anticipated.

While this paper focuses on hazard identification and prioritisation, other applications of the rDEM and sensitivity framework include habitat restoration and/or floodwater mitigation. Restoration of geomorphic complexity is an important habitat characteristic for conserving imperilled species. Localising near-threshold areas could be a means of implementing process-based restoration with greater efficiency by guiding designs that leverage the threshold (where threshold breach is desirable) or mitigate sensitivity by reinforcing thresholds (where threshold breach is undesirable). Similarly, depressions may be desirable areas for attenuating flood peaks and could be screened based on channel-migration (avulsion) tolerance.

5.8 Conclusion

The societal need to address river avulsions as hazards necessitates a functional approach that is not well-served by a literature body sharply partitioned by geomorphic setting. Topographic advantage, the degree to which a present watercourse is elevated above other potential paths, provides a common denominator across geomorphic settings and can be rapidly assessed using relative-elevation DEMs (rDEMs) detrended using the stream as a baseline datum. The empirical, GIS-based analysis environment make rDEMs a rapid and highly-accessible approach for landscape-screening. Aside from localising potential hot-spots, they facilitate inferences on processes and/or topographic evolution and processes.

Differentiating the “setup” phase of the traditional two-step river avulsion conceptual model into preparation (dynamic) and preconditioning (static) factors better aligns the model with other threshold-based geomorphic sub-fields, specifically slope stability. It is highly relevant to hazard management as it can also aid focus mitigation types and level of effort, for example, by distinguishing relevant spatiotemporal scales, data resolution, and/or feasibility to influence. This is further helped by advancing visualisation of the traditional avulsion threshold model to 1) differentiate channel and receiving area preparation, 2) incorporation of sensitivity as an inverse function of the distance between the two, and 3) representation that sensitivity can increase or decrease due to variation in either. A framework based on preparation sensitivity offers applications that provide unity and are more inclusive of processes (e.g., glacial impingement, volcanic filling, tectonic displacement, or outburst flooding) that not well-captured by existing conceptual models.

While the rDEM process is highly accessible with relatively straightforward implementation to localise potential hot-spots, geomorphic process interpretation remains expert-driven at the present level of framework development. A good example is provided by the case of avulsions induced by coseismic displacement where adjacent streams intersect the same fault (i.e., experiencing comparable slip) are likely out-of-phase in terms of avulsion occurrence. Thus, specialist knowledge and experience are required for understanding how processing potentially biases results as well as for classification, prioritisation, and identification of lines of investigation. Opportunities to make framework application more accessible include increasing frequency and resolution of geospatial data capture and creating data processing pipelines. For example, differencing a time-series of rDEMS, could be used to identify trends in bed aggradation and/or overbank relief. Present and future, the proposed screening aids identification of a necessary condition (topographic advantage) for avulsion to occurs and guide more intensive investigation hydraulic, hydrodynamic, or morphodynamic modelling efforts.

Summary of Thesis Chapter 5

Chapter 5 consolidates avulsion factors across various subfields of geomorphology, distils a common denominator framework, and provides a rapid screening method that is both scientifically novel and offers great potential utility to hazard managers. Differentiation of Phase 1 (the 'set-up') of the traditional two-phase conceptual model into preparation and precondition components is novel in discretising the roles of twenty-nine factors identified in the literature and providing conceptual standardisation consistent with the slope-stability sub-field of geomorphology. The proposed GIS-based approach for screening landscape-scale data demonstrates ability to identify reach-scale hot-spots when applied across a large extent of the Ruamāhanga catchment. The relative-elevation based method enhances visualisation of topographic advantage and facilitates rapid inference of potential contributing mechanisms. When hot-spots placed into the proposed sensitivity-based conceptual framework, localities can be prioritised for subsequent attention. Due to unresolved quality control issues identified between overlapping LiDAR flights, Chapter 5 ingests a single DEM. As such, it represents the spatially-explicit potential for change. However, the same method could be applied to a DEM-of-Difference to represent, for example, spatially-explicit rates of sedimentation or other preparation and preconditioning factors. Even in the absence of measured vertical change, the spatially-continuous and landscape-scale nature of Chapter 5 reveals a very high-degree of spatially-explicit variability in sensitivity that underscores the need for identifying and understanding geomorphic context. The high density and variable nature of tectonic forcing contributes to a stark lack of spatial uniformity in the Ruamāhanga catchment's gravel bed rivers and sets-up exploration of riverscape, decadal-scale vertical bed dynamics (Chapter 6) and increasing planimetric uniformity (Chapter 7).

Chapter 6

Persistent control of vertical bed dynamics by active faults in unconfined gravel-bed rivers

Introduction to Chapter 6 of Thesis

Chapter 6 follows on the spatial variability and differential morphodynamic potential identified in the previous chapter by exploring vertical bed dynamics in relation to river intersections with active geologic structures. The landscape perspective of Chapter 5 is refined to a single river (riverscape-scale) for a 22-year time-series of benchmarked cross-sections. Epochs of directly measured change range from three to five years while the active tectonic framing implicitly incorporates multi-century temporal scaling. Chapter 6 uses the relative-elevation method from Chapter 5 to enhance visualisation and enable profile extraction from adjacent terraces to support a hypothesis of tectonic back-tilting. It builds upon Chapter 5's graphical and descriptive exploration of active tectonic control on alluvial rivers and streams and addresses thesis objective 'iii' by documenting persistent compartmentalisation of vertical channel behaviours along an unconfined river corridor during an interseismic period.

This chapter is in preparation as a manuscript for Nature Communications: Earth and Environment as

Conley, W.C., McColl, S.T., Fuller, I.C., Tunnicliffe, J.F., Stahl, T., Macklin, M.G. (In Prep). Persistent control of vertical bed dynamics by active faults in unconfined gravel-bed rivers.

As a consequence of the typical concise style of a Nature paper, much of the information is presented as supplementary information.

6.1 Abstract

Fluvial control by tectonic processes has been explored at millennial and orogen scales and more recently at annual and reach scales associated with fault rupture. Fluviotectonic dynamics operating between these time-scales are relatively unexplored. I use a time-series of six surveys of thirty monumented cross-sections, collected over twenty-two years, to evaluate change in bed material storage (bed change) in an unconfined gravel bed river within an active New Zealand forearc basin. The 16-kilometre study reach crosses four active oblique strike-slip faults and several folds. I analyse metrics of bed change and relate spatial patterns to surface deformation interpreted from a 1 m LiDAR-derived elevation model. Incremental changes between surveys at the same station are noisy as are net bed changes through time with neither metric revealing clear patterns. By contrast, patterns of total bed change accumulated over the time-series reveals spatial coherence with intersecting geologic structures Relatively little total bed change occurs at cross-sections located close to uplifted axes and greater total bed change is generally observed at cross-sections downstream of such intersections and/or coinciding with back-tilting. I conclude that bed change compartmentalisation by active geologic structures along an unconfined alluvial river is detectable, spatially coherent, and persistent during an interseismic period.

6.2 Introduction

Tectonic deformation is a primary control of regional landscape gradient and fluvial morphodynamic expression. Deformation effects on network geometry, channel pattern and long-profile are well-documented (cf. Schumm et al., 2000; Bull, 2009; Burbank and Anderson, 2012). Early work comprised of descriptive correlations of channel planform (e.g. Adams, 1980; Ouchi, 1985; Holbrook and Schumm, 1999), migration (e.g. Cotton, 1941; Nanson, 1980), depositional patterns (Burbank, 1992) and their collective integration (e.g. Alexander et al., 1994) between alluvial rivers and tectonics at regional scales. Investigations over the last two decades have favoured uplifted, erosional, bedrock-controlled, and geomorphically-confined landscapes, often at orogen and multi-millennial scales (e.g. Whipple and Tucker, 1999; Kirby and Whipple, 2001; Snyder et al., 2003a; Duvall et al., 2004; Wobus et al., 2006; Kirby and Whipple, 2012).

Advances in topographic measurement, indirect subsurface exploration and geospatial analyses have enabled characterisation of reach-scale alluvial dynamics at discrete millennial scales (Amos and Burbank, 2007) as well as documentation of annual to sub-decadal changes in bed material storage (bed change) and knickpoint retreat to co-seismic rupture (Yanites et al., 2010; Huang et al., 2013). However, the bulk of research has targeted higher relief, confined settings with comparatively little attention to unconfined alluvial reaches. While slope is the prevailing hydraulic parameter across studies at all scales, width variation has generally been considered at broad scales using values derived from drainage area (e.g. Snyder et al., 2003a; Duvall et al., 2004) with some field validation; exceptions include rare reach-scale investigation of paleochannel widths (e.g. Amos and Burbank, 2007). To my knowledge, coupling of active, interseismic tectonics and bed change at segment to reach-scales over sub-decadal to decadal time periods has not been investigated for unconfined rivers.

Modelling of alluvial river processes identifies signal detection difficulties (sensu Straub et al., 2020) which, perhaps, has discouraged fluviotectonic field investigation in unconfined alluvial settings. While studies of well-dated alluvial and bedrock-controlled rivers worldwide show clear evidence of Quaternary climate and anthropogenic forcing over sub-decadal to millennial timescales (Macklin et al., 2012), unpacking a fluviotectonic signal is hindered by scaling issues between tectonic and alluvial processes, particularly during interseismic periods. Differential magnitudes of tectonic

deformation (millimetres per year) versus erosion/deposition rates (centimetres to metres per year) challenge change assessment. Standard approaches using drainage area, channel gradient, topographic ratios, bedrock incision, or profile inflections (Snyder et al., 2003b; Kirby and Whipple, 2012) are not well-suited for multi-thread channels, especially in unconfined settings. Tailored methodological approaches are necessary to address the challenges of detecting signals in this geomorphic domain.

Traditional conceptualisations of channel profile response to fault rupture were developed largely to explain terrace flights and consider the immediate redistribution of channel materials proximal to a planar rupture, without consideration of fluvial dynamics (Figure 6-1, left). Numerical modelling of asymmetric subsidence has shown aggradation rates and channel stacking vary spatially, especially in back-tilted basin settings (Heller and Paola, 1996). I hypothesise that persistent control by active tectonic structures can partition decadal bed change in unconfined alluvial rivers during interseismic periods (Figure 6-1, right). I apply a novel combination of detrended high-resolution terrain analysis with a time-series of permanent cross-sections to evaluate field-scale spatial coherence of sub-decadal bed change and geologic structures in an active forearc basin. Use of the term "bed" should be interpreted as all substrate within the active zone of the river over the period of study. In this manner, it includes materials that could be considered "floodplain" at discrete points in time.

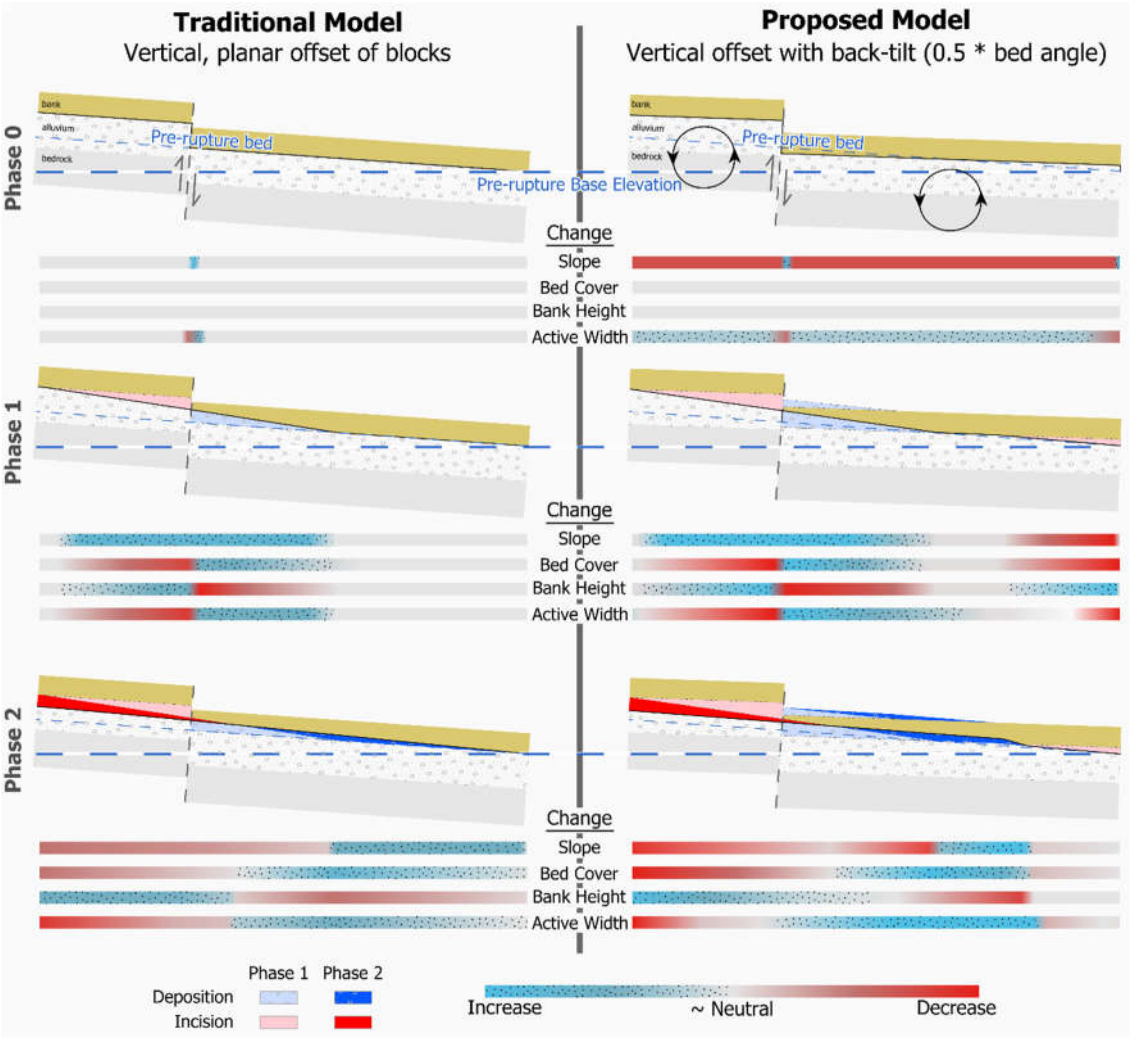

Figure 6-1. Left: traditional concept of vertical offset on river profile and sediment redistribution (after Lensen (1964) and Carne et al. (2011)). Right: Same geodetic offset as left side of graphic coupled with back-tilt.

6.3 Setting and study area

New Zealand straddles a plate boundary (Figure 6-2, inset) where net motions of the Australian and Pacific plates are in oblique opposition, with the southern North Island experiencing 3-8 millimetres per year of upper-plate shortening (Nicol et al., 2007). The study area, within the forearc basin east of the Tararua axial range, is primarily characterised by oblique strike-slip faulting (Figure 6-2, middle). Active faults exhibit primary dextral motion, often with secondary dip-slip (GNS Science, 2020). The lower Waingawa River (Figure 6-2, top) is unconfined (Figure 6-2, bottom), gravel-bedded, lacks tributaries in its lower 15 km (XS 1-28), slopes between 0.005 and 0.01 m/m and has a relatively straight active braidplain alignment between 80 and 230 metres wide. It crosses four active faults, including the Wairarapa Fault which ruptured in 1855, and other tectonic structures (Figure 6-2, top), has a Late Quaternary terrace paralleling nearly the entire river (Figure 6-3A), and minimal intrusion of fixed human infrastructure (see Supplementary Materials for reach and catchment detail).

6.4 Methods

Cross-sectional surveys enable evaluation of bed change, network propagation, and disturbance responses by capturing vertical and width changes (Tunnicliffe et al., 2017). I differenced thirty permanent cross-sections sequentially in time across six surveys (1989-2011) to produce five epochs of change for the lower Waingawa River. Morphotectonic structures were mapped at 1:3,000 map scale using 1-metre absolute and 5-metre detrended (relative elevation to stream channel) elevation models derived from airborne LiDAR. Relative and absolute elevation profiles of terrace and channel alignments were extracted from the DEMs to further define morphotectonic structure boundaries and zones of distributed uplift of up to 350 metres wide (Figure 6-3A, boxes). Spatiotemporal patterns of change in the cross-section data were then compared with the morphotectonic results. Detailed methods are provided in the Supplemental Materials.

6.5 Results

6.5.1 Morphotectonics

My morphotectonic mapping of four major areas of known active deformation (Figure 6-3A; A-A', C-C', E-E', and F-F') agrees with previously mapped structures (GNS Science Active Faults Database) but reveals greater complexity and additional structures. Back-tilting appears evident upstream of A, B, C, and F (Figure 6-3C). Lineament B-B' is likely a monocline or plunging extension of an anticline mapped by Lee and Begg (2002). Most notable is the Skeets Road Lineament (D-D') which I've inferred based on deformation of the low terrace and the 100-year floodplain.

6.5.2 Channel dynamics

The evaluation of different quantitative expressions of cross-section areal change indicates differing suitability for practical representation of channel dynamics. Cumulative total bed change is the most useful for spatial partitioning (Figure 6-3D), particularly when values are normalised by the mean of their respective epoch (Figure 6-3E). By contrast, changes between individual surveys are noisy (Figure 6-3F and G), though some pattern is detectable for total change when normalised. Net change reflects the importance of tailoring metrics to purpose: while valuable for sediment budgeting, it is not a useful indicator of at-a-station dynamics. The clearest results emerge when cumulative frequency contours (all sections across all epochs) are co-plotted with normalised cumulative bed change (Figure 6-3E). Because the cumulative frequency contours integrate time, the sharp gradients exhibited in proximity to major structures support the premise of cumulative fluvial

response.

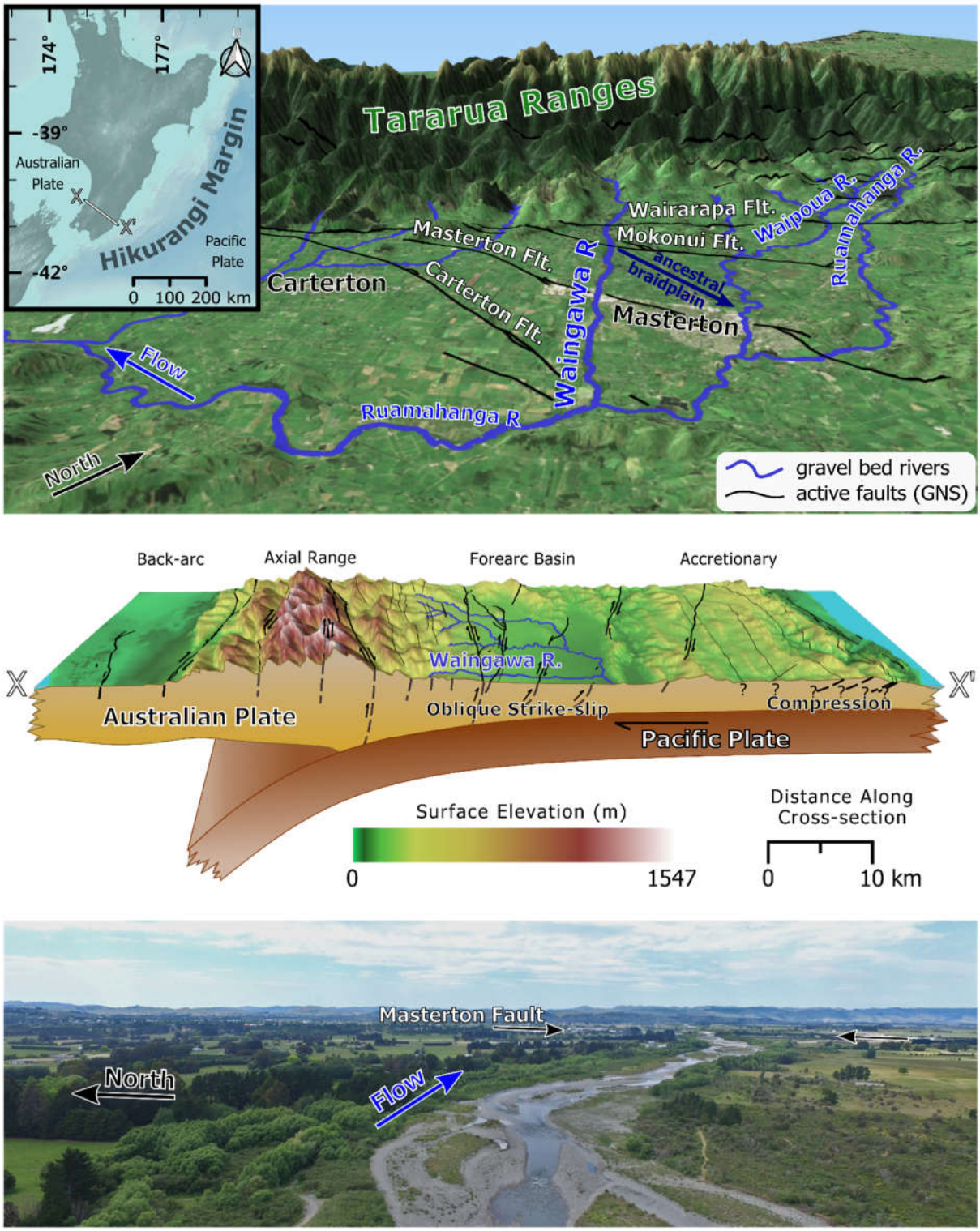

Figure 6-2. Inset: Vicinity map of study area (data: NIWA and LINZ). Top: Oblique view from SE of the upper-Ruamāhanga catchment gravel bed rivers draining the high relief Tararua Ranges (data: LINZ, GNS Science, Sentinel-2, author). Middle: The study area lies in a forearc basin and drains the eastern slopes of the North Island's major hydrographic divide (after Lee and Begg (2002); data: LINZ and GNS Science). Bottom: downstream view of the Waingawa River from the vicinity of ~XS 18 is typical of unconfined conditions through most of the study area, Masterton Fault is ~3 kilometres downstream (photo: WC).

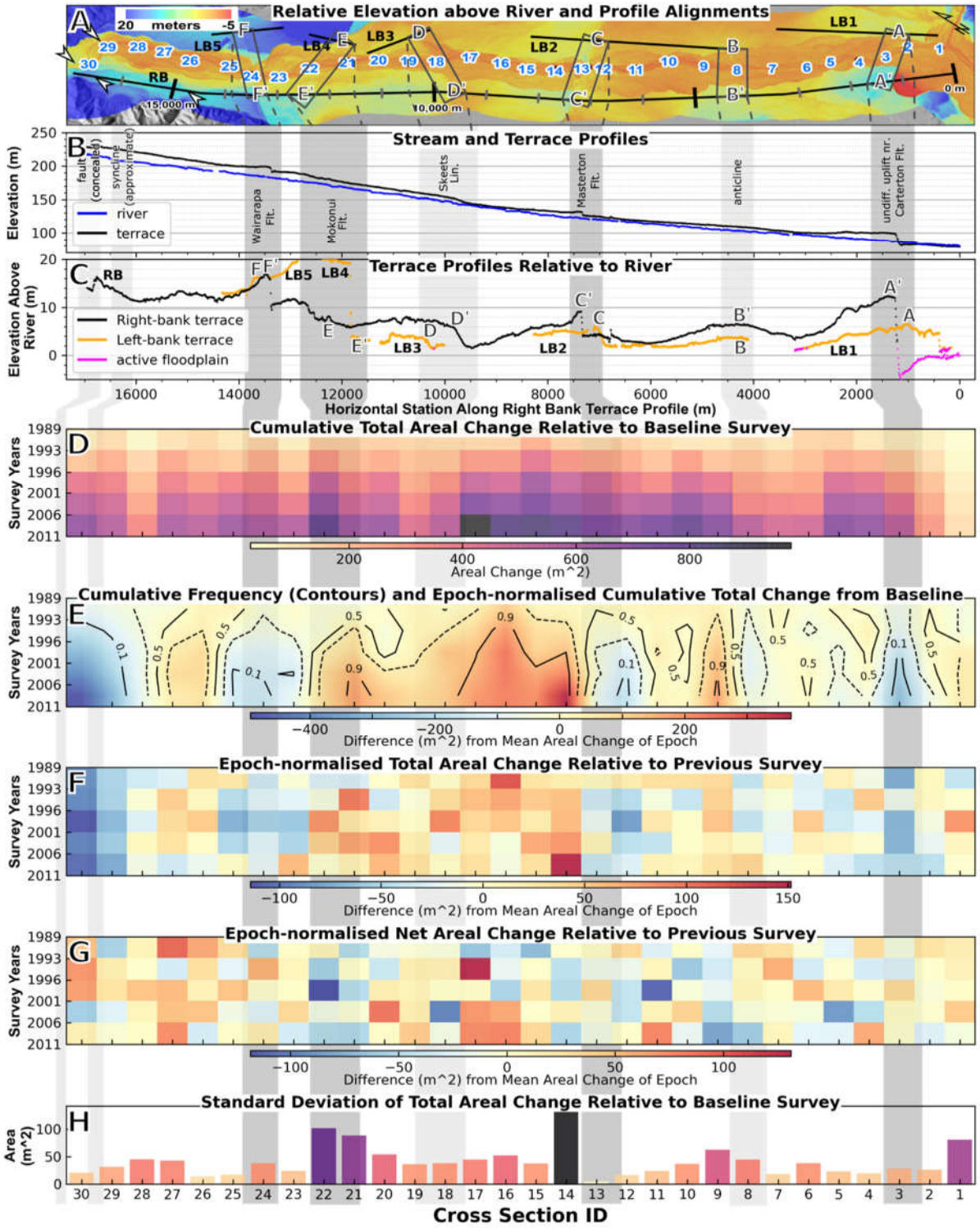

Figure 6-3. Waingawa River bed change context. Dark grey vertical bars: morphotectonic zones confirmed with GNS Active Faults Database. Light grey vertical bars: morphotectonic zones identified solely by the mapping (B-B' and D-D'). Arrows: concealed structures (see Supplement, Figure S6-7). (A) Plan-view of cross-section locations and terrace profile alignments over detrended DEM; 'LB1' – 'LB5' are the left-bank terrace profiles 1-5, respectively; 'RB' is the right-bank terrace profile. (B) absolute elevation profiles along-channel and right-bank (RB) terrace, (C) relative-elevation terrace profiles, (D) cumulative total bed change for each of five epochs relative to the initial (1989) survey, (E) cumulative total change from baseline normalised by mean of each epoch, cumulative frequency contours overplotted, (F) normalised total change relative to previous survey, (G) normalised net change from previous survey (H) standard deviation of total change relative to baseline.

6.5.3 Spatial coherence of tectonics and channel dynamics

I find that cross-sectional bed change is generally partitioned by intersecting geologic structures (Figure 6-3D-E) where relatively little fluvial change occurs in proximity to uplift axes, especially at the Wairarapa, Masterton and Carterton faults. Within-section variation over time also diminishes notably at the Masterton and Wairarapa faults (Figure 6-3H). The most intense cumulative bed change occurs within subreaches overlying likely up-stream portions of back-tilted strata; particularly, cross-sections 9-11, 16-17, 21, and 26-27.

6.6 Discussion

The spatial distribution of observed cross-sectional behaviours (Figure 6-3) is generally consistent with my conceptual model (Figure 6-1, right). The extent of bed change is lower (reduced dynamics) in proximity of most uplifted structural intersections and with greater (enhanced dynamics) in sub-reaches of inferred back-tilt as indexed by low and high standard deviations, respectively (Figure 6-3H). This behaviour in back-tilted zones is consistent with Heller and Paola's (1996) back-tilted models which consistently exhibit increased up-basin channel stacking density. While my results (Figure 6-3G) do not address aggradation or avulsion specifically, I surmise that general patterns of channel activity should follow. My results are also consistent with hypotheses of back-tilt influence on channel pattern posited by Schumm (1986) and Burbank and Anderson (2012, p. 260).

Observed reduction in cumulative dynamics near major structures likely results from marginally greater boundary resistance and/or local hydraulic effects. Active belt narrowing observed at the Wairarapa and Masterton faults is consistent with reductions expected of local gradient increases of rivers crossing *en echelon* fault segments (Hopkins and Dawers, 2015). Each of the major fault intersections, upon rupturing, becomes analogous to an entrenched fan-head (sensu stage 3 of Davies and Korup (2007)) that acts as a nozzle with downstream flow expansion. Unlike a purely alluvial fan-head, strike slip faulting further controls the hydraulic aperture of each nozzle and, indirectly, the nature of downstream sedimentation diffusion. Related to my conceptual model (Figure 6-1, right), incision propagates upstream from vicinity of the fault intersection(s) and mobilised sediments are transferred downstream of the faults and the depositional front advances through time. Though not shown in the graphic, the downstream deposition enhances lateral channel activity which remobilises floodplain and bed materials. The aperture effect associated with strike-slip faults may increase sediment storage on the margins given backwatering and a longer flow path although this is not reflected in one-dimensional visualisation of the channel profile.

In this geomorphically unconfined setting, initial post-rupture hydraulic control related to incision diminishes through time moderated by boundary resistance as lateral fluvial re-working occurs. Active channel and floodplain width is progressively recovered, with post-rupture confinement near "nozzles" persisting for longer as higher magnitude discharges are needed for hydraulic control engagement (sensu Miller, 1994). Relatively greater transport capacity at these controls increases sedimentation downstream of these nodes that, in combination with back-tilt, produces thicker alluvial fills and relative relief variations that increase potential for lateral migration and overbank flow (Figure 6-4).

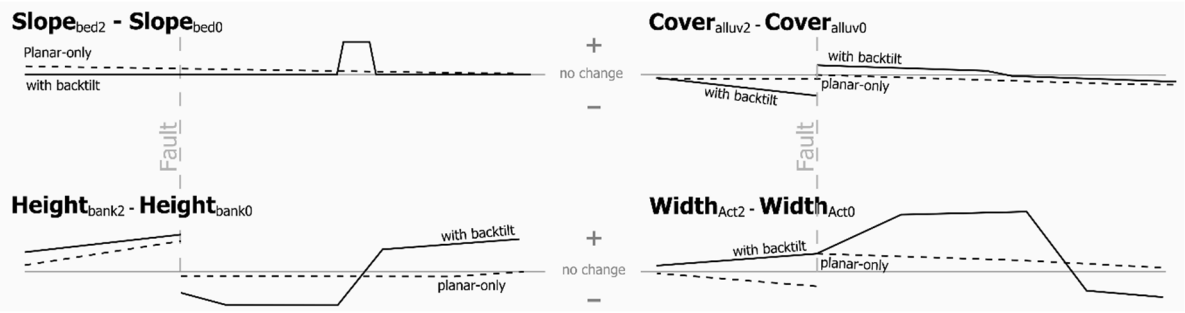

Figure 6-4. Comparison of conceptualised net river profile response of four metrics between two deformation response models (Figure 6-1).

These changes in hydraulic geometry are moderated by differential resistance of boundary material. Proximal to structures, boundary resistance of otherwise granular, largely non-cohesive active channel sediments to hydraulic shear may be enhanced by: A) closer proximity to and greater resistance from direct rock control (cf. Duvall et al., 2004; Goudie, 2016) where transient lithic-fluvial contacts occur (Supplement, Figure S3A-D); B) local recruitment of fines weathered from local bedrock (i.e. Neogene mudstone, high in cohesive fines with rapid disintegration; Supplement, Figure S3B); C) alteration or cementation of alluvial covers from coseismic fluid migration/intrusion. By contrast, areas of thicker sedimentary fills in back-tilted zones downstream of structures have greater potential (frequency and/or magnitude) for reworking.

6.6.1 Anomalous behaviour at the Mokonui Fault

Unlike the other major structures, channel dynamics at the Mokonui Fault exhibit enhanced dynamics (Figure 6-3H, XS 21-22), comparable to back-tilted subreaches. Terrace height (Figure 6-3A and C, E’ on LB terrace) between the Mokonui and Wairarapa faults is the highest in the study area but is coupled with greater valley bottom width and muted morphotectonic expression due to lateral fluvial re-working that seems out-of-place. A braidplain of the ancestral Waingawa River diverges from the modern active belt in this vicinity (Figure 6-3A, ~XS 21; Supplement, Figure S6-5) and is directed toward the Waipoua River upstream of the town of Masterton (Figure 6-2, top). A portion of the braidplain was active during an avulsion in the late-1860s and is considerably younger than the 16-26 ka age (Begg and Johnston, 2000) of its broader mapping unit. The avulsion (subsequently rediverted by local residents) suggests an aggradation episode which may have signalled the arrival of a pulse of coseismically transferred sediments from the 1855 earthquake. See Supplemental Materials for details.

The reach between the Mokonui and Wairarapa faults crosses the proximal zone where the Mokonui Fault splays from the Wairarapa Fault and exhibits distributed uplift (Figure 6-3B-C, between RB profile stations 12,500 and 13,250). This likely contributes to the reach’s modest incision and rank as the steepest (~0.010 m/m) within the study area. Enhanced sediment transfer from this sub-reach to the Mokonui Fault, which occurs within the likely diffusive zone of this zone, may translate to greater lateral activity such that fluvial reworking masks (or shreds) tectonic signatures. Coupled with the tendency for regional (a.k.a. nodal) avulsions to occur up-basin in back-tilted scenarios (Heller and Paola, 1996), the valley unit in proximity and immediately downstream of the Mokonui Fault may be particularly sensitive and predisposed to avulsion.

6.7 Summary

Waingawa River channel dynamics over a 22-year period exhibit spatial coherence with and partitioning by multiple active geologic structures. Cross-sectional bed change diminishes in

proximity of active faults with lesser effects observed at supplemental structures identified by high-resolution morphotectonic mapping. Bed change appears to be enhanced between structures, particularly in areas of apparent back-tilt. While spatial partitioning of channel dynamics is evident when areal change is accumulated over the entire time series, changes between individual surveys and net change are much noisier. This underscores the importance of the manner in which changes are assessed and suggests a time-dependent shift of control from autogenic fluvial/hydraulics between surveys (~3-5 year increments) to mixed or transitional control by active tectonics over decadal time-scales in the absence of near-field coseismic forcing. I conclude that morphological control of alluvial bed change is spatially coherent with geologic structures and persistent during interseismic periods.

6.8 Acknowledgements

This work was supported by Greater Wellington Regional Council, Massey University, and FluvioTec, LLC. Allison Pfeiffer provided valuable feedback on data presentation.

6.9 Supplemental material

6.9.1 Tectonic and Geomorphic Setting

New Zealand straddles a major plate boundary with the North Island (NI) occupying the Australian Plate (Figure 6-2, inset) and the South Island mainly sitting on the Pacific Plate. Opposing net northeast motion of the Australian Plate and southwest motion of the Pacific Plate coupled with the sigmoidal inflection of the plate boundary from the east coast to the west coast south of the study area effectively creating a giant releasing bend. The majority of the strain is accommodated on the plate boundary with approximately 3-8 millimetres per year of upper-plate shortening occurring on the southern NI (Nicol et al., 2007). Upper-plate strain manifests differentially along an axis normal to the plate boundary (Figure 6-2, inset X-X'), and my study area is primarily characterised by oblique strike-slip faulting (Figure 6-2, middle).

Major active faults in the study area exhibit primary dextral motion, often with secondary dip-slip (GNS Science, 2020). Except for the Wairarapa Fault, slip rates and motion are not well-constrained. The persistence of scarps and observation of other faults in the region indicate co-seismic rupturing behaviour is typical of larger events. The Wairarapa Fault's 1855 rupture is the single largest terrestrial dextral displacement documented globally, reaching an 18.7 metre local maximum (Rodgers and Little, 2006). Field observation of scarps along many faults in the region indicates rupturing behaviour is typical of larger events. Except for the Wairarapa Fault, slip rates and motion are poorly-constrained regionally.

Vertical and horizontal deformation varies along the Wairarapa Fault with general northward diminution (Grapes, 1991). Structural investigation has focused on the Southern and Central sections of the Wairarapa Fault (Figure 6-2, south of where the Carterton Fault splays). Along-strike inflection in deformation magnitude (Grapes, 1991, Figure 6, vicinity of site 14) occurs in vicinity of the Carterton Fault's bifurcation and suggests broader surficial distribution of seismic energy northward across the landscape. My exploration of a 1 metre LiDAR-derived elevation model indicates active faults (particularly the Carterton, Masterton, and Northern section of the Wairarapa Fault) crossed by the Waingawa River exhibit segmentation features including overlapping step-overs, bulges and rents within similarly narrow bands (~350 metres) similar to those documented by Carne and Little (2012) in the Central section of the Wairarapa Fault.

The lower Waingawa River (Figure 6-2, top) has mostly uniform drainage area and is well-suited tectonically for this exploration. It is unconfined (Figure 6-2, bottom), lacks tributaries in its lower 15 kilometres (XS 1-28), slopes between 0.005 and 0.01 m/m and has a relatively straight active braidplain alignment that varies between 80 and 230 metres. It drains the high relief Tararua Ranges which have a greywacke core and mudstone foothills. Channel boundaries in the study area are almost entirely composed of Holocene and Late Pleistocene alluvium overlying Neogene mudstones. Review of aerial photography indicates active channel mudstone contacts are small (10s of m^2), infrequent, temporally-intermittent and limited to the vicinity of the Wairarapa and Mokonui Faults. Within the study area, it also crosses four active faults and other tectonic structures (Figure 6-2, top), a Late Quaternary terrace that parallels nearly the entire river (Figure 6-3A), and minimal intrusion of fixed human infrastructure. Two bridge crossings and a lumber mill intrude on the 100-year floodplain along a 300 metre sub-reach where the Masterton Fault crosses the river.

6.9.2 Methods

I evaluate areal changes between six cross-section survey campaigns of thirty bench-marked cross-sections to characterise sub-kilometre channel dynamics of the lower Waingawa River. I compare spatiotemporal patterns of change with geologic structures to evaluate patterns and spatial coherence.

6.9.2.1 Cross-sectional bed change

Though somewhat coarse by modern standards, cross-sectional surveys provide temporal resolution not afforded by remote-sensing methods and enable evaluation of channel bed change, network propagation, and disturbance responses (Tunnicliffe et al., 2017). Perhaps more importantly, they are the only high-accuracy, long-term data record in many areas. Greater Wellington Regional Council (GWRC) initiated cross-sectional surveys of the Waingawa River in 1989 at thirty locations spaced approximately 450 metres apart along the lower 16.5 kilometres of the river. Monuments were constructed at one or both ends of each section for datum-control to improve precision through time. Re-surveys occurred in 1993, 1996, 2001, 2006, 2011 and 2017. Data from 2017 were excluded from my analysis as they exhibited unresolvable vertical and horizontal datum shifts whose magnitude exceeded expected fluvial changes. For any given cross-section, the horizontal extents surveyed varied through time with most re-surveys terminating where it was believed to tie-in with an unchanged surface from the previous survey.

I differenced surveys sequentially to identify change extents for each cross-section over the period-of-record (POR). As any given survey might be less extensive than the change extents for the POR, I forward-filled extents missing from re-surveys using earlier surveys to facilitate apples-to-apples comparison through the POR. Thus, my assumption is prior stasis as opposed to potential exclusion of known changes. At each cross-section survey station, comparisons were made of each survey and its predecessor in time (t_i, t_{i-1}) to determine the cross-sectional area of deposition and erosion over time within the limits of the surveyed line. *Net bed change* for each epoch at each cross-section is the difference between erosion and deposition. *Total bed change* is the sum of the absolute values of erosion and deposition. *Cumulative total bed change* is the summation of total bed change from baseline for all epochs of a given cross-section up to (and including) a given re-survey year.

The study area is managed under a “fairway” scheme with channel shifts permitted within preferred and buffered corridors. Management treatments such as willow plantings and rock barbs/groynes comprising native alluvium are the primary impositions to constrain migration outside of the buffer. Within the preferred corridor, vegetation is maintained in an early seral state with periodic local realignments performed mechanically. Gravel extraction occurs periodically, with the vast majority

within ~1.5 kilometres downstream of the bridges (XS 11/12) though documentation is insufficient to assess its effect on individual cross-sections. To reduce potential noise associated with variable inter-survey river discharge and/or management between epochs, I normalised measures of areal change by the mean for their respective epochs.

Cumulative bed change was normalised by computing the mean for all values of an epoch, then subtracting the mean from each value. This emphasises patterns of within-epoch ordering and improves comparisons across epochs by reduces the variable effects river flows and human management between epochs.

Because the entire study zone is within a managed river setting, there is potential for human modifications to influence cross-sectional change directly and indirectly. I envisage scenarios where management actions could cancel, amplify, or dampen change, but records do not exist to determine if, when, where, or how much. Given general river management biases favouring stability, I loosely assume human actions would dampen these relationships. To account for these unknowns, I normalised the cumulative bed change for each epoch by computing the mean for all values of an epoch, then subtracting the mean from each value. I believe such epoch-normalisation moderates potential differential effects between any two surveys by providing a ranking or index that permits more standardised comparison between epochs. This normalisation emphasises within-epoch ordering, cleans-up within- and between-section relationships and enables better tracking of each section through time.

6.9.2.2 Geologic Structure and Deformation

I conducted morphotectonic mapping and interpretation at 1:5,000 map scale or better using LiDAR-derived elevation models. A combination of 1 metre absolute-elevation and 5 metre relative-elevation models were used. Morphotectonic approaches have been shown to have high precision for feature extraction in palaeoseismic investigations (Manighetti et al., 2020) and, while less temporally discrete than detailed stratigraphic study (e.g. Grapes, 1991; Carne et al., 2011), the approaches are complementary. For my purposes, the broader spatial context of a topographic approach is more robust, by avoiding complications inherent in extrapolating highly localised stratigraphic interpretation in a highly segmented tectonic regime.

The relative-elevation DEM was generated by down-sampling the 1 metre (absolute elevation) model to 5 metres using minimum aggregation to minimise the effect of non-ground artefacts. In other words, reprocessing produced a 5x5 cell whose elevation value equals the minimum value of the twenty-five cells occupying the same footprint. Then, a moving-window process (after Dilts et al., 2010) was applied with a 1,500 metre radius using the active channel centreline as the baseline (Figure S6-5). I cross-correlated common structures in proximity to coarser (1:250,000) published data (GNS Science, 2020) or maps (Begg and Johnston, 2000) as a means of confirming general presence, alignment and tilt of features (Figure S6-6 and Figure S6-7). Given cross-sectional spacing, fault segmentation (Carne and Little, 2012), and scale of this analysis, I consider deformation in zones over discrete lines (vertical bands in Figure 6-3).

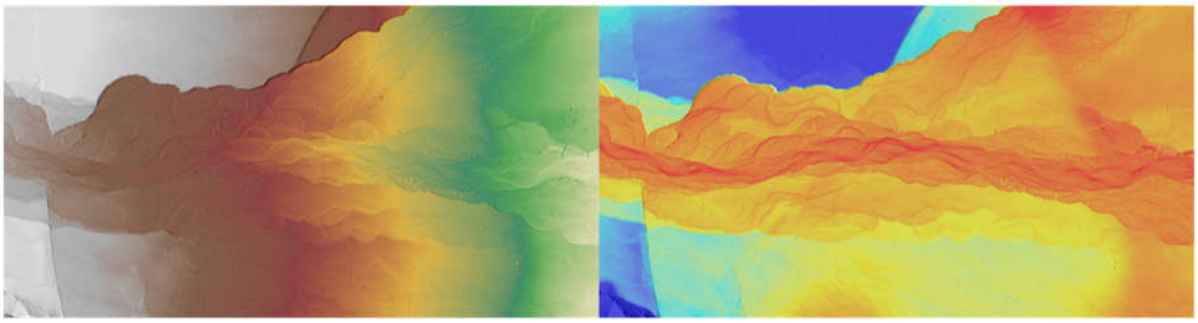

Figure S6-5. Comparison of absolute elevation DEM (left) and detrended DEM normalised to the Waingawa River profile (right). Both have a 40% transparency and are superimposed over a hillshade with the min/max if their respective colorramps scaled to viewable area.

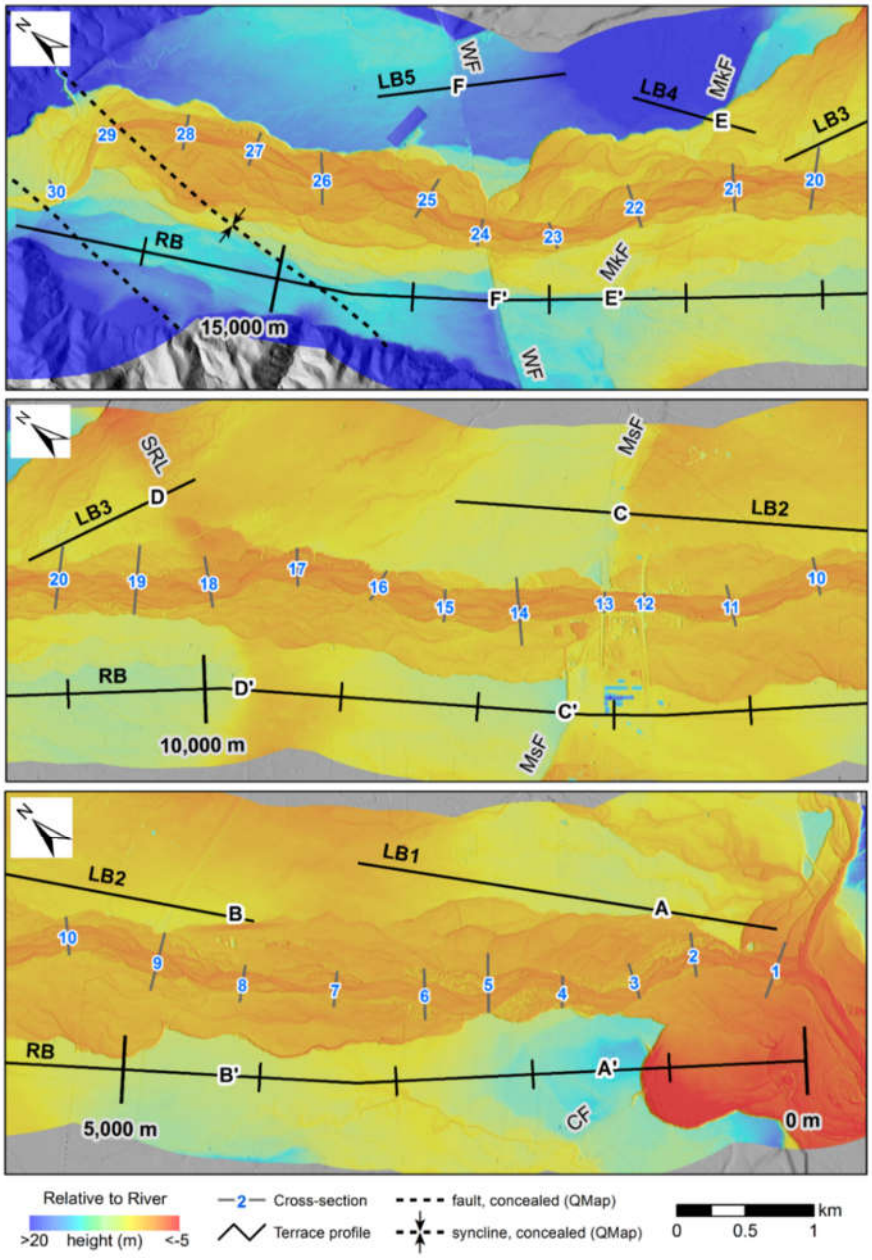

Figure S6-6. Features and annotation from Figure 6-3 at 1:35,000 map scale. CF = Carterton Fault, MsF = Masterton Fault, SRL = Skeets Road Lineament, MkF = Mokonui Fault, WF = Wairarapa Fault.

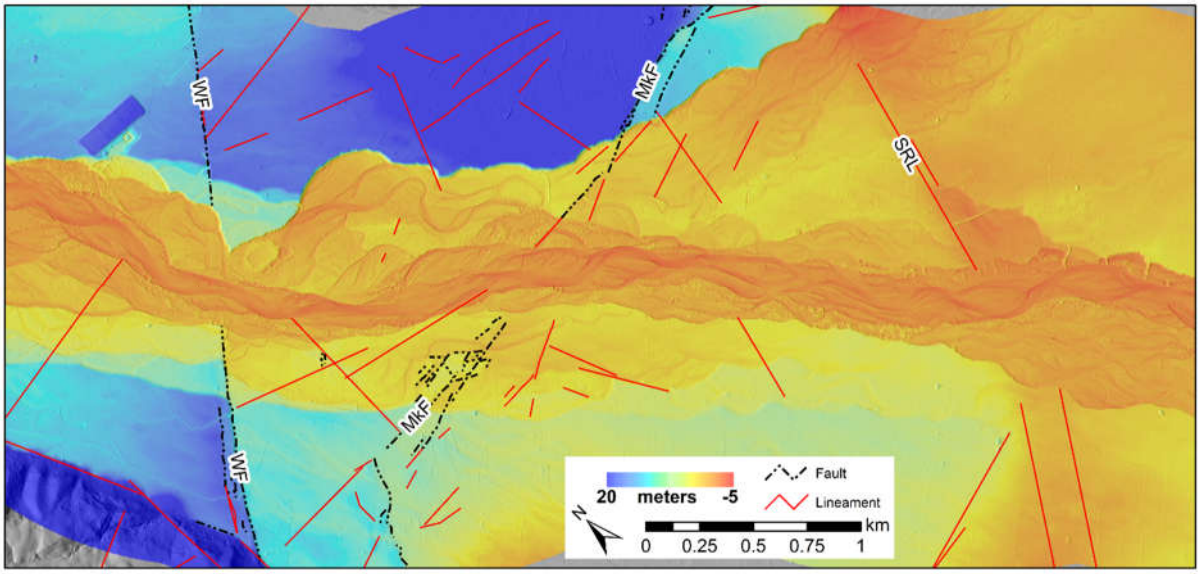

Figure S6-7. Detrended DEM of the study area between the Wairarapa Fault (WF) and Skeets Road Lineament (SRL). Main scarp of Mokonui Fault (MF) is labelled. Blue rectangle indicates general geodetic location of photos in Figure S6-8 (DEM is not representative of the active channel belt at time of photos).

The exploration of a 1 metre LiDAR-derived elevation model indicates active faults (particularly the Carterton, Masterton, and Northern section of the Wairarapa Fault) crossed by the Waingawa River exhibit segmentation features including overlapping step-overs, bulges and rents within similarly narrow bands (~350 metres) similar to those documented by Carne and Little (2012) in the Central section of the Wairarapa Fault. Considering this and cross-section spacing, I treat the structures in Figure 6-3 as a zone as opposed to discrete lines. Along-strike inflection in deformation magnitude (Figure 6 in Grapes, 1991, vicinity of site 14) occurs in vicinity of the Carterton Fault's bifurcation and suggests broader surficial distribution of seismic energy northward across the landscape.

6.9.2.3 Terrace and Channel Profiles

River planform was manually-digitised from 0.3 metre digital orthoimagery collected in 2012 from the centreline of the active belt and the trunk river (Ruamāhanga) confluence as the zero-point. Deformation of adjacent Holocene and late-Pleistocene alluvial terraces (sensu Amos et al., 2007) was determined along alignments manually-digitised to transect major vertical inflections with the general aim of minimising horizontal distance and deflection from river planform. All horizontal profile positions were referenced to the right-bank (south) terrace profile as it runs nearly the entire length of the study area. Elevation values for terrace and river profiles were extracted from both the absolute (Figure 6-3B) and relative elevation (Figure 6-3C) DEMs to refine localisation of structural boundaries and zones of more diffuse uplift.

6.9.2.4 Deformation

Geomorphic interpretations of deformation (Keller, 1986; Wobus et al., 2006; Masoud and Koike, 2011) are enhanced by hillshade or otherwise enhanced high-resolution renderings of topography (Figure 6-3A-C). In particular, I found that detrending topography by reprojecting the landscape relative to the river channel profile enhanced inference of floodplain and terrace deformation (Figure 6-3A) and tilting at landscape scale (Figure 6-3C).

I assume that terrace deformation accumulates across rupture cycles and the river has mostly (or fully) relaxed relative to the last major co-seismic disruption (1855). By normalising surrounding topography to the river, tilting of tectonic units can be more robustly inferred from vertical offsets

and slope of the terrace treads from the relative-elevation model than the absolute model. Thus, detrended topography (reprojected relative to the river profile) not only enhances visualisation of offsets and uplift, but enables detection of serial back-tilting, the latter of which may be more properly characterised as *relative* back-tilt given lack of data on bedrock depth and the nature of contacts with overlying soil strata.

Back-tilting (Figure 6-1) produces more complex stream slope relationships over more of the reach and generally thicker sedimentary sequences. Phase 1 is a period of rapid adjustment [minutes to months] initiated by rupture and dominated by headcut dynamics. Phase 2 reflects ongoing adjustments beyond the proximal disturbance where interactions with autogenic processes occur, but the system may not have relaxed. Side-tilt relative to the valley axis coupled with a syncline that strikes sub-parallel to the river upstream of the Wairarapa Fault (Figure S6-6) complicates interpretation beyond the scope of this paper and is not considered further.

6.9.3 Supplemental Discussion

I suggest that reduced cumulative bed change in proximity to major controlling structures results from marginally greater boundary resistance and/or local hydraulic effects. Narrowing of the active channel belt observed at the Wairarapa and Masterton faults is consistent with width reductions expected of local gradient increases where rivers cross en echelon fault segments (Hopkins and Dawers, 2015) supporting hydraulics as a partial control. Aside from the known importance of direct rock control (Duvall et al., 2004; Goudie, 2016), I suggest that river sediments in proximity to bedrock exhumed at the active fault structures may have higher cohesion. Gouge generation (Engelder, 1974) and alteration (e.g. Boulton et al., 2012) are known to occur along faults and via coseismic fluid migration/intrusion may cause cementation of alluvial covers which, I hypothesise, could also enhance local bank resistance of otherwise granular, largely non-cohesive active channel sediments to hydraulic shear in proximity to the faults.

At my sites, the Neogene mudstone bedrock being exhumed in proximity to the faults is high in cohesive fines content and rapidly breaks down (Figure S6-8B). Fault gouge and alteration coupled with direct weathering of mudstone, create potential for local enrichment of cohesive fines. Review of archival aerial photographic records reveals intermittent daylighting of a few, small (tens of square metres) patches of bedrock strath in this sub-reach. Field observations from 2018 and 2019 during channel incision episode provide some evidence of this in the field and hypothesise boundary-related differences could include 1) closer proximity to and greater resistance of the bedrock (Figure S6-8, A-D); 2) increased potential for recruitment of fines weathered locally from local bedrock (mudstone; (Figure S6-8B); 3) induration, cementation, or local fines enrichment of alluvial covers resulting from coseismic fluid migration/intrusion.

The diversion node for the ancestral Waignawa River braidplain occurs in this vicinity (Figure 6-3A, ~XS 21; Supplement, Figure S6-6) and is directed toward the Waipoua River upstream of the town of Masterton (Figure 6-2, top). A portion of the ancestral braidplain was re-activated during an avulsion in 1867 or 1868 (Correspondence, 1884). Occurring roughly twelve years following the 1855 Wairarapa earthquake (M 8.1), the avulsion coupled with heightened flooding in the decade following the earthquake (Correspondence, 1884), suggest an aggradation episode which may have signalled the arrival of a pulse of coseismically-transferred sediments.

Several factors may predispose this area to heightened fluvial dynamics, particularly during periods of enhanced sediment delivery. The top of the strath (Figure S6-8, A and C) slope in roughly the same direction and gradient as the Waingawa River, supporting the hypothesis that control transitions intermittently between tectonic and fluvial processes. Clusters of small reverse faults (Figure S6-8C)

which strike roughly normal to the strike of the Mokunui Fault (Figure S6-8D) may further add to non-linear complexities of fluviotectonic responses. While I don't specifically evaluate the likelihood of the Waingawa River to reoccupy its ancestral braidplain, the combination of morphologic interpretation, consistency of the avulsion node's setting with literature, and historic record of avulsion suggest a predisposition exists. The prevalence of human development in unconfined settings and predominant temporal duration of interseismic periods enhances the importance of identifying spatial units that pose disproportionate uncertainty (if not greater risk) to adjacent human interests such as inferred in areas I have identified.

Figure S6-8. Active channel bedrock exposures in the diffuse uplift zone between the Mokonui and Wairarapa faults revealed during an incision episode in 2018-2019: (A) poorly-sorted, fining-up sequence of low terrace between Mokonui and Wairarapa faults exhibits considerably greater fines enrichment than active alluvium with top of bedrock strath sloping in same general orientation as river; (B) active joint-controlled weathering of bedrock (mudstone) strath along a fluvial erosion scarp within active the river channel witnessed over the course of one week and a single sub-annual recurrence flow event; (C) cluster of small (vertical throw = 0.04-0.45 metre), steeply dipping (75-86°) secondary reverse faults visible in an erosional scarp of bedrock strath capped by active alluvium (top of surface is inundated by ~1.5-year recurrence discharge). (D) strike (dashed lines) of small reverse fault cluster (panel 'C') is oblique to the Mokonui fault (~700 metres downstream) and parent rock shows considerable fracture uncharacteristic of usually massive mudstone strata away from deformed areas.

Summary of Thesis Chapter 6

The partitioning of vertical alluvial behaviours demonstrated in Chapter 6 suggests morphologic forcing by active tectonics is detectable on timeframes much shorter than rupture intervals and can persist well into (>130 years) the interseismic period. This counters general scientific perceptions which constrain the role of active tectonics on fluvial geomorphology to co-seismic rupturing, slope-based sediment transfer, bedrock control, and/or floodplain confinement transitions. The high degree of along profile variation is a caution for managers tempted to apply uniform templates and/or treatments based on averaged conditions. Further, fluvial signals may be subtle, discernible over many years, and require multiple lines of evidence to detect. The theme of multiple lines of evidence for detecting subtle fluvial signals continues in Chapter 7 expanded to multiscale scope (riverscape and sub-reach) and dimensionality (planimetric and volumetric changes).

Chapter 7

Scale-dependent morphodynamic patterns of stability and sensitisation in managed rivers

Introduction to Chapter 7 of Thesis

Chapter 7 investigates planimetric and 3-dimensional time-series at multi-decadal and event scales, respectively, to characterise and contrast channel responses to river management. Within the thesis framing of spatiotemporal channel dynamics, it supplements the spatially continuous, point-in-time, planimetric approach of Chapter 5 as well as Chapter 6's aggregation of spatially-discrete sub-decadal vertical bed data. It continues the spatially explicit change theme of the thesis by incorporating both Type 2 and Type 4 change detections (sensu Chapter 4) for a) decadal, riverscape-scale and b) event-based, segment-scale investigation representing the end-members of human scale river management. The results of the case study described in Chapter 4 guide decadal analysis and interpretation while the classification is used for quality control and framing of both decadal and event-based change detection. The event-based analysis in Chapter 7 uses very-high resolution (UAS-derived) imagery and topography to identify patterns of sedimentation and erosion relevant to follow-on refinement suitable for priority areas identified based on Chapter 5. Chapter 6 results lend to interpretation of generally low catchment sediment supply to the study area enabling framing of dynamics as reworking of existing valley floor sediments. Chapter 7 addresses thesis objectives iv(a), iv(b) and iv(c) with the crux being establishing amplified morphodynamic sensitivity to routine hydrologic events coherent with recent flood protection earthworks.

This chapter is in preparation as a manuscript for Science of Total Environment as:

Conley, W.C., Fuller, I.C., McColl, S.T. (In Prep). Scale-dependent morphodynamic patterns of channel stability and sensitisation in managed rivers.

7.1 Abstract

Increased channel stability and reduced river belt footprints are two common river management aims. While usually implemented concurrently, such aims may conflict on a first-principles level since width and length reductions associated with footprint-reduction, for an unmodified hydrologic regime, will shift sediment transport relationships in favour of increased mobility for some period. While management implementation occurs incrementally through localised physical modifications of channel(s) and/or floodplain(s), geomorphic effects may lag and/or accumulate over time. The complexity of interactions within and between natural and human processes, coupled with highly variable temporal relationships (and often inadequate records) of geomorphic effectiveness, make efficacy evaluations across spatiotemporal scales rare. I evaluate long and short-term records of active belt width and supplement with sub-seasonal, high-resolution morphologic differencing to assess congruence between management aims for an unregulated, multi-thread wandering gravel-bed river under a "training" management guided by regime equations. A sixty-nine-year trend of decreasing width (-48%) and increasing width uniformity (-62% standard deviation) converges on current design dimensions at the riverscape scale (~18 kilometres).

Evaluation of high-resolution (0.1 metre) repeat topography and morphological sediment budgeting for a ~3.5-kilometre reach over a two-month series of discharge events found highly variable geomorphic behaviours at the subreach (~1,000 metres) scale. Highly dynamic subreaches had tight spatiotemporal coupling with recent (~9-30 months) in-channel earthworks and roughly fivefold greater volumetric changes than adjacent, untreated reaches. Differential volumetric change was evident (0.35 metre threshold) during an epoch with instantaneous peak flow magnitude approximately one-half the mean annual flood. The peaked nature of volumetric changes combined with propagation of incision upstream and aggradation downstream suggests sediment-generating process origins internal to the disturbed subreaches. Multiple lateral shifts of the primary wetted channel between 30 and 50 metres during the epoch including an event with mean annual flood recurrence frequency (Q_{MAF}). Channel shifts occurred in subreaches influenced by training and were generally coherent with channel units experiencing aggradation. Aggradation of treatment-influenced sediments produced up to 16 metre of bank erosion and multiple instances where primary and secondary channel activity increased outside of the design fairway.

Practices that minimise long-term active belt width while countering shorter-term stability aims indicate an anti-pattern I call the "fairway paradox". Resolving the paradox requires reconciliation of conflicting design philosophies and river training actions. For example, well-connected multi-thread channel forms demonstrated greater short-term stability in the contemporary river environment. The wider "buffer" corridor generally contains these channels as well as the active channels for all but the 1940s era channel alignments. Rethinking existing targets for corridor pattern and dimension is warranted with a wider buffer corridor and less rigid fairway enforcement as a starting point for a management regime where less frequent intervention produces more routine stability.

7.2 Introduction

Increased channel stability and minimised river footprint are primary aims of many river management regimes. In geomorphology, stability concepts generally imply approximate balance of matter inflows and outflows (Osterkamp, 2008) with accommodation for adjustments in position or form up to some intrinsic threshold condition identified from system behaviour (Newson, 2002; Brierley and Fryirs, 2005). By contrast, river management practice tends toward more subjective, human-based framing more consistent with engineering definitions such as "the tendency…to perform…within *acceptable* limits…" (Neuendorf, 2005) or "…the *right* balance…without long-

term…sediment deposition or erosion" (Fischenich, 2000). Independent of human-imposed values, changes in river systems are reflected in channel and floodplain forms variably driven by sediment movement and storage (Lane and Richards, 1997; Church, 2015). The nature of such changes is determined by the interactions between sediment, fluid forces and topographic boundaries and resistance elements that vary and hierarchically nest in space and time (cf. Fryirs and Brierley, 2012) with investigations increasingly interested in scale-dependency (e.g. Recking et al., 2012; Venditti et al., 2019). Consequently, stability evaluation is not possible until spatial and, especially, temporal framings are defined.

Management operations that reduce river footprint (inclusive of floodplain and inundation zones) commonly include flood hydrograph attenuation (e.g., storage reservoirs), local alterations of hydraulic conditions that produce steeper, deeper, and/or less resistant fluvially-active zones (e.g., levees, groynes, realignment, vegetation removal) and direct reduction of sediment supply (e.g., gravel extraction). The geomorphic signals that emerge from human alteration of boundary conditions vary over space and time (Hoffmann et al., 2010; Macklin and Lewin, 2015) and similar actions in different systems may produce opposing outcomes depending on system connectivity (Salant et al., 2006). Despite well-documented limitations, computational approaches e.g., downstream hydraulic geometry and/or regime-based approaches) often provide the numerical basis for design of narrower corridors (cf. Ferguson, 1986; Carson and Griffiths, 1987). Such corridors may be achieved incrementally over appreciable spatial extents (many kilometres) by sequences of management actions (e.g., "training") that interact and nest with natural processes over many years. The interactions with natural processes may be sufficiently interwoven that multiple, suitably-scaled data sources must be used (e.g. Downs et al., 2013) to help discretise human from natural signals, if discretisation is possible at all.

Interactions of physical processes across scales make coarse-bedded rivers challenging to measure, analyse, and manage (Piégay et al., 2006). Though typically composing 15% or less of total sediment yield for most rivers (Knighton, 1998), coarse sediments (gravel and larger) exert a disproportionately high influence on channel morphologies (Leopold, 1992; Martin and Church, 1995; Church, 2006). Coarse-bedded rivers are known for having temporally variable bed transport (Klingeman and Emmett, 1982; Reid et al., 1985) with variable morphological expressions (Moog and Whiting, 1998; Martin and Jerolmack, 2013; Misset et al., 2020). Stability is dependent on changes in sediment supply and transport capacity (Church, 1983) and directional transfer (lateral vs down-river) can vary with flood magnitude (Weber and Pasternack, 2017). Over longer periods (years), hydrologic variability is recognised for influencing forms and behaviours (Bledsoe and Watson, 2001; Welber et al., 2012; Kidová et al., 2016) which may shift over still longer timeframes (decades) given longer-term controls such as flood-rich and flood-poor periods (Macklin et al., 2006; Toone et al., 2014; Kidová et al., 2016). These behaviours may cluster and/or cycle over centuries to millennia (Macklin et al., 1998; Macklin et al., 2002) and result from (or produce) differing degrees of change sensitivity (Clement and Fuller, 2007).

Here, I consider *sensitivity* as the degree to which a change in controls will produce and propagate detectable geomorphic change (sensu Brunsden and Thornes, 1979). Sensitivity can be expected to vary within and across systems and the very nature of sensitivity may change (Figure 5-1, also, cf. Fryirs (2017)). If the change in sensitivity means a change in control is more likely to be absorbed (i.e., negative feedback) the respective system may be considered *de-sensitised*, such as when it becomes less-responsive to a given flow (or a higher flow becomes necessary to generate a given change). By contrast, a *sensitised* system will be more likely to change and/or propagate

sedimentary signals for a given driving force such as where greater geomorphic change is produced than may have otherwise. The act(s) of making a system sensitised is/are considered s*ensitisation*.

Lane and Richards (1997) identify investigation of short timescale and local spatial scales as critical to understanding sensitivity of non-linear systems. While such studies have revealed otherwise undetectable changes and processes (Lane and Richards, 1997; Lindsay and Ashmore, 2002), high frequency (e.g., daily or flow event) morphologic sampling in fluvial settings remains relatively rare. This is particularly true in the context of geomorphic effectiveness where most studies make linkages to flow frequencies no more frequent than the mean annual flood (Q_{MAF}, 2.33-year recurrence interval). With some exception (e.g., Lane et al., 1995; Bakker et al., 2019), routine flows receive comparatively little attention for sediment transport and sub-annual frequency flows have been generally ignored for geomorphic effectiveness.

Bizzi and Lerner (2015) use stream power to quantitatively characterise channel sensitivity and several different duration-based measures of flow intensity (e.g. excess discharge, shear, energy, and/or power) have been related to geomorphic effectiveness for cross-scale comparisons within and between systems (Phillips and Jerolmack, 2014; Gilet et al., 2020). Lisenby et al. (2017) propose volumetric change as a standard indicator of geomorphic work which is facilitated by the well-established approach of morphologic sediment budgeting (e.g. Fuller et al., 2002; Brasington et al., 2003; Wheaton et al., 2010b) and ever greater access to high-resolution topographic data sets making understanding of mass and energy transfers increasingly feasible over broader, spatially-continuous extents (Passalacqua et al., 2015).

In this chapter, I contrast stability for endmembers of management-relevant scales. I use interpretation of archival aerial imagery to explore a multi-decadal riverscape trend of braidplain width as an indicator of stability for a wandering, gravel-bed New Zealand river under a training-style management regime. I use high-resolution, UAS-derived orthoimagery and topography for a nested segment (~3.5 kilometres) of the same river to evaluate event-based ($\leq Q_{MAF}$) morphodynamic responses for reaches subjected to different treatments and timing. I relate differential responses (i.e., stability) to the same flows as a matter of *sensitisation* and focus discussion on how the same regime-based principles that accomplish decadal narrowing aims also drive event-based reach instability.

7.3 Study Area

The study area is located within the Ruamāhanga River catchment near the southern end of New Zealand's North Island (Figure 7-1). The Waingawa River is approximately 45 kilometres long with a 151 square kilometre rain-driven catchment that drains the crest of southern North Island's axial mountains, the Tararua Range. Mean annual precipitation varies from ~4,600 millimetres per year along the crest to ~1,300 millimetres per year (MfE, 2021) in the upper reaches of the study area. Catchment hydrology is unregulated and flashy with very steep rising and falling limbs (Figure 7-3).

This study focuses on the unconfined, downstream reaches where the river is gravel to small boulder bedded with 0.005 to 0.01 (m/m) gradient. Bed material (surface) in the upper half of the Area-of-Interest (AOI) ranges between ~250-350 and ~140-210 millimetres for the D_{84} and D_{50}, respectively, while the D_{50} varies between 42-62 and D_{84} varies between ~58-110 millimetres in the downstream half (Christensen, 2013, Appendix C). Channel forms are multi-threaded with early aerial imagery exhibiting island-braided or wandering channel patterns and imagery from the last forty years appearing more braided-like.

Late Quaternary fluvial terraces generally define the margins of the 100-year floodplain, though active channel contact is rare except in some locations upstream of the Wairarapa Fault. There is minimal channel intrusion of fixed human infrastructure with only two bridge crossings, both occurring within 100 metres of each other where the Masterton Fault crosses the river. Channel boundaries are almost entirely composed of Holocene and Late Pleistocene alluvium overlying Neogene mudstones. Review of decadal aerial photography (see Chapter 4, this thesis) at the riverscape scale indicates active channel mudstone contacts are limited to the vicinity of the Wairarapa and Mokonui faults, small and infrequent.

The surrounding land-use is typically agricultural with increasing subdivision for rural lifestyle. A mid-1990s report on the nearby Ruamāhanga River notes an "emphasis on farming all available land to the river edge, leaving no margin for natural river erosion/accretion processes" (Heslop, 1996, p. 2) and a general intolerance of even minor amounts of erosion.

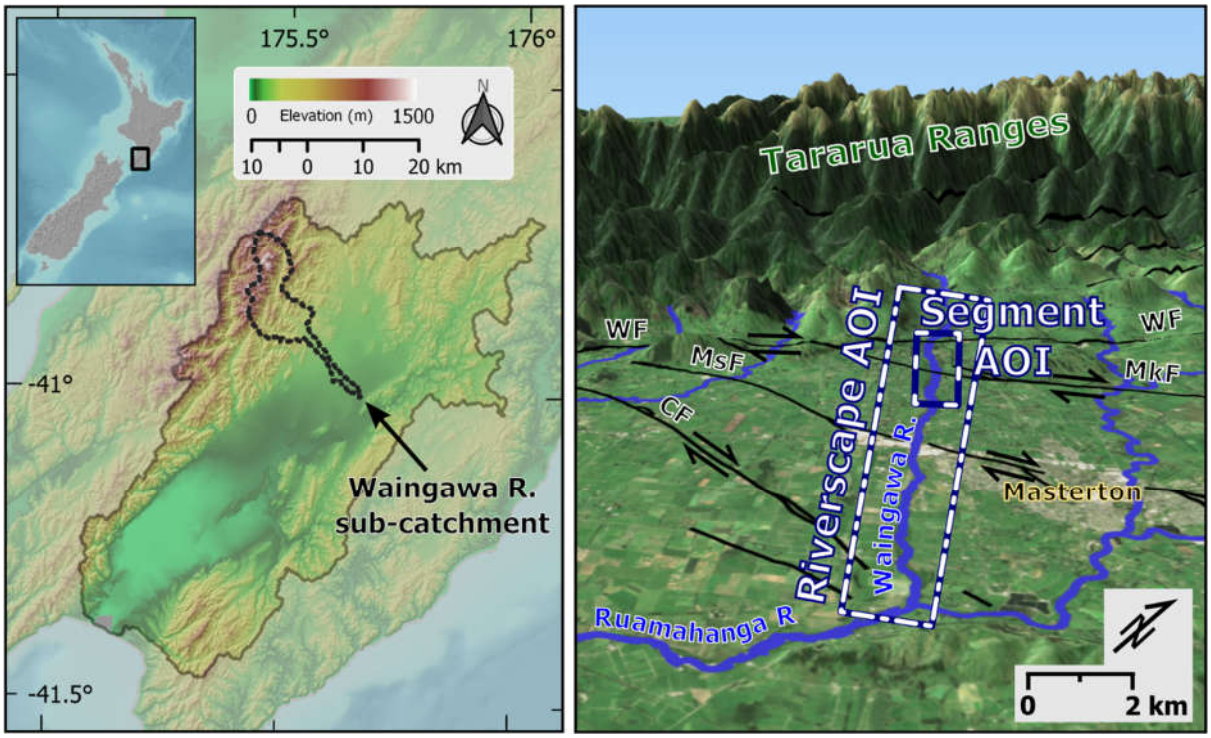

Figure 7-1. Left: The Waingawa River study area is located within the southern North Island's Ruamāhanga catchment. Right: The Waingawa River exits the Tararua Ranges as an unconfined river and crosses, multiple active tectonic structures (WF: Wairarapa Fault, MsF: Masterton Fault, MkF: Mokonui Fault, CF: Carterton Fault) over its ~15-kilometre course to the Ruamāhanga River confluence. Data: NIWA, LINZ, Sentinel-2, GNS Science, and authors.

7.3.1 Sediment supply

Catchment-derived inputs are limited by the tributary structure which only has confluences in the upper 500 metres of the study area. A review of benchmarked cross-section data (Figure 6-3E and F)) suggests consistently low relative dynamics of the two most-upstream cross-sections (XS 29 and XS 30). Epoch-normalised results, where the mean of total change across all cross-sections for that epoch is subtracted from the total change of each XS value within that epoch, show the upstream the upstream cross-sections accumulating the least amount of change over the 22-year period of record (Figure 6-3E). I interpret this as indicative of relatively low catchment sediment supply during that time. This is supported by qualitative aerial photographic review of upstream reaches that suggests low degrees of change in channel alignment or bar features. Thus, the inference is that,

between 1989 and 2011, channel dynamics were driven by reworking of alluvial valley fills within the study area, modulated by the tectonic structures, as opposed an influx or high variability sediment supply from upstream.

7.3.2 Areas of Interest (AOIs)

7.3.2.1 Riverscape scale

For multidecadal analysis at riverscape scale (Figure 7-1, "Riverscape AOI"), I consider the 17.8 kilometres (mean braid plain centreline over multi-decadal record) between the Atiwhakatu Stream confluence and the mouth of the Waingawa River where it meets the Ruamāhanga River. Drainage area at the upstream end of the AOI is 118 square kilometres (78% of total catchment area).

7.3.2.2 Segment scale

Sub-annual, segment-scale analysis (Figure 7-1, "Segment AOI") focuses on 4 km between the Skeets Road Lineament and Wairarapa Fault (10.7 – 14.7 kilometres upstream of where it joins the Ruamāhanga River). Woody vegetation colonisation in the segment AOI is very rapid with observed vertical growth exceeding one meter in under twelve months (inclusive of colonisation) for *Lupinus* spp.

7.3.3 River Management Regime

The primary, stated management aim and approach the for the Waingawa and nearby rivers is to "establish a stable channel alignment through the adoption of design channel fairways with vegetative buffer on either side of the river" (Harley, 2014). Since approximately the early-1990s, this aim has been operationally implemented using planimetric boundaries established in GIS where the *fairway* (channel) is an inner corridor desired to contain the active channel/belt and the *buffer* delineates the outermost acceptable active channel limits (Figure 7-2). The buffer boundary follows of natural geomorphic features in some locations while the fairway appears as a purely sinusoidal human construct. Collectively, the channel and buffer are known as the *design lines*. In-channel and floodplain heavy equipment treatments are used to *train* the active channel/belt into the fairway including channel realignment, blocking secondary channels, removing bars, extracting gravel, ripping-armour, stripping vegetation, and constructing bank groynes. Dormant pole plantings (*Salix* and *Populus* spp.) are used to reinforce groynes, banks, and unwanted channels. Constructed forms and slopes are field-determined by equipment operators, generally without survey control or stake-out.

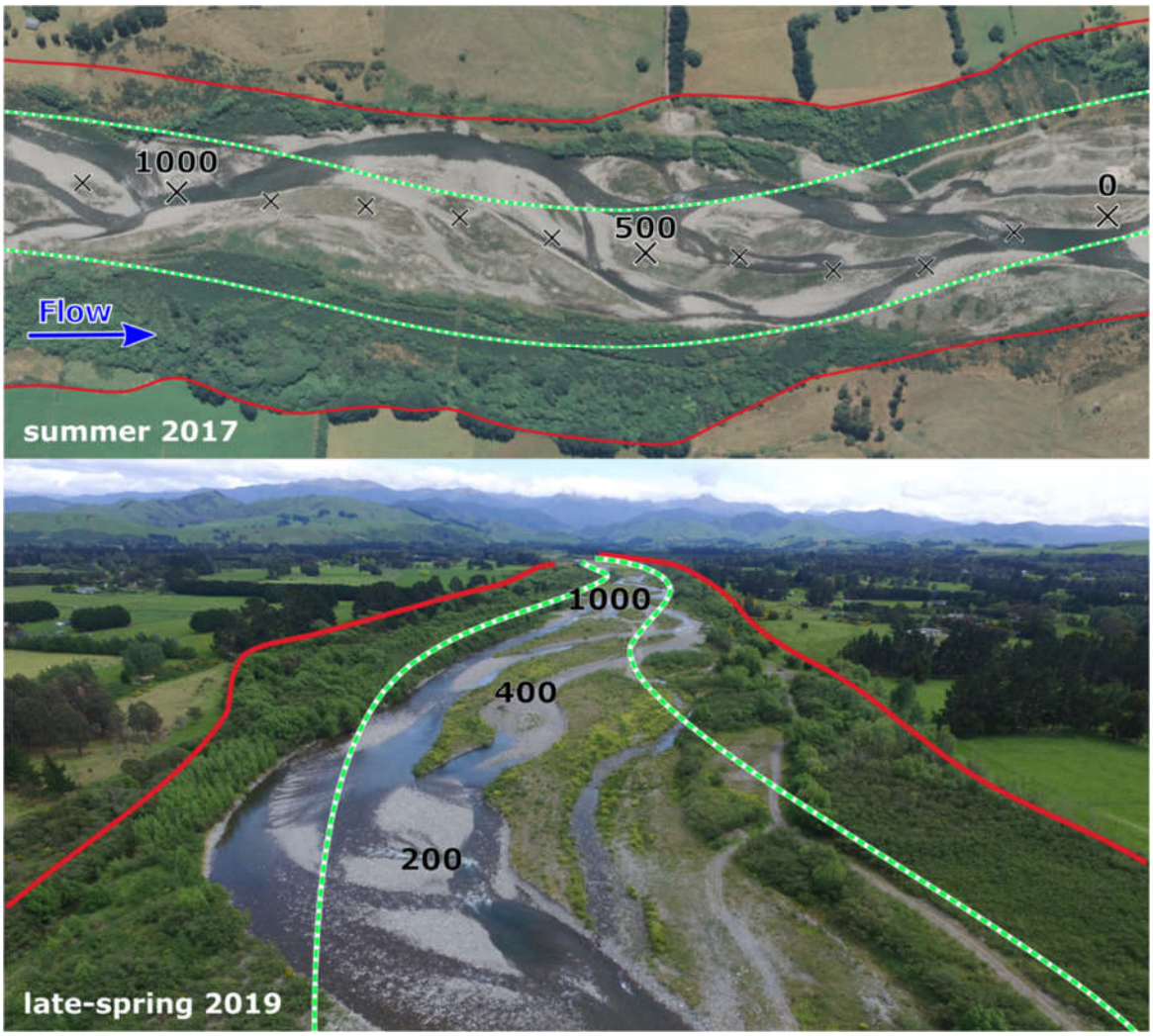

Figure 7-2. Management boundaries (design lines) are composed of an inner channel fairway (green & white lines) and outer buffer (red lines). Top: Downstream portion of the segment AOI (vicinity of valley-KM 10) with accurate 2019 design lines superimposed over the most recent (2017) regional orthoimage. Bottom: Upstream-looking oblique photo of same reach with 2019 design lines transposed from the shapefile over an orthoimage of imagery acquired on the same date as the oblique image. Lines represent the same geodetic position in both images. Numeric annotation indicates stationing (m) along the centreline used for event-scale analysis of the segment AOI.

7.4 Methods

This study considers the same river at two different spatiotemporal scales: a riverscape over many decades and a nested segment over many-decades and a single season. Geographic and statistical distributions of active belt width were used to evaluate riverscape scale changes. At the segment scale, the spatial distribution of volumetric change and changes in primary channel position were evaluated. All spatial data were evaluated in the same Coordinate Referencing System (NZTM 2000, EPSG: 2193).

7.4.1 Riverscape scale change

Active channel belt width was used to assess patterns of change at the riverscape scale over a 69-year period. Greater Wellington Regional Council (GWRC) provided polylines of active belt boundaries digitised for each of eight sets of aerial photography from 1941 to 2010 for the lower ~17 kilometres of the Waingawa River as part of a previous study (Christensen, 2013). Digital

photomosaics were also received from GWRC (e.g., *Figure 4-3* and *Figure 4-4*) corresponding to each year of polylines. Given data lineage by others and the lack of metadata, I conducted a suitability screening of both the imagery (cf. Chapter 4, this thesis) and polylines before proceeding with analysis.

Source imagery for the first three years (1941, 1961, and 1989) was originally collected with metric cameras and multiple overlapping passes at scales between 1:16,000 and 1:54,000. Scan quality was highly variable and geodetic control ranges between 16 and 87 m RMSE (Table 4-5, *Figure 4-8*). Source images for the remaining years were collected via single-pass, low-elevation images using non-metric camera, prints were scanned and stitched, then georeferenced by GWRC personnel. Spot-checking coregistration and geodetic control using common, identifiable points to the same reference imagery (2012 orthomosaic) suggests maximum errors up to about 10 m, though RMSE is likely closer to 5-7 metres. Comparison of polylines to respective source images suggests they were digitised at 1:15,000 or coarser and represent an easily-identified, contiguous active belt corridor. Corridors defined by the polylines are generally inclusive of islands but appear to exclude sedimentologically-active floodplain and floodplain channels. The earliest year (1941) predates widespread availability of heavy equipment and is presumed to best reflect (an unknown portion of) morphological conditions prior to widespread direct human channel modifications. Given earlier clearance of native forest, none of the years were considered pristine.

Given the very wide range and magnitude of geodetic control quality (cf. Chapter 4, this thesis), variety of image acquisition materials and methods, and coarse digitisation scale, the polyline time-series was determined to be unsuitable for absolute, spatially-explicit change detection (e.g. channel migration or locational probability analysis (e.g. Graf, 2000)). However, because the ratio of channel width to frame width was relatively small, polylines were considered acceptable for along-profile evaluation of width (i.e., a second order change detection *sensu* Table 4-6), particularly for bulk statistical comparison across the riverscape. Consequently, for analysis, I treat width as a scalar quantity with changes visualised in terms of geographic and statistical distributions. Aside from avoiding false assumptions of precision, this approach precludes complete reprocessing of mosaics and/or manual quantification of thousands of at-a-point displacement vectors that exceeded project resources.

To characterise riverscape active belt width, I started by converting each pair of inherited polylines (representing right and left margins) to a polygon. Then, I generated a centreline for each polygon using a Voronoi-based approach with 20 metre densification and Euclidean distance. Next, I created cross-sectional lines (n = 896 +/- 6) at 20 metre spacing along and perpendicular to each centreline. Finally, I clipped cross-sections to the active belt polygon for each photo set, respectively. The length of each polyline represents the width of the belt at a given location along the profile for that particular year. As guided by my suitability assessment (above) comparison is performed in bulk as a statistical population for each year. Individual cross-sections were not compared between years.

7.4.2 Segment scale changes

At the segment scale I made four collections of high-resolution aerial photography over a two-month period to assess the magnitude and patterns of planimetric and volumetric river changes associated an increasing sequence of discharge events up to the mean annual flood (Q_{MAF}). Data for segment-scale evaluation has excellent geodetic control and is suitable for fourth order change detection (Table 4-6). The highest-resolution data (low-elevation photogrammetry) is considered in terms of within-season spatially explicit volumetric change while high-elevation orthoimagery is used to

assess multi-decadal relationships. Both sets of data involve the use of Structure-from-Motion processing to create tightly controlled spatially-continuous topographic models and orthoimagery.

7.4.2.1 Structure from Motion (SfM)

Seasonal time series – Four low-elevation aerial photograph collections (surveys) were made by Unmanned Aircraft System (UAS) in November and December 2019 interspersed between flow events with peak magnitudes up to the mean annual flood (Q_{MAF}). Peak flows between the surveys ranged between 34 and 291 cumecs determined from 5-minute gage records from GWRC's gage at Kaituna (Figure 7-3), for which the published Q_{MAF} magnitude is 289 cumecs (GWRC, 2021a). Thus, event maxima captured by this study account for a range of discharge peaks 0.12 to 1.01 times the Q_{MAF}.

Horizontal and vertical control were established by using ground control points (GCPs) marked and surveyed in advance of the first and third collections. GCPs consisted of a mix of fabric and painted targets with geodetic control established by RTK-quality survey (Trimble R10 base and Rover). GCPs were generally located on the periphery of the change detection AOI with maximum 250 metre spacing and surveyed within three days of the first and third aerial collections. Aerial acquisition of RGB images occurred with a DJI Phantom 3 Pro at 70 metres above ground level in programmed missions using Litchi control software. Each mission was flown twice, one with a crossing pattern and nadir camera orientation (achieving a minimum 60% side-lap and 70% forward-lap) and one longitudinally (perpendicular to crossing lines) with a forward-looking, high-angle oblique (~70°) camera angle, to maximise photo overlap and reduce radial lens distortion (James and Robson, 2014).

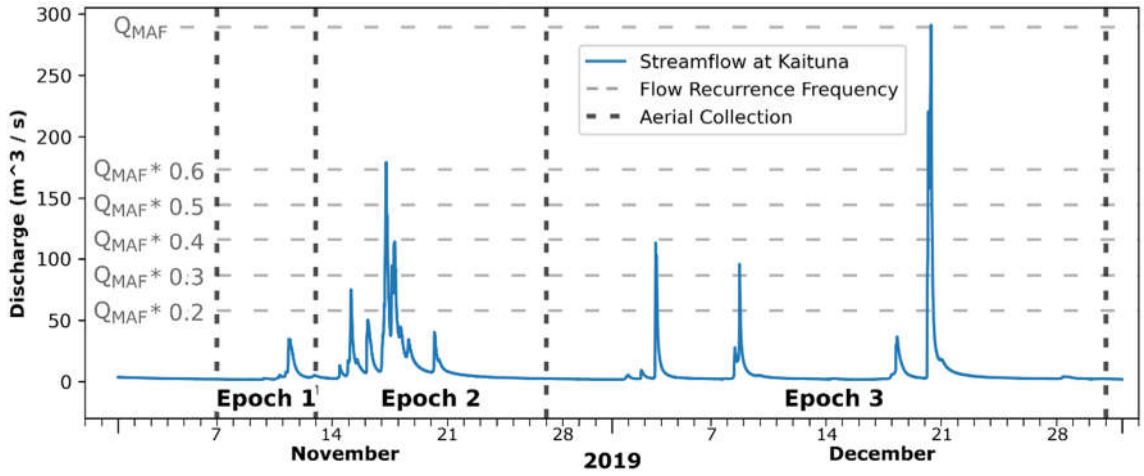

Figure 7-3. Waingawa River discharge at Kaituna (5-minute data,(GWRC, 2021a)) relative to the aerial collections that define each change detection epoch.

All field survey (ground) points were corrected in Trimble Business Center (v5.20) and referenced to common temporary benchmarks (TBMs). TBM coordinates were established by static occupation of at least 30 hours (cumulative), differentially corrected against a nearby (~15kilometres, WRPA) continuously operating GNSS station. Structure-from-Motion was performed using MetaShape v1.5.1 using georeferencing and calibration from approximately 50 well-distributed GCPs, and 'highest quality' alignment and 'high quality' dense cloud settings. A subset (approximately 1/3) of GCPs was reserved during creation of each model to facilitate independent model validation (see Supplemental Materials). Validation using independent GCPs was not possible for the 31-December collection as a sizable proportion (~30%) were excluded due to disturbance or destruction and remaining points were necessary for model creation. A 0.1 metre resolution DEM and a 0.05 metre

RGB orthoimage were created for each survey. DEMs for each survey were concurrent with the other three DEMs.

Historic time series – At the segment scale I used a tightly geodetically-controlled orthoimage time-series to visualise river planform changes relative to design lines over 54-year period. I supplemented commercially-produced orthomosaics from 2012 and 2017 by creating orthomosaics for 1963 and 1983 using high-quality scans acquired from RetroLens (https://retrolens.co.nz/). Horizontal control was established manually using common, fixed, unchanged points identifiable in both the 2012 orthomosaic and year historic images. Once horizontal (XY) points were established, Z-values were extracted from a 1 metre DEM to establish vertical control. The DEM is derived from LiDAR acquisition during the same year and season as the 2012 orthomosaic used for horizontal control. These were processed in MetaShape v1.5.1 using 'highest-quality' filtering to generate finished imagery better than 0.8 metre resolution.

7.4.2.2 Geomorphic Change Detection

Geomorphic change was assessed using the seasonal high-resolution DEM time-series to provide spatially-explicit and spatially-continuous accounting of sediment sources, storage, and sinks (Fuller et al., 2003a). Change computations involved subtracting the previous DEM from a given DEM in the time-series to generate error-thresholded DEMs-of-Difference (DoDs) using Standalone Geomorphic Change Detection (GCD) software (Wheaton et al. (2010b), v7.5.0, http://gcd.riverscapes.xyz/). The process was conducted iteratively to remove vegetation effects. An initial un-thresholded pass created raw DEMs for visual evaluation of actual topographic change vs. apparent model-based changes. Based on inspection, a vertical threshold envelope was determined and used to filter-out non-real values. It was also used to assist digitisation (in combination with high-resolution orthoimagery) of mask polygons to exclude pixels from further analyses (e.g., where vegetation produced false signals). This effectively resulted in the active braid network (sensu Egozi and Ashmore, 2009) where masking of selected channel boundaries minimised vegetation effects. Water clarity during all surveys was excellent with the deepest (~2.5 metre) points visible within the wetted channel. Bathymetric surfaces were manually inspected for consistency with field observation. Bathymetric distortion associated with refraction was assumed to be consistent across surveys. Because pixel-based changes were considered in bulk by units (see next subsection) consistently across the study area, distortion effects are not considered to bias results in a manner that would patterns of change detection.

A second GCD pass was then performed using the mask and a Minimum Level of Detection (mLoD) value of 0.35 metre. The mLoD was determined using the equation of Hugenholtz et al. (2013) that defines a mLoD threshold by combining errors from the two datasets being compared:

$$T = \pm 3 \times \sqrt{RMSE_1{}^2 + RMSE_2{}^2}$$

Calculations of *T* were made for all sequential comparisons for both model and independent control points and produced values between 0.227 and 0.300 metre. I used the largest value of T and added a 0.05 metre safety factor to exclude residual vegetation effects and implemented thresholding with a 0.35 metre threshold. While this may result in under-representation of shallow surfaces (sensu Brasington et al., 2000), it provided greatest certainty that observed patterns of change intensity between the thresholded DEMs-of-difference (DoD) were real. Thus, changes presented here are highly conservative and biased low or, in other words, the distribution and magnitude of actual changes exceed changes reported in this chapter.

7.4.2.3 Change Units

A series of adjacent polygons was developed to ensure sequential, ordered common geographic units were compared across surveys. Such approaches are well-established for sediment budgeting (Fuller et al., 2002; Wheaton et al., 2010b) and also enable summarising/discretising other spatially-continuous parameters (e.g. Alber and Piegay, 2011; Kidová et al., 2016; Gregory et al., 2019). The survey extent polygons were dissolved, then a common centreline was created. An iterative process was undertaken where cross-section lines were generated perpendicular to centreline at 20 metre increments and evaluated. If any intersected, then an additional increment of smoothing was applied to the centreline and cross-sections were recreated until no intersections occurred within the perimeter of the dissolved perimeter polygon. Polygon budgeting units were then created to facilitate summarising volumetric change and channel movement by cutting the dissolved perimeter polygon by the cross-section lines.

7.4.2.4 Wetted primary channel position (seasonal)

To identify magnitude and patterns of low-water channel planform change associated with the Q_{MAF}, edges of the primary wetted channel were manually digitised at 1:1,000 scale from RGB orthoimagery for 27-November and 31-December surveys and a common centreline was generated. Cross-sections were generated at 10 metre increments along the centreline and projected to the left and right edges of each survey respectively. The magnitude and direction of change for each edge was determined by the point where each cross-section intersected the primary wetted channel centreline by survey.

To enable comparison with volumetric change results, a set of cross-sections was generated along the common survey centreline at 10 metre increments and projected to the wetted channel centreline. The 10-metre survey centreline cross-sections were offset from the budget units such that two cross-sections lay within each budget unit without interesting polygon boundaries. Finally, the points (and respective edge attributes) from the wetted channel centreline were snapped to the closest 10 metre survey line and projected to the survey centreline such that volumetric change and wetted channel change could be plotted concurrently using the survey centreline as a common reference.

7.4.2.5 Decadal active belt position and migration relative to design lines

Historic channel occurrence within the design lines was assessed for the Segment AOI using high-quality historic orthomosaics I produced (1963 and 1983; 7.4.2.2) and publicly available high-quality orthoimagery (2012 and 2017). Imagery was suitable for fourth order change detection (cf. Table 4-6) which encompasses a 54-year period. The 2012 and 2017 orthomosaics (0.3-metre resolution) were commercially produced with coregistration of the 2017 mosaic 0.9 metre 95% confidence (Table 4-5) compared to the reference 2012 image. Coregistration of the 1963 and 1983 orthomosaics was assessed by spot-checking to the 2012 reference and has maximum point displacements of 2.1 metres. Using the spot-check ratio from the 2017 orthomosaic (Table 4-5), suggests 3.25 metres as a conservative 95% confidence coregistration estimate. Collectively, these layers provide a high degree of positional certainty for multidecadal analysis. The shapefile of the GWRC 2019 design lines was used as a fixed reference to assess channel extents digitised from the orthoimage time series.

7.4.2.6 Hydrologic threshold for geomorphic effectiveness

Many studies note difficulty and uncertainty associated with identifying thresholds of motion (e.g. Phillips and Jerolmack, 2014). I constrain the hydrologic threshold for geomorphic effectiveness

empirically, using two lines of evidence based on multiple field observations between May 2017 and March 2019. Preliminary ground surveys and SfM collections across a range of flows provided the basis for identifying thresholds of geomorphic effectiveness and particle mobility. Event-based sampling found unit-scale erosion and deposition following events with peak recurrence of 0.2 to 0.3 * Q_{MAF} (e.g., Figure 7-4) with patch-scale redistribution of gravels observed as frequent as 0.1 * Q_{MAF} events.

Flow disturbance of painted GCPs after flow events presented an opportunity to characterise event-scale particle movements (Figure 7-5). Painted particles dispersed from GCPs were searched for using a systematic grid pattern that extended up to 5 m downstream from the last observable clast. When a tracer was observed, its position was recorded with RTK GPS to assess the distance travelled, and its β-axis length estimated or measured with a ruler. Particle-scale surveys were conducted on an *ad hoc* basis as time was available. Though limited in scope and largely descriptive in nature, this work provides the first empirical data for establishing particle mobility and geomorphic effectiveness thresholds for Wairarapa rivers. Because these event-based particle surveys were neither systematic, nor random, I do not present reach or segment-scale statistical summaries as representativeness cannot be characterised. However, based on a weight-of-the-evidence approach across multiple geomorphic surfaces and multiple events, I consider the 0.2 * Q_{MAF} discharge (57 cumecs) robust threshold for thresholding geomorphic effectiveness and use it for calculations of excess discharge.

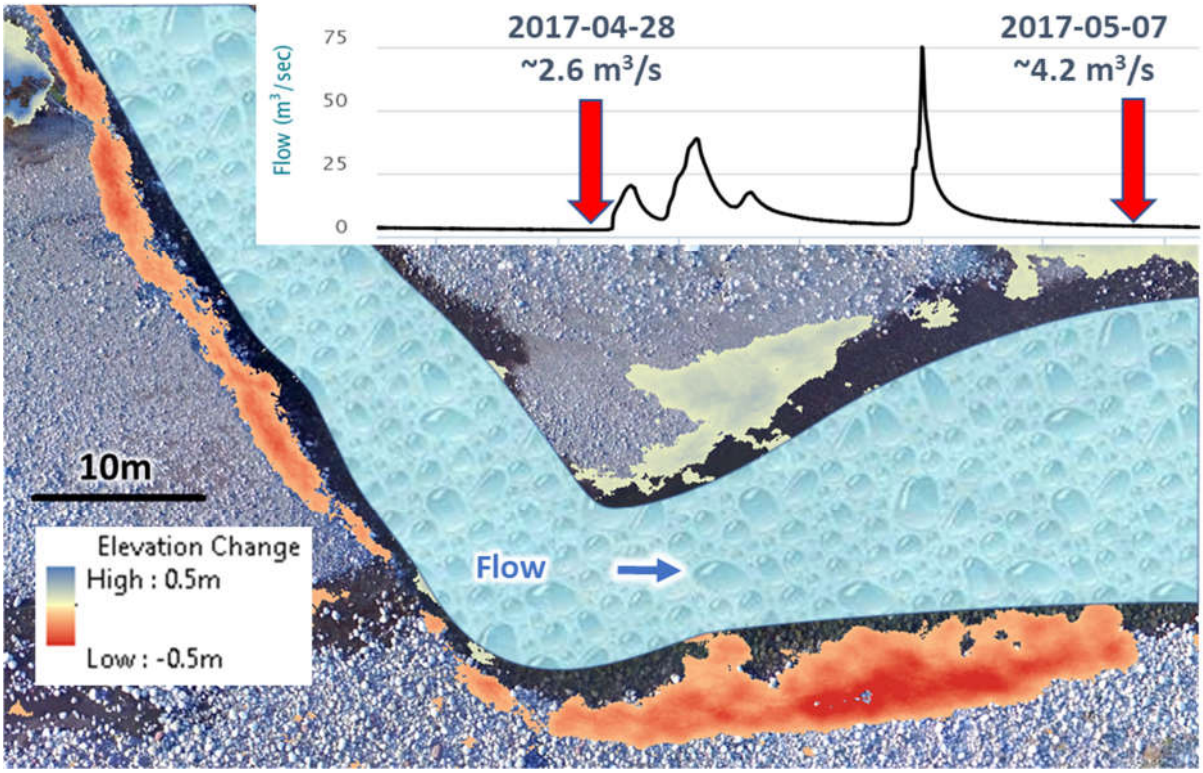

Figure 7-4. Local erosion and deposition along channel margins associated with a ~0.25 * Q_{MAF} recurrence event indicative of unit-scale geomorphic effectiveness. Wetted channel is masked as surface turbulence during re-survey exceeded the mLoD threshold of the analysis.

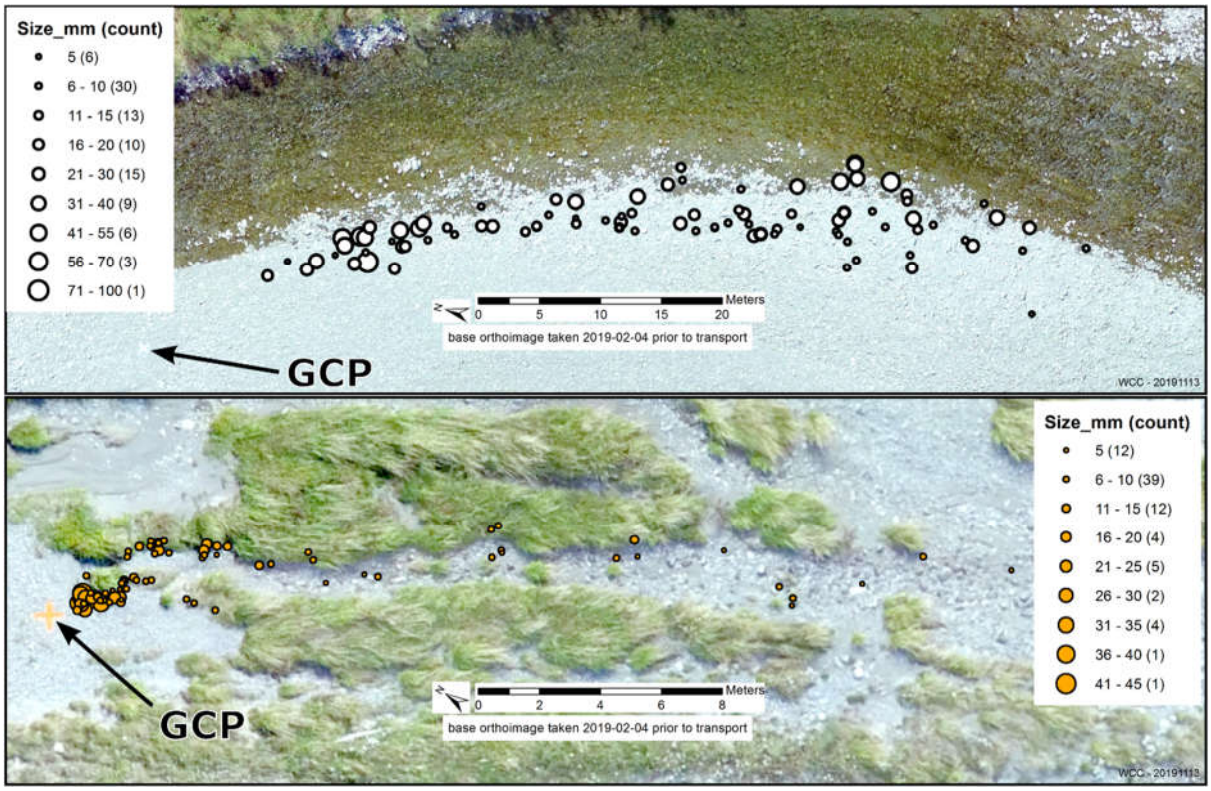

*Figure 7-5. Spatial distribution of tracer particles originating from GCPs following a ~ 0.2 * Q_{MAF} event. Top: Lateral bar adjacent to primary channel. Bottom: Intermittent floodplain channel.*

7.5 Results

7.5.1 Decadal change at riverscape scale

Between 1941 and 2010, there is a pronounced trend of riverscape narrowing and increasing uniformity. The 1941 riverscape exhibits the highest geographic variability in the time series with distinct geographic clusters with cyclic transitions between narrow and wide (Figure 7-6) that is also indicated by a very wide and flat statistical population (Figure 7-7). Variability is still present in 1961 with many transitions between wide and flat reaches remaining in comparable areas to 1941 (Figure 7-6) though much diminished width magnitudes and an obvious shift toward narrower conditions (Figure 7-7). In the 1989, 1993, 1996, and 2000 members, wider reaches largely disappear though a few persist as remnants noted by lighter colour bands (Figure 7-6) and retaining a bit of a right-tailed skew (Figure 7-7). The statistical distribution in 2006 and 2010 approximates a normal curve indicative of highly uniform width conditions (Figure 7-7).

Narrowing occurs relatively early in the time series with the biggest jump between 1941 (mean = 241 metres) and 1961 (mean = 166 metres), then gradual narrowing subsequently (Figure 7-7). Low-end range values are fairly constant through time, though the upper tail values (inclusive of outliers) shift toward smaller values. While mean width diminishes progressively through time, the mode is largely stationary from 1989 and after (Figure 7-7). The trend toward increased uniformity is present throughout the timeseries but develops later and more gradually. The 1961-1989 epoch shows the greatest change characterised by the single biggest reduction (24 m) in standard deviation over the period of record (Figure 7-7). The 1961-1989 epoch also exhibits the greatest graphical shift in kurtosis (i.e., flatness) from highly negative to positive. Since 1993, roughly 75% of the widths in any given year (top of 'box') have been less than the 25th percentile width in 1941 (Figure 7-7, bottom left, horizontal line).

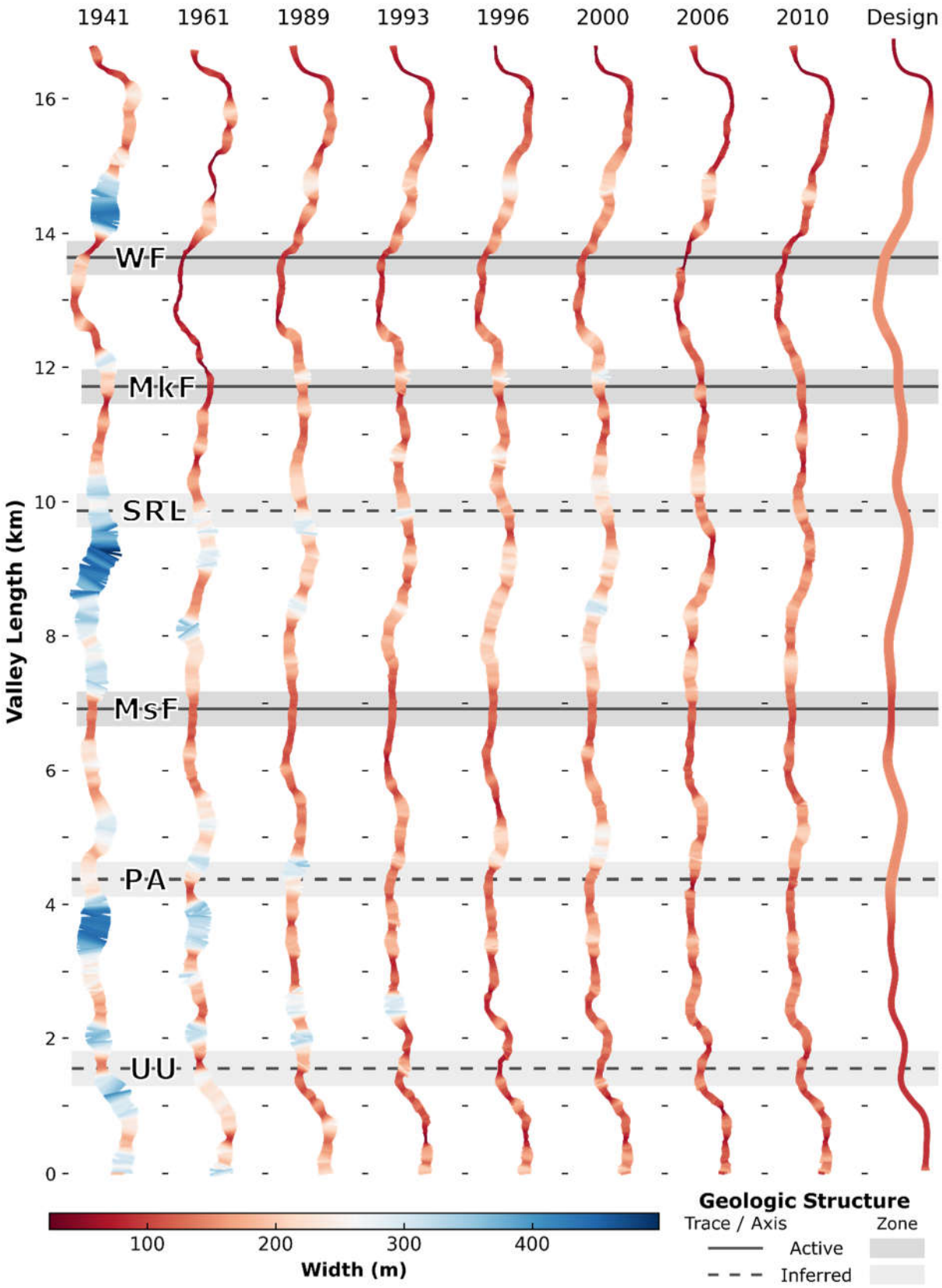

Figure 7-6. Choropleth plots by year for active belt widths of the lower Waingawa River superimposed over major geologic structure (active: NZAFD; inferred: authors per Chapter 6). WF: Wairarapa Fault, MkF: Mokonui Fault, SRL: Skeets Road lineament, MsF: Masterton Fault, PA: plunging anticline, UU: undifferentiated uplift. Lack of colour contrast indicates increasing uniformity.

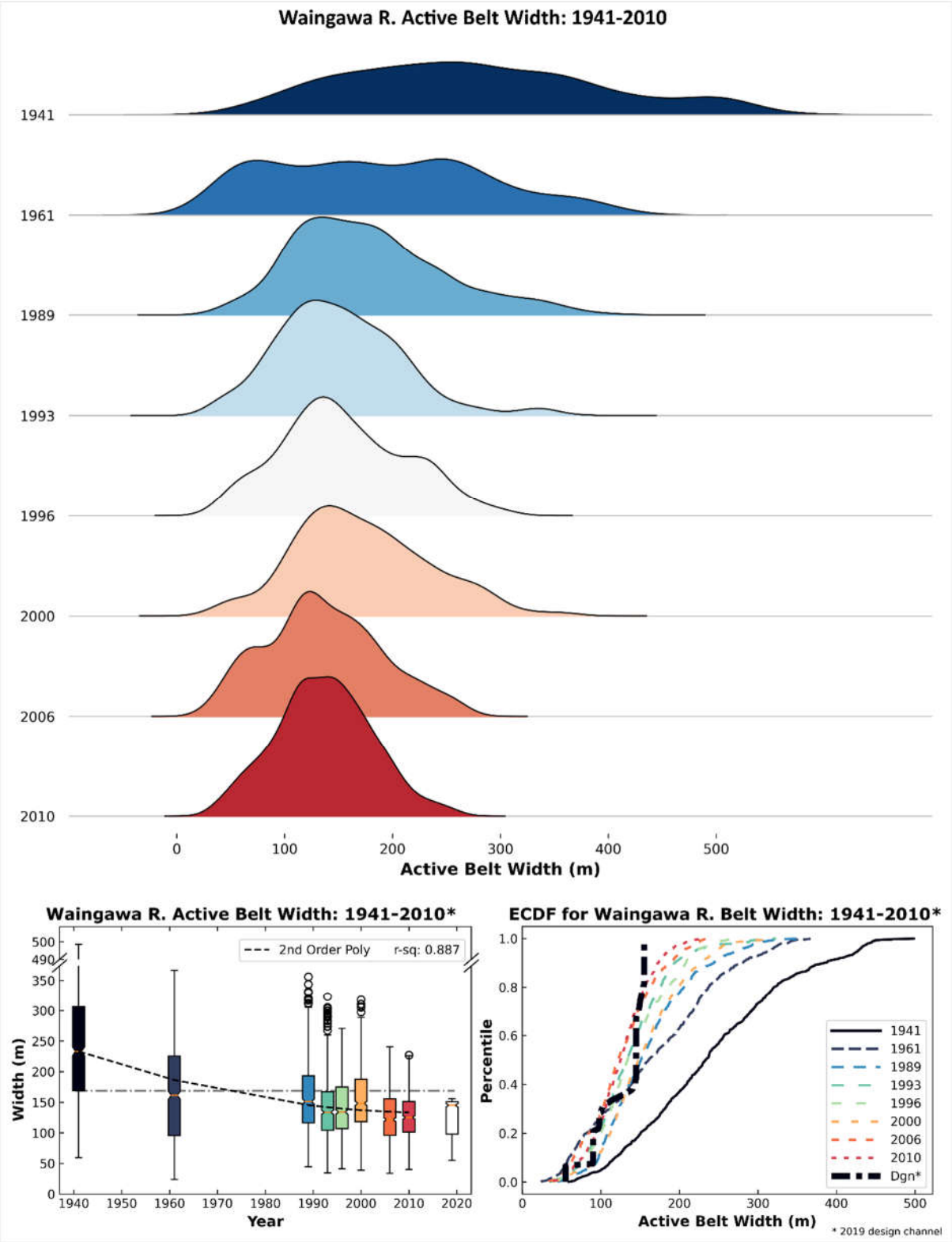

Figure 7-7. Active belt widths by year. Top: Ridge plot indicating narrower widths (shift to left) with a tighter and more uniform statistical distribution through time. Bottom Left: Central tendency, range and interquartile range of widths diminish through time with second-order polynomial regression showing a convergent relationship on 2019 design width (white box). Bottom Right: Empirical cumulative frequency plots (using same colour coding as lower left plot) exhibit truncation and steepening consistent with trends in ridge and box plots; an ECDF of the design width is overplotted for reference.

The geographic pattern of width distribution in 1941 (~pre-disturbance) and, to a degree, subsequent years shows spatial correlation with crossing geologic structure. In particular, narrower belts occur near uplifted areas (Figure 7-6; WF, MkF, MsF, PA, and UU) consistent with prevailing theory (see Chapter 6, this thesis). Notably wider areas tend to occur in between structures which is also expected in a back-tilting scenario proposed in Chapter 6. Within the broader riverscape trend of diminishing width and variation, there are sub-units of relatively greater (within-year) width that persist (e.g., Figure 7-6, Valley km (Vkm) 3.3 and 14.7) or occasionally re-form (e.g. Figure 7-6, Vkm 2.5, 5.1, 7.5 and 8.5) in proximity to those of 1941.

Diminishing widths and variability through time converge statistically on the 2019 design lines (Figure 7-7, bottom). A second-order polynomial regression (Figure 7-7, bottom left, curved line) was fit to visualise the apparent asymptotic nature of the narrowing trend (in terms of absolute width) that converges on the design distribution. Because of non-homogeneity of variance across time-series members, I neither interpolate nor extrapolate the relationship for predictive purposes. The synthetic nature of design channel widths is particularly stark when one considers the highly skewed boxplot (Figure 7-7, bottom left) and cumulative frequency distribution (Figure 7-7, bottom right, heavy hashed line).

7.5.2 Segment scale dynamics

7.5.2.1 Decadal position and migration

Several key relationships become evident when comparing the high-quality orthoimage series (coregistration ~3 m or better) to the current design lines (Figure 7-8). The active belt has generally occurred within the 2019 'buffer' since 1963. The 1963 corridor appears to have a lower composition of bare gravel than subsequent years and generally greater vegetative cover on medial features that reflects more natural conditions consistent with the first two (kurtotic) histograms in (Figure 7-7, top). The 1960s mark the onset of extensive earthworks within the Ruamāhanga catchment's gravel bed rivers. The 1983 corridor is a wider expanse of bare gravel indicative of an expansion period and breaks-out of the fairway margins in multiple places. The 1983 image is the first to integrate the effects of substantial earthworks. It also includes two of the three largest discharge events on record within three years (1980 and 1982) of the 1983 photo. Though the 1983 belt appears generally less sinuous than 1963, the breakouts appear more abundant and with greater displacements. Expansion and the shift toward break-out behaviour could well be a response to the first hydraulic 'test' of those initial decades of management. Graphically, the smoothness of the fairway margins is inconsistent with the at-a-time irregularity of the 1963 and 1983 belts. Despite general statistical convergence with design lines (Figure 7-7) and a qualitatively better 'fit' in 2012 and 2017 (Figure 7-8), the active belt is not fully contained by the design fairway in any of the images and the location of containment breaches shift over time. Channel evolution required the sequence of forms also suggests more frequent, but unrepresented dynamics.

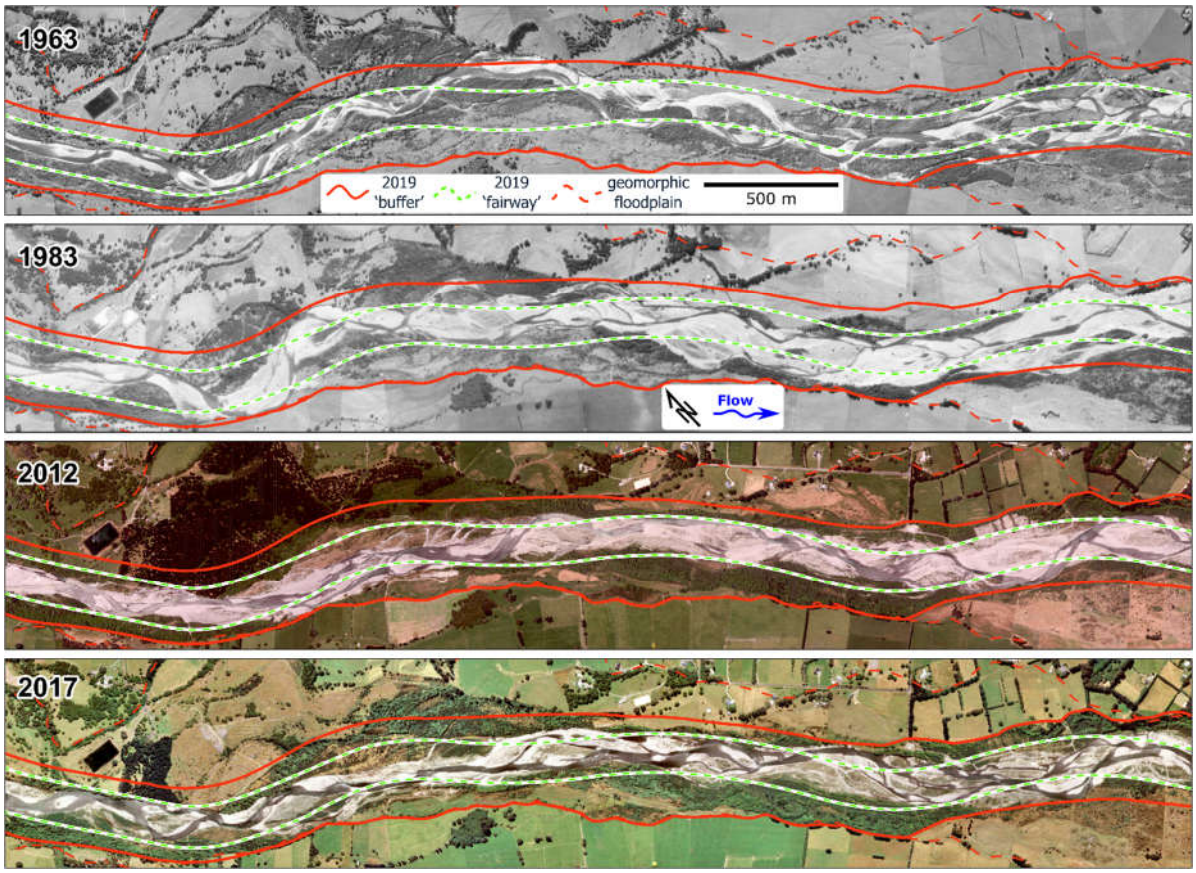

Figure 7-8. High-quality decadal orthoimage series from 1963 to 2017 for the Segment AOI with the 2019 design lines superimposed.

7.5.2.2 Event discharge and geomorphic work potential

In contrast to diminishing variability through time at the riverscape scale, a high degree of variability in channel change exists at the segment and finer scales. Both hydrologic and geomorphic variation were captured and emerge in both space and time even at sub-annual frequency discharges. Peak discharges for each of the three change detection epochs varied in magnitude and duration (Table 7-1). The maximum discharge (34.6 cumecs) in Epoch 1 did not equal or exceed the discharge threshold. Three peaks exceeded the threshold during Epoch 2 with a 179.2 cumecs maximum and a total excess duration of 16.4 hours. Epoch 3 also had three peaks of excess discharge including the largest discharge of the sampling period, which magnitude slightly exceeded the Q_{MAF}. Despite having the largest discharge, the duration of total excess flow in Epoch 3 was roughly three hours less than Epoch 2. However, discharge during Epoch 3 delivered almost twice as much total excess volume of water (the discharge in cumecs for each 5-minute increment reported by the gage times 300 seconds). When total effective volume is normalised by the cumulative duration of all excess flows, "excess discharge" (Table 7-1), doubles for Epoch 3 increasing the potential for geomorphic work.

Table 7-1. Peak water discharge characteristics for events by epoch. The excess discharge threshold is 57 m^3/s.

Epoch	# of Peaks > Threshold	Total Excess Duration (hrs)	Instantaneous Maximum (m^3/s)	Total Excess Water Volume (m^3)	Excess Discharge (m^3/s)
1	0	0	34.6	0	0
2	3	16.4	179.2	2,217,737	37.5
3	3	13.3	290.8	4,058,646	85.1

7.5.2.3 Geomorphic Change

As expected, geomorphic change between epochs varied proportionately with excess discharge. Surprisingly, considerable within-epoch spatial variation occurred for epochs with excess discharge, with the greatest contrasts occurring in Epoch 3. The spatial distribution of variation groups into four reaches, numbered 1-4 from the bottom of the segment (Figure 7-9).

Temporal change (with discharge) – The total quantity of change during Epoch 1 was relatively small and may reflect vegetation effects not eliminated by masking and thresholding (Table 7-2). A modest increase in change occurs during Epoch 2 with the onset of discharges exceeding the effectiveness threshold. Areal and volumetric change for the entire segment increase roughly twenty-fold in Epoch 3 compared to Epoch 2. Thus, while more excess discharge caused more change as expected, the relationship is notably non-linear and scales more with discharge than duration.

Table 7-2. Areal and volumetric changes in absolute units by epoch and reach. Total areal change is the sum (in m) of all cells where a vertical change exceeding the mLoD occurred. Total volumetric change is the sum of the absolute thresholded change volume. Refer to Figure 7-9 for reach location.

	Total Areal Change (m^2)			**Total Volumetric Change (m^3)**		
	Epoch 1	**Epoch 2**	**Epoch 3**	**Epoch 1**	**Epoch 2**	**Epoch 3**
Reach 1	375	1007	25,698	385	595	17,192
Reach 2	373	381	5,303	346	383	2,949
Reach 3	387	1,971	32,684	429	1,274	23,613
Reach 4	n/a	n/a	1,207	n/a	n/a	676
Total	1,135	3,359	64,892	1,160	2,252	44,430

Spatial distribution of change – Change intensity occurs in distinct spatial groupings at reach and sub-reach scales for epochs during which excess discharge occurred (Table 7-2 and Table 7-3). At reach-scale, absolute change in highly active reaches (1 and 3) is an order of magnitude greater than less active reaches (2 and 4). The differences could be partly attributed to reach size, so to standardise comparison across reaches, absolute thresholded changes (Table 7-2) were divided by reach area (Table 7-3). After normalisation, the mean areal change of highly active reaches (31.7%) is almost five times greater than the mean of the less active reaches (6.6%) for Epoch 3 (Figure 7-11). Similarly, the mean normalised absolute change of highly active reaches (0.222 m/m^2) for Epoch 3 is six times greater than the mean of the less active reaches (0.037 m/m^2).

Table 7-3. Areal and total volumetric changes normalised by reach area.

	Normalised Areal Change (%)			**Normalised Volumetric Change (m^3/m^2)**		
	Epoch 1	**Epoch 2**	**Epoch 3**	**Epoch 1**	**Epoch 2**	**Epoch 3**
Reach 1	0.4	1.0	26.8	0.004	0.006	0.179
Reach 2	0.6	0.6	8.0	0.005	0.006	0.044
Reach 3	0.5	2.4	36.6	0.005	0.015	0.265
Reach 4	n/a	n/a	5.1	n/a	n/a	0.029

While the relative geographic ordering of reaches is similar for both epochs 2 and 3, the spatial extent of the most intense changes (Reaches 1 and 3) is larger following Epoch 3 (Figure 7-9 and Figure 7-10) which provides the basis for delineation (Figure 7-9). Shifts of the primary wetted channel (Figure 7-9, left panel and Figure 7-10, bottom-right) generally coincide with reaches exhibiting greater overall change. Within highly active reaches there is some evidence of headward incision particularly ca. centreline station (STA) 300 to 600 to 750 (possibly 950) and STA 2900 to 3150 to 3300 for Epochs 1, 2, and 3, respectively.

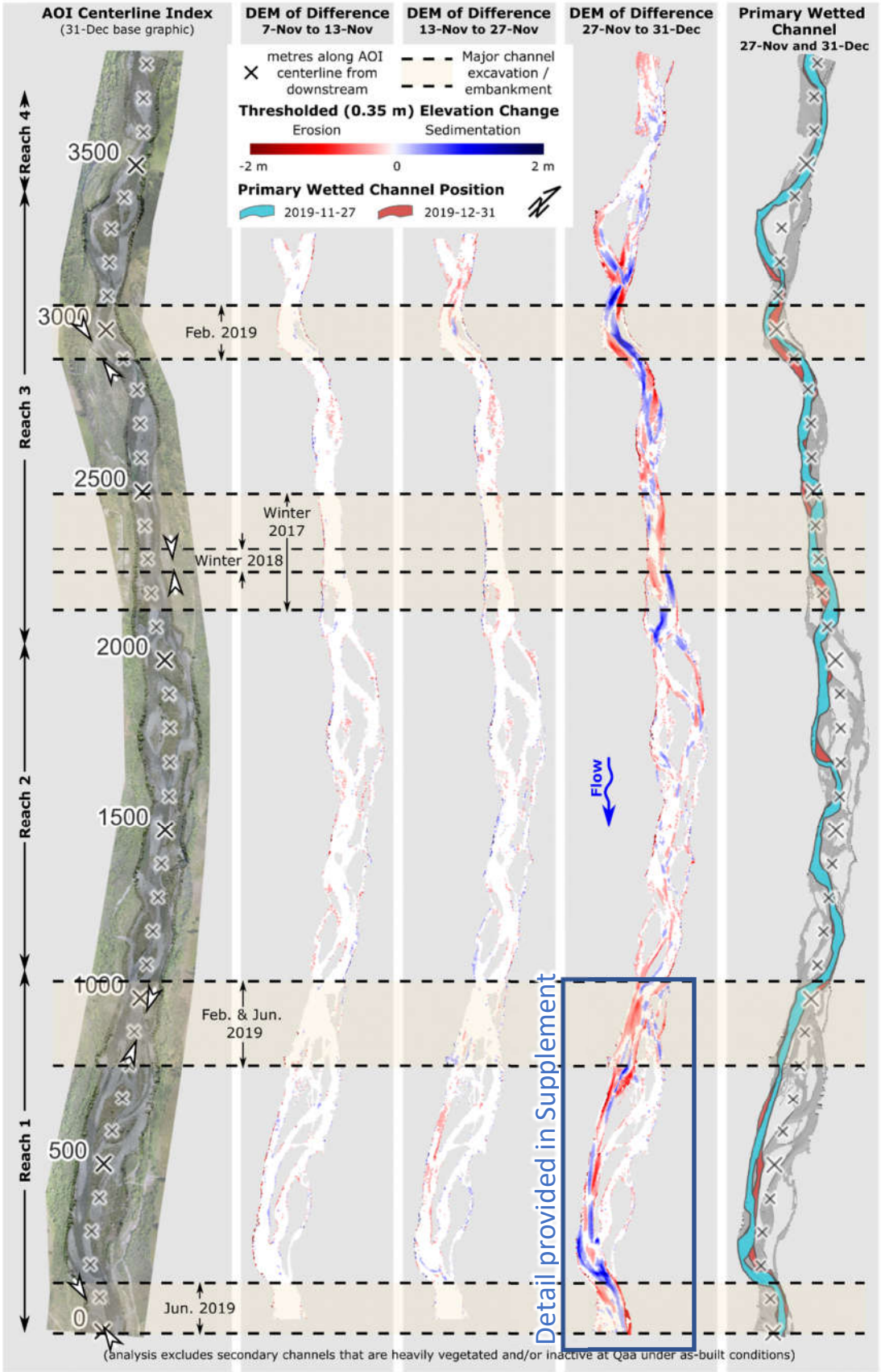

Figure 7-9. Change in the segment AOI with index (left), DoDs by epoch (middle three panels, labelled accordingly), and primary wetted channel alignments (right). Horizontal zones delineate areas of mechanical treatment with white arrows indicating berms construction to block channels. An annotated DoD for Reach 1 is provided in Supplemental Materials.

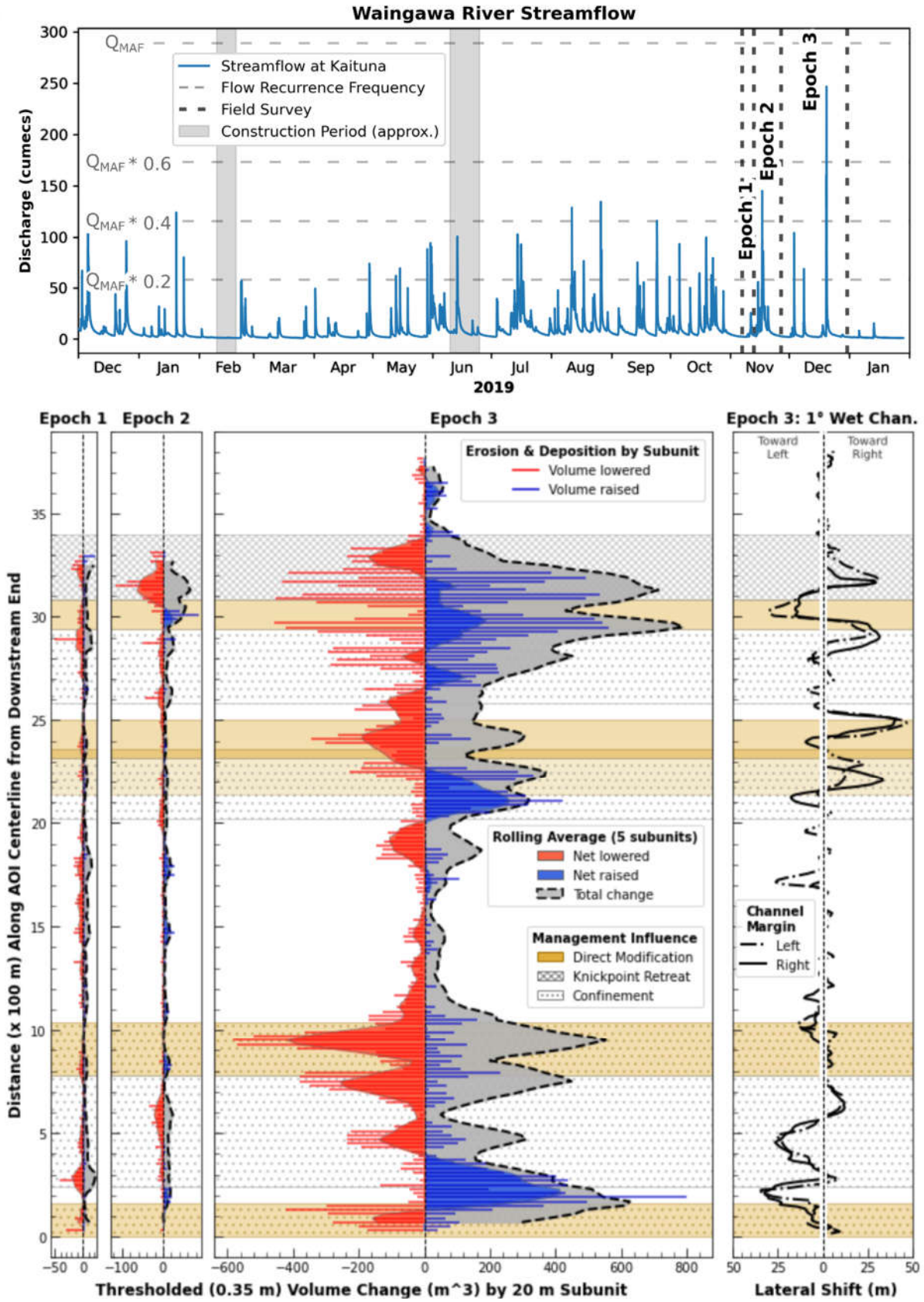

Figure 7-10. Top: Hydrograph for the Waingawa River at Kaituna for 2019 with field surveys and approximate construction periods. Bottom: Thresholded volumetric change by subunit (sediment budget blocks, 20 metres along profile) with the lateral change in the wetted primary channel during the final epoch (bottom-right).

There is consistent paring of aggrading sub-reaches (Figure 7-10, 'Net raised') downstream of incising sub-reaches (Figure 7-10, 'Net lowered') with little exception. Sub-reaches exhibiting the most intense changes are spatially coupled with locations of major active channel grading (i.e. earthworks) during an observation period that began in May 2017. Of these, most notable are embankments constructed to block side channels in the vicinity of STA 950, 2250, and 2950 (Figure 7-9, left panel).

While Epoch 1 lacks distinct reach-scale differences, the spatial distribution of thresholded change in the vicinity of STA 300 and 2900 (Figure 7-10) is consistent with field-observed bed changes. The consistent amount of reach-scale change during Epoch 1 (Table 7-2) may also indicate some base level of vegetation presence in the terrain models and their effect on the DEM-of-Difference.

7.6 Discussion

7.6.1 Riverscape narrowing and uniformity

A key aspect of multiscale analysis is the exploration of correspondence (or non-correspondence) and scaling of trends and processes. Results of decadal analysis (Figure 7-6 and Figure 7-7) could be considered an indicator of increased stability and, potentially, validation of long-term flood protection efforts. However, such interpretation must be constrained to the time and context of the data, as indicated by segment-scale decadal results (Figure 7-8).

Piégay et al. (2006) proposed a conceptual model of river change with an *expansion* phase characterised by frequent lateral shifts during periods of high sediment supply and *contraction* occurring where narrowing and incision result from low sediment supply. The definitive trend of the Waingawa River toward a narrower belt and increasing uniformity over the multi-decadal period is generally consistent with contraction.

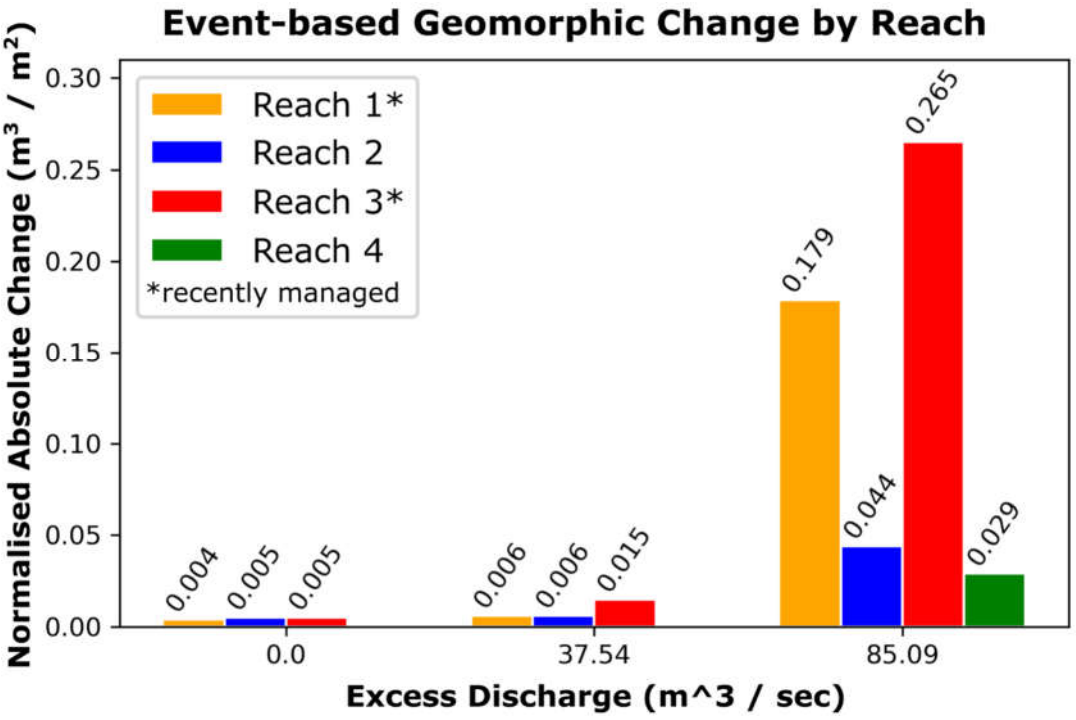

Figure 7-11. Geomorphic change by reach for three different time-integrated events with 0.0, 37.54, and 85.09 m^3/sec of excess discharge representing epochs 1, 2, and 3, respectively. The 0.004-0.005 values associated with Epoch 1 appear to be related to be perimeter effects of masking polygons and are considered as the residual (post-thresholding) background noise present across all epochs.

The catchment and broader region have experienced relative quiescence in terms of natural hazards during the study period. The last earthquake to generate MM VII shaking within the catchment was in 1942 and major storms generating regional-scale land-sliding have largely spared the area. By comparison, six earthquakes generated MM VII+ or greater shaking in the region between 1848 and 1942 (cf. Downes, 1995), including the 1855 Wairarapa earthquake (MM IX-X) that produced rupturing on both sides of the river. Thus, a case could be made that the Waingawa River was emerging from a period of sediment enrichment early in the photo series with subsequent entrenchment occurring as sediment supply diminished. Reduced mean width but maintenance of relative variability (i.e., flat histogram shape) between 1941 and 1961 could be characteristic of this.

Liébault and Piégay (2002) attributed widespread, long-term narrowing of many gravel bed rivers in eastern France to reductions in catchment sediment supply and increased floodplain stability associated with afforestation and abandonment of riparian agriculture. Floodplain accretion can also result in narrowing (e.g. Schumm and Lichty, 1963) and the presence of vegetation produces narrower, deeper channels (Manners et al., 2014; Mao et al., 2020). Narrowing and floodplain terrestrialisation typically co-occurs with reduced braiding and increased stability (e.g., Liébault and Piégay, 2002; Surian, 2006; Marchese et al., 2017; Mao et al., 2020; Tena et al., 2020).

However, my (qualitative) photo-interpretation suggests the opposite for the Waingawa River as it has shifted from a generally multi-threaded wandering form to increased presence of braided signatures (cf. Wheaton et al., 2013). While this is counter to global narrowing trends, it is consistent with increased sediment transport, reductions in floodplain vegetation and diminished resistance (e.g., absence of large wood). Thus, while some degree of natural entrenchment cannot be ruled-out, it is worth considering other explanations.

The tendency of flood control efforts to narrow floodplains and increase riverscape uniformity is widespread in New Zealand and abroad (Hohensinner et al., 2014; Gregory et al., 2019; Tena et al., 2020; Fuller et al., 2021; Kidova et al., 2021). In the Waingawa, the photo-interpretation identifies isolated human signatures of morphologic change in the earliest photography (1941), but suggests management into the early 1980s favoured discrete, localised manipulations associated with abstraction, realignment, and gravel extraction. This is consistent with an evaluation of flood protection records noting that concerted, isolated channel works began in the 1960s (Williams, 1990). Most of the channel adjustment over this time is likely to be linked to river control works, with little evidence of catchment-derived sediment pulses. Minimal variation in belt width upstream of ~Rkm 16 (Figure 7-6) is interpreted as general absence of catchment-derived sediment pulses and may even indicate regime behaviour (i.e., where geometry is in a quasi-equilibrium state with sediment transport). This inference is also generally supported by cross-section data (Figure 6-3) which, other than some net change at XS 30 in the mid-1990s, shows no clear signatures of a pulse (cf. Cui et al., 2003; Sims and Rutherfurd, 2017) in upper reaches. This apparent absence of a catchment-based sedimentary signal implicates local sediment sources as drivers of morphological changes within the AOIs. Given the absence of significant tributaries, valley floor sediments are the most probable source, thus implicating erosion of bed and banks as the chief recruitment mechanism.

While the 1943-1963 epoch correlates with the “Great Acceleration” of the Anthropocene (cf. Steffen et al., 2015), I cannot rule out that the observed contraction could also reflect relaxation following earlier coseismic sediment enrichment. Therefore, I suspect riverscape change during this time is a mix of natural and human signatures (e.g. Downs et al., 2013), but nonetheless suggest that observed changes since the 1960s are largely human-forced as acted upon by flooding given 1) operational records indicating more active management co-occurring with the greatest change in

variation (Figure 7-7, 1961-1989), 2) absence of a catchment sedimentary signal, 3) changes in the statistical distribution of width that converge on fairway design dimensions, and, perhaps most importantly 4) the counter-trend of increase of braided forms (opposite to that expected with natural contraction).

7.6.2 Reach-scale instability

In-channel disturbance by humans is widely recognised for effects on channel form and boundary composition (Kondolf, 1997b) and in-channel mining has been identified as the most influential factor on local form and process (e.g. Graf, 2000) in some systems. Within the study area, gravel extraction is used for both commodity production and as a source of armour for reinforcing fairway margins. Within the segment AOI, effects are best considered from a force-balance perspective as management actions decrease resisting forces along the boundary as well as increase driving force of the water itself

Repeat field observations of bed and floodplain structure indicate that treatments modify both sediment structure and hydraulic conditions in ways that increase sediment transport capacity by decreasing resisting force (Figure 7-12) and/or increasing driving force (Figure 7-13). The mechanisms by which treatments were observed to decrease resistance can be grouped into four categories: 1) armour removal, 2) reduced particle shielding, 3) surface disruption/tillage associated with uprooting vegetation, and 4) reduction/removal of barforms (reduced form-roughness). These outcomes co-occur (either deliberately or as by-product) with operational reshaping of hydraulic geometry that increase unit flow depth and local slope.

The width signals of local sediment recruitment at riverscape scale (Figure 7-6) come into focus in the segment AOI. While the spatial correlation between treated areas seem quite clear, diffusive effects associated from re-working that occurred between completion of in-channel operations and the earliest (7 November) survey extend morphologic change signals upstream and downstream (Figure 7-9 and Figure 7-10; detail provided for Reach 1 in Supplemental Materials). Reach scale sediment pulses originate from mobilisation of channel (Reach 3) and floodplain (Reach 1) sediments, move through sub-reaches confined to a single channel, then gain (or create) access to broader areas in the general manner described by Cui et al. (2003). While there is an intermediate zone of translation in both instances, the outcome seems primarily dispersive at the reach exits. In the case of Reach 3, this is more difficult to determine due to active knickpoint migration appearing to generate multiple pulses (discussed below).

Though the mechanics of downstream transfer is not critical to my premise, it is worth noting that the pulses interact differently within the AOI. The pulses generated from the two main source zones in 2019 (~ STA 1000 and 3000) seem to largely translate through sub-reaches with higher banks until encountering less-confined sections at which point there is a shift to dispersion with considerable lateral sediment transfer occurring (see Supplemental Figure S7-16 for example of Reach 1)). The translative expression appears more visible in the erosive signal (Figure 7-10, subplots for epochs 1, 2 and 3) However, the morphological response in the receiving zones from Reaches 1 and 3 are quite different. At STA 2000 to 2150, the main effect is bar and floodplain accretion. In the vicinity of STA 100 to 300, a greater degree of channel filling occurred seemingly due to greater bank heights (related to incision following operations in 2017), which produced lateral erosion that recruited supplemental sediments and seems to reflect both sensitivity of transport capacity to changes in width/depth ratio (sensu Dust and Wohl, 2012) and the importance of bank erosion in braiding and maintaining capacity (cf. Wheaton et al., 2013). These differential responses are similar to

observations of Wathen and Hoey (1998) and reflected in the primary wetted channel response (Figure 7-10, D).

Figure 7-12. Selected examples of substrate characteristics in the segment AOI. A: A mature (though still mobile) bed armor layer. B: floodplain channel prior to flow augmentation from channel realignment C and D: Vicinity of STA 9+50 where inlet capacity of floodplain channel was increased C: as-built condition on 2019-02-21 looking downstream following armor removal and excavation (directed to B) D: same location looking upstream two days later following the first freshet (57.9 cumec peak). Total discharge (distributed across all channels) in the second photo is approximately 5 cumecs greater, but considerable reworking and winnowing has already begun. E: As-built conditions in a gravel extraction zone (material source for bank groynes) to enlarge channel capacity (E) and close-up of grain size distribution (F) from the inlet area shown in C and D.

STA 2200 is the approximate downstream end of the upper artificially confined zone and channel changes intensify as flow-separation occurs. I selected STA 2000 as the downstream end of Reach 3 as that is where direct sedimentation effects seemed to end following the 22-Dec flow event. It is worth noting that bed deflation between STA 1800 and 2000 (Figure 7-9) may be an indirect effect as flow became directed toward the left-hand channel. While transient bed incision has been suggested immediately downstream of a sediment pulse front by 1D numerical modelling (e.g. An et al., 2017), I include this zone in Reach 2 due to its indirect nature recognising that this makes the change signal of the background condition greater than otherwise. The keen observer will notice a similar condition for the boundary between reaches 3 and 4 (Figure 7-9), where deposition at the inlet to the left channel near STA 3400 occurred and potentially augments flow in the right channel

where scour is observed. Given differences in relative intensity between the deposition and erosion coupled with *a priori* vertical bed instability (visible in Epoch 2), I consider headward knickpoint migration into the excavated area to be a greater driver of bed deflation at the upstream end of Reach 3.

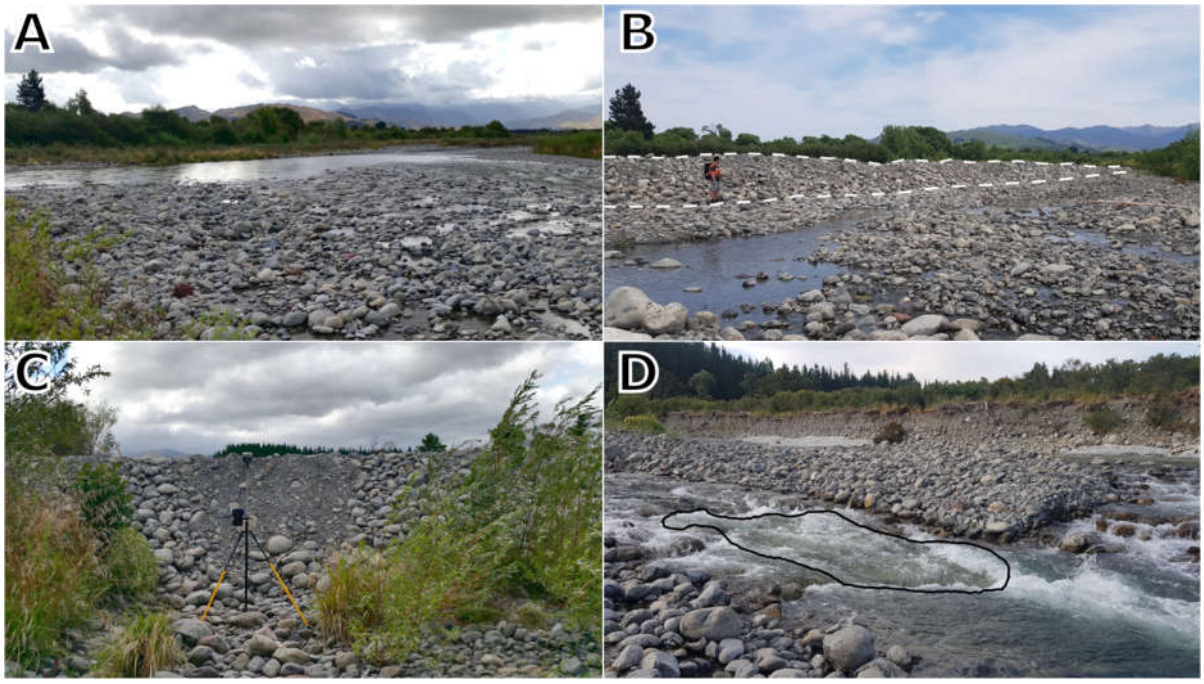

Figure 7-13. Example conditions in vicinity of constructed channel blockages with berms constructed of native, granular materials. Top: Upstream view of primary channel in vicinity of STA 950 on 23-Feb. 2019 (A) and same location/view on 26-Nov. 2019 several months after dozer-constructed berm creation (B; primary channel is on the other side of the berm and person is 1.85 m tall). This area is included within the detailed graphic for Reach 1 in Supplemental Materials. Bottom: As-built view of 2 m high berm shaped by an excavator looking upstream from isolated secondary channel vicinity of STA 2950 on 27-Feb. 2019 (C) and newly revealed bedrock in the invert of the primary channel ~STA 3100 on 27 Nov. 2019 (D) following headward incision from treatment area.

7.6.2.1 Interpreting morphological response

Several conditions factor into the spatially variable geomorphic responses observed, including, differential changes in channel gradient, confinement, and surface condition. Increased velocity and its derivatives (energy and power) is a first-order response to increased channel gradient, such as where the flow path was straightened from STA 500 to 900. Similarly, increased flow confinement (such as near STA 950, 2300, and 2950 following construction of side-channel blockages) is also know to produce differentially greater geomorphic change to the same flow event (Magilligan, 1992; Fuller, 2007). It has been suggested that surface condition (e.g. ground cover) at the time of a flood also influences the type and magnitude of geomorphic response (Toone et al., 2014). Management actions were observed to alter surface conditions of both the channel and floodplain within the AOI.

Management treatments modify local channel surfaces directly and indirectly, with both producing finer bed textures. Armor layer disruption, such as extractions that occurred at STA 900 and 3000, can dramatically increase sediment supply (Lenzi et al., 2004) with increased vertical mixing (Haschenburger, 2013; Houbrechts et al., 2015) increasing available volume. Further, extraction destroys bed structure, such as imbrication observed prior to treatment, which could otherwise reduce sediment transport by orders of magnitude (Church et al., 1998). Bed fining resulting from direct armor removal as well as indirectly by realignment of flow onto floodplains and small side channels within the fairway lowers the force necessary for mobility (cf. Hjulstrøm, 1939; Miller et al.,

1977). The high sand content of the bed subgrade and floodplain channels in the AOI (Figure 7-12) likely contributes to higher transport rates (Wilcock et al., 2001) and distances (Hassan et al., 1992) in units where armour is disrupted/removed.

I have observed flood protection operations remove vegetation from surfaces within the segment AOI fairway annually to bi-annually with the intent of reducing floodwater surface elevations. However, channel geometry management based on equilibrium channel theory assumes (requires) static channel boundaries. Thus, recurrent vegetation removal ignores two decades of literature recognising colonial vegetation as a primary control of sediment dynamics (e.g. Millar, 2000; Corenblit et al., 2009), pioneer landforms (Gurnell et al., 2012) and general contributions to stability (see reviews by Corenblit et al., 2007; Stoffel and Wilford, 2012; and/or Curran and Hession, 2013). Given the criticality of vegetation in preventing braiding (cf. Tal and Paola, 2007; Braudrick et al., 2009) and concentrating flow into fewer, more persistent channels (Welber et al., 2012), removal of vegetation can be expected to promote less-stable morphologic responses than might otherwise occur. The result is amplified as evolutionary processes that contribute to and reinforce more stable morphologies (e.g. Bertoldi et al., 2011) such as soil development (Bätz et al., 2015) and trapping of propagules and large wood ('LW'; Gurnell et al., 2005) are truncated or undone. LW in particular, enhances the persistence of hydraulic units (Abbe and Montgomery, 2003) and a combination of vegetation and LW is shown by flume-based research to produce the lowest braiding indices (Mao et al., 2020). Thus, the morphological re-setting associated with vegetation (and LW) removal on the Waingawa River prevents longer-term processes such as riparian forest development that might otherwise contribute to more stable multi-thread forms evident in the 1941 and 1961 imagery, which may indicate higher bedload transport capacity (e.g. Li et al., 2016b). The importance of resistance in general in system stability receives special emphasis in Brunsden (2001) and the importance of vegetation specifically in granular bank cohesion is sufficiently recognised that it is explicitly included in some downstream channel geometry (i.e. regime) models (e.g. Eaton and Church, 2007).

7.6.2.2 The “Fairway Paradox”

By reducing vegetation and increasing sediment supply, Waingawa River management actions promote two key mechanisms known to encourage less-stable channel forms (cf. Piégay et al., 2006). Despite mechanistic complexity, differential reach-scale patterns of dynamics in the segment AOI can be understood on conceptual grounds and explained from first principles. For a given discharge: 1) removing surface substrate (armour and structure) from the intended channel alignment leaves a finer substrate gradation (decreases resisting force), 2) removing bank and floodplain vegetation reduces effective substrate cohesion (decreases resisting force), 3) removing vegetation decreases hydraulic roughness which tends to increase local velocity (increases driving force), 4) blocking active channels and/or side channels concentrates increases velocity and depth (increases driving force), 5) realignment of discharge into a shorter flow path increases slope and thereby velocity, energy, and power (increases driving force). Doing any one of these things can be expected to increase substrate mobility. Doing all of them concurrently alters force balance that not only enhances particle mobility at the location of treatment, but can, as observed, propagate upstream and downstream signals that produce reach scale geomorphic change at a given discharge. This suite of effects is problematic for any management approach intending stability as an outcome, even more so for those based equilibrium channel theory. Thus, removal of resistance elements (vegetation, armour, etc) in the interest of reducing flood stage and/or constraining river footprint effectively counters concurrent management aims of stability. I call this anti-pattern (sensu Brown et al., 1998) the *fairway paradox*. Linkages to river-training coupled with complex ecogeomorphic

interactions interwoven in space and time invites/necessitates discussion underpinning application of regime theory.

7.6.3 Regime fitness-for-purpose

Based on my observations, the fairway boundaries appear to be regarded as reasonably 'hard' targets where routine (annual or sub-annual) earthmoving is undertaken as the channel(s) get out-of-line. This seems to occur even where a buffer exists beyond the channel alignment and without regard for an alignment's stability prior to treatment. Thus, a binary form-based decision-point prevails, a channel's stability is irrelevant if it is outside the fairway.

For example, the side channel in Reach 3 that was blocked-off in February 2019 (Figure 7-9, ~ STA 2950), had been showing signs of sedimentation, woody vegetation establishment and reduced scour from January 2018 through February 2019. Despite exhibiting favourable behaviour and occurring almost (but not completely) within the fairway lines, earthworks were conducted anyways because of some (uncharacterised) potential for channelised flow outside of the fairway.

Regime- and *threshold channel* equations provide the quantitative basis underlying dimension and form of the Waingawa design fairway (cf. Williams, 1990) as part of an opinion-based process that includes visual curve-fitting using aerial photography and review of benchmarked cross-section data. Regime and threshold channel approaches can be derived to solve for various hydraulic geometry parameters (channel width, mean depth, mean slope and/or mean velocity) though their specific and respective degree of influence in Waingawa design conditions is not explicitly clear. Threshold channel approaches are generally depth-slope based while regime approaches traditionally are based on water discharge (e.g. Lacey, 1929; Leopold and Maddock Jr, 1953) though often include other independent variables. *Rational regime* approaches (e.g. Eaton et al., 2004; Eaton and Church, 2011) are more recent multi-parameter models which often use scaling factors such as dimensionless unit stream power (e.g. Eaton and Church, 2011) or dimensionless width and discharge (e.g. Métivier et al., 2017) to better represent transfers of fluid energy or momentum to the channel boundary.

7.6.3.1 Suitability of regime-based application

Due to some variability in application of these terms across investigators, practitioners, and time, I clarify my use. The various *threshold channel* equations (a.k.a. *equilibrium cross-section* per Knighton (1998)) incorporate suites of conditions such that bed materials along all parts of the channel boundary are on the verge of movement. The essential assumption and intended outcome of threshold channel application for design purposes is that a boundary doesn't deform. Thus, management scenarios are necessarily intolerant of exchange between bed and bank materials. Thus, a fundamental tension exists when applied to alluvial rivers where such exchanges are intrinsic behaviours. In such cases, it is wise to constrain objectives to (very) short time periods, although it has also been suggested (Pfeiffer et al., 2017) that naturally-occurring threshold channels (i.e. where median grain size begins moving at bankfull stage) may simply indicate low sediment supply.

Regime equations implicitly integrate time on the premise that, given enough time, channels will self-adjust to some prevailing suite of hydrologic and sedimentologic conditions such that material entering the reach equals material exiting the reach. Management application of regime approaches tends to focus on manipulations of channel width to either diminish bank erosion or enhance bed erosion. Traditional models treated water discharge as the sole independent determinant of changes in mean width, mean depth and mean slope (e.g. Leopold and Maddock Jr, 1953). Later models supplement discharge by a sediment term (either transport rate or calibre related), but application

remains particularly challenged for multi-thread channels as the discharge received by a particular channel is not independent of sediment dynamics (Gaurav et al., 2017). Rational regime approaches developed over the last several decades address such limitations and increasingly accommodate some form of resistance either by stratifying data sets (e.g. by vegetation class, e.g. Hey and Thorne (1986)) or by adding explicit terms for channel form (e.g. width/depth) and/or bank strength (e.g. Eaton et al., 2010). Instances of the former have provided some degree of regionalised design guidance while the latter have successfully been applied to differentiating conditions pertinent to channel pattern stability/instability. On this last note, it is important to recognise that transitions between channel patterns, referred to as thresholds (sensu Schumm (1973)), are not to be confused with *threshold channels*.

Both regime and threshold channel theory rest upon the equilibrium channel concept, also known as "a graded stream" originating with (Gilbert, 1877) and classically-defined by Mackin (1948, p. 464) as:

> *"one in which, over a period of years, slope is delicately adjusted to provide, with available discharge and the prevailing channel characteristics, just the velocity required for transportation of all of the load supplied from above."*

Henderson (1966) provides a more explicit connection between being "in regime" and an equilibrium state where slope and cross-section are in adjustment such that sediment transport equals sediment supply. While considerable effort has gone into developing and applying regime and threshold channel relationships over the years, significant questions remain over their utility for design purposes, particularly with multi-thread gravel-bed rivers like the Waingawa.

Davies and McSaveney (2006) note that starting with a channel in its natural state of adjustment (i.e. maximised for local transport capacity), any channel adjustment tips the regime to a less efficient state more likely to incur sedimentation, including in artificially-confined cases where accelerated rates may occur (Lane et al., 2007; Beagley et al., 2020a). In their seminal review, Carson and Griffiths (1987) repeatedly express strong reservations about the application of regime equations to natural gravel-bed channels for design purposes and Bledsoe and Watson (2001) describe how use of canal-based regime equations to compute widths for natural streams directly biased stream power estimates. Some improvements have been made to broaden applicability (e.g. Parker et al., 2007; Dunne and Jerolmack, 2020) with some promise for predicting widths of individual threads of multi-thread channels (Gaurav et al., 2017). However, some authors explicitly acknowledge limited engineering-scale applicability (sensu Dunne and Jerolmack, 2020). Because many regime equations consider width a dependent variable of sediment supply rate, their application to braided rivers (where width and transport capacity are interdependent (e.g. Recking et al., 2016; Gaurav et al., 2017)) is tenuous with ample potential for latent, undocumented collinearity to bias predictions.

There are also persistent issues of dogma that continue to drive practice, such as the notion that confining a braided stream to a single channel will improve stability by increasing transport capacity (cf. Carson and Griffiths, 1987) even in the general absence of long-term field-scale success and counter-evidence accumulates (e.g. Lane et al., 2007; Wheaton et al., 2013). On practical grounds, there remain issues of misfit precision given regime relationships plot in log-log numerical space (often with considerable scatter) while river managers get phone calls from riparian owners conditioned to expecting operational action when a few metres of bank erosion occurs. As such, the precision mismatch is unresolvable on technical grounds and it is pragmatic to examine the underlying assumptions necessary for rationalising application of regime theory.

First, the notion of self-adjustment toward equilibrium is implicitly one of a negative feedback regime where perturbance of one or more hydraulic variables are absorbed and dampened by the others. Therefore, systems with positive feedbacks (that enhance non-equilibrium) cannot be in regime. This is accommodated by Mackin's discussion that stresses importance of recognition and differentiation between streams where equilibrium is 1) maintained, 2) transitioning, or 3) does not exist. A second implicit assumption is that, if present, an equilibrium form can be identified. Most often, this frequently defaults to the 'bankfull' channel, which has been widely correlated morphologically with flow recurrence between 1.6 and 2.4. However, differing methodologies for bankfull identification can significantly influence results (Navratil et al., 2006). Perhaps even more importantly, the geomorphic relevance of bankfull as a morphologic indicator of dominant discharge stage is usually assumed. However, this assumption can be problematic as bar-full may be more effective (Biedenharn and Thorne, 1994; Downs et al., 2016) and active channel width (as evidenced by bankfull) may be more indicative of the magnitude of the most recent major storm (Graf, 2000). That said, there is some support for constructive floodplains (or bars) in some fine-grained systems representing the current hydro-sedimentological regimes (Naito and Parker, 2019).

As a general observation, it has been suggested that the flow recurrence interval to generate bankfull conditions in New Zealand rivers is much higher than the mean annual flood (Mosley and Jowett, 1999) and that the banks of many coarse-bed NZ rivers may be better indicators of recent erosive events (Carson and Griffiths, 1987). I find this generally true and, in my experience with NZ rivers, consider the banks of many NZ gravel rivers as destructive forms whose overbank relevance is more indicative of a historic condition or regime than a present one. Specific to the Waingawa River, I find the combination of much stage variation over short profile distances and persistence of forms resulting from earth-moving operations in cross-section indicative of very low 'bankfull' relevance.

Beyond such implicit assumptions, explicit assumptions of equilibrium channel application can be explored by combining Mackin's and Henderson's definitions in a more linear manner. Thus, I might expect that: some recurrent and generalisable water discharge over "a period of years" acting upon a river reach will produce a form where sediment load received from upstream equals the sediment load exiting the reach. This can be further reduced: some range of flow variation, consistently applied over a period of years while other controls are held constant may generate reach-scale equilibrium.

I consider "period of years" to be the most salient point as it is frequently lost given the vast prevalence of applications that substitute single metrics of assumed geomorphic relevance (e.g., dominant discharge) for the intended range of driving/maintaining conditions. While Mackin (1948) specifically noted the significance of discharge distribution (rare high water events vs extended low-water periods vs. a specific bed forming stage) on stream character, he considered the ultimate relevance lacking, instead emphasising "over a period of years" as the unit where equilibrium is maintained. Despite often blunt, long-standing calls for its end (e.g. Carson and Griffiths, 1987), use of a single *dominant discharge* is widely persistent in practice (including the Waingawa River) for simplicity of characterisation and computation. Regime-based studies that explicitly account for hydrologic variability (Navratil and Albert, 2010; Naito and Parker, 2019) remain rare. Mackin doubles-down on "period-of-years" by noting his deliberate use of the timeframe as representing some "constancy of controlling conditions." The plurality of *conditions* is further telling as it acknowledges the spectrum of stream responses to changes in hierarchically-nested controls as a function of the rate at which such changes occur.

7.6.3.2 Contrasting Waingawa River regimes

As a thought exercise, I consider two different effectiveness thresholds for the segment AOI results using the past decade as the "period of years". The hydrology (Figure 7-14, top) is very favourable for such comparison as it comprised entirely floods of routine magnitude (~Q_{MAF} or smaller). I assume that my empirically defined threshold (see Methods, this chapter) is static over the period. Fluvial recovery/relaxation times following large sedimentary events have not been reported for New Zealand rivers, but Izumiyama et al. (2020) report a range of 1-19 years for recovery from large sediment supply episodes for Japanese rivers with similar climate, relief, and tectonic activity. Thus, I will consider a decade (the mid-point) as a "period of years" for Discussion purposes.

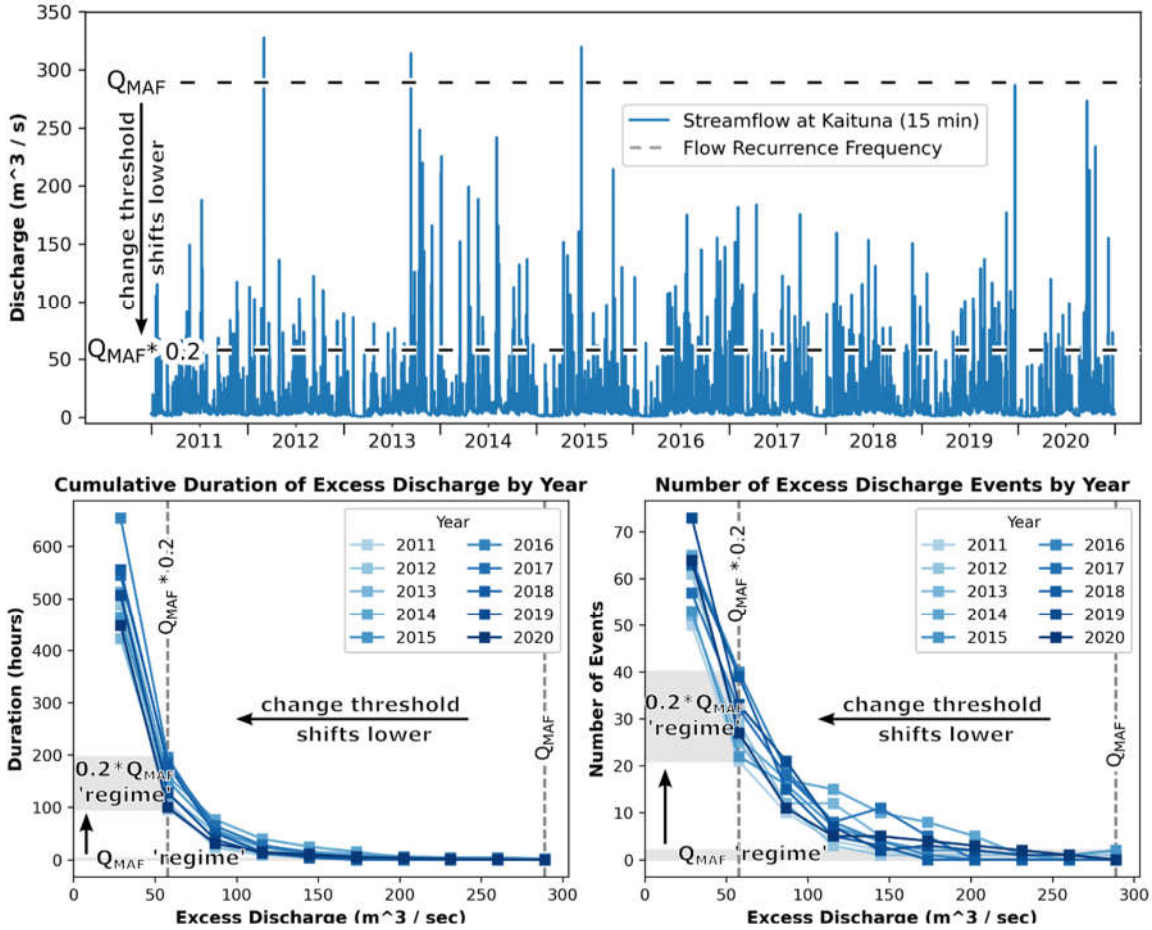

*Figure 7-14. As the threshold at which channel change occurs shifts to lower flow magnitude, the behavioural regime of the river becomes more active. Top: A lower flow threshold (0.2 * Q_{MAF}) intersects many more runoff events than a higher flow threshold (0.2 * Q_{MAF}) as indicated for the Waingawa River from 2011 through 2020. Bottom: As the flow threshold decreases, intraannual frequency and interannual variability both increase. Cumulative duration of excess discharge by year (left) and number of excess discharge events for 1/10th fractions of the Q_{MAF} by year (right). Grey boxes contrast the geomorphic effectiveness 'regimes' of the last decade for the present, anthropogenically-forced regime with an effectiveness threshold of 0.2 * Q_{MAF} and a hypothetical regime where Q_{MAF} is the effectiveness threshold.*

Comparing my observed (0.2 * Q_{MAF}) effectiveness threshold for the segment AOI to the Q_{MAF} shows not only an increase in duration (Figure 7-14, bottom-left), but also much greater inter-annual variability. Over the decade, cumulative effectiveness duration is 310 times greater (Table 7-4) for threshold at 20% of Q_{MAF} than at the Q_{MAF} and maximum within-year duration increase by 88 times. Given the flashiness of the hydrology, it is also prudent to consider the number of effective instances (Figure 7-14, bottom-right) as each rising limb presents an opportunity for change potentially

independent of duration effects. The total number of instances over the decade is roughly 60 times greater at the higher frequency threshold and the range within any given year increases by an order of magnitude (Table 7-4).

This last point is particularly important as the *annual ranges* over a "period-of-years" may serve as a simple proxy of the respective 'regimes' (Figure 7-14, bottom, grey rectangles). Thus, the current 'regime' is one of low threshold of motion, high annual variability, and high spatiotemporal sensitivity to standard flood flows (Q_{MAF} and larger). A question can be framed in terms of the potential for geomorphic change relative to channel maintenance:

> *Given limited time and money to maintain some condition, is it preferable to perform similar levels of maintenance zero to two times in a year, or 21 to 40 times per year?*

*Table 7-4. Count and duration summary statistics for mean annual flood (Q_{MAF}) and 0.2*Q_{MAF} from 2011 to 2020 (inclusive).*

Flow Frequency	Duration (hours)				Count (#)			
	Cumulative	Annual			Cumulative	Annual		
		Mean	Range	Std		Mean	Range	Std
Q_{MAF}	4.6	0.5	0.0 - 2.2	0.75	5	0.5	0 - 2	0.81
0.2 * Q_{MAF}	1,431.2	143.1	96.2 - 195.5	34.9	294	29.4	21 - 40	6.21

Specific to the application of equilibrium channel theory, such a question is better framed over the entire period as Mackin discusses the need to tolerate (and not confuse) local, short-term changes in bed elevation with "true shiftings of the equilibrium". On this last point, he draws the analogy to differentiating between weather and climate. Thus, in his mind, an increase in bed elevation at one or more sequential riffles (or other hydraulic controls) would not be considered aggradation until the condition had persisted through the whatever range of flow conditions and time was customary for that reach to maintain equilibrium. Thus, interannual consideration prevents mistaking adjustments resulting from seasonal shifts in transport thresholds (cf. Moog and Whiting, 1998; Martin and Conklin, 2018) or geomorphic effectiveness (e.g. Misset et al., 2020). Because flow sequencing can also control transport distances (Rainato et al., 2020), volumes (Reid et al., 1985), and rates (Mao, 2018) as well as mechanism dominance (Wheaton et al., 2013), a longer timeframe is more likely accommodate resulting variation on form.

Morphological responses to treatments observed over short timeframes also present point-in-time interpretive peril if channel evolution context is not accounted for as morphological changes non-linearly influence field-scale bedload prediction (Recking et al., 2016). This is particularly important as most operational settings tend to have a bias-for-action. That is, river authorities go do stuff to the river, often without a sufficient period of observation, under the premise that doing something is better than nothing. With great prescience, Mackin (1948, p. 508) confidently predicted (and cautioned against) this:

> *"…a safe general implication is that the engineer who alters natural equilibrium relations…will often find that he has a bull by the tail and is unable to let go—as he continues to correct or suppress undesirable phases of the chain reaction of the stream to the initial "stress"…*

This dynamic indeed seems to be the case on the Waingawa and neighbouring rivers and had strong implications for the high-resolution study design. Originally including three other rivers, the study design was iteratively revised to shorter timeframes on fewer rivers as it became apparent the high

frequency and magnitude of disturbance was incompatible with my sampling resources. During the study period, treated areas seem to demonstrate positive feedbacks that elevate the magnitude of response for a given excess discharge, a response that is fundamentally incompatible with either equilibrium channel or regime theories. In using a regime-based approach in a non-equilibrium river, Simon and Thorne (1996) demonstrate very poor prediction of field-measured geometries by the Chang (1980) equations which generally underpredicted width by up to 90%. Channel interventions appear to both lower the recurrence threshold of motion to such a regular frequency that action begets more action and near constant tinkering becomes the regime. As one action translocates instability to another location (sensu Brookes, 1985), a game of whack-a-mole develops. I observed several instances of this, most notably where sediments translocated from the treated area in the vicinity STA 1900 enhanced lateral shifts outside the fairway near STA 200 (Figure 7-2 and Figure 7-9). Thus, the system is more of a dis-climax regime defined by the magnitude and frequency of river management operations where equilibrium-channel concepts simply do not apply, and related design approaches cannot reasonably be expected to deliver stability aims.

7.6.4 Channel Sensitisation

Sensitivity is an essential component of geomorphic stability (Brunsden, 2001) and classically defined as the degree to which a "given change in the controls of a system will produce a sensible, recognisable, and persistent response" (Brunsden and Thornes, 1979, p. 476). Though generally considered as a system-level property (cf. Fryirs, 2017) I make broader consideration as the degree to which a change in controls will produce and propagate detectable geomorphic change. My application at the reach/segment scale is consistent with "Interpretation 1" (ratio of disturbing and resisting forces) of Downs and Gregory (1995) who differentiated sensitivity into four interpretations.

Fuller (2007) found confined reaches had the greatest geomorphic responses to a 100-year flood while gross morphology was unchanged in reaches where there was general floodplain connectivity. I observe similar results in the Waingawa, where confined reaches (1 and 3) showed substantial vertical changes across the entire channel with very active lateral forcing at confinement transitions while reaches 2 and 4 (well-connected to its secondary channel structure) showed very little change. Historically, such spatially-variable geomorphic response have generally been explained as a matter of floodplain and valley controls associated with discrete, high-magnitude, low-frequency events (e.g. Magilligan, 1992; Miller, 1995; Fuller, 2007) though time-integrated effects of buried controls within the active channel have also been documented (Hoyle et al., 2008). This association with large, infrequent changes is arguably more consistent with the persistence element of the classic sensitivity definition.

I do not disagree with either the system-level application nor the persistence concept but do recognise that rigid adherence to either or both may miss geomorphic responses to changes in controls at some scales that could have important system-level effects in sum and be overlooked by standard sampling increments (e.g., inter-annual to sub-decadal). Thus, my more nuanced view of sensitivity considers the high spatial contrast of the reaches to the same, frequent discharge as indicative of being in a sensitised state at the time of discharge. In my usage, the state of being sensitised means a given driving force will be more likely to cause geomorphic change (persistent or not) and/or propagate sedimentary signals. It is a function of *preparation* and/or *preconditioning* (see Chapter 5, this thesis) and may be considered as a precursor to or component of system-level sensitivity. Specific to the segment AOI, the dynamic factors that shift force-balance in favour of a geomorphic response (bed fining, flow realignment to steeper paths, flow concentration, reduced bank cohesion) are a matter of preparation.

It is important to note that the coarse temporal nature of the historic aerial photo record doesn't facilitate direct quantitative comparison of event-based change frequency or intensity over extended time. This is because longer time gaps are more likely to represent conditions between disturbances (flood or human) as vegetation becomes re-established. This does not affect the validity of my results as I do not assert changes in frequency over time even though inference based on descriptive lines of evidence (e.g., disappearance of well-established channels and more mature island vegetation, increased confinement) suggests the likelihood. The key point is that the observed event-based, reach-scale changes nest within the decadal, segment-scale trends and provide granular, process-based insights of mechanisms consistent with dynamics that explain decadal-scale trends.

In the absence of explicit definition of stability and spatiotemporal outcomes intended by management it is not possible to evaluate management actions objectively. However, such ambiguity does afford socio-political space for assigning changes due to routine flows as the river-just-being-a-river while blaming-the-flood for changes associated with standard flood recurrence intervals.

Managing alluvial rivers for stability with any set of fixed dimensions implicitly requires stationarity assumptions that become particularly important in the application of equilibrium channel concepts and derivations such as regime theory. The number of Waingawa River events generating excess discharge and their cumulative duration from year-to-year ranges by a factor of two and becomes increasingly less stationary as the threshold of geomorphic effectiveness becomes more frequent. Evaluated over a ten-year period, the observed threshold of 20% of the mean annual flood (0.2 * Q_{MAF}) was 311 and 59 times greater than the mean annual flood (Q_{MAF}) in terms of cumulative duration and excess event occurrence, respectively. Sensitisation caused by flood protection operations seems to be the main cause of sub-annual sediment transport non-stationarity. Thus, a shift to operations that decrease the frequency of geomorphic change will better approximate satisfaction of stationarity assumptions fundamental to regime-based assumptions underlying the management scheme.

Given no basis for assumed stationarity at century- to millennial-scale due to climate shifts and active tectonic forcing, the prospects for regime-based stability are even lower in the long-term. Considering pre-management spatial distribution of active belt variability as indicative of riverscape response to tectonic forcing, the multidecadal riverscape narrowing and uniformity trend may merely be masking indicators of infrequent but inevitable changes in boundary conditions. Thus, there is great potential for inhabitants and managers conditioned to the status quo to be surprised when the present period of weather and tectonic quiescence ends, and primary controls reassert themselves. Resolving the 'fairway paradox' requires revisiting fairway dimensions and design philosophies where operations (e.g., channel straightening and vegetation removal) aimed at minimising stage-discharge relationships diminish stability of channel boundaries fundamentality required for application of equilibrium channel theory. If a regime-based approach for establishing dimensions is to be retained, then approaches that incorporate greater active channel and floodplain resistance will be necessary.

Considering this reach-scale sensitisation over the extended (~50+ years) timeframe the Waingawa has experienced mechanical interventions, it can be reasonably inferred from my segment-scale results that sediments are being mobilised from valley fill storage more frequently than they would otherwise during that time. This heightened system-level sensitivity lends support to my interpretation of flood history and channel form in the 1983 high-quality orthoimage (Figure 7-8). It also provides insight to forms that may result following the next infrequent, high magnitude event as

an example of assessing future adjustments scenarios (cf. Lisenby et al., 2020). Making this linkage of feedbacks between spatial scales addresses as one of the five key needs in understanding human roles in fluvial geomorphic change (cf. Gregory, 2006).

7.7 Conclusion

Evaluation at two different spatiotemporal scales leads to different conclusions of stability for this rain-driven, wandering gravel-bed river. A multidecadal trend of progressive narrowing and uniformity of active riverscape belt width contrasts strongly with amplified sediment dynamics at reach and event scales. Substantial change variation occurs at the reach-scale with subreaches exhibiting the most intense changes tightly coupled to recent (<3 years) flood protection operations. The most intense changes associated with sub-annual to mean annual-frequency floods occurred where side channel access was blocked and/or where as-built conditions left non-armour bed materials exposed. The contrast between decadal narrowing compliant with management aims and decreased short-term stability that increases maintenance requirements is an anti-pattern I call the *fairway paradox*. Resolving such anthropogenic sensitisation requires revisiting river training philosophies (i.e., straighter, narrower active belts) and actions (e.g., removal of barforms, harvesting the largest bed particles, and stripping island vegetation) that minimise water surface elevation as intended, but also amplify sediment dynamics and channel movement. Well-connected multi-thread forms within existing design buffers offer a promising pattern and dimension to begin reconciling the presently competing aims of lower floodwater elevation and channel stability. The wider “buffer” corridor generally contains these channels as well as the active channels for all but the 1940s era channel alignments. This implicates less rigid focus on fairways and a greater emphasis on the buffer corridor as a starting point for less frequent interventions which, by extension, could produce more routine stability.

7.8 Acknowledgements

Menno Diersmann, Amelia Horne, Brent Vermolen, Ada Conley, and Declan Conley are thanked for their field assistance and commitment to the rigorous schedule. Jon Tunnicliffe provided valuable input for framing event-based patterns of change.

7.9 Supplemental Material

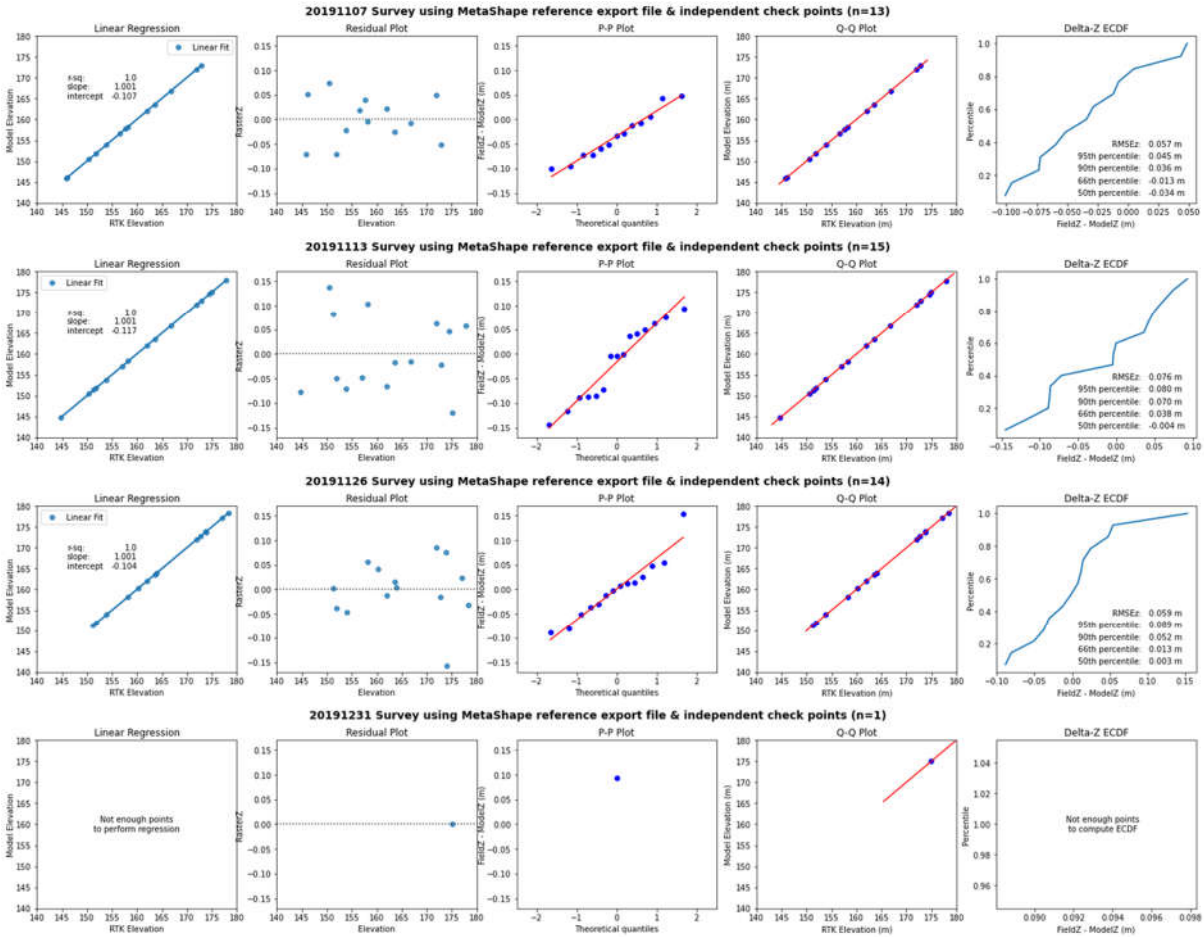

Figure S7-15. Positional quality of structure-from-motion models using independent (non-model) ground control points (GCPs).

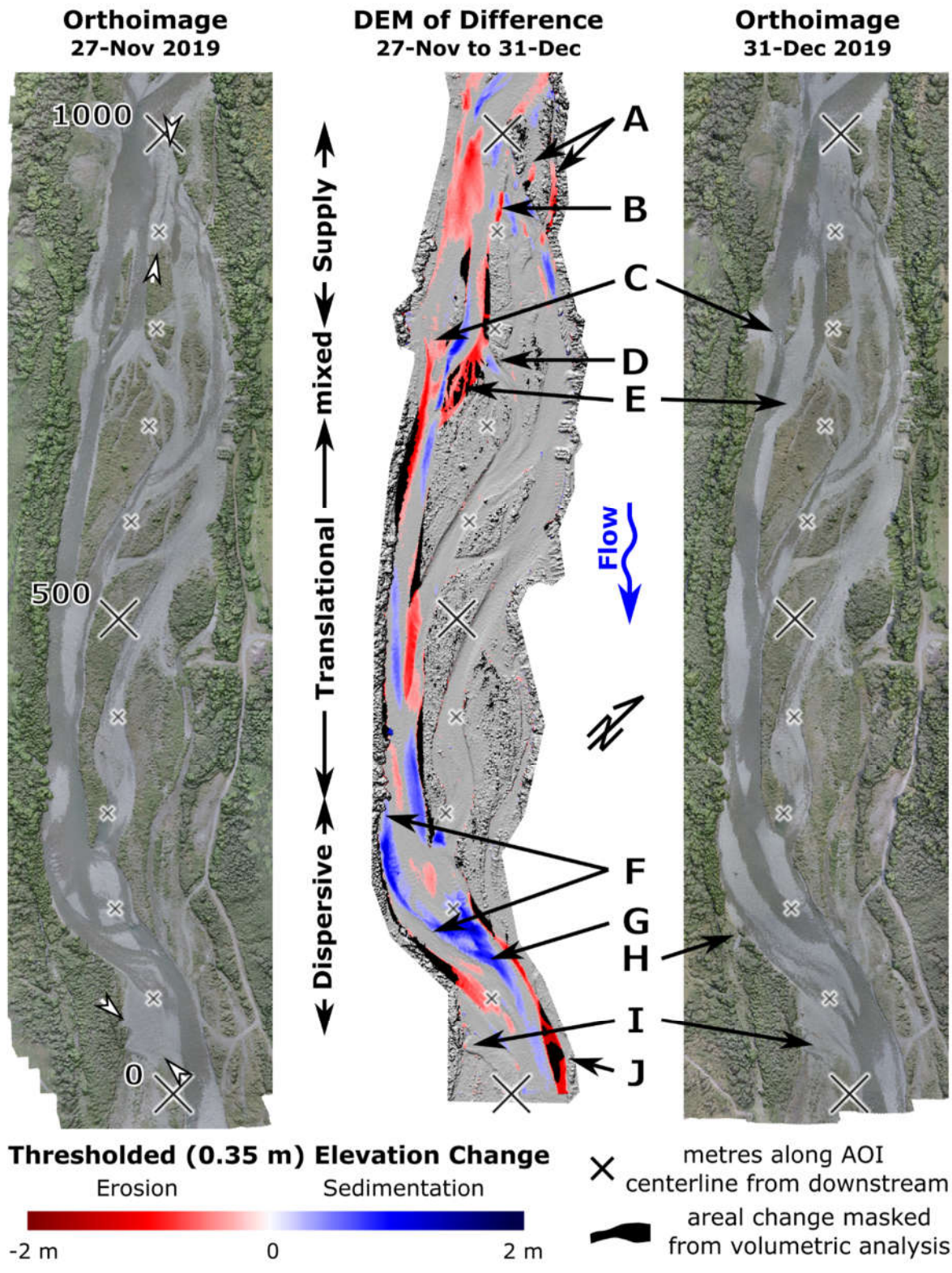

Figure S7-16. Reach 1 detail for Epoch 3, inclusive of the highest discharge event (Q_{MAF} recurrence). White arrows (left panel) indicate locations of berms constructed c. June 2019 (e.g., Figure 7-13B). The sub-reach (~ STA 800-1000) in vicinity of the upper berm and channel works is mainly a sediment source as adjustments continue five months after disturbance. Within this area, two side channels to river-left (A) of the upper berm gained capacity via headward incision. This could be due to lowering of the tailwater depth at their confluence with the (former) main channel and/or greater inflow due to primary channel flanking upstream. If the latter, combined with breach of the constructed berm (B), capacity of the as-built channel may have been under-

sized. The next sub-reach downstream (~STA 700-800) is a mix of processes and behaviours with headward knickpoint retreat (C) in the right-hand channel acting as a source, localised dispersion (D) at a channel difluence, and downstream translation (E). Once flow is mostly confined to a single channel with higher banks (STA 300-700), downstream sediment transfer is largely translational with lateral bar development driving switching of the low-water channel and recruitment of bank sediments. Downstream of STA 300, the active cross-section is substantially wider and behaviour is largely dispersive. Substantial accretion of a pre-existing crescentic bar (F) occurred with dissection and transfer from the slip-faces into the primary channel (G) with subsequent re-working. Erosion of the right bank during Epoch 3 daylighted surface inflow of a pre-existing side-channel (H) entraining sufficient flow for bed scour and vegetation stripping to occur locally within the side channel and increasing its conveyance capacity. This could be the beginning of flanking of control works where a channel blockage (I) was previously graded and flow becomes largely re-confined to a single channel. Coupled with bar accretion on the opposite side of the primary channel (G), this channelisation increases pressure on the left bank (J) where the greatest degree of lateral erosion (>15 metres) was observed in the AOI during Epoch 3.

Summary of Thesis Chapter 7

Chapter 7 characterises and contrasts the morphodynamic endmembers (multi-decadal and event scales) of human-based river management. Trends and differential responses are evaluated within the context of the regime-based framing that guides river management in the study area. Considered over many decades, the narrowing trend of the active belt is favourable to flood protection aims. However, differentially high-frequency morphological change of reaches recently experiencing flood protection earthwork implicates the same management regime as a destabilising agent. Thus, this chapter provides novel quantitative and conceptual exploration of the management paradox created by river management traditions of co-managing for low flood stage and channel stability. The earliest planimetric distributions from the multi-decadal analysis supplement and validate partitioning of fluvial behaviours by active tectonic structures introduced by vertical dynamics in Chapter 6. The persistence of morphological control by tectonics evident from the earliest data (1941, 86 years post-rupture) begs the temporal significance of more recent trends toward channel uniformity associated with an era of active management. This also casts doubt on persistence of those trends when catchment sediment yield elevates and/or tectonically-driven changes to slope (cf. Chapter 6) and cross-sectional hydraulics (e.g., strike-slip displacement) occur.

Chapter 8

Synthesis

My overarching aim in this thesis is to deepen understanding of gravel bed river dynamics in New Zealand's upper Ruamāhanga River catchment across spatiotemporal scales in a manner that is scientifically novel and fills management-relevant information gaps. The importance of fluvial morphodynamics is increasingly recognized in flood hazard assessment (Slater et al., 2015; Staines and Carrivick, 2015; Slater, 2016; Call et al., 2017; Naylor et al., 2017) in ways that may exceed climate change effects (Lane et al., 2007). Morphodynamic interactions and controls nest hierarchically in space and time (Fryirs and Brierley, 2012) and understanding these linkages and spatiotemporal scales in river-system adjustments is an essential foundation of effective catchment management (Macklin and Lewin, 1997). This thesis seeks to enhance such understanding in support of effective and sustainable fluvial hazard-related decision-making in the Ruamāhanga catchment.

Broadly, my thesis contributes to calls for transdisciplinary hazard assessment (Mills, 2005; United Nations Office for Disaster Risk Reduction, 2019a), improving data quality in hazard assessment (United Nations Office for Disaster Risk Reduction, 2019a), communicating uncertainty (Thorne, 2002), understanding dynamic conditioning between flood events (Naylor et al., 2017), assessing future adjustment scenarios (Lisenby et al., 2020), and establishing multiscale feedback linkages to understand human roles in geomorphic change (Gregory, 2006). Chapters 4-7 address coregistration quality assessment (thesis objective 'i'), multi-scale screening of avulsion hazard (thesis objectives 'ii'), active tectonic partitioning of alluvial bed dynamics (thesis objectives 'iii'), and multi-scale human morphodynamic signatures (thesis objectives 'iv'), respectively. Collectively, my thesis addresses three of four trajectories in the field of geomorphology identified by Church (2010), specifically: reconciliation of representations across spatiotemporal scales, comprehension of process and landform history complexity, and increased recognition of anthropogenic dominance in modifying terrestrial surfaces. This chapter makes coherent linkages within and between chapters, highlights novelty, draws conclusions for investigators and practitioners, and identifies further lines of investigation.

8.1 Linkages within- and between-chapters

Ensuring the same spatial units are being compared through time is a critical component for any assessment of spatially-explicit change. Uncertainty that the same units are compared is a data quality matter of positional accuracy (cf. Unwin, 1995) and quantitative characterisation generally involves comparison of common, unmodified ground features relative to a single 'true' reference (e.g. Gurnell, 1997; Fisher and Tate, 2006; Hughes et al., 2006; James et al., 2012; Lea and Legleiter, 2016b; Lallias-Tacon et al., 2017). Despite recognition that a single, spatially-averaged metric cannot characterize the spatial distribution of error (e.g. Hunter and Goodchild, 1993; Unwin, 1995; Fisher and Tate, 2006; James et al., 2012; James et al., 2019), root-mean-squared-error (RMSE) remains the standard metric for minimum change detection thresholding for GIS-based studies in fluvial geomorphology (Grabowski and Gurnell, 2016). The first section of Chapter 4 heightens end-user awareness of the problem by presenting a numerical model to illustrate how very different forms of positional error resulting from random and/or systematic effects can converge to produce the exact

same RMSE, which if left undifferentiated may affect interpretation. Because a more comprehensive approach to assessment has yet to emerge, the second section of Chapter 4 proposes a workflow based on a time-series of photomosaics that span a very wide range of quality. A visual and semi-quantitative exploratory stage (Stage 1) precedes a more rigorous quantitative stage (Stage 2) where error is characterised by three components: 1) displacement magnitude, 2) consistency of displacement direction, and 2) geographic distribution. Ultimately, the role of error in data suitability determinations is study-specific (Chrisman, 1982; Hunter and Goodchild, 1993; Lillesand et al., 2015) given the need to balance intrinsic data properties with context of use (Deitrick and Edsall, 2008). However, the lack of a common framework for more comprehensive evaluation and/or communicating such judgment calls can challenge apples-to-apples comparison across studies. To address this gap, the final section of Chapter 4 presents a suitability framework. A hierarchy of change detection is proposed based on analytical intent that specifically considers whether comparisons are quantitative or qualitative, scalar or vector, and their physical dimensionality. A spectrum of analyses from 'Type 0' (e.g., spatially aggregated presence / absence) to 'Type 4' (e.g., spatially-explicit volumetric change) is accommodated and qualitatively scaled to positional quality needs for each of the Stage 2 components. Evaluation is assisted by a graphical framework that also considers spatial scale. In addressing thesis objective 'i', Chapter 4 meets a need of objectively assessing, framing, and communicating pre-existing GIS data sets that were unsuitable for certain forms of analysis (e.g., channel migration). The challenge of framing and communicating suitability within the thesis also reflects a global need related to spatial data "democratisation"(e.g. Butler, 2006; Devillers et al., 2010; Gomez et al., 2015) where data acquisition, processing, and analysis are increasingly driven by end-users that often lack specialisation in processing geospatial data. Thus, Chapter 4 meets study-specific needs while also addressing more general calls to improve data uncertainty communication within geomorphology (Thorne, 2002; Hooke, 2019) and globally (United Nations Office for Disaster Risk Reduction, 2019a). Specific to the thesis aim of advancing multi-scale understanding of river dynamics within the Ruamāhanga catchment, Chapter 4's case study provides the basis for evaluating the decadal time-series suitability and framing multi-scale morphodynamics in Chapter 7.

Specific to the theme of Ruamāhanga morphodynamics, Chapter 5 takes a landscape- to reach-scale view of the infrequent, but consequential phenomenon of river avulsions. Despite awareness of the general potential for the Ruamāhanga's alluvial rivers to change course and substantial management effort constraining them to desired planimetric boundaries, avulsion potential has not received systematic evaluation and is notably absent from regional multi-hazard reviews (e.g. Grant, 2005; Dawe, 2007). Only the Waingawa River paleochannel near Plain has received substantive descriptive treatment (cf. Williams, 1990) though there is also concern regarding the Waiohine River near Greytown. The high degree of spatiotemporal variation in cause, style, frequency, and consequence across riverscapes and settings (e.g., Flood and Hampson, 2014; Valenza et al., 2020) has resulted in bodies of literature fragmented between sub-fields that impedes systematic landscape-scale analysis and field application. One review (Kleinhans et al., 2013) grouped research by geomorphic setting into alluvial fan, braided channel, lowland river, and delta bodies of literature in the interest of framing bifurcation-scale investigation. Alternatively, descriptive groupings of style have been made to characterise palaeostratigraphic process sequences (Jones and Hajek, 2007). However, these represent spatiotemporal end-members that leave a substantial gap where contemporary landscapes or riverscape scales are of interest. To address literature fragmentation and organise in a manner better suited for application, Chapter 5 reframes Phase 1 (the "set-up" or "destabilising" phase) of the standard two-phase conceptual model (Jones and Schumm, 1999; Smith, 2003; Slingerland and Smith, 2004) into preparation and precondition components that differentiate

factors based on their dynamic or static nature, respectively (cf. Glade and Crozier, 2005). Twenty-nine factors compiled across geomorphic sub-fields are qualitatively graded along the revised conceptual spectrum to reflect their individual tendencies to span phases as well as differentiate phase-specific roles between factors (Table 5-1). Though important, consolidation and organisation of factors only provides an initial step given much of the related information requires time-averaged assumptions, modelling, and/or data collections infeasible or cost-prohibitive for many managers at landscape scales. Chapter 5 selects topographic advantage as a common denominator across many factors and adapts a riparian habitat processing method (Dilts et al., 2010) into an approach that facilitates spatial refinement of reach scale avulsion hot-spots (e.g. Czuba and Foufoula-Georgiou, 2015) in an efficient, low-cost manner using landscape-scale data (DEM) and software (GIS) commonly accessible to managers. Finally, because triggers often rapidly occur and their mitigation may not be feasible, Chapter 5 organises and discusses reach-scale hot-spots across a spectrum of geomorphic settings in terms of preparation sensitivity to provide a proactive perspective with greater potential for refined assessment and/or pre-mitigation. Collectively, by consolidating factors across various subfields, developing a common screening framework, and refining conceptual models, Chapter 5 addresses thesis objective 'ii' and delivers both scientific novelty and greater functional utility for hazard management.

The high degree of landscape complexity and tectonic forcing revealed in Chapter 5 invites more detailed focus on a single river in Chapter 6. While Chapter 5 represents inferred potential for long-term (centuries to millennia) spatially-explicit change, Chapter 6 considers a 22-year time-series of benchmarked cross-sectional surveys to explore persistent, interseismic active tectonic control of vertical bed dynamics. Traditional conceptual models of spatiotemporal scaling (McDowell et al., 1990; Frostick and Jones, 2002) imply the lower end of tectonic control (inclusive of sediment supply) occurring on the order of 10^4 or 10^5 years, though more recent empirical work has characterised tectonic influence on reach-scale alluvial dynamics at millennial scale (e.g. Amos and Burbank, 2007). More recently, morphological effects of bed material storage and knickpoint retreat have been documented on annual to sub-decadal timeframes for channels experiencing co-seismic rupture (Yanites et al., 2010; Huang et al., 2013). Considering non-linear temporal diffusion, peak expression of responses are episodic with a frequency scaled by rupture periodicity. Rupture frequency for mapped faults intersecting the Waingawa River range between 700 and 2000 years (Dawe, 2007) although sequencing has not been established and direct channel deformation likely occurs more frequently assuming not all ruptures will be in-phase across faults. The last known rupture was in 1855, 134 years before establishment of the cross-section scheme. Standard approaches using drainage area, channel gradient, topographic ratios, bedrock incision, or profile inflections (e.g. Snyder et al., 2003b; Kirby and Whipple, 2012) are not well-suited for multi-thread alluvial channels, especially in unconfined settings so we sought a more tailored methodological approach to detecting signals in this geomorphic domain. Standard cross-sectional sediment budgeting (i.e. net change and/or discretisation into erosion and deposition components (cf. Brewer and Passmore, 2002)) was unconvincing (Figure 6-3G), however, patterns begin to emerge using the absolute value of change (total dynamics) accumulated over sequential surveys (Figure 6-3D). Upon normalising total dynamics values for each cross-section instance by the difference from mean of its respective epoch then interpolating within and between epochs more persistent behaviours become more discrete and coherent with projections of intersecting tectonic structures. Use of the relative-elevation DEM generated in Chapter 5 to extract profiles from adjacent terraces is novel methodological development that facilitated visualisation of tectonic deformation (Figure 6-3C). Spatial coherence between dynamic behaviour and inferred back-tilting within the study site is consistent with numerical modelling suggesting greater dynamism in back-tilted basin settings (cf.

Heller and Paola, 1996). Chapter 6 advances conceptual models of channel profile response to vertical rupture (originally developed to explain terrace flights and redistribute eroded channel materials from the hanging wall of a planar rupture) by incorporating back-tilting and overbank sedimentation to give a richer picture of fluvial dynamics. The most intriguing contrast of the model proposed in Chapter 6 (Figure 6-1) with the traditional model (Lensen, 1964; Carne et al., 2011) is the wider spatial distribution of adjustment and mixing of erosion and deposition on the same block owing to reach-scale change in slope. The field-scale partitioning of vertical alluvial behaviours coherent with geologic structures demonstrated in Chapter 6 suggests morphologic forcing by active tectonics is detectable on timeframes much shorter than rupture intervals and persist well into (>130 years) the interseismic period. Beyond addressing thesis objective 'iii', it builds upon the results of Chapter 5 documenting tectonic control of contemporary alluvial rivers and streams in the Ruamāhanga and more complex fluvial behaviours than suggested at face value in generally low-relief terrain.

The net cross-sectional record between 1989 and 2011 indicates general incision of the Waingawa River (Christensen, 2013), however net changes within and between epochs (Figure 6-3G) indicate a high degree of spatial variability in erosion and deposition. Fresh unit-scale erosion and deposition observed during initial field visits following routine discharges suggested a good degree of morphodynamic activity was going unsampled by the coarse nature of GWRC's monitoring (~500 m cross-section spacing, sampled every 3-5 years). Further, because channel conditions, forms, and dimensions at the onset of the cross-sectional monitoring (and present management scheme) reflected two or three decades of earth-moving actions there is a need to consider longer-term trends and forms that pre-date widespread management influence. In addressing thesis objective 'iv', Chapter 7 also answers calls in the scientific literature to establish relationships needed for assessing future adjustment scenarios (cf. Lisenby et al., 2020) and increase understanding of human roles in fluvial geomorphic change by linking feedbacks between spatial scales (cf. Gregory, 2006). A multi-scale, spatially-continuous approach is used to characterise and contrast the morphodynamic end-members of human-scale management of the Waingawa River. A multi-decadal Type 2 change detection (cf. Chapter 4, this thesis) finds increasing narrowing and uniformity at riverscape-scale based on a 69-year period of aerial photography. Narrowing (as indicated by central tendency of the statistical distribution) is already evident by 1961 (the second time-step) while uniformity (as indicated by shape of statistical distributions (i.e. kurtosis)) has a later onset more tightly linked with the onset of active management with progressive subsequent tail-trimming that converges on contemporary design widths indicating long-term effects of river training. Lane and Richards (1997) identify investigation of short time-scale and local spatial scales as critical to understanding sensitivity of non-linear systems, though such investigation remains generally rare. Chapter 7 takes an event-based approach to empirically establish a magnitude-frequency context for geomorphic change and investigate differential reach-scale stability for a segment nested within the multi-decadal analysis. Rigorous geodetic control across repeat UAS-missions produces very-high resolution imagery and topography (James and Robson, 2014) and supports a Type 4 change detection that, when interspersed with runoff events of differing excess discharge (relative to empirical change threshold), reveals discrete, differential reach-scale stability. The least stable reaches are spatially coherent with recent active channel earthworks and morphological sediment budgeting (cf. Fuller et al., 2002; Brasington et al., 2003; Wheaton et al., 2010b) exhibits roughly six times more (area normalised) volumetric change from an average annual magnitude discharge event. Considered together, results from the two scales explored in Chapter 6 provide a novel juxtaposition of river management effects. The multi-decadal narrowing of the active belt reflects a general consistency with flood protection aims and is likely aided by earthmoving actions. By

contrast, differentially high morphological changes of reaches recently experiencing flood protection earthworks implicates actions implemented as part of the same management regime as a destabilising agent and supports a hypothesis of channel sensitization. Moreover, high change in recently managed reaches associated with high-frequency, low-magnitude discharges relevant to channel conditioning between large floods (sensu Naylor et al., 2017) and has broad implications for regime-based management schemes where over-prescription of earthwork creates disclimax regimes that necessitate more work through time. This *fairway paradox* is an antipattern indicative of how routine interventions to reduce hydraulic resistance in support of constraining flood footprints concurrently amplify morphodynamic response and, thus subvert near-term channel stability aims. The multi-decadal and event-based results in isolation both make important contributions by documenting the spatiotemporally variable nature of geomorphic signals associated with human alteration of boundary conditions (sensu Hoffmann et al., 2010; Macklin and Lewin, 2015). Chapter 7 is the first instance in the fluvial geomorphic literature where multi-scale juxtaposition has been used to identify an anti-pattern making it both highly scientifically novel and, if taken to heart, very useful for river management.

8.2 Conclusions

The contributions of this thesis can be grouped into 1) methods, 2) multi-scale morphodynamics, and 3) management applications each of which have different, but equally important, value to investigators and practitioners alike.

Methodological advances made by this thesis address data quality underpinning spatially-explicit change detection, scale refinement to identify potential change hotspots, inferences of geologic structure, and co-integration of scales. The validity of any spatially-explicit change detection rests on the degree to which the data are properly aligned in space, yet researchers use a single averaged metric (RMSE) for thresholding. Practitioners frequently assume alignment and skip formal assessment. Chapter 4 provides a numerical model and case demonstrating uncharacterised uncertainty resulting from both scenarios, presents a multi-parameter workflow for assessing coregistration and scales to a hierarchy of change analysis types. This fills a major gap for establishing fitness-for-purpose of geospatial time-series data. Chapter 5 provides high-level novelty by consolidating factors across geomorphic sub-fields and refining the standard two-phase conceptual model of avulsion into three-phases that supports a sensitivity-based decision framework. A landscape-scale GIS method that locally detrends widely available data (DEM) by specific stream channel alignment(s) highlights potential reach-scale hotspots and supports sensitivity interpretation. The locally detrended DEM provides additional utility in Chapter 6 highlighting topographic complexity of low-relief unconfined settings, enhanced visualisation of geologic lineaments, and inference regarding tectonic deformation (e.g., back-tilt). As a matter of signal detection, absolute change accumulated across sub-decadal epochs in Chapter 6 was better able to differentiate dynamic hot and cool spots over the period of record than the standard sediment budgeting approach using net values. Chapter 7 uses multi-decadal and event-based lines of evidence to identify hot and cool areas of dynamics across scales normally treated in isolation that, when juxtaposed, facilitates anti-pattern recognition.

The presence of the study area within a forearc basin along a major plate boundary provides an active tectonic theme throughout the chapters that provides novel results for unconfined alluvial rivers at human scales in fluviotectonics, a field that is generally dominated by longer-term results from confined rivers within uplifted orogens or, more recently, short-term responses to co-seismic rupture. Chapter 5 highlights different forms of tectonic forcing within and adjacent to low-relief

settings revealing high spatial complexity within a fairly small spatial extent (~600 km^2). Though earlier work in the Ruamāhanga catchment documented channel displacements at several localities, it was used to inform slip-rates and/or landform evolution without exploration of hazard. Explicit ties between coseismic displacement and hazard potential, illustration and discussion of complex-response, and identification of out-of-phase avulsions of adjacent streams along the same fault are specific instances of fluviotectonic novelty in Chapter 5. Spatial coherence between channel dynamics and back-tilting in Chapter 6 provides the first field-based evidence I'm aware of in support of numerical modelling presented by (Heller and Paola, 1996). Chapter 6 generally upholds conventional wisdom that tectonic controls dominate over longer periods of time while alluvial processes prevail in the shorter term. However, no timeframes have been established. In this regard, the detectable partitioning of alluvial dynamics accumulated over a twenty-two-year period of record beginning 134 years after the most recent rupture provides food-for-thought. With fluviotectonic relationships as a backdrop, this thesis also advances knowledge of anthropogenic forcing in fluvial morphodynamics. Multi-decadal riverscape narrowing of the statistical and geographic distributions coupled with progressive uniformity (less kurtotic) and convergence with present management specifications indicates the generally intended influence of 'training' actions on riverscape stability. However, the spatial coherence of amplified event-based volumetric change in recently 'trained' reaches presents an antipattern where actions that support a stability aim at one scale are clearly destabilise at another scale. This is indicative of sensitization that can be expected to diffuse non-linearly for any given reach, though may persist as a distributed system state through time.

From the ground, detecting the subtle geomorphic controls and fluvial expressions over the near-flat expanse of the Wairarapa's valley floor challenges the eye of even a seasoned geomorphologist. Thus, it is understandable that the general public and river managers have developed perceptions resulting in uniform application of template-based treatments based on averaged conditions. The geomorphic hot-spots identified in Chapter 5 reveal a very high degree of process complexity within low- and higher relief areas alike inferred from a static (one-off LiDAR) data set. Time-series analysis in Chapter 6 confirms and supplements this finding by identifying dynamic hot-spots along 15 km of the Waingawa River. However, aside from accumulated total change, cross-section data yielded relatively little morphodynamic insight due to spatiotemporal misfit between the sampling regime and distribution of fluvial processes. While the unexpected recurrence of earth moving operations within field sites prevented implementation of the original thesis scope, the adapted study design was able to document differential rates of reach-scale geomorphic change within 3.5 km of the Waingawa River. Differences in sensitivity were spatially coherent with recent river training actions related to 'fairway' management that concentrate flow and reduce resistance within specified planimetric boundaries. The inferred shift in local force-balance produces desired gains in hydraulic efficiency (to constrain horizontal and vertical flood extent) while subverting stability aims is the antipattern I call the *fairway paradox*. Chapters 6 and 7 both point to reworking of existing valley floor sediments as a symptom and driver of contemporary Waingawa River morphodynamics and support the inference that catchment sediment supply plays a comparatively small role for the periods evaluated. The dominance of local bank and bed sediment exchange establishes the Waingawa as a non-equilibrium channel. Collectively, the high degree of variation in geomorphic controls and process expression provides a strong caution against application of uniform templates, particularly where non-equilibrium channels invalidate assumptions required for regime-based prescriptions.

A glimpse of the future is possible by considering contemporary patterns of riverscape-scale alluvial dynamics (Chapter 6) and inference from pre-disturbance planimetric patterns (Chapter 7) in the

context of landscape-scale controls (Chapter 5). Correspondence between belt-width variability in the earliest data (1941, 86 years post-rupture; Chapter 7) and tectonic structures indicates the underlying control template and probable form distribution. Persistent spatial coherence of vertical dynamics with the same structures 134 years post-rupture (Chapter 6) suggests ongoing influence of the same geomorphic template. Thus, it should be considered that management-based trends and current form may simply be a veneer enabled by a period of quiescence. Considering the 1983 aerial imagery was taken within two years of the first and third largest discharges in the hydrologic record, the widened, unstable channel forms (Chapter 7) could well indicate the extent and rapidity with which the river might ignore training.

The aims of this thesis have been successfully met and significantly contribute to integrating multiple lines of evidence across scales to identify fluvial morphodynamic relationships in the Ruamāhanga Catchment. Despite overall success, the geographic breadth and detail of change detection originally envisaged was necessarily reduced by mitigating inefficiencies associated with recurrent heavy equipment disturbance to field sites and unexpectedly high amount of time spent assessing and re-processing archival data. The scope envisaged, but not accomplished, within this thesis as well as questions inspired by present findings provide ample follow-on opportunities described in the *Future research: Needs and opportunities* section.

8.3 Future research: needs and opportunities

This thesis provides the first multiscale investigation of gravel-bed rivers in the Ruamāhanga catchment. Completion of this initial, necessarily broad scope has identified and helps to frame both further research and needed supporting measures to facilitate future research.

8.3.1 Making landscape-scale avulsion screening more objective

The avulsion screening framework developed and described in this thesis provides a high-level structure suitable for landscape-scale identification and prioritisation of potential sites for follow-on investigation. However, implementation is largely dependent on the interpreter's experience and understanding of geomorphic processes and, thus, limits implementation to a limited pool. As there will likely be interest from the engineering and ecological communities, application could become more inclusive by adding a landscape unit component that constrains and/or grades likelihood of relevant processes. A tool that quantifies relative depth to overbank could be work using a one-off data source if truly bare-earth. Coupling of the landscape-scale, relative-elevation approach of Chapter 5 with the time-series DoD-based approach of Chapter 7 could be used provide a more process-based and quantitative foundation to avulsion sensitivity by, for example, incorporating spatially-continuous sedimentation rates relative to channel depth.

8.3.2 Short term channel evolution

Qualitatively, propagation of morphologic change from disturbance centres correlated with flood protection treatments appear to follow expected diffusion patterns. Graf (1977) suggests geomorphic relaxation times follow more universal laws and may be useful for assessing human impacts on landform processes. These can be expected to involve non-linear shifts in geomorphic effectiveness (Lisenby et al., 2017) and so local, empirical relationships will need to be a starting point. A high-resolution time series that establishes pre-treatment effectiveness rates then tracks post-treatment evolution incrementally could establish both recovery time as well as spatial extents and rates over which geomorphic effects propagate. As-built topographic surveys (inclusive of bathymetry) should be compulsory for all river works and capture an extent that facilitates evaluation of potential upstream, downstream, and lateral changes. Surveys should be conducted

prior to reshaping by runoff events, include the active belt width, begin upstream at approximately five times the river works envelope length from the upstream extent of the river works, and proceed downstream to five times the envelope length of river works from the downstream extent of the river works. These extents should be reviewed for adequacy following several iteration as empirical data becomes available. As least one follow-on survey three to four months following completion and/or following the first effective runoff event should also be compulsory.

8.3.3 Climate

Despite being all the rage, climate effects are noticeably absent from this thesis. This is partly out of necessity to generate a focused work. Given massive efforts and budgets being presently placed into climate research, not addressing climate may, ironically, be more novel. With regard to flood inundation, it's been suggested that the role of morphodynamics may exceed climate change effects (Lane et al., 2007). While climate forcing certainly plays a role in morphodynamics, signal detection is both more expensive and less clear than active tectonics in terms of ties to archival data records. Nonetheless, a review of forty-four North Island catchments (Clement and Fuller, 2007) noted that fluvial sensitivity (as determined from terrace records) increased during the Holocene with Wairarapa rivers (as evidenced by terrace formation (preservation) particularly sensitive to variable sediment supply). Given the more refined picture of tectonic deformation and effects on alluvial rivers in the Wairarapa produced by this thesis, two lines of follow-on work would be highly valuable: 1) establishing spatiotemporally-refined process domains that integrate climate reconstruction, sedimentation and deformation rates, and channel positions will require subsurface characterisation and dating to inform how Wairarapa Rivers have responded to past forcing and 2) model-based work to assess how changes in storm intensity, duration, and frequency might compound already complex tectonic and human forcing. For example, these topics in concert will be particularly helpful for informing how geomorphic behavioural areas of the lower Ruamāhanga catchment will shift with sea level rise and also how increased sedimentation rates along the Tararua mountain front will influence channel migration.

8.3.4 Multi-scale tectonic forcing and multi-hazard flood modelling

My work has identified a previously unrecognised degree of tectonic deformation and influence on rivers within the Ruamāhanga catchment. Implications range, for example, from the long-term influence of synclinal folds as important places to acknowledge will have higher flood risk to near-instantaneous shifts in hydraulic boundaries associated with fault ruptures. In particular, spatial concurrence of the avulsion node, fault intersection, and enhanced alluvial dynamics warrants further investigation under rupturing, outburst flood, and enhanced sediment supply conditions that are frequently co-seismically linked. For example, topographic evaluation conducted (but not presented) during this work suggests the longest stopbank at the head of the Waingawa's palaeobraidplain is anchored into the fault trace of the Mokonui Fault. What happens the next time the Mokonui Fault ruptures? Will tectonic displacement increase or decrease topographic advantage (and braidplain reactivation potential)? What if there's an outburst from a landslide dam failure within hours or days (i.e., prior to repair)? How long will it take for the sediment pulse(s) to arrive (and peak) at the site? How will embankments perform under lateral forcing from the advancing sediment pulse? Further questions include: how do the tectonic signals persist? Are the proximal explanations I posited sufficient or does inter-seismic creep or deformation occurring from far-field earthquakes play a role? Or, perhaps, some combination thereof? If local enrichment of fines contributes to increased hydraulic bank resistance at shorter timescales, what are the covariants that cause such zones of rock damage to be prone to more rapid drainage development at landscape evolution timescales (sensu Roy et al., 2016) and visibly occurring within the active channel between

the Mokonui and Wairarapa faults? Further, more detailed examination of fault kinematics should be conducted where ruptures may be expected to have a damming effect, such as where the Masterton Fault crosses the Ruamāhanga River. Perhaps most importantly, what happens in the years following the next rupture of the Wellington Fault when massive quantities of sediment are delivered to the Wairarapa valley floor?

8.3.5 Ecological and habitat relationships

Ecological relationships are beyond the scope of this thesis but are essential to freshwater management and addressing principles of Te Mana o te Wai. Channel and substrate stability in particular affect macroinvertebrate species richness (Death and Winterbourn, 1994; Townsend et al., 1997) and fish assemblages (Poff and Allan, 1995). Given greater instability of reaches experiencing earth moving treatments and multi-year duration of effects (Chapter 7) and the nearly continuous spatial extent of operations across all rivers within managed schemes, lost habitat function represents an important gap in the state-of-knowledge. As there are no undisturbed reaches to serve as study control, an ultrahigh-resolution approach such as used in Chapter 7 would be the most pragmatic. Segment- or reach-scale investigation would be the most manageable, though greater spatial extent while maintaining the same resolution would be more powerful. Ideally, there would be several collections prior to treatment, collections immediately before and immediately after treatment, and several collections following treatment. This would afford characterisation of pre-disturbance state and trend, nature and magnitude of disturbance, and duration and trajectory of recovery.

8.3.6 Filtering (or preventing) vegetation from SfM point clouds

As a technique, Structure-from-Motion (SfM) is something of a marvel and provided relatively rapid field collection of high-quality, spatially-continuous data. However, passive 3-band sensing (i.e., RGB) is far less suited to characterisation of study segments than an active sensor (e.g., LiDAR) due to (high) vegetation growth rates that generally exceeded underlying geomorphic change. Considerable post-processing effort was expended to produce (unsatisfactory) bare-earth models, but ultimately vegetated areas were masked-out. Machine-learning techniques offer excellent promise to automate image segmentation (masking) and filtering in the near future. Inclusion of a fourth band (near-IR) in future collections would enable more efficient processing with or without machine learning.

8.3.7 Archival data management

Several practices associated with archival data that would greatly conserve and focus future research resources by third parties (e.g., Massey PGG) include 1) data accessibility, 2) data consistency, and 3) data version control. Historic cross-section and hydrology data were initially delivered by GWRC in a proprietary format (*.hts) which, even once the proper software was acquired, cross-section data was shockingly difficult to export. Constraints of this data format have been previously noted (e.g. Basher and Fisher, 2013) and while a Python Application Programming Interface (API) now exists, much better documentation is needed. Hilltop software has a highly niche user-base and improving data access will facilitate analyses by a far broader pool of investigators familiar with more analytically powerful environments (e.g., Matlab, Python, or even Excel) and produce richer findings. The need for data consistency in New Zealand's flood protection data has also been previously noted (Giberson, 2019). Documentation (i.e., metadata) would streamline the data suitability process and possibly result in less data being thrown-out. For example, the standard metadata fields in Hilltop were either null or contained an aggregated value (e.g., a single date for all cross-sections collected during a particular survey campaign) that prevented assessment of how

discharges during data collection may have influenced consistency. The absence of control points or common, unmodified surfaces within each cross-section prevents assessment of local, survey-specific errors and challenges establishing thresholds for change detection over the time-series. Lack of clear version control also created much uncertainty when reviewing data. Multiple groups of the same cross-sections often existed without any indication of which was the most current or how they were different. In all cases, delivery of a single, most current set (in csv format) would generally be preferable. Further, between 2017 and 2020, the Massey Physical Geography Group (PGG) received three deliveries of the Waingawa cross-section data for 1989-2011 each of which produced different results that varied, on-average, ~0.23 m vertically from the prior set. For example, change magnitude differences (2020 values minus 2018 values) ranges from -1.49 to 0.89 m for individual cross-section/epoch instances. These 'changes' are due solely to data versioning as the RL-offset values of the field points are unchanged. Particularly problematic are instances of reversals of geomorphic process. For example, between 1996 and 2001 cross-section 27 exhibits 0.153 m of *deposition* in the 2018 dataset but 1.162 m of *erosion* in the 2020 dataset. Given replication as a central tent of the scientific method, this caused considerable concern for our results as we re-checked over the course of the project. Thus, considerable effort was made to identify the source of non-replication and determined edits to the horizontal boundaries (used to compute mean bed elevation) were responsible. In other words, though point values (RL – elevation), the set of points used in computing mean bed elevation changed. In the future, it is recommended such corrections be made prior to delivery such that a single 'best' data set can be analysed (unless requested otherwise).

8.3.8 Human-forcing in fluvial morphodynamics

Aerial photographic review of all gravel-bed rivers in the Ruamāhanga catchment found exactly zero alluvial reaches that might indicate reference (i.e., un-modified by human action) conditions. In other words, there is not a single unconfined alluvial gravel reach in the Ruamāhanga catchment that can be considered to be functioning in a 'natural' manner. Increasing recognition of the high frequency, magnitude, and geographic distribution of human influence throughout Earth systems and processes has spawned general scientific agreement that the time in which we live deserves its own classification on the geologic timescale: the Anthropocene. In fluvial systems, anthropogenic (i.e., human) forcing may equal, dampen, amplify, or swamp signals of other geomorphic controls. However, unwinding mixed signals is a major impediment to deeper understanding. Two areas where managers can greatly assist researchers globally also apply to the Ruamāhanga: 1) improved record-keeping and accessibility may enable un-mixing of signals and 2) discretising operations and measurements to prevent signal mixing.

The largest impediment to coherent morphodynamic analysis of archival data was a lack of operational documentation at suitable spatiotemporal scales to facilitate discretisation of drivers. For example, without knowing what management actions occurred where, to what degree, and how much time had elapsed (e.g., streamflow history) before or after a cross-section was surveyed could lead to much false interpretation if attempted at too granular a scale. Did deposition and lateral migration occur because of a human-forced realignment upstream? Did incision occur naturally or because downstream excavation lowered local base level? Consequently, while change can be measured as vertical gain or loss between any two surveys of a cross-section, morphodynamics cannot be reasonably inferred without knowledge of site history in-between (and preferably preceding). The aggregation of gravel extraction volumes by river prior to 2001 provides much less opportunity for specific insight than subsequent records where volumes are tied to geographic

points. While improved spatiotemporal resolution of records since 2001 can produce higher quality gravel budgets, it lacks sufficient dimension and spatial resolution for morphodynamic insight.

Establishing a high-quality data record of channel changes that discretely control for human and natural driving forces, respectively (see “Short term channel evolution” section) is the foundation for building greater understanding of river behaviours. Compulsory as-built documentation as standard operating procedure would greatly improve learning potential for both retrospective and predictive purposes.

Discretizing and/or isolating drivers is a foundation of most research design. At the outset, this research attempted to proactively isolate ongoing human influence by requesting either operational suspension within study reaches or close coordination such that surveys could be conducted immediately before and after operations. Decision-makers gave precedence to routine flood protection operations with post-hoc notification except in one instance. The co-mingled effects present in data from initial epochs confounded establishing morphodynamic relationships with annual sediment budgets. Several iterations of study design progressively increased sampling frequency to gain signal isolation and decreased the number of segments to minimize costs of such unplanned sampling. Ultimately, the first fifteen field campaigns and related pre-processing from two sites were abandoned and only the spring 2019 surveys from the Waingawa River are included in this thesis. This is the only three-epoch sequence where morphologic change between surveys (n=4) can be solely assigned to hydrology. Operational suspension and/or *a priori* notifications will avoid future inefficiency greatly assist researchers deliver quality results in a timely manner.

8.4 Closing

Further questions and research needs aside, this thesis advances global knowledge of multi-scalar fluvial geomorphic relationships and provides a foundation for more effective and sustainable flood and erosion hazard decision-making in the Ruamāhanga catchment by:

1. Highlighting the need for formal data quality assessment of spatially-referenced time-series (e.g. archival aerial imagery) and contributing a methodology to improve confidence and communication of fitness-for-purpose in geomorphic change detection practice.
2. Developing a landscape-scale screening framework to address and streamline river avulsion hazard identification and prioritisation across geomorphic settings.
3. Evaluating detectability, persistence, and spatial compartmentalisation of unconfined vertical bed dynamics by active geologic structures during an interseismic period.
4. Juxtaposing multi-decadal, riverscape trends with event-based morphodynamics to identify contrary river behaviours resulting from the same management regime.

Collectively, this thesis highlights the importance of identifying different controls on river behaviour and the scales on which they operate. It also casts substantive doubt on the sustainability of applying uniform design conditions based on theory and averages where empirical evidence shows diverse riverscapes with variable and spatially explicit geomorphic controls. As such, this is the first work of its kind in NZ and possibly globally in this combination of spatiotemporal scales, providing a robust template and foundation for future investigations of these dynamic geomorphic systems.

References

1884a, THE FLOOD, Wairarapa Standard, Volume Volume XVII, Issue 1605, https://paperspast.natlib.govt.nz/newspapers/WAIST18840903.2.9?end_date=31-12-1900&items_per_page=10&page=4&query=Waingawa+Plain&snippet=true&sort_by=byDA&start_date=01-01-1880&type=ARTICLE#print

1884b, THE FLOOD (followup), Wairarapa Standard, Volume Volume XVII, Issue 1606,

1884c, GENERAL NEWS, New Zealand Times, Volume Volume XLIII, Issue 7270, https://paperspast.natlib.govt.nz/newspapers/NZTIM18840912.2.33?end_date=31-12-1900&items_per_page=10&page=4&query=Waingawa+Plain&snippet=true&sort_by=byDA&start_date=01-01-1880&type=ARTICLE

103rd Congress of the United States, 1994, National Flood Insurance Reform Act of 1994, *in* States, r. C. o. t. U., ed., 42 U.S.C. Sec. 4001: Washington, D.C., p. 33, https://www.fema.gov/sites/default/files/2020-07/national-flood-insurance-reform-1994.pdf

(FGDC), F. G. D. C., 1998, Geospatial Positioning Accuracy Standards, Part 3: National Standard for Spatial Data Accuracy, Volume FGDC-STD-007.3-1998: Reston, VA, p. 28,

Abbe, T. B., and Montgomery, D. R., 2003, Patterns and processes of wood debris accumulation in the Queets river basin, Washington: Geomorphology, v. 51, no. 1-3, p. 81-107, 10.1016/S0169-555X(02)00326-4.

Adams, D., 2005, The Hitchhiker's Guide to the Galaxy, New York, Del Rey Books,

Adams, J., 1980, Active tilting of the United States midcontinent: Geodetic and geomorphic evidence: Geology, v. 8, no. 9, p. 442-446, 10.1130/0091-7613(1980)8<442:Atotus>2.0.Co;2.

Alber, A., and Piegay, H., 2011, Spatial disaggregation and aggregation procedures for characterizing fluvial features at the network-scale: Application to the Rhone basin (France): Geomorphology, v. 125, no. 3, p. 343-360, 10.1016/j.geomorph.2010.09.009.

Alexander, J., Bridge, J. S., Leeder, M. R., Collier, R. E. L., and Gawthorpe, R. L., 1994, Holocene meander-belt evolution in an active extensional basin, southwestern Montana: Journal of Sedimentary Research, v. 64, no. 4b, p. 542-559, 10.1306/d4267fff-2b26-11d7-8648000102c1865d.

Allan, A. J. N., 2014, Te Kāuru Upper Ruamāhanga: A floodplain management plan for the Upper Wairarapa Valley, Phase 1 Summary: Greater Wellington Regional Council; GWRC,

Allan, A. J. N., and Girvan, R., 2015, Te Kauru Upper Ruamahanga Floodplain Management Plan: Phase 2 - Vision and Aims: Greater Wellington Regional Council,

Allen, J. R. L., 1965, A review of the origin and characteristics of recent alluvial sediments: Sedimentology, v. 5, no. 2, p. 89-191, https://doi.org/10.1111/j.1365-3091.1965.tb01561.x.

-, 1974, Reaction, relaxation and lag in natural sedimentary systems: General principles, examples and lessons: Earth-Science Reviews, v. 10, no. 4, p. 263-342, https://doi.org/10.1016/0012-8252(74)90109-3.

Amos, C. B., and Burbank, D. W., 2007, Channel width response to differential uplift: Journal of Geophysical Research: Earth Surface, v. 112, no. F2, https://doi.org/10.1029/2006JF000672.

Amos, C. B., Burbank, D. W., Nobes, D. C., and Read, S. A. L., 2007, Geomorphic constraints on listric thrust faulting: Implications for active deformation in the Mackenzie Basin, South Island, New Zealand: Journal of Geophysical Research: Solid Earth, v. 112, no. B3, https://doi.org/10.1029/2006JB004291.

An, C., Cui, Y., Fu, X., and Parker, G., 2017, Gravel-bed river evolution in earthquake-prone regions subject to cycled hydrographs and repeated sediment pulses: Earth Surface Processes and Landforms, v. 42, no. 14, p. 2426-2438, 10.1002/esp.4195.

Ancey, C., and Pascal, I., 2020, Estimating Mean Bedload Transport Rates and Their Uncertainty: Journal of Geophysical Research: Earth Surface, v. 125, no. 7, p. e2020JF005534, https://doi.org/10.1029/2020JF005534.
Anderson, H., and Webb, T., 1994, New-Zealand Seismicity - Patterns Revealed By The Upgraded National-Seismograph-Network: New Zealand Journal of Geology and Geophysics, v. 37, no. 4, p. 477-493, <Go to ISI>://WOS:A1994PZ23300005
Anderson, S., and Pitlick, J., 2014, Using repeat lidar to estimate sediment transport in a steep stream: Journal of Geophysical Research: Earth Surface, v. 119, no. 3, p. 621-643, https://doi.org/10.1002/2013JF002933.
Anderson, S. W., 2019, Uncertainty in quantitative analyses of topographic change: error propagation and the role of thresholding: Earth Surface Processes and Landforms, v. 44, no. 5, p. 1015-1033, 10.1002/esp.4551.
Ashmore, P. E., 1991, How do gravel-bed rivers braid?: Canadian journal of earth sciences, v. 28, no. 3, p. 326-341,
Ashworth, P. J., Best, J. L., and Jones, M., 2004, Relationship between sediment supply and avulsion frequency in braided rivers: Geology, v. 32, no. 1, p. 21-24, 10.1130/g19919.1.
Ashworth, P. J., Best, J. L., and Jones, M. A., 2007, The relationship between channel avulsion, flow occupancy and aggradation in braided rivers: insights from an experimental model: Sedimentology, v. 54, no. 3, p. 497-513, https://doi.org/10.1111/j.1365-3091.2006.00845.x.
Aslan, A., Autin, W. J., and Blum, M. D., 2005, Causes of River Avulsion: Insights from the Late Holocene Avulsion History of the Mississippi River, U.S.A: Journal of Sedimentary Research, v. 75, no. 4, p. 650-664, 10.2110/jsr.2005.053.
Aslan, A., Blum, M., Smith, N., and Rogers, J., 1999, Contrasting styles of Holocene avulsion, Texas Gulf coastal plain, USA: Fluvial sedimentology VI, v. 28, p. 193-209,
ASPRS, A. S. f. P. a. R. S., 1989, Interim accuracy standards for large scale line maps: Photogrammetric Engineering and Remote Sensing, v. 55, p. 1038-1040,
Atkinson, C. L., Allen, D. C., Davis, L., and Nickerson, Z. L., 2018, Incorporating ecogeomorphic feedbacks to better understand resiliency in streams: A review and directions forward: Geomorphology, v. 305, p. 123-140, https://doi.org/10.1016/j.geomorph.2017.07.016.
Baker, V., 1977, Stream-channel response to floods, with examples from central Texas: GSA Bulletin, v. 88, no. 8, p. 1057-1071, 10.1130/0016-7606(1977)88<1057:Srtfwe>2.0.Co;2.
Baker, V., and Costa, J., 1987, Flood power, *in* Mayer, L., and Nash, D., eds., Catastrophic flooding, Volume 18: Boston, Allen & Unwin;,
Baker, V. R., 2007, Flood hazard science, policy, and values: A pragmatist stance: Technology in Society, v. 29, no. 2, p. 161-168, https://doi.org/10.1016/j.techsoc.2007.01.004.
Bakker, M., Antoniazza, G., Odermatt, E., and Lane, S. N., 2019, Morphological Response of an Alpine Braided Reach to Sediment-Laden Flow Events: Journal of Geophysical Research: Earth Surface, v. 124, no. 5, p. 1310-1328, 10.1029/2018jf004811.
Bakker, M., and Lane, S. N., 2017, Archival photogrammetric analysis of river–floodplain systems using Structure from Motion (SfM) methods: Earth Surface Processes and Landforms, v. 42, no. 8, p. 1274-1286, 10.1002/esp.4085.
Ballance, P., 2017, New Zealand Geology: an illustrated guide, Geoscience Society of New Zealand,
Bannister, C., 1940, Early history of the Wairarapa, Cadsonbury Publications, http://ezproxy.massey.ac.nz/login?url=https://search.ebscohost.com/login.aspx?direct=true&AuthType=ip,cookie,url,uid&db=cat00245a&AN=massey.b1571619&site=eds-live&scope=site&authtype=sso&custid=s3027306
Barrand, N. E., Murray, T., James, T. D., Barr, S. L., and Mills, J. P., 2009, Optimizing photogrammetric DEMs for glacier volume change assessment using laser-scanning derived ground-control points: Journal of Glaciology, v. 55, no. 189, p. 106-116, 10.3189/002214309788609001.
Barredo, J. I., 2009, Normalised flood losses in Europe: 1970–2006: Nat. Hazards Earth Syst. Sci., v. 9, no. 1, p. 97-104, 10.5194/nhess-9-97-2009.

Basher, L. R., and Fisher, P., 2013, River-cross-section data from the Wakapuaka and Whangamoa rivers: analysis of data 2007–2012 and implications for managing gravel extraction: Landcare Research,

Bätz, N., Verrecchia, E. P., and Lane, S. N., 2015, The role of soil in vegetated gravelly river braid plains: more than just a passive response?: Earth Surface Processes and Landforms, v. 40, no. 2, p. 143-156, 10.1002/esp.3631.

Beagley, R., Davies, T., and Eaton, B., 2020a, Past, present and future behaviour of the Waiho River, Westland, New Zealand: A new perspective, New Zealand Hydrological Society, v. 1, 41–61 p, 10.3316/informit.447098163966961.

-, 2020b, Past, present and future behaviour of the Waiho River, Westland, New Zealand: A new perspective: Journal of Hydrology (New Zealand), v. 59, no. 1, p. 41,

Beckman, N. D., and Wohl, E., 2014, Carbon storage in mountainous headwater streams: The role of old-growth forest and logjams: Water Resources Research, v. 50, no. 3, p. 2376-2393, https://doi.org/10.1002/2013WR014167.

Begg, J., Brown, L., Gyopari, M., and Jones, A., 2005, A review of geology - with a groundwater bias: Institute of Geological and Nuclear Science

Begg, J., and Johnston, M., 2000, Geology of the Wellington Area: Institute of Geological and Nuclear Sciences,

Begg, J. G., Villamore, P., Zachariasen, J., and Litchfield, N., 2001, Palaeoseismic assessment of the active Masterton and Carterton Faults, Wairarapa: GNS Science,

Benda, L., Poff, N. L., Miller, D., Dunne, T., Reeves, G., Pess, G., and Pollock, M., 2004, The network dynamics hypothesis: How channel networks structure riverine habitats: Bioscience, v. 54, no. 5, p. 413-427, 10.1641/0006-3568(2004)054[0413:tndhhc]2.0.co;2.

Bertin, S., and Friedrich, H., 2018, Effect of surface texture and structure on the development of stable fluvial armors: Geomorphology, v. 306, p. 64-79, https://doi.org/10.1016/j.geomorph.2018.01.013.

Bertoldi, W., 2012, Life of a bifurcation in a gravel-bed braided river: Earth Surface Processes and Landforms, v. 37, no. 12, p. 1327-1336, 10.1002/esp.3279.

Bertoldi, W., Gurnell, A. M., and Drake, N. A., 2011, The topographic signature of vegetation development along a braided river: Results of a combined analysis of airborne lidar, color air photographs, and ground measurements: Water Resources Research, v. 47, no. 6, 10.1029/2010wr010319.

Biedenharn, D. S., and Thorne, C. R., 1994, Magnitude-frequency analysis of sediment transport in the lower Mississippi river: Regulated Rivers: Research & Management, v. 9, no. 4, p. 237-251, https://doi.org/10.1002/rrr.3450090405.

Biedenharn, D. S., Thorne, C. R., and Watson, C. C., 2000, Recent morphological evolution of the Lower Mississippi River: Geomorphology, v. 34, no. 3, p. 227-249, https://doi.org/10.1016/S0169-555X(00)00011-8.

Bierman, P. R., and Montgomery, D. R., 2014, Key Concepts in Geomorphology, New York, W.H. Freeman and Co., xiv, 494, [422] pages p,

Bird, S., Hogan, D., and Schwab, J., 2010, Photogrammetric monitoring of small streams under a riparian forest canopy: Earth Surface Processes and Landforms, v. 35, no. 8, p. 952-970, 10.1002/esp.2001.

Bizzi, S., and Lerner, D. N., 2015, The Use of Stream Power as an Indicator of Channel Sensitivity to Erosion and Deposition Processes: River Research and Applications, v. 31, no. 1, p. 16-27, 10.1002/rra.2717.

Bledsoe, B. P., and Watson, C. C., 2001, Logistic analysis of channel pattern thresholds: meandering, braiding, and incising: Geomorphology, v. 38, no. 3, p. 281-300, https://doi.org/10.1016/S0169-555X(00)00099-4.

Boulton, C., Carpenter, B. M., Toy, V., and Marone, C., 2012, Physical properties of surface outcrop cataclastic fault rocks, Alpine Fault, New Zealand: Geochemistry, Geophysics, Geosystems, v. 13, no. 1, https://doi.org/10.1029/2011GC003872.
Bouwer, L., Crompton, R., Faust, E., Hoppe, P., and Pielke, R., 2007, Disaster management: Confronting disaster losses: Science, v. 318, p. 753, 10.1126/science.1149628.
Bouwer, L. M., 2011, Have Disaster Losses Increased Due to Anthropogenic Climate Change?: Bulletin of the American Meteorological Society, v. 92, no. 1, p. 39-46, 10.1175/2010bams3092.1.
Bouwer, L. M., Bubeck, P., and Aerts, J. C. J. H., 2010, Changes in future flood risk due to climate and development in a Dutch polder area: Global Environmental Change, v. 20, no. 3, p. 463-471, https://doi.org/10.1016/j.gloenvcha.2010.04.002.
Bracken, L. J., Turnbull, L., Wainwright, J., and Bogaart, P., 2015, Sediment connectivity: a framework for understanding sediment transfer at multiple scales: Earth Surface Processes and Landforms, v. 40, no. 2, p. 177-188, 10.1002/esp.3635.
Brasington, J., Langham, J., and Rumsby, B., 2002, Sensitivity of morphometric estimates of sediment transport in large gravel-bed rivers, International Symposium on Remote Sensing, Volume 4545, SPIE, https://doi.org/10.1117/12.453679
-, 2003, Methodological sensitivity of morphometric estimates of coarse fluvial sediment transport: Geomorphology, v. 53, no. 3-4, p. 299-316, 10.1016/s0169-555x902)00320-3.
Brasington, J., and Richards, K., 2007, Reduced-complexity, physically-based geomorphological modelling for catchment and river management: Geomorphology, v. 90, no. 3-4, p. 171-177, 10.1016/j.geomorph.2006.10.028.
Brasington, J., Rumsby, B. T., and McVey, R. A., 2000, Monitoring and modelling morphological change in a braided gravel-bed river using high resolution GPS-based survey: Earth Surface Processes and Landforms, v. 25, no. 9, p. 973-990, 10.1002/1096-9837(200008)25:9<973::aid-esp111>3.0.co;2-y.
Brasington, J., Vericat, D., and Rychkov, I., 2012, Modeling river bed morphology, roughness, and surface sedimentology using high resolution terrestrial laser scanning: Water Resources Research, v. 48, 10.1029/2012wr012223.
Braudrick, C. A., Dietrich, W. E., Leverich, G. T., and Sklar, L. S., 2009, Experimental evidence for the conditions necessary to sustain meandering in coarse-bedded rivers: Proceedings of the National Academy of Sciences, v. 106, no. 40, p. 16936, 10.1073/pnas.0909417106.
Brazier, R. E., Puttock, A., Graham, H. A., Auster, R. E., Davies, K. H., and Brown, C. M. L., 2021, Beaver: Nature's ecosystem engineers: WIREs Water, v. 8, no. 1, p. e1494, https://doi.org/10.1002/wat2.1494.
Brecher, H., 1986, Surface velocity determination on large polar glaciers by aerial photogrammetry: Annals of Glaciology, v. 8, p. 22-26,
Brewer, P. A., and Passmore, D. G., 2002, Sediment budgeting techniques in gravel-bed rivers: Geological Society, London, Special Publications, v. 191, no. 1, p. 97-113, 10.1144/gsl.sp.2002.191.01.07.
Bridge, J. S., and Leeder, M. R., 1979, A simulation model of alluvial stratigraphy: Sedimentology, v. 26, no. 5, p. 617-644, 10.1111/j.1365-3091.1979.tb00935.x.
Brierley, G., Fryirs, K., Cullum, C., Tadaki, M., Huang, H. Q., and Blue, B., 2013, Reading the landscape: Integrating the theory and practice of geomorphology to develop place-based understandings of river systems: Progress in Physical Geography, v. 37, no. 5, p. 601-621, 10.1177/0309133313490007.
Brierley, G. J., 2010, Landscape memory: the imprint of the past on contemporary landscape forms and processes: Area, v. 42, no. 1, p. 76-85, 10.1111/j.1475-4762.2009.00900.x.
Brierley, G. J., Brooks, A. P., Fryirs, K., and Taylor, M. P., 2005, Did humid-temperate rivers in the Old and New Worlds respond differently to clearance of riparian vegetation and removal of

woody debris?: Progress in Physical Geography: Earth and Environment, v. 29, no. 1, p. 27-49, 10.1191/0309133305pp433ra.
Brierley, G. J., and Fryirs, K. A., 2005, Geomorphology and river management: applications of the river styles framework, Carlton, Victoria, Australia, Blackwell,
Brierley, G. J., Hikuroa, D. C., Friedrich, H., Fuller, I. C., Brasington, J., Hoyle, J., Tunnicliffe, J., Allen, K., and Measures, R., 2021, Why we should release New Zealand's strangled rivers to lessen the impact of future floods, The Conversation: The Conversation, The Conversation,
Brizga, S. O., and Finlayson, B. L., 1990, Channel avulsion and river metamorphosis: The case of the Thomson River, Victoria, Australia: Earth Surface Processes and Landforms, v. 15, no. 5, p. 391-404, https://doi.org/10.1002/esp.3290150503.
Brogan, D. J., MacDonald, L. H., Nelson, P. A., and Morgan, J. A., 2019, Geomorphic complexity and sensitivity in channels to fire and floods in mountain catchments: Geomorphology, v. 337, p. 53-68, https://doi.org/10.1016/j.geomorph.2019.03.031.
Brookes, A., 1985, Traditional engineering methods, physical consequences and alternative practices: Progress in Physical Geography: Earth and Environment, v. 9, no. 1, p. 44-73, 10.1177/030913338500900103.
Brooks, A. P., Brierley, G. J., and Millar, R. G., 2003, The long-term control of vegetation and woody debris on channel and flood-plain evolution: Insights from a paired catchment study in southeastern Australia: Geomorphology, v. 51, no. 1-3, p. 7-29, 10.1016/S0169-555X(02)00323-9.
Brown, W., Malveau, R., McCormick, S., and Mowbray, T., 1998, AntiPatterns: Refactoring Software, Architectures, and Projects in Crisis, John Wiley and Sons,
Brunsden, D., 2001, A critical assessment of the sensitivity concept in geomorphology: CATENA, v. 42, no. 2, p. 99-123, https://doi.org/10.1016/S0341-8162(00)00134-X.
Brunsden, D., and Thornes, J., 1979, Landscape sensitivity and change: Transactions of the Institute of British Geographers, v. 4, no. 4, p. 463-484,
Brunsdon, C., 1995, Estimating probability surfaces for geographical point data: An adaptive kernel algorithm: Computers & Geosciences, v. 21, no. 7, p. 877-894, https://doi.org/10.1016/0098-3004(95)00020-9.
Bryant, M., Falk, P., and Paola, C., 1995, Experimental study of avulsion frequency and rate of deposition: Geology, v. 23, no. 4, p. 365-368, 10.1130/0091-7613(1995)023<0365:Esoafa>2.3.Co;2.
Bubeck, P., Kreibich, H., Penning-Rowsell, E. C., Botzen, W. J. W., de Moel, H., and Klijn, F., 2017, Explaining differences in flood management approaches in Europe and in the USA – a comparative analysis: Journal of Flood Risk Management, v. 10, no. 4, p. 436-445, https://doi.org/10.1111/jfr3.12151.
Bull, W. B., 1979, Threshold Of Critical Power In Streams: Geological Society of America Bulletin, v. 90, no. 5, p. 453-464, 10.1130/0016-7606(1979)90<453:tocpis>2.0.co;2.
Bull, W. B., 2009, Tectonically Active Landscapes, Chichester, UK, Wiley-Blackwell, 1 online resource (x, 326 pages) p, http://ezproxy.massey.ac.nz/login?url=http://onlinelibrary.wiley.com/book/10.1002/9781444312003
Bunny, T., Thompson, M., and Keenan, L., 2014, Water allocation in the Ruamāhanga whaitua: Greater Wellington Regional Council,
Burbank, D. W., 1992, Causes of recent Himalayan uplift deduced from deposited patterns in the Ganges basin: Nature, v. 357, no. 6380, p. 680-683,
Burbank, D. W., and Anderson, R. S., 2012, Tectonic Geomorphology, Chichester, UK, Wiley-Blackwell, http://ezproxy.massey.ac.nz/login?url=http://onlinelibrary.wiley.com/book/10.1002/9781444345063
Butler, D., 2006, The web-wide world: Nature, v. 439, no. 7078, p. 776-778, 10.1038/439776a.
Butler, D. R., 2019, Zoogeomorphology, International Encyclopedia of Geography, p. 1-6, https://doi.org/10.1002/9781118786352.wbieg1119.pub2.

Butler, D. R., Anzah, F., Goff, P. D., and Villa, J., 2018, Zoogeomorphology and resilience theory: Geomorphology, v. 305, p. 154-162, https://doi.org/10.1016/j.geomorph.2017.08.036.
Call, B. C., Belmont, P., Schmidt, J. C., and Wilcock, P. R., 2017, Changes in floodplain inundation under nonstationary hydrology for an adjustable, alluvial river channel: Water Resources Research, v. 53, no. 5, p. 3811-3834, https://doi.org/10.1002/2016WR020277.
Carbonneau, P., Fonstad, M. A., Marcus, W. A., and Dugdale, S. J., 2012, Making riverscapes real: Geomorphology, v. 137, no. 1, p. 74-86, https://doi.org/10.1016/j.geomorph.2010.09.030.
Carbonneau, P. E., Lane, S. N., and Bergeron, N., 2006, Feature based image processing methods applied to bathymetric measurements from airborne remote sensing in fluvial environments: Earth Surface Processes and Landforms, v. 31, no. 11, p. 1413-1423, 10.1002/esp.1341.
Carbonneau, P. E., and Piegay, H., 2012, Introduction: The Growing Use of Imagery in Fundamental and Applied River Sciences, Fluvial Remote Sensing for Science and Management: Oxford, U.K., Wiley-Blackwell, 10.1002/9781119940791.ch1.
Carley, J. K., Pasternack, G. B., Wyrick, J. R., Barker, J. R., Bratovich, P. M., Massa, D. A., Reedy, G. D., and Johnson, T. R., 2012, Significant decadal channel change 58–67years post-dam accounting for uncertainty in topographic change detection between contour maps and point cloud models: Geomorphology, v. 179, p. 71-88, https://doi.org/10.1016/j.geomorph.2012.08.001.
Carne, R. C., and Little, T. A., 2012, Geometry and scale of fault segmentation and deformational bulging along an active oblique-slip fault (Wairarapa fault, New Zealand): Geological Society of America Bulletin, v. 124, no. 7-8, p. 1365-1381, 10.1130/b30535.1.
Carne, R. C., Little, T. A., and Rieser, U., 2011, Using displaced river terraces to determine Late Quaternary slip rate for the central Wairarapa Fault at Waiohine River, New Zealand: New Zealand Journal of Geology and Geophysics, v. 54, no. 2, p. 217-236, 10.1080/00288306.2010.532224.
Carson, M. A., and Griffiths, G. A., 1987, Bedload transport In gravel channels: Journal of Hydrology (New Zealand), v. 26, no. 1, p. 1-151, http://www.jstor.org.ezproxy.massey.ac.nz/stable/43944586
Cerovski-Darriau, C., and Roering, J. J., 2016, Influence of anthropogenic land-use change on hillslope erosion in the Waipaoa River Basin, New Zealand: Earth Surface Processes and Landforms, v. 41, no. 15, p. 2167-2176, 10.1002/esp.3969.
Chadwick, A. J., Lamb, M. P., and Ganti, V., 2020, Accelerated river avulsion frequency on lowland deltas due to sea-level rise: Proceedings of the National Academy of Sciences, v. 117, no. 30, p. 17584-17590, 10.1073/pnas.1912351117.
Chakraborty, T., Kar, R., Ghosh, P., and Basu, S., 2010, Kosi megafan: Historical records, geomorphology and the recent avulsion of the Kosi River: Quaternary International, v. 227, no. 2, p. 143-160, https://doi.org/10.1016/j.quaint.2009.12.002.
Chandler, J., and Cooper, M., 1989, The extraction of positional data from historical photographs and their application to geomorphology: The Photogrammetric Record, v. 13, no. 73, p. 69-78,
Chang, H. H., 1980, Geometry of Gravel Streams: Journal of the Hydraulics Division, v. 106, no. 9, p. 1443-1456, doi:10.1061/JYCEAJ.0005504.
Chappell, P. R., 2014, The Climate and Weather of Wellington Region: NIWA, https://niwa.co.nz/sites/niwa.co.nz/files/Wellington%20Climate%20WEB_0.pdf, https://niwa.co.nz/sites/niwa.co.nz/files/Wellington%20Climate%20WEB_0.pdf
Chen, Y., Overeem, I., Kettner, A. J., Gao, S., and Syvitski, J. P. M., 2015, Modeling flood dynamics along the superelevated channel belt of the Yellow River over the last 3000 years: Journal of Geophysical Research: Earth Surface, v. 120, no. 7, p. 1321-1351, https://doi.org/10.1002/2015JF003556.

Chen, Y., Syvitski, J. P. M., Gao, S., Overeem, I., and Kettner, A. J., 2012, Socio-economic Impacts on Flooding: A 4000-Year History of the Yellow River, China: AMBIO, v. 41, no. 7, p. 682-698, 10.1007/s13280-012-0290-5.
Chorley, R. J., 1972, Spatial analysis in geomorphology, London, Routledge,
-, 1978, Bases for theory in geomorphology, *in* Embleton, C., Brunsden, D., and Jones, D. K., eds., Geomorphology: present problems and future prospects, Oxford University Press,
Chorley, R. J., and Kennedy, B. A., 1971, Physical geography: a systems approach, Prentice Hall,
Chrisman, N., 1982, The role of quality information in the long-term functioning of a Geographic Information System: Cartographica, v. 21,
Chrisman, N. R., 1991, The error component in spatial data: Geographical information systems, v. 1, no. 12, p. 165-174,
Christensen, K., 2013, Upper Wairarapa Floodplain Management Plan: Phase 1 Geomorphology, *in* Protection, F., ed.: Wellington, Greater Wellington Regional Council, p. 113,
Church, M., Records of recent geomorphological events, *in* Proceedings British geomorphological research group. Symposium1980, p. 13-29.
Church, M., 1983, Pattern of Instability in a Wandering Gravel Bed Channel, *in* Collinson, J. D., and Lewin, J., eds., Modern and Ancient Fluvial Systems: Boston, Blackwell, p. 169-180, 10.1002/9781444303773.ch13.
-, 2006, Bed material transport and the morphology of alluvial river channels, Annual Review of Earth and Planetary Sciences, Volume 34, p. 325-354, 10.1146/annurev.earth.33.092203.122721.
Church, M., 2010, The trajectory of geomorphology: Progress in Physical Geography - PROG PHYS GEOG, v. 34, p. 265-286, 10.1177/0309133310363992.
-, 2013, Refocusing geomorphology: Field work in four acts: Geomorphology, v. 200, p. 184-192, https://doi.org/10.1016/j.geomorph.2013.01.014.
-, 2015, Channel Stability: Morphodynamics and the Morphology of Rivers, *in* Rowiński, P., and Radecki-Pawlik, A., eds., Rivers – Physical, Fluvial and Environmental Processes: Cham, Springer International Publishing, p. 281-321, 10.1007/978-3-319-17719-9_12.
Church, M., and Ferguson, R. I., 2015, Morphodynamics: Rivers beyond steady state: Water Resources Research, v. 51, no. 4, p. 1883-1897, 10.1002/2014WR016862.
Church, M., Hassan, M. A., and Wolcott, J. F., 1998, Stabilizing self-organized structures in gravel-bed stream channels: Field and experimental observations: Water Resources Research, v. 34, no. 11, p. 3169-3179, 10.1029/98wr00484.
Cienciala, P., Melendez Bernardo, M., Nelson, A. D., and Haas, A. D., 2022, Interdecadal variation in sediment yield from a forested mountain basin: The role of hydroclimatic variability, anthropogenic disturbances, and geomorphic connectivity: Science of The Total Environment, v. 826, p. 153876, https://doi.org/10.1016/j.scitotenv.2022.153876.
Clapuyt, F., Vanacker, V., and Van Oost, K., 2016, Reproducibility of UAV-based earth topography reconstructions based on Structure-from-Motion algorithms: Geomorphology, v. 260, no. Supplement C, p. 4-15, https://doi.org/10.1016/j.geomorph.2015.05.011.
Clark, K., Howarth, J., Litchfield, N., Cochran, U., Turnbull, J., Dowling, L., Howell, A., Berryman, K., and Wolfe, F., 2019, Geological evidence for past large earthquakes and tsunamis along the Hikurangi subduction margin, New Zealand: Marine Geology, v. 412, p. 139-172, https://doi.org/10.1016/j.margeo.2019.03.004.
Clement, A. J. H., and Fuller, I. C., 2007, Fluvial responses to environmental change in the North Island, New Zealand, during the past c. 30 ka recorded in river terrace sequences: a review and model for river behaviour: New Zealand Journal of Geology and Geophysics, v. 50, no. 2, p. 101-116, <Go to ISI>://WOS:000248197900004
Clement, A. J. H., Whitehouse, P. L., and Sloss, C. R., 2016, An examination of spatial variability in the timing and magnitude of Holocene relative sea-level changes in the New Zealand

archipelago: Quaternary Science Reviews, v. 131, p. 73-101, https://doi.org/10.1016/j.quascirev.2015.09.025.
Collins, B. D., Dickerson-Lange, S. E., Schanz, S., and Harrington, S., 2019, Differentiating the effects of logging, river engineering, and hydropower dams on flooding in the Skokomish River, Washington, USA: Geomorphology, v. 332, p. 138-156, https://doi.org/10.1016/j.geomorph.2019.01.021.
Conley, W., 2015, Fluvial Reconnaissance of Rock Creek and Selected Tributaries with Implications for Anadromous Salmonid Habitat Management: United States Department of Energy, Bonneville Power Administration, P153764, https://www.cbfish.org/Document.mvc/Viewer/P153764, https://www.cbfish.org/Document.mvc/Viewer/P153764
Conley, W., Fuller, I. C., McColl, S. T., Tunnicliffe, J., and Macklin, M. G., Morphotectonics as a landscape template for assessing sediment transfers and flood vulnerability, *in* Proceedings Geoscience Society of New Zealand, Auckland, 2017a, https://doi.org/10.6084/m9.figshare.19210098.v1.
Conley, W. C., Fuller, I. C., Macklin, M., McColl, S. T., Death, R. G., and Tunnicliffe, J. F., Vulnerability zone identification and river channel change sensitivity in the Ruamāhanga catchment, *in* Proceedings 5th Biennial Symposium of the International Society for River Science, Hamilton, NZ, 2017-11-20 2017b, https://doi.org/10.6084/m9.figshare.19243287.
Cooke, R. V., and Doornkamp, J. C., 1990, Geomorphology in environmental management: a new introduction: Oxford, Oxford University Press (OUP), p. xxiv + 410 pp, https://www.cabdirect.org/cabdirect/abstract/19931975249
Corenblit, D., Davies, N. S., Steiger, J., Gibling, M. R., and Bornette, G., 2015, Considering river structure and stability in the light of evolution: feedbacks between riparian vegetation and hydrogeomorphology: Earth Surface Processes and Landforms, v. 40, no. 2, p. 189-207, 10.1002/esp.3643.
Corenblit, D., Steiger, J., Gurnell, A. M., Tabacchi, E., and Roques, L., 2009, Control of sediment dynamics by vegetation as a key function driving biogeomorphic succession within fluvial corridors: Earth Surface Processes and Landforms, v. 34, no. 13, p. 1790-1810, https://doi.org/10.1002/esp.1876.
Corenblit, D., Tabacchi, E., Steiger, J., and Gurnell, A. M., 2007, Reciprocal interactions and adjustments between fluvial landforms and vegetation dynamics in river corridors: A review of complementary approaches: Earth-Science Reviews, v. 84, no. 1, p. 56-86, https://doi.org/10.1016/j.earscirev.2007.05.004.
Correspondence, 1884, CORRESPONDENCE, Wairarapa Daily Times, Volume Volume 6, Issue 1798, https://paperspast.natlib.govt.nz/newspapers/WDT18840926.2.8?end_date=31-12-1900&items_per_page=10&page=4&query=Waingawa+Plain&snippet=true&sort_by=byDA&start_date=01-01-1880&type=ARTICLE
Costa, J. E., and O'Connor, J. E., 1995, Geomorphically Effective Floods, *in* Costa, J. E., Miller, A. J., Potter, K. W., and Wilcock, P. R., eds., Natural and Anthropogenic Influences in Fluvial Geomorphology, Volume 89: Washington, D.C. USA, American Geophysical Union, p. 45-56, 10.1029/GM089p0045.
Cotton, C., 1941, Notes on Two Transverse-Profile Geomorphic Problems: Trans. R. Soc. NZ, v. 71, p. 1-5,
Cotton, C., 1945, Geomorphology: An Introduction to the Study of Landforms, Wellington, NZ, Whitcombe and Tombs Ltd.,
Coulthard, T. J., Hicks, D. M., and Van De Wiel, M. J., 2007, Cellular modelling of river catchments and reaches: Advantages, limitations and prospects: Geomorphology, v. 90, no. 3–4, p. 192-207, https://doi.org/10.1016/j.geomorph.2006.10.030.

Coulthard, T. J., and Van De Wiel, M. J., 2007, Quantifying fluvial non linearity and finding self organized criticality? Insights from simulations of river basin evolution: Geomorphology, v. 91, no. 3–4, p. 216-235, https://doi.org/10.1016/j.geomorph.2007.04.011.

Council, G. W. R., 2014, Summary report for Ruamahanga Whaitua Committee: Hydrological sustems of the Ruamahanga catchment,

Cowgill, E., 2007, Impact of riser reconstructions on estimation of secular variation in rates of strike–slip faulting: Revisiting the Cherchen River site along the Altyn Tagh Fault, NW China: Earth and Planetary Science Letters, v. 254, no. 3, p. 239-255, https://doi.org/10.1016/j.epsl.2006.09.015.

Croissant, T., Steer, P., Lague, D., Davy, P., Jeandet, L., and Hilton, R. G., 2019, Seismic cycles, earthquakes, landslides and sediment fluxes: Linking tectonics to surface processes using a reduced-complexity model: Geomorphology, v. 339, p. 87-103, https://doi.org/10.1016/j.geomorph.2019.04.017.

Croke, J., Fryirs, K., and Thompson, C., 2016, Defining the floodplain in hydrologically-variable settings: implications for flood risk management: Earth Surface Processes and Landforms, v. 41, no. 14, p. 2153-2164, https://doi.org/10.1002/esp.4014.

Cucchiaro, S., Maset, E., Cavalli, M., Crema, S., Marchi, L., Beinat, A., and Cazorzi, F., 2020, How does co-registration affect geomorphic change estimates in multi-temporal surveys?: GIScience & Remote Sensing, p. 1-22, 10.1080/15481603.2020.1763048.

Cui, Y., Parker, G., Lisle, T. E., Gott, J., Hansler-Ball, M. E., Pizzuto, J. E., Allmendinger, N. E., and Reed, J. M., 2003, Sediment pulses in mountain rivers: 1. Experiments: Water Resources Research, v. 39, no. 9, https://doi.org/10.1029/2002WR001803.

Curran, J. C., and Hession, W. C., 2013, Vegetative impacts on hydraulics and sediment processes across the fluvial system: Journal of Hydrology, v. 505, p. 364-376, https://doi.org/10.1016/j.jhydrol.2013.10.013.

Curran, J. H., Loso, M. G., and Williams, H. B., 2017, Glacial conditioning of stream position and flooding in the braid plain of the Exit Glacier foreland, Alaska: Geomorphology, v. 293, p. 272-288, https://doi.org/10.1016/j.geomorph.2017.06.004.

Czuba, J. A., and Foufoula-Georgiou, E., 2015, Dynamic connectivity in a fluvial network for identifying hotspots of geomorphic change: Water Resources Research, v. 51, no. 3, p. 1401-1421, https://doi.org/10.1002/2014WR016139.

D'Arcy, M., and Whittaker, A. C., 2014, Geomorphic constraints on landscape sensitivity to climate in tectonically active areas: Geomorphology, v. 204, p. 366-381, https://doi.org/10.1016/j.geomorph.2013.08.019.

Davies, T. R., Edwards, L., and Woodhouse, C., 2014, Waiohine FMP Phase 3 Detailed Option 7 Assessment, W01866504,

Davies, T. R., and McSaveney, M. J., 2006, Geomorphic constraints on the management of bedload-dominated rivers: Journal of Hydrology (Wellington North), v. 45, no. 2, p. 111-130, <Go to ISI>://BIOABS:BACD200700124857

Davies, T. R. H., and Korup, O., 2007, Persistent alluvial fanhead trenching resulting from large, infrequent sediment inputs: Earth Surface Processes and Landforms, v. 32, no. 5, p. 725-742, https://doi.org/10.1002/esp.1410.

Davies, T. R. H., McSaveney, M. J., and Clarkson, P. J., 2003, Anthropic aggradation of the Waiho River, Westland, New Zealand: Microscale modelling: Earth Surface Processes and Landforms, v. 28, no. 2, p. 209-218, 10.1002/esp.449.

Davis, W. M., 1899, The Geographical Cycle: The Geographical Journal, v. 14, no. 5, p. 481-504, 10.2307/1774538.

Dawe, I., 2007, Updated Hazard and Risk Analysis for the Wellington Region CDEM Group Plan: Civil Defence,

de Haas, T., Densmore, A. L., den Hond, T., and Cox, N. J., 2019, Fan-Surface Evidence for Debris-Flow Avulsion Controls and Probabilities, Saline Valley, California: Journal of Geophysical Research: Earth Surface, v. 124, no. 5, p. 1118-1138, https://doi.org/10.1029/2018JF004815.
de Moel, H., van Alphen, J., and Aerts, J. C. J. H., 2009, Flood maps in Europe – methods, availability and use: Nat. Hazards Earth Syst. Sci., v. 9, no. 2, p. 289-301, 10.5194/nhess-9-289-2009.
De Rose, R. C., and Basher, L. R., 2011, Measurement of river bank and cliff erosion from sequential LIDAR and historical aerial photography: Geomorphology, v. 126, no. 1-2, p. 132-147,
Death, R. G., and Winterbourn, M. J., 1994, Environmental Stability and Community Persistence: A Multivariate Perspective: Journal of the North American Benthological Society, v. 13, no. 2, p. 125-139, 10.2307/1467232.
Deitrick, S., and Edsall, R., 2008, Making uncertainty usable: Approaches for visualizing uncertainty information, Geographic Visualization: Concepts, Tools and Applications, p. 277-291,
Dépret, T., Riquier, J., and Piégay, H., 2017, Evolution of abandoned channels: Insights on controlling factors in a multi-pressure river system: Geomorphology, v. 294, p. 99-118, https://doi.org/10.1016/j.geomorph.2017.01.036.
Devillers, R., Desjardin, É., and De Runz, C., 2019, Imperfection of Geographic Information: Concepts and Terminologies, Imperfection of Geographic Information, p. 11-24, 10.1002/9781119507284.ch2.
Devillers, R., Stein, A., Bédard, Y., Chrisman, N., Fisher, P., and Shi, W., 2010, Thirty Years of Research on Spatial Data Quality: Achievements, Failures, and Opportunities: T. GIS, v. 14, p. 387-400, 10.1111/j.1467-9671.2010.01212.x.
Dietrich, W. E., Kirchner, J. W., Ikeda, H., and Iseya, F., 1989, Sediment supply and the development of the coarse surface layer in gravel-bedded rivers: Nature, v. 340, no. 6230, p. 215-217, 10.1038/340215a0.
Dilts, T., Yang, J., and Weisberg, P., 2010, Mapping Riparian Vegettation with Lidar Data: Predicting plant community distribution using height above river and flood height, ArcUser, Volume Winter: Redlands, CA, ESRI, p. 18-21, http://www.cabnr.unr.edu/weisberg/downloads/
Diplas, P., Dancey, C. L., Celik, A. O., Valyrakis, M., Greer, K., and Akar, T., 2008, The Role of Impulse on the Initiation of Particle Movement Under Turbulent Flow Conditions: Science, v. 322, no. 5902, p. 717-720, doi:10.1126/science.1158954.
Donovan, M., and Belmont, P., 2019, Timescale dependence in river channel migration measurements: Earth Surface Processes and Landforms, v. 44, no. 8, p. 1530-1541, https://doi.org/10.1002/esp.4590.
Dow, S., Snyder, N. P., Ouimet, W. B., Martini, A. M., Yellen, B., Woodruff, J. D., Newton, R. M., Merritts, D. J., and Walter, R. C., 2020, Estimating the timescale of fluvial response to anthropogenic disturbance using two generations of dams on the South River, Massachusetts, USA: Earth Surface Processes and Landforms, v. n/a, no. n/a, 10.1002/esp.4886.
Downes, G., 2006, The 1904 Ms6.8 Mw7.0-7.2 Cape Turnagain, New Zealand, earthquake: Bulletin of the New Zealand Society for Earthquake Engineering, v. 39, no. 4, p. 25,
Downes, G., Dowrick, D., Smith, E., and Berryman, K., 1999a, The 1934 Pahiatua earthquake sequence: Bulletin of the New Zealand Society for Earthquake Engineering, v. 32, no. 4, 10.5459/bnzsee.32.4.221-245.
-, 1999b, The 1934 Pahiatua earthquake sequence: analysis of observational and instrumental data,
Downes, G. L., 1995, Atlas of isoseismal maps of New Zealand earthquakes: Institute of Geological and Nuclear Sciences,
Downes, G. L., Dowrick, D. J., Van Dissen, R. J., Taber, J. J., Hancox, G. T., and Smith, E. G. C., 2001, The 1942 Wairarapa, New Zealand, earthquakes: Bulletin of the New Zealand Society for Earthquake Engineering, v. 34, no. 2, 10.5459/bnzsee.34.2.125-157.

Downs, P. W., 1995, Estimating the probability of river channel adjustment: Earth Surface Processes and Landforms, v. 20, no. 7, p. 687-705, https://doi.org/10.1002/esp.3290200710.
Downs, P. W., Dusterhoff, S. R., and Sears, W. A., 2013, Reach-scale channel sensitivity to multiple human activities and natural events: Lower Santa Clara River, California, USA: Geomorphology, v. 189, p. 121-134, https://doi.org/10.1016/j.geomorph.2013.01.023.
Downs, P. W., and Gregory, K. J., 1995, Approaches to River Channel Sensitivity: The Professional Geographer, v. 47, no. 2, p. 168-175, https://doi.org/10.1111/j.0033-0124.1995.00168.x.
Downs, P. W., Soar, P. J., and Taylor, A., 2016, The anatomy of effective discharge: the dynamics of coarse sediment transport revealed using continuous bedload monitoring in a gravel-bed river during a very wet year: Earth Surface Processes and Landforms, v. 41, no. 2, p. 147-161, https://doi.org/10.1002/esp.3785.
Downton, M. W., and Pielke, R. A., 2005, How accurate are disaster loss data? The case of US flood damage: Natural Hazards, v. 35, no. 2, p. 211-228,
Dowrick, D. J., 1996, The Modified Mercalli earthquake intensity scale: Bulletin of the New Zealand Society for Earthquake Engineering, v. 29, no. 2, 10.5459/bnzsee.29.2.92-106.
Dumont, J. F., Santana, E., Valdez, F., Tihay, J. P., Usselmann, P., Iturralde, D., and Navarette, E., 2006, Fan beheading and drainage diversion as evidence of a 3200-2800 BP earthquake event in the Esmeraldas-Tumaco seismic zone: A case study for the effects of great subduction earthquakes: Geomorphology, v. 74, no. 1, p. 100-123, https://doi.org/10.1016/j.geomorph.2005.07.011.
Dunne, K. B. J., and Jerolmack, D. J., 2020, What sets river width?: Science Advances, v. 6, no. 41, p. eabc1505, 10.1126/sciadv.abc1505.
Dust, D., and Wohl, E., 2012, Conceptual model for complex river responses using an expanded Lane's relation: Geomorphology, v. 139-140, p. 109-121, https://doi.org/10.1016/j.geomorph.2011.10.008.
Duvall, A., Kirby, E., and Burbank, D., 2004, Tectonic and lithologic controls on bedrock channel profiles and processes in coastal California: Journal of Geophysical Research: Earth Surface, v. 109, no. F3, https://doi.org/10.1029/2003JF000086.
Dykes, R., Fuller, I. C., Macklin, M. G., and Death, R., 2015, An assessment of data and research in the Ruamhanga River catchment: Innovative River Solutions, Institute of Agriculture and Environment,
East, A. E., Logan, J. B., Mastin, M. C., Ritchie, A. C., Bountry, J. A., Magirl, C. S., and Sankey, J. B., 2018, Geomorphic Evolution of a Gravel-Bed River Under Sediment-Starved Versus Sediment-Rich Conditions: River Response to the World's Largest Dam Removal: Journal of Geophysical Research: Earth Surface, v. 123, no. 12, p. 3338-3369, https://doi.org/10.1029/2018JF004703.
Eaton, B. C., and Church, M., 2007, Predicting downstream hydraulic geometry: A test of rational regime theory: Journal of Geophysical Research: Earth Surface, v. 112, no. F3, https://doi.org/10.1029/2006JF000734.
Eaton, B. C., and Church, M., 2011, A rational sediment transport scaling relation based on dimensionless stream power: Earth Surface Processes and Landforms, v. 36, no. 7, p. 901-910, https://doi.org/10.1002/esp.2120.
Eaton, B. C., Church, M., and Millar, R. G., 2004, Rational regime model of alluvial channel morphology and response: Earth Surface Processes and Landforms, v. 29, no. 4, p. 511-529,
Eaton, B. C., Millar, R. G., and Davidson, S., 2010, Channel patterns: braided, anabranching, and single-thread: Geomorphology, v. 120, no. 3, p. 353-364,
Egozi, R., and Ashmore, P., 2009, Experimental analysis of braided channel pattern response to increased discharge: Journal of Geophysical Research: Earth Surface, v. 114, no. F2, https://doi.org/10.1029/2008JF001099.
El Ashrey, M., 1967, Shoreline features and thier changes: Photogrammetric Engineering, v. 33, p. 184-189,

Engelder, J. T., 1974, Cataclasis and the Generation of Fault Gouge: GSA Bulletin, v. 85, no. 10, p. 1515-1522, 10.1130/0016-7606(1974)85<1515:Catgof>2.0.Co;2.
Ethridge, F., Skelly, R., Bristow, C. S., Smith, N., and Rogers, J., 1999, Avulsion and crevassing in the sandy, braided Niobrara River: complex response to base-level rise and aggradation, Volume 28, Wiley Online Library, p. 179-191,
European Environment Agency, World Health Organization, and JRC, 2008, Impacts of Europe's changing climate – 2008 indicator-based assessment, European Environment Agency,, https://www.eea.europa.eu/publications/eea_report_2008_4/pp1-19_CC2008Executive_Summary.pdf, https://www.eea.europa.eu/publications/eea_report_2008_4/pp1-19_CC2008Executive_Summary.pdf
European Parliament and the Council of the European Union, 2007, Directive on the assessment and management of flood risks (2007/60/EC), *in* Union, E. P. a. t. C. o. t. E., ed., Volume (2007/60/EC, https://eur-lex.europa.eu/legal-content/EN/TXT/?uri=CELEX:32007L0060
Faisal, I. M., Kabir, M. R., and Nishat, A., 1999, Non-structural flood mitigation measures for Dhaka City: Urban Water, v. 1, no. 2, p. 145-153, https://doi.org/10.1016/S1462-0758(00)00004-2.
Ferguson, A. P., and Ashley, W. S., 2017, Spatiotemporal analysis of residential flood exposure in the Atlanta, Georgia metropolitan area: Natural Hazards, v. 87, no. 2, p. 989-1016, 10.1007/s11069-017-2806-6.
Ferguson, R. I., 1977, Meander migration: equilibrium and change, *in* Gregory, K. J., ed., River Channel Changes: Chichester, Wiley, p. 235-248,
Ferguson, R. I., 1986, Hydraulics and hydraulic geometry: Progress in Physical Geography: Earth and Environment, v. 10, no. 1, p. 1-31, 10.1177/030913338601000101.
Ferguson, R. I., 1993, Understanding braiding processes in gravel-bed rivers: progress and unsolved problems: Geological Society, London, Special Publications, v. 75, no. 1, p. 73-87, 10.1144/gsl.sp.1993.075.01.03.
Ferguson, R. I., Prestegaard, K. L., and Ashworth, P. J., 1989, Influence of sand on hydraulics and gravel transport in a braided gravel bed river: Water Resources Research, v. 25, no. 4, p. 635-643, https://doi.org/10.1029/WR025i004p00635.
Ferguson, R. I., and Werritty, A., 1983, Bar Development and Channel Changes in the Gravelly River Feshie, Scotland, *in* Collinson, J. D., and Lewin, J., eds., Modern and Ancient Fluvial Systems: Boston, Blackwell, p. 181-193, 10.1002/9781444303773.ch14.
First Street Foundation, 2020a, The First National Flood Risk Assessment: Defining America's Growing Risk: First Street Foundation, https://firststreet.org/flood-lab/published-research/2020-national-flood-risk-assessment-highlights/, https://firststreet.org/flood-lab/published-research/2020-national-flood-risk-assessment-highlights/
-, 2020b, First Street Foundation Flood Model (FSF-FM) Technical Methodology Document: First Street Foundation, https://assets.firststreet.org/uploads/2020/06/FSF_Flood_Model_Technical_Documentation.pdf, https://assets.firststreet.org/uploads/2020/06/FSF_Flood_Model_Technical_Documentation.pdf
Fischenich, C., 2000, Glossary of Stream Restoration Terms,
Fisher, P. E., and Tate, N. J., 2006, Causes and consequences of error in digital elevation models: Progress in Physical Geography, v. 30, no. 4, p. 467-489, 10.1191/0309133306pp492ra.
Fisher, P. F., 1991, Spatial data sources and data problems: Geographical information systems: principles and applications, v. 1, p. 175-189,
Flood Risk Management and River Control Review Steering Group, 2008, Meeting the Challenges of Future Flooding in New Zealand: NZ Ministry for the Environment, https://www.mfe.govt.nz/sites/default/files/meeting-challenges-of-future-flooding-in-

nz.pdf, https://www.mfe.govt.nz/sites/default/files/meeting-challenges-of-future-flooding-in-nz.pdf
Flood, Y. S., and Hampson, G. J., 2014, Facies And Architectural Analysis To Interpret Avulsion Style and Variability: Upper Cretaceous Blackhawk Formation, Wasatch Plateau, Central Utah, U.S.A: Journal of Sedimentary Research, v. 84, no. 9, p. 743-762, 10.2110/jsr.2014.59.
Fonstad, M. A., Dietrich, J. T., Courville, B. C., Jensen, J. L., and Carbonneau, P. E., 2013, Topographic structure from motion: a new development in photogrammetric measurement: Earth Surface Processes and Landforms, v. 38, no. 4, p. 421-430, 10.1002/esp.3366.
Fonstad, M. A., and Marcus, W. A., 2005, Remote sensing of stream depths with hydraulically assisted bathymetry (HAB) models: Geomorphology, v. 72, no. 1-4, p. 320-339,
Formento-Trigilio, M. L., Burbank, D. W., Nicol, A., Shulmeister, J., and Rieser, U., 2003, River response to an active fold-and-thrust belt in a convergent margin setting, North Island, New Zealand: Geomorphology, v. 49, no. 1-2, p. 125-152, 10.1016/s0169-555x(02)00167-8.
Fremier, A. K., Yanites, B. J., and Yager, E. M., 2018, Sex that moves mountains: The influence of spawning fish on river profiles over geologic timescales: Geomorphology, v. 305, p. 163-172, https://doi.org/10.1016/j.geomorph.2017.09.033.
Frostick, L. E., and Jones, S. J., 2002, Impact of periodicity on sediment flux in alluvial systems: grain to basin scale: Geological Society, London, Special Publications, v. 191, no. 1, p. 81-95, 10.1144/gsl.sp.2002.191.01.06.
Fryirs, K., 2013, (Dis)Connectivity in catchment sediment cascades: a fresh look at the sediment delivery problem: Earth Surface Processes and Landforms, v. 38, no. 1, p. 30-46, 10.1002/esp.3242.
Fryirs, K., and Brierley, G. J., 2010, Antecedent controls on river character and behaviour in partly confined valley settings: Upper Hunter catchment, NSW, Australia: Geomorphology, v. 117, no. 1-2, p. 106-120, 10.1016/j.geomorph.2009.11.015.
Fryirs, K. A., 2017, River sensitivity: a lost foundation concept in fluvial geomorphology: Earth Surface Processes and Landforms, v. 42, no. 1, p. 55-70, https://doi.org/10.1002/esp.3940.
Fryirs, K. A., and Brierley, G. J., 2012, Geomorphic analysis of river systems: an approach to reading the landscape, Chichester, UK, John Wiley & Sons,
Fryirs, K. A., Brierley, G. J., Preston, N. J., and Kasai, M., 2007, Buffers, barriers and blankets: The (dis)connectivity of catchment-scale sediment cascades: Catena, v. 70, no. 1, p. 49-67, 10.1016/j.catena.2006.07.007.
Fuller, I., 2014, Towards an Understanding of Catchment-scale Sediment Dynamics: Cascades & Connectivity in Steepland Systems: International Journal of Erosion Control Engineering, v. 7, p. 1-8, 10.13101/ijece.7.
Fuller, I. C., 2007, Geomorphic Work during a “150-Year” Storm: Contrasting Behaviors of River Channels in a New Zealand Catchment: Annals of the Association of American Geographers, v. 97, no. 4, p. 665-676,
Fuller, I. C., 2008, Geomorphic impacts of a 100-year flood: Kiwitea Stream, Manawatu catchment, New Zealand: Geomorphology, v. 98, no. 1, p. 84-95, https://doi.org/10.1016/j.geomorph.2007.02.026.
Fuller, I. C., 2010, Waingawa River Channel Change 1943-2009: A Quantitative Geomorphological Analysis: Massey University,
Fuller, I. C., Death, R. G., Garcia, J. H., Trenc, N., Pratt, R., Pitiot, C., Matoš, B., Ollero, A., Neverman, A., and Death, A., 2021, An index to assess the extent and success of river and floodplain restoration: Recognising dynamic response trajectories and applying a process-based approach to managing river recovery: River Research and Applications, v. 37, no. 2, p. 163-175, https://doi.org/10.1002/rra.3672.
Fuller, I. C., Gilvear, D. J., Thoms, M. C., and Death, R. G., 2019a, Framing resilience for river geomorphology: Reinventing the wheel?: River Research and Applications, v. 35, no. 2, p. 91-106, 10.1002/rra.3384.

Fuller, I. C., Large, A. R. G., Charlton, M. E., Heritage, G. L., and Milan, D. J., 2003a, Reach-scale sediment transfers: An evaluation of two morphological budgeting approaches: Earth Surface Processes and Landforms, v. 28, no. 8, p. 889-903, 10.1002/esp.1011.

Fuller, I. C., Large, A. R. G., and Milan, D. J., 2003b, Quantifying channel development and sediment transfer following chute cutoff in a wandering gravel-bed river: Geomorphology, v. 54, no. 3-4, p. 307-323, 10.1016/s0169-555x(02)00374-4.

Fuller, I. C., Macklin, M. G., Toonen, W. H. J., Turner, J., and Norton, K., 2019b, A 2000 year record of palaeofloods in a volcanically-reset catchment: Whanganui River, New Zealand: Global and Planetary Change, v. 181, p. 102981, https://doi.org/10.1016/j.gloplacha.2019.102981.

Fuller, I. C., and Marden, M., 2011, Slope-channel coupling in steepland terrain: A field-based conceptual model from the Tarndale gully and fan, Waipaoa catchment, New Zealand: Geomorphology, v. 128, no. 3-4, p. 105-115, 10.1016/j.geomorph.2010.12.018.

Fuller, I. C., Passmore, D. G., Heritage, G. L., Large, A. R. G., Milan, D. J., and Brewer, P. A., 2002, Annual sediment budgets in an unstable gravel-bed river: the River Coquet, northern England: Geological Society, London, Special Publications, v. 191, no. 1, p. 115-131, 10.1144/gsl.sp.2002.191.01.08.

Fuller, I. C., Richardson, J. M., Basher, L., Dykes, R. C., and Vale, S. S., 2011, Responses to river management? Geomorphic change over decadal and annual timescales in two gravel-bed rivers in New Zealand, *in* Molina, D. A., ed., River channels: types, dynamics and changes, Nova Science Publishers, Inc.,

Fuller, I. C., Riedler, R. A., Bell, R., Marden, M., and Glade, T., 2016a, Landslide-driven erosion and slope-channel coupling in steep, forested terrain, Ruahine Ranges, New Zealand, 1946-2011: Catena, v. 142, p. 252-268, 10.1016/j.catena.2016.03.019.

Fuller, T. K., Gran, K. B., Sklar, L. S., and Paola, C., 2016b, Lateral erosion in an experimental bedrock channel: The influence of bed roughness on erosion by bed load impacts: Journal of Geophysical Research: Earth Surface, v. 121, no. 5, p. 1084-1105, 10.1002/2015jf003728.

Gaeuman, D., Schmidt, J. C., and Wilcock, P. R., 2005, Complex channel responses to changes in stream flow and sediment supply on the lower Duchesne River, Utah: Geomorphology, v. 64, no. 3, p. 185-206, https://doi.org/10.1016/j.geomorph.2004.06.007.

Galia, T., and Škarpich, V., 2016, Do the coarsest bed fractions and stream power record contemporary trends in steep headwater channels?: Geomorphology, v. 272, p. 115-126, https://doi.org/10.1016/j.geomorph.2015.07.047.

Gaurav, K., Tandon, S. K., Devauchelle, O., Sinha, R., and Métivier, F., 2017, A single width–discharge regime relationship for individual threads of braided and meandering rivers from the Himalayan Foreland: Geomorphology, v. 295, p. 126-133, https://doi.org/10.1016/j.geomorph.2017.07.004.

Gessesse, G. D., Fuchs, H., Mansberger, R., Klik, A., and Rieke-Zapp, D. H., 2010, Assessment of Erosion, Deposition and Rill Development On Irregular Soil Surfaces Using Close Range Digital Photogrammetry: The Photogrammetric Record, v. 25, no. 131, p. 299-318, 10.1111/j.1477-9730.2010.00588.x.

Ghani, M. A., 1978, Late Cenozoic vertical crustal movements in the southern North Island, New Zealand: New Zealand Journal of Geology and Geophysics, v. 21, no. 1, p. 117-125, 10.1080/00288306.1978.10420728.

Giberson, C., 2019, Hiding in Plain Sight (Summary), Tonkin and Taylor, https://www.tonkintaylor.co.nz/media/1290/gibersonplus2019plushidingplusinplusfullplussitecleaned.pdf

Gibling, M. R., and Davies, N. S., 2012, Palaeozoic landscapes shaped by plant evolution: Nature Geoscience, v. 5, no. 2, p. 99-105, 10.1038/ngeo1376.

Gibling, M. R., Davies, N. S., Falcon-Lang, H. J., Bashforth, A. R., DiMichele, W. A., Rygel, M. C., and Ielpi, A., 2014, Palaeozoic co-evolution of rivers and vegetation: a synthesis of current

knowledge: Proceedings of the Geologists' Association, v. 125, no. 5, p. 524-533, https://doi.org/10.1016/j.pgeola.2013.12.003.
Gilbert, G. K., 1877, Report on the geology of the Henry Mountains, http://pubs.er.usgs.gov/publication/70039916, 10.3133/70039916.
Gilet, L., Gob, F., Gautier, E., Houbrechts, G., Virmoux, C., and Thommeret, N., 2020, Hydro-morphometric parameters controlling travel distance of pebbles and cobbles in three gravel bed streams: Geomorphology, v. 358, p. 107117, https://doi.org/10.1016/j.geomorph.2020.107117.
Gill, J., and Malamud, B., 2014, Reviewing and visualizing the interactions of natural hazards: Reviews of Geophysics, v. 52, p. 680–722, 10.1002/2013RG000445.
Gilvear, D., and Bryant, M. D., 2016, Analysis of remotely sensed data for fluvial geomorphology and river science, Tools in Fluvial Geomorphology, John Wiley & Sons, Ltd, p. 103-132, 10.1002/9781118648551.ch6.
Gilvear, D., and Bryant, R., 2003, Analysis of Aerial Photography and Other Remotely Sensed Data, *in* Kondolf, M., and Piegay, H., eds., Tools in Fluvial Geomorphology, p. 133-168,
Gilvear, D., Winterbottom, S., and Sichingabula, H., 2000, Character of channel planform change and meander development: Luangwa River, Zambia: Earth Surface Processes and Landforms, v. 25, no. 4, p. 421-436, 10.1002/(sici)1096-9837(200004)25:4<421::Aid-esp65>3.0.Co;2-q.
Gilvear, D. J., Waters, T. M., and Milner, A. M., 1995, Image analysis of aerial photography to quantify changes in channel morphology and instream habitat following placer mining in interior Alaska: Freshwater Biology, v. 34, no. 2, p. 389-398, 10.1111/j.1365-2427.1995.tb00897.x.
Glade, T., and Crozier, M. J., 2005, The Nature of Landslide Hazard Impact, *in* Glade, T., Anderson, M. G., and Crozier, M. J., eds., Landslide Hazard and Risk: Chichester, John Wiley & Sons, p. 21-60,
GNS Science, 2017, How often do earthquakes occur along the fault?, Volume 2017: Wellington, GNS Science, https://www.gns.cri.nz/Home/Learning/Science-Topics/Earthquakes/Major-Faults-in-New-Zealand/Wellington-Fault/How-often-do-earthquakes-occur-along-the-fault
-, 2020, Active Faults Database: Wellington, GNS, https://data.gns.cri.nz/af/
-, 2021, Earthquake Catalogue, https://www.geonet.org.nz/data/types/eq_catalogue
Gomez, C., Oguchi, T., and Evans, I. S., 2015, Spatial analysis in geomorphology (1): Present directions, from collection to processing: Geomorphology, v. 242, p. 1-2, https://doi.org/10.1016/j.geomorph.2015.04.026.
Goodchild, M. F., Spatial accuracy 2.0, *in* Proceedings Proceedings of the eighth international symposium on spatial accuracy assessment in natural resources and environmental sciences2008, Volume 1, Citeseer, p. 1-7.
Gordon, M., 2012, Hydrological statistics for surface water monitoring sites in the Wellington region: Greater Wellington Regional Council,
Goudie, A. S., 2016, Quantification of rock control in geomorphology: Earth-Science Reviews, v. 159, p. 374-387, https://doi.org/10.1016/j.earscirev.2016.06.012.
Grabowski, R. C., and Gurnell, A. M., 2003, Using historical data in fluvial geomorphology, *in* Kondolf, G. M., and Piegay, H., eds., Tools in Fluvial Geomorphology: Chichester, John Wiley & Sons, Ltd, p. 77-101, 10.1002/9781118648551.ch4.
-, 2016, Using historical data in fluvial geomorphology, Tools in Fluvial Geomorphology, John Wiley & Sons, Ltd, p. 56-75, 10.1002/9781118648551.ch4.
Graf, W., 1977, The Rate Law in Fluvial Geomorphology: American Journal of Science, v. 277, p. 178-191, 10.2475/ajs.277.2.178.
Graf, W. L., 2000, Locational probability for a dammed, urbanizing stream: Salt River, Arizona, USA: Environmental Management, v. 25, no. 3, p. 321-335,
-, 2008, Sources of uncertainty in river restoration research, River restoration: Managing the uncertainty in restoring physical habitat, Wiley, p. 15-19,

Grant, G. E., O'Connor, J., and Safran, E., 2017, Excursions in fluvial (dis)continuity: Geomorphology, v. 277, no. Supplement C, p. 145-153, https://doi.org/10.1016/j.geomorph.2016.08.033.
Grant, H., 2005, Natural hazards - background report: Greater Wellington Regional Council,
Grapes, R., 1988, Geology And Revegetation Of An 1855 Landslide, Ruamahanga River, Kopuaranga, Wairarapa: Tuatara, v. 30, no. 1, p. 77-83, http://nzetc.victoria.ac.nz/tm/scholarly/tei-Bio30Tuat01-t1-body-d10.html
-, 2000, Magnitude Eight Plus: New Zealand's Biggest Earthquake, Wellington, NZ, Victoria University Press,
Grapes, R., and Downes, G., 1997, The 1855 Wairarapa, New Zealand, Earthquake - Analysis of historical data: Bulletin of the New Zealand Society for Earthquake Engineering, v. 30, no. 4, p. 271-368, 10.5459/bnzsee.30.4.271-368.
Grapes, R. H., 1991, Aggradation Surfaces And Implications For Displacement Rates Along The Wairarapa Fault, Southern North Island, New-Zealand: Catena, v. 18, no. 5, p. 453-469, 10.1016/0341-8162(91)90049-4.
Graveleau, F., Strak, V., Dominguez, S., Malavieille, J., Chatton, M., Manighetti, I., and Petit, C., 2015, Experimental modelling of tectonics–erosion–sedimentation interactions in compressional, extensional, and strike–slip settings: Geomorphology, v. 244, no. Supplement C, p. 146-168, https://doi.org/10.1016/j.geomorph.2015.02.011.
Gregory, K. J., 1979, River Channels, *in* Gregory, K. J., ed., Man and Environmental Processes: New York, Routledge, 10.4324/9780429051708.
Gregory, K. J., 2006, The human role in changing river channels: Geomorphology, v. 79, no. 3-4, p. 172-191,
Gregory, S., Wildman, R., Hulse, D., Ashkenas, L., and Boyer, K., 2019, Historical changes in hydrology, geomorphology, and floodplain vegetation of the Willamette River, Oregon: River Research and Applications, p. 12, 10.1002/rra.3495.
Guha-Sapir, D., 2020, Emergency Disasters Data Base (EM-DAT),, *in* UCLouvain, C., ed.: Brussels, Belgium, Centre for Research on the Epidemiology of Disasters, https://public.emdat.be/
Gupta, A., 1983, High-Magnitude Floods and Stream Channel Response, Modern and Ancient Fluvial Systems, p. 219-227, https://doi.org/10.1002/9781444303773.ch17.
Gupta, A., and Fox, H., 1974, Effects of high-magnitude floods on channel form: A case study in Maryland Piedmont: Water Resources Research, v. 10, no. 3, p. 499-509, https://doi.org/10.1029/WR010i003p00499.
Gupta, N., Kleinhans, M. G., Addink, E. A., Atkinson, P. M., and Carling, P. A., 2014, One-dimensional modeling of a recent Ganga avulsion: Assessing the potential effect of tectonic subsidence on a large river: Geomorphology, v. 213, p. 24-37, https://doi.org/10.1016/j.geomorph.2013.12.038.
Gurnell, A., 2014, Plants as river system engineers: Earth Surface Processes and Landforms, v. 39, no. 1, p. 4-25, 10.1002/esp.3397.
Gurnell, A., Tockner, K., Edwards, P., and Petts, G., 2005, Effects of deposited wood on biocomplexity of river corridors: Frontiers in Ecology and the Environment, v. 3, no. 7, p. 377-382, 10.1890/1540-9295(2005)003[0377:Eodwob]2.0.Co;2.
Gurnell, A. M., 1997, Channel change on the River Dee meanders, 1946–1992, from the analysis of air photographs: Regulated Rivers: Research & Management, v. 13, no. 1, p. 13-26, 10.1002/(sici)1099-1646(199701)13:1<13::Aid-rrr420>3.0.Co;2-w.
-, 1998, The hydrogeomorphological e•ects of beaver dam-building activity: Progress in Physical Geography: Earth and Environment, v. 22, no. 2, p. 167-189, 10.1177/030913339802200202.
Gurnell, A. M., Bertoldi, W., and Corenblit, D., 2012, Changing river channels: The roles of hydrological processes, plants and pioneer fluvial landforms in humid temperate, mixed load, gravel bed rivers: Earth-Science Reviews, v. 111, no. 1, p. 129-141, https://doi.org/10.1016/j.earscirev.2011.11.005.

Gurnell, A. M., Downward, S. R., and Jones, R., 1994, Channel planform change on the river dee meanders, 1876–1992: Regulated Rivers: Research & Management, v. 9, no. 4, p. 187-204, 10.1002/rrr.3450090402.
GWRC, 2021a, Waingawa River streamflow at Kaituna, http://graphs.gw.govt.nz/?siteName=Waingawa%20River%20at%20Kaituna&dataSource=Flow
GWRC, G. W. R. C., 2021b, Environmental Monitoring and Research, Volume 2021, https://graphs.gw.govt.nz/
Hajek, E. A., and Edmonds, D. A., 2014, Is river avulsion style controlled by floodplain morphodynamics?: Geology, v. 42, no. 3, p. 199-202, 10.1130/g35045.1.
Hajek, E. A., Heller, P. L., and Sheets, B. A., 2010, Significance of channel-belt clustering in alluvial basins: Geology, v. 38, no. 6, p. 535-538, 10.1130/g30783.1.
Hajek, E. A., and Wolinsky, M. A., 2012, Simplified process modeling of river avulsion and alluvial architecture: Connecting models and field data: Sedimentary Geology, v. 257-260, p. 1-30, https://doi.org/10.1016/j.sedgeo.2011.09.005.
Ham, D. G., and Church, M., 2000, Bed-material transport estimated from channel morphodynamics: Chilliwack River, British Columbia: Earth Surface Processes and Landforms, v. 25, no. 10, p. 1123-1142, 10.1002/1096-9837(200009)25:10<1123::aid-esp122>3.0.co;2-9.
Hansford, M. R., and Plink-Björklund, P., 2020, River discharge variability as the link between climate and fluvial fan formation: Geology, v. 48, no. 10, p. 952-956, 10.1130/g47471.1.
Harbert, S. A., Duvall, A. R., and Tucker, G. E., 2018, The Role of Near-Fault Relief Elements in Creating and Maintaining a Strike-Slip Landscape: Geophysical Research Letters, v. 45, no. 21, p. 11,683-611,692, https://doi.org/10.1029/2018GL080045.
Harley, G., 2014, Te Kauru Upper Ruamahanga: Current River and Flood Risk Management, *in* Protection, F., ed.: Wellington, Greater Wellington Regional Council, p. 192,
Harvey, A. M., 2001, Coupling between hillslopes and channels in upland fluvial systems: implications for landscape sensitivity, illustrated from the Howgill Fells, northwest England: CATENA, v. 42, no. 2, p. 225-250, https://doi.org/10.1016/S0341-8162(00)00139-9.
-, 2002, Effective timescales of coupling within fluvial systems: Geomorphology, v. 44, no. 3-4, p. 175-201, 10.1016/s0169-555x(01)00174-x.
Harvey, G. L., Henshaw, A. J., Brasington, J., and England, J., 2019, Burrowing Invasive Species: An Unquantified Erosion Risk at the Aquatic-Terrestrial Interface: Reviews of Geophysics, v. 57, no. 3, p. 1018-1036, https://doi.org/10.1029/2018RG000635.
Harwood, K., and Brown, A. G., 1993, Fluvial processes in a forested anastomosing river: Flood partitioning and changing flow patterns: Earth Surface Processes and Landforms, v. 18, no. 8, p. 741-748, 10.1002/esp.3290180808.
Haschenburger, J. K., 2013, Tracing river gravels: Insights into dispersion from a long-term field experiment: Geomorphology, v. 200, p. 121-131, https://doi.org/10.1016/j.geomorph.2013.03.033.
Hassan, M. A., Church, M., and Ashworth, P. J., 1992, Virtual Rate And Mean Distance Of Travel Of Individual Clasts In Gravel-Bed Channels: Earth Surface Processes and Landforms, v. 17, no. 6, p. 617-627, 10.1002/esp.3290170607.
Hassan, M. A., Gottesfeld, A. S., Montgomery, D. R., Tunnicliffe, J. F., Clarke, G. K. C., Wynn, G., Jones-Cox, H., Poirier, R., MacIsaac, E., Herunter, H., and Macdonald, S. J., 2008, Salmon-driven bed load transport and bed morphology in mountain streams: Geophysical Research Letters, v. 35, no. 4, 10.1029/2007gl032997.
Heckmann, T., Cavalli, M., Cerdan, O., Foerster, S., Javaux, M., Lode, E., Smetanová, A., Vericat, D., and Brardinoni, F., 2018, Indices of sediment connectivity: opportunities, challenges and limitations: Earth-Science Reviews, v. 187, p. 77-108, https://doi.org/10.1016/j.earscirev.2018.08.004.

Heckmann, T., and Schwanghart, W., 2013, Geomorphic coupling and sediment connectivity in an alpine catchment — Exploring sediment cascades using graph theory: Geomorphology, v. 182, p. 89-103, https://doi.org/10.1016/j.geomorph.2012.10.033.
Heller, P. L., and Paola, C., 1996, Downstream changes in alluvial architecture; an exploration of controls on channel-stacking patterns: Journal of Sedimentary Research, v. 66, no. 2, p. 297-306, 10.1306/d4268333-2b26-11d7-8648000102c1865d.
Henderson, F. M., 1966, Open Channel Flow, Macmillan:, 522 p,
Hendrery, S., 2017, Did November's 7.8 shake create a 'quake lake' in the Tararuas?, Stuff.com, https://www.stuff.co.nz/environment/90608086/did-novembers-78-shake-create-a-quake-lake-in-the-tararuas
Heritage, G., Fuller, I. C., Charlton, M., Brewer, P., and Passmore, D., 1998, CDW photogrammetry of low relief fluvial features: accuracy and implications for reach-scale sediment budgeting: Earth Surface Processes and Landforms: The Journal of the British Geomorphological Group, v. 23, no. 13, p. 1219-1233,
Herzig, A., Dymond, J. R., and Marden, M., 2011, A gully-complex model for assessing gully stabilisation strategies: Geomorphology, v. 133, no. 1, p. 23-33, https://doi.org/10.1016/j.geomorph.2011.06.012.
Heslop, I., 1995, The Upper Ruamahanga River & Floodplain Investigation Phase 1 - Issues: Wellington Regional Council,
-, 1996, The Upper Ruamahanga River & Floodplain Investigation Phase 2 - Options: Wellington Regional Council,
Hey, R. D., and Thorne, C. R., 1986, Stable channels with mobile gravel beds: Journal of Hydraulic engineering, v. 112, no. 8, p. 671-689,
Hickin, E. J., 1983, River Channel Changes: Retrospect and Prospect, *in* Collinson, J. D., and Lewin, J., eds., Modern and Ancient Fluvial Systems: Boston, Blackwell, p. 59-83, 10.1002/9781444303773.ch5.
Hicks, D. M., Shankar, U., McKerchar, A. I., Basher, L., Lynn, I., Page, M., and Jessen, M., 2011, Suspended sediment yields from New Zealand rivers: Journal of Hydrology (New Zealand), v. 50, no. 1, p. 81-142, www.jstor.org/stable/43945015
Hicks, M., Duncan, M., Walsh, J., Westaway, R., and Lane, S., 2002, New views of the morphodynamics of large braided rivers from high-resolution topographic surveys and time-lapse video: IAHS-AISH Publication,
Hill, R. D., 1963, The Vegetation of the Wairarapa in Mid-Nineteenth Century: Tuatara, v. 11, no. 2,
Hjulstrøm, F., Transportation of debris by moving water, *in* Proceedings Recent Marine Sediments; A Symposium, Tulsa, Oklahoma, 1939,
Hoffmann, T., Thorndycraft, V. R., Brown, A. G., Coulthard, T. J., Damnati, B., Kale, V. S., Middelkoop, H., Notebaert, B., and Walling, D. E., 2010, Human impact on fluvial regimes and sediment flux during the Holocene: Review and future research agenda: Global and Planetary Change, v. 72, no. 3, p. 87-98, https://doi.org/10.1016/j.gloplacha.2010.04.008.
Hohensinner, S., Jungwirth, M., Muhar, S., and Schmutz, S., 2014, Importance of multi-dimensional morphodynamics for habitat evolution: Danube River 1715–2006: Geomorphology, v. 215, p. 3-19, https://doi.org/10.1016/j.geomorph.2013.08.001.
Holbrook, J. M., and Schumm, S. A., 1999, Geomorphic and sedimentary response of rivers to tectonic deformation: a brief review and critique of a tool for recognizing subtle epeirogenic deformation in modern and ancient settings: Tectonophysics, v. 305, p. 287-306,
Hood, G. A., and Larson, D. G., 2015, Ecological engineering and aquatic connectivity: a new perspective from beaver-modified wetlands: Freshwater Biology, v. 60, no. 1, p. 198-208, https://doi.org/10.1111/fwb.12487.
Hooke, J., 2003, Coarse sediment connectivity in river channel systems: a conceptual framework and methodology: Geomorphology, v. 56, no. 1, p. 79-94, https://doi.org/10.1016/S0169-555X(03)00047-3.

Hooke, J. M., 2015, Variations in flood magnitude–effect relations and the implications for flood risk assessment and river management: Geomorphology, v. 251, p. 91-107, https://doi.org/10.1016/j.geomorph.2015.05.014.
-, 2019, Changing landscapes: Five decades of applied geomorphology: Geomorphology, https://doi.org/10.1016/j.geomorph.2019.06.007.
Hooke, J. M., and Kain, J. P., 1983, Historical Change in the Physical Environment: A Guide to Sources and Techniques, London, Butterworth,
Hopkins, M. C., and Dawers, N. H., 2015, Changes in bedrock channel morphology driven by displacement rate increase during normal fault interaction and linkage: Basin Research, v. 27, no. 1, p. 43-59, https://doi.org/10.1111/bre.12072.
Houbrechts, G., Levecq, Y., Peeters, A., Hallot, E., Van Campenhout, J., Denis, A.-C., and Petit, F., 2015, Evaluation of long-term bedload virtual velocity in gravel-bed rivers (Ardenne, Belgium): Geomorphology, v. 251, p. 6-19, https://doi.org/10.1016/j.geomorph.2015.05.012.
Hoyle, J., Brooks, A., Brierley, G., Fryirs, K., and Lander, J., 2008, Spatial variability in the timing, nature and extent of channel response to typical human disturbance along the Upper Hunter River, New South Wales, Australia: Earth Surface Processes and Landforms, v. 33, no. 6, p. 868-889, https://doi.org/10.1002/esp.1580.
Hsu, L., Martin, R. L., McElroy, B., Litwin-Miller, K., and Kim, W., 2015, Data management, sharing, and reuse in experimental geomorphology: Challenges, strategies, and scientific opportunities: Geomorphology, v. 244, p. 180-189, https://doi.org/10.1016/j.geomorph.2015.03.039.
Huang, M.-W., Pan, Y.-W., and Liao, J.-J., 2013, A case of rapid rock riverbed incision in a coseismic uplift reach and its implications: Geomorphology, v. 184, p. 98-110, https://doi.org/10.1016/j.geomorph.2012.11.022.
Hugenholtz, C. H., Whitehead, K., Brown, O. W., Barchyn, T. E., Moorman, B. J., LeClair, A., Riddell, K., and Hamilton, T., 2013, Geomorphological mapping with a small unmanned aircraft system (sUAS): Feature detection and accuracy assessment of a photogrammetrically-derived digital terrain model: Geomorphology, v. 194, no. Supplement C, p. 16-24, https://doi.org/10.1016/j.geomorph.2013.03.023.
Hughes, M. L., McDowell, P. F., and Marcus, W. A., 2006, Accuracy assessment of georectified aerial photographs: Implications for measuring lateral channel movement in a GIS: Geomorphology, v. 74, no. 1-4, p. 1-16, 10.1016/j.geomorph.2005.07.001.
Hunter, G. J., and Goodchild, M., Managing uncertainty in spatial databases: Putting theory into practice, *in* Proceedings Papers from the Annual Conference-Urban and Regional Information Systems Association1993, Urisa Urban and Regional Information Systems, p. 15-15.
Hunter, N. M., Bates, P. D., Horritt, M. S., and Wilson, M. D., 2007, Simple spatially-distributed models for predicting flood inundation: A review: Geomorphology, v. 90, no. 3–4, p. 208-225, https://doi.org/10.1016/j.geomorph.2006.10.021.
Hutchings, J., Williams, J., and Lawson, L., 2019, Central Government Co-investment in River Management for Flood Protection: Critical Adaptation to Climate Change for a More Resilient New Zealand: Taranaki Regional Council, https://www.trc.govt.nz/assets/Documents/Research-reviews/hazards/FloodControlCoInvestment2019.pdf, https://www.trc.govt.nz/assets/Documents/Research-reviews/hazards/FloodControlCoInvestment2019.pdf
Inoue, T., Izumi, N., Shimizu, Y., and Parker, G., 2014, Interaction among alluvial cover, bed roughness, and incision rate in purely bedrock and alluvial-bedrock channel: Journal of Geophysical Research: Earth Surface, v. 119, no. 10, p. 2123-2146, 10.1002/2014jf003133.

Insurance Council of New Zealand, 2014, Protecting New Zealand from Natural Hazards: Insurance Council of New Zealand, https://www.icnz.org.nz/fileadmin/Assets/PDFs/icnz-protecting-nz-from-natural-hazards-2014.pdf, https://www.icnz.org.nz/fileadmin/Assets/PDFs/icnz-protecting-nz-from-natural-hazards-2014.pdf

International Commission for the Protection of the Rhine, 2002, Non structural flood plain management. Measures and their effectiveness: International Commission for the Protection of the Rhine,

Izumiyama, H., Uchida, T., Horie, K., and Sakurai, W., 2020, Characteristics of sediment dynamics following large-scale sediment supply events in mountain watersheds in Japan: Geomorphology, v. 367, p. 107301, https://doi.org/10.1016/j.geomorph.2020.107301.

James, L. A., 1999, Time and the persistence of alluvium: River engineering, fluvial geomorphology, and mining sediment in California: Geomorphology, v. 31, no. 1–4, p. 265-290, https://doi.org/10.1016/S0169-555X(99)00084-7.

James, L. A., Hodgson, M. E., Ghoshal, S., and Latiolais, M. M., 2012, Geomorphic change detection using historic maps and DEM differencing: The temporal dimension of geospatial analysis: Geomorphology, v. 137, no. 1, p. 181-198, https://doi.org/10.1016/j.geomorph.2010.10.039.

James, M., 2017, Precision maps and 3-D uncertainty-based topographic change detection with structure-from-motion photogrammetry,

James, M., and Robson, S., 2012, Straightforward reconstruction of 3D surfaces and topography with a camera: Accuracy and geoscience application: J. Geophysical Research, v. 117, p. F03017, 10.1029/2011JF002289.

James, M. R., Chandler, J. H., Eltner, A., Fraser, C., Miller, P. E., Mills, J. P., Noble, T., Robson, S., and Lane, S. N., 2019, Guidelines on the use of structure-from-motion photogrammetry in geomorphic research: Earth Surface Processes and Landforms, v. 44, no. 10, p. 2081-2084, 10.1002/esp.4637.

James, M. R., Pinkerton, H., and Robson, S., 2007, Image-based measurement of flux variation in distal regions of active lava flows: Geochemistry, Geophysics, Geosystems, v. 8, no. 3, 10.1029/2006gc001448.

James, M. R., and Robson, S., 2014, Mitigating systematic error in topographic models derived from UAV and ground-based image networks: Earth Surface Processes and Landforms, v. 39, no. 10, p. 1413-1420, 10.1002/esp.3609.

James, M. R., Robson, S., d'Oleire-Oltmanns, S., and Niethammer, U., 2017, Optimising UAV topographic surveys processed with structure-from-motion: Ground control quality, quantity and bundle adjustment: Geomorphology, v. 280, no. Supplement C, p. 51-66, https://doi.org/10.1016/j.geomorph.2016.11.021.

Javernick, L., Brasington, J., and Caruso, B., 2014, Modeling the topography of shallow braided rivers using Structure-from-Motion photogrammetry: Geomorphology, v. 213, p. 166-182, 10.1016/j.geomorph.2014.01.006.

Jensen, J., 2000, Remote Sensing of the Environment: An Earth Resource Perspective, New Jersey, Prentice Hall, Prentice Hall Series in Geographic Information Science, 550 p,

Jerolmack, D. J., and Mohrig, D., 2007, Conditions for branching in depositional rivers: Geology, v. 35, no. 5, p. 463-466, 10.1130/g23308a.1.

Jerolmack, D. J., and Paola, C., 2007, Complexity in a cellular model of river avulsion: Geomorphology, v. 91, no. 3–4, p. 259-270, https://doi.org/10.1016/j.geomorph.2007.04.022.

-, 2010, Shredding of environmental signals by sediment transport: Geophysical Research Letters, v. 37, no. 19, doi:10.1029/2010GL044638.

Jiao, R., Herman, F., and Seward, D., 2017, Late Cenozoic exhumation model of New Zealand: Impacts from tectonics and climate: Earth-Science Reviews, v. 166, p. 286-298, https://doi.org/10.1016/j.earscirev.2017.01.003.

Johnson, J. M., Munasinghe, D., Eyelade, D., and Cohen, S., 2019, An integrated evaluation of the National Water Model (NWM)–Height Above Nearest Drainage (HAND) flood mapping methodology: Nat. Hazards Earth Syst. Sci., v. 19, no. 11, p. 2405-2420, 10.5194/nhess-19-2405-2019.

Johnson, J. P. L., 2016, Gravel threshold of motion: a state function of sediment transport disequilibrium?: Earth Surf. Dynam., v. 4, no. 3, p. 685-703, 10.5194/esurf-4-685-2016.

Johnson, M. F., Reid, I., Rice, S. P., and Wood, P. J., 2009, Stabilization of fine gravels by net-spinning caddisfly larvae: Earth Surface Processes and Landforms, v. 34, no. 3, p. 413-423, https://doi.org/10.1002/esp.1750.

Johnson, M. F., Rice, S. P., and Reid, I., 2011, Increase in coarse sediment transport associated with disturbance of gravel river beds by signal crayfish (Pacifastacus leniusculus): Earth Surface Processes and Landforms, v. 36, no. 12, p. 1680-1692, 10.1002/esp.2192.

Jones, H. L., and Hajek, E. A., 2007, Characterizing avulsion stratigraphy in ancient alluvial deposits: Sedimentary Geology, v. 202, no. 1, p. 124-137, https://doi.org/10.1016/j.sedgeo.2007.02.003.

Jones, L. S., and Harper, J. T., 1998, Channel avulsions and related processes, and large-scale sedimentation patterns since 1875, Rio Grande, San Luis Valley, Colorado: GSA Bulletin, v. 110, no. 4, p. 411-421, 10.1130/0016-7606(1998)110<0411:Caarpa>2.3.Co;2.

Jones, L. S., and Schumm, S. A., 1999, Causes of avulsion: an overview, Fluvial sedimentology VI, Volume 28, Wiley Online Library, p. 171-178,

Jongman, B., Winsemius, H. C., Aerts, J. C. J. H., Coughlan de Perez, E., van Aalst, M. K., Kron, W., and Ward, P. J., 2015, Declining vulnerability to river floods and the global benefits of adaptation: Proceedings of the National Academy of Sciences, v. 112, no. 18, p. E2271-E2280, 10.1073/pnas.1414439112.

Kamp, P. J. J., 1992, Landforms of Wairarapa: A Geological Perspective, *in* Soons, J. M., and Selby, M. J., eds., Landforms of New Zealand, John Wiley & Sons Incorporated, p. 255-,

Keen-Zebert, A., Tooth, S., Rodnight, H., Duller, G. A. T., Roberts, H. M., and Grenfell, M., 2013, Late Quaternary floodplain reworking and the preservation of alluvial sedimentary archives in unconfined and confined river valleys in the eastern interior of South Africa: Geomorphology, v. 185, p. 54-66, https://doi.org/10.1016/j.geomorph.2012.12.004.

Keenan, L., Thompson, M. and Mzila, D., 2012, Freshwater allocation and availability in the Wellington region: state and trends: Greater Wellington Regional Council,

Keller, E., Adamaitis, C., Alessio, P., Anderson, S., Goto, E., Gray, S., Gurrola, L., and Morell, K., 2019, Applications in geomorphology: Geomorphology, p. 106729, https://doi.org/10.1016/j.geomorph.2019.04.001.

Keller, E. A., 1986, Investigation of Active Tectonics: Use of Surficial Earth Processes, *in* Council, N. R., ed., Active Tectonics: Impact on Society: Washington, DC, The National Academies Press, p. 136-147, doi:10.17226/624.

Khan, S., Fryirs, K., and Bizzi, S., 2021, Modelling sediment (dis)connectivity across a river network to understand locational-transmission-filter sensitivity for identifying hotspots of potential geomorphic adjustment: Earth Surface Processes and Landforms, v. n/a, no. n/a, https://doi.org/10.1002/esp.5213.

Kidová, A., Lehotský, M., and Rusnák, M., 2016, Geomorphic diversity in the braided-wandering Belá River, Slovak Carpathians, as a response to flood variability and environmental changes: Geomorphology, v. 272, p. 137-149, https://doi.org/10.1016/j.geomorph.2016.01.002.

Kidova, A., Radecki-Pawlik, A., Rusnák, M., and Plesiński, K., 2021, Hydromorphological evaluation of the river training impact on a multithread river system (Belá River, Carpathians, Slovakia): Scientific Reports, v. 11, 10.1038/s41598-021-85805-2.

Kidson, J. W., 2000, An analysis of New Zealand synoptic types and their use in defining weather regimes: International Journal of Climatology, v. 20, no. 3, p. 299-316, https://doi.org/10.1002/(SICI)1097-0088(20000315)20:3<299::AID-JOC474>3.0.CO;2-B.

Kirby, E., and Whipple, K., 2001, Quantifying differential rock-uplift rates via stream profile analysis: Geology, v. 29, no. 5, p. 415-418, 10.1130/0091-7613(2001)029<0415:qdrurv>2.0.co;2.
Kirby, E., and Whipple, K. X., 2012, Expression of active tectonics in erosional landscapes: Journal of Structural Geology, v. 44, p. 54-75, 10.1016/j.jsg.2012.07.009.
Kirby, R. P., 1991, Measurement Of Surface Roughness In Desert Terrain By Close Range Photogrammetry: The Photogrammetric Record, v. 13, no. 78, p. 855-875, 10.1111/j.1477-9730.1991.tb00753.x.
Kleinhans, M. G., Ferguson, R. I., Lane, S. N., and Hardy, R. J., 2013, Splitting rivers at their seams: bifurcations and avulsion: Earth Surface Processes and Landforms, v. 38, no. 1, p. 47-61, 10.1002/esp.3268.
Klingeman, P. C., and Emmett, W. W., 1982, Gravel bedload transport processes, *in* Hey, R. D., Bathurst, J. C., and Thorne, C. R., eds., Gravel Bed Rivers: New York, John Wiley, p. 141-169,
Knighton, D., 1998, Fluvial Forms and Processes: A New Perspective, London, Taylor and Francis,
Knox, J. C., 1972, Valley alluviation in southwestern Wisconsin: Annals of the Association of American Geographers, v. 62, no. 3, p. 401-410, 10.1111/j.1467-8306.1972.tb00872.x.
Kondolf, G. M., 1994, Geomorphic and environmental effects of instream gravel mining: Landscape and Urban Planning, v. 28, no. 2, p. 225-243, https://doi.org/10.1016/0169-2046(94)90010-8.
Kondolf, G. M., 1997a, Application of the pebble count notes on purpose, method, and variants: JAWRA Journal of the American Water Resources Association, v. 33, no. 1, p. 79-87, 10.1111/j.1752-1688.1997.tb04084.x.
Kondolf, G. M., 1997b, PROFILE: hungry water: effects of dams and gravel mining on river channels: Environmental management, v. 21, no. 4, p. 533-551,
Korup, O., 2004, Landslide-induced river channel avulsions in mountain catchments of southwest New Zealand: Geomorphology, v. 63, no. 1, p. 57-80, https://doi.org/10.1016/j.geomorph.2004.03.005.
Kovanen, D. J., and Slaymaker, O., 2004, Glacial imprints of the Okanogan Lobe, southern margin of the Cordilleran Ice Sheet: Journal of Quaternary Science, v. 19, no. 6, p. 547-565, https://doi.org/10.1002/jqs.855.
Kreibich, H., Bubeck, P., Van Vliet, M., and De Moel, H., 2015, A review of damage-reducing measures to manage fluvial flood risks in a changing climate: Mitigation and Adaptation Strategies for Global Change, no. 6,
Kritikos, T., and Robinson, T. R., 2014, Earthquake-generated landslide assessment of the Waiohine Catchment, Wellington: Department of Geological Sciences, University of Canterbury,
Kuhnle, R. A., 1992, Bed load transport during rising and falling stages on two small streams: Earth Surface Processes and Landforms, v. 17, no. 2, p. 191-197, https://doi.org/10.1002/esp.3290170206.
Kuo, C.-W., and Brierley, G., 2014, The influence of landscape connectivity and landslide dynamics upon channel adjustments and sediment flux in the Liwu Basin, Taiwan: Earth Surface Processes and Landforms, v. 39, no. 15, p. 2038-2055, 10.1002/esp.3598.
Kuo, C.-W., and Brierley, G. J., 2013, The influence of landscape configuration upon patterns of sediment storage in a highly connected river system: Geomorphology, v. 180, p. 255-266, 10.1016/j.geomorph.2012.10.015.
Lacey, C., 1929, Stable channels in alluvium: Proceedings of the Instituion of Civil Engineers, v. 229, p. 259-384,
LaChapelle, E., 1962, Assessing Glacier Mass Budgets by Reconnaissance Aerial Photography: Journal of Glaciology, v. 4, no. 33, p. 290-297, doi:10.3189/S0022143000027593.
Lallias-Tacon, S., Liébault, F., and Piégay, H., 2017, Use of airborne LiDAR and historical aerial photos for characterising the history of braided river floodplain morphology and vegetation responses: CATENA, v. 149, p. 742-759, https://doi.org/10.1016/j.catena.2016.07.038.

Lane, S. N., 2000, The Measurement of River Channel Morphology Using Digital Photogrammetry: The Photogrammetric Record, v. 16, no. 96, p. 937-961, 10.1111/0031-868x.00159.
Lane, S. N., and Chandler, J. H., 2003, Editorial: the generation of high quality topographic data for hydrology and geomorphology: new data sources, new applications and new problems: Earth Surface Processes and Landforms, v. 28, no. 3, p. 229-230, 10.1002/esp.479.
Lane, S. N., James, T. D., and Crowell, M. D., 2000, Application of Digital Photogrammetry to Complex Topography for Geomorphological Research: The Photogrammetric Record, v. 16, no. 95, p. 793-821, 10.1111/0031-868x.00152.
Lane, S. N., and Richards, K. S., 1997, Linking River Channel Form and Process: Time, Space and Causality Revisited: Earth Surface Processes and Landforms, v. 22, no. 3, p. 249-260, 10.1002/(SICI)1096-9837(199703)22:3<249::AID-ESP752>3.0.CO;2-7.
Lane, S. N., Richards, K. S., and Chandler, J. H., 1993, Developments in photogrammetry; the geomorphological potential: Progress in Physical Geography: Earth and Environment, v. 17, no. 3, p. 306-328, 10.1177/030913339301700302.
Lane, S. N., Richards, K. S., and Chandler, J. H., 1995, Morphological Estimation of the Time-Integrated Bed Load Transport Rate: Water Resources Research, v. 31, no. 3, p. 761-772, 10.1029/94wr01726.
-, 1996, Discharge and sediment supply controls on erosion and deposition in a dynamic alluvial channel: Geomorphology, v. 15, no. 1, p. 1-15, https://doi.org/10.1016/0169-555X(95)00113-J.
Lane, S. N., Tayefi, V., Reid, S. C., Yu, D., and Hardy, R. J., 2007, Interactions between sediment delivery, channel change, climate change and flood risk in a temperate upland environment: Earth Surface Processes and Landforms, v. 32, no. 3, p. 429-446, https://doi.org/10.1002/esp.1404.
Lane, S. N., Westaway, R. M., and Murray Hicks, D., 2003, Estimation of erosion and deposition volumes in a large, gravel-bed, braided river using synoptic remote sensing: Earth Surface Processes and Landforms, v. 28, no. 3, p. 249-271, 10.1002/esp.483.
Langridge, R. M., Ries, W. F., Litchfield, N. J., Villamor, P., Van Dissen, R. J., Barrell, D. J. A., Rattenbury, M. S., Heron, D. W., Haubrock, S., Townsend, D. B., Lee, J. M., Berryman, K. R., Nicol, A., Cox, S. C., and Stirling, M. W., 2016, The New Zealand Active Faults Database: New Zealand Journal of Geology and Geophysics, v. 59, p. 86-96, 0.1080/00288306.2015.1112818.
Langridge, R. M., Townsend, D., and Persaud, M., 2003, Paleoseismic assessment of the active Mokonui Fault, Wairarapa: Institute of Geological and Nuclear Sciences,
Latocha, A., 2014, Geomorphic connectivity within abandoned small catchments (Stołowe Mts, SW Poland): Geomorphology, v. 212, p. 4-15, https://doi.org/10.1016/j.geomorph.2013.04.030.
Lawler, D. M., 1993, The measurement of river bank erosion and lateral channel change: a review: Earth surface processes and landforms, v. 18, no. 9, p. 777-821,
Lea, D. M., and Legleiter, C. J., 2016a, Mapping spatial patterns of stream power and channel change along a gravel-bed river in northern Yellowstone: Geomorphology, v. 252, p. 66-79, 10.1016/j.geomorph.2015.05.033.
-, 2016b, Refining measurements of lateral channel movement from image time series by quantifying spatial variations in registration error: Geomorphology, v. 258, p. 11-20, 10.1016/j.geomorph.2016.01.009.
Leddy, J. O., Ashworth, P. J., and Best, J. L., 1993, Mechanisms of anabranch avulsion within gravel-bed braided rivers: observations from a scaled physical model: Geological Society, London, Special Publications, v. 75, no. 1, p. 119-127, 10.1144/gsl.Sp.1993.075.01.07.
Lee, J. M., and Begg, J., 2002, Geology of the Wairarapa Area: Institute of Geological and Nuclear Sciences, 0478097506,

Leeder, M. R., 1977, A Quantitative Stratigraphic Model for Alluvium, with Special Reference to Channel Deposit Density and Interconnectedness: Canadian Society of Petroleum Geologists, v. Memoir 5, p. 587-596,
Legleiter, C. J., and Marston, R. A., 2013, Introduction to the special issue: The field tradition in geomorphology: Geomorphology, v. 200, p. 1-8, https://doi.org/10.1016/j.geomorph.2013.06.004.
Leier, A. L., DeCelles, P. G., and Pelletier, J. D., 2005, Mountains, monsoons, and megafans: Geology, v. 33, no. 4, p. 289-292, 10.1130/g21228.1.
Lensen, G., and Vella, P., The Waiohine River Faulted Terrace Sequence1971,
Lensen, G. J., 1964, The general case of progressive fault displacement of flights of degradational terraces: New Zealand Journal of Geology and Geophysics, v. 7, p. 864-870,
Lenzi, M. A., Mao, L., and Comiti, F., 2004, Magnitude-frequency analysis of bed load data in an Alpine boulder bed stream: Water Resources Research, v. 40, no. 7, 10.1029/2003wr002961.
-, 2006, Effective discharge for sediment transport in a mountain river: Computational approaches and geomorphic effectiveness: Journal of Hydrology, v. 326, no. 1, p. 257-276, https://doi.org/10.1016/j.jhydrol.2005.10.031.
Leopold, L. B., 1992, Sediment Size That Determines Channel Morphology, Dynamics of Gravel-Bed Rivers, 297-311 p, <Go to ISI>://WOS:A1992BX19P00014
Leopold, L. B., and Maddock Jr, T., 1953, The hydraulic geometry of stream channels and some physiographic implications, 252, http://pubs.er.usgs.gov/publication/pp252, 10.3133/pp252.
Leopold, L. B., Wolman, M. G., and Miller, J. P., 1964, Fluvial processes in geomorphology, Courier Corporation, 522 p,
Lewin, J., 1977, River Channel Changes, Chichester, Wiley,
Lewin, J., Davies, B., and Wolfenden, P., 1977, Interactions between channel change and historic mining sediments, River channel changes, Wiley Chichester, p. 353-367,
Lewin, J., and Manton, M. M. M., 1975, Welsh floodplain studies: The nature of floodplain geometry: Journal of Hydrology, v. 25, no. 1, p. 37-50, https://doi.org/10.1016/0022-1694(75)90037-2.
Li, G., West, A. J., Densmore, A. L., Hammond, D. E., Jin, Z., Zhang, F., Wang, J., and Hilton, R. G., 2016a, Connectivity of earthquake-triggered landslides with the fluvial network: Implications for landslide sediment transport after the 2008 Wenchuan earthquake: Journal of Geophysical Research: Earth Surface, v. 121, no. 4, p. 703-724, https://doi.org/10.1002/2015JF003718.
Li, T., Li, J., and Zhang, D. D., 2020, Yellow River flooding during the past two millennia from historical documents: Progress in Physical Geography: Earth and Environment, v. 44, no. 5, p. 661-678, 10.1177/0309133319899821.
Li, Z. W., Yu, G. A., Brierley, G., and Wang, Z. Y., 2016b, Vegetative impacts upon bedload transport capacity and channel stability for differing alluvial planforms in the Yellow River source zone: Hydrology and Earth System Sciences, v. 20, no. 7, p. 3013-3025, 10.5194/hess-20-3013-2016.
Liang, M., Voller, V. R., and Paola, C., 2015, A reduced-complexity model for river delta formation – Part 1: Modeling deltas with channel dynamics: Earth Surf. Dynam., v. 3, no. 1, p. 67-86, 10.5194/esurf-3-67-2015.
Liao, K.-H., 2014, From flood control to flood adaptation: a case study on the Lower Green River Valley and the City of Kent in King County, Washington: Natural Hazards, v. 71, no. 1, p. 723-750, 10.1007/s11069-013-0923-4.
Liébault, F., and Piégay, H., 2002, Causes of 20th century channel narrowing in mountain and piedmont rivers of southeastern France: Earth Surface Processes and Landforms, v. 27, no. 4, p. 425-444, https://doi.org/10.1002/esp.328.
Lillesand, T., Kiefer, R. W., and Chipman, J., 2015, Remote sensing and image interpretation, John Wiley & Sons,

Limited, A. N., 2018, Wellington 0.3m Rural Aeiral Photos (2016-2017), *in* (GWRC), G. W. R. C., ed., Land Information New Zealand (LINZ), https://data.linz.govt.nz/layer/95496-wellington-03m-rural-aerial-photos-2016-2017/metadata/

Lindsay, J. B., and Ashmore, P. E., 2002, The effects of survey frequency on estimates of scour and fill in a braided river model: Earth Surface Processes and Landforms, v. 27, no. 1, p. 27-43, 10.1002/esp.282.

Lisenby, P. E., Croke, J., and Fryirs, K. A., 2017, Geomorphic effectiveness: a linear concept in a non-linear world: Earth Surface Processes and Landforms, p. n/a-n/a, 10.1002/esp.4096.

Lisenby, P. E., Fryirs, K. A., and Thompson, C. J., 2020, River sensitivity and sediment connectivity as tools for assessing future geomorphic channel behavior: International Journal of River Basin Management, v. 18, no. 3, p. 279-293, 10.1080/15715124.2019.1672705.

Lisle, T. E., 1995, Effects of Coarse Woody Debris and its Removal on a Channel Affected by the 1980 Eruption of Mount St. Helens, Washington: Water Resources Research, v. 31, no. 7, p. 1797-1808, https://doi.org/10.1029/95WR00734.

Litchfield, N. J., and Berryman, K. R., 2005, Correlation of fluvial terraces within the Hikurangi Margin, New Zealand: implications for climate and baselevel controls: Geomorphology, v. 68, no. 3, p. 291-313,

Little, T. A., Van Dissen, R., Schermer, E., and Carne, R., 2009, Late Holocene surface ruptures on the southern Wairarapa fault, New Zealand: Link between earthquakes and the uplifting of beach ridges on a rocky coast: Lithosphere, v. 1, no. 1, p. 4-28, 10.1130/l7.1.

Lloyd's of London, 2018, A world at risk: Closing the insurance gap, https://www.lloyds.com/_test/library/understanding-risk/a-world-at-risk, https://www.lloyds.com/_test/library/understanding-risk/a-world-at-risk

Lowell, K., On the incorporation of uncertainty into spatial data systems, *in* Proceedings GIS LIS-INTERNATIONAL CONFERENCE-1992, Volume 2, American Society for Photogrammetry and Remote Sensing, p. 484-484.

Luce, C. H., and Black, T. A., 1999, Sediment production from forest roads in western Oregon: Water Resources Research, v. 35, no. 8, p. 2561-2570, https://doi.org/10.1029/1999WR900135.

-, 2001, Spatial and Temporal Patterns in Erosion from Forest Roads, Land Use and Watersheds: Human Influence on Hydrology and Geomorphology in Urban and Forest Areas, p. 165-178, https://doi.org/10.1029/WS002p0165.

Macfarlane, W. W., Wheaton, J. M., Bouwes, N., Jensen, M. L., Gilbert, J. T., Hough-Snee, N., and Shivik, J. A., 2017, Modeling the capacity of riverscapes to support beaver dams: Geomorphology, v. 277, p. 72-99, https://doi.org/10.1016/j.geomorph.2015.11.019.

Mackey, B., Roering, J., and McKean, J., 2009, Long-term kinematics and sediment flux of an active earthflow, Eel River, California: Geology, v. 37, no. 9, p. 803-806,

Mackey, S. D., and Bridge, J. S., 1995, Three-dimensional model of alluvial stratigraphy; theory and applications: Journal of Sedimentary Research, v. 65, no. 1b, p. 7-31, 10.1306/d42681d5-2b26-11d7-8648000102c1865d.

Mackin, J. H., 1948, Concept of the graded river: GSA Bulletin, v. 59, no. 5, p. 463-512, 10.1130/0016-7606(1948)59[463:Cotgr]2.0.Co;2.

Macklin, M. G., Benito, G., Gregory, K. J., Johnstone, E., Lewin, J., Michczyńska, D. J., Soja, R., Starkel, L., and Thorndycraft, V. R., 2006, Past hydrological events reflected in the Holocene fluvial record of Europe: CATENA, v. 66, no. 1, p. 145-154, https://doi.org/10.1016/j.catena.2005.07.015.

Macklin, M. G., Fuller, I. C., Lewin, J., Maas, G. S., Passmore, D. G., Rose, J., Woodward, J. C., Black, S., Hamlin, R. H. B., and Rowan, J. S., 2002, Correlation of fluvial sequences in the Mediterranean basin over the last 200ka and their relationship to climate change: Quaternary Science Reviews, v. 21, no. 14, p. 1633-1641, https://doi.org/10.1016/S0277-3791(01)00147-0.

Macklin, M. G., and Lewin, J., 1989, Sediment Transfer And Transformation Of An Alluvial Valley Floor - The River South Tyne, Northumbria, UK: Earth Surface Processes and Landforms, v. 14, no. 3, p. 233-246, 10.1002/esp.3290140305.
-, 1997, Channel, floodplain and drainage basin response to environmental change, *in* Thorne, C. R., Hey, R. D., and Newson, M. D., eds., Applied fluvial geomorphology for river engineering and management: Chichester, John Wiley & Sons, p. 15-45,
Macklin, M. G., and Lewin, J., 2008, Alluvial responses to the changing Earth system: Earth Surface Processes and Landforms, v. 33, no. 9, p. 1374-1395, 10.1002/esp.1714.
-, 2015, The rivers of civilization: Quaternary Science Reviews, v. 114, p. 228-244, https://doi.org/10.1016/j.quascirev.2015.02.004.
Macklin, M. G., Lewin, J., and Woodward, J. C., 2012, The fluvial record of climate change: Phil. Trans. R. Soc. A., http://doi.org.ezproxy.massey.ac.nz/10.1098/rsta.2011.0608.
Macklin, M. G., Passmore, D. G., and Newson, M. D., 1998, Controls of Short- and Long-term River Instability: Processes and Patterns in Gravel-bed Rivers, Tyne Basin, England, *in* Klingeman, P. C., Beschta, R. L., Komar, P. D., and Bradley, J. B., eds., Gravel-Bed Rivers in the Envvironment, Volume IV: Highlands Ranch, Colorado, Water Resources Publications, LLC,
Madej, M. A., 2001, Erosion and sediment delivery following removal of forest roads: Earth Surface Processes and Landforms, v. 26, no. 2, p. 175-190, https://doi.org/10.1002/1096-9837(200102)26:2<175::AID-ESP174>3.0.CO;2-N.
Magilligan, F. J., 1992, Thresholds and the spatial variability of flood power during extreme floods: Geomorphology, v. 5, no. 3–5, p. 373-390, https://doi.org/10.1016/0169-555X(92)90014-F.
Magilligan, F. J., Phillips, J. D., James, L. A., and Gomez, B., 1998, Geomorphic and Sedimentological Controls on the Effectiveness of an Extreme Flood: The Journal of Geology, v. 106, no. 1, p. 87-96, 10.1086/516009.
Mai, T., Mushtaq, S., Reardon-Smith, K., Webb, P., Stone, R., Kath, J., and An-Vo, D.-A., 2020, Defining flood risk management strategies: A systems approach: International Journal of Disaster Risk Reduction, v. 47, p. 101550, https://doi.org/10.1016/j.ijdrr.2020.101550.
Makaske, B., Maathuis, B. H. P., Padovani, C. R., Stolker, C., Mosselman, E., and Jongman, R. H. G., 2012, Upstream and downstream controls of recent avulsions on the Taquari megafan, Pantanal, south-western Brazil: Earth Surface Processes and Landforms, v. 37, no. 12, p. 1313-1326, 10.1002/esp.3278.
Manawatu Times, 1917, Severe Earthquake, Manawatu Times, Volume XL: Palmerston North, NZ, p. 5, https://paperspast.natlib.govt.nz/newspapers/MT19170807.2.37
Manighetti, I., Perrin, C., Gaudemer, Y., Dominguez, S., Stewart, N., Malavieille, J., and Garambois, S., 2020, Repeated giant earthquakes on the Wairarapa fault, New Zealand, revealed by Lidar-based paleoseismology: Scientific Reports, v. 10, no. 1, p. 2124, 10.1038/s41598-020-59229-3.
Manners, R. B., Schmidt, J. C., and Scott, M. L., 2014, Mechanisms of vegetation-induced channel narrowing of an unregulated canyon river: Results from a natural field-scale experiment: Geomorphology, v. 211, p. 100-115, 10.1016/j.geomorph.2013.12.033.
Mao, L., 2012, The effect of hydrographs on bed load transport and bed sediment spatial arrangement: Journal of Geophysical Research: Earth Surface, v. 117, no. F3, https://doi.org/10.1029/2012JF002428.
-, 2018, The effects of flood history on sediment transport in gravel-bed rivers: Geomorphology, https://doi.org/10.1016/j.geomorph.2018.08.046.
Mao, L., Ravazzolo, D., and Bertoldi, W., 2020, The role of vegetation and large wood on the topographic characteristics of braided river systems: Geomorphology, v. 367, p. 107299, https://doi.org/10.1016/j.geomorph.2020.107299.
Marchese, E., Scorpio, V., Fuller, I., McColl, S., and Comiti, F., 2017, Morphological changes in Alpine rivers following the end of the Little Ice Age: Geomorphology, v. 295, p. 811-826, https://doi.org/10.1016/j.geomorph.2017.07.018.

Marcus, W. A., and Fonstad, M. A., 2008, Optical remote mapping of rivers at sub-meter resolutions and watershed extents: Earth Surface Processes and Landforms: The Journal of the British Geomorphological Research Group, v. 33, no. 1, p. 4-24,
Marcus, W. A., and Fonstad, M. A., 2010, Remote sensing of rivers: the emergence of a subdiscipline in the river sciences: Earth Surface Processes and Landforms, v. 35, no. 15, p. 1867-1872, 10.1002/esp.2094.
Martin, R. L., and Jerolmack, D. J., 2013, Origin of hysteresis in bed form response to unsteady flows: Water Resources Research, v. 49, no. 3, p. 1314-1333, https://doi.org/10.1002/wrcr.20093.
Martin, S. E., and Conklin, M. H., 2018, Tracking channel bed resiliency in forested mountain catchments using high temporal resolution channel bed movement: Geomorphology, v. 301, p. 68-78, https://doi.org/10.1016/j.geomorph.2017.10.026.
Martin, Y., and Church, M., 1995, Bed-material transport estimated from channel surveys: Vedder River, British Columbia: Earth Surface Processes and Landforms, v. 20, no. 4, p. 347-361,
Masoud, A. A., and Koike, K., 2011, Morphotectonics inferred from the analysis of topographic lineaments auto-detected from DEMs: Application and validation for the Sinai Peninsula, Egypt: Tectonophysics, v. 510, no. 3, p. 291-308, https://doi.org/10.1016/j.tecto.2011.07.010.
Masteller, C. C., and Finnegan, N. J., 2017, Interplay between grain protrusion and sediment entrainment in an experimental flume: Journal of Geophysical Research: Earth Surface, v. 122, no. 1, p. 274-289, https://doi.org/10.1002/2016JF003943.
Masteller, C. C., Finnegan, N. J., Turowski, J. M., Yager, E. M., and Rickenmann, D., 2019, History-Dependent Threshold for Motion Revealed by Continuous Bedload Transport Measurements in a Steep Mountain Stream: Geophysical Research Letters, v. 46, no. 5, p. 2583-2591, https://doi.org/10.1029/2018GL081325.
McCarthy, T. S., Ellery, W. N., and Stanistreet, I. G., 1992, Avulsion mechanisms on the Okavango fan, Botswana: the control of a fluvial system by vegetation: Sedimentology, v. 39, no. 5, p. 779-795, https://doi.org/10.1111/j.1365-3091.1992.tb02153.x.
McDowell, P. F., Webb III, T., and Bartlein, P. J., 1990, Long-term environmental change, *in* Turner II, B. L., Clarck, W. C., Kates, R. W., Richards, J. F., Mathews, J. T., and Meyer, W. B., eds., The Earth As Transformed by Human Actions: Global and Regional Changes in the Biosphere over the Past 300 Years: Victoria, Australia, Cambridge University Press, p. 143-162,
McLaren, J., 2002, A Night of Terror: Wairarapa's 1942 earthquake, Wairarapa Archive,
McSaveney, E., 2009, Floods - New Zealand's number one hazard, Te Ara - the Encyclopedia of New Zealand, http://www.TeAra.govt.nz/en/floods/1
Merriam-Webster, 2020, Merriam-Webster's Online Dictionary, https://www.merriam-webster.com/dictionary/dynamics
Métivier, F., Lajeunesse, E., and Devauchelle, O., 2017, Laboratory rivers: Lacey's law, threshold theory, and channel stability: Earth Surf. Dynam., v. 5, no. 1, p. 187-198, 10.5194/esurf-5-187-2017.
MfE, 2021, https://data.mfe.govt.nz/layer/53314-average-annual-rainfall-19722013/
Michalková, M., Piégay, H., Kondolf, G. M., and Greco, S. E., 2011, Lateral erosion of the Sacramento River, California (1942–1999), and responses of channel and floodplain lake to human influences: Earth Surface Processes and Landforms, v. 36, no. 2, p. 257-272, 10.1002/esp.2106.
Milan, D. J., Heritage, G. L., and Large, A. R. G., 2002, Tracer pebble entrainment and deposition loci: influence of flow character and implications for riffle-pool maintenance: Geological Society, London, Special Publications, v. 191, no. 1, p. 133-148, 10.1144/gsl.sp.2002.191.01.09.
Millar, R. G., 2000, Influence of bank vegetation on alluvial channel patterns: Water Resources Research, v. 36, no. 4, p. 1109-1118, 10.1029/1999wr900346.

Miller, A. J., 1994, Debris-fan constrictions and flood hydraulics in river canyons: Some implications from two-dimensional flow modelling: Earth Surface Processes and Landforms, v. 19, no. 8, p. 681-697, 10.1002/esp.3290190803.
-, 1995, Valley Morphology and Boundary Conditions Influencing Spatial Patterns of Flood Flow, *in* Costa, J. E., Miller, A. J., Potter, K. W., and Wilcock, P. R., eds., Natural and Anthropogenic Influences in Fluvial Geomorphology, Volume 89: Washington, D.C. USA, American Geophysical Union, p. 57-81, 10.1029/GM089p0057.
Miller, M. C., McCave, I. N., and Komar, P. D., 1977, Threshold of sediment motion under unidirectional currents: Sedimentology, v. 24, no. 4, p. 507-527, https://doi.org/10.1111/j.1365-3091.1977.tb00136.x.
Mills, E., 2005, Insurance in a Climate of Change: Science, v. 309, no. 5737, p. 1040-1044, 10.1126/science.1112121.
Ministry of Business Innovation and Employment, 2020, New Zealand Now: Natural Disasters, Volume 2020, www.newzealandnow.govt.nz/live-in-new-zealand/safety/natural-disasters
Misset, C., Recking, A., Legout, C., Bakker, M., Bodereau, N., Borgniet, L., Cassel, M., Geay, T., Gimbert, F., Navratil, O., Piegay, H., Valsangkar, N., Cazilhac, M., Poirel, A., and Zanker, S., 2020, Combining multi-physical measurements to quantify bedload transport and morphodynamics interactions in an Alpine braiding river reach: Geomorphology, v. 351, p. 106877, https://doi.org/10.1016/j.geomorph.2019.106877.
Mohleji, S., and Pielke, R., 2014, Reconciliation of Trends in Global and Regional Economic Losses from Weather Events: 1980–2008: Natural Hazards Review, v. 15, no. 4, p. 04014009, doi:10.1061/(ASCE)NH.1527-6996.0000141.
Mohrig, D., Heller, P. L., Paola, C., and Lyons, W. J., 2000, Interpreting avulsion process from ancient alluvial sequences: Guadalope-Matarranya system (northern Spain) and Wasatch Formation (western Colorado): GSA Bulletin, v. 112, no. 12, p. 1787-1803, 10.1130/0016-7606(2000)112<1787:Iapfaa>2.0.Co;2.
Monckton, C. G., 1994, An investigation into the spatial structure of error in digital elevation data: Innovations in GIS, v. 1, p. 201-211,
Montgomery, D. R., 1999, Process domains and the river continuum: Journal of the American Water Resources Association, v. 35, no. 2, p. 397-410, 10.1111/j.1752-1688.1999.tb03598.x.
Moody, J. A., 2017, Residence times and alluvial architecture of a sediment superslug in response to different flow regimes: Geomorphology, v. 294, p. 40-57, https://doi.org/10.1016/j.geomorph.2017.04.012.
Moody, L., 2008, Memo to the Salmon Recovery Funding Board: Large Woody Materials, *in* Office, G. s. S. R., ed.: Olympia, WA, p. 22,
Moog, D. B., and Whiting, P. J., 1998, Annual hysteresis in bed load rating curves: Water Resources Research, v. 34, no. 9, p. 2393-2399, https://doi.org/10.1029/98WR01658.
Moretto, J., Rigon, E., Mao, L., Picco, L., Delai, F., and Lenzi, M. A., 2014, Channel adjustments and island dynamics in the Brenta River (Italy) over the last 30 years: River Research and Applications, v. 30, no. 6, p. 719-732, 10.1002/rra.2676.
Morozova, G., Smith, N., and Rogers, J., 1999, Holocene avulsion history of the lower Saskatchewan fluvial system, Cumberland Marshes, Saskatchewan-Manitoba, Canada: Fluvial sedimentology VI, v. 28, p. 231-249,
Motha, J., Bradley, B., Paterson, J., Lee, R., Thomson, E., Tarbali, K., Huang, J., Schill, C., Polak, V., and Lagrava, D., 2020, Cybershake NZ v20.8: New Zealand simulation-based probabilistic seismic hazard analysis, https://hdl.handle.net/10092/101435
Mount, N., and Louis, J., 2005, Estimation and propagation of error in measurements of river channel movement from aerial imagery: Earth Surface Processes and Landforms, v. 30, no. 5, p. 635-643, 10.1002/esp.1172.
Murray, A. B., 2007, Reducing model complexity for explanation and prediction: Geomorphology, v. 90, no. 3–4, p. 178-191, https://doi.org/10.1016/j.geomorph.2006.10.020.

Nadler, C. T., and Schumm, S. A., 1981, Metamorphosis of South Platte and Arkansas Rivers, eastern Colorado: Physical Geography, v. 2, no. 2, p. 95-115, 10.1080/02723646.1981.10642207.
Naito, K., and Parker, G., 2019, Can Bankfull Discharge and Bankfull Channel Characteristics of an Alluvial Meandering River be Cospecified From a Flow Duration Curve?: Journal of Geophysical Research: Earth Surface, v. 124, no. 10, p. 2381-2401, https://doi.org/10.1029/2018JF004971.
Nanson, G. C., 1980, A Regional Trend to Meander Migration: The Journal of Geology, v. 88, no. 1, p. 100-108, 10.1086/628477.
Nanson, G. C., 1986, Episodes of vertical accretion and catastrophic stripping: A model of disequilibrium flood-plain development: GSA Bulletin, v. 97, no. 12, p. 1467-1475, 10.1130/0016-7606(1986)97<1467:Eovaac>2.0.Co;2.
Nanson, G. C., and Hickin, E. J., 1986, A statistical analysis of bank erosion and channel migration in western Canada: GSA Bulletin, v. 97, no. 4, p. 497-504, 10.1130/0016-7606(1986)97<497:Asaobe>2.0.Co;2.
Nash, D., 1994, Effective Sediment-Transporting Discharge from Magnitude-Frequency Analysis: The Journal of Geology, v. 102, no. 1, p. 79-95, 10.1086/629649.
National Research Council, 1982, Committee on a Levee Policy for the National Flood Insurance Program: National Academy Press,
Navratil, O., and Albert, M. B., 2010, Non-linearity of reach hydraulic geometry relations: Journal of Hydrology, v. 388, no. 3, p. 280-290, https://doi.org/10.1016/j.jhydrol.2010.05.007.
Navratil, O., Albert, M. B., Hérouin, E., and Gresillon, J. M., 2006, Determination of bankfull discharge magnitude and frequency: comparison of methods on 16 gravel-bed river reaches: Earth Surface Processes and Landforms, v. 31, no. 11, p. 1345-1363, doi:10.1002/esp.1337.
Naylor, L. A., Spencer, T., Lane, S. N., Darby, S. E., Magilligan, F. J., Macklin, M. G., and Möller, I., 2017, Stormy geomorphology: geomorphic contributions in an age of climate extremes: Earth Surface Processes and Landforms, v. 42, no. 1, p. 166-190, 10.1002/esp.4062.
Nelson, A., and Dubé, K., 2016, Channel response to an extreme flood and sediment pulse in a mixed bedrock and gravel-bed river: Earth Surface Processes and Landforms, v. 41, no. 2, p. 178-195, https://doi.org/10.1002/esp.3843.
Nelson, J. M., Logan, B. L., Kinzel, P. J., Shimizu, Y., Giri, S., Shreve, R. L., and McLean, S. R., 2011, Bedform response to flow variability: Earth Surface Processes and Landforms, v. 36, no. 14, p. 1938-1947, 10.1002/esp.2212.
Neuendorf, K. K., 2005, Glossary of geology, Springer Science & Business Media,
Neverman, A. J., 2018, Quantifying bed stability : the missing tool for establishing mechanistic hydrological limits : a thesis presented in partial fulfilment of the requirements for the degree of Doctor of Philosophy in Geography at Massey University, Palmerston North, New Zealand [Doctor of Philosophy (PhD) Doctoral]: Massey University.
Newson, M., 1980, The geomorphological effectiveness of floods—a contribution stimulated by two recent events in mid-wales: Earth Surface Processes, v. 5, no. 1, p. 1-16, 10.1002/esp.3760050102.
Newson, M. D., 2002, Geomorphological concepts and tools for sustainable river ecosystem management: Aquatic Conservation: Marine and Freshwater Ecosystems, v. 12, no. 4, p. 365-379, https://doi.org/10.1002/aqc.532.
Nicholas, A. P., Aalto, R. E., Sambrook Smith, G. H., and Schwendel, A. C., 2018, Hydrodynamic controls on alluvial ridge construction and avulsion likelihood in meandering river floodplains: Geology, v. 46, no. 7, p. 639-642, 10.1130/G40104.1.
Nicol, A., Mazengarb, C., Chanier, F., Rait, G., Uruski, C., and Wallace, L., 2007, Tectonic evolution of the active Hikurangi subduction margin, New Zealand, since the Oligocene: Tectonics, v. 26, no. 4, https://doi.org/10.1029/2006TC002090.

Nicoll, T. J., and Hickin, E. J., 2010, Planform geometry and channel migration of confined meandering rivers on the Canadian prairies: Geomorphology, v. 116, no. 1, p. 37-47, https://doi.org/10.1016/j.geomorph.2009.10.005.
Nienhuis, J. H., Törnqvist, T. E., and Esposito, C. R., 2018, Crevasse Splays Versus Avulsions: A Recipe for Land Building With Levee Breaches: Geophysical Research Letters, v. 45, no. 9, p. 4058-4067, https://doi.org/10.1029/2018GL077933.
NIWA, N. I. o. W. a. A. R., 1999-2000, Meteorological Hazards Relevant to Wairarapa Engineering Lifeline: National Institute of Water and Atmospheric Research; NIWA,
Nobre, A. D., Cuartas, L. A., Hodnett, M., Rennó, C. D., Rodrigues, G., Silveira, A., Waterloo, M., and Saleska, S., 2011, Height Above the Nearest Drainage – a hydrologically relevant new terrain model: Journal of Hydrology, v. 404, no. 1, p. 13-29, https://doi.org/10.1016/j.jhydrol.2011.03.051.
Noda, A., 2016, Forearc basins: Types, geometries, and relationships to subduction zone dynamics: GSA Bulletin, v. 128, no. 5-6, p. 879-895, 10.1130/B31345.1.
Norman, J. W., 1969, Photo-interpretation of boulder clay areas as an aid to engineering geological studies: Quarterly Journal of Engineering Geology and Hydrogeology, v. 2, no. 2, p. 149-157,
O'Connell, P. E., and O'Donnell, G., 2014, Towards modelling flood protection investment as a coupled human and natural system: Hydrol. Earth Syst. Sci., v. 18, no. 1, p. 155-171, 10.5194/hess-18-155-2014.
O'Connor, J., Smith, M. J., and James, M. R., 2017, Cameras and settings for aerial surveys in the geosciences:Optimising image data: Progress in Physical Geography: Earth and Environment, v. 41, no. 3, p. 325-344, 10.1177/0309133317703092.
O'Connor, J. E., Jones, M. A., and Haluska, T. L., 2003, Flood plain and channel dynamics of the Quinault and Queets Rivers, Washington, USA: Geomorphology, v. 51, no. 1, p. 31-59, https://doi.org/10.1016/S0169-555X(02)00324-0.
O'Loughlin, C. L., 1969, Streambed investigations in a small mountain catchment: New Zealand Journal of Geology and Geophysics, v. 12, no. 4, p. 684-706, 10.1080/00288306.1969.10431106.
Osborne, J., 2010, Arguing to Learn in Science: The Role of Collaborative, Critical Discourse: Science, v. 328, no. 5977, p. 463-466, 10.1126/science.1183944.
Osterkamp, W. R., 2008, Annotated definitions of selected geomorphic terms and related terms of hydrology, sedimentology, soil science and ecology, 2008-1217, http://pubs.er.usgs.gov/publication/ofr20081217, 10.3133/ofr20081217.
Ouchi, S., 1985, Response of alluvial rivers to slow active tectonic movement: GSA Bulletin, v. 96, no. 4, p. 504-515, 10.1130/0016-7606(1985)96<504:Roarts>2.0.Co;2.
Ouchi, S., 2005, Development of offset channels across the San Andreas fault: Geomorphology, v. 70, no. 1, p. 112-128, https://doi.org/10.1016/j.geomorph.2005.04.004.
Oxenham, S., 1993, Waiohine, Greytown, NZ.,
Parker, G., Wilcock, P. R., Paola, C., Dietrich, W. E., and Pitlick, J., 2007, Physical basis for quasi-universal relations describing bankfull hydraulic geometry of single-thread gravel bed rivers: Journal of Geophysical Research: Earth Surface, v. 112, no. F4, https://doi.org/10.1029/2006JF000549.
Parliament, N. Z., 1991, Resource Management Act (as amended 30 September 2020), Volume 1991 No. 69: New Zealand Legistions, Parliamentary Council Office, https://www.legislation.govt.nz/act/public/1991/0069/latest/DLM234389.html
Parliament, N. Z. P. N., 2002, Civil Defense Emergency Management Act, CDEM, 2002 No. 33: Wellington, NZ, https://www.legislation.govt.nz/act/public/2002/0033/51.0/DLM149789.html
Passalacqua, P., Belmont, P., Staley, D. M., Simley, J. D., Arrowsmith, J. R., Bode, C. A., Crosby, C., DeLong, S. B., Glenn, N. F., Kelly, S. A., Lague, D., Sangireddy, H., Schaffrath, K., Tarboton, D. G., Wasklewicz, T., and Wheaton, J. M., 2015, Analyzing high resolution topography for

advancing the understanding of mass and energy transfer through landscapes: A review: Earth-Science Reviews, v. 148, p. 174-193, https://doi.org/10.1016/j.earscirev.2015.05.012.
Patterson, L. A., and Doyle, M. W., 2009, Assessing Effectiveness of National Flood Policy Through Spatiotemporal Monitoring of Socioeconomic Exposure1: JAWRA Journal of the American Water Resources Association, v. 45, no. 1, p. 237-252, https://doi.org/10.1111/j.1752-1688.2008.00275.x.
Patton, P. C., and Baker, V. R., 1976, Morphometry and floods in small drainage basins subject to diverse hydrogeomorphic controls: Water Resources Research, v. 12, no. 5, p. 941-952, https://doi.org/10.1029/WR012i005p00941.
Perrin, C., Manighetti, I., and Gaudemer, Y., 2016, Off-fault tip splay networks: A genetic and generic property of faults indicative of their long-term propagation: Comptes Rendus Geoscience, v. 348, no. 1, p. 52-60, https://doi.org/10.1016/j.crte.2015.05.002.
Pfeiffer, A. M., Finnegan, N. J., and Willenbring, J. K., 2017, Sediment supply controls equilibrium channel geometry in gravel rivers: Proceedings of the National Academy of Sciences, v. 114, no. 13, p. 3346-3351, 10.1073/pnas.1612907114.
Phillips, C. B., and Jerolmack, D. J., 2014, Dynamics and mechanics of bed-load tracer particles: Earth Surf. Dynam., v. 2, no. 2, p. 513-530, 10.5194/esurf-2-513-2014.
Phillips, J. D., 2002, Geomorphic impacts of flash flooding in a forested headwater basin: Journal of Hydrology, v. 269, no. 3, p. 236-250, https://doi.org/10.1016/S0022-1694(02)00280-9.
-, 2003, Sources of nonlinearity and complexity in geomorphic systems: Progress in Physical Geography: Earth and Environment, v. 27, no. 1, p. 1-23, 10.1191/0309133303pp340ra.
Phillips, J. D., 2006, Evolutionary geomorphology: thresholds and nonlinearity in landform response to environmental change: Hydrol. Earth Syst. Sci., v. 10, no. 5, p. 731-742, 10.5194/hess-10-731-2006.
Phillips, J. D., 2007, The perfect landscape: Geomorphology, v. 84, no. 3, p. 159-169, https://doi.org/10.1016/j.geomorph.2006.01.039.
-, 2009, Changes, perturbations, and responses in geomorphic systems: Progress in Physical Geography: Earth and Environment, v. 33, no. 1, p. 17-30, 10.1177/0309133309103889.
-, 2016, Vanishing point: Scale independence in geomorphological hierarchies: Geomorphology, v. 266, no. Supplement C, p. 66-74, https://doi.org/10.1016/j.geomorph.2016.05.012.
Pickup, G., and Rieger, W. A., 1979, A conceptual model of the relationship between channel characteristics and discharge: Earth Surface Processes, v. 4, no. 1, p. 37-42, https://doi.org/10.1002/esp.3290040104.
Piégay, H., Grant, G., Nakamura, F., and Trustrum, N., 2006, Braided river management: from assessment of river behaviour to improved sustainable development, *in* Sambrook Smith GH, Best, J., Bristow, C., and Petts, G., eds., Braided Rivers: Process, Deposits, Ecology and Management, Volume 36: Oxford, UK, Blackwell, p. 257-276,
Piégay, H., Mathias Kondolf, G., Toby Minear, J., and Vaudor, L., 2015, Trends in publications in fluvial geomorphology over two decades: A truly new era in the discipline owing to recent technological revolution?: Geomorphology, v. 248, p. 489-500, https://doi.org/10.1016/j.geomorph.2015.07.039.
Pielke, R. A., 1999, Nine Fallacies of Floods: Climatic Change, v. 42, no. 2, p. 413-438, 10.1023/A:1005457318876.
Pinter, N., 2005, One Step Forward, Two Steps Back on U.S. Floodplains: Science, v. 308, no. 5719, p. 207-208, 10.1126/science.1108411.
Poff, N. L., and Allan, J. D., 1995, Functional Organization of Stream Fish Assemblages in Relation to Hydrological Variability: Ecology, v. 76, no. 2, p. 606-627, https://doi.org/10.2307/1941217.
Pollock, M. M., Beechie, T. J., and Jordan, C. E., 2007, Geomorphic changes upstream of beaver dams in Bridge Creek, an incised stream channel in the interior Columbia River basin, eastern Oregon: Earth Surface Processes and Landforms, v. 32, no. 8, p. 1174-1185, https://doi.org/10.1002/esp.1553.

Pollock, M. M., Beechie, T. J., Wheaton, J. M., Jordan, C. E., Bouwes, N., Weber, N., and Volk, C., 2014, Using Beaver Dams to Restore Incised Stream Ecosystems: BioScience, v. 64, no. 4, p. 279-290, 10.1093/biosci/biu036.

Polvi, L. E., and Wohl, E., 2012, The beaver meadow complex revisited – the role of beavers in post-glacial floodplain development: Earth Surface Processes and Landforms, v. 37, no. 3, p. 332-346, https://doi.org/10.1002/esp.2261.

Puttock, A., Graham, H. A., Carless, D., and Brazier, R. E., 2018, Sediment and nutrient storage in a beaver engineered wetland: Earth Surface Processes and Landforms, v. 43, no. 11, p. 2358-2370, https://doi.org/10.1002/esp.4398.

Quigley, M., Dissen, R. V., Villamor, P., Litchfield, N., Barrell, D., Furlong, K., Stahl, T., Duffy, B., Bilderback, E., Noble, D., Townsend, D., Begg, J., Jongens, R., Ries, W., Claridge, J., Klahn, A., Mackenzie, H., Smith, A., Hornblow, S., Nicol, R., Cox, S., Langridge, R., and Pedley, K., 2010, Surface rupture of the Greendale Fault during the Darfield (Canterbury) earthquake, New Zealand: Bulletin of the New Zealand Society for Earthquake Engineering, v. 43, no. 4, 10.5459/bnzsee.43.4.236-242.

Rainato, R., Mao, L., and Picco, L., 2020, The effects of low-magnitude flow conditions on bedload mobility in a steep mountain stream: Geomorphology, v. 367, p. 107345, https://doi.org/10.1016/j.geomorph.2020.107345.

Raven, E. K., Lane, S. N., and Bracken, L. J., 2010, Understanding sediment transfer and morphological change for managing upland gravel-bed rivers: Progress in Physical Geography, v. 34, no. 1, p. 23-45, 10.1177/0309133309355631.

Recking, A., 2012, Influence of sediment supply on mountain streams bedload transport: Geomorphology, v. 175-176, no. Supplement C, p. 139-150, https://doi.org/10.1016/j.geomorph.2012.07.005.

Recking, A., Liébault, F., Peteuil, C., and Jolimet, T., 2012, Testing bedload transport equations with consideration of time scales: Earth Surface Processes and Landforms, v. 37, no. 7, p. 774-789, https://doi.org/10.1002/esp.3213.

Recking, A., Piton, G., Vazquez-Tarrio, D., and Parker, G., 2016, Quantifying the Morphological Print of Bedload Transport: Earth Surface Processes and Landforms, v. 41, no. 6, p. 809-822, https://doi.org/10.1002/esp.3869.

Reid, I., Frostick, L. E., and Layman, J. T., 1985, The incidence and nature of bedload transport during flood flows in coarse-grained alluvial channels: Earth Surface Processes and Landforms, v. 10, no. 1, p. 33-44, https://doi.org/10.1002/esp.3290100107.

Reid, J. B., 1992, The Owens River as a Tiltmeter for Long Valley Caldera, California: The Journal of Geology, v. 100, no. 3, p. 353-363, 10.1086/629637.

Reid, L. M., and Dunne, T., 1984, Sediment production from forest road surfaces: Water Resources Research, v. 20, no. 11, p. 1753-1761, https://doi.org/10.1029/WR020i011p01753.

Reid, S. C., Lane, S. N., Berney, J. M., and Holden, J., 2007a, The timing and magnitude of coarse sediment transport events within an upland, temperate gravel-bed river: Geomorphology, v. 83, no. 1, p. 152-182, https://doi.org/10.1016/j.geomorph.2006.06.030.

Reid, S. C., Lane, S. N., Montgomery, D. R., and Brookes, C. J., 2007b, Does hydrological connectivity improve modelling of coarse sediment delivery in upland environments?: Geomorphology, v. 90, no. 3–4, p. 263-282, https://doi.org/10.1016/j.geomorph.2006.10.023.

Rennie, C. D., and Church, M., 2010, Mapping spatial distributions and uncertainty of water and sediment flux in a large gravel bed river reach using an acoustic Doppler current profiler: Journal of Geophysical Research-Earth Surface, v. 115, 10.1029/2009jf001556.

Rennó, C. D., Nobre, A. D., Cuartas, L. A., Soares, J. V., Hodnett, M. G., Tomasella, J., and Waterloo, M. J., 2008, HAND, a new terrain descriptor using SRTM-DEM: Mapping terra-firme rainforest environments in Amazonia: Remote Sensing of Environment, v. 112, no. 9, p. 3469-3481, https://doi.org/10.1016/j.rse.2008.03.018.

Renwick, W. H., 1992, Equilibrium, disequilibrium, and nonequilibrium landforms in the landscape: Geomorphology, v. 5, no. 3–5, p. 265-276, https://doi.org/10.1016/0169-555X(92)90008-C.
Replumaz, A., Lacassin, R., Tapponnier, P., and Leloup, P. H., 2001, Large river offsets and Plio-Quaternary dextral slip rate on the Red River fault (Yunnan, China): Journal of Geophysical Research: Solid Earth, v. 106, no. B1, p. 819-836, https://doi.org/10.1029/2000JB900135.
Richards, K., 1979, Channel Adjustment to Sediment Pollution by the China Clay Industry in Cornwall, England, *in* Rhodes, D., and Williams, G., eds., Adjustments of the fluvial system: Dubuque, IA, Kendall/Hunt Pub. Co., p. 309-331, http://ezproxy.massey.ac.nz/login?url=http://search.ebscohost.com/login.aspx?direct=true&db=cat00245a&AN=massey.b1027921&site=eds-live&scope=site
Richards, K., Brasington, J., and Hughes, F., 2002, Geomorphic dynamics of floodplains: ecological implications and a potential modelling strategy: Freshwater Biology, v. 47, no. 4, p. 559-579, 10.1046/j.1365-2427.2002.00920.x.
Richards, K., Chandra, S., and Friend, P., 1993, Avulsive channel systems: characteristics and examples: Geological Society, London, Special Publications, v. 75, no. 1, p. 195-203, 10.1144/gsl.Sp.1993.075.01.12.
Richards, K. S., 1984, Book reviews: Historical change in the physical environment: Progress In Physical Geography, v. 8, no. 1, p. 147-150,
Richardson, J., 2013, Are the Northland rivers of New Zealand in synchrony with global Holocene climate change? : a thesis presented in partial fulfilment of the requirements for the degree of Doctor of Philosophy in Geography at Massey University, Palmerston North, New Zealand [Doctor of Philosophy (Ph.D.) Doctoral]: Massey University.
Richardson, J. M., Fuller, I. C., Holt, K. A., Litchfield, N. J., and Macklin, M. G., 2013, Holocene river dynamics in Northland, New Zealand: The influence of valley floor confinement on floodplain development: Geomorphology, v. 201, p. 494-511, 10.1016/j.geomorph.2013.07.022.
Rickenmann, D., 2020, Effect of Sediment Supply on Cyclic Fluctuations of the Disequilibrium Ratio and Threshold Transport Discharge, Inferred From Bedload Transport Measurements Over 27 Years at the Swiss Erlenbach Stream: Water Resources Research, v. 56, no. 11, p. e2020WR027741, https://doi.org/10.1029/2020WR027741.
Rodgers, D., and Little, T., 2006, World's largest coseismic strike-slip offset: The 1855 rupture of the Wairarapa Fault, New Zealand, and implications for displacement/length scaling of continental earthquakes: Journal of Geophysical Research: Solid Earth, v. 111, no. B12,
Rodrigues, S., Breheret, J.-G., Macaire, J.-J., Greulich, S., and Villar, M., 2007, In-channel woody vegetation controls on sedimentary processes and the sedimentary record within alluvial environments: a modern example of an anabranch of the River Loire, France: Sedimentology, v. 54, no. 1, p. 223-242, 10.1111/j.1365-3091.2006.00832.x.
Roth, D. L., Finnegan, N. J., Brodsky, E. E., Cook, K. L., Stark, C. P., and Wang, H. W., 2014, Migration of a coarse fluvial sediment pulse detected by hysteresis in bedload generated seismic waves: Earth and Planetary Science Letters, v. 404, p. 144-153, https://doi.org/10.1016/j.epsl.2014.07.019.
Röthlisberger, V., Zischg, A. P., and Keiler, M., 2017, Identifying spatial clusters of flood exposure to support decision making in risk management: Science of The Total Environment, v. 598, p. 593-603, https://doi.org/10.1016/j.scitotenv.2017.03.216.
Roy, S. G., Koons, P. O., Upton, P., and Tucker, G. E., 2016, Dynamic links among rock damage, erosion, and strain during orogenesis: Geology, v. 44, no. 7, p. 583-586, 10.1130/g37753.1.
Royal, C., 2011, 2011, Cultural values for the Wairarapa waterways report: Prepared by Ohau Plants Ltd,
Rumsby, B. T., Brasington, J., Langham, J. A., McLelland, S. J., Middleton, R., and Rollinson, G., 2008, Monitoring and modelling particle and reach-scale morphological change in gravel-bed rivers: Applications and challenges: Geomorphology, v. 93, no. 1–2, p. 40-54, https://doi.org/10.1016/j.geomorph.2006.12.017.

Salant, N. L., Renshaw, C. E., and Magilligan, F. J., 2006, Short and long-term changes to bed mobility and bed composition under altered sediment regimes: Geomorphology, v. 76, no. 1–2, p. 43-53, https://doi.org/10.1016/j.geomorph.2005.09.003.
Salinger, M. J., Renwick, J. A., and Mullan, A. B., 2001, Interdecadal Pacific Oscillation and South Pacific climate: International Journal of Climatology, v. 21, no. 14, p. 1705-1721, https://doi.org/10.1002/joc.691.
Sanders, H., Rice, S. P., and Wood, P. J., 2021, Signal crayfish burrowing, bank retreat and sediment supply to rivers: A biophysical sediment budget: Earth Surface Processes and Landforms, v. 46, no. 4, p. 837-852, https://doi.org/10.1002/esp.5070.
Schaffrath, K. R., Belmont, P., and Wheaton, J. M., 2015, Landscape-scale geomorphic change detection: Quantifying spatially variable uncertainty and circumventing legacy data issues: Geomorphology, v. 250, p. 334-348, https://doi.org/10.1016/j.geomorph.2015.09.020.
Schick, A. P., Lekach, J., and Hassan, M. A., 1987, Vertical exchange of coarse bedload in desert streams: Geological Society, London, Special Publications, v. 35, no. 1, p. 7-16, 10.1144/gsl.Sp.1987.035.01.02.
Schmitt, R. J. P., Bizzi, S., and Castelletti, A., 2016, Tracking multiple sediment cascades at the river network scale identifies controls and emerging patterns of sediment connectivity: Water Resources Research, v. 52, no. 5, p. 3941-3965, https://doi.org/10.1002/2015WR018097.
Schumm, S., 1973, Geomorphic thresholds and complex response of drainage systems: Fluvial geomorphology, v. 6, p. 69-85,
Schumm, S., and Lichty, R., 1965, Time, space and causality in geomorphology. American Journal of Science 263, 110-19,
Schumm, S. A., 1977, The fluvial system,
Schumm, S. A., 1979, Geomorphic Thresholds: The Concept and Its Applications: Transactions of the Institute of British Geographers, v. 4, no. 4, p. 485-515, 10.2307/622211.
-, 1986, Alluvial River Response to Active Tectonics, *in* Council, N. R., ed., Active Tectonics: Impact on Society: Washington, DC, The National Academies Press, p. 280, doi:10.17226/624.
Schumm, S. A., 1991, To Interpret the Earth: Ten ways to be wrong, Cambridge University Press,
Schumm, S. A., Dumont, J. F., and Holbrook, J. M., 2000, Active tectonics and alluvial rivers, New York, Cambridge University Press,
Schumm, S. A., and Lichty, R. W., 1963, Channel widening and flood-plain construction along Cimarron River in southwestern Kansas, 352D, http://pubs.er.usgs.gov/publication/pp352D, 10.3133/pp352D.
Schwendel, A. C., and Fuller, I. C., 2011, Connectivity in forested upland catchments and associated channel dynamics: The eastern Ruahine Range: Journal of Hydrology (Wellington North), v. 50, no. 1, Sp. Iss. SI, p. 205-225, <Go to ISI>://BIOABS:BACD201100427831
Scown, M. W., Thoms, M. C., and De Jager, N. R., 2015, Floodplain complexity and surface metrics: Influences of scale and geomorphology: Geomorphology, v. 245, no. 0, p. 102-116, http://dx.doi.org/10.1016/j.geomorph.2015.05.024.
Sear, D. A., Newson, M. D., and Thorne, C. R., 2010, Guidebook of applied fluvial geomorphology, Victoria, Australia, Thomas Telford Ltd, 257 p,
Shugar, D. H., Clague, J. J., Best, J. L., Schoof, C., Willis, M. J., Copland, L., and Roe, G. H., 2017, River piracy and drainage basin reorganization led by climate-driven glacier retreat: Nature Geoscience, v. 10, no. 5, p. 370-+, 10.1038/ngeo2932.
Sieh, K. E., and Jahns, R. H., 1984, Holocene activity of the San Andreas fault at Wallace Creek, California: GSA Bulletin, v. 95, no. 8, p. 883-896, 10.1130/0016-7606(1984)95<883:Haotsa>2.0.Co;2.
Simon, A., and Thorne, C. R., 1996, Channel adjustment of an unstable coarse-grained stream: Opposing trends of boundary and critical shear stress, and the applicability of extremal hypotheses: Earth Surface Processes and Landforms, v. 21, no. 2, p. 155-180, 10.1002/(sici)1096-9837(199602)21:2<155::Aid-esp610>3.0.Co;2-5.

Sims, A. J., and Rutherfurd, I. D., 2017, Management responses to pulses of bedload sediment in rivers: Geomorphology, v. 294, no. Supplement C, p. 70-86, https://doi.org/10.1016/j.geomorph.2017.04.010.
Singers, N., Crisp, P., and Spearpoint, O., 2018, Forest ecosystems of the Wellington Region, https://www.gw.govt.nz/assets/Our-Environment/Environmental-monitoring/Environmental-Reporting/Forest-ecosytems-of-the-Wellington-region-reduced.pdf, https://www.gw.govt.nz/assets/Our-Environment/Environmental-monitoring/Environmental-Reporting/Forest-ecosytems-of-the-Wellington-region-reduced.pdf
Sinha, R., 2008, Kosi: Rising Waters, Dynamic Channels and Human Disasters: Economic and Political Weekly, v. 43, no. 46, p. 42-46, http://www.jstor.org.ezproxy.massey.ac.nz/stable/40278180
-, 2009, The Great avulsion of Kosi on 18 August 2008: Current Science, v. 97, no. 3, p. 429-433, http://www.jstor.org.ezproxy.massey.ac.nz/stable/24112012
Slater, L. J., 2016, To what extent have changes in channel capacity contributed to flood hazard trends in England and Wales?: Earth Surface Processes and Landforms, v. 41, no. 8, p. 1115-1128, https://doi.org/10.1002/esp.3927.
Slater, L. J., Singer, M. B., and Kirchner, J. W., 2015, Hydrologic versus geomorphic drivers of trends in flood hazard: Geophysical Research Letters, v. 42, no. 2, p. 370-376, https://doi.org/10.1002/2014GL062482.
Slingerland, R., and Smith, N. D., 1998, Necessary conditions for a meandering-river avulsion: Geology, v. 26, no. 5, p. 435-438, 10.1130/0091-7613(1998)026<0435:Ncfamr>2.3.Co;2.
-, 2004, River avulsions and their deposits: Annual Review of Earth and Planetary Sciences, v. 32, no. 1, p. 257-285, 10.1146/annurev.earth.32.101802.120201.
Smart, G. M., and McKerchar, A. I., 2010, More Flood Disasters in New Zealand: J. Hydrology (NZ), v. 49, no. 2, p. 69-78,
Smith, M. J., Chandler, J., and Rose, J., 2009, High spatial resolution data acquisition for the geosciences: kite aerial photography: Earth Surface Processes and Landforms, v. 34, no. 1, p. 155-161, 10.1002/esp.1702.
Smith, M. J., and Pain, C. F., 2009, Applications of remote sensing in geomorphology: Progress in Physical Geography: Earth and Environment, v. 33, no. 4, p. 568-582, 10.1177/0309133309346648.
Smith, N. D., 2003, Avulsion, *in* Middleton, G. V., Church, M. J., Coniglio, M., Hardie, L. A., and Longstaffe, F. J., eds., Encyclopedia of Sediments and Sedimentary Rocks: Dordrecht, Springer Netherlands, p. 34-36, 10.1007/978-1-4020-3609-5_16.
Smith, N. D., Cross, T. A., Dufficy, J. P., and Clough, S. R., 1989, Anatomy of an avulsion: Sedimentology, v. 36, no. 1, p. 1-23, https://doi.org/10.1111/j.1365-3091.1989.tb00817.x.
Smith, R. D., Sidle, R. C., and Porter, P. E., 1993a, Effects on bedload transport of experimental removal of woody debris from a forest gravel-bed stream: Earth Surface Processes and Landforms, v. 18, no. 5, p. 455-468, https://doi.org/10.1002/esp.3290180507.
Smith, R. D., Sidle, R. C., Porter, P. E., and Noel, J. R., 1993b, Effects of experimental removal of woody debris on the channel morphology of a forest, gravel-bed stream: Journal of Hydrology, v. 152, no. 1, p. 153-178, https://doi.org/10.1016/0022-1694(93)90144-X.
Snyder, N. P., Whipple, K. X., Tucker, G. E., and Merritts, D. J., 2003a, Channel response to tectonic forcing: field analysis of stream morphology and hydrology in the Mendocino triple junction region, northern California: Geomorphology, v. 53, no. 1, p. 97-127, https://doi.org/10.1016/S0169-555X(02)00349-5.
-, 2003b, Importance of a stochastic distribution of floods and erosion thresholds in the bedrock river incision problem: Journal of Geophysical Research: Solid Earth, v. 108, no. B2, https://doi.org/10.1029/2001JB001655.

Sofia, G., Masin, R., and Tarolli, P., 2017, Prospects for crowdsourced information on the geomorphic 'engineering' by the invasive Coypu (Myocastor coypus): Earth Surface Processes and Landforms, v. 42, no. 2, p. 365-377, https://doi.org/10.1002/esp.4081.
Soong, T. W., and Zhao, Y., 1994, The Flood and Sediment Characteristics of the Lower Yellow River in China: Water International, v. 19, no. 3, p. 129-137, 10.1080/02508069408686216.
Spector, S., Cradock-Henry, N. A., Beaven, S., and Orchiston, C., 2019, Characterising rural resilience in Aotearoa-New Zealand: a systematic review: Regional Environmental Change, v. 19, no. 2, p. 543-557, 10.1007/s10113-018-1418-3.
Staines, K. E. H., and Carrivick, J. L., 2015, Geomorphological impact and morphodynamic effects on flow conveyance of the 1999 jökulhlaup at sólheimajökull, Iceland: Earth Surface Processes and Landforms, v. 40, no. 10, p. 1401-1416, https://doi.org/10.1002/esp.3750.
Standards New Zealand, 2008, NZS 9401:2008 Managing flood risk - A process standard, https://www.standards.govt.nz/touchstone/business/2008/nov/managing-flood-risk/
Steffen, W., Broadgate, W., Deutsch, L., Gaffney, O., and Ludwig, C., 2015, The trajectory of the Anthropocene: The Great Acceleration: The Anthropocene Review, v. 2, no. 1, p. 81-98, 10.1177/2053019614564785.
Stephens, T. A., and Bledsoe, B. P., 2020, Probabilistic mapping of flood hazards: Depicting uncertainty in streamflow, land use, and geomorphic adjustment: Anthropocene, v. 29, p. 100231, https://doi.org/10.1016/j.ancene.2019.100231.
Stewart, A., 2014, Land use and water quality: Greater Wellington Regional Council,
Stirling, M. W., Litchfield, N., Villamor, P., Van Dissen, R., Nicol, A., Pettinga, J., Barnes, P., Langridge, R., Little, T., and Barrell, D., 2017, The Mw7. 8 2016 Kaikōura earthquake: Surface fault rupture and seismic hazard context: Bulletin of the New Zealand Society for Earthquake Engineering, v. 50, no. 2, p. 73-84,
Stock, J. D., and Montgomery, D. R., 1999, Geologic constraints on bedrock river incision using the stream power law: Journal of Geophysical Research: Solid Earth, v. 104, no. B3, p. 4983-4993, 10.1029/98JB02139.
Stoffel, M., and Wilford, D. J., 2012, Hydrogeomorphic processes and vegetation: disturbance, process histories, dependencies and interactions: Earth Surface Processes and Landforms, v. 37, no. 1, p. 9-22, 10.1002/esp.2163.
Stojmirovic, G., 1998, Waingawa River Management Scheme: 5 Year Review: Greater Wellington Regional Council,
Stoll, S., Breyer, P., Tonkin, J. D., Früh, D., and Haase, P., 2016, Scale-dependent effects of river habitat quality on benthic invertebrate communities — Implications for stream restoration practice: Science of The Total Environment, v. 553, p. 495-503, https://doi.org/10.1016/j.scitotenv.2016.02.126.
Stouthamer, E., and Berendsen, H. J. A., 2000, Factors Controlling the Holocene Avulsion History of the Rhine-Meuse Delta (The Netherlands): Journal of Sedimentary Research, v. 70, no. 5, p. 1051-1064, 10.1306/033000701051.
-, 2001, Avulsion Frequency, Avulsion Duration, and Interavulsion Period of Holocene Channel Belts in the Rhine-Meuse Delta, The Netherlands: Journal of Sedimentary Research, v. 71, no. 4, p. 589-598, 10.1306/112100710589.
Stouthamer, E., and Berendsen, H. J. A., 2007, Avulsion: The relative roles of autogenic and allogenic processes: Sedimentary Geology, v. 198, no. 3, p. 309-325, https://doi.org/10.1016/j.sedgeo.2007.01.017.
Stover, S. C., and Montgomery, D. R., 2001, Channel change and flooding, Skokomish River, Washington: Journal of Hydrology, v. 243, no. 3, p. 272-286, https://doi.org/10.1016/S0022-1694(00)00421-2.
Straub, K. M., Duller, R. A., Foreman, B. Z., and Hajek, E. A., 2020, Buffered, Incomplete, and Shredded: The Challenges of Reading an Imperfect Stratigraphic Record: Journal of

Geophysical Research: Earth Surface, v. 125, no. 3, p. e2019JF005079, https://doi.org/10.1029/2019JF005079.
Stubbe, F., 1981, A Changing Riverscape 1854 to 1880: The Lower Waiohine Catchment, Greytown, Wairarapa [Honours Honours]: Victoria University of Wellington.
Surian, N., 2006, Effects of Human Impact on Braided River Morphology: Examples from Northern Italy, Braided Rivers, p. 327-338, https://doi.org/10.1002/9781444304374.ch16.
Surian, N., Ziliani, L., Comiti, F., Lenzi, M. A., and Mao, L., 2009, Channel Adjustments And Alteration Of Sediment Fluxes In Gravel-Bed Rivers Of North-Eastern Italy: Potentials And Limitations For Channel Recovery: River Research and Applications, v. 25, no. 5, p. 551-567, 10.1002/rra.1231.
Syvitski, J. P., and Brakenridge, G. R., 2013, Causation and avoidance of catastrophic flooding along the Indus River, Pakistan: GSA Today, v. 23, no. 1, p. 4-10,
Tacconi, P., Rinaldi, M., Moretti, S., and Matteini, M., 1990, Monitoring of particle movement on Virginio gravel bed stream, Third International Workshop on Gravel-Bed Rivers; Dynamics of Gravel-Bed Rivers: Florence, Italy,
Taha, Z. P., and Anderson, J. B., 2008, The influence of valley aggradation and listric normal faulting on styles of river avulsion: A case study of the Brazos River, Texas, USA: Geomorphology, v. 95, no. 3–4, p. 429-448, https://doi.org/10.1016/j.geomorph.2007.07.014.
Tal, M., and Paola, C., 2007, Dynamic single-thread channels maintained by the interaction of flow and vegetation: Geology, v. 35, no. 4, p. 347-350, 10.1130/G23260A.1.
Tangi, M., Bizzi, S., Fryirs, K., and Castelletti, A., 2022, A Dynamic, Network Scale Sediment (Dis)Connectivity Model to Reconstruct Historical Sediment Transfer and River Reach Sediment Budgets: Water Resources Research, v. 58, no. 2, p. e2021WR030784, https://doi.org/10.1029/2021WR030784.
Tanoue, M., Hirabayashi, Y., and Ikeuchi, H., 2016, Global-scale river flood vulnerability in the last 50 years: Scientific Reports, v. 6, no. 1, p. 36021, 10.1038/srep36021.
Tavares da Costa, R., Zanardo, S., Bagli, S., Hilberts, A. G. J., Manfreda, S., Samela, C., and Castellarin, A., 2020, Predictive Modeling of Envelope Flood Extents Using Geomorphic and Climatic-Hydrologic Catchment Characteristics: Water Resources Research, v. 56, no. 9, p. e2019WR026453, https://doi.org/10.1029/2019WR026453.
Temme, A. J. A. M., Keiler, M., Karssenberg, D., and Lang, A., 2015, Complexity and non-linearity in earth surface processes – concepts, methods and applications: Earth Surface Processes and Landforms, v. 40, no. 9, p. 1270-1274, 10.1002/esp.3712.
Tena, A., Piégay, H., Seignemartin, G., Barra, A., Berger, J. F., Mourier, B., and Winiarski, T., 2020, Cumulative effects of channel correction and regulation on floodplain terrestrialisation patterns and connectivity: Geomorphology, v. 354, p. 107034, https://doi.org/10.1016/j.geomorph.2020.107034.
Thomaz, E. L., and Peretto, G. T., 2016, Hydrogeomorphic connectivity on roads crossing in rural headwaters and its effect on stream dynamics: Science of The Total Environment, v. 550, p. 547-555, https://doi.org/10.1016/j.scitotenv.2016.01.100.
Thompson, C. S., 1982, The weather and climate of the Wairarapa region, New Zealand: Meteorological Service,
Thoms, M. C., Piégay, H., and Parsons, M., 2018, What do you mean, 'resilient geomorphic systems'?: Geomorphology, v. 305, p. 8-19, https://doi.org/10.1016/j.geomorph.2017.09.003.
Thorne, C., and Lewin, J., 1979, Bank processes, bed material movement and planform development in a meandering river, *in* Rhodes, D., and Williams, G., eds., Adjustments of the Fluvial System, Volume 10: Dubuque, Iowa, Kendall/Hunt p. 117-137,
Thorne, C. R., 2002, Geomorphic analysis of large alluvial rivers: Geomorphology, v. 44, no. 3, p. 203-219, https://doi.org/10.1016/S0169-555X(01)00175-1.
Thornes, J. B., and Brunsden, D., 1977, Geomorphology and Time, London, Methuen,

Tobin, G. A., 1995, The Levee Love Affair: A Stormy Relationship?: JAWRA Journal of the American Water Resources Association, v. 31, no. 3, p. 359-367, https://doi.org/10.1111/j.1752-1688.1995.tb04025.x.
Toone, J., Rice, S. P., and Piégay, H., 2014, Spatial discontinuity and temporal evolution of channel morphology along a mixed bedrock-alluvial river, upper Drôme River, southeast France: Contingent responses to external and internal controls: Geomorphology, v. 205, p. 5-16, https://doi.org/10.1016/j.geomorph.2012.05.033.
Törnqvist, T. E., and Bridge, J. S., 2002, Spatial variation of overbank aggradation rate and its influence on avulsion frequency: Sedimentology, v. 49, no. 5, p. 891-905, https://doi.org/10.1046/j.1365-3091.2002.00478.x.
Törnqvist, T. r. E., 1994, Middle and late Holocene avulsion history of the River Rhine (Rhine-Meuse delta, Netherlands): Geology, v. 22, no. 8, p. 711-714, 10.1130/0091-7613(1994)022<0711:Malhah>2.3.Co;2.
Townsend, C. R., Scarsbrook, M. R., and Dolédec, S., 1997, Quantifying Disturbance in Streams: Alternative Measures of Disturbance in Relation to Macroinvertebrate Species Traits and Species Richness: Journal of the North American Benthological Society, v. 16, no. 3, p. 531-544, 10.2307/1468142.
Townsend, D., Begg, J., Villamor, P., and Lukovic, B., 2002, Late Quaternary displacement of the Mokonui Fault, Wairarapa, NEw Zealand: A preliminary assessment of earthquake generating potential: Institute of Geological and Nuclear Sciences,
Trewick, S., and Bland, K. J., 2011, 153-183 Fire and slice: Palaeogeography for biogeography at New Zealand's North Island/ South Island juncture: Journal of the Royal Society of New Zealand iFirst, v. 2011, 10.1080/03036758.2010.549493.
Trimble, S. W., and Cooke, R. U., 1991, Historical Sources For Geomorphological Research In The United States: The Professional Geographer, v. 43, no. 2, p. 212-228, 10.1111/j.0033-0124.1991.00212.x.
Tseng, C.-M., Lin, C.-W., Dalla Fontana, G., and Tarolli, P., 2015, The topographic signature of a major typhoon: Earth Surface Processes and Landforms, v. 40, no. 8, p. 1129-1136, https://doi.org/10.1002/esp.3708.
Tuckman, B. W., 1965, Developmental sequence in small groups: Psychological Bulletin, v. 63, no. 6, p. 384-399, 10.1037/h0022100.
Tunnicliffe, J., Brierley, G., Fuller, I. C., Leenman, A., Marden, M., and Peacock, D., 2017, Reaction and relaxation in a coarse-grained fluvial system following catchment-wide disturbance: Geomorphology, https://doi.org/10.1016/j.geomorph.2017.11.006.
Tunnicliffe, J. F., and Church, M., 2011, Scale variation of post-glacial sediment yield in Chilliwack Valley, British Columbia: Earth Surface Processes and Landforms, v. 36, no. 2, p. 229-243, 10.1002/esp.2093.
Turley, M., Hassan, M. A., and Slaymaker, O., 2021, Quantifying sediment connectivity: Moving toward a holistic assessment through a mixed methods approach: Earth Surface Processes and Landforms, v. n/a, no. n/a, https://doi.org/10.1002/esp.5191.
Turner, D., Lucieer, A., and Watson, C., 2012, An Automated Technique for Generating Georectified Mosaics from Ultra-High Resolution Unmanned Aerial Vehicle (UAV) Imagery, Based on Structure from Motion (SfM) Point Clouds: Remote Sensing, v. 4, no. 5, p. 1392, http://www.mdpi.com/2072-4292/4/5/1392
Turowski, J. M., Yager, E. M., Badoux, A., Rickenmann, D., and Molnar, P., 2009, The impact of exceptional events on erosion, bedload transport and channel stability in a step-pool channel: Earth Surface Processes and Landforms, v. 34, no. 12, p. 1661-1673, https://doi.org/10.1002/esp.1855.
UNDRR, 2015, The human cost of weather-related disasters 1995-2015: Centre for Research on the Epidemiology of Disasters (CRED)

United Nations Office for Disaster Risk Reduction (UNDRR),

United Nations Office for Disaster Risk Reduction, 2019a, Global assessment report on disaster risk reduction 2019, https://www.undrr.org/publication/global-assessment-report-disaster-risk-reduction-2019, 978-92-1-004180-5.
-, 2019b, UNDRR Annual Report 2019, https://www.undrr.org/publication/undrr-annual-report-2019, https://www.undrr.org/publication/undrr-annual-report-2019
United Nations Office for Disaster Risk Reduction, and International Science Council, 2020, Hazard definition and classification review, https://www.undrr.org/publication/hazard-definition-and-classification-review, https://www.undrr.org/publication/hazard-definition-and-classification-review
Unwin, D. J., 1995, Geographical information systems and the problem of'error and uncertainty': Progress in Human Geography, v. 19, no. 4, p. 549-558,
Ureña-Cámara, M. A., Nogueras-Iso, J., Lacasta, J., and Ariza-López, F. J., 2019, A method for checking the quality of geographic metadata based on ISO 19157: International Journal of Geographical Information Science, v. 33, no. 1, p. 1-27, 10.1080/13658816.2018.1515437.
Valenza, J. M., Edmonds, D. A., Hwang, T., and Roy, S., 2020, Downstream changes in river avulsion style are related to channel morphology: Nature Communications, v. 11, no. 1, p. 2116, 10.1038/s41467-020-15859-9.
Van Dissen, R. J., and Berryman, K. R., 1996, Surface rupture earthquakes over the last similar to 1000 years in the Wellington region, New Zealand, and implications for ground shaking hazard: Journal of Geophysical Research-Solid Earth, v. 101, no. B3, p. 5999-6019, 10.1029/95jb02391.
Vella, P., Upper Pleistocene succession in the inland part of Wairarapa Valley, New Zealand, *in* Proceedings Transactions of the Royal society of New Zealand1963a, Volume 2, p. 62-78.
-, 1963b, Upper Pleistocene succession in the inland part of Wairarapa Valley, New Zealand,
Venditti, J. G., Dietrich, W. E., Nelson, P. A., Wydzga, M. A., Fadde, J., and Sklar, L., 2010, Mobilization of coarse surface layers in gravel-bedded rivers by finer gravel bed load: Water Resources Research, v. 46, no. 7, https://doi.org/10.1029/2009WR008329.
Venditti, J. G., Li, T., Deal, E., Dingle, E., and Church, M., 2019, Struggles with stream power: Connecting theory across scales: Geomorphology, p. 106817, https://doi.org/10.1016/j.geomorph.2019.07.004.
Vericat, D., Brasington, J., Wheaton, J., and Cowie, M., 2009, Accuracy Assessment Of Aerial Photographs Acquired Using Lighter-Than-Air Blimps: Low-Cost Tools For Mapping River Corridors: River Research and Applications, v. 25, no. 8, p. 985-1000, 10.1002/rra.1198.
Viles, H., 2016, Technology and geomorphology: Are improvements in data collection techniques transforming geomorphic science?: Geomorphology, v. 270, p. 121-133, https://doi.org/10.1016/j.geomorph.2016.07.011.
-, 2019, Biogeomorphology: Past, present and future: Geomorphology, p. 106809, https://doi.org/10.1016/j.geomorph.2019.06.022.
Wainwright, J., Parsons, A. J., Cooper, J. R., Gao, P., Gillies, J. A., Mao, L., Orford, J. D., and Knight, P. G., 2015, The concept of transport capacity in geomorphology: Reviews of Geophysics, v. 53, no. 4, p. 1155-1202, 10.1002/2014rg000474.
Wairarapa Daily Times, 1917, Notices, Wairarapa Daily Times, , Volume 43 Masterton, p. 1, https://paperspast.natlib.govt.nz/newspapers/WDT19170817.2.2.3
Wald, D. J., Quitoriano, V., Heaton, T. H., and Kanamori, H., 1999, Relationships between Peak Ground Acceleration, Peak Ground Velocity, and Modified Mercalli Intensity in California: Earthquake Spectra, v. 15, no. 3, p. 557-564, 10.1193/1.1586058.
Walker, F., and Allen, M. B., 2012, Offset rivers, drainage spacing and the record of strike-slip faulting: The Kuh Banan Fault, Iran: Tectonophysics, v. 530-531, p. 251-263, https://doi.org/10.1016/j.tecto.2012.01.001.

Walley, Y., Tunnicliffe, J., and Brierley, G., 2017, The influence of network structure upon sediment routing in two disturbed catchments, East Cape, New Zealand: Geomorphology, https://doi.org/10.1016/j.geomorph.2017.10.029.
Walstra, J., Dixon, N., and Chandler, J. H., 2007, Historical aerial photographs for landslide assessment: two case histories: Quarterly Journal of Engineering Geology and Hydrogeology, v. 40, no. 4, p. 315-332, 10.1144/1470-9236/07-011.
Wang, N., and Grapes, R., 2008, Infrared-stimulated luminescence dating of late Quaternary aggradation surfaces and their deformation along an active fault, southern North Island of New Zealand: Geomorphology, v. 96, no. 1-2, p. 86-104, 10.1016/j.geomorph.2007.07.016.
Ward, J., 1989, The Four-Dimensional Nature of Lotic Ecosystems: Journal of the North American Benthological Society, v. 8, no. 1, p. 2-8, 10.2307/1467397.
Ward, P. D., Montgomery, D. R., and Smith, R., 2000, Altered River Morphology in South Africa Related to the Permian-Triassic Extinction: Science, v. 289, p. 1740-1743,
Wathen, S. J., and Hoey, T. B., 1998, Morphological controls on the downstream passage of a sediment wave in a gravel-bed stream: Earth Surface Processes and Landforms, v. 23, no. 8, p. 715-730, https://doi.org/10.1002/(SICI)1096-9837(199808)23:8<715::AID-ESP877>3.0.CO;2-0.
Weber, M. D., and Pasternack, G. B., 2017, Valley-scale morphology drives differences in fluvial sediment budgets and incision rates during contrasting flow regimes: Geomorphology, v. 288, p. 39-51, https://doi.org/10.1016/j.geomorph.2017.03.018.
WELA, W. E. L. A., 2003, Natural Hazards in the Wairarapa, Risk to Lifelines from Natural Hazards, p. 54,
Welber, M., Bertoldi, W., and Tubino, M., 2012, The response of braided planform configuration to flow variations, bed reworking and vegetation: the case of the Tagliamento River, Italy: Earth Surface Processes and Landforms, v. 37, no. 5, p. 572-582, 10.1002/esp.3196.
Wells, N. A., and Dorr, J. A., Jr., 1987, Shifting of the Kosi River, northern India: Geology, v. 15, no. 3, p. 204-207, 10.1130/0091-7613(1987)15<204:Sotkrn>2.0.Co;2.
Wemple, B. C., and Jones, J. A., 2003, Runoff production on forest roads in a steep, mountain catchment: Water Resources Research, v. 39, no. 8, https://doi.org/10.1029/2002WR001744.
Wemple, B. C., Jones, J. A., and Grant, G. E., 1996, Channel network extension by logging roads in two basins, western cascades, oregon: JAWRA Journal of the American Water Resources Association, v. 32, no. 6, p. 1195-1207, https://doi.org/10.1111/j.1752-1688.1996.tb03490.x.
Wemple, B. C., Swanson, F. J., and Jones, J. A., 2001, Forest roads and geomorphic process interactions, Cascade Range, Oregon: Earth Surface Processes and Landforms, v. 26, no. 2, p. 191-204, https://doi.org/10.1002/1096-9837(200102)26:2<191::AID-ESP175>3.0.CO;2-U.
Werritty, A., and Ferguson, R., 1980, Pattern changes in a Scottish braided river over 1, 30, and 200 years, *in* Cullingford, R. A., Davidson, D. A., and Lewin, J., eds., Timescales in Geomorphology: Brisbane, John Wiley and Sons, p. 53-68,
Westaway, R. M., Lane, S. N., and Hicks, D. M., 2000, The development of an automated correction procedure for digital photogrammetry for the study of wide, shallow, gravel-bed rivers: Earth Surface Processes and Landforms, v. 25, no. 2, p. 209-226, <Go to ISI>://WOS:000085315600009
Westbrook, C. J., Cooper, D. J., and Baker, B. W., 2006, Beaver dams and overbank floods influence groundwater–surface water interactions of a Rocky Mountain riparian area: Water Resources Research, v. 42, no. 6, https://doi.org/10.1029/2005WR004560.
Wester, T., Wasklewicz, T., and Staley, D., 2014, Functional and structural connectivity within a recently burned drainage basin: Geomorphology, v. 206, p. 362-373, https://doi.org/10.1016/j.geomorph.2013.10.011.

Westoby, M. J., Brasington, J., Glasser, N. F., Hambrey, M. J., and Reynolds, J. M., 2012, 'Structure-from-Motion' photogrammetry: A low-cost, effective tool for geoscience applications: Geomorphology, v. 179, p. 300-314, 10.1016/j.geomorph.2012.08.021.
Wheaton, J., Darby, S., and Sear, D., 2008, The Scope of Uncertainties in River Restoration, *in* Darby, S. E., and Sear, D. A., eds., River Restoration: Managing the Uncertainty in Restoring Physical Habitat, Wiley, p. 21-32, 10.1002/9780470867082.ch3.
Wheaton, J. M., Bouwes, N., Mchugh, P., Saunders, C., Bangen, S., Bailey, P., Nahorniak, M., Wall, E., and Jordan, C., 2018, Upscaling site-scale ecohydraulic models to inform salmonid population-level life cycle modeling and restoration actions – Lessons from the Columbia River Basin: Earth Surface Processes and Landforms, v. 43, no. 1, p. 21-44, 10.1002/esp.4137.
Wheaton, J. M., Brasington, J., Darby, S. E., Kasprak, A., Sear, D., and Vericat, D., 2013, Morphodynamic signatures of braiding mechanisms as expressed through change in sediment storage in a gravel-bed river: Journal of Geophysical Research-Earth Surface, v. 118, no. 2, p. 759-779, 10.1002/jgrf.20060.
Wheaton, J. M., Brasington, J., Darby, S. E., Merz, J., Pasternack, G. B., Sear, D., and Vericat, D., 2010a, Linking Geomorphic Changes To Salmonid Habitat At A Scale Relevant To Fish: River Research and Applications, v. 26, no. 4, p. 469-486, 10.1002/rra.1305.
Wheaton, J. M., Brasington, J., Darby, S. E., and Sear, D. A., 2010b, Accounting for uncertainty in DEMs from repeat topographic surveys: improved sediment budgets: Earth Surface Processes and Landforms, v. 35, no. 2, p. 136-156, 10.1002/esp.1886.
Whipple, K. X., and Dunne, T., 1992, The influence of debris-flow rheology on fan morphology, Owens Valley, California: GSA Bulletin, v. 104, no. 7, p. 887-900, 10.1130/0016-7606(1992)104<0887:Tiodfr>2.3.Co;2.
Whipple, K. X., and Tucker, G. E., 1999, Dynamics of the stream-power river incision model: Implications for height limits of mountain ranges, landscape response timescales, and research needs: Journal of Geophysical Research: Solid Earth, v. 104, no. B8, p. 17661-17674, 10.1029/1999JB900120.
Wilcock, P. R., Kenworthy, S. T., and Crowe, J. C., 2001, Experimental study of the transport of mixed sand and gravel: Water Resources Research, v. 37, no. 12, p. 3349-3358, https://doi.org/10.1029/2001WR000683.
Williams, G., 1990, Waingawa River Management Study Hazard Assessment, G. and E. Williams Consultants, Ltd. 84 p.
Williams, G., 2000, Tauherenikau Delta - options for the future management of the lower Tauherenikau River: G & E Williams Consultants,
Williams, G., 2010, Waingawa River - Scheme Review (Draft: June 2010): G & E Williams Consultants, Ltd,
Williams, G. P., 1978, Bank-full discharge of rivers: Water Resources Research, v. 14, no. 6, p. 1141-1154, https://doi.org/10.1029/WR014i006p01141.
Williams, M., Zalasiewicz, J., Davies, N., Mazzini, I., Goiran, J.-P., and Kane, S., 2014, Humans as the third evolutionary stage of biosphere engineering of rivers: Anthropocene, v. 7, p. 57-63, https://doi.org/10.1016/j.ancene.2015.03.003.
Wing, O. E. J., Bates, P. D., Neal, J. C., Sampson, C. C., Smith, A. M., Quinn, N., Shustikova, I., Domeneghetti, A., Gilles, D. W., Goska, R., and Krajewski, W. F., 2019, A New Automated Method for Improved Flood Defense Representation in Large-Scale Hydraulic Models: Water Resources Research, v. 55, no. 12, p. 11007-11034, https://doi.org/10.1029/2019WR025957.
Winterbottom, S. J., 2000, Medium and short-term channel planform changes on the Rivers Tay and Tummel, Scotland: Geomorphology, v. 34, no. 3, p. 195-208, https://doi.org/10.1016/S0169-555X(00)00007-6.
Winterbottom, S. J., and Gilvear, D. J., 1997, Quantification of channel bed morphology in gravel-bed rivers using airborne multispectral imagery and aerial photography: Regulated Rivers:

Research & Management, v. 13, no. 6, p. 489-499, 10.1002/(SICI)1099-1646(199711/12)13:6<489::AID-RRR471>3.0.CO;2-X.
Wishart, D., Warburton, J., and Bracken, L., 2008, Gravel extraction and planform change in a wandering gravel-bed river: The River Wear, Northern England: Geomorphology, v. 94, no. 1, p. 131-152, https://doi.org/10.1016/j.geomorph.2007.05.003.
Wobus, C., Whipple, K. X., Kirby, E., Snyder, N. P., Johnson, J., Spyropolou, K., Crosby, B., and Sheehan, D., 2006, Tectonics from topography: Procedures, promise, and pitfalls, *in* Willett, S. D., Hovius, N., Brandon, M. T., and Fisher, D. M., eds., Tectonics, Climate, and Landscape Evolution, Volume 398, p. 55-74, 10.1130/2006.2398(04).
Wohl, E., 2010, Mountain Rivers Revisited, American Geophysical Union, Water Resources Monograph 19, Washington, D.C., 573 p.
-, 2013, The complexity of the real world in the context of the field tradition in geomorphology: Geomorphology, v. 200, p. 50-58, https://doi.org/10.1016/j.geomorph.2012.12.016.
Wohl, E., 2014, Time and the rivers flowing: Fluvial geomorphology since 1960: Geomorphology, v. 216, p. 263-282, 10.1016/j.geomorph.2014.04.012.
Wohl, E., 2015, Legacy effects on sediments in river corridors: Earth-Science Reviews, v. 147, p. 30-53, https://doi.org/10.1016/j.earscirev.2015.05.001.
Wohl, E., Brierley, G., Cadol, D., Coulthard, T. J., Covino, T., Fryirs, K. A., Grant, G., Hilton, R. G., Lane, S. N., Magilligan, F. J., Meitzen, K. M., Passalacqua, P., Poeppl, R. E., Rathburn, S. L., and Sklar, L. S., 2019, Connectivity as an emergent property of geomorphic systems: Earth Surface Processes and Landforms, v. 44, no. 1, p. 4-26, 10.1002/esp.4434.
Wolman, M. G., and Eiler, J. P., 1958, Reconnaissance study of erosion and deposition produced by the flood of August 1955 in Connecticut: Eos, Transactions American Geophysical Union, v. 39, no. 1, p. 1-14, https://doi.org/10.1029/TR039i001p00001.
Wolman, M. G., and Gerson, R., 1978, Relative scales of time and effectiveness of climate in watershed geomorphology: Earth Surface Processes, v. 3, no. 2, p. 189-208, https://doi.org/10.1002/esp.3290030207.
Wolman, M. G., and Miller, J. P., 1960, Magnitude and Frequency of Forces in Geomorphic Processes: The Journal of Geology, v. 68, no. 1, p. 54-74, 10.1086/626637.
Wood, H. O., and Neuman, F., 1931, Modified Mercalli Intensity scale of 1931: Bulletin of the Seismological Society of America, v. 21, no. 4, p. 7,
Yager, E. M., Turowski, J. M., Rickenmann, D., and McArdell, B. W., 2012, Sediment supply, grain protrusion, and bedload transport in mountain streams: Geophysical Research Letters, v. 39, no. 10, https://doi.org/10.1029/2012GL051654.
Yanites, B. J., Tucker, G. E., Mueller, K. J., and Chen, Y.-G., 2010, How rivers react to large earthquakes: Evidence from central Taiwan: Geology, v. 38, no. 7, p. 639-642, 10.1130/g30883.1.
Yellen, B., Woodruff, J. D., Cook, T. L., and Newton, R. M., 2016, Historically unprecedented erosion from Tropical Storm Irene due to high antecedent precipitation: Earth Surface Processes and Landforms, v. 41, no. 5, p. 677-684, https://doi.org/10.1002/esp.3896.
Yu, G.-a., Brierley, G., Huang, H. Q., Wang, Z., Blue, B., and Ma, Y., 2014, An environmental gradient of vegetative controls upon channel planform in the source region of the Yangtze and Yellow Rivers: Catena, v. 119, p. 143-153, 10.1016/j.catena2014.02.010.
Zachariasen, J., Villamor, P., Lee, J., Lukovic, B., and Begg, J., 2000, Late Quaternary Faulting of the Masterton and Carterton Faults, Wairarapa, New Zealand: Institute of Geological and Nuclear Sciences; IGNS,
Zawiejska, J., Wyżga, B., and Radecki-Pawlik, A., 2015, Variation in surface bed material along a mountain river modified by gravel extraction and channelization, the Czarny Dunajec, Polish Carpathians: Geomorphology, v. 231, p. 353-366, https://doi.org/10.1016/j.geomorph.2014.12.026.

Zhang, L. M., Zhang, S., and Huang, R. Q., 2014, Multi-hazard scenarios and consequences in Beichuan, China: The first five years after the 2008 Wenchuan earthquake: Engineering Geology, v. 180, p. 4-20, https://doi.org/10.1016/j.enggeo.2014.03.020.

Zhang, S., Ma, Y., Chen, F., Liu, J., Chen, F., Lu, S., Jiang, L., and Li, D., 2020, A new method for supporting interpretation of paleochannels in a large scale — Detrended Digital Elevation Model Interpretation: Geomorphology, v. 369, p. 107374, https://doi.org/10.1016/j.geomorph.2020.107374.

Zheng, X., Tarboton, D. G., Maidment, D. R., Liu, Y. Y., and Passalacqua, P., 2018, River Channel Geometry and Rating Curve Estimation Using Height above the Nearest Drainage: JAWRA Journal of the American Water Resources Association, v. 54, no. 4, p. 785-806, https://doi.org/10.1111/1752-1688.12661.

Appendix A – Statements of Contribution

MASSEY UNIVERSITY
TE KUNENGA KI PŪREHUROA
UNIVERSITY OF NEW ZEALAND

GRADUATE RESEARCH SCHOOL

STATEMENT OF CONTRIBUTION
DOCTORATE WITH PUBLICATIONS/MANUSCRIPTS

We, the student and the student's Main Supervisor, certify that all co-authors have consented to their work being included in the thesis and they have accepted the student's contribution as indicated below in the Statement of Originality.

Student name:	William Campbell Conley Jr
Name/title of main supervisor:	Professor Ian C. Fuller
In which chapter is the manuscript/published work?	Chapter 4

Please select one of the following three options:

○	The manuscript/published work is published or in press • Please provide the full reference of the research output:
○	The manuscript is currently under review for publication – please indicate: • The name of the journal: • The percentage of the manuscript/published work that was contributed by the student: % • Describe the contribution that the student has made to the manuscript/published work:
●	It is intended that the manuscript will be published, but it has not yet been submitted to a journal

Student's signature:	
Main supervisor's signature:	

This form should appear at the end of each thesis chapter/section/appendix submitted as a manuscript/ publication or collected as an appendix at the end of the thesis.

MASSEY UNIVERSITY
TE KUNENGA KI PŪREHUROA
UNIVERSITY OF NEW ZEALAND

GRADUATE RESEARCH SCHOOL

STATEMENT OF CONTRIBUTION
DOCTORATE WITH PUBLICATIONS/MANUSCRIPTS

We, the student and the student's Main Supervisor, certify that all co-authors have consented to their work being included in the thesis and they have accepted the student's contribution as indicated below in the Statement of Originality.

Student name:	William Campbell Conley Jr
Name/title of main supervisor:	Professor Ian C. Fuller
In which chapter is the manuscript/published work?	Chapter 5

Please select one of the following three options:

○	The manuscript/published work is published or in press • Please provide the full reference of the research output:
○	The manuscript is currently under review for publication – please indicate: • The name of the journal: • The percentage of the manuscript/published work that was contributed by the student: % • Describe the contribution that the student has made to the manuscript/published work:
●	It is intended that the manuscript will be published, but it has not yet been submitted to a journal

Student's signature:	
Main supervisor's signature:	

This form should appear at the end of each thesis chapter/section/appendix submitted as a manuscript/ publication or collected as an appendix at the end of the thesis.

MASSEY UNIVERSITY
TE KUNENGA KI PŪREHUROA
UNIVERSITY OF NEW ZEALAND

GRADUATE RESEARCH SCHOOL

STATEMENT OF CONTRIBUTION
DOCTORATE WITH PUBLICATIONS/MANUSCRIPTS

We, the student and the student's Main Supervisor, certify that all co-authors have consented to their work being included in the thesis and they have accepted the student's contribution as indicated below in the Statement of Originality.

Student name:	William Campbell Conley Jr
Name/title of main supervisor:	Professor Ian C. Fuller
In which chapter is the manuscript/published work?	Chapter 6

Please select one of the following three options:

○	The manuscript/published work is published or in press • Please provide the full reference of the research output:
○	The manuscript is currently under review for publication – please indicate: • The name of the journal: • The percentage of the manuscript/published work that was contributed by the student: % • Describe the contribution that the student has made to the manuscript/published work:
●	It is intended that the manuscript will be published, but it has not yet been submitted to a journal

Student's signature:	
Main supervisor's signature:	

This form should appear at the end of each thesis chapter/section/appendix submitted as a manuscript/ publication or collected as an appendix at the end of the thesis.

MASSEY UNIVERSITY
TE KUNENGA KI PŪREHUROA
UNIVERSITY OF NEW ZEALAND

GRADUATE RESEARCH SCHOOL

STATEMENT OF CONTRIBUTION
DOCTORATE WITH PUBLICATIONS/MANUSCRIPTS

We, the student and the student's Main Supervisor, certify that all co-authors have consented to their work being included in the thesis and they have accepted the student's contribution as indicated below in the Statement of Originality.

Student name:	William Campbell Conley Jr
Name/title of main supervisor:	Professor Ian C. Fuller
In which chapter is the manuscript/published work?	Chapter 7

Please select one of the following three options:

○	The manuscript/published work is published or in press • Please provide the full reference of the research output:
○	The manuscript is currently under review for publication – please indicate: • The name of the journal: • The percentage of the manuscript/published work that was contributed by the student: % • Describe the contribution that the student has made to the manuscript/published work:
●	It is intended that the manuscript will be published, but it has not yet been submitted to a journal

Student's signature:	
Main supervisor's signature:	

This form should appear at the end of each thesis chapter/section/appendix submitted as a manuscript/ publication or collected as an appendix at the end of the thesis.